

Washington University in St. Louis

Washington University Open Scholarship

All Theses and Dissertations (ETDs)

1-1-2011

The Hydrology And Geochemistry Of Urban And Rural Watersheds In East-Central Missouri

Elizabeth Hasenmueller

Washington University in St. Louis

Follow this and additional works at: <https://openscholarship.wustl.edu/etd>

Recommended Citation

Hasenmueller, Elizabeth, "The Hydrology And Geochemistry Of Urban And Rural Watersheds In East-Central Missouri" (2011). *All Theses and Dissertations (ETDs)*. 585.

<https://openscholarship.wustl.edu/etd/585>

This Dissertation is brought to you for free and open access by Washington University Open Scholarship. It has been accepted for inclusion in All Theses and Dissertations (ETDs) by an authorized administrator of Washington University Open Scholarship. For more information, please contact digital@wumail.wustl.edu.

WASHINGTON UNIVERSITY IN ST. LOUIS

Department of Earth & Planetary Sciences

Dissertation Examination Committee:

Robert E. Criss, Chair

Jeffrey G. Catalano

Daniel E. Giammar

William R. Lowry

Jill D. Pasteris

Jennifer R. Smith

THE HYDROLOGY AND GEOCHEMISTRY OF URBAN AND RURAL
WATERSHEDS IN EAST-CENTRAL MISSOURI

by

Elizabeth A. Hasenmueller

A dissertation presented to the
Graduate School of Arts and Sciences
of Washington University in
partial fulfillment of the
requirements for the degree
of Doctor of Philosophy

December 2011

Saint Louis, Missouri

ABSTRACT OF THE DISSERTATION

THE HYDROLOGY AND GEOCHEMISTRY OF URBAN AND RURAL
WATERSHEDS IN EAST-CENTRAL MISSOURI

by

Elizabeth A. Hasenmueller

Doctor of Philosophy in Earth & Planetary Sciences

Washington University in St. Louis, 2011

Professor Robert E. Criss, Chairperson

This dissertation examines the physical hydrology and geochemistry of surface waters and shallow groundwaters in east-central Missouri, USA, to determine how runoff differs in flow and quality between urban and natural watersheds. The study employs high frequency in situ monitoring of relevant water quality parameters in tandem with lab analyses of major and minor elements and stable isotope concentrations to address degradation of watersheds by land development and other human activities. Chapter 3 of this dissertation compares three watersheds and their tributaries, each with differing levels of urban land use, which were monitored for more than one year to document their hydrologic and geochemical character. Urban streams were characterized by flashier responses to storm perturbations and had reduced baseflow components compared to rural streams. Rural streams had smaller hydrologic and geochemical variations, higher baseflow, and longer lag times following storm perturbations. Urban and suburban streams were commonly polluted with salts and nutrients, and chemical compositions

could change rapidly. Continuous monitoring data demonstrate increased seasonal and diurnal variability in urban systems, and show that infrequent and arbitrary sampling regimes in both urban and rural systems can under- or overestimate loads by 100-fold. Chapter 4 examines regional boron (B) concentrations. In contrast to previous work that attributes B contamination of surface waters and groundwaters to wastewaters and fertilizers, this study found that the largest contributor of B to local waters was municipal drinking water used for urban lawn irrigation. Chapter 5, a comparative study of springs in east-central Missouri, establishes contaminant background levels in shallow groundwaters and quantitatively establishes that springs proximal to St. Louis and adjoining suburbs have the most degraded water quality. The impacted springs display the same water quality problems as urban surface waters including high Cl (> 230 ppm), low dissolved oxygen (DO; < 5 ppm), and high *Escherichia coli* (*E. coli*; > 206 cfu/100 mL). In addition, the residence times for contaminants typically range from a few months to two years and approximate stable isotope residence times. Chapter 6 discusses a novel technique to determine the subterranean environment of groundwaters using field measurements of DO and pH. Springs draining vadose cave passages have higher DO and pH values than “phreatic” springs that have no known cave passage because of the equilibration of DO with overlying cave air and the simultaneous degassing of dissolved CO₂. Degassing processes also affect the saturation state of minerals such as calcite, with cave springs having the highest degree of saturation with respect to calcite. Taken together, these chapters provide a unique archive of regional water hydrology and geochemistry, and demonstrate previously unknown sources and transport mechanisms for several chemical constituents.

ACKNOWLEDGEMENTS

There are many thanks owed to the many people who have helped me complete this dissertation and requisite research. First, I would like to thank my advisor, Robert Criss; without his guidance and support I could have never completed this project. I would also like to thank my dissertation committee, including Jeffrey Catalano, Daniel Giammar, William Lowry, Jill Pasteris, and Jennifer Smith, for their suggestions to improve this manuscript.

Fieldwork, bacterial analyses, and chemical analyses (including wet chemical, ICP-OES, and ICP-MS analyses) were funded by subcontracts for two 319 Grants from the Watershed Management Plan Development Grant Program, which were provided by the U.S. Environmental Protection Agency through the Missouri Department of Natural Resources to the University Department of Public Works (Grant No. G06-NPS-18) and the Missouri Botanical Garden (Grant No. G09-NPS-13), and personally by Robert Criss. Stable isotope analyses were funded predominantly by Robert Criss, but in part by 319 Grant No. G06-NPS-18. ICP-OES and ICP-MS analyses were performed at the Nano Research Facility (NRF) of Washington University, a member of the National Nanotechnology Infrastructure Network (NNIN), which is supported by the National Science Foundation under Grant No. ECS-0335765.

I gratefully acknowledge Washington University for support, including teaching assistantships and a Graduate School of Arts and Sciences Dean's Dissertation Fellowship that funded my final year of graduate research. Additional funding from the Missouri Space Grant Consortium and research assistantships from the 319 Grants are

recognized. Summer support from the Earth and Planetary Sciences Department through Wheeler Fellowships is also greatly appreciated.

William Winston provided indispensable guidance and training in the field, lab, and with ArcGIS software. Jeffrey Catalano and Jennifer Smith are thanked for valuable discussion and mentoring, and Kate Nelson and Yujie Xiong are thanked for their assistance in data analysis on the ICP-OES and ICP-MS. Trish Reilly's advice and discussion for the 319 Grant projects was exceptionally helpful. I would also like to thank Susan McCrary and Nicholas Bauer from the Metropolitan St. Louis Sewer District (MSD) for their help and cooperation. I have had many field and laboratory assistants whose involvement with sampling excursions and sample processing has been invaluable, and I greatly appreciate all who have helped me over the years. Support from my friends inside and outside the department made all the difference in the completion of this project.

Most of all I thank my parents, who encouraged me to pursue my education, and my husband, Jeremy, whose love and support made this project possible.

TABLE OF CONTENTS

ABSTRACT OF THE DISSERTATION	ii
ACKNOWLEDGEMENTS	iv
LIST OF TABLES	xv
LIST OF FIGURES	xvii
CHAPTER 1: Introduction	1
1.1. Background	1
1.2. Regional Setting	1
<i>1.2.1. Climate</i>	2
<i>1.2.2. Karst Terrains</i>	2
<i>1.2.3. Hydrology</i>	4
1.2.3.1. Surface Waters	4
1.2.3.2. Shallow Groundwaters	5
1.3. Isotope Hydrology	6
<i>1.3.1. Isotopic Composition of Rainfall</i>	7
1.4. Generation and Character of Runoff and Land Use	8
<i>1.4.1. Flood Waters and Chemographs</i>	8
<i>1.4.2. Effects of Land Use</i>	9
1.4.2.1. Water Quality	10
1.5. Remediation Efforts	13
1.6. Objectives of the Current Study	13
1.7. References	15

CHAPTER 2: Methods and Data	20
2.1. Fieldwork and Sampling	20
2.1.1. <i>Precipitation Samples</i>	20
2.1.2. <i>Grab Samples</i>	21
2.1.2.1. <i>Grab Sample Preparation</i>	22
2.1.2.2. <i>Field Sample Collection</i>	22
2.1.2.3. <i>In Situ Field Measurements</i>	23
2.1.3. <i>Autosamplers</i>	24
2.1.3.1. <i>Autosampler Bottle Preparation</i>	24
2.1.3.2. <i>Autosampler Installations, Specifications, and Operational Modes</i>	24
2.1.4. <i>Continuous Monitoring Sensors</i>	26
2.2. Laboratory Methods	28
2.2.1. <i>IR-MS Analysis: Hydrogen and Oxygen Isotopes</i>	28
2.2.2. <i>Inductively Coupled Plasma Optical Emission Spectrometry (ICP-OES) and Inductively Coupled Plasma Mass Spectrometry (ICP-MS) Analyses</i>	29
2.2.3. <i>Wet Chemical Analysis</i>	30
2.2.4. <i>Microbial Analysis</i>	30
2.2.5. <i>Quality Assurance/Quality Control (QA/QC)</i>	31
2.3. Data Treatment and Interpretative Methods	31
2.3.1. <i>Drift Corrections for Continuous Monitoring Devices</i>	31
2.3.2. <i>HCO₃⁻, fCO₂, and fO₂ Calculations</i>	32

2.3.3. <i>Hydrograph Separations</i>	33
2.3.4. <i>Theoretical Hydrograph</i>	34
2.4. Data Tables	35
2.5. References	36
CHAPTER 3: New insight into urban watershed dynamics using high frequency in situ monitoring in three streams and their tributaries, east-central Missouri	47
Abstract	47
3.1. Introduction	48
3.1.1. <i>Significance of Floods</i>	48
3.1.2. <i>Shortcomings of Available Datasets</i>	49
3.1.3. <i>Study Design</i>	52
3.2. Description of Study Sites	55
3.2.1. <i>Fox Creek</i>	56
3.2.2. <i>Grand Glaize Creek</i>	57
3.2.3. <i>River des Peres</i>	58
3.2.3.1. <i>Deer Creek</i>	60
3.2.1.3.1. <i>Black Creek</i>	60
3.3. Methods	61
3.4. Results	63
3.4.1. <i>Response to Storm Perturbation</i>	63
3.4.1.1. <i>March – April, 2008 Events: Fox, Grand Glaize, and Black Creeks</i>	63
3.4.1.1.1. <i>Fox Creek</i>	64

3.4.1.1.2. <i>Grand Glaize Creek</i>	65
3.4.1.1.3. <i>Black Creek</i>	67
3.4.1.2. May 2008 Event: Fox, Grand Glaize, and Black Creeks.	70
3.4.1.2.1. <i>Fox Creek</i>	70
3.4.1.2.2. <i>Grand Glaize Creek</i>	71
3.4.1.2.3. <i>Black Creek</i>	73
3.4.1.3. July 2008 Event: Fox and Black Creeks	75
3.4.1.3.1. <i>Fox Creek</i>	75
3.4.1.3.2. <i>Black Creek</i>	77
3.4.1.4. September 2008 Event (Hurricane Gustav): Fox Creek ..	79
3.4.1.5. April 2010 Event: RP1, RP2, and HMP	80
3.4.1.5.1. <i>Ruth Park, RP1</i>	81
3.4.1.5.2. <i>Ruth Park, RP2</i>	82
3.4.1.5.3. <i>Heman Park, HMP</i>	84
3.5. Discussion	85
3.5.1. <i>Isotope Hydrology and Hydrograph Separation</i>	85
3.5.2. <i>Geochemical Response during Storm Perturbations</i>	87
3.5.2.1. SpC and Major Elements	88
3.5.2.1.1. <i>Small-Scale SpC Features</i>	89
3.5.2.1.1.1. First Flush Events	90
3.5.2.1.1.2. Transient SpC Minima.....	91
3.5.2.2. Turbidity	92
3.5.2.3. Elements Positively Correlated with Discharge	92

3.5.3. <i>Seasonal Variations</i>	93
3.5.4. <i>Diurnal Variations</i>	97
3.5.5. <i>Water Quality Differences in Natural and Artificial Channels</i>	98
3.5.6. <i>Load Estimates</i>	99
3.5.6. <i>Theoretical Hydrograph Models</i>	101
3.5.8. <i>Observed Hysteresis Behaviors</i>	103
3.5.8.1. <i>Proposed Hysteresis Explanations</i>	106
3.6. Conclusions	107
3.7. References	111
CHAPTER 4: Determining the source of boron in east-central Missouri surface waters and groundwaters	168
Abstract	168
4.1. Introduction	169
4.1.1. <i>Sources of B</i>	169
4.1.1.1. <i>Wastewaters</i>	171
4.1.1.2. <i>Fertilizers</i>	172
4.1.2. <i>Use of B Isotopes</i>	173
4.1.3. <i>Urban Irrigation</i>	174
4.1.4. <i>Study Design</i>	175
4.2. Description of Study Sites	176
4.2.1. <i>Continuously Monitored Sites</i>	176
4.2.1.1. <i>Upper River des Peres</i>	176
4.2.1.1.1. <i>Ruth Park 1 (RP1)</i>	177

4.2.1.1.2. <i>Ruth Park 2 (RP2)</i>	177
4.2.1.1.3. <i>Heman Park (HMP)</i>	178
4.2.1.2. <i>Surface Runoff</i>	178
4.2.1.2.1. <i>10920 Chalet Court (CHA)</i>	178
4.2.1.2.2. <i>8360 Cornell Avenue (CORN)</i>	179
4.2.1.2.3. <i>Mt. Calvary Church and Adjacent Neighborhood (MTC)</i>	179
4.2.2. <i>Grab Sample Sites: Surface Waters, Groundwaters, and End- members</i>	179
4.2.3. <i>Additional Data</i>	180
4.3. Methods	180
4.4. Results and Discussion	181
4.4.1. <i>Regional B Concentrations</i>	181
4.4.2. <i>Relationship between B Concentrations and Discharge</i>	182
4.4.2.1. <i>Urban Watersheds: The River des Peres</i>	182
4.4.2.2. <i>Surface Runoff</i>	183
4.4.2.3. <i>Examples of Positive Correlations between B and Discharge</i>	184
4.4.3. <i>B Sources and End-members</i>	185
4.4.3.1. <i>Atmospheric Deposition</i>	185
4.4.3.2. <i>Road Salt Contamination</i>	185
4.4.3.3. <i>Organic Rich Leachates</i>	186
4.4.3.4. <i>Wastewaters</i>	187

4.4.3.5. Fertilizers	189
4.4.3.6. Lawn Irrigation	190
4.4.3.6.1. B Concentrations along the Missouri River....	191
4.5. Conclusions.....	192
4.6. References.....	194
CHAPTER 5: Magnitude, timescales, and geographic variations of groundwater contamination.....	214
Abstract.....	214
5.1. Introduction.....	215
5.1.1. <i>Regional Hydrologic Setting.....</i>	216
5.2. Methods.....	217
5.2.1. <i>Samples</i>	217
5.3. Results and Discussion.....	217
5.3.1. <i>Water Quality Results</i>	217
5.3.1.1. SpC, Na, and Cl	218
5.3.1.2. DO.....	220
5.3.1.3. <i>E. coli</i>	221
5.3.1.4. Nutrients.....	222
5.3.1.5. B.....	224
5.3.1.6. Trace Metals.....	224
5.3.1.7. Stable Isotopes	225
5.3.1.8. Timescales of Contaminant Residence	226
5.4. Conclusions.....	228

5.5. References	230
CHAPTER 6: A novel technique to discover open cave passage in karst spring systems	245
Abstract	245
6.1. Introduction	247
<i>6.1.1. Geophysical Cave Detection</i>	248
<i>6.1.2. Chemical Basis</i>	249
6.2. Description of Study Sites	252
6.3. Methods	253
6.4. Results and Discussion	254
<i>6.4.1. Dissolved Oxygen and pH</i>	254
<i>6.4.2. Calcite Saturation</i>	258
<i>6.4.3. Total Suspended Solids and E. coli</i>	259
<i>6.4.4. Stable Isotopes</i>	260
6.5. Conclusions	261
6.6. References	262
CHAPTER 7: Conclusions and Future Work	277
7.1. Conclusions	277
7.2. Future Research	280
7.3. References	284
APPENDIX A: Ladue Rainfall	285
APPENDIX B: Fox Creek Data	294
APPENDIX C: Grand Glaize Creek Data	302

APPENDIX D: Sugar Creek Data.....	309
APPENDIX E: River des Peres at Morgan Ford Rd. Data.....	310
APPENDIX F: Upper River des Peres Data.....	312
APPENDIX G: Upper River des Peres ICP-MS Data.....	324
APPENDIX H: Upper River des Peres ICP-OES Data.....	330
APPENDIX I: Deer Creek Data	336
APPENDIX J: Black Creek Data	338
APPENDIX K: Spring Data.....	348
APPENDIX L: Wastewater Treatment Plant Data	360

LIST OF TABLES

CHAPTER 2

Table 2.1. Field collection protocols and analytical procedures for individual analytes	38
Table 2.2. Handheld water quality equipment specifications	39
Table 2.3. Monitoring locations, equipment, and time frames	40
Table 2.4. Continuous monitoring sensors specifications	41
Table 2.5. Elements and detection limits measured with ICP-OES	42
Table 2.6. Elements and detection limits measured with ICP-MS	43

CHAPTER 3

Table 3.1. Sampling location information	118
Table 3.2. Rainfall amounts and isotopic character for selected discharge responses	119
Table 3.3. Baseflow contributions during five storm induced pulses	120
Table 3.4. Average and maximum baseflow contributions determined by isotope hydrograph separation for all discharge perturbations	121
Table 3.5. Weighted average daily load estimates for various water quality parameters calculated using grab samples and continuous monitoring data	122
Table 3.6. Simple average of various water quality parameters calculated using grab samples and continuous monitoring data	123
Table 3.7. Average <i>b</i> values for discharge responses at various sampling sites	124

CHAPTER 4

Table 4.1. Site descriptions for runoff sampling locations	199
---	-----

Table 4.2. Average values for various water quality parameters for surface runoff, municipal drinking and wastewaters, surface streams, groundwaters, runoff, and other potential B end-members	200
Table 4.3. Field measurements, major element, isotope, and bacterial analyses of wastewater influent and effluent	201
Table 4.4. Minor and trace element analyses of wastewater influent and effluent	202
Table 4.5. Chemical composition of selected homeowner and agricultural fertilizers. .	203
Table 4.6. B concentrations along the Missouri River	204

CHAPTER 5

Table 5.1. Concentration means and ranges for selected water quality constituents compared to global average values	234
Table 5.2. Time constants of isotopic and SpC response for select springs	236

CHAPTER 6

Table 6.1. Concentration means and ranges for selected water quality constituents for various types of waters.....	268
Table 6.2. Concentration means and ranges for selected water quality constituents for archival phreatic and cave spring data	269

LIST OF FIGURES

CHAPTER 2

Figure 2.1. Typical autosampler field installation44

Figure 2.2. Typical in situ continuous water quality monitoring device field installation
.....45

Figure 2.3. Typical in situ water level sensor field installation46

CHAPTER 3

Figure 3.1. Graph of average and record discharge versus basin area for rivers and
streams in Missouri125

Figure 3.2. Graph of average and record discharge versus basin area for the sampling
sites in the study.....126

Figure 3.3. Delineated watershed boundaries on a digital elevation model for east-
central Missouri127

Figure 3.4. Delineated watershed boundaries on a soil map for east-central Missouri .129

Figure 3.5. Delineated watershed boundaries on a bedrock map for east-central Missouri
.....132

Figure 3.6. Delineated watershed boundaries on a relief and population density map for
east-central Missouri.....133

Figure 3.7. Delineated watershed boundaries on a land use map for east-central Missouri
.....134

Figure 3.8. Fox Creek monitoring location.....135

Figure 3.9. Grand Glaize Creek monitoring location.....	136
Figure 3.10. Historical and present day images of the River des Peres monitoring location.....	137
Figure 3.11. Black Creek monitoring location.....	138
Figure 3.12. Turbidity versus TSS	139
Figure 3.13. The hydrologic, isotopic, and geochemical responses for Fox, Grand Glaize, and Black Creeks during five rainfall in March – April 2008.....	140
Figure 3.14. Hysteresis loops for the March 26 discharge event at Black Creek	142
Figure 3.15. Hysteresis loops for the March 31 – April 1 discharge event at Black Creek.	143
Figure 3.16. The hydrologic, isotopic, and geochemical responses for Fox, Grand Glaize, and Black Creeks during a May 7 – 8, 2008 discharge event	144
Figure 3.17. The hydrologic, isotopic, and geochemical responses for Fox and Black Creeks for a July 9, 2008 discharge event	146
Figure 3.18. The observed precipitation and the hydrologic, isotopic, and geochemical responses at Fox Creek during Hurricane Gustav, September 14, 2008	148
Figure 3.19. The discharge at Ruth and Heman Parks in response to an April 2, 2010 discharge event.....	150
Figure 3.20. The hydrologic, isotopic, and geochemical responses for the Southwest Branch and the Upper River des Peres for an April 2, 2010 discharge event.....	151
Figure 3.21. Isotope and SpC hydrograph separation comparison for a May 7 – 8, 2008 discharge event at Fox, Grand Glaize, and Black Creeks.....	153

Figure 3.22. Seasonal monitoring data for Fox Creek, Grand Glaize Creek, and the River des Peres.....	154
Figure 3.23. Seasonal monitoring data for the Upper River des Peres sites	156
Figure 3.24. Seasonal isotopic data from all monitoring sites	158
Figure 3.25. The Southwest Branch of the Upper River des Peres field sites	160
Figure 3.26. The measured and predicted discharge variations for Fox, Grand Glaize, and Black Creeks	162
Figure 3.27. The measured and predicted discharge variations for the Upper River des Peres	164
Figure 3.28. The isotopic hydrograph separation of storm flow and δD - $\delta^{18}O$ plots for two discharge events at the Orangeville Rise (Lakey and Krothe, 1996).....	165
Figure 3.29. Possible causes of hysteresis	166
Figure 3.30. Locations of CSOs in St. Louis City and County.....	167

CHAPTER 4

Figure 4.1. Relief map of east-central Missouri showing sampling locations	205
Figure 4.2. Sample sites and delineated watershed boundaries on a land use map for east-central Missouri.....	206
Figure 4.3. The positive correlation of B and major elements with SpC.....	207
Figure 4.4. Discharge and B concentrations for an April 2 – 3 event at the Upper River des Peres monitoring locations	208
Figure 4.5. The relationship between B concentration and discharge for surface runoff	209

Figure 4.6. Typical surface runoff responses	210
Figure 4.7. The relationship between B and selected elements	211
Figure 4.8. B concentrations along the Missouri River	212

CHAPTER 5

Figure 5.1. Relief and population density map of east-central Missouri showing sampling locations	237
Figure 5.2. Spring water quality parameters plotted against the UTM easting	238
Figure 5.3. Na and Cl concentrations for various waters plotted against SpC and United States road salt usage	240
Figure 5.4. The pH versus DO for springs and streams	242
Figure 5.5. Comparison of $\delta^{18}\text{O}$ and SpC values for Lewis and Rockwoods Springs...	243

CHAPTER 6

Figure 6.1. Relief map of east-central Missouri showing sample locations	270
Figure 6.2. Cave maps.....	271
Figure 6.3. The pH versus DO for phreatic springs and cave springs	272
Figure 6.4. The pH versus DO for phreatic springs and cave springs traverses	273
Figure 6.5. The pH and DO versus distances for phreatic springs and cave springs	274
Figure 6.6. $\log\text{Ca}^{2+}$ versus $\log f\text{CO}_2$	275
Figure 6.7. δD and $\delta^{18}\text{O}$ and for various water samples	276

Chapter 1: Introduction

1.1. Background

Water is an essential resource covering over 70% of the Earth's surface; however, most water is too saline for human consumption and use. Less than 3% of the hydrosphere is freshwater, and of this, only about 25% is accessible, with the majority of the available water being groundwater. Familiar surface water bodies such as lakes, streams, and rivers make up less than 0.02% of the hydrosphere (Gleick, 1996).

It is important to understand the sources and mechanisms that reduce the quality of these limited freshwater supplies. Anthropogenic pollutants can significantly degrade water resources, and while the relationship between land development and the hydrologic and geochemical character of streams and springs has been studied extensively, many key relationships are not well understood. Stream and shallow groundwater degradation caused by urbanization involves multiple contaminant sources with complex pathways to aquatic environments. The time scales and mechanisms with which contaminants and water move through the environment are important factors controlling the severity of pollution. This research examines the relationships between land use and water quality degradation by comparing natural and altered systems.

1.2. Regional Setting

East-central Missouri is a densely vegetated region with abundant rainfall and rugged topography (Vandike, 1995). The region lies in the northern part of the Ozark Plateaus province, and is predominantly underlain by Paleozoic limestone, dolostone, sandstone, and shale units. These sedimentary rocks gently dip away from the St. Francois Mountains, a regional uplift with a core of Precambrian igneous rocks

(Fenneman, 1938). The high precipitation rates and topography promote interactions among flowing, aggressive surface waters and groundwaters and the soluble carbonate rocks, a process which has led to the extensive development of karst features including abundant sinkholes, caves, springs, seeps, and losing and gaining streams (Criss et al., 2009). This topography is a major control for the hydrology of the region, and results in enhanced interconnectivity of surface waters and groundwaters.

1.2.1. Climate

The climate of Missouri is temperate, with an average air temperature of 13.5°C. Temperatures fluctuate seasonally from lows near -10°C in the winter to highs near 35°C in the late summer. Average annual precipitation for the area is approximately 100 cm, based on long-term records of the National Weather Service (NWS) at Lambert-St. Louis International Airport (National Oceanic and Atmospheric Administration [NOAA], 2011); most of this precipitation occurs as rain. Evapotranspiration rates for the area are approximately 70 cm/year based on regional estimates (Vandike, 1995). A simple water budget for local features can be calculated using this information:

$$\text{Runoff} = \text{Precipitation} - \text{Evapotranspiration} \pm \text{Change in Groundwater Storage}$$

Another estimate of average runoff in the region can be calculated by dividing the average annual discharge by the drainage area of local rivers. Using long-term records of discharge at gauging stations in St. Louis area, the estimated average regional runoff is 8.7×10^{-3} cms/km² (Criss, 2001).

1.2.2. Karst Terrains

Carbonic and organic acids dissolved in surface waters enhance the dissolution of carbonate rocks as they move through the subsurface. Dissolution is enhanced along joints, fractures, and bedding planes in limestones and dolostones, and over time this

action leads to the development of large voids and conduit systems in the subsurface. These openings enhance an aquifer's ability to store and rapidly transport large quantities of water (White, 1988). "Karst" refers to the landforms produced by this dissolution process, and mature karst terrains are characterized by numerous features including sinkholes, springs, seeps, and losing or gaining streams. Subsurface drainage in these systems is important or dominant, allowing the vertical penetration of meteoric precipitation to enhance the exchange of contaminants between surface water and groundwaters.

Karst development is highly variable and depends on climatic conditions, rock type, and the amount of exposed rock. It is commonly understood that dissolution rates also depend on the amount of dissolved CO₂ and organic acids; for example, pure water in a closed system can dissolve about 13 ppm of calcite before the solution is saturated, while pure water in equilibrium with the atmosphere (e.g., $P_{\text{CO}_2} = 10^{-3.5}$ bar) is able to dissolve > 70 ppm of calcite (Stumm and Morgan, 1981). Further dissolution may occur as result of soil waters coming in contact with soluble carbonate rocks. Soil air has a much higher concentration of CO₂ (usually $10^{-2.5}$ to $10^{-1.5}$ bar), a product of respiration and decay of organic matter (Troester and White, 1984; White, 1988; Langmuir, 1997).

Lithology can have a major impact on the amount of karstification in a given area. Of the common carbonates, dolomite is the least soluble, calcite has intermediate solubility, and high-Mg calcite and aragonite are the most soluble (James and Choquette, 1984). The purity of the carbonate host rock (i.e., amount of clay and sand content), grain size, texture, and porosity also play important roles in host rock solubility. Ford and Williams (1989) found that fine grained rocks are typically more soluble.

Additionally, climate can also impact karst terrain formation and various authors have found relationships between limestone dissolution and runoff (Gams, 1972), precipitation (Pulina, 1971), and temperature (Smith and Atkinson, 1976). In general, carbonate dissolution increases with higher amounts of precipitation.

1.2.3. Hydrology

1.2.3.1. Surface Waters

The mechanisms by which precipitation moves to river channels and into the subsurface has been studied and modeled extensively. Horton (1933) originally proposed that overland flow, produced when rainfall exceeds the infiltration capacity of the subsurface, is the dominant mechanism supplying water to streams. However, subsequent geochemical studies (Pinder and Jones, 1969; Fritz et al., 1976; Sklash et al., 1976; Freeze and Cherry, 1979; Sklash and Farvolden, 1979; Frederickson and Criss, 1999) demonstrate that infiltration rates are usually greater than most rainfall rates. Thus, when rainfall infiltrates, it displaces preexisting groundwater into stream channels (Hewlett and Hibbert, 1967).

Streams derive their water directly or indirectly from precipitation events. Some of this water may have its origin as overland flow, but generally much of the water in streams originally infiltrated and traveled to the channel as interflow through soils or as baseflow through rock. During low flows, stream discharge is predominantly derived from groundwaters, while high flows are a combination of this baseflow component and recent event water (Ward and Trimble, 2004). Surface waters can exhibit dynamic changes in discharge and chemical constituents, and their responses are affected by numerous factors including the drainage area, topography, watershed shape and

orientation, geology, interflow, and, perhaps most importantly, the soil and land use (Ward and Trimble, 2004).

Streams in east-central Missouri are extremely diverse in nature, ranging from small streams and rivers to the large Missouri and Mississippi Rivers. Just above St. Louis, the Illinois, Missouri, and Mississippi Rivers combine into what is called the Middle Mississippi. Below the confluence with the Missouri River, the Mississippi River has an average discharge of 5,000 cms, but can reach up to 28,000 cms during severe flooding as seen during the Great Flood of 1993 (U.S. Geological Survey [USGS], 2011). The smaller Meramec River drains 10,300 km² in central Missouri, and is fast, clear, and relatively unimpacted river with an average discharge of 90 cms, but flows can range from lows of 6 cms to almost 5,000 cms during extreme flooding, as in 1936 (USGS, 2011). In addition, Missouri has many smaller rivers and streams that drain a few hundred square kilometers or less. Many of these smaller features are impacted to varying degrees by different types of land use and development.

1.2.3.2. Shallow Groundwaters

Groundwater aquifers can underlie vast regions, retain water for long periods of time, and transport subsurface waters across large distances. Aquifer recharge occurs when meteoric precipitation and surface waters either directly or diffusely percolate through the overlying soils and bedrock. During subsurface residence, interactions between the water and the host soils and rock impart a unique chemical signature.

Discharge from an aquifer occurs where the water table intersects the Earth's surface, and the groundwater can emerge as a spring or seep. Connections that join surface water and groundwater resources facilitate the mutual exchange of water,

suspended sediments, bacteria, and dissolved material (including contaminants), but these interactions are often difficult to observe and quantify. Often drill holes or other intrusive investigations are expensive and impractical, and in many areas the subsurface environment is not well characterized. Springs, however, provide a natural interface between surface topography and groundwater reservoirs (Fetter, 1994). Spring water carries the integrated signature of the processes that occur from the time surface waters penetrate into the subsurface to when the water emerges at the spring orifice. These chemical signatures carry information about the aquifer residence time (Fredrickson and Criss, 1999; Winston and Criss, 2004), geologic composition and structure (Williams, 2008), recharge area (Rose et al., 1996; Larsen et al., 2001), transport processes (James et al., 2000), and the contributions of various end-members during storm induced discharge responses (Lee and Krothe, 2001; Winston and Criss, 2004).

East-central Missouri features a diverse suite of springs that range from small (with average discharges of < 0.0001 cms) to large, “first magnitude” springs, and the largest, Big Spring, has an impressive average discharge of 12.5 cms (Vineyard and Feder, 1982). Spring systems vary from nearly pristine to highly impacted urban systems, and many springs have been destroyed by urban land development.

1.3. Isotope Hydrology

Stable isotope analysis is an extremely useful tool for determining the origins of water in streams and springs, and has provided novel insight about flooding processes (Freeze and Cherry, 1979; Clark and Fritz, 1997; Frederickson and Criss, 1999). Isotope data can be used in conjunction with other geochemical measurements to determine pollution sources. Hydrogen and oxygen isotopes provide a conservative, double-

isotopic tracer system that is intrinsic to the water molecule (Fritz et al., 1976; Criss, 1999). Because of phase transitions and meteorological factors, the isotopic compositions of waters vary geographically (Dansgaard, 1964). Moreover, at a given site, the values exhibit seasonal variations on which short term changes are superimposed. Thus, the isotopic character of rainfall at a given location exhibits a distinctive time-series of variations (e.g., Frederickson and Criss, 1999; International Atomic Energy Agency [IAEA], 2004).

The δD and $\delta^{18}O$ values of water samples can be used to determine the component of stream or spring flow that originates from rainwater versus groundwater, provided that the isotopic compositions of each end-member are distinct (Sklash et al., 1976; Sklash and Farvolden, 1979). When a large volume of rainwater encounters the interconnected surface water and groundwater system, the increase in head is hydraulically transmitted through the phreatic zone causing increased discharge at a basin outlet (Freeze and Cherry, 1979; Criss, 1997; Criss and Winston, 2003). Baseflow is typically older soil water or groundwater that has migrated through the soil mantle or aquifer, which may have a unique isotopic character compared to rainwater. Thus, the percentage of groundwater and recent rainwater that constitutes the total stream flow can be determined using hydrograph separation techniques (Pinder and Jones, 1969; Freeze and Cherry, 1979). This behavior has been documented by many geochemical and isotopic studies (Freeze and Cherry, 1979; Dreiss, 1989; Vandike, 1992).

1.3.1. Isotopic Composition of Rainfall

Average δD and $\delta^{18}O$ values of rainfall in the St. Louis region are close to -45‰ and -7.0‰, respectively, but the value of individual storms can range from as low as -

214‰ and -28‰ to as high as +18‰ and +1‰ (Appendix A). Bi-monthly composites from Ladue, MO, follow cycloid seasonal patterns (Criss, 1999) with heavier isotopic values occurring in the spring and summer months and lighter isotopic values occurring in the winter, primarily due to temperature effects (Dansgaard 1964; Criss, 1999). Kinetic fractionation effects that accompany the evaporation of seawater lead to a consistent correlation between δD and $\delta^{18}O$ values in rainwater that produce the Meteoric Water Line (MWL) which is defined by the relationship:

$$\delta D = 8 \cdot \delta^{18}O + 10 \text{ (Craig, 1961)}$$

Because stream and spring waters in Missouri are derived from meteoric precipitation and generally do not experience the same evaporative enrichment observed in lakes, these waters generally plot on the MWL (Criss, 1999).

1.4. Generation and Character of Runoff and Land Use

Floods are one of the most familiar and frequent natural disasters in the world (Smith and Ward, 1998). Flood problems do not simply arise from too much water, but include the insidious, low quality of that water, which promotes the spread of contaminants and disease. It is thus important to understand how flood waters originate, what reservoirs are involved, and what chemical processes and transport mechanisms accompany these events.

1.4.1. Flood Waters and Chemographs

Stream water chemistry during and following discharge pulses can reveal important information about the flow paths of both baseflow and event water components. Variations in flood water chemistry cannot be explained by simple dilution of baseflow by rainwater (Lee and Krothe, 2001). Simple dilution would predict that all

dissolved ions in the stream water would be negatively correlated with discharge. However, the concentrations of some dissolved ions actually increase during increased discharge, while others decrease but may not show uniform dilution response (Edwards, 1973; Walling and Foster, 1975; Miller and Drever, 1977; Winston and Criss, 2002; 2004).

During rainfall, soil pore spaces are filled, and as this water migrates through the soil, it reacts with pollutants, mineral phases, and organic phases. Processes include ion exchange with solid phases, sorption/desorption, precipitation/dissolution of soluble salts, and complexation/decomplexation (Du Laing et al., 2009). These waters can contribute substantially to stream discharge during flood events (Kennedy et al., 1986; Walling and Webb, 1986). The concentrations of these ions vary with discharge and when these ions are plotted against time it produces a characteristic chemograph.

1.4.2. Effects of Land Use

The small streams in the St. Louis region have been variously impacted by urbanization. Storm water runoff patterns, erosion and sedimentation rates, water quality, and the overall health of the aquatic ecosystems have been modified, generally for the worse. In urban environments, impervious surfaces such as roads, parking lots, and rooftops inhibit the penetration of meteoric waters into the subsurface, and, consequently, surface runoff can flow more rapidly into streams and rivers (Paul and Meyer, 2001). This produces abnormally rapid and high peak flows, and the resulting hydrographs are characterized by sharp, but asymmetrical peaks, with both the rising and recession limbs changing rapidly (Criss and Winston, 2003). The decreased infiltration capacity of urban

watersheds often causes perennial streams to become intermittent because much of the flow is rapidly delivered following rainfall.

In contrast, natural discharge responses exhibit lower peak flows, slower rising limb responses, and more gradual attenuation to baseflow conditions on the recessional limb. This behavior reflects the greater retention of water by prairie and forest soils after storm events, which can then recharge the groundwater in natural environments.

1.4.2.1. Water Quality

Urban development leads to severe water quality degradation, not only for the obvious reason that urban environments have higher concentrations of chemical contaminants, but also because of decreased infiltration capacity of soils, which reduces the amount of filtration and bioremediation that can occur before event water reaches receiving waters. Impervious surfaces lead to reduced water quality because they accumulate pollutants deposited from the atmosphere, leaked from vehicles, applied intentionally (i.e., road salts, pesticides, and fertilizers), emitted from industrial operations, or derived from other sources. During storms, these accumulated surface pollutants are entrained in runoff and rapidly delivered to aquatic systems. Studies have consistently demonstrated that urban pollutant concentrations are directly related to watershed imperviousness (Schueler, 1987).

Additionally, impervious surfaces both absorb and reflect heat, and during the summer months, pavement and building areas can have local air and ground temperatures that are approximately 5°C warmer than the prairies and forests that they replace. Stream temperatures throughout the summer are increased in urban watersheds, and the degree of

warming appears to be directly related to the imperviousness of the contributing watershed (Galli, 1991).

Moreover, higher peak flows and the loss of vegetation in urban watersheds and riparian zones amplify erosion and sedimentation problems (Horowitz, 2009). Bank widening, channel incision, cut bank erosion, and channel scour are common results of the increased erosive power of the high peak flows of urban streams, and often these streams are almost completely disconnected from their flood plains due to deep incision (Criss and Wilson, 2003). Higher flows also wash away the fine grained sediments leaving inhospitable channels armored with coarse gravel.

Bank erosion can threaten homes, businesses, roads, bridges, sewer lines, and many other kinds of structures built along streams and rivers. Removal of vegetation also causes soil loss in the watershed, which in turn increases sediment input to the stream. Direct human activities including construction can also drastically increase sediment loads in developed watersheds. Increases in suspended solid loads stress fish populations and decrease light penetration necessary for aquatic plant growth.

Even chemicals that are relatively benign, such as Na and Cl from road salt, can be disastrous to aquatic ecosystems when delivered as concentration spikes during urban flood pulses (Shock et al., 2003). East-central Missouri typically has several snowfall events every year, and salts used to keep roads, parking lots, and sidewalks free of ice rapidly dissolve in surface waters when the snow and ice melt (Oberts et al., 2000). Spring rains flush these surface waters into the shallow groundwater, and the latter can retard salt delivery into the summer months.

Landscaping practices are another potential source of pollutants in urban runoff. Turf management chemicals including fertilizers and pesticides used by homeowners, golf courses, and public parks can add nutrients and toxic compounds to runoff (Arnolds and Gibbons, 1996). Schueler (1995) showed a direct link between the chemicals found in lawn care products and reduced water quality. While questions remain about the relative contributions of nutrients from turf management practices, it is clear that the type, quantity, and timing of the materials used have a substantial impact on water quality.

Trace metals are often elevated in urban areas by emissions, wear, and leakage from vehicles. Contributions of these trace elements to local waters include metals in tailpipe exhaust, tire and brake pad wear, motor oil, grease, gasoline leaks, and vehicle rust. For example, tire wear is a substantial source of toxic metals including Zn, Pb, Cu, and Cd, and the concentrations of these elements around roads often exceed acute toxicity levels (McKenzie et al., 2009). Combined sewer overflows (CSOs), sanitary sewer overflows (SSOs), sewer leaks, and pet wastes can all contribute trace elements, pathogens, and undesirable nutrient loads to storm water (Haile, 1996).

All of the aforementioned sources can significantly reduce ecosystem health. The Missouri Department of Conservation (MDC) lists only Fox Creek in St. Louis County as a priority stream that remains healthy (Missouri Department of Conservation [MDC], 2011). However, most streams in the area have impacted biodiversity, and even Fox Creek has undergone considerable change. St. Louis is an ideal location to study the differing effects of land use on the hydrologic cycle because it is a densely populated (1,990 people/km² in the City of St. Louis; U.S. Census, 2010) city that features a variety

of stream and land uses, including urban, commercial, residential, agricultural, and rural land use.

1.5. Remediation Efforts

Due to the deleterious effects of urban land use, many national and local regulations have been developed to mitigate water quality and volume issues. Best management practices (BMPs) are now being developed or required to reduce runoff volumes, peak flows, and pollutant loads by increasing evapotranspiration, detention, or infiltration of water, and by using native plant species to remove pollutants. Several types of BMPs are widely utilized, including: biofiltration, bioretention, infiltration and detention basins, erosion and sediment control, silt fences, swales, and wetlands, among others (U.S. Environmental Protection Agency [EPA], 2011).

1.6. Objectives of the Current Study

The sources and transport mechanisms of surface runoff and its associated pollutants into streams and shallow groundwater systems remain poorly understood. The current study was undertaken to investigate the hydrologic and geochemical behavior of surface waters and groundwater in response to seasonal fluctuations, transient storm perturbations, and land use, by using a comparative approach. To meet the objectives of the study, frequent measurements of key parameters such as stage, temperature, specific conductivity (SpC), turbidity, pH, major and minor elements, and D and ¹⁸O stable isotopes were made. These measurements were accomplished by deploying continuous, in situ monitoring devices as well as by collecting thousands of physical samples.

Chapter 2 describes the standard field, lab, and data processing methods used in this study. Chapter 3 discusses a database of temporally indexed physical and chemical

parameters that represent the hydrologic and geochemical response of urban and rural streams in St. Louis City and County, on scales that range from individual storm pulses to seasonal fluctuations. Chapter 3 uses isotope hydrograph separations to identify the magnitude and timing of event water and pre-existing groundwater (baseflow) components that combine to produce flood waters. Chapter 4 examines potential end-member sources that contribute to the background B levels in surface waters and groundwaters, and identifies an unexpected major source. Chapter 5 establishes the extent and origin of contamination in regional shallow groundwaters, and includes results for several major and trace elements. Chapter 6 presents a novel means to determine whether spring waters encountered air-filled passages while in the subsurface. Chapter 7 summarizes the results of the study and outlines many avenues for continued research.

1.7. References

- Arnold, C.L., and Gibbons, C.J., 1996, Impervious surface coverage: The emergence of a key environmental indicator: *Journal of the American Planning Association*, v. 62, p. 247-249.
- Clark, I., and Fritz, P., 1997, *Environmental isotopes in hydrogeology*: New York, Lewis Publishers, 328 p.
- Craig, H., 1961, Isotopic variations in meteoric waters: *Science*, v. 133, p. 1702-1703.
- Criss, R.E., 1997, New formulation for the hydrograph, time constants for stream flow, and the variable character of base flow: *Transactions American Geophysical Union*, v. 78, p. 317.
- Criss, R.E., 1999, *Principles of stable isotope distribution*: Oxford, Oxford University Press, 254 p.
- Criss, R.E., 2001, Hydrogeology of Tyson Research Center, Lone Elk County Park, and West Tyson County Park, eastern Missouri: Tyson Valley (ex) Army Powder Storage Farm Site File, EPA Region 7, 58 p.
- Criss, R.E., Osburn, G.R., and House, R. S., 2009, The Ozark Plateaus: Missouri, *in* Palmer, A.N. and Palmer M.V., eds., *Caves and Karst of the USA*: National Speleological Society, Huntsville, Ala., p. 156-170.
- Criss, R.E. and Wilson, D.A., 2003, Rivers of the St. Louis Confluence Region, *in* Criss, R.E., and Wilson, D.A., eds., *At the confluence: Rivers, floods, and water quality in the St. Louis region*: St. Louis, MBG Press, p. 10-29.
- Criss, R.E., and Winston, W.E., 2003, Hydrograph for small basins following intense storms: *Geophysical Research Letters*, v. 30, p. 1,314.
- Dansgaard, W., 1964, Stable isotopes in precipitation: *Tellus*, v. 16, p. 436-468.
- Dreiss, S.J., 1989, Regional scale transport in a karst system: 1. Component separation of spring flow hydrographs: *Water Resources Research*, v. 25, p. 117-125.
- Du Laing, G., Rinklebe, J., Vandecasteele, B., Meers, E., and Tack, F.M.G., 2009, Trace metal behaviour in estuarine and riverine floodplain soils and sediments: A review: *Science of the Total Environment*, p. 3,972-3,985.
- Edwards, A.M.C., 1973, The variation of dissolved constituents with discharge in some Norfolk rivers: *Journal of Hydrology*, v. 18, p. 219-242.

Fenneman, N.M., 1938, Physiography of eastern United States: New York, McGraw-Hill Book Company, Inc., 714 p.

Fetter, C.W., 1994, Applied hydrology: New Jersey, Prentice-Hall, 691 p.

Freeze, R.A., and Cherry, J.A., 1979, Groundwater: Englewood Cliffs, N.J., Prentice-Hall, 604 p.

Frederickson, G.C., and Criss, R.E., 1999, Oxygen isotope relations in karst springs, east-central Missouri and southwestern Illinois: *Chemical Geology*, v. 157, p. 303-317.

Fritz, P., Cherry, J.A., Weyer, K.U., and Sklash, M., 1976, Storm run-off analysis using environmental isotopes and major ions, *in* Interpretation of environmental isotopes and hydrochemical data in groundwater hydrology: International Atomic Energy Agency, Vienna, p. 111-130.

Ford, D.C., and Williams, P.W., 1989, Karst geomorphology: London, Unwin Hyman, 601 p.

Galli, J., 1991, Thermal impacts associated with urbanization and stormwater management best management practices. Metropolitan Washington Council of Governments: Washington, D.C., Maryland Department of Environment, 188 p.

Gams, I., 1972, Effect of runoff on corrosion intensity in the northwest Dinaric karst: Cave Research Group of Great Britain, *Transactions.*, v. 14, p. 78-83.

Gleick, P.H., 1996, Water resources, in Schneider, S.H., ed., *Encyclopedia of climate and weather*, vol. 2: New York, Oxford University Press, p. 817-823.

Haile, R.W., Alamillo, J., Barret, K., Cressey, R., Dermond, J., Glasser, A., Harawa, N., Harmon, P., Harper, J., McGee, C., Millikan, R.C., Nides, M., and J.S. Witte, 1996, An epidemiological study of possible adverse health effects of swimming in Santa Monica Bay: Los Angeles, Santa Monica Bay Restoration Project, p. 7-8.

Hewlett, J.D., and Hibbert, A.R., 1967, Factors affecting the response of small watersheds to precipitation in humid area, *in* Sopper, W.E., and Lull, H.W., eds., *Forest hydrology*: Oxford, Pergamon Press, p. 275-290.

Horowitz, A.J., 2009, Monitoring suspended sediments and associated chemical constituents in urban environments: Lessons from the city of Atlanta, Georgia, USA Water Quality Monitoring Program: *Journal of Soils and Sediments*, v. 9, no. 4, p. 342-363.

Horton, R.E., 1933, The role of infiltration in the hydrologic cycle: *Transactions American Geophysical Union*, v. 14, p. 446-460.

International Atomic Energy Agency, 2004, International Atomic Energy Agency, Isotope Hydrology Information System: The ISOHIS Database: International Atomic Energy Agency Web page, <http://isohis.iaea.org>.

James, E.R, Manga, M., Rose, T.P., and Hudson, G.B., 2000, The use of temperatures and isotopes of O, H, C and noble gases to determine the pattern and spatial extent of groundwater flow: *Journal of Hydrology*, v. 237, p. 100-112.

James, N.P., and Choquette, P.W., 1984, Diagenesis. 6. Limestone-the seafloor diagenic environment: *Geoscience Canada*, v. 10, p. 162-179.

Kennedy, V.C., Kendall, C., Zellweger, G.W., Wyerman, T.A., and Avanzino, R.J., 1986, Determination of the components of stormflow using water chemistry and environmental isotopes, Mattole River Basin, California: *Journal of Hydrology*, v. 84, p. 107-140.

Langmuir, D., 1997, *Aqueous environmental geochemistry: Upper Saddle River, New Jersey*, Prentice-Hall, 600 p.

Larsen, D., Swihart, G.H., and Xiao, Y., 2001, Hydrochemistry and isotope composition of springs in Tecopa Basin, southeastern California, USA: *Chemical Geology*, v. 179, p. 17-35.

Lee, F.S, and Krothe, N.C., 2001, A four-component mixing model for water in a karst terrain in south-central Indiana, USA. Using solute concentrations and stable isotopes as tracers: *Chemical Geology*, v. 179, p. 129-143.

McKenzie, E.R., Money, J.E., Green, P.G., and Young, T.M., 2009, Metals associated with stormwater-relevant brake and tire samples: *Science of the Total Environment*, v. 407, p. 5,855-5,860.

Miller, W.R., and Drever, J.I., 1977, Water chemistry of a stream following a storm, Absaroka Mountains, Wyoming: *Geological Society of America Bulletin*, v. 88, p. 286-290.

Missouri Department of Conservation, 2011, LaBarque Creek watershed: Conservation opportunity area: Missouri Department of Conservation Web page, <http://mdc.mo.gov/>.

National Oceanic and Atmospheric Administration (NOAA), 2011, National Weather Service (NWS) Weather: NWS Web page, <http://www.weather.gov/>.

Oberts, G., Marsalek, J., and Viklander, M., 2000, Review of water quality impacts of winter operation of urban drainage: *Water Quality Research Journal of Canada*, v. 35, p. 781-808.

Paul, M.J., and Meyer, J.L., 2001, Streams in the urban landscape: *Annual Review of Ecology and Systematics*, v. 32, p. 333-365.

- Pinder, G.F., and Jones, J.F., 1969, Determination of ground-water component of peak discharge from the chemistry of total runoff: *Water Resources Research*, v. 5, p. 438-445.
- Pulina, M., 1971, Observations on the chemical denudation of some karst areas of Europe and Asia: *Studia Geomorphologica Carpatho-Balcanica*, v. 5, p. 79-92.
- Rose, T.P., Davisson, M.L., and Criss, R.E., 1996, Isotope hydrology of voluminous cold springs in fractured rock from an active volcanic region, northeastern California: *Journal of Hydrology*, v. 179, 207-236.
- Schueler, T.R., 1987, Controlling urban runoff: A practical manual for planning and designing urban BMPs: Metropolitan Washington Council of Governments, Department of Environmental Programs, 240 p.
- Schueler, T., 1995, Urban pesticides: From the lawn to the stream: *Watershed Protection Techniques*, v. 2, p. 247-253.
- Shock, E.L., Carbery, K., Noblit, N., Schnall, B., Kogan, P., Rovito, S., Berg, A., and Liang, J., 2003, Water and solute sources in an urban stream, River des Peres, St. Louis, Missouri, in Criss, R.E., and Wilson, D.A., eds., *At the confluence: Rivers, floods, and water quality in the St. Louis region*: St. Louis, MBG Press, p. 150-160.
- Sklash, M.G., and Farvolden, R.N., 1979, The role of groundwater in storm runoff: *Journal of Hydrology*, v. 43, p. 45-65.
- Sklash, M.G., Farvolden, R.N., and Fritz, P., 1976, A conceptual model of watershed response to rainfall, developed through the use of oxygen-18 as a natural trace: *Canadian Journal of Earth Science*, v. 13, p. 271-283.
- Smith, D.I., and Atkinson, T.C., 1976, Process, landforms and climate in limestone regions, in Derbyshire, E., ed., *Geomorphology and climate*: London, Wiley, p. 369-409.
- Smith, K., and Ward, R., 1998, *Floods: Physical processes and human impacts*: Chichester, John Wiley and Sons, 394 p.
- Stumm, W., and Morgan, J.J., 1981, *Aquatic chemistry*, 2nd ed.: New York, John Wiley 780 p.
- Troester, J.W., and White, W.B., 1984, Seasonal fluctuations in the carbon dioxide partial pressure in a cave atmosphere: *Water Resources Research*, v. 20, p. 153-156.
- U.S. Census, 2010, Population density date: 2010 U.S. Census Web page, <http://2010.census.gov/2010census/>.

U.S. Environmental Protection Agency, 2011, Drinking water contaminants: Drinking Water Contaminants Web page, <http://water.epa.gov/drink/contaminants/index.cfm>.

U.S. Geological Survey, 2011, USGS Real-time data for Missouri: USGS Real-time data for Missouri Web page, <http://waterdata.usgs.gov/mo/nwis/rt>.

Vandike, J.E., 1992, The hydrogeology of the Bennett Spring area, Laclede, Dallas, Webster, and Wright counties, Missouri: Missouri Department of Natural Resources Water Resources Report 38, 112 p.

Vandike, J.E., 1995, Surface water resources of Missouri: Missouri Department of Natural Resources Water Resources Report 45, 121 p.

Vineyard, J., and Feder, G.L., 1982, Springs of Missouri: Missouri Department of Natural Resources Water Resources Report 29, 266 p.

Walling, D.E., and Foster, I.D.L., 1975, Variations in the natural chemical concentrations: *Journal of Hydrology*, v. 26, p. 237-244.

Walling, D.E., and Webb, B.W., 1986, Solutes in river systems, *in* Trudgill, S.T., ed., *Solute processes*: New York., John Wiley, p. 251-327.

Ward, A.D., and Trimble, S.W., 2004, *Environmental hydrology*, 2nd ed.: Boca Raton, Florida, CRC Press, 475 p.

White, W.B., 1988, *Geomorphology and hydrology of karst terrains*: New York, Oxford University Press, 464 p.

Williams, P.W., 2008, The role of the epikarst in karst and cave hydrogeology: a review: *International Journal of Speleology*, v. 37, p. 1-10.

Winston, W.E., and Criss, R.E., 2002, Geochemical variations during flash flooding, Meramec Basin, May 2000: *Journal of Hydrology*, v. 265, p. 149-163.

Winston, W.E., and Criss, R.E., 2004, Dynamic hydrologic and geochemical response in a perennial karst spring: *Water Resources Research*, v. 40, W05106.

Chapter 2: Methods and Data

This chapter addresses field sampling, laboratory analyses, and data treatment methods and procedures that are discussed in the subsequent chapters. Methods specific to a chapter are discussed in that chapter's methods section. All geographic coordinates are given in Universal Transverse Mercator (UTM) NAD83 for Zone 15.

2.1. Fieldwork and Sampling

2.1.1. Precipitation Samples

Precipitation samples were collected in 10.2 cm (4 inch) diameter, private rain gauges located in St. Louis (UTM: 734572, 4281304), Ladue (UTM: 725896, 4277671), and Washington (UTM: 676582, 4266241), MO. Precipitation was collected by the author in St. Louis (2007 – 2011), Robert Criss in Ladue (1995 – 2011), and William Winston in Washington (2000 – 2008). Precipitation was typically collected immediately after a storm event in order to reduce isotopic enrichment in the sample through evaporation.

Two types of samples were obtained to characterize seasonal isotopic variability and to identify the isotopic character of individual pulses. Bimonthly “composite” samples were collected at Ladue, and consist of an aliquot of the homogenized mix of all precipitation that fell during a half month period. Rainfall samples were removed from the gauge after each storm and combined in a larger vessel and held until the 15th or end of each month and then were analyzed. Composite samples were collected to track seasonal isotopic variations and to model the residence times for surface water and groundwater systems in the area. There is an extensive record of composite samples dating back to 1995 (see Appendix A). Individual samples of selected precipitation

events were also analyzed for δD and $\delta^{18}O$ values and some were analyzed for major and trace elements. Generally, individual storm samples were collected at the completion of a storm event, but for some precipitation events subsamples were collected on shorter time scales to further characterize the storm. The purpose of collecting individual storm samples was to identify the temporal variability of the mixing end-members that constitute stream discharge using isotopic and geochemical hydrograph separation techniques. The data for the precipitation station nearest to the stream of interest were used for hydrograph separations.

Rainfall records for Valley Park and Lambert-St. Louis International Airport in St. Louis, MO are published on the internet by the U.S. Geological Survey (USGS, 2011; gaging station: 07019185; UTM: 720316, 4271936) and the National Weather Service (NWS; National Oceanic and Atmospheric Administration [NOAA], 2011; UTM: 728947, 4291462), respectively, and are reported in 15- and 60-minute intervals, respectively. These data were used to identify temporal variations in rainfall during individual storm events.

2.1.2. Grab Samples

Grab samples were collected upon each visit to a field site. They represented individual, discrete samples, and upon delivery to the laboratory, underwent isotopic, geochemical, and bacterial analyses. For the purpose of quantifying the characteristics of a water body or wastewater discharge, one grab sample is not generally considered sufficient. Repeated sampling to generate a time series is the method applied throughout this study.

2.1.2.1. Grab Sample Preparation

Prior to sample collection, all sampling vessels were properly cleaned and prepared for target analytes. Bottles were then segregated based on analyte to prevent cross contamination. All bottles used for sampling were triple rinsed in deionized water (DI water) to remove any debris or residues that might contaminate the sample. After rinsing, all glassware were dried in a clean drying oven (75°C) and all plastic bottles were air dried on clean drying racks. Some analytes required additional special treatment, such as acid washing, triple rinsing with ultra pure water (18.2 MΩ•cm Elga Maxima; Tramontano et al., 1987), or autoclaving. Parameters that were routinely measured are listed in Table 2.1 along with the appropriate container type, container preparation, collection volume, required preservative measures, analytical method, holding time, and sample volume needed to conduct each analysis.

2.1.2.2. Field Sample Collection

During site visits, grab samples for each analyte were collected in tandem with field measurements (see 2.1.2.3. In Situ Field Measurements) at each sampling location. When samples were collected, nitrile gloves were used to protect the sample from contamination and personnel from water-borne diseases. Inclusion of large incidental materials such as sticks, leaves, and aquatic organisms was avoided during sampling. During sample collection for flowing bodies of water, care was taken to not disturb the water above the point of collection. Straight channels exhibit laminar flow and may require long distances for lateral and vertical mixing; thus when sampling at the confluences of two or more streams, samples were collected at a point where complete

mixing has occurred. When sampling at bridge locations, samples were collected in the middle of the flowing stream to ensure a well-mixed, representative sample.

Although the collection of most grab samples was accomplished by simply submerging the sample container into the water body of interest, grab samples were also variously collected by use of peristaltic pumps, buckets, and Kemmerer and Van Dorn bottles; but only when these vessels were appropriate for the parameter being sampled (e.g., one would not use a brass sampler for metal analyses). These devices were thoroughly rinsed with DI water between each use and triple rinsed in the water being sampled prior to actual sample acquisition to avoid cross contamination with previous sites or the water used to cleanse the vessel between sampling events.

2.1.2.3. In Situ Field Measurements

Field measurements of temperature, specific conductivity (SpC), turbidity, dissolved oxygen (DO), and pH were made using handheld meters concurrently with grab sample collection during site visits. At field sites with in situ monitoring devices, these measurements were made to check the accuracy of the sensors and determine if there were any calibration issues. The model and manufacturer for each handheld device are listed in Table 2.2, along with the instrumental range and accuracy.

All meters were calibrated according to the manufacturers' specifications before field excursions to ensure accuracy. Measurements were taken directly in the stream of interest when possible. In situ measurements were collected at a well-mixed point in the stream where the sensors could be fully immersed and elevated above the streambed. When sampling from a bridge or other structure was necessary, an appropriate vessel was filled and then measurements were obtained from that sample. Measurements on a

discrete sample volume were conducted promptly to ensure that parameters such as temperature, turbidity, DO, and pH remain at their ambient levels.

2.1.3. Autosamplers

In addition to grab samples, many samples were collected by autosamplers (Figure 2.1A). In particular, ISCO brand portable samplers were utilized to automatically collect up to 24 sequential samples into individual containers that could then be analyzed individually or manually composited into one container. Aliquots from the autosampler were transferred to appropriate bottles upon return to the lab. Comparison between temporally equivalent grab samples and samples that remained inside the autosampler for up to two weeks indicates that isotopic enrichment from evaporation was minimal and differences were within analytical error.

2.1.3.1. Autosampler Bottle Preparation

All autosampler bottles were prepared in a manner suited for the target analyte (Table 2.1). The appropriate bottle type was employed according to the type of parameters being studied. Standard high density polyethylene (HDPE) plastic bottles were acceptable for isotopic investigations, but samples intended for chemical or biological analyses were collected in one-time use ISCO ProPak™ bags or standard bottles that were cleaned and/or autoclaved to avoid cross contamination (Figure 2.1B).

2.1.3.2. Autosampler Installations, Specifications, and Operational Modes

Typical autosampler installations involved placing the device in a secure housing unit, such as a utility box or other suitable enclosure, which could withstand occasional high water events (Figure 2.1C). A section of PVC pipe was often used to protect the suction tubing, and was run from the secure housing unit to the water body. The PVC

pipe was long enough to protect the tubing and also included numerous holes where it was submerged in the stream to allow free circulation of water around the intake strainer so that samples could be collected. The intake line was suspended at mid-depth in the stream to obtain as representative a sample as possible (see Figure 2.1D).

Two types of automated sample collection devices were used: ISCO models 6712 and 3700. These units differ in their programming functions and ability to accept various peripheral devices such as acoustic stage recorders and continuous monitoring sensors, with the 6712 model featuring the most advanced functions. If the ISCO unit was not equipped with an acoustic stage recorder (see 2.1.4. Continuous Monitoring Sensors section), a 1640 Liquid Level Sampler Actuator was used (Figure 2.1D), which is a device operated in conjunction with an ISCO sampler to begin a sampling routine when the liquid level reaches a predetermined height.

Sample collection timing was controlled by programming the individual autosamplers. For background samples, a fixed interval of typically 24 to 48 hours was used to capture the ambient conditions in a stream. Storm flow sampling was triggered based on a set time or by a rise in water level if the sampler was equipped with a stage sensor or actuator. Storm samples were collected at much higher frequency than the background samples, with intervals usually being 5 to 15 minutes for runoff samples and 15 to 120 minutes for stream samples. These intervals were chosen to capture the rapid compositional variations that occur during these transient flow events. For streams, these time intervals were chosen to permit acquisition of samples representing pre-storm baseflow and on the rising and recessional limbs of the hydrograph. Rural streams and

large rivers respond to precipitation more slowly than storm water runoff, urban streams, or smaller streams, and accordingly, require less frequent sampling.

Each autosampler collection cycle included an initial air purge and rinsing cycles of the sample tubing, followed by filling of the sample bottle with a specified volume (usually 1 L), then a final purge of the line. The device records the time and date when each bottle was filled, along with ancillary data, and any associated error messages. Samples did not remain in the unit longer than the stipulated holding times for a given analyte (see Table 2.1).

ISCO autosamplers were in operation at several field locations including: Fox Creek in Allenton, Grand Glaize in Valley Park, four locations on the River des Peres in University City and St. Louis, Black Creek in Brentwood, 10920 Chalet Ct. in Creve Coeur, 8360 Cornell Ave. in University City, and Mt. Calvary Church in Brentwood, MO. These locations, along with the type of autosamplers, type of continuous monitoring device, and years of operation are listed in Table 2.3.

2.1.4. Continuous Monitoring Sensors

In addition to the ISCO autosampler units, continuous monitoring devices were deployed at many of the study sites. Two types of continuous monitoring equipment were used including those capable of measuring a suite of water quality parameters (e.g., the YSI 6600 V2 and YSI 600R Sondes) and those that record water level (e.g., the YSI Level Scout, a vented pressure transducer, and ISCO 710 Ultra Sonic Flow Module). Locations and years of operation for each of these devices are listed in Table 2.3. It should be noted that uninterrupted operation of these devices was not always possible due

to equipment malfunctions, removal for calibration, and removal during the winter to avoid freezing.

The water quality monitoring probes recorded data at 5-minute intervals or less. The YSI 6600 V2 Sondes were equipped to measure water quality parameters in situ and include: temperature, SpC, turbidity, DO, pH, Cl, $\text{NH}_3\text{-N}$, $\text{NH}_4^+\text{-N}$, and $\text{NO}_3^-\text{-N}$, and the YSI 600 was equipped to measure temperature, SpC, DO, and pH (results from the DO sensors were often unreliable when compared to grab sample measurements, and these data have not been used in this study). The YSI Level Scouts were used to continuously measure the water level and temperature of storm runoff. These devices recorded data at 1- to 2-minute intervals. The ISCO 710 Ultra Sonic Flow Module measured water level at 5-minute intervals or less. Table 2.4 lists the devices used in this study, and describes the measured parameters, accuracy, and ranges for these instruments.

Typical installations of the YSI 6600 and YSI 600R continuous monitoring devices involve a section of PVC pipe with a locking cap to discourage theft or tampering. The PVC pipe was long enough to protect the device and included numerous holes to allow free circulation of water around the sensors. The PVC tubing was attached to bridge abutments or rebar poles were driven into the bank or streambed so that contact with floating debris did not dislodge the equipment (Figure 2.2A). The YSI Level Scouts were secured vertically in storm sewers using rebar (Figure 2.3). The ISCO 710 Ultra Sonic Flow Modules were attached to bridges or tree branches that crossed above the stream channel.

Sensors on the YSI 6600 and YSI 600 Sondes were calibrated biweekly to ensure accuracy and to evaluate their condition (Figure 2.2B). The YSI Level Scout and the

ISCO 710 Ultra Sonic Flow Module were factory calibrated. A two-point calibration was used for the pH sensor and the ion specific electrodes (ISE; e.g., Cl, NH₃-N, NH₄⁺-N, and NO₃⁻-N sensors), while one-point calibrations were used for all other sensors on the instruments, as specified by the manufacturer. During calibration visits, the data were downloaded and routine maintenance was performed. Calibration results and field measurements were used to verify and correct any systematic drift or static bias in the raw continuous records. A linear adjustment was performed to correct for these behaviors (see 2.3.3. Drift Corrections for Continuous Monitoring Devices).

2.2. Laboratory Methods

Individual analyses were conducted according to procedures listed in Table 2.1. Ultra pure DI water was used for all wet chemistry work and nitrile gloves were worn to maintain sample integrity. Detailed procedures for each analysis are discussed in the following sections.

2.2.1. IR-MS Analysis: Hydrogen and Oxygen Isotopes

Stable isotope analyses of D and ¹⁸O for untreated water samples were measured by isotope ratio mass spectrometry (IR-MS) using an automatic Thermo Finnigan MAT 252 mass spectrometer with a peripheral PAL device. The D and ¹⁸O isotope data are reported in the conventional manner (Craig, 1961), as δD and δ¹⁸O values in parts per thousand (or per mil) deviations from Standard Mean Ocean Water (SMOW):

$$\delta D_{sample} = 1000 \times \left(\frac{(D/H)_{sample} - (D/H)_{SMOW}}{(D/H)_{SMOW}} \right)$$

$$\delta^{18}O_{sample} = 1000 \times \left(\frac{\left(\left(\frac{{}^{18}O}{{}^{16}O} \right)_{sample} - \left(\frac{{}^{18}O}{{}^{16}O} \right)_{SMOW} \right)}{\left(\frac{{}^{18}O}{{}^{16}O} \right)_{SMOW}} \right)$$

The δD values of sample waters were determined by reacting 1.0 μL of water with metallic chromium at 800°C to produce hydrogen gas, prior to analysis in the mass spectrometer; precision is $\pm 1.0\text{‰}$ (Nelson and Dettman, 2001). The $\delta^{18}O$ values were determined by equilibrating 0.5 mL of the water sample with a 0.3% CO_2/He gas mixture at 1 bar for 16 – 24 hours at 26.5°C, and analyzing the CO_2 gas; precision is $\pm 0.1\text{‰}$ (Epstein and Mayeda, 1953). Every run included several standards and duplicates and triplicates of samples to check the precision and accuracy of analytical procedures.

2.2.2. Inductively Coupled Plasma Optical Emission Spectrometry (ICP-OES) and Inductively Coupled Plasma Mass Spectrometry (ICP-MS) Analyses

All samples slated for ICP-OES and ICP-MS analyses were collected and processed using the techniques outlined in U.S. Environmental Protection Agency (EPA) Method 200.7 (U.S. Environmental Protection Agency, 1990) and EPA Method 200.8 (U.S. Environmental Protection Agency, 1994), respectively. Water samples were processed to remove particles and stabilize compositions for storage prior to major and trace element analyses on the ICP-OES and ICP-MS. Samples were drawn under vacuum through 0.2 μm nylon filter paper and then individual aliquots for ICP-OES and ICP-MS were decanted in clean, acid-washed 50 mL polypropylene (PP) plastic centrifuge tubes. Samples that were analyzed by the ICP-OES and ICP-MS were acidified with a 0.5% HCl/2.0% HNO_3 acid matrix to $pH < 1$ with trace metal grade HCl and HNO_3 to ensure that all aqueous species remained soluble and did not react with the vessel wall. Samples were then stored under refrigeration until analysis.

Chemical analyses for major elements, B, and Sr were measured using a Perkin-Elmer Optima 7300DV ICP-OES, and instrument operation and data processing were

performed with the WinLab32™ software. Analyses for trace elements were performed using a Perkin-Elmer ELAN DRC II ICP-MS, and instrument operation and data processing were performed with the ELAN® software. Samples were measured automatically in triplicate by the ICP-OES and ICP-MS software and the results were averaged. Relative standard deviation (RSD) values were less than 5%. In addition, during each run blanks, references standards (TraceCERT® and Perkin-Elmer Pure Plus), and duplicate and triplicate samples were analyzed to check the precision and accuracy of analytical procedures; lab accuracy was $\pm 5\%$. Detection limits for each element are listed in Tables 2.5 and 2.6.

2.2.3. *Wet Chemical Analysis*

Wet chemical analyses of water samples were performed in the manner described in Table 2.1, and major elements, nutrients, and total suspended solids (TSS) were measured using EPA-approved methods: Cl (digital titration; Hach, 2005d), NH_4^+ -N (spectrophotometry Nessler; Hach, 2005a), NO_3^- -N (spectrophotometry chromotropic acid; Hach, 2005e), total P as orthophosphate (spectrophotometry ascorbic acid; Hach 2005c; 2005b), and TSS (EPA, 1971; see Table 2.1).

2.2.4. *Microbial Analysis*

Coliform bacteria are universally found in the guts of mammals and are easy to culture. Their presence is used to indicate other pathogenic organisms associated with fecal contamination, which makes them ideal for monitoring water quality. Around 60 to 90% of total coliforms are fecal coliforms, and of these more than 90% are *Escherichia* (usually *E. coli*). *E. coli* and total coliform colonies were measured in untreated water

samples using the IDEXX Colilert reagent and 97-well Quanti-Tray®; this EPA approved method has a most probable number range limit of 1 to 2420 cfu/100 mL.

2.2.5. Quality Assurance/Quality Control (QA/QC)

Accurate results were ensured through a regular system of QA/QC procedures. The practices outlined below were employed to test for accuracy, to ensure repeatability and sample stability, and to evaluate the possibility that materials in the raw samples might interfere with the analytical tests. The accuracy of each analytical technique was tested by measurement of known standard materials. Matrix spikes, consisting of a known quantity and concentration of a standard solution, were added to raw water samples collected in the field or by the autosamplers to ensure there are no interferences in the raw samples that would lead to incorrect results.

Field, laboratory, and reagent blanks were analyzed to ensure that no systematic errors were introduced by sample collection or analytical methods. Duplicate field and laboratory samples were analyzed to ensure sample stability and analytical reproducibility. Field duplicates were separate samples taken concurrently at the same location, while laboratory duplicates were analyses of a new aliquot of a given sample taken from the same sample container. Most QA/QC procedures showed variations of less than 10% in accuracy and precision.

2.3. Data Treatment and Interpretative Methods

2.3.1. Drift Corrections for Continuous Monitoring Devices

Over time the measurements for some of the sensors on the continuous monitoring devices drifted linearly; typically by less than 20%. The probes most prone to drift were the ISE sensors (e.g., Cl, NH₃-N, NH₄⁺-N, and NO₃⁻-N). Drift corrections

were applied to the data collected by these sensors. The baseline drift correction used for sensors that required a one-point calibration is:

$$C = m + \left(\frac{t}{\sum t}\right) \cdot (s_i - s_f)$$

where C is the drift corrected parameter value, m is the uncorrected, in situ measurement of the parameter of interest, t is the time interval of interest divided by the total time, $\sum t$, s_i is the value of the calibration standard, and s_f is the measured value of the calibration standard after drift has occurred (i.e., before calibration). The drift correction used for a two-point calibration is:

$$a_t = a_i + \left(\frac{t}{\sum t}\right) \cdot (a_i - a_f)$$

$$b_t = b_i - \left(\frac{t}{\sum t}\right) \cdot (b_i - b_f)$$

$$C = \left(\frac{m - a_t}{b_t - a_t}\right) (b_i - a_i) + a_i$$

where C , m , and t are the same as for the one-point calibration equation, a_t and b_t are the drift corrections using the lower and higher concentration calibration standard, respectively, a_i and b_i are the values of the lower and higher calibration standards, respectively, and a_f and b_f are the measured values for the lower and higher concentration calibration standards after drift has occurred and before calibration, respectively.

2.3.2. HCO_3^- , $f\text{CO}_2$, and $f\text{O}_2$ Calculations

HCO_3^- is the dominant anion in carbonate-hosted waters, such as those in this study, but concentrations are not stable over the time period that samples remain in the autosampler because of CO_2 degassing. Therefore, concentrations of HCO_3^- were calculated using ion balancing for the measured major ions (including the cations: Ca^{2+} ,

Mg²⁺, Na⁺, K⁺, and NH₄⁺-N and the anions: Cl⁻, NO₃⁻-N, PO₄³⁻, SO₄²⁻-S, and SiO₄⁴⁻-Si) and pH. The *f*CO₂, *f*O₂, and carbonate alkalinity were calculated using Geochemist's Workbench Standard 8.0 using major element and pH data.

2.3.3. *Hydrograph Separations*

Storm events often result in flooding in streams and springs. Interest in flood mitigating has led to the development of models in the hope of identifying source water contribution to flood waters. Mixing studies based on conservative geochemical tracers can be used to quantitatively resolve the discharge hydrograph into incoming precipitation (event water) or groundwater (baseflow) components. In many temperate environments the major component of flooding is the baseflow constituent (Sklash and Farvolden, 1979; Buttle, 1994), and this component is typically greater than 50% of the discharge event (Hooper and Shoemaker, 1986; Brown et al., 1999). However, the baseflow component can be much larger, as found by Caissie et al. (1996) and Winston and Criss (2002). Various tracers can be used as long as they are conservative, including SpC (Caissie et al., 1996), individual ions (Pinder and Jones, 1969), or stable isotopes (Sklash and Farvolden, 1979; Lakey and Krothe, 1996).

Both isotopic and chemical tracers were employed in this study to distinguish between event water and baseflow in several streams during discharge events. Application of this method is possible when a precipitation sample from the individual event was collected and the pre-storm condition baseflow was characterized. The rainfall and baseflow must be chemically and isotopically consistent or subsamples must be collected so that no other sources confuse the mixing calculation. There must also be a significant difference between the rainfall event and the baseflow, and no more than two

end-members can affect the system. However, this is not the case in most circumstances, and these complications are discussed in detail in Chapter 3.

The relationship for two end-member mixing (i.e., baseflow and event water for most systems) takes the form:

$$Q_t C_t = Q_a C_a + Q_b C_b$$

where Q is the discharge, C is the concentration or isotopic δ -value for any conservative parameter, and the subscripts represent the total (t) discharge or concentration and the respective discharge or concentration for end-member components a and b . Because conservative tracers are used, this relationship can be solved to obtain the fraction X of discharge derived from baseflow, which is equal to Q_b/Q_t . Using isotopes as an example (Sklash and Farvolden, 1979), the result is:

$$X_{baseflow} = \frac{\delta^{18}O_{stream} - \delta^{18}O_{rain}}{\delta^{18}O_{baseflow} - \delta^{18}O_{rain}}$$

2.3.4. Theoretical Hydrograph

Criss and Winston (Criss, 1997; Criss and Winston, 2003; 2006; 2008) have developed a quantitative hydrograph model, and have shown that different watersheds have self-similar hydrographs but different time constants (Winston and Criss, 2004).

The theoretical hydrograph is simulated by the following equation:

$$\frac{Q}{Q_{max}} = \left(\frac{2eb}{3t}\right)^{3/2} e^{-b/t}$$

where Q is the discharge at time t , Q_{max} is peak discharge, b is the response time constant, and e is Euler's number. The theoretical lag time between the storm event at $t = 0$ and the subsequent flow peak is equal to $2b/3$. The model is able to generate full flood pulse behavior including the rising limb, the crest, and the recessional limb (Criss and Winston,

2003; 2006; 2008; Winston and Criss, 2004).

2.4. Data Tables

Results from field measurements, isotope, chemical, and bacterial analyses are tabulated in Appendices A – L. All measurements were made in the manner described in the preceding sections. Some of the processed samples included in these tables may not be discussed in the current study. They are included for completeness and to provide an archival database.

2.5. References

Brown, V.A., McDonnell, J.J., Burns, D.A., and Kendall, C., 1999, The role of event water, a rapid shallow flow component, and catchment size in summer stormflow: *Journal of Hydrology*, v. 217, p. 171-190.

Buttle, J.M., 1994, Isotope hydrograph separations and rapid delivery of pre-event water from drainage basins: *Progress in Physical Geography*, v. 18, p. 16-41.

Caissie, D., Pollock, T.L., and Cunjak, R.A., 1996, Variations of stream water chemistry and hydrograph separation in a small drainage basin: *Journal of Hydrology*, v. 178, p. 137-157.

Craig, H., 1961, Standard for reporting concentrations of deuterium and oxygen-18 in natural waters: *Science*, v. 133, p. 1,833-1,834.

Criss, R.E., 1997, New formulation for the hydrograph, time constants for stream flow, and the variable character of base flow: *Transactions American Geophysical Union*, v. 78, p. 317.

Criss, R.E., and Winston, W.E., 2003, Hydrograph for small basins following intense storms: *Geophysical Research Letters*, v. 30, p. 1,314.

Criss, R.E., and Winston, W.E., 2006, Comparative hydraulic diffusivities of chemical and physical parameters in watersheds with hierarchies of flow paths: *Geological Society of America Abstracts with Programs*, v. 38, p. 463.

Criss, R.E., and Winston, W.E., 2008, Properties of a diffusive hydrograph and the interpretation of its single parameter: *Mathematical Geology*, v. 40, p. 313-325.

Epstein, S., and T. Mayeda, 1953, Variation of O-18 content of waters from natural sources: *Geochimica et Cosmochimica Acta*, v. 4, p. 213-224.

Hach, 2005a, Method 8038: Nitrogen, ammonia: Nessler Method: Hach Company, 6 p.

Hach, 2005b, Method 8048: Phosphorus: Reactive (orthophosphate) method: Hach Company, 6 p.

Hach, 2005c, Method 8190, Phosphorus: Total digestion: Hach Company, 4 p.

Hach, 2005d, Method 8206: Chloride, mercuric nitrate, *in* Digital titrator model 16900 manual: Hach Company, p. 67-68.

Hach, 2005e, Method 10020: Nitrate: Chromotropic acid method: Hach Company, 4 p.

- Hooper, R.P. and Shoemaker, C.A., 1986, A comparison of chemical and isotopic hydrograph separations: *Water Resources Research*, v. 22, p. 1,444-1,454.
- Horiba, 2006, U-10 Water quality checker instruction manual: Horiba, LTD.
- Lakey, B., and Krothe, N.C., 1996, Stable isotopic variation of storm discharge from a perennial karst spring, Indiana: *Water Resources Research*, v. 32, p. 721-731.
- Nelson, S.T., and Dettman, D., 2001, Improving hydrogen isotope ratio measurements for on-line chromium reduction systems: *Rapid Communications in Mass Spectrometry*, v. 15, p. 2,301-2,306.
- National Oceanic and Atmospheric Administration, 2011, National Weather Service (NWS) Weather: National Weather Service Web page, <http://www.weather.gov/>.
- Pinder, G.F., and Jones, J.F., 1969, Determination of ground-water component of peak discharge from the chemistry of total runoff: *Water Resources Research*, v. 5, p. 438-445.
- Sklash, M.G., and Farvolden, R.N., 1979, The role of groundwater in storm runoff: *Journal of Hydrology*, v. 43, p. 45-65.
- Tramontano, J.M., Scudlark, J.R., and Church, T.M., 1987, A method for the collection, handling, and analysis of trace metals in precipitation: *Environmental Science & Technology*, v. 21, p. 749-753.
- U.S. Environmental Protection Agency, 1971, Method 160.2: Residue, non-filterable (gravimetric, dried at 103-105°C): U.S. Environmental Protection Agency, 3 p.
- U.S. Environmental Protection Agency, 1990, Method 200.7: Determinations of metals and trace elements in water and wastes by inductively coupled plasma-atomic emission spectrometry: U.S. Environmental Protection Agency, Revision 3.0, 58 p.
- U.S. Environmental Protection Agency, 1994, Method 200.8: Determinations of trace elements in waters and wastes by inductively coupled plasma-mass spectrometry: U.S. Environmental Protection Agency, Revision 5.4, 51 p.
- U.S. Geological Survey, 2011, USGS Real-time data for Missouri: USGS Real-time data for Missouri Web page, <http://waterdata.usgs.gov/mo/nwis/rt>.
- Winston, W.E., and Criss, R.E., 2002, Geochemical variations during flash flooding, Meramec Basin, May 2000: *Journal of Hydrology*, v. 265, p. 149-163.
- Winston, W.E., and Criss, R.E., 2004, Dynamic hydrologic and geochemical response in a perennial karst spring: *Water Resources Research*, v. 40, W05106.

Table 2.1. Field collection protocols and analytical procedures for individual analytes.

Parameter	Field Collection				Laboratory Analysis			
	Container	Preparation	Collection Volume	Preservation	Analytical Method	Holding Time	Analysis Volume	Performance Range or Detection Limits
D/H Isotope Ratio	Airtight Glass	Triple rinse bottle with DI water, drying oven	30 mL	None	Nelson and Dettman, 2001	Indefinite*	1 µL	-1000 to 1000 ‰
¹⁸O/¹⁶O Isotope Ratio	Airtight Glass	Triple rinse bottle with DI water, drying oven	30 mL	None	Epstein and Mayeda, 1953	Indefinite*	0.5 mL	-1000 to 1000 ‰
TSS	HDPE Plastic	Triple rinse bottle with DI water, air dry, triple rinse with sample	500 mL	Refrigerate	EPA Method 160.2, EPA, 1971	28 days	100 mL	4 to 20,000 ppm
Cl	HDPE Plastic	Triple rinse bottle with DI water, air dry, triple rinse with sample	500 mL	Refrigerate	Digital titration: Hach Method 8206 (Hach, 2005d)	7 days	100 mL	10 to 8,000 ppm
NH₄⁺-N†	HDPE Plastic	Triple rinse bottle with DI water, air dry, acid wash (HCl), triple rinse with DI, triple rinse with sample	500 mL	H ₂ SO ₄ to pH < 2, Refrigerate	Spectrophotometry Chromotrophic Acid Method: Hach Method 10020 (Hach, 2005e)	28 days	1 mL	0.2 to 30.0 ppm NO ₃ ⁻ -N
NO₃⁻-N†	HDPE Plastic	Triple rinse bottle with DI water, air dry, acid wash (HCl), triple rinse with DI, triple rinse with sample	500 mL	H ₂ SO ₄ to pH < 2, Refrigerate	Spectrophotometry Nessler Method: Hach Method 8038 (Hach, 2005a)	28 days	25 mL	0.02 to 2.50 ppm NH ₄ ⁺ -N
Total PO₄³⁻	Glass	Triple rinse bottle with DI water, air dry, triple rinse with sample	100 mL	H ₂ SO ₄ to pH < 2, Refrigerate	Spectrophotometry Acid Persulfate Digestion: Hach Method 8190 (Hach, 2005c) and Ascorbic Acid: Hach Method 8048 (Hach, 2005b)	2 days	25 mL	0.02 to 2.50 ppm PO ₄ ³⁻
Major Elements (ICP-OES Analysis)‡	PP Plastic	Triple rinse bottle with ultra pure DI water, drying oven, acid wash (HNO ₃), triple rinse with sample	50 mL	0.2 µm filter, 2% HNO ₃ /0.5% HCl to pH < 1	EPA ICP-OES Method 200.7: EPA, 1990	28 days	5 mL	See Table 2.5
Trace Elements (ICP-MS Analysis)‡	PP Plastic	Triple rinse bottle with ultra pure DI water, drying oven, acid wash (HNO ₃), triple rinse with sample	50 mL	0.2 µm filter, 2% HNO ₃ /0.5% HCl to pH < 1	EPA ICP-MS Method 200.8: EPA, 1994	28 days	5 mL	See Table 2.6
<i>E. coli</i>/Total Coliform	Sterile PP Plastic	Triple rinse bottle with DI water, air dry, autoclave (>121°C for 40 minutes), triple rinse with sample	500 mL	Refrigerate	IDEXX Colilert System (97 well tray)	0.25 days	100 mL	0 to 2,420 cfu/100 mL (undiluted sample)

*Container must be airtight to prevent evaporative enrichment.

†Nitrogen species can be collected in the same 500 mL container.

‡ICP-OES and ICP-MS species can be collected in the same 500 mL container.

Table 2.2. Handheld water quality equipment specifications.

Model	Manufacturer	Parameter	Range	Accuracy*
YSI 30	YSI Environmental	SpC	0 – 200 mS/cm	± 0.5%
		Salinity	0 – 80 ppt	± 2%
		Temperature	-5 – 95°C	± 0.1°C
YSI 550 A	YSI Environmental	DO	0 – 20 ppm	± 2% of reading or 0.3 ppm
		Temperature	-5 – 95°C	± 0.1°C
YSI 60	YSI Environmental	pH	0 – 14	± 0.02
		Temperature	-5 – 75°C	± 0.1°C
YSI EcoSense pH 10	YSI Environmental	pH	0 – 14	± 0.02
		Temperature	0 – 99.9°C	± 0.3°C
IQ125	IQ Scientific	pH	2 – 12	± 0.1
2100P	Hach	Turbidity	0 – 1000 NTU	± 2%
U-10	Horiba	Temperature	0 – 50°C	± 0.3°C
		SpC	0 – 100 mS/cm	± 1% of full scale
		Turbidity	0 – 800 NTU	± 3% of full scale
		DO	0 – 19.9 ppm	± 0.1 ppm
		pH	1 – 14	± 0.05

*The larger value is used for parameters that have more than one accuracy value given.

Table 2.3. Monitoring locations, equipment, and time frames.

Location*	Type of Feature	Abbreviation	Grab Sampling	Autosampler	Years of Operation	Continuous Monitoring Device	Years of Operation
Fox Creek	Stream	FOX	2007 – 2008	ISCO 3700	2007 – 2008	YSI6600	2007 – 2008
Grand Glaize Creek	Stream	GG@Q	2007 – 2008	ISCO 3700	2008	YSI6600	2007 – 2008
Sugar Creek	Stream	SGR	2007 – 2008	–	–	–	–
River des Peres @ Morgan Ford Rd.	Stream	RDP	2007 – 2008	–	–	YSI6600	2007 – 2008
Southwest Branch of the Upper River des Peres @ Ruth Park, McKnight Rd. Site	Stream	RP1	2009 – 2010	ISCO 6712	2009 – 2010	YSI6600	2009 – 2010
Southwest Branch of the Upper River des Peres @ Ruth Park, Downstream Woodland Site	Stream	RP2	2009 – 2010	ISCO 3700	2009 – 2010	YSI6600	2009 – 2010
Upper River des Peres @ Heman Park	Stream	HMP	2009 – 2010	ISCO 6712	2009 – 2010	YSI6600	2009 – 2010
Deer Creek @ Litzsinger Rd.	Stream	DCL	2008	–	–	–	–
Deer Creek @ Ladue	Stream	DC@MAC	2008	–	–	–	–
Deer Creek @ Maplewood	Stream	DC@BB	2008	–	–	–	–
Sebago Creek	Stream	SEB	2008	–	–	–	–
Two Mile Creek	Stream	TMW	2008	–	–	–	–
Black Creek	Stream	BCK	2004 – 2009	ISCO 6712	2004 – 2009	YSI600	2004 – 2009
Chalet Ct.	Surface Runoff	CHA	2010 – 2011	ISCO 3700	2010 – 2011	YSI Level Scout	2010 – 2011
Cornell Ave.	Surface Runoff	CORN	2009 – 2011	ISCO 3700	2009 – 2011	YSI Level Scout	2010 – 2011
Mt. Calvary Church	Surface Runoff	MTC	2010 – 2011	ISCO 3700	2010 – 2011	YSI Level Scout	2010 – 2011

*Detailed information about each sampling location is provided in Chapter 3, Table 3.1.

Table 2.4. Continuous monitoring sensors specifications.

Manufacturer Model	Parameters Measured	Range	Accuracy*
YSI 6600 V2 Sonde	Temperature	-5 – 50°C	± 0.15°C
	SpC	0 – 100 mS/cm	± 0.5% of the reading + 0.001mS/cm
	Turbidity	0 – 1000 NTU	± 2% of the reading or 0.3 NTU
	DO	0 – 50 ppm	0-20 ppm: ± 1% of the reading or ± 0.1 ppm 20-50 ppm: ± 15% of the reading
	pH	0 – 14	± 0.2
	Cl	0 – 200 ppm	± 15% of the reading or 5 ppm
	NH ₃ -N	0 – 200 ppm	± 10% of the reading or 2 ppm
	NH ₄ ⁺ -N	0 – 200 ppm	± 10% of the reading or 2 ppm
YSI 600R	NO ₃ -N	0 – 200 ppm	± 10% of the reading or 2 ppm
	Temperature	-5 – 45°C	± 0.15°C
	SpC	0 – 100 mS/cm	± 0.5% of the reading + 0.001mS/cm
	DO	0 – 20 ppm	0-20 ppm: ± 2% of the reading or ± 0.2 ppm 20-50 ppm: ± 6% of the reading
YSI Level Scout	pH	0 – 12	± 0.2
	Temperature	-5 – 50°C	± 0.2°C
ISCO 710 Ultrasonic Flow Module	Level	0 – 760 cm	±0.3 cm
	Level	30.5 – 335 cm away from the sensor	±0.03 cm

*The higher value is used for parameters that have more than one accuracy value given.

Table 2.5. Elements and detection limits measured with ICP-OES. Values reported in ppm.

Element	Detection Limit*
Ca	0.06
K	0.1
Mg	0.02
Na	0.2
S	0.06
Si	0.03
B	0.002
Sr	0.002

*Detection limits reported as the operational limits of the test and reported as the concentration corresponding to a signal three times the noise of the background.

Table 2.6. Elements and detection limits measured with ICP-MS. Values reported in ppb.

Element	Detection Limit*
Al	0.04
Ba	0.008
Cd	0.006
Co	0.003
Cr	0.04
Cu	0.02
Fe	0.09
Ga	0.007
Li	0.09
Mn	0.006
Mo	0.006
Ni	0.01
Pb	0.003
Rb	0.003
Zn	0.09

*Detection limits reported as the operational limits of the test and reported as $\left(\frac{3 \times \sqrt{\text{blank intensity}}}{\text{standard intensity} - \text{blank intensity}} \right) \times \text{concentration of the standard}$.



Figure 2.1. Typical autosampler field installation: (A) an ISCO Model 3700 autosampler; (B) a carousel filled with disposable ISCO ProPak™ bags; (C) the utility box and PVC pipe housing; and (D) the PVC pipe housing and the 1640 Liquid Level Sampler Actuator.



Figure 2.2. Typical in situ continuous water quality monitoring device field installation:
(A) a continuous water quality monitoring device housed in PVC pipe and (B) a YSI 6600 continuous monitoring device and its calibration standards.



Figure 2.3. Typical in situ water level sensor field installation in a storm sewer to measure runoff water level.

Chapter 3: New insight into urban watershed dynamics using high frequency in situ monitoring in three streams and their tributaries, east-central Missouri

Abstract

High frequency monitoring of relevant water quality parameters in conjunction with isotopic measurements are used in this study to quantify the hydrologic and geochemical differences between watersheds with differing land use and to address their degradation by human activities. Three watersheds and their tributaries, including a rural, suburban, and urban watershed, were monitored for a period of more than one year to assess their hydrologic and geochemical character. The urban stream and its tributaries are characterized by flashier responses to storm perturbation and have reduced baseflow components during these events, while hydrologic and geochemical parameters in the rural stream exhibits fewer extreme excursions from baseflow values and longer lag times (4-fold longer) during discharge perturbations. The urban and suburban streams are commonly degraded with respect to specific conductivity (SpC), turbidity, dissolved oxygen (DO), Na, Cl, nutrient, and trace metal contents, and their concentrations change rapidly. Water quality and storm water delivery in urban streams are mitigated in part by reconstructing natural channels that can increase baseflow contribution by 15% and reduce Cl, nutrient, and bacterial loads. Continuous monitoring data demonstrate increased seasonal and diurnal variability in urban systems, and temperature measurements indicate smaller seasonal groundwater contributions to baseflow in these systems. Further, infrequent and arbitrary sampling regimes can result in under- or overestimation of chemical and sediment loads by 100-fold, including consistent underestimation of Cl loads following winter road salt application.

3.1. Introduction

3.1.1. Significance of Floods

In the urban areas of St. Louis City and County, surface water composition may be influenced by many factors, both natural and human-induced. Anthropogenic organic and inorganic contaminants can stem from numerous point and non-point sources throughout the watershed. Organic contaminants, whether from wastewaters, animal manures, debris dumping, or landscape management of commercial and residential properties, create several problems including health risks, low DO, increased water temperatures, and large debris accumulations. Inorganic contaminants can be toxic to aquatic organisms that inhabit these environments.

Transient storm events, especially in urbanized areas, produce substantial runoff that mobilizes and transports pollutants at rates that can dwarf their delivery during normal flows. Further, flood waters exacerbated by urban development can damage and destroy homes and property. This process is usually most severe during the spring in humid regions, and the scale of these events can range from minor nuisances to life threatening disasters. Floods are regarded as the most frequent, ubiquitous, and familiar natural hazards and globally account for approximately one-third of all disasters (Gleick, 1993; Smith and Ward, 1998). In the United States alone, flooding causes average annual economic losses exceeding \$2 billion, and flash flooding is the primary cause of weather related deaths (National Oceanic and Atmospheric Administration; NOAA, 2011b).

Of particular importance are flash floods on small creeks and rivers, which occur rapidly and unexpectedly (Ogden et al., 2000), and feature enormous excursions from

normal flow conditions (Figure 3.1). These hydrologic pulses represent intense perturbations to watersheds that transport large amounts of sediments and mobilize nutrients and pollutants (e.g., Borah et al., 2003; Vicars-Groening and Williams, 2007).

In small catchments, flood hydrographs are characterized by rapid increases in discharge that result in a sharp discharge peak followed by a more gradual return to normal flow conditions. Factors involved in flash flooding include high rainfall intensity, protracted rainfall duration, reduced vegetation, land development, steep topography, and basin slope. Urban watersheds are particularly vulnerable to flash flooding due to the high percentage of impervious surface, such as roads, roofs, sidewalks, and parking lots (Konrad, 2003). Analyses from this study of more than 500 pulses from 12 regional streams support the theoretical model of Criss and Winston (2008a). The model is based on the diffusion equation and Darcy's law (see Chapter 2, Section 2.5.8. Theoretical Hydrograph) to explain these excursions, where the magnitude and timing of flow variations are driven by the theoretical response to detailed meteorological records (Criss and Winston, 2008a,b). The model also explains the first-order response of several other physical and chemical parameters, which are initiated by the same pulse but respond with their own intrinsic timescales (Winston and Criss, 2004).

3.1.2. Shortcomings of Available Datasets

For many constituents of environmental concern, the vast majority of the average annual load can be delivered in only a few days (Wallace et al., 2009). Numerous studies have estimated the significant loads delivered by flood waters in rural (Mott and Steele, 1991; Winston and Criss, 2002) and urban environments (Smullen et al., 1999; Phillips and Bode, 2004). However, these studies typically rely on infrequent sampling regimes,

and, therefore, cannot accurately quantify the magnitude or timing of these geochemical pulses which adversely affect stream health (Roberts, 1997; Horowitz, 2009).

Relatively few small catchments in the United States are instrumented for flow, and these installations are rarely capable of measuring key water quality parameters. Variations of individual chemical constituents (chemographs) are also not well-documented because few studies sample frequently enough to observe any rapid changes that occur on the short time scale of the flash flood process (Tomlinson and De Carlo, 2003; Harris and Heathwaite, 2005). Knowledge of the behavior of flash floods is accordingly limited, and quantifying the associated spectrum of transport phenomena represents a significant goal for hydrologic science.

Previous attempts have been constrained by technological and economic limitations, and, consequently, lacked the capacity to observe real-time changes in the concentrations of individual ions. Further, many sampling devices measure only a few constituents. Thus, most studies estimate solute concentrations based on regression techniques and a few seasonal samples (Cohn et al., 1989; Driver and Troutman, 1989). Others rely on composite sampling to determine an event mean concentration (EMC) that is then used to characterize annual loads (e.g., Bannerman et al., 1996). These composites are typically collected on flow or time-based intervals by automated sampling devices that may not collect samples during periods of maximum flow or solute concentration.

Some studies have begun to incorporate newer technologies that allow the continuous monitoring of some parameters and illustrate the potential for discovery that these observational advances represent. Christensen (2001) deployed sensors in rural

Rattlesnake Creek in south-central Kansas to continuously monitor temperature, SpC, turbidity, DO, and pH. Site-specific regression equations were then developed based on analysis of four low flow samples plus five “wet” flow samples taken during different storms to estimate the concentration of other constituents such as suspended sediments, NO_3^- -N, and Cl. However, traditional regression coefficient methods cannot capture the rich patterns of concentration variability, in part because many chemical constituents exhibit hysteresis patterns during storm flow that depend on individual transport timescales (Toler, 1965; Miller and Drever, 1977; Evans and Davies, 1998). Moreover, Leecaster et al. (2002) determined that no fewer than 12 flow-interval samples are required to accurately characterize the load delivered during a single storm event.

In short, limitations of previous work include the total lack of rapid sample collection to capture the dramatic variations that occur during flooding, a reliance on too few physical samples to define the relationships among parameters, no systematic investigation of regional behaviors, no consideration of the hysteresis response of key parameters, and overuse of simplistic regression analysis. In addition, there has been little recognition that seasonal differences can affect the response of some parameters and produce complex relationships among easily measured parameters such as SpC. Advantages of continuous monitoring devices include more accurate quantification of the timing and magnitude of water quality extremes, a more representative image of overall water quality, and a better understanding of watershed response to storm events (Jarvie et al., 2001). Continuous and high frequency datasets offer a more representative view of actual transport processes and facilitate a shift from arbitrarily selected sampling regimes, and their study could help to optimize discrete sampling schemes.

3.1.3. Study Design

In this study, three different watersheds including rural Fox Creek, suburban Grand Glaize Creek, and urban River des Peres were investigated. Monitoring sites were located proximal to U.S. Geological Survey (USGS) gaging stations near the mouths of the streams. Additional sampling locations within the River des Peres and Grand Glaize Creek watersheds were also monitored. These include four continuous monitoring sites (two at the Southwest Branch of the Upper River des Peres, one at the Upper River des Peres, and one at Black Creek) and five grab sample sites (all in the Deer Creek basin: Sebago Creek, Two Mile Creek, and three locations along the main stem) in the River des Peres watershed and one grab sample site (Sugar Creek) in the Grand Glaize Creek watershed (see Table 3.1). These additional sites were selected to assess nested basin behavior.

Continuous monitoring devices were deployed alongside autosampling units that collect physical samples to verify the accuracy of the sensors and for isotopic analysis (see Chapter 2, Table 2.3 for equipment specifications and monitoring time frames). Extensive study of storm responses took place at Fox Creek, Grand Glaize Creek, the two locations on the Southwest Branch of the Upper River des Peres, the Upper River des Peres, and Black Creek. Geochemical monitoring was concurrent at Fox, Grand Glaize, and Black Creeks from 2007 to 2008 and at the Upper River des Peres Sites including Ruth Park 1 (RP1), Ruth Park 2 (RP2), and Heman Park (HMP) sampling sites from 2009 to 2010 (Table 2.3). While storm events may be temporally disparate, overall perturbation responses are still comparable between basins. These efforts created a detailed record of watershed scale hydrologic and geochemical behavior, which are used

to study the timing and magnitude of watershed response to several factors including urbanization, basin size, and diurnal and seasonal variations.

By coupling the high frequency datasets with stable isotope methods (e.g., Sklash and Farvolden, 1979; Hooper and Shoemaker, 1986; Lakey and Krothe, 1996) this study provides a unique and reliable means to deconvolve the sources of individual chemical constituents in stream flow. Winston and Criss (2004) have documented that the magnitudes and relative proportions of these sources vary dynamically during storm flow in a karst spring. Application of the Criss and Winston (2003) hydrograph model to the associated hydrologic and geochemical responses yields a quantitative measure of the timing and magnitude of each response that facilitates basin intercomparison. Detailed characterization of watershed attributes, causal precipitation events, and subsequent hydrologic and geochemical variations have been employed to identify consistent response patterns for given watersheds, and are used to develop predictive models.

This study addresses advancement in watershed theory, methods, and models as well as watershed response to precipitation events, including surface water generation and transport, by employing a network of sensors and applying subsequent datasets to basin and regional modeling efforts. It investigates, interprets, and intercompares detailed observational datasets of hydrologic and geochemical responses in three basins with different levels of urbanization.

Flood pulses were actively sampled and continuously monitored for more than one year at each site to quantify seasonal differences and to characterize a sufficient number of events to allow adequate comparison between the basins. Results include field measurements, stable isotope and geochemical analyses of water, and continuous records

of temperature, SpC, turbidity, DO, pH, $\text{NH}_4^+\text{-N}$, $\text{NO}_3^-\text{-N}$, and Cl. This study also compiles regional discharge records, climate and rainfall data, and GIS datasets (including topography, soil, geology, population density, and land use maps) to quantify storm and watershed characteristics, permitting intercomparison of each basin's response.

The outcome of these field investigations has provided a unique dataset that allows quantification of several significant, fundamental questions including:

- 1) How much do peak flows increase and recession rates shorten, as a function of urbanization as characterized by land use data?
- 2) How does the isotopically-identified baseflow fraction vary during an individual storm, differ from storm to storm, and differ from urban to suburban to woodland settings?
- 3) How much does the transport of suspended sediment, as characterized by the turbidity, increase due to increases in flood severity caused by urbanization?
- 4) What is the hierarchy of transport timescales for the different chemical and physical parameters in each basin and is this hierarchy consistent? Does urbanization shorten the transport timescales of any individual parameters and by how much?
- 5) Which chemical parameters are most closely associated with the isotopically-identified baseflow fraction, and which correlate most closely with the event water fraction?
- 6) How does the transport of individual solutes depend on storm and basin characteristics?
- 7) Are stream temperature variations during flood pulses more pronounced in urban settings?

- 8) How well does an infrequent sampling protocol quantify the loads of particulates and individual solutes transported by streams in small basins?

3.2. Description of Study Sites

The St. Louis region is a unique area for the study of hydrologic phenomena. Features range from the large Mississippi and Missouri Rivers to small creeks, and the USGS currently maintains 39 real-time surface water monitoring stations to quantify discharge values in St. Louis City and County. The watersheds selected for intensive sampling in this study vary in catchment size by three orders of magnitude, and the area above various gaging stations and sampling sites, effective catchment area, and other gaging station information are provided for each site in Table 3.1. Basin area for all the watersheds is correlated with mean discharge (Figure 3.2). The three larger basins (Fox Creek, Grand Glaize Creek, and River des Peres) were carefully chosen to compare the effects of urbanization on hydrologic and geochemical response. Consideration was also given to basin proximity in order to minimize meteorological differences since the predominant storm path in this region is from southwest to northeast. The selected basins therefore are aligned to intersect the same storm events.

The basins are all located in east-central Missouri within 40 km of St. Louis; easing the logistical problems associated with the ambitious field component of this project. Existing geospatial datasets were compiled for each watershed and include basin topography, soil type distributions, geology, population demographics, and land use/land cover (Figures 3.3 – 3.7). These datasets provide the basis for defining spatial and surficial metrics for each basin and allow correlation between basin parameters and hydrologic and geochemical response.

3.2.1. Fox Creek

Fox Creek (Figures 3.3, 3.8) has a drainage area of 46 km² and is the most westerly of the study sites, draining the largely rural parts of western St. Louis County and eastern Franklin County. It joins the Meramec River, a subbasin in the lower Mississippi River basin, from the north near Allenton, MO. Basin elevation ranges from 245 m at the headwaters to 133 m at the confluence with the Meramec River. The geology predominantly consists of several Ordovician limestone and dolostone units (Figure 3.5). Properties in the watershed are large and dispersed and include a few small farms (Figure 3.7). While the watershed is largely rural, it is beginning to experience residential and commercial growth, and a major highway (I-44) crosses this basin near its confluence with the Meramec River. The highest population density in the watershed is in Allenton (295 people/km²; Figure 3.6).

Fox Creek is considered by the Missouri Department of Conservation (MDC) to be a priority stream that remains healthy. In marked contrast to streams closer to the urban areas surrounding St. Louis, it hosts more than 40 species of fish (Missouri Department of Conservation; MDC, 2011). For instance, Antire Creek, located 16 km east of Fox Creek, only hosts three species of fish (MDC, 2011). Fox Creek serves as the rural end-member for the interbasin comparison. A USGS gaging station located next to the ISCO autosampler and continuous monitoring device was in operation from 2007 to 2008 on the lower reaches of the creek. Average discharge at Fox Creek at the Allenton gaging station is 0.51 cms but can reach more than 226.5 cms during flash flood conditions (USGS, 2011).

3.2.2. *Grand Glaize Creek*

Grand Glaize Creek (Figure 3.9), with an area of 61 km², is an impacted suburban stream located in the Meramec River basin. It is situated near the interstate highway bypass (I-270) that surrounds the greater metropolitan St. Louis area, and basin elevations range from 120 to 200 m (Figure 3.3). The watershed is underlain predominantly by Mississippian limestones, but the basin geology also includes Pennsylvanian shales in the eastern portion of the watershed (Figure 3.5). This basin exhibits extensive residential development with the most densely populated areas containing 465 people/km² (Figure 3.6).

Approximately 60% of the land use is classified as urban (Figure 3.7), but the watershed lacks the extensive highway and commercial developments of the River des Peres watershed. The stream is included on the Missouri 2002, 2006, 2008, and 2010 303(d) lists for high Hg, high Cl, bacterial contamination, and low DO, respectively (MoDNR, 2011b). Development throughout the basin has affected the hydrologic response by increasing the magnitude and reducing the duration of flood events, producing marked erosion and channel incision. Wildlife has been heavily impacted by development in the basin, and the stream only hosts 10 species of fish (MCD, 2005).

The autosampler and continuous monitoring device were located next to a USGS gaging station in Valley Park, MO, with a 13-year record (the station was later moved slightly upstream due to structural issues with this bridge). The average discharge at this station since 1998 is 0.68 cms, but flows can exceed 169.9 cms during flash flood conditions (USGS, 2011; Table 3.1). A second USGS gaging station (07019150) is located upstream on the main stem of Grand Glaize Creek near Manchester, MO, and a

third one is located on the Sugar Creek tributary (07019175) in Kirkwood, MO. In addition to the extensive sampling and monitoring at the Valley Park site, bi-weekly grab samples were collected at the Sugar Creek gaging station.

3.2.3. *River des Peres*

The River des Peres is a large (295 km²), highly degraded watershed draining St. Louis City and the eastern portion of St. Louis County (42 municipalities). Elevations in this watershed range from 200 m in the headwaters to 140 m at its confluence with the Mississippi River (Figure 3.3). The geology of the basin consists predominantly of the Meramecian Series limestones in the southwest and Pennsylvanian shales in the northeast (including the Black Creek basin; Figure 3.5), and these units are overlain by Quaternary loess soils (Lutzen and Rockaway, 1989; Harrison, 1997; Figure 3.4).

River des Peres has the highest average population density (1,990 people/km²; Figure 3.6) and the highest percentage of urban land coverage (> 90% urban land coverage; Figure 3.7) of the watersheds in the study. The river extends approximately 30 km through the St. Louis area before discharging into the Mississippi River. Most of the main stem (> 80%) was straightened and channelized using a system of tunnels, pipelines, and canals during the River des Peres Sewerage and Drainage Works project (1924 to 1931) in an attempt to mitigate flooding issues and alleviate severe water quality issues associated with accidental and intentional use of the river as an open sewer (Corbett, 1997; Shock et al., 2003; ASCE, 2011; Figure 3.10). Because hundreds of storm sewers channel the runoff from roads, parking lots, houses, institutional, commercial, and industrial properties into the stream, flow rates of the River des Peres can range from virtually zero to more than 700 cms in the lower basin (USGS, 2011).

The River des Peres and its tributaries represent extremely impacted urban streams that respond rapidly to rainfall. The main stem has been listed on the Missouri 2006 and 2010 303(d) lists for high Cl and low DO, respectively (MoDNR, 2011b). Undesirable levels of these constituents are caused by a combination of pulses of road salt, nutrients from fertilizers, combined sewer overflows (CSOs), and animal wastes (see subsequent sections). The watershed hosts 134 CSOs along its reaches, and about 50 overflows per year discharge 24,000,000 m³ annually (Metropolitan St. Louis Sewer District; MSD, 2011). Due to the poor condition of this watershed, it serves as the urbanized end member for this comparative study.

Autosamplers and continuous monitoring devices were deployed at two locations on the Southwest Branch of the Upper River des Peres in Ruth Park and one location on the Upper River des Peres in Heman Park (University City, MO). The Lower River des Peres at Morgan Ford Rd. (St. Louis, MO) was outfitted with only a continuous monitoring device. The monitoring site farthest upstream, which is located in Ruth Park at McKnight Rd. (RP1), was equipped with an acoustic stage recorder. The second monitoring site (RP2) was located 320 m downstream of RP1 in a wooded portion of the park, downstream of a golf course and a mulching facility. The third monitoring station was located in Heman Park (HMP) below the confluence of the Southwest Branch, the main stem of the Upper River des Peres, and an unnamed tributary. This station was located 795 m downstream of a USGS gaging station (07010022). The lowermost monitoring location encompassed the majority of the River des Peres watershed and was located near the Morgan Ford Rd. bridge next to a USGS gaging station (07010097). This site was frequently affected by backwater from the Mississippi River. Within the

River des Peres Watershed there are several tributaries, including Deer Creek and its smaller tributary Black Creek, which are both discussed in the subsequent sections.

3.2.3.1. Deer Creek

The Deer Creek watershed drains approximately 95 km² of densely populated St. Louis County (970 people/km²; see Figures 3.3, 3.6). The three major tributaries to Deer Creek are Black, Sebago, and Two Mile Creeks. More than 80% of the land use in the watershed is residential development (Figure 3.7). Large areas of impervious surface cause streams within the Deer Creek watershed to be subject to frequent flash flooding events. Discharge responses to storm perturbation are sharp and often damage residential and commercial structures (such as manufacturing buildings, industrial parks, and retail shops). Water quality threats to the main stem and tributaries include storm water runoff from impervious surfaces, debris and trash, sediment from streambed and bank erosion, and pollutants associated with combined sewer overflow (CSO) and sanitary sewer overflow (SSO). However, Deer Creek and its tributary Black Creek were recently classified for use as irrigation, livestock, and wildlife waters and as cool and cold water fisheries, indicating a change in public attitude toward the benefits of these creeks (MoDNR, 2011a).

3.2.1.3.1. *Black Creek*

Black Creek, a small tributary (22 km²) to Deer Creek and the River des Peres, drains the predominantly urban region of the St. Louis suburb, Brentwood, MO (Figure 3.3). Approximately 90% of the land is commercial development (Figure 3.7) and much of the main reach of Black Creek flows in cement-walled channels or culverts. The watershed is highly impacted and is prone to flash flooding even after only moderate

amounts (< 2 cm) of precipitation. Consequently, significant channel alterations were made to accommodate high flows from impervious areas (Figure 3.11). Two major highways cross the Black Creek basin and are significant sources of road runoff, while numerous commercial facilities constitute additional sources for anthropogenic pollutants. The stream also features CSOs, as well as several detention basins used for flood control. Flash floods in this area have recently increased in frequency and forced several small businesses to relocate away from the creek.

An automatic sampling device equipped with an acoustic stage recorder and continuous monitoring device (which was run intermittently for temperature, SpC, and pH) were located only 208 m upstream of a USGS gaging station with 7 years of record. Average discharge over the 7 years of record at Black Creek is 0.23 cms but has reached more than 141.6 cms during flash flooding (U.S. Geological Survey, 2011; Table 3.1). The installation was destroyed by severe flooding on September 14, 2008.

3.3. Methods

Field sampling techniques, field equipment specifications and periods of operations, laboratory procedures, and data processing procedures (i.e., hydrograph separations and estimations of artificial hydrographs) are outlined in Chapter 2. For convenience, δD and $\delta^{18}O$ values will always be listed in that order, and this relationship will be used when the specific isotope ratio is not specified.

For this study, total suspended solids (TSS) were not measured on field samples for comparison with turbidity values measured in the field or lab. TSS have been measured in the subsequent analyses of similar waters, and given the robust correlation between the two parameters for local surface and groundwaters ($R^2 = 0.90$; Figure 3.12),

turbidity will be used as a proxy for TSS. Notable exceptions are organic rich wastewaters and mulch leachates, which do not follow the same trend. These samples have different particle properties, and therefore, display a unique trend (Figure 3.12).

Rainfall amount, temporal distribution, and intensity were obtained from hourly records from the National Weather Service (NWS) weather station at Lambert – St. Louis Internal Airport in St. Louis, MO, and from USGS gaging station 07019185 equipped with a rain gauge in Valley Park, MO. The isotopic composition of precipitation was determined in samples collected at private rain gauges in St. Louis, Ladue, and Washington, MO, to obtain a wide spatial distribution of rainfall events. If the isotopic character for rainfall samples varied between sampling sites at St. Louis, Ladue, or Washington, MO, the data for the precipitation station closest to a given basin were used for hydrograph separations.

Baseflow conditions are defined by the stage, SpC, and isotopic composition measured at the sites prior to initiation of a flow pulse. Baseflow conditions are characterized by δD and $\delta^{18}O$ values that are close to the weighted, long term average of local meteoric precipitation and by SpC values near the seasonal range for the stream. Event water consists of recent precipitation that has infiltrated the watershed and SpC is relatively low compared to baseflow. Event extremes for physical and chemical parameters (i.e., temperature, SpC, nutrients, etc.) are taken from the continuous monitoring device records, when available, and compared to field and laboratory analyses. The next section contains the data treatment for the five investigated pulses and causal precipitation events, and is followed by discussion and interpretations.

3.4. Results

3.4.1. Response to Storm Perturbation

Each watershed has a unique volumetric, chemical, and isotopic response to a given storm perturbation. Moreover, different basins exhibit distinct responses to the same storm. Multiple storm-induced perturbations occurred at the sites, and nearly 80 events were sampled at the six autosampler locations since the equipment was deployed. Not all of these discharge events will be discussed here, and several of these pulses are not suitable for detailed study due to equipment malfunction, spatially variable rainfall, insignificant perturbations from baseflow, or the lack of significant differences between the isotopic character of baseflow and incoming precipitation.

Five discharge events at Fox Creek, Grand Glaize Creek, Black Creek, and the three Upper River des Peres locations have been selected for detailed comparative study of their isotopic and chemical responses. Not all of the monitoring sites discussed in the study (including, Sugar Creek, River des Peres at Morgan Ford Rd., and all of the Deer Creek locations except Black Creek) were equipped with continuous monitoring or autosampling equipment, and consequently, isotopic and chemical analyses of flood perturbations for these sites were not available. The physical and isotopic character of the causal precipitation events has been compiled to facilitate the comparison of these discharge responses (Table 3.2).

3.4.1.1. March – April 2008 Events: Fox, Grand Glaize, and Black Creeks

A series of samples representing several discharge events were collected in the early spring of 2008 at Fox, Grand Glaize, and Black Creeks (Figure 3.13). The rainfall events that triggered these perturbations are listed in Table 3.2. All of the rainfall events

were isotopically distinct from each stream's baseflow. The relative increases in discharge depended on both the particular stream site and the particular storm, but in general, Fox Creek had the most dampened hydrologic and geochemical responses of the three basins and Black Creek had the most dynamic responses. Baseflow contributions to each pulse event are shown in Table 3.3 and the results for individual basins responses are discussed below.

3.4.1.1.1. Fox Creek

In every case, Fox Creek exhibited the most subdued response to the various March – April storm perturbations, responding with discharge peaks that were low and broad. The March 26 and March 27 event peaks overlapped and the baseflow fraction for these events was 79%. During the next event on March 30, the baseflow component was reduced to 59% of the total discharge volume. The maximum discharge for all the events was less than 5 cms with the exception of the March 31 – April 1 event, which reached a peak discharge of 35.3 cms (Figure 3.13A). The March 31 – April 1 rainfall event was the largest of the five (32% larger than the preceding event), but the discharge response was not proportional to the rainfall and was almost 9-fold larger than the event on the day before, due to saturated basin conditions. Stable isotope values changed minimally during the perturbation and varied less than 13‰ and 0.7‰ during the monitoring period (Figure 3.13B).

The stream temperature variations were complex, due to the daily changes in ambient air temperature, but small ($< 0.2^{\circ}\text{C}$) changes occurred following the March 26 and 31 events (Figure 3.13C). SpC was initially 480 $\mu\text{S}/\text{cm}$ and dropped to 230 $\mu\text{S}/\text{cm}$ during the March 26 perturbation, and during this decline several transient minima were

observed. The lowest SpC was observed after the March 31 – April 1 event, when SpC decreased to 126 $\mu\text{S}/\text{cm}$ 20 minutes after peak discharge (Figure 3.13D). For most of the discharge response, turbidity pulses remained less than 250 NTU; however, during the large March 31 event, turbidity reached 845 NTU on the rising limb of the discharge pulse (Figure 3.13D).

DO and pH patterns were complex during this series of events because of the diurnal oscillations of these parameters due to aquatic photosynthesis. These daily patterns were superimposed on the storm pulse signals. However, during the storm perturbations, both DO and pH tended to increase (Figure 3.13E). Baseflow Cl prior to these events was 45 ppm, and increased to 50 ppm on the rising limb of the first storm perturbation. Cl subsequently diluted to 23 ppm, though transient minima similar to those that occurred in the SpC data were observed. Cl reached its lowest value (11 ppm) on the recessional limb of the large March 31 event (Figure 3.13F). NH_4^+ -N remained relatively constant during all of the perturbations. NO_3^- -N had a more dynamic response than NH_4^+ -N and typically increased by 0.5 ppm at the onset of a discharge pulse (Figure 3.13G).

3.4.1.1.2. Grand Glaize Creek

Peak discharges at Grand Glaize Creek were higher than those at Fox Creek for all events; in part because of the larger watershed size (e.g., the Grand Glaize Creek basin is approximately 1.5 times larger). However, if the area of the Grand Glaize Creek watershed is scaled to that of Fox Creek, the discharge peaks for this series of events are 3-fold larger than those at Fox Creek. Further, the discharge pulses at Grand Glaize

Creek also featured shorter rising and recessional limb responses than Fox Creek, indicating that the water moved through the basin more rapidly.

During the March 26 event, stream flow increased from 0.03 cms to 20.8 cms, with 49% of the discharge perturbation composed of event water, which was substantially less than the baseflow fraction observed at Fox Creek. The event hydrograph also displayed the same double peak as Fox Creek, but did not exhibit the broad peak response (Table 3.3; Figure 3.13A). Isotopic changes were more extreme than those observed at Fox Creek, and the maximum enrichment of δD at Grand Glaize Creek was to a value of -27‰ compared to -47‰ at Fox Creek (Figure 3.13B).

Baseflow during the March 31 – April 1 event was 0.14 cms and had δD and $\delta^{18}O$ values of -41‰ and -6.4‰. Peak discharge for this event was 47.0 cms and the maximum isotopic enrichment for the event produced values of -30‰ and -4.9‰, which occurred on the rising limb of the discharge pulse (Figure 3.13B). The April 3 rainfall event was isotopically depleted, and as a result, a maximum depletion to -48‰ for δD and -7.4‰ for $\delta^{18}O$ was observed on the recessional limb of the event (Figure 3.13B).

Like Fox Creek, Grand Glaize Creek's water temperature patterns featured complex, superimposed patterns. However, the temperature excursions were more extreme at Grand Glaize Creek, and ranged from 7.3 – 13.4°C. The largest temperature change associated with the discharge pulse was observed during the March 31 – April 1 event (> 2°C; Figure 3.13C). Baseflow SpC was substantially higher at Grand Glaize Creek (1,328 $\mu S/cm$) than Fox Creek. The SpC reached a minimum of 206 $\mu S/cm$ during the March 31 – April 1 event (Figure 3.13D). Turbidity peaks were higher and shorter

than at Fox Creek, and the maximum observed turbidity (1120 NTU) occurred on the March 30 event (Figure 3.13D).

DO and pH extremes were also larger at Grand Glaize Creek, and varied by up to 30% and 0.6 units, respectively. The DO invariably increased during the rising limb of the discharge event. The pH commonly increased during the series of storm perturbations, but decreases were observed during the March 30 and April 3 events (Figure 3.13E). Cl values were four times higher than at Fox Creek, and the minimum value of 29 ppm was reached during the March 31 – April 1 event (Figure 3.13F). The NH_4^+ -N levels were 20-fold higher than those at Fox Creek, and increased by 0.5 ppm during the first two events. After these events, NH_4^+ -N was diluted by subsequent storm perturbations. During the largest discharge response (March 31 – April 1), NH_4^+ -N decreased sharply by almost 2 ppm (Figure 3.13G). NO_3^- -N concentrations diluted during the first three discharge perturbations, but then increased (by about 0.2 ppm) as a result of the next two events. During the final April 3 event, dilution of NO_3^- -N was observed once again (Figure 3.13G).

3.4.1.1.3. *Black Creek*

Black Creek was analyzed only for δD and $\delta^{18}\text{O}$, SpC, and turbidity during the five discharge events. The first rainfall event on March 26 induced a 50-fold change in discharge, where baseflow was 0.03 cms and peak flow was 15.7 cms. Black Creek featured the lowest baseflow components of all the sites during these perturbations (Table 3.3; Figure 3.13A). Baseflow conditions were characterized by isotope values of -56‰ and 8.0‰, SpC of 1,456 $\mu\text{S}/\text{cm}$, and turbidity of 2 NTU, and the maximum excursions from these values were -21‰ and 4.3‰, 303 $\mu\text{S}/\text{cm}$, and 1,453 NTU (Figure 3.13B, D).

SpC reached a minimum value of 279 $\mu\text{S}/\text{cm}$ 1.5 hours after peak flow and did not recover to pre-storm flow values before the next storm pulse (Figure 3.13D). Two maxima were observed in the turbidity data; the first was observed at the onset of the rising limb (1,268 NTU) and the second was observed during peak discharge (Figure 3.13D).

Data from this event produced an unusual and wide hysteresis loop when δD and $\delta^{18}\text{O}$ were plotted (Figure 3.14A). At the widest part of the loop, there was a difference of 10‰ for δD and 1.5‰ for $\delta^{18}\text{O}$. The maximum excursion from the meteoric water line (MWL; Craig, 1961), 10‰ for δD and 1.5‰ for $\delta^{18}\text{O}$, occurred at peak discharge (asterisk), which had δD and $\delta^{18}\text{O}$ values of -21‰ and -5.4‰. Both SpC and turbidity also produce hysteresis loops when plotted against $\delta^{18}\text{O}$ (Figure 3.14B).

No samples were collected until the March 30 discharge event. Because of the preceding rainfall events, the “baseflow” prior to this storm was likely a mix of recent event water and deeper, older reservoirs. Pre-event water was characterized by -42‰ and -6.4‰, 1,197 $\mu\text{S}/\text{cm}$, and 13 NTU for the isotopic composition, SpC, and turbidity, respectively, and during the event these values reached extremes of -31‰ and -5.0‰, 384 $\mu\text{S}/\text{cm}$, and 211 NTU, respectively (Figure 3.13B, D). A longer sampling interval of 2 hours was used during the event, and the extremes all occur in the same sample which was collected shortly after peak discharge. SpC recovered to near baseflow conditions 1.2 days later. Hysteresis patterns are observed in the SpC and turbidity data when plotted against isotope data; however, in this and subsequent events strong δD - $\delta^{18}\text{O}$ hysteretic effects are not observed as in the March 26 event (Figure 3.14), nor are they observed in any of the other basins.

Another discharge event at Black Creek followed a day later on March 31, 2008. The rainfall event that triggered the pulse deposited 2.6 cm of rain and occurred between 16:00 and 20:00 on March 31. There was over a 100-fold change in discharge, where baseflow was 0.14 cms and peak discharge was 17.5 cms (Figure 3.13A). The rainfall collected at Ladue (-22‰, -3.8‰) and Washington (-25‰, -4.7‰) differed from the δD and $\delta^{18}O$ values of creek baseflow (-44‰ and -6.6‰). The largest excursion from baseflow value occurred 15 minutes after peak flow, with values of -20‰ and -4.3‰ (Figure 3.13B).

Baseflow for this event had values of 1,360 $\mu S/cm$ and 33 NTU for SpC and turbidity, respectively. SpC reached its lowest value (210 $\mu S/cm$) during the recessional limb and recovered to 1,230 $\mu S/cm$ one day later (Figure 3.13D). Turbidity reached its highest value (1200 NTU) on the rising limb of the pulse and recovered to 30 NTU by the end of the sampling period (Figure 3.13D). A hysteresis loop was not observed when the isotope data were plotted (Figure 3.15A), but when SpC data were plotted against $\delta^{18}O$, a large open loop was observed (Figure 3.15B). A narrow loop was observed when turbidity was plotted in the same manner (Figure 3.15B).

The final event documented in this series occurred on April 3. The isotopic composition, SpC, and turbidity for baseflow were -42‰ and -6.5‰, 1,559 $\mu S/cm$, and 21 NTU, respectively. Event extremes were 5.4 cms, -53‰ and -8.0‰ (this event is the only one in which isotopic depletion was observed), 322 $\mu S/cm$, and 80 NTU. SpC did not recover by the end of the sampling period 0.5 days later and was 830 $\mu S/cm$ (Figure 3.13A, B, D).

3.4.1.2. May 2008 Event: Fox, Grand Glaize, and Black Creeks

On May 7 – 8 a discharge event was simultaneously collected at Fox, Grand Glaize, and Black Creeks. The event occurred after a relatively dry period when only 0.48 cm of rain had fallen five days prior to the May 7 event. Rain fell in several increments on the basin: 0.78 cm at 7:00 on May 7, 2.48 cm from 13:00 – 23:30 on May 7, 2.28 cm from 1:00 – 12:30 on May 8, and 0.2 cm from 9:30 – 11:00 on May 9 (Table 3.2), resulting in a total of 5.73 cm. Separate rain samples were collected for isotopic analysis from Washington and St. Louis, MO (Table 3.2). A composite sample of May 7 – 8 precipitation collected at Ladue had δD and $\delta^{18}O$ values of -32‰ and -5.4‰, which was approximately the same as the weighted average of the individual St. Louis (-31‰ and -5.3‰) and Washington (-34‰ and -5.8‰) precipitation samples. Again, during this event Fox Creek showed the most dampened response. The results for each site from this event are discussed below.

3.4.1.2.1. Fox Creek

Fox Creek had the most dampened response of the three watersheds to the May 2008 rainfall events. The discharge perturbation for the first rainfall event on May 7 was minimal when compared to Grand Glaize and Black Creeks. At Fox Creek, there were only two low, broad discharge peaks (Figure 3.16A). Baseflow was initially 0.09 cms, but increased to 5.7 cms at 20:00, following the 13:00 – 23:30 May 7 storm event. The largest event occurred at 11:15 on May 8 and produced a peak discharge of 8.5 cms. There was no observable response to the 9:30 – 11:00 May 9 rainfall (Figure 3.16A). Fox Creek's isotopic response to the storm perturbation was minimal. Baseflow was characterized by isotope values of -44‰ and -6.8‰, and the maximum excursion from

these values (-39‰ and -6.1‰) was observed on the recessional limb of the second discharge peak. By 11:00 on May 12, Fox Creek returned to near ambient baseflow conditions with isotope values of -43‰ and -6.6‰ (Figure 3.16B).

A small temperature excursion on the rising limb of the first discharge response ($< 0.5^{\circ}\text{C}$) was superimposed on the diurnal temperature variations (Figure 3.16C). SpC dropped gradually from 500 $\mu\text{S}/\text{cm}$ (baseflow level) to its lowest value of 210 $\mu\text{S}/\text{cm}$, which was observed on the falling limb of the second event. SpC had not recovered to pre-storm baseflow levels by the time an event on May 11 occurred (Figure 3.16D). Turbidity was initially 1 NTU and rose to a maximum value of 213 NTU prior to peak discharge during the first event. The second discharge event induced another increase in suspended sediments, but both turbidity responses at Fox Creek produced low, broad peaks. Fox Creek reached 4 NTU prior to the May 11 event (Figure 3.16D).

The baseflow pH value was 7.5, but increased to almost 7.8 during the onset of the pulse event. The pH remained in the 7.6 – 8.0 range for the remainder of the perturbation, but the response was complex as it was superimposed on diurnal changes (Figure 3.16E). Baseflow Cl concentrations were slightly more than 40 ppm, but gradually decreased to 10 ppm (Figure 3.16F). $\text{NH}_4^+\text{-N}$ remained relatively constant (about 0.2 ppm) throughout the perturbation, while $\text{NO}_3^-\text{-N}$ increased more than 1.5 ppm during the event (Figure 3.16G).

3.4.1.2.2. *Grand Glaize Creek*

Like Fox Creek, the May 2008 storm events resulted in several discharge perturbations at Grand Glaize Creek. However, the hydrographs for Grand Glaize Creek were markedly different from those for Fox Creek. Peak shapes were sharper and peak

discharge was more than 4 times that at Fox Creek when the basin area difference was taken into account. Baseflow was initially 0.42 cms, but increased to 3.5 cms at 9:20 following the 7:00 May 7 rainfall. The second discharge perturbation followed the 13:00 – 23:30 May 7 storm event, and resulted in a more complex discharge response than the one observed at Fox Creek. However, Grand Glaize Creek only had two distinct peaks during the complex event while Black Creek had three (see next section). The larger of these two peaks occurred at 16:10 on May 7 and was 22.0 cms. The largest event sampled during the study period had a peak discharge of 58.0 cms and occurred at 10:00 on May 8. There was no observed response to the 9:30 – 11:00 May 9 rainfall (Figure 3.16A).

A stream sample collected on May 7 at 8:40 had δD and $\delta^{18}O$ values of -33‰ and -5.2‰, respectively. Samples collected during the first small discharge event were depleted, but during the onset of the second complex discharge event there was isotopic enrichment. The most enriched Grand Glaize Creek sample, which was collected at peak discharge during the second event, reached a maximum value of -20‰ and -3.8‰ (Figure 3.16B). During the middle of this complex event, the isotopic composition of the rainfall changed, and the isotopic character of Grand Glaize Creek once again became depleted. The creek subsequently began to return to baseflow values, but there was a small isotopic enrichment in association with the third and largest event (Figure 3.16C).

SpC initially dropped from nearly 1,200 $\mu S/cm$ to 380 $\mu S/cm$ after peak discharge, reaching a minimum of 290 $\mu S/cm$ during the largest discharge event (Figure 3.16D). This SpC minimum approximately coincided with the maximum contribution of event water. The SpC recovered to 400 $\mu S/cm$, but the in situ monitoring data show that

complex SpC behavior occurred during the transition to lower values in response to the storm pulse. When transient minima such as these were observed, they were typically associated with changes in the slope of the event hydrograph. The initial downward trend occurred when the event water component began to crest and baseflow was still rising or was cresting at a slower rate. Transitions to lower values occurred when the baseflow component was declining relative to the event water component (Figure 3.16A, D).

Turbidity was initially < 2 NTU, but increased to almost 880 NTU on the rising limb of the first event, then dropped 50 NTU only to rise again to 437 NTU at the onset of the second flood pulse. The final turbidity value at the end of the monitoring period was 24 NTU (Figure 3.16D). The initial pH value was 7.5 but dropped slightly to 7.3 during the complex event. On the rising limb of the third event, the pH rose sharply by 0.4 units, then dropped by approximately the same amount at peak discharge (Figure 3.16E). The Cl level during baseflow was more than 160 ppm and its dilution during the flood pulse mirrored the pattern observed in the SpC (Figure 3.16D, F). Like Fox Creek, NH_4^+ -N concentrations remained steady during the monitoring period, but were generally about 0.3 ppm higher than those observed at Fox Creek (Figure 3.16G). However, the NO_3^- -N concentration was lower than the concentration at Fox Creek. NO_3^- -N diluted on the rising limb of the largest event, but increased to a maximum of 0.8 ppm during peak flow and the recession limb (Figure 3.16G).

3.4.1.2.3. Black Creek

The May 2008 rainfall events caused rapid flow variations at Black Creek, and unlike Fox Creek and Grand Glaize Creek, all of the rainfall events resulted in discharge perturbations. Baseflow was initially 0.03 cms, but increased to 3.8 cms at 7:30

following the rainfall at 7:00 on May 7. The second flood pulse occurred following the 13:00 – 23:30 May 7 storm event. These discharge variations were more complex than both Fox and Grand Glaize Creeks, with three distinct responses superimposed on each other (the largest of which occurred at 15:00 on May 7 and was 5.9 cms). The largest discharge perturbation that occurred during the sampling period had a peak discharge of 10.4 cms and took place at 8:00 on May 8. Finally, a small response was observed on May 9 at 11:00 associated with the 9:30 – 11:00 May 9 rainfall (Figure 3.16A). All of these events had considerably larger peak flows than Fox Creek despite the difference in basin area (e.g., the basin area of Fox Creek is 3-fold larger than the Black Creek basin).

Black Creek was by far the most isotopically variable of the three basins during these storm pulses. A sample collected prior to the flood on May 6 had δD and $\delta^{18}O$ values of -40‰ and -6.3‰. The samples collected on the rising limb of the first discharge response were depleted isotopically, the stream became increasingly enriched during the second event until it reached a maximum value of -11.5‰ and -3.0‰ (Figure 3.16B), which was very similar to the rainfall value of -9‰ and -2.3‰. Later, flood waters progressed toward the isotopic composition of the third increment of rain collected at St. Louis (-55‰ and -8.0‰; Table 3.2; Figure 3.16B). The last samples were collected on the rising limb of the largest discharge event and progressed toward the isotopic composition of the May 8 rain samples (Table 3.2; Figure 3.16B).

SpC was initially 1,550 $\mu S/cm$ during baseflow, but reached its lowest value of 250 $\mu S/cm$ toward the end of the second, complex discharge event. There was a slight recovery to 440 $\mu S/cm$ in the last sample collected during the monitoring period (Figure 3.16D). Turbidity was initially low (2 NTU), but increased rapidly to 649 NTU during

the rising limb of the first discharge event. It then dropped steadily until the next complex event, during which turbidity levels only rose to 398 NTU (Figure 3.16D). The pH dropped more than a full pH unit on the rising limb of the complex discharge event, but gradually returned to 7.2 (Figure 3.16E).

3.4.1.3. July 2008 Event: Fox and Black Creeks

A July 8 – 9 storm-driven pulse was sampled at both Fox and Black Creeks. The timing, intensity, and isotopic composition of the precipitation were variable between the two basins (Table 3.2), but the antecedent moisture conditions at the two sites were similar and the event followed a relatively dry period when there had been no precipitation in either basin since July 3, 2008. This discharge perturbation was unique because it was the only observed response at Fox Creek that had a higher storm flow component than baseflow component.

3.4.1.3.1. Fox Creek

There were two periods of rainfall on the Fox Creek basin, and no changes in discharge were observed after the first precipitation event in which 0.76 cm of rain was deposited. The second period of rainfall produced a 45-fold increase in flow, and peak discharge was 4.3 cms (Figure 3.17A). The isotopic composition of the rainfall was extremely depleted for a summer rainfall event (-80‰ and -11.3‰), while baseflow had typical isotopic values for regional waters in summer (-39‰ and -6.0‰). The maximum isotopic excursion observed during this event was -69‰ and -9.5‰. This event was unique for the Fox Creek watershed because it was the only observed discharge perturbation that resulted in a larger storm flow component than baseflow component. Baseflow comprised only 29% of the total discharge flow during the event. Furthermore,

45 minutes after peak discharge, storm flow reached a maximum of 92% of the total flow (Figure 3.17A). The isotopic character of the stream water reached almost pre-storm flow conditions by the end of the sampling period 2.3 days after peak discharge (Figure 3.17B).

The water temperature signal was complex, and as observed in the previously discussed events, was superimposed on diurnal oscillations. Following the onset of the discharge event, the temperature increased 0.4°C, then abruptly decreased 1°C (Figure 3.17C). The temperature increase corresponded to the slight change in slope on the rising limb of the discharge peak, and the decrease occurred concomitant with peak discharge. Baseflow SpC was 564 µS/cm and reached a transient minimum of 224 µS/cm, which occurred following the break in slope on the rising limb. SpC began to recover after this break, but then continued to drop and reached a minimum of 185 µS/cm, after which it returned to near baseflow conditions 3.4 days later (Figure 3.17D). Turbidity increased to 751 NTU prior to peak flow and returned to near-ambient conditions (9 NTU) nearly a day later (Figure 3.17D). The cause of anomalous turbidity spikes observed after the discharge event is uncertain. These peaks were not associated with any rainfall or discharge perturbations and could be the result of sensor malfunction. However, simultaneous increases in SpC, $\text{NH}_4^+\text{-N}$, $\text{NO}_3^-\text{-N}$, and Cl, were observed (Figure 3.17D, F), but there were no observed changes in water temperature, DO, or pH (Figure 3.17C, E). This indicates that neither a single probe nor an entire unit malfunction was likely. This anomaly was probably associated with macroorganisms activity around the sensors.

The DO and pH increased 20% and 0.2 units, respectively, on the rising limb of the storm flow event; however, these signals were superimposed on diurnal oscillations

(Figure 3.17E). Baseflow Cl concentration was approximately 35 ppm, but decreased to 12 ppm during the rising limb of the discharge event. Cl levels then recovered, but subsequently dropped to 11 ppm during the recessional limb and eventually recovered to pre-storm flow conditions 2.6 days later. NO_3^- -N and NH_4^+ -N showed the opposite behavior of Cl, and increased 0.6 ppm and 0.1 ppm during the discharge peak (Figure 3.17F).

3.4.1.3.2. *Black Creek*

There were three periods of rainfall on the Black Creek basin during this event rather than the two observed at Fox Creek (Table 3.2; Figure 3.17A). The first rainfall event was small (0.08 cm), but produced a 7-fold increase in discharge (Figure 3.17A). The two subsequent rainfall events were larger (0.76 and 0.71 cm) and the average isotopic composition of all the rainfall samples was -51‰ and -6.9‰ (Table 3.2; Figure 3.17A). The second rainfall event produced the largest discharge response at Black Creek, and flow was increased from 0.05 to 2.1 cms (Figure 3.17A). A sample of baseflow collected on July 6 had an isotopic composition of -25‰ and -4.4‰, and the maximum excursion from these baseflow values occurred during the recessional limb of the storm flow event and was -7.1‰ and -50‰ (Figure 3.17B).

A sharp change in temperature occurred on the rising limb of the first large storm-induced pulse. Temperature dropped nearly 2°C and made a sharp recovery of 1.5°C, but decreased subsequently as ambient air temperatures dropped during the night. During the second of the large discharge response, temperature again increased about 2°C, but the peak was broader and lasted for the majority of the discharge event (Figure 3.17C). Baseflow SpC was 800 $\mu\text{S}/\text{cm}$ and increased to 965 $\mu\text{S}/\text{cm}$ during a small discharge

perturbation at the beginning of the monitoring period. During the first large storm SpC decreased to a minimum of 427 $\mu\text{S}/\text{cm}$, and during the second large event SpC decreased to 308 $\mu\text{S}/\text{cm}$. It reached baseflow levels 3.4 days after attaining its minimum value (Figure 3.17D). The turbidity response was more subdued than in the Fox Creek basin, and the maximum turbidity (209 NTU) occurred during the first large event. The second large event reached a maximum of 87 NTU (Figure 3.17D). The baseflow pH at Black Creek was higher (8.8) and more variable than the pH observed at Fox Creek. During the rising limb of the first large discharge event, the pH increased sharply almost a full pH unit, reaching its maximum value at peak flow during the first event. During the second large discharge event, there was a small (0.15 unit) increase in the pH (Figure 3.17E).

3.4.1.4. September 2008 Event (Hurricane Gustav): Fox Creek

In September 2008, two exceptionally intense rainfall events occurred in Missouri as a result of Hurricanes Gustav and Ike. In less than a 24-hour period on September 4, 2008, Hurricane Gustav delivered precipitation totals of 9.37 cm at St. Louis, 9.80 cm at Ladue, 7.87 cm at Lambert – St. Louis Internal Airport (Figure 3.18-1; NOAA, 2011a) and 8.31 cm at Valley Park, MO (USGS, 2008).

Hurricane Gustav was succeeded by Hurricane Ike (September 14, 2008), which had slightly higher rainfall totals (11.63 cm at Lambert – St. Louis Internal Airport; NOAA, 2011a). However, due to rapid delivery of most of this precipitation in a 6-hour interval combined with the high antecedent moisture conditions, Hurricane Ike caused massive flash flooding throughout Missouri, killing four people and damaging homes, roads, and multiple USGS gaging stations. A discharge pulse caused by Hurricane Gustav was monitored at Fox Creek and is discussed in the following section, but

unfortunately, the larger response caused by Hurricane Ike was not monitored as it damaged the Washington University field equipment at both Fox and Black Creeks.

The maximum discharge during the Hurricane Gustav flooding event occurred approximately 13 hours after the rainfall event began and reached 24.6 cms (Figure 3.18-2A). The resulting hydrograph had two superimposed discharge peaks. The isotope values for baseflow were -37‰ and -6.0‰ (Figure 3.18-2B). There were two distinct enrichments peaks that coincided with the rising limb of the first discharge peak, and these excursions occurred after the first two increments of rain (Figure 3.18-2A, B). The first and larger peak reached a maximum enrichment of -32‰ and -5.3‰. As flow increased at Fox Creek, its isotopic composition became more depleted and reached values of -42‰ and -6.7‰ during peak flow (Figure 3.18-2B). Hydrograph separations show that during the event 59% of the discharge consisted of baseflow, and the lowest baseflow contribution (27%) was observed 1 hour after peak discharge (Figure 3.18-2A). The baseflow fraction preceded the storm flow fraction in both the first and second discharge peaks. Interestingly, the baseflow fraction in this event was 30% higher than the much smaller event that occurred in July 2008, despite the much larger precipitation volume (more than 8 times larger).

The water temperature was initially about 21°C, though a decreasing trend was apparent prior to the discharge perturbation. At the onset of the rising limb, the temperature dropped rapidly to 19.8°C and recovered to pre-flood conditions in 5 hours, after which it continued to decline (Figure 3.18-2C). Baseflow SpC was 611 $\mu\text{S}/\text{cm}$ and reached a minimum of 157 $\mu\text{S}/\text{cm}$, though the declining SpC trend was punctuated by five transient minima, all of which were associated with changes in rainfall intensity

(Figure 3.18-2D). The pre-storm flow turbidity level was 1 NTU and reached a maximum of 347 NTU on the rising limb of the event; though the turbidity peak was complex. A second turbidity peak reaching 157 NTU occurred on the rising limb of the second discharge peak (Figure 3.18-2D).

There were minor oscillations in the DO, pH, $\text{NH}_4^+\text{-N}$, and Cl data that are likely artifacts (Figure 3.18-2E, F). Still, general trends are observed in these data. Both DO and pH increased 10% and 0.3 units, respectively, during the flooding event (Figure 3.18-2E). Cl was diluted by 80% with the onset of event water in the system, while $\text{NH}_4^+\text{-N}$ increased 0.35 ppm in parallel with turbidity (Figure 3.18-2F).

3.4.1.5. April 2010 Event: RP1, RP2, and HMP

On April 2 – 3, 2010 a discharge event was simultaneously sampled in the Upper River des Peres watershed at RP1, RP2, and HMP. Antecedent moisture conditions were relatively high because of spring rains, with the most recent event prior to April 2 occurring on March 28 (0.69 cm of rain). Rain fell in two increments on the basin: 0.20 cm between 20:00 – 22:00 April 2 and 0.86 cm from 0:00 – 3:00 April 3. Separate rain samples were collected for isotopic analysis at St. Louis, MO (Table 3.2). The first rainfall event was isotopically enriched (-25‰ and -4.2‰), while the second event was depleted (-62‰ and -9.1‰). HMP generally showed the most subdued hydrologic and geochemical responses to the rainfall. At the Ruth Park sites, RP1 had a larger storm flow component than RP2. The discharge responses to the rainfall event are shown on the same scale in Figure 3.19 and the hydrologic, isotopic, and geochemical responses are shown in Figure 3.20.

3.4.1.5.1. Ruth Park, RP1

Following the first rainfall event, discharge at RP1 increased by 0.1 cms, but the response was broad and flattened, and did not have a typical hydrograph peak shape. The second increment of rainfall induced a more typical discharge peak with a maximum of 1.25 cms (Figures 3.19, 3.20A). The maximum isotopic enrichment (-32‰ and -4.4‰) occurred on the rising limb of the event and was similar to isotopic composition of the first rainfall (Figure 3.20B; Table 3.2). After the second rainfall event, the flood waters became depleted, reaching -59‰ and -9.0‰ (Figure 3.20B). A hydrograph separation indicates that the baseflow fraction was small and comprised only 9% of the total storm flow. After peak discharge, the baseflow component reached a minimum of 0% of the total discharge (Figure 3.20A).

The most obvious pattern in temperature was the diurnal oscillation of water temperature; however, superimposed on this signal were two small but sharp decreases in water temperature (Figure 3.20C). Baseflow SpC was elevated (1,693 $\mu\text{S}/\text{cm}$) compared to rural stream end-members. SpC reached a minimum of 214 $\mu\text{S}/\text{cm}$ during the recessional limb of the discharge event, 14 hours after it began to rain, and attenuated to near baseflow levels (1,676 $\mu\text{S}/\text{cm}$) 2.3 days after reaching its minimum value (Figure 3.20D). Two turbidity spikes were observed that coincided with the two rainfall pulses, having maximum values of 99 NTU and 163 NTU, respectively (Figure 3.20D).

The complex DO and pH patterns observed in the other basins were also seen at RP1, but despite these complications, two simultaneous peaks in both DO and pH were observed and correlate to increased discharge (Figure 3.20D, E). DO rose by almost 10%

for both perturbations, which likely was the result of more turbulent flow during the discharge (Figure 3.20E).

Major elements including Na, Cl, Ca, Mg, S, and Si, tended to decrease as discharge increased. The largest reductions in concentration were observed in Ca (81%), Na (91%), and Cl (89%). However, during the rising limb of the event, small increases in NH_4^+ -N, Na, Cl, Ca, Mg, S, and Si were observed. The concentration spikes in major elements were most easily observed in the continuous monitoring data for Cl (Figure 3.20F, G). Minor elements generally showed reductions in concentration as well, but Fe and Al exhibited more complex behavior. A transient minimum in Fe occurred on the rising limb of the discharge event. Fe reached its lowest value on the recessional limb, after which it slowly recovered. Al concentrations were initially low (2 ppb) but increased during the recessional limb of the event before returning to near ambient baseflow levels (Figure 3.20E).

3.4.1.5.2. Ruth Park, RP2

Discharge was not gauged at RP2, but given its proximity to the RP1 station, the RP1 discharge measurements are a close approximation (Figures 3.19, 3.20). The isotopic response at RP2 was similar to RP1, but was more dampened. On the rising limb of the event, the maximum isotopic enrichment observed at RP2 (-27‰ and -4.6‰), was almost the same as the response at RP1; however, the largest isotopic depletion observed at RP2 was only -57‰ and -8.4‰ (Figure 3.20B), and the isotope hydrograph separation indicated that there was a larger baseflow component (23%) in the downstream site. This is consistent with the natural channel between the RP1 and RP2 sites, which facilitates the displacement of groundwater into the stream channel.

The diurnal variations in temperature at RP2 were more pronounced than at RP1 (Figure 3.20C). This disparity resulted because a large pool (approximately 1 m in depth during normal flow conditions) formed at the RP1 site following attempts to dam the area around the culvert to reduce erosion during high flow events. However, because RP2 is not dammed, the water depth is significantly shallower, having a maximum depth of less than 0.25 m during normal flow conditions. Consequently, water temperatures at this site rapidly equilibrate with ambient air temperature, and temperature perturbations at RP2 during this event featured larger, broader peaks than at the RP1 site (Figure 3.20C). The SpC response at RP2 was more dampened than at RP1, and the baseflow SpC level was 1,517 $\mu\text{S}/\text{cm}$; almost 200 $\mu\text{S}/\text{cm}$ lower than RP1.

A SpC increase similar to the one observed at RP1 occurred on the rising limb of the event, but again, values were lower than at RP1 (1,710 $\mu\text{S}/\text{cm}$; 40 $\mu\text{S}/\text{cm}$ lower than RP1). SpC reached a minimum value of 265 $\mu\text{S}/\text{cm}$ (50 $\mu\text{S}/\text{cm}$ higher than RP1) on the recessional limb of the event. There were only three transient SpC minima during the smooth reduction of SpC toward its minimum value instead of five as observed at RP1 (Figure 3.20D). This is likely the result of the rapid delivery of event water in the upstream cement-lined channel. The first turbidity perturbation at RP2 was not fully captured by the continuous monitoring equipment due to instrument calibration, but laboratory measurements of turbidity indicate that the RP2 response was comparable to RP1. The maximum turbidity level during the first perturbation was 64 NTU. During the second event, the turbidity reached a maximum of 203 NTU (20% higher than the response at RP1; Figure 3.10D). Both DO and pH increased concomitantly during the

flood pulse, and as a result of turbulent flow, DO increased more than 30%. RP2 displayed larger, broader DO and pH peaks than RP1 (Figure 3.20E).

The major element concentrations and patterns at RP2 were similar to those at RP1. These elements initially increased during the “first flush” event, then subsequently diluted (Figure 3.20F, G). High resolution Cl data have a similar pattern to SpC, and both parameters exhibited concurrent transient minima. Likewise, minor elements generally experienced dilution, with the exception of Fe and Al, which both sharply increased on the recessional limb before returning to baseflow levels. The increases in Fe and Al did not coincide with the turbidity maximum as observed in other studies (e.g., Stueber and Criss, 2005), and therefore, it is unlikely that these elements are associated with small clay particles. The Fe and Al patterns could represent input from another water source, perhaps from the mulching facility or golf course nearby, but the runoff volume from the mulching operation is volumetrically insignificant. Moreover, runoff from both of these sources would be characterized by increased turbidity and nutrient concentration, which were not observed. The cause of this increase is more likely explained by the concomitant decrease in pH. The more acidic interflow waters likely leached these elements from the soil, but more work is needed to verify this relationship.

3.4.1.5.3. Heman Park, HMP

HMP had a similar but more subdued hydrologic and geochemical responses than both the Ruth Park sites, despite its larger maximum discharge (8.63 cms at HMP compared to 1.25 cms at Ruth Park). The catchment area is larger at HMP (Table 3.2) and includes contributions from the Upper River des Peres main stem and an unnamed tributary (Figure 3.3). HMP had the largest baseflow component of the three sites (62%

of the total discharge response and a minimum baseflow value of 17%; Figure 3.20A). Because of equipment malfunctions, temperature, SpC, turbidity, DO, Cl, and nutrient levels were not monitored continuously; however, SpC, turbidity, and Cl were measured in the lab. Isotopic response on the rising limb of the event reached a maximum enrichment of -43‰ and -6.8‰, and the maximum depletion (-56‰ and -8.5‰) was observed on the recessional limb (Figure 3.20B). SpC and turbidity responses were also dampened (Figure 3.20D). Baseflow SpC at HMP was 100 $\mu\text{S}/\text{cm}$ lower than RP2, and reached a minimum of 383 $\mu\text{S}/\text{cm}$ (Figure 3.20D). Unlike the Ruth Park sites, there was only one turbidity peak, which reached a maximum of 109 NTU (Figure 3.20D). Major element concentrations in baseflow were typically 10 – 25% lower than the Ruth Park sites, and 10 – 30% higher during peak flow (Figure 3.20F, G). Trace element concentrations were also much lower than the Ruth Park sites, with the exception of B and Li which were 35% and 20% higher, respectively (Figure 3.20H).

3.5. Discussion

3.5.1. Isotope Hydrology and Hydrograph Separation

Comparisons of nearly 80 flood responses using a suite of isotopic data from March 2008 to September 2010 clarify the relative contributions of baseflow and event water during rainfall-driven flood responses in urban and rural streams. Using the equations discussed in Chapter 2, stream isotopic values during flood pulses were used for hydrograph separations (see storm perturbation graphs in the Results sections, this chapter). The isotopic hydrograph separations reveal that baseflow discharge in all of the studied streams is derived from longer-term, shallow groundwaters, though groundwater inputs in the urban end-members are reduced. High flow conditions represent the

combined and rapid delivery of both baseflow and event water components. The event water mostly travels along transient shallow flowpaths and can constitute a significant portion of the total discharge during a storm pulse. Further, the event water proportion during flooding is enhanced dramatically with increased urban land use. The urban end-members that have the highest population densities and percentage of urban land cover in the watershed (Figures 3.6, 3.7) also have the highest storm flow component, and for precipitation events of 1.5 cm or greater, event water typically comprises > 60% of the total discharge in urban streams though it often approaches 100% of the discharge component near peak flow (Table 3.4). In contrast, for discharge perturbations in the rural Fox Creek, event water usually comprises about 35% of the total discharge; however, Fox Creek can reach more than 90% event water at peak discharge (Table 3.4).

Isotope hydrograph separations show that baseflow and event flow components exhibit characteristics common to the overall discharge hydrograph shape, including the slopes of rising and recessional limbs as well as the peak shape. Baseflow and event flow hydrographs generally rise together, but either baseflow or event water may dominate the total discharge signal. In some cases, the slopes of individual discharge curves exhibit subtle differences due to changes in the proportion of the flow components. Urban end-members typically have a higher storm flow component, which tends to be delivered on the rising limb before the baseflow component. Rural end-members generally have higher baseflow components, and unlike urban systems, the delivery of this component dominates the rising limb because of higher infiltration rates that hydraulically force baseflow into the streams (Table 3.4). However, even natural systems can be overwhelmed by storm water when antecedent moisture conditions or rainfall intensity

are high or basin slopes are steep. Moreover, though the Fox Creek watershed features minor urban development and is heavily forested today (thus, representing the “rural” end-member), it has undergone significant modification through the last two centuries, including clear cutting and farming activities. These practices alter basin soils and infiltration rates, and based on the relatively short average lag time for Fox Creek (less than 90 minutes, see subsequent sections) compared to lag times observed in Pennsylvania streams by Sheeder et al. (2002), the watershed likely has not recovered from historical activities.

Other factors besides land use, including the rainfall amount and intensity, antecedent moisture conditions, and input of exotic waters (CSOs, SSOs, and interbasin transfers in urban systems), influence the hydrologic and geochemical response of these watersheds. Rainfall events as small as 0.05 cm and with an intensity of 0.02 cm/hour can trigger discharge responses in developed areas such as Black Creek, the Southwest Branch of the Upper River des Peres, and the Upper River des Peres. In contrast, in the rural Fox Creek watershed, rainfall events as large as 0.8 cm and with an intensity of nearly 0.4 cm/hour may cause no discharge response. Pre-event rainfall that occurs closer to the storm pulse has a greater impact on the hydrologic response than older storms, and this result was extensively documented for a karst spring near St. Louis (Winston, 2001).

3.5.2. Geochemical Response during Storm Perturbations

The precise response of the chemograph during a given storm event varies from storm to storm as a result of many controlling factors (Miller and Drever, 1977). These

geochemical perturbations are discussed in detail for SpC, turbidity, and major and trace elements in the flowing sections.

3.5.2.1. SpC and Major Elements

The form and timing of the SpC response are affected by concentration differences in the chemical constituents of surface and subsurface flow components, and by the timing of the delivery of these contributions (Anderson and Burt, 1982). Water may also flow by different routes through the soil during different phases of a storm event, and therefore, will have differential access to exchangeable or soluble material that may be distributed unevenly through the soil (Spraggs, 1976).

Despite these complications, SpC generally exhibits the same timing as isotopic perturbations during discharge events. This correlation indicates that fluctuations in SpC can be used as a proxy for event water contributions under certain circumstances. Hydrograph separations using SpC demonstrate similar trends in baseflow and storm flow contributions to isotope hydrograph separations (see Figure 3.21). However, because ions can be added to dilute rainfall from throughfall, the ground surface, and the shallow subsurface, it is difficult to estimate the effective SpC of the “event water.” As a consequence, if the SpC of the event water is underestimated, the volumetric importance of that component will likewise be underestimated and vice versa. Additionally, the isotopic composition of the streams usually returns to normal levels prior to the recovery of SpC, suggesting more complex processes are occurring than simple mixing.

In natural systems, the SpC level in the baseflow is the product of water-rock and water-soil interactions and remains relatively stable over time, except for seasonal variations which are discussed later (see 3.5.3. Seasonal Variations section). In detail,

SpC fluctuates during storm events due to the influences of different source waters and transport processes. At the beginning of a discharge event, the response of the SpC is delayed due to the separate transport mechanisms at work for each flow component. Stream discharge increases rapidly due to hydraulic forcing, but SpC responds more slowly since this flow is initially dominated by displaced pre-event water that has been in contact with the host rock and soils long enough to attain the background SpC level. In some cases there is a sharp, transient SpC increase or spike at the onset of a discharge pulse that is seasonally related (see 3.5.2.1.1. Small-Scale SpC Features and 3.5.3. Seasonal Variations sections).

Coinciding with the rising limb of most discharge hydrographs, SpC undergoes a significant reduction, commonly more than 50% in rural streams and up to 95% in urban streams, that usually precedes the discharge peak and marks the arrival of the event water in the stream. Minimum SpC invariably follows the discharge maximum in rural streams like Fox Creek, typically by more than 60 minutes and roughly corresponds to the point where the volumetric event water contribution reaches a fractional maximum relative to the baseflow component. However, in urban environments minimum SpC follows the discharge peak typically by only 30 minutes, and in some cases it can be concurrent with peak discharge. Recovery to the initial SpC value occurs slowly, and usually lags behind the loss of the event water component indicating the variable nature of baseflow SpC.

3.5.2.1.1. Small-Scale SpC Features

During the onset of a pulse event, SpC can exhibit complex behavior including significant positive or negative fluctuations, and these small increases and decreases in SpC are superimposed on the general dilution curve associated with discharge events.

Commonly, “first flush” events, in which the concentrations of major elements temporally increase, proceed the onset of the general discharge trend. These events are often succeeded by small decreases in SpC during the general dilution trend and have been observed elsewhere (Winston, 2001).

3.5.2.1.1.1. First Flush Events

The major ions, including Na and Cl present in winter road salt, are major components of the characteristic “first flush” concentration spike that often occurs on the rising limb of the springtime discharge pulse. This “flushing” effect, whereby soluble material is accumulated during the pre-storm period and then transported into the stream during the beginning period of the storm, has been noted in many other rivers, streams, and springs (Hendrickson and Krieger, 1960; Edwards, 1973; Walling and Foster, 1975; Winston, 2001). Many events discussed in this study, including the July 2008 and April 2010 events (Figures 3.17, 3.20), provide typical examples of this type of spike. The rising limb of the discharge hydrograph is accompanied by a sharp (about 50 ppm), transient increase in Cl that corresponds to increased SpC. This flushing effect begins upon the arrival of the event water, and is expectedly associated with higher Na concentrations.

Other major element data for the April 2010 storm indicate that the concentrations of other elements are also temporally increased during these flushing spikes, including Ca, Mg, S, and Si species. These concentration spikes are a result of event water and displaced baseflow rapidly mobilizing ions from the ground surface and soils. Other studies have noted that during the first flush high levels of pollutants are discharged into the receiving waters (Lee and Bang, 2000). In areas with significant urban land use,

storm water runoff has been identified as one of the leading causes of degradation in the quality of receiving waters during the first flush. The concentration peak may vary for different pollutants during the same storm event and for the same watershed during different storm events, a phenomenon observed elsewhere (Gupta and Saul, 1996; Lee et al., 2002). However, because it was not possible to measure many of the major element concentrations on a continuous basis, detailed information about their behavior is not available. The magnitude of the flushing event can vary, but exhibits seasonal dependence (Figure 3.22), with larger spikes occurring during the early spring. This is contrary to previous studies that have observed the largest and most prominent first flush spikes following dry basin conditions in urban areas (Klein, 1981; Kang et al., 2009).

3.5.2.1.1.2. Transient SpC Minima

All of the observed pulses in all the basins showed a transient minimum in SpC during the smooth reduction of SpC toward the minimum value (i.e., small decreases followed by recoveries in SpC superimposed on the larger dilution trend), and these minima always accompany a change in the slope of the event water component. The change in SpC is caused by the different contributions of the individual flow components, and is observed when the event water contribution begins to increase relative to the baseflow component. The reversal of the downward trend in SpC takes place when the event water component begins to crest and baseflow is still rising or is cresting at a slower rate. The reduction in SpC resumes when the baseflow component undergoes a rate change and begins to decline more rapidly than the event water component. A notable example of this occurred during the July 2008 storm event at Fox and Black Creeks (Figure 3.17).

3.5.2.2. Turbidity

The average TSS load during both low and high flow conditions is a significant measure of the physical and aesthetic degradation of watersheds as well as a good indicator of other pollutants, particularly nutrients and metals that are carried on the surfaces of sediment in suspension. The delivery of suspended solids during discharge events is generally more rapid than the variations observed in the isotopic and SpC data. Rainfall events rapidly wash particles and debris into streams, but these sources are quickly exhausted, resulting in decreased turbidity at the onset of peak flow. Moreover, turbidity levels can fluctuate during a discharge perturbation as result of changes in the rainfall intensity.

On the rising limb of most discharge pulses suspended loads increase by up to four orders of magnitude. Suspended loads in urban streams are further augmented by soil erosion and street runoff, and TSS loads in these streams can dwarf these loads in rural streams because of enhanced runoff, a phenomenon that was also observed by Brezonik and Stadelmann (2002). In urban environments, turbidity levels are often 5 to 10-fold larger than their rural counterparts for the same storm. Further, the onset of the turbidity peak is usually shortened in urban streams and is commonly 15 to 30 minutes earlier than turbidity peaks in rural settings.

3.5.2.3. Elements Positively Correlated with Discharge: Fe and Al

Ion exchange can regulate the transport of specific ions in floodwaters, and is therefore crucial in determining the fate of heavy metals or other chemical pollutants. Cation exchange, in which one ion is replaced for another on a solid surface, occurs during rainfall events when the water composition of the soil column is changed. This

results in both the readjustment of the starting water composition and the ion exchangers in the soil. The process can significantly alter the water chemistry throughout a flood cycle in a process known as ion-chromatography (Appelo and Postma, 2007).

During the April 2010 storm perturbation, Fe and Al concentrations at RP2 increased during the falling limb of the discharge pulse, which was likely the result of cation exchange processes in the basin soils. There have been several instances of observed increases of cation concentration in floodwaters due to cation exchange. Shand et al. (2005) observed a positive correlation between pH and Al during high flow for river waters, where proton exchange may have been responsible for the mobilization of Al. However, other elements in the Shand et al. (2005) study were observed to decrease significantly with flow, including: Na, Cl, Ca, Mg, SO_4^{2-} , Cu, Ni, and Sr. Winston and Criss (2004) observed that Fe, Al, B, Cu, and Pb were positively correlated with spring discharge while overall SpC of the floodwaters decreased.

3.5.3. Seasonal Variations

Continuous monitoring data provide a robust means to analyze seasonal variations in watersheds and document substantial differences in the character of various basins. Seasonal oscillations in temperature, SpC, DO, pH, and Cl are shown in Figures 3.22 and 3.23. There are some gaps in the data due to equipment malfunctions or to issues such as siltation, which can erode the DO membrane and cause low pH due to anoxia, for example. In the case of the River des Peres at Morgan Ford Rd., continuous monitoring data for April through June of 2008 are not included in this study because of back flooding from the Mississippi River at this site.

In the three larger watersheds (Fox Creek, Grand Glaize Creek, and the River des Peres at Morgan), as air temperatures decreased in the winter months, predictably water temperatures decreased as well (Figure 3.22A). However, Fox Creek experienced dampened seasonal and diurnal temperature changes, while River des Peres had the most extreme temperature changes and often changed by $> 5^{\circ}\text{C}$ per day. Moreover, Fox Creek never reached freezing temperatures due to groundwater input into the stream, which is reflected in the seasonal isotope data (discussed below; Figure 3.24), and the storm pulse hydrograph separations. The coldest temperature measured at Fox Creek (1.3°C) occurred on February 21, 2008 after a prolonged cold period when the average air temperature had been -5°C during the preceding week. Grand Glaize Creek exhibited larger temperature extremes than Fox Creek, and reached 0°C several times during the winter. Moreover, water temperatures at Grand Glaize Creek were on average 2.5°C higher than Fox Creek during the spring of 2008. River des Peres maintained 0°C temperatures for most of January and February of 2008, and, as previously mentioned, it had the largest daily temperature variations. Further, thicker ice and persistent ice cover were observed in the field at the Grand Glaize Creek and River des Peres sites.

For much of the winter, the three Upper River des Peres monitoring sites experienced sustained ice cover, and to prevent damage the continuous monitoring, devices were not deployed during this time. Temperature measurements collected during the spring and summer show that HMP had the least variable daily temperature changes, followed by RP1, then RP2 (Figure 3.23A). In general, the water temperature at RP1 was lower, and is a result of a small dammed area below the McKnight Rd. culvert. RP2 was most variable because it had the shallowest water depth.

Lower DO was observed at all the sites in the late summer and early fall, due to decreased discharge (Balls et al., 1996) and increased organic loads from algal blooms and leaf litter (Figures 3.22B, 3.23B). At all of the River des Peres monitoring sites, DO oscillated almost 100% during warmer periods (Figures 3.22B, 3.23B) when photosynthetic algae were most active. These oscillations were less pronounced at Fox Creek, and commonly varied less than 30% (Figure 3.22B). The Upper River des Peres experienced the most anoxic conditions, and low DO was commonly observed at night (Figures 3.22B, 3.23B).

Oscillations in pH also tended to be larger in the summer months for the same reason that oscillations were observed in the DO signal. The pH was largely circum neutral for all the sampling locations, but Fox and Grand Glaize Creeks had more dampened responses than the River des Peres sites, which exhibited large pH increases of up to 3.5 units (reaching maximum values of 11) associated with surface runoff events (Figures 3.22C, 3.23C). Grand Glaize Creek and River des Peres had higher average pH (7.6 and 7.7, respectively) than Fox Creek (7.0). RP1 had the highest average pH of the sites in the Upper River des Peres (7.6), followed by HMP (7.3), and RP2 (7.1).

Springtime is normally characterized by high precipitation in this region, and average monthly rainfall in May and June is approximately 10.2 cm. Springtime discharge pulses typically have higher peaks and as a result of the increased discharge these pulses exhibit larger geochemical variations than those in the late summer and fall. For instance, SpC can change substantially as Na and Cl accumulated during winter road salt applications are flushed from roads, soil, and shallow groundwater reservoirs (Figures 3.22D, E). SpC is strongly correlated to Na and Cl concentrations in urban and

impacted environments, and they are often the prevailing ions in these systems, in contrast to natural carbonate hosted systems dominated by Ca, Mg, and HCO_3^- ions.

The simple average of SpC observed by the continuous monitoring is 670 $\mu\text{S}/\text{cm}$ at Fox Creek, 1,350 $\mu\text{S}/\text{cm}$ at Grand Glaize Creek, and 1,230 $\mu\text{S}/\text{cm}$ at the River des Peres. Continuous measurements for the Upper River des Peres sites had lower averages than the grab samples because continuous monitoring took place primarily in the summer months while grab samples were collected year round. The simple averages of SpC for grab samples are 1,431 $\mu\text{S}/\text{cm}$, 1,319 $\mu\text{S}/\text{cm}$, and 1,180 $\mu\text{S}/\text{cm}$ at RP1, RP2, and HMP, respectively. Snow melt runoff measurements corroborate the conclusion that road salt is the dominant contributor of Na and Cl to these systems, as melt runoff can have SpC levels exceeding 36,000 $\mu\text{S}/\text{cm}$ and Cl levels of almost 14,000 ppm. Contamination from road salt applications persisted throughout the year in baseflow because of contamination of the shallow groundwater. Thus, there was elevated background SpC during the summer months long after road salt application (Figures 3.22D, E; 3.23D, E).

Surprisingly, Cl spikes due to winter road salting were the highest at Grand Glaize Creek. As mentioned before, Grand Glaize Creek was on the Missouri 303d list for Cl contamination (MoDNR, 2011b). Differences between Grand Glaize Creek and the River des Peres may be a result of different road salting practices in Valley Park and St. Louis, respectively, but other studies have found that SpC levels in the River des Peres can reach 10,000 $\mu\text{S}/\text{cm}$ (Shock et al., 2003), nearly 3,000 $\mu\text{S}/\text{cm}$ higher than those observed in this study. Determining the exact salt application rates in these watersheds is extremely difficult because of number of municipalities involved and lack of well-

maintained salting records. Cl spikes at Fox Creek were more subdued, but the stream waters still exceeded the acute Cl contamination levels on four occasions (Figure 3.22E).

Because the continuous monitoring devices could not be deployed in the winter time at the Upper River des Peres sites, Cl road salt spikes were not recorded (Figure 3.23E). Grab samples indicate that winter Cl levels were frequently high at these sites and reached 1,400 ppm; however, the winter data collected at Fox Creek, Grand Glaize Creek, and the River des Peres indicate that peak Cl levels are likely much higher. The Cl concentrations in the Upper River des Peres remained above regulatory limits for chronic Cl contamination (230 ppm) even in the spring and summer months, and on several occasions exceeds the acute Cl contamination level (860 ppm), which indicates extensive Cl contamination of the shallow groundwater (Figure 3.23E).

Isotope data further establish that less urbanized streams have more dampened seasonal responses. Figure 3.24A, B shows isotope data from bi-weekly grab sampling for all the monitored sites. Fox Creek exhibited the smallest variations in isotopic values, and all of the sites in the River des Peres watershed showed more isotopic variability. In Figure 3.24C, the standard deviation of temperature has been plotted against the standard deviation of $\delta^{18}\text{O}$, and illustrates that the less urbanized end-members tend to be less seasonally variable. One exception is RP1, which has less variable water temperatures, a result of the deep pool at the site.

3.5.4. Diurnal Variations

In addition to providing insight into seasonal variations, the continuous monitoring data have revealed greater detail regarding the day to day behavior of these streams. The data indicate there are significant diurnal oscillations in water temperature

as a result of the daily fluctuations in air temperature from solar heating. Other constituents fluctuate as well, including:

- 1) the pH, which increases as a result of the removal of dissolved CO₂ in the water by photosynthetic algal growth during the hours of maximum solar radiance. Stream water becomes more acidic at night when photosynthetic activities stop and the production of CO₂ from respiration becomes dominant;
- 2) the DO, which changes for the same reason as pH, whereby DO increases during the day due to photosynthetic processes and then decreases at night when these biologic pathways are inactive;
- 3) the N-species, which decrease during the day due to biological use;
- 4) and the SpC and Cl increase slightly during the day because of higher evaporations rates, a result corroborated by small, daily variations in discharge, where discharge decreases during the day.

All of these effects are most pronounced in the summer months when evaporation rates and biological activity are highest.

3.5.5. Water Quality Differences in Natural and Artificial Channels

The examination of the proximal Ruth Park sites (RP1 and RP2), which are located less than 320 m apart, reveals that stream channel form can appreciably control baseflow contributions and geochemistry. The Southwest Branch of the Upper River des Peres is almost entirely channelized upstream of the RP1 site; however, between the RP1 and RP2 sites a more natural channel is present in a wooded area (Figure 3.25). The April 2010 storm pulse data exemplify the importance of these differences between the two sites. The baseflow component at RP2 is enhanced by almost 15% (Figure 3.20), and

additional hydrograph separations indicate this is a typical result (Table 3.4). Further, the concentrations of $\text{NH}_4^+\text{-N}$, $\text{NO}_3^-\text{-N}$, total PO_4^{3-} , Cl, and *Escherichia coli* (*E. coli*) are reduced in the short length of natural channel between the two sites (Tables 3.5, 3.6). Turbidity and DO are the only parameters that are adversely affected at the downstream site. The turbidity at RP1 is anomalously low because the upstream channel is concrete-lined and the presence of a plunge pool allows settling of suspended particles at this site (the site has been artificially dammed to help mitigate erosion; Figure 3.25). Increased turbidity at the RP2 site is likely a result of the erosive force of water leaving the artificial channel and entering the natural, sediment-walled channel downstream. Grab sample data indicate higher DO at RP2, but continuous monitoring data indicated that DO is lower at this site than RP1.

3.5.6. Load Estimates

Analysis of chemograph response to discharge perturbations is limited when only autosampling devices are used, and the detailed continuous monitoring datasets have resolved storm perturbation response behavior at these sites. As mentioned earlier, these devices resolve peak shapes for first flushing events for SpC and Cl. Further, these data show significant changes in temperature (which may increase or decrease depending on the temperature of the storm water), DO (generally increases due to increased turbulence), and pH (typically increases and often shows complex responses). Moreover, temperature, DO, and pH cannot be measured accurately on samples collected by the automated samplers if sample recovery is not immediate because these values change rapidly. The concentration of N-species can either increase or decrease during storm

perturbations, depending on relevant pre-storm basin conditions that may include fertilizer applications, antecedent rainfall, and time of year.

Further, when continuous monitoring datasets are compared to those from infrequent sampling regimes, it is clear that many parameters are significantly under- or overestimated by the infrequent sampling regimes. Using discharge data from either proximal USGS gaging stations or stage data from this study, loads were calculated for water quality parameters using the continuous monitoring devices and grab samples (see Table 3.5). Load estimations are based on discharge-weighted averages for each parameter using the following relationship:

$$\left(\frac{\sum Q \cdot m \cdot t}{\sum t} \right)$$

where Q is discharge (cms), m is the water quality parameter of interest (the unit depending on the parameter), and t is the time interval between samples (days, i.e., 0.00347 days for 5 minute data intervals). Simple averages of the same parameters are given in Table 3.6.

TSS loads are almost always overestimated by grab sampling, and at the River des Peres Morgan Ford Rd. site, the grab sample TSS load estimate is overestimated by up to almost 90% (Tables 3.5, 3.6). This is surprising because one might expect that the rapid transfer of suspended solids during storm flow would increase the average turbidity determined by the continuous monitoring devices. Lab and field turbidity measurements show that sensor calibration is not the reason for this disparity (see section 3.4.1. Response to Storm Perturbation), and thus, the averages are likely skewed because of infrequent sampling. On a few occasions sampling regimes were modified to recover samples and to operate and maintain ISCO autosamplers during flooding events; thus,

these “grab” samples overestimate the TSS loads of the preceding two weeks. It should be noted that turbidity measurements made by both handheld and continuous monitoring devices represent minimum sediment loads, since these methods only measure suspended particles and do not take wash or bed loads into account.

DO averages are also somewhat overestimated by grab sampling regimes (by up to 5-fold; Tables 3.5, 3.6), a result that is almost certainly due to the fact that all grab samples are collected during the day when photosynthetic oxygen production is at its highest. In contrast, Cl concentrations are underestimated by grab sampling regimes typically by 50% because large Cl pulses from road salting are missed when streams are sampled arbitrarily and infrequently (Tables 3.5, 3.6). NO_3^- -N estimated loads are underestimated and NH_4^+ -N loads are overestimated by grab sampling (Tables 3.5, 3.6). These differences are likely a result of both the diurnal cycling of these species as well as their rapid and variable concentration changes during high flow conditions.

3.5.7. Theoretical Hydrograph Models

In order to quantify the physical response of each watershed and subwatershed, a theoretical hydrograph based on the Darcy’s law and the diffusion equation (Criss, 1997; Criss and Winston, 2003; 2008a,b) was used. Discharge hydrograph models were made for the May 2008 event at Fox, Grand Glaize, and Black Creeks (Figure 3.26) and the April 2010 event at RP1 and HMP (Figure 3.27). The rainfall-driven model uses evapotranspiration rates measured by Van Bavel (1961) and fitted with a bell curve by Criss and Winston (2008a). The model accurately predicts the flow variations of these basins and shows that the basin time constant (b) varies depending on the level of development in the basin. Fox Creek’s discharge responses are characterized by the

longest response time of all the basins and lower peak discharges and slower rising and falling limbs. This is quantified by its b value (0.09) and the corresponding theoretical lag time (~ 85 minutes; Table 3.7). The suburban (e.g., Grand Glaize Creek) and urban end-members (e.g., Black Creek, RP1, and HMP) show little variation in b (e.g., 0.02 to 0.03, respectively), and the theoretical lag time for all these sites ranges from 20 to 30 minutes. This result indicates that the hydrologic response of all these creeks is impacted, and these basins exhibit rapidly changing hydrographs with higher peak flows.

Model fits of b for other discharge events at these sites (not shown in Table 3.7) indicate that b values vary between events for all the basins. For instance, b was equal to 0.045 for Fox Creek during a larger discharge event in March of 2008, which had a peak flow of 40 cms. This may indicate that despite being relatively undeveloped compared to the other sites, Fox Creek is somewhat impacted, so the basin's infiltration capacity can be overwhelmed during large rainfall events. Other factors besides urbanization may affect b values including basin size, slope, and shape and soil type. Winston and Criss (2004) observed that antecedent moisture conditions caused variations in b . Further modeling is needed to completely characterize the ranges of b values for each of these sites.

Additionally, the theoretical model assumes that watershed response to precipitation in many small humid basins is dominated by, or mimics, diffusive processes. As rainfall infiltrates the soil, it causes an increase in head that is hydraulically transmitted through the phreatic zone, causing a rise in discharge at the basin outlet. It presumes that this process can be approximated using diffusion theory and Darcy's law, and it does not consider channel transport. As a consequence, the

model does not fit data for the urban basin end-members as well as the rural end-members because of the larger event water component in these systems (see Figure 3.27).

3.5.8. *Observed Hysteresis Behaviors*

Previous studies have established that large chemical and isotopic variations in streams accompany variations in discharge (e.g., Hendrickson and Kreiger, 1960). An even more surprising finding is that the correlations between ion concentrations and discharge rarely define simple linear or curvilinear responses (Miller and Drever, 1977; Walling and Webb, 1986). Rather, hysteresis loops are commonly found where the correlated variables follow cyclic paths; for example, between concentration and discharge. In particular, at the same discharge rate, the concentrations of dissolved ions may differ between the rising and falling limbs (Hendrickson and Kreiger, 1964; Toler, 1965; Miller and Drever, 1977; Walling and Webb, 1986; Evans and Davies, 1998). Similar hysteresis loops have been observed for many different parameters including SpC, turbidity, and particular dissolved cations and anions (Hendrickson and Kreiger, 1964; Porter, 1975; Miller and Drever, 1977; Walling and Webb, 1986; House and Warwick, 1998; Evans and Davies, 1998; Criss et al., 2007; this study).

A wide range of causes, even numerous causes for a given stream, has been proposed to account for the hysteresis phenomenon. Miller and Drever (1977) suggested that the hysteresis loops produced in a storm event in the North Fork of the Shoshone River, Wyoming, are a result of solution of material in the soil zone, dilution of baseflow, selective weathering of ferromagnesium minerals, and leaching of biological materials. Total and individual solute concentrations are commonly higher during the rising limb

compared to the falling limb, which they suggest represents flushing out of soluble material that has accumulated from weathering or farm activity prior to the storm.

In contrast, Walling and Webb (1986) suggest that hysteretic behavior may result from differences in the relative timing of chemographs and hydrographs or the relative form of the solute and discharge responses. Several factors may influence the form or timing of flood chemographs, which subsequently generate hysteresis loops when these parameters are plotted against one another. Further, the form and timing of solute response may also be affected by contrasts in the chemical concentration of surface and subsurface flow components and by the timing of delivery of these contributions (Anderson and Burt, 1982). Water may flow by different routes through the soil during different phases of a storm event, and will have differential access to soluble material which may be distributed unevenly through the soil (Spraggs, 1976). Basin size may also contribute to hysteretic effects due to tributary effects or geological heterogeneities (Hendrickson and Krieger, 1960). In large river systems, the contributions of individual tributaries can significantly affect the form and timing of solute response downstream (Walling and Webb, 1980). In addition to storm period fluctuations, solute levels may also respond to variations in discharge and to other controlling factors over a variety of other time scales. For instance, diurnal oscillations have been reported for total and individual solute concentrations (Sharp, 1969; this study), and annual patterns of solute behavior have also been identified for many rivers (Feller and Kimmins, 1979; Houston and Brooker, 1981; this study).

Lastly, it has been proposed that hysteretic effects may be due to a third mixing component and that traditional, two-component mixing models that only consider

baseflow and precipitation are almost always inaccurate (Kennedy et al., 1986; DeWalle et al., 1988; Lee and Krothe, 2001). The importance of soil water to stream flow has been known for some time, and in locations where water from soils makes a significant chemically and/or isotopically distinct contribution to runoff, a third mixing component may need to be considered (Kennedy et al., 1986). Evaporated soil waters can be significantly enriched in D and ^{18}O (by up to 70‰ for δD and 16‰ for $\delta^{18}\text{O}$) in the first tens of centimeters below the surface (Zimmermann et al., 1967; Barnes and Allison, 1983; Allison et al., 1983). Further, soils also contain large volumes of soluble material that can be observed in discharge events (Miller and Drever, 1977). These soil waters may be sufficiently voluminous and isotopically distinct to be recognized in flood hydrographs (DeWalle et al., 1988; Lakey and Krothe, 1996). Other mixing components may include combined sewer overflows (CSOs) and sanitary sewer overflows (SSOs) in more urbanized watersheds, assuming the municipal water source is isotopically distinct from the watershed of interest (Kracht, 2007). These sources may also be detected by increases in *E. coli* and total coliform bacteria as well as industrial and household chemicals. Additionally, detention basins used for flood mitigation may also be a source of isotopically distinct waters due to evaporation.

Hysteresis loops analogous to those described above have been observed in the δD and $\delta^{18}\text{O}$ isotopic responses of discharge events in the Orangeville Rise, a karst spring in southern Indiana (Lakey and Krothe, 1996) as well as Black Creek (this study). The hysteresis loops observed by Lakey and Krothe (1996) show both a complex evolution of flood waters that are above the MWL as well as a simple loop pattern below the MWL (Figure 3.28A, B). Their suggested explanation is that the isotopic shifts to the left of

MWL observed in an October 1990 discharge event after drought conditions are due to inputs of soil and epikarst water, while shifts to the right of the MWL observed in an April 1991 flood after a period of high recharge are due to water from vadose zone storage. However, they do not suggest a mechanism by which this process occurs.

3.5.8.1. Proposed Hysteresis Explanations

The Criss and Winston quantitative hydrograph model has shown that different watersheds have self-similar hydrographs but different time constants (Winston and Criss, 2004). Hysteretic effects can be explained by this model in terms of the different time constants for the various parameters. For instance, if two parameters have different b values for the same causal storm event, when these parameters are plotted against one another they generate hysteretic behavior (Figure 3.29A). Hysteretic behavior may also be a result of three or more mixing components. If the relative proportions of any of these three end members vary, a loop (or other distinct path) will plot within the area bounded by the tie lines of the three components (Figure 3.29B).

Hysteretic effects in δD and $\delta^{18}O$ plots were minor with the exception of the March 26, 2008, event at Black Creek. The δD and $\delta^{18}O$ mixing was typically centered on or above the MWL. Hysteresis loops completely below the MWL were not seen in this study, unlike those observed by Lakey and Krothe (1996). Additionally, the width of the loops, the rotation sense, and position relative to the MWL varied for a given storm or hydrologic feature. The width of the hysteresis loops does not appear to be correlated to the amount of rainfall in the weeks preceding the sampled discharge event. Hysteresis is commonly observed when SpC or turbidity is plotted against $\delta^{18}O$, but not always (Criss et al., 2007). The pH did not have as pronounced hysteretic effects as SpC and turbidity,

which is likely due to the small variations in pH during these events. Chemical hysteresis is likely a result of differences in response timing between chemical parameters and $\delta^{18}\text{O}$ and has been studied extensively in this region (Criss and Winston, 2003; Winston and Criss, 2004).

There are several well-documented cases of waters with isotopic compositions that plot above the MWL: (1) deep saline brines of the Canadian Shield (Frape et al., 1984), (2) pore waters in sediments of the oceanic crust (Lawrence and Gieskes, 1981), and (3) landfill leachates (Baedecker and Back, 1979). While these sources are not present in the watersheds in this study, a similar process to the ^{18}O depletion seen in pore waters may occur in the carbonate host rock. Sedimentary pore waters are depleted in ^{18}O relative to the MWL when low-temperature exchange between the water and rocks has occurred. This exchange process may occur in the studied watersheds and reservoirs of ^{18}O -depleted water may be large enough at certain times to be eluted from the epikarst into the streams.

3.6. Conclusions

The study improves understanding of the natural processes that govern hydrologic behaviors at the watershed scale using a successful theoretical model (Criss and Winston, 2003) to simulate the response of these systems and to predict their behavior in future situations. The hydrologic, isotopic, and geochemical responses of several streams with differing land use have been examined during low and high flow conditions to characterize response timing, season and diurnal patterns, pollutant loads, and hysteretic effects in these features. Observations of linked geochemical behaviors during the study period have furthered understanding of transport processes in urban environments. Storm

events cause rapid discharge and geochemical variations in streams, and particularly in urban streams, and these variations are well simulated by the Criss and Winston theoretical hydrograph.

The outcome of the field investigations in both rural and urban watersheds has provided a unique dataset that helps address and quantify several significant, fundamental questions about the effect of land use on stream hydrologic and geochemical response. Dynamic response to precipitation events includes significant increases in discharge, reductions in SpC and major element concentrations, increases in turbidity, and variable patterns in nutrients and minor elements. Urban stream hydrographs are characterized by sharp rising limbs (i.e., lag times of less than 25 minutes), increased peak flows (by nearly an order of magnitude), shortened recession rates (often by several days), and dramatically reduced baseflow fractions compared to their rural counterparts. In rural systems, the initial discharge pulse consists of baseflow that has been hydraulically displaced through the phreatic zone, while the event water is physically delivered through surface runoff or the vadose zone.

The isotopically-identified baseflow fraction varies during individual storms, differs from storm to storm, and differs from urban to suburban to woodland settings. During individual storms, baseflow is commonly the dominant end-member in rural systems, and the largest relative contribution of baseflow is observed during the rising limb as stream discharge increases rapidly due to hydraulic forcing. This is confirmed by delayed SpC minima, which follow the relatively constant SpC values observed during the rising limb, since rising limb flow consists of displaced pre-event water. The larger storm flow fraction is observed during the recession limb of the pulse when shallow

flow paths are activated. In contrast, in urban settings storm flow typically dominates the rising limb, and higher baseflow fractions are observed on the recessional limb, a result of the rapid transfer of surface runoff into these systems.

The hierarchy of transport timescales for the different chemical and physical parameters in each basin varies, with SpC and the major elements having the longest response times and turbidity having the shortest response time. Moreover, urbanization shortens the transport timescales of individual parameters. Transport of suspended sediment, as characterized by the turbidity, increases substantially due to an increase in flood severity caused by urbanization. TSS loads can increase nearly 5-fold in urban settings and the peak width of these perturbations is shortened.

The major elements, including Na, Cl, Ca, Mg, S, and Si are most closely associated with the isotopically-identified baseflow fraction. However, this becomes more complicated during winter when road salting occurs. During this time Na and Cl are highly concentrated in melt waters, and subsequently in runoff from the first few storms. In contrast, sharp perturbations of temperature, turbidity, DO, pH, and NO_3^- -N correlate most closely with the event water fraction. The transport of these individual solutes depends on storm and basin characteristics, and can be affected by the time of year, antecedent moisture conditions, and land use. For instance, impervious surface area speeds the transport of suspended solids and reduces a watershed's ability to dampen temperature changes caused by precipitation events. Temperature variations are amplified by increased urban land coverage, and can differ from their rural counterparts by 2°C or more, depending on the ambient air temperature.

Finally, when monitoring the variability between rural and urban watersheds, an infrequent sampling protocol does not accurately quantify the loads of particulates and individual solutes transported by the streams. Continuous monitoring devices provide high resolution datasets that document rapid changes in solutes and other physical parameters. For comparison, an arbitrary, infrequent sampling regime often misses first flushing events in SpC and Cl and can lead to large errors in load estimates.

Fundamentally, unimpacted watersheds show more dampened hydrologic and geochemical responses than urban watersheds. Impervious surfaces and anthropogenic contamination cause flashier responses and result in the rapid transmission of pollutants into surface waters. However, even the so-called “rural” end-member in this study (Fox Creek) demonstrates significant impairment, including shortened lag times due to historical land use and increased SpC and Cl concentrations due to road salt application.

3.7. References

- Allison, G.B., Barnes, C.J., and Hughes, M.W. 1983, The distribution of deuterium and ^{18}O in dry soils, 2. Experimental: *Journal of Hydrology*, v. 64, p. 377-397.
- American Society of Civil Engineers, 2011, River des Peres Sewage and Drainage Works: American Society of Civil Engineers Web page, <http://www.asce.org/>.
- Anderson, M.G., and Burt, T.P., 1982, The contribution of throughflow to storm runoff: An evaluation of a chemical mixing model: *Earth Surfaces Processes and Landforms*, v. 7, p. 565-574.
- Appelo, C.A.J., and Postma, D., 2007, *Geochemistry, groundwater and pollution*, 2nd ed.: Leiden., A.A. Balkema Publishers, 649 p.
- Baedecker, M.J., and Back, W., 1979, Hydrogeological processes and chemical reactions at a landfill: *Ground Water*, v. 7, p. 429-437.
- Balls, P.W., Brockie, N., Dobson, J., and Johnston, W., 1996, Dissolved oxygen and nitrification in the Upper Forth Estuary during summer (1982–92): patterns and trends: *Estuarine, Coastal and Shelf Science*, v. 42, p. 117-134.
- Bannerman, R.T., Legg, A.D., and Greb, S.R., 1996, Quality of Wisconsin stormwater, 1989–94: U.S. Geological Survey Open-File Report 96-458, 26 p.
- Barnes, C.J., and Allison, G.B., 1983, The distribution of deuterium and ^{18}O in dry soils, 1. Theory: *Journal of Hydrology*, v. 60, p. 141-156.
- Borah, D.K., Bera, M., and Shaw, S., 2003, Water, sediment, nutrient, and pesticide measurements in an agricultural watershed in Illinois during storm events: *Transactions of the American Society of Agricultural Engineers*, v. 46, p. 657-674.
- Brezonik, P.L., and Stadelmann, T.H., 2002, Analysis and predictive models of stormwater runoff volumes, loads, and pollutant concentrations from watersheds in the Twin Cities metropolitan area, Minnesota, USA: *Water Research*, v. 36, p. 1,743-1,757.
- Christensen, V.G., 2001, Characterization of surface-water quality based on real-time monitoring and regression analysis, Quivira National Wildlife Refuge, south-central Kansas, December 1998 through June 2001: U.S. Geological Survey Water Resources Investigations Report 01-4248, 28 p.
- Cohn, T.A., DeLong, L.L., Gilroy, E.J., Hirsch, R.M., and Wells, D.K., 1989, Estimating constituent loads: *Water Resources Research*, v. 25, p. 937-942.

Corbett, K.T., 1997, Draining the metropolis: The politics of sewers in nineteenth century St. Louis *in* Hurley, A., ed., *Common fields: An environmental history of St. Louis*: St. Louis, Missouri Historical Society, p. 107-125.

Craig, H., 1961, Isotopic variations in meteoric waters: *Science*, v. 133, p. 1,702-1,703.

Criss, R.E., 1997, New formulation for the hydrograph, time constants for stream flow, and the variable character of base flow: *Transactions American Geophysical Union*, v. 78, p. 317.

Criss, R.E., 2003, Character and origin of floodwaters, *in* Criss, R.E., and Wilson, D.A., eds. *At the confluence: Rivers, floods, and water quality in the St. Louis region*: St. Louis, MBG Press, p. 75-87.

Criss, R.E., Davisson, M.L., Surbeck, H., and Winston, W.E., 2007, Isotopic techniques, *in* Drew, D., and Goldscheider, N., eds., *Methods in karst hydrogeology*: London, Taylor & Francis, Ch. 7, p. 123-145.

Criss, R.E., and Winston, W.E., 2003, Hydrograph for small basins following intense storms: *Geophysical Research Letters*, v. 30, p. 1,314.

Criss, R.E., and Winston, W.E., 2008a, Discharge predictions of a rainfall-driven theoretical hydrograph compared to common models and observed data: *Water Resources Research*, v. 44, W10407.

Criss, R.E., and Winston, W.E., 2008b, Properties of a diffusive hydrograph and the interpretation of its single parameter: *Mathematical Geology*, v. 40, p. 313-325.

DeWalle, D.R., Swistock, B.R., and Sharpe, W.E., 1988, Three-component tracer model for stormflow on a small Appalachian forested catchment: *Journal of Hydrology*, v. 104, p. 301-310.

Driver, N., and Troutman, B., 1989, Regression models for estimating urban storm-runoff quality and quantity in the United States: *Journal of Hydrology*, v. 109, p. 221-236.

Edwards, A.M.C., 1973, The variation of dissolved constituents with discharge in some Norfolk rivers: *Journal of Hydrology*, v. 18, p. 219-242.

Evans, C., and Davies, T.D., 1998, Causes of concentration/discharge hysteresis and its potential as a tool for analysis of episode hydrochemistry: *Water Resources Research*, v. 34, p. 129-137.

Feller, M.C., and Kimmins, J.P., 1979, Chemical characteristics of small streams near Haney in Southern British Columbia: *Water Resources Research*, v. 15, p. 247-258.

Frape, S.K., Fritz, P., and McNutt, R.H., 1984, Water-rock interaction and chemistry of groundwaters from the Canadian Shield: *Geochimica et Cosmochimica Acta*, v. 48, p. 1,617-1,627.

Gleick, P.H., ed., 1993, *Water in crisis: A guide to the world's fresh water resources*: New York, Oxford University Press, 504 p.

Gupta, K., and Saul, A.J., 1996, Specific relationships for the first flush load in combined sewer flows: *Water Research*, v. 30, p. 1,244-1,252.

Harris, G., and Heathwaite, A.L., 2005, Inadmissible evidence: Knowledge and prediction in land and riverscapes: *Journal of Hydrology*, v. 304, p. 3-19.

Harrison, R.W., 1997, Bedrock geologic map of the St. Louis 30' × 60' Quadrangle, Missouri and Illinois: U.S. Geological Survey Miscellaneous Investigation Series Map I-2533, scale 1:100,000.

Hendrickson, G.E., and Krieger, R.A., 1960, Relationship of chemical quality of water to stream discharge in Kentucky: Report of the 21st International Geological Congress, Copenhagen, Part 1, p. 66-75.

Hendrickson, G.E., and Krieger, R.A., 1964, Geochemistry of natural waters of the Blue Grass Region, Kentucky: U.S. Geological Survey Water Supplies Paper 1700, 125 p.

Hooper R.P., and Shoemaker, C.A., 1986, A comparison of chemical and isotopic hydrograph separation: *Water Resources Research*, v. 22, p. 1,444-1,454.

Horowitz, A.J., 2009, Monitoring suspended sediments and associated chemical constituents in urban environments: Lessons from the city of Atlanta, Georgia, USA Water Quality Monitoring Program: *Journal of Soils and Sediments*, v. 9, p. 342-363.

House, W.A., and Warwick, M.S., 1998, Hysteresis of the solute concentration/discharge relationship in rivers during storms: *Water Research*, v. 32, p. 2,279-2,290.

Houston, J.A., and Brooker, M.P., 1981, A comparison of nutrient sources and behaviour in two lowland subcatchments of the River Wye: *Water Research*, v. 15, p. 49-57.

Kang, J.H., Lee, Y.S., Ki, S.J., Cha, S.M., Cho, K.H., Kim, and J.H., 2009, Characteristics of wet and dry weather heavy metal discharges in the Yeongsan Watershed, Korea: *Science of the Total Environment*, v. 407, p. 3,482-3,493.

Kennedy, V.C., Kendall, C., Zellweger, G.W., Wyerman, T.A., and Avanzino, R.J., 1986, Determination of the components of stormflow using water chemistry and environmental isotopes, Mattole River Basin, California: *Journal of Hydrology*, v. 84, p. 107-140.

- Klein, M., 1981, Dissolved material transport—the flushing effect in surface and subsurface flow: *Earth Surface Processes and Landforms*, v. 6, p. 173-178.
- Konrad, C.P., 2003, Effects of urban development on floods: U.S. Geological Survey Fact Sheet FS-076-03, p. 1-4.
- Kracht, O., 2007, Tracer-based hydrograph separation methods for sewer systems [Ph.D. thesis]: Zurich, Swiss Federal Institute of Technology, p. 15-18.
- Lakey, B., and Krothe, N.C., 1996, Stable isotopic variation of storm discharge from a perennial karst spring, Indiana: *Water Resources Research*, v. 32, p. 721-731.
- Lawrence, J.R., and Gieskes, J.M., 1981, Constraints on water transport and alteration in the oceanic crust from the isotopic composition of pore water: *Geophysical Research Letters*, v. 86, p. 7,924-7,934.
- Lee, J.H., and Bang, K.W., 2000, Characterization of urban stormwater runoff: *Water Research*, v. 34, p. 1,773-1,780.
- Lee, J.H., Bang, K.W., Ketchum Jr., L.H., Choe, J.S., and Yu, M.J., 2002, First flush analysis of urban storm runoff: *Science of the Total Environment*, v. 293, p. 163-175.
- Lee, F.S., and Krothe, N.C., 2001, A four-component mixing model for water in a karst terrain in south-central Indiana, USA. Using solute concentrations and stable isotopes as tracers: *Chemical Geology*, v. 179, p. 129-143.
- Leecaster, M.K., Schiff, K., and Tiefenthaler, L.L., 2002, Assessment of efficient sampling designs for urban stormwater monitoring: *Water Research*, v. 36, p. 1,556-1,564.
- Lutzen, E.E., and Rockaway, J.D., Jr., 1989, Engineering geologic map of St. Louis County, Missouri: Missouri Department of Natural Resources, Open File Map 89-256-EG.
- Metropolitan St. Louis Sewer District, 2011, Metropolitan St. Louis Sewer District: Metropolitan St. Louis Sewer District Web page, <http://www.stlmsd.com/home>.
- Miller, W.R., and Drever, J.I., 1977, Water chemistry of a stream following a storm, Absaroka Mountains, Wyoming: *Geological Society of America Bulletin*, v. 88, p. 286-290.
- Missouri Department of Conservation, 2011, LaBarque Creek watershed: Conservation opportunity area: Missouri Department of Conservation Web page, <http://mdc.mo.gov/>.
- Missouri Department of Natural Resources, 2011a, Code of State Regulations (CSR): Division 20, Chapter 7 – Water Quality, Table H – Stream Classifications and Use

Designations: <http://www.sos.mo.gov/adrules/csr/current/10csr/10c20-7.pdf>. Revised 9-30-2009.

Missouri Department of Natural Resources, 2011b, Missouri Department of Natural Resources: Missouri Department of Natural Resources Web page, <http://www.dnr.mo.gov/>.

Missouri Spatial Data Information Service. Data Resources (MSDIS), 2011, Missouri Spatial Data Information Service: University of Missouri Web site, <http://www.msdis.missouri.edu>.

Mott, D.N., and Steele, K.F., 1991, Effects of pasture runoff on water chemistry, Buffalo National River, USA *in* Sediment and stream water quality in a changing environment: Trends and explanation, (Proceedings of the Vienna Symposium, August 1991): International Association of Hydrological Sciences Publication 203, p. 229-238.

National Oceanic and Atmospheric Administration (NOAA), 2011a, National Weather Service (NWS) Weather: NWS Web page, <http://www.weather.gov/>.

National Oceanic and Atmospheric Administration (NOAA), 2011b, National Weather Service (NWS) Weather: NWS Flood Loss Data Web page, http://nws.noaa.gov/oh/hic/flood_stats/Flood_loss_time_series.shtml

Ogden, F.L., Sharif, H.O., Senarath, S.U.S., Smith, J.A., Baeck, M.L., and Richardons, J.R., 2000, Hydrologic analysis of the Fort Collins, Colorado, flash flood of 1997: *Journal of Hydrology*, v. 228, p. 82-100.

Phillips, P.J., and Bode, R.W., 2004, Pesticides in surface water runoff in south-eastern New York State, USA: Seasonal and stormflow effects on concentrations: *Pest Management Science*, v. 60, p. 531-543.

Porter, K.S., 1975, Transport in streams: Nitrogen and phosphorus, *in* Porter, K.S., ed., Food production, waste and the environment: New York, Ann Arbor Science.

Roberts, G., 1997, The influence of sampling frequency on streamflow chemical loads: *Water and Environment Journal*, v. 11, p. 114-118.

Shand, P., Haria, A.H., Neal, C., Griffiths, K.J., Goody, D.C., Dixon, A.J., Hill, T., Buckley, D.K., and Cunningham, J.E., 2005, Hydrochemical heterogeneity in an upland catchment: further characterisation of the spatial, temporal and depth variations in soils, streams and groundwater of the Plynlimon forested catchment, Wales: *Hydrology and Earth System Sciences*, v. 9, p. 612-644.

Sharp, J.V.A., 1969, Time-dependent behaviour of water chemistry in hydrologic systems: *Transactions American Geophysical Union*, v. 50, p. 141.

Sheeder, S.A., Ross, J.D., and Carlson, T.N., 2002, Dual urban and rural hydrograph signals in three small watersheds: *Journal of the American Water Resources Association*, v. 38, p. 1027-1040.

Shock, E.L., Carbery, K., Noblit, N., Schnall, B., Kogan, P., Rovito, S., Berg, A., and Liang, J., 2003, Water and solute sources in an urban stream, River des Peres, St. Louis, Missouri, *in* Criss, R.E., and Wilson, D.A., eds. *At the confluence: Rivers, floods, and water quality in the St. Louis region*: St. Louis, MBG Press, p. 150-160.

Sklash, M.G., and Farvolden, R.N., 1979, The role of groundwater in storm runoff: *Journal of Hydrology*, v. 43, p. 45-65.

Smith, K., and Ward, R., 1998, *Floods: Physical processes and human impacts*: Chichester, John Wiley and Sons, 394 p.

Smullen, J.T., Shallcross, A.L., and Cave, K.A., 1999, Updating the US nationwide urban runoff quality data base: *Water Science and Technology*, v. 39, p. 9-16.

Spraggs, G., 1976, Solute variations in a local catchment: *The Southern Hampshire Geographer*, v. 8, p. 1-14.

St. Louis Planning Commission, uncredited 1916 photo: Files of the City Planning Commission.

Stueber, A.M., and Criss, R.E., 2005, Origin and transport of dissolved chemicals in a karst watershed, southwestern Illinois. *Journal of American Water Resources Association*, v. 41, p. 267-290.

Toler, L.G., 1965, Relationship between chemical quality and water discharge in Spring Creek, southern Georgia: U.S. Geological Survey Professional Paper 525-C, p. C206-C208.

Tomlinson, M.S., and De Carlo, E.H., 2003, The need for high resolution time series data to characterize Hawaiian streams: *Journal of the American Water Resources Association*, v. 39, p. 113–123.

U.S. Census, 2010, Population Density Date: 2010 U.S. Census Web page, <http://2010.census.gov/2010census/>.

U.S. Department of Agriculture, 2011, USDA Web Soil Survey: Web Soil Survey Web page, <http://websoilsurvey.nrcs.usda.gov/app/HomePage.htm>.

U.S. Geological Survey, 2011, USGS Real-time data for Missouri: USGS Real-time data for Missouri Web page, <http://waterdata.usgs.gov/mo/nwis/rt>.

- Van Bavel, C.H.M., 1961, Lysimetric measurements of evapotranspiration rates in the eastern United States: *Soil Science Society of America Proceedings*, v. 25, p. 138-141.
- Vicars-Groening, J., and Williams, H.F.L., 2007, Impact of urbanization on storm response of White Rock Creek, Dallas, TX: *Environmental Geology*, v. 51, p. 1,263-1,269.
- Wallace, J., Stewart, L., Hawdon, A., Keen, R., Karim, F., and Kemei, J., 2009, Flood water quality and marine sediment and nutrient loads from the Tully and Murray catchments in north Queensland, Australia: *Marine and Freshwater Research*, v. 60, p. 1,123–1,131.
- Walling, D.E., and Foster, I.D.L., 1975, Variations in the natural chemical concentrations: *Journal of Hydrology*, v. 26, p. 237-244.
- Walling, D.E., and Webb, B.W., 1980, The spatial dimension in the interpretation of stream solute behaviour: *Journal of Hydrology*, v. 47, p. 129-149.
- Walling, D.E., and Webb, B.W., 1986, Solutes in river systems, *in* Trudgill, S.T., ed., *Solute processes*: New York, John Wiley, p. 251-327.
- Winston, W.E., 2001, Dynamic response of an eastern Missouri karst spring to seasonal and storm induced perturbations [Master thesis]: St. Louis, Washington University in St. Louis, 225 p.
- Winston, W.E., and Criss, R.E., 2002, Geochemical variations during flash flooding, Meramec Basin, May 2000: *Journal of Hydrology*, v. 265, p. 149-163.
- Winston, W.E., and Criss, R.E., 2003, Flash flooding in the Meramec Basin, May 2000 *in* Criss, R.E., and Wilson, D.A., eds., *At the confluence: Rivers, floods, and water quality in the St. Louis region*: St. Louis, MBG Press, p. 88-95.
- Winston, W.E., and Criss, R.E., 2004, Dynamic hydrologic and geochemical response in a perennial karst spring: *Water Resources Research*, v. 40, W05106.
- Zimmermann, U., Ehhalt, D., and Münnich, K.O., 1967, Soil water movement and evapotranspiration: Changes in the isotopic composition of the water *in* *Proceedings Symposium on Isotopes in Hydrology*, Vienna, 1966: Vienna, International Atomic Energy Agency, p. 567-584.

Table 3.1. Sampling location information.

Sample Location	Stream Order	USGS Gaging Station Number*	UTM Coordinates (NAD83, Zone 15)		USGS Gage Location Description	Period of Record	Hydrologic Unit†	Drainage Basin	Gaging Station Drainage Area (km ²)	Watershed Area (km ²)	Datum of Gage NAVD88 (m)	Average Discharge (cms)	Peak Discharge (cms)
			Easting (m)	Northing (m)									
Fox Creek	4	07017115	701550	4263800	On left downstream abutment of Old Hwy. 66 bridge 1.3 km west of Allenton.	July 2007 to May 2009	07140102	Lower Mississippi Basin Meramec Subbasin	39.1	46.3	139.1	0.50	229.9
Grand Glaize	4	07019185	720316	4271936	On right upstream abutment of Quinette Rd. bridge, 2.7 km north of I-44, 2.9 km west of I-270, and 5.6 km upstream of the confluence with the Meramec River.	May 1997 to present	07140102	Lower Mississippi Basin Meramec Subbasin	56.5	61.4	128	0.69	170.8
Sugar Creek	3	07019175	720887	4272840	On left upstream abutment of Barrett Station Rd. bridge, 3.7 km north of I-44, and 1.8 km west of I-270.	June 1997 to present	07140102	Lower Mississippi Basin Meramec Subbasin	13.2	13.3	128.3	0.17	65.4 (Stage = 4.63 m, Highest Stage = 6.09 m)
River des Peres @ St. Louis	5	07010097	736722	4271385	On right downstream abutment of Morgan Ford Rd. bridge, 1.0 km north of I-55, 3.4 km east of Mackenzie Rd., and 3.9 km upstream of the confluence with the Mississippi River.	Feb. 2002 to present	07140101	Lower Mississippi Basin	213.7	295	119.0	2.06	710.8
River des Peres @ University City	3	07010022	732843	4283362	On left downstream abutment of Purdue Ave. bridge, 6.1 km south of I-70, 3.2 km east of I-170, and 0.2 km south of Olive Blvd.	Sept. 1997 to present	07140101	Lower Mississippi Basin	23.2	23.5	149.9	0.30	143.0
Southwest Branch of the Upper River des Peres @ McKnight	1	NA	729968	4283766	On left downstream abutment of McKnight Rd. bridge, 0.3 km west of I-170, and 0.2 km south of Olive Blvd.	Apr. 2010 to Aug. 2010	07140101	Lower Mississippi Basin	2.8	2.8	167.9	0.07‡	9.4
Deer Creek @ Maplewood	4	07010086	732932	4275701	On right downstream abutment of Big Bend Rd. bridge, 0.7 km north of I-44, 0.7 km east of Lindbergh Blvd., and 1 km upstream of the confluence with the River Des Peres drainage channel.	July 1996 to present	07140101	Lower Mississippi Basin River Des Peres Subbasin	94.5	95.5	126.7	0.88	291.7
Deer Creek @ Ladue	-	07010075	729647	4277499	On left upstream bank by the Rock Hill Quarry, on McCarthy Construction Co. complex, 8 km east of I-270, 1.5 km south of I-64/40, 0.3 km west of McKnight Rd.	May 2001 to present	07140101	Lower Mississippi Basin River Des Peres Subbasin	64.2	64.2	138.6	0.61	288.8
Deer Creek @ Litzinger Rd. in Ladue	-	07010055	728531	4278180	On left downstream abutment of Litzinger Rd. bridge, 1 km south of I-40, 1.1 km west of Hanley Rd., and 1.8 km north of Manchester Rd.	June 2001 to present	07140101	Lower Mississippi Basin River Des Peres Subbasin	31.1	31.1	136.9	0.35	279.8
Sebago Creek	2	07010070	728345	4277313	On left downstream abutment of Old Warson Rd. bridge, 1.8 km south of I-40, 1.2 km west of Hanley Rd., and 1 km north of Manchester Rd.	July 2001 to Oct. 2005, Aug. 2006 to present	07140101	Lower Mississippi Basin River Des Peres Subbasin	10.5	10.6	141.3	0.06	64.6
Two Mile Creek	3	07010061	727539	4277871	On left downstream abutment of Trent Dr. bridge, 1.2 km south of I-40, 2.4 km west of Hanley Rd., and 1.9 km north of Manchester Rd.	May 2002 to present	07140101	Lower Mississippi Basin River Des Peres Subbasin	16.7	17.2	143.2	0.23	89.2
Black Creek	3	07010082	731821	4277607	On right upstream abutment of Litzinger Rd., 1.4 km south of I-40, 0.3 km west of Hanley Rd., and 0.6 km north of Manchester Rd.	Mar. 2004 to present	07140101	Lower Mississippi Basin River Des Peres Subbasin	15.0	22.4	131.3	0.23	147.2

Data compiled from USGS (2011).

*All USGS gages types: water-stage recorders and crest-stage gage.

†Hydrologic unit explanation: (1) Accounting Unit 071401 – Upper Mississippi-Meramec: The Mississippi River Basin below the confluence with and excluding the Missouri River Basin to the confluence with the Ohio River, excluding the Kaskaskia River Basin, Illinois and Missouri, area = 29,000 km²; (2) Cataloging Units: (A) 07140101 – Cahokia-Joachim, Illinois and Missouri, area = 4,270 km²; (B) 07140102: Meramec, Missouri, area = 5,520 km².

‡Discharge calculated from stage data collected in this study.

Table 3.2. Rainfall amounts and isotopic character at St. Louis (S), Ladue (L), and Washington (W), MO compared to rainfall totals from Lambert – St. Louis International Airport (NOAA, 2011) and Valley Park, MO (USGS, 2011) for selected discharge responses.

Site	Number of Samples	Time Span	Precipitation (cm)		Isotopic Values (‰)		Weighted Average (‰)		NWS @ Lambert (60 min intervals)	USGS @ Valley Park (15 min intervals)
			Subtotal	Total	δD	$\delta^{18}O$	δD	$\delta^{18}O$		
L	1	3/26/08 15:00 – 3/27/08 7:15	NA	3.45	-11	-3.6	NA	NA	3.28	2.59
S	1	3/27/08 20:15 – 3/28/08 0:15	NA	1.03	-10	-3.2	NA	NA	0.43	0.91
L	1	3/30/08 5:15 – 3/31/08 20:00	NA	3.56	-22	-3.8	NA	NA	3.71	4.32
W	1	3/30/08 5:15 – 3/31/08 20:00	NA	4.21	-25	-4.7	NA	NA		
S	1	4/3/08 4:45 – 20:15	NA	1.76	-56	-8.3	NA	NA	2.08	1.78
L	1	4/3/08 4:45 – 20:15	NA	1.80	-41	-6.7	NA	NA		
W	1	4/3/08 4:45 – 20:15	NA	2.00	-50	-7.9	NA	NA		
S	1	5/6/08 18:00 – 5/7/08 10:40	0.99	5.62	-54	-7.9	-31	-5.3	4.98	5.61
	2	5/7/08 10:40 – 18:45	1.86		-9	-2.3				
	3	5/7/08 18:45 – 5/8/08 6:40	1.22		-55	-8				
	4	5/8/08 6:40 – 20:00	1.55		-25	-4.3				
L	1	5/7/08 6:00 – 5/8/08 19:00	NA	5.66	-32	-5.4	NA	NA	-34	-5.8
W	1	5/7/08 6:30 – 18:30	1.85	4.97	-46	-6.7				
	2	5/7/08 18:30 – 5/8/08 6:30	1.28		-29	-5.6				
	3	5/8/08 6:30 – 18:30	1.84		-25	-5.1				
L	1	7/8/08 8:00 – 7/9/08 5:00	NA	2.03	-51	-6.9	NA	NA	1.55	1.55
W	1	7/8/08 8:00 – 7/9/08 5:00	NA	1.12	-80	-11.3	NA	NA		
S	1	9/3/08 23:15 – 9/4/08 17:45	NA	9.40	-45	-7.1	NA	NA	7.87	8.23
L	1	9/3/08 23:15 – 9/4/08 17:45	NA	9.80	-39	-6.4	NA	NA		
S	1	4/2/10 20:00 – 22:00	0.69	1.24	-25	-4.6	-41	-6.7	1.07	NA
	2	4/3/10 0:00 – 3:00	0.55		-62	-9.1				
L	1	4/2/10 20:00 – 4/3/10 3:00	NA	1.40	-42	-6.9	NA	NA		

NA = Not Applicable or Not Available.

Table 3.3. Baseflow contributions during five March – April 2008 storm induced pulses at Fox, Grand Glaize, and Black Creeks.

Date	Percent Baseflow Component		
	Fox Creek	Grand Glaize Creek	Black Creek
March 26 – 27	79%	49%	30%
March 27 – 28	79%	NA	NA
March 30	59%	76%	52%
March 31 – April 1	NA	48%	27%
April 3	NA	53%	60%

NA = Not Available.

Table 3.4. Average and maximum baseflow contributions determined by isotope hydrograph separation for all discharge perturbations.

Percent Storm Flow Component	Fox Creek	Grand Glaize Creek	Black Creek	RP1	RP2	HMP
Average	36%	44%	67%	78%	62%	64%
Maximum	92%	100%	100%	100%	100%	100%

Table 3.5. Weighted average daily load estimates for various water quality parameters calculated using grab samples and continuous monitoring data.

Parameter	Calculation Method	FOX	SGR	GG	BCK	RDP	RP1	RP2	HMP
TSS* (kg/day)	Continuous	378	NA	701	NA	1,999	56	92	876
	Grab	989	244	1,991	471	15,645	62	106	290
DO (kg/day)	Continuous	356	NA	564	NA	1,589	33	23	31
	Grab	399	168	557	157	1,582	42	47	150
Cl (kg/day)	Continuous	4,327	NA	23,403	NA	70,304	2,309	1,107	5,267
	Grab	2,134	4,990	17,074	8,776	19,632	1,311	1,239	3,451
NO₃⁻-N (kg/day)	Continuous	48	NA	109	NA	409	10	4.8	60
	Grab	30	17	66	23	267	5.4	4.4	12
NH₄⁺-N (kg/day)	Continuous	3.46	NA	36	NA	224	0.60	0.06	2.1
	Grab	3.9	1.9	12	28	139	4.0	2.5	13
Total PO₄³⁻ (kg/day)	Grab	9.1	4.1	20	16	119	3.4‡	3.1‡	6.7‡
<i>E. coli</i> (cfu/day) †	Grab	41342 (0%)	>70,018 (5%)	>414,093 (8%)	>283,037 (38%)	>2,017,627 (41%)	>105,650 (50%)	>100,850 (50%)	>486,311 (67%)
Discharge (cms)		0.50	0.17	0.69	0.23	2.06	0.07	~0.07	0.30

*TSS is calculated from turbidity measurements.

†Numbers in parentheses represent the percent of *E. coli* measurements that were off-scale. The detection limit was used for the calculation so the measurement represents the minimum load.

‡Less than 5 measurements, which were made in June – August.

NA = Not Available.

Table 3.6. Simple average of various water quality parameters calculated using grab samples and continuous monitoring data.

Parameter	Calculation Method	FOX	SGR	GG	BCK	RDP	RP1	RP2	HMP
TSS* (mg/L)	Continuous	8.7	NA	11.8	NA	11.2	9.23	15.2	33.8
	Grab	22.9	16.6	33.4	23.7	87.9	10.2	17.5	11.2
DO (mg/L)	Continuous	8.3	NA	9.5	NA	8.9	5.5	3.8	1.2
	Grab	9.2	11.4	9.3	7.9	8.9	6.9	7.7	5.8
Cl (mg/L)	Continuous	100.2	NA	392.6	NA	395.0	381.8	183.0	203.2
	Grab	49.4	339.7	286.4	441.6	110.3	216.7	204.9	133.2
NO ₃ ⁻ -N (mg/L)	Continuous	1.1	NA	1.8	NA	2.3	1.7	0.8	2.3
	Grab	0.7	1.2	1.1	1.2	1.5	0.9	0.7	0.5
NH ₄ ⁺ -N (mg/L)	Continuous	0.08	NA	0.60	NA	1.3	0.10	0.01	0.08
	Grab	0.09	0.13	0.20	1.39	0.78	0.66	0.42	0.51
Total PO ₄ ³⁻ (mg/L)	Grab	0.21	0.28	0.33	0.83	0.67	0.56‡	0.51‡	0.26‡
<i>E. coli</i> (cfu/100 mL)†	Grab	96	477	695	1,424	1,134	1,747	1,668	1,876
Discharge (cms)		0.50	0.17	0.69	0.23	2.06	0.07	~0.07	0.30

*TSS is calculated from turbidity measurements.

†Numbers in parentheses represent the percent of *E. coli* measurements that were off-scale. The detection limit was used for the calculation so the measurement represents the minimum load.

‡Less than 5 measurements, which were made in June – August.

NA = Not Available.

Table 3.7. Average b values for discharge responses at various sampling sites.

Parameter	May 2008 Event			April 2010 Event	
	Fox Creek	Grand Glaize Creek	Black Creek	RP1	HMP
b (days)	0.09	0.03	0.02	0.02	0.02
Theoretical Peak Lag Time: $2b/3$ (minutes)	85	30	20	20	20
Scalar	5	40	10	3	15
Contributing Drainage Area at Gaging Station (km ²)	39.1	56.5	15.0	2.8	23.2

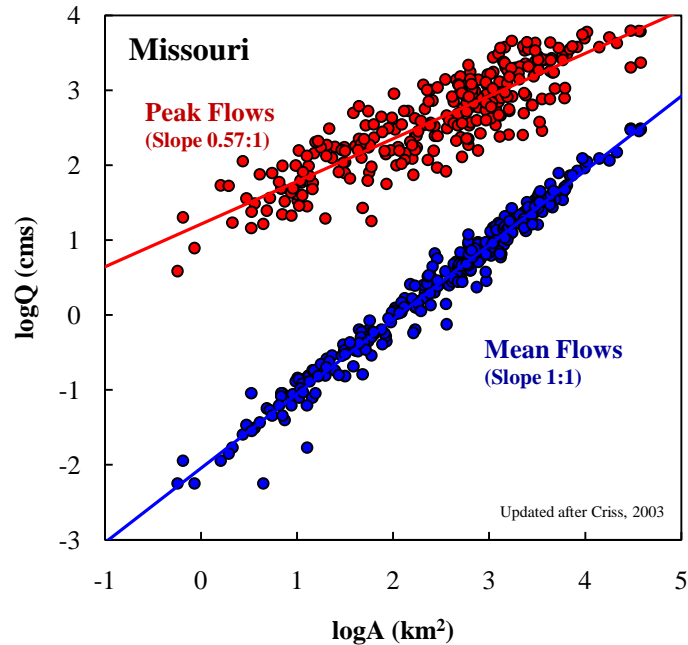


Figure 3.1. Graph of average (blue circles) and record (red circles) discharge versus basin area for rivers and streams in Missouri (data from USGS, 2011). Average discharge has a strong, 1:1 correlation with basin size that differs from the trend for record flows. Consequently, flash flood flows on small rivers can be 1000 times larger than mean flow (slope = 0.57:1). Note that the periods of record for the smallest basins are relatively short and record flows will likely increase as observations continue. Mean flows on the largest rivers (not shown; see Criss, 2003) lie below the mean flow regression line because their watersheds include the dry western plains. Figure updated after Criss, 2003.

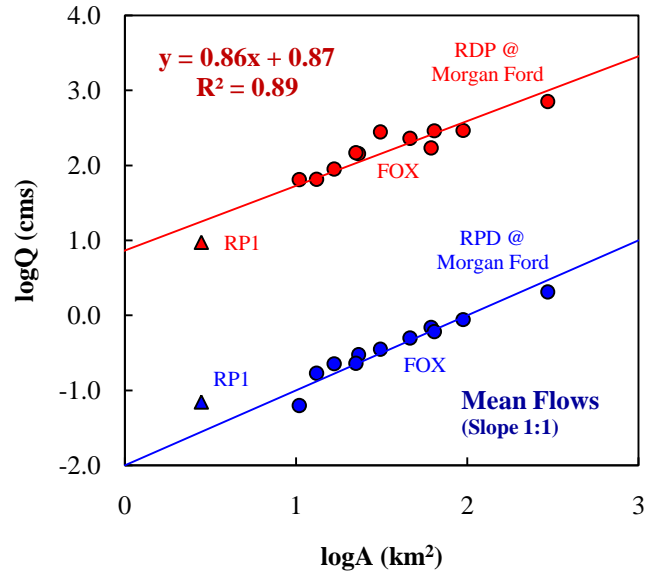


Figure 3.2. Graph of average discharge versus basin area for the sampling sites in the study. The mean flows for the streams in this study have the same 1:1 slope observed in Figure 3.1 and by Criss et al., 2003. However, peak flow has a 0.86:1 slope that is not understood. Data quality, historical archive, interbasin transfer, or the fact that the majority of the peak flows in these basins are a result of Hurricane Ike (September 14, 2008) may result in the relative differences in slope between peak flows for these features and peak flows for Missouri streams in Figure 3.1. Note that discharge data for RP1 (triangles) were measured by this study, while discharge data for all the other basins (circles) were measured by the USGS.

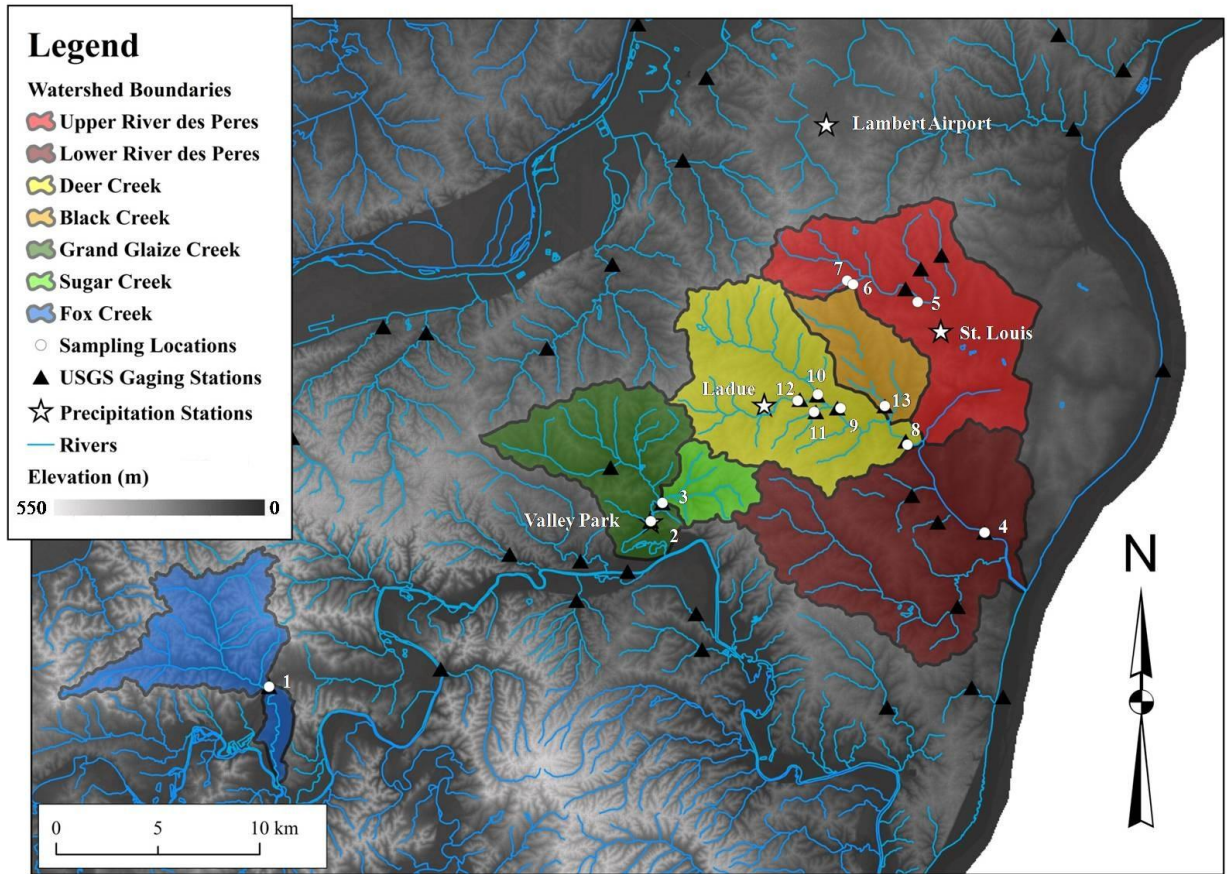
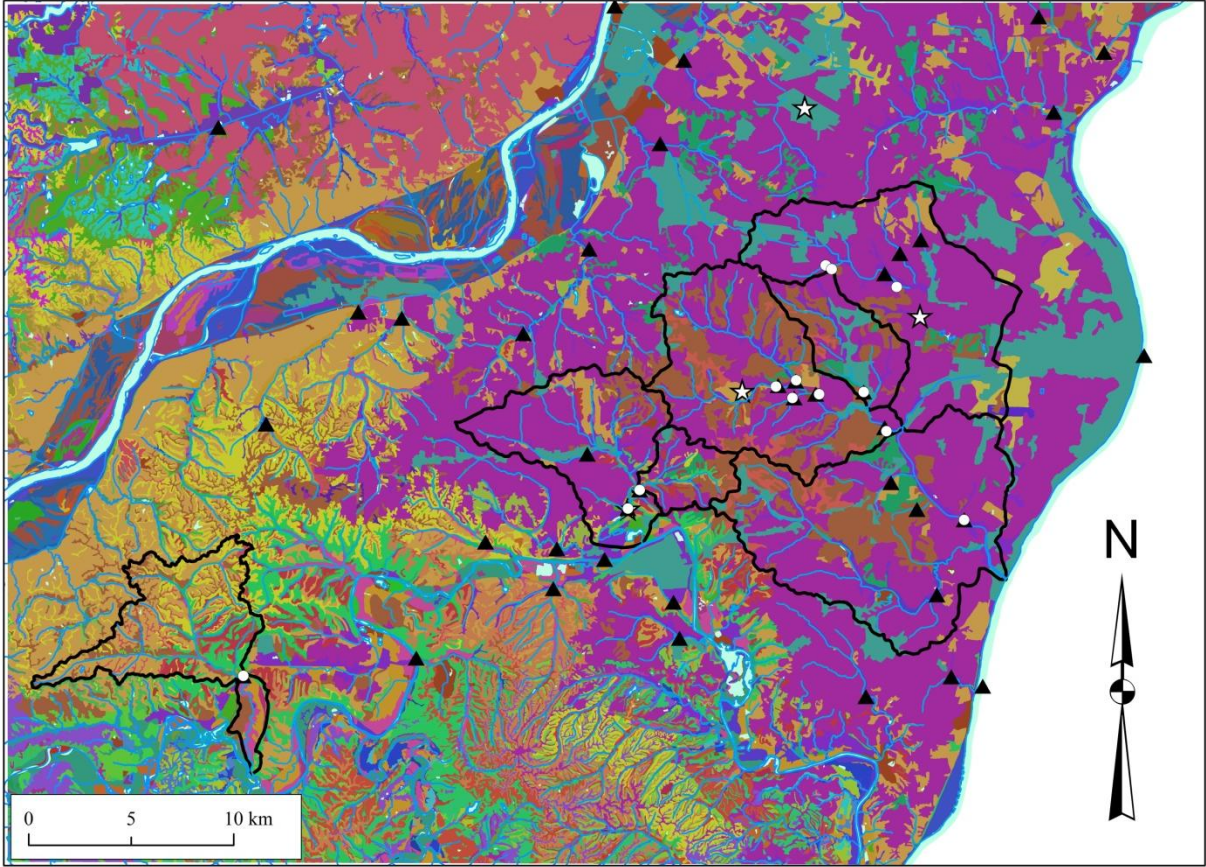


Figure 3.3. The delineated watershed boundaries on a digital elevation model for east-central Missouri. Sampling and equipment locations are shown (white circles) along with USGS stream gaging stations (black triangles). The St. Louis and Ladue precipitation collection stations are labeled; the Washington station is off-scale and lies 15 km west of the map area. Also labeled are the Lambert-St. Louis International Airport and Valley Park weather stations operated by NOAA and USGS, respectively. Sampling locations are labeled: (1) Fox Creek, (2) Grand Glaize Creek, (3) Sugar Creek, (4) River des Peres at St. Louis, (5) Upper River des Peres at University City, (6) Southwest Branch of the Upper River des Peres at Ruth Park, (7) Southwest Branch of the Upper River des Peres at McKnight Rd., (8) Deer Creek at Maplewood, (9) Deer Creek at Ladue, (10) Deer Creek at Litzinger Rd. in Ladue, (11) Sebago Creek, (12) Two Mile Creek, and (13) Black Creek. The elevation ranges from 390 m in the southwest to 110 m along the Mississippi River in the southeast. The 60 m digital elevation model basemap data are from the USGS (MSDIS, 2011).



Legend

- Sampling Locations
 - ▲ USGS Gaging Stations
 - Rivers
 - ☆ Precipitation Stations
 - Soils
- | | |
|---|---|
| <ul style="list-style-type: none"> ■ Arents ■ Armster ■ Auxvasse ■ Blake ■ Bloomsdale ■ Booker ■ Brussels-Rock ■ Caneyville ■ Cedargap ■ Crider ■ Crider-Menfro ■ Deible ■ Dockery ■ Dumps, Sand Piles ■ Edinburg ■ Elsay ■ Fishpot-Urban ■ Freesburg ■ Gabriel ■ Gasconade-Rock ■ Gatewood ■ Gatewood-Gasconade ■ Gladden ■ Goss ■ Hartville ■ Harvester-Urban ■ Hatton ■ Haymond ■ Haymond-Relfe ■ Haynie ■ Haynie-Treloar-Blake ■ Herrick ■ Hodge ■ Holstein ■ Horsecreek ■ Iva ■ Iva-Urban ■ Kaintuck ■ Kennebec ■ Keswick ■ Landes ■ Landfills ■ Lindley ■ Lowmo ■ Lowmo-Peers ■ Menfro ■ Menfro-Gate ■ Menfro-Goss ■ Menfro-Urban ■ Mexico ■ Minnith ■ Miscellaneous Water ■ Moko-Rock ■ Moniteau | <ul style="list-style-type: none"> ■ Nevin ■ Nevin-Urban ■ Parkville ■ Peers ■ Peers-Lowmo-SansDessein ■ Perche ■ Pevely ■ Pevely-Holstein ■ Pits ■ Possumtrot ■ Racoon ■ Ramsey-Rock ■ Razort ■ Rueter ■ SansDessein ■ Sarpy ■ Sarpy-Treloar ■ Sensabaugh ■ Sonsac ■ Sturkie ■ Tanglenook ■ Treloar-Sarpy-Kenmoor ■ Twomile ■ Udorthents ■ Union ■ Urban Land ■ Urban Land-Deible ■ Urban Land-Freeburg ■ Urban Land-Goss ■ Urban Land-Harvester ■ Urban Land-Horsecreek ■ Urban Land-Razort ■ Urbanlan-Orthents ■ Useful Silt Loam ■ Useful-Gatewood ■ Waldron ■ Water ■ Weingarten ■ Weller ■ Westerville ■ Wideman ■ Wilbur ■ Winfield ■ Wrengart |
|---|---|

Figure 3.4. Delineated watershed boundaries on a soil map for east-central Missouri.

Soil data are from the U.S. Department of Agriculture (USDA, 2011).

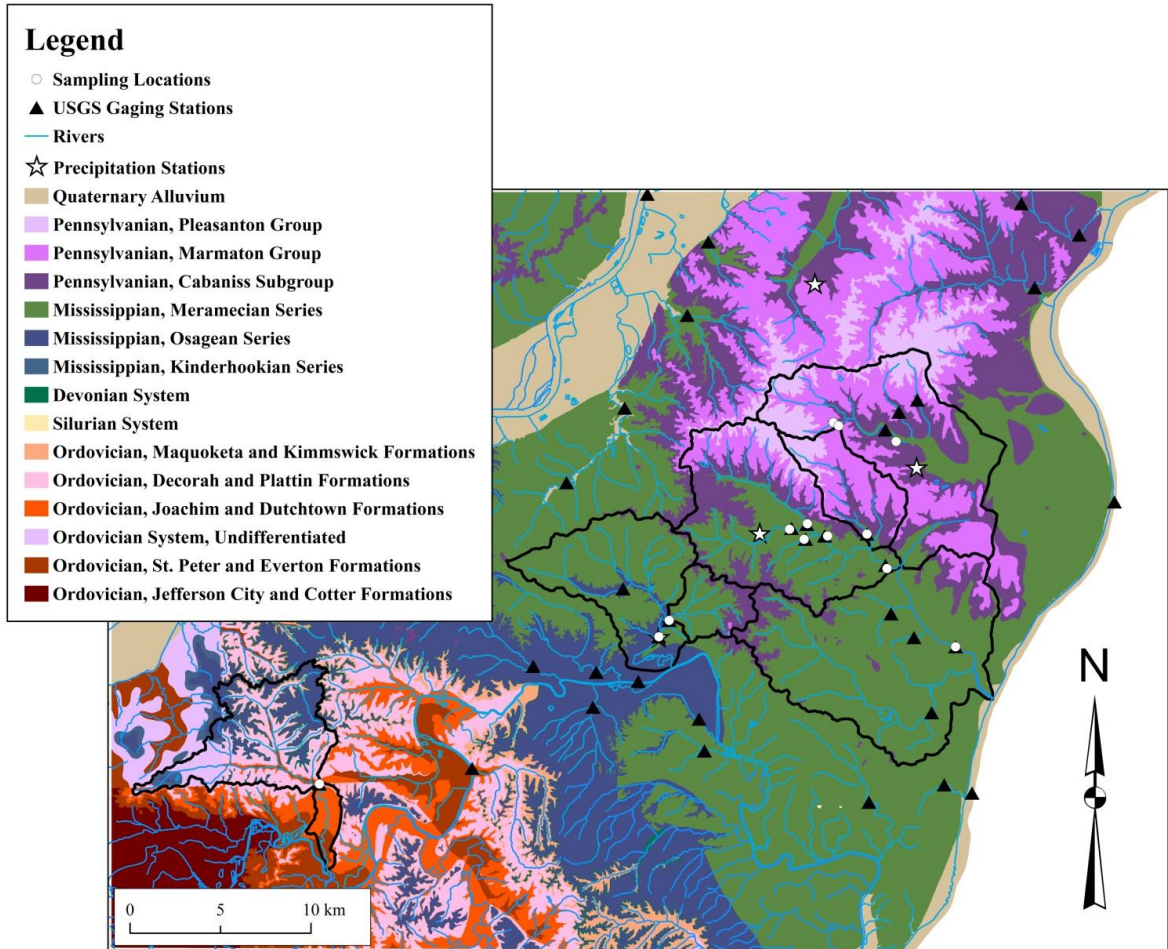


Figure 3.5. Delineated watershed boundaries on a bedrock map for east-central Missouri. Common lithologies include carbonates, shales, and sandstones and units range in age from Ordovician to Quaternary for this area. Bedrock data are from the MoDNR (MSDIS, 2011).

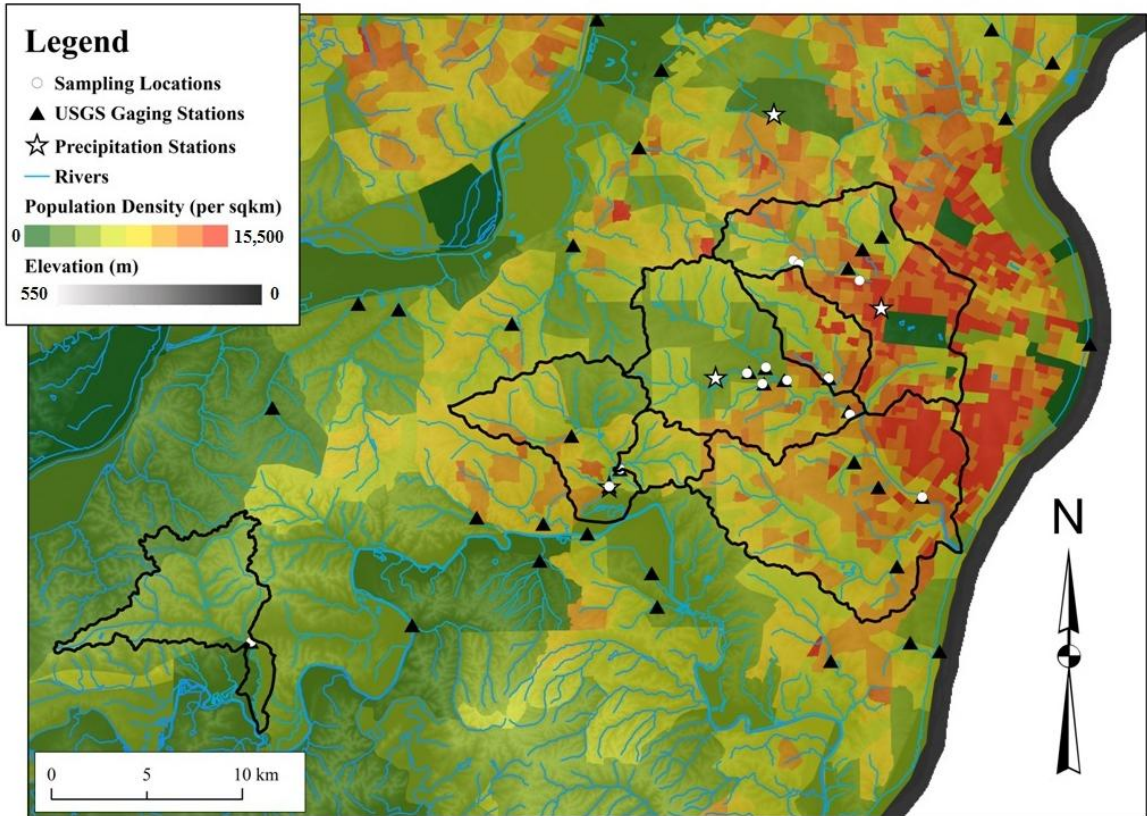


Figure 3.6. Delineated watershed boundaries on a relief and population density map for east-central Missouri. Digital elevation model basemap data are from the USGS (MSDIS, 2011); overlain on the DEM is population density data from the 2010 U.S. Census (U.S. Census, 2010).

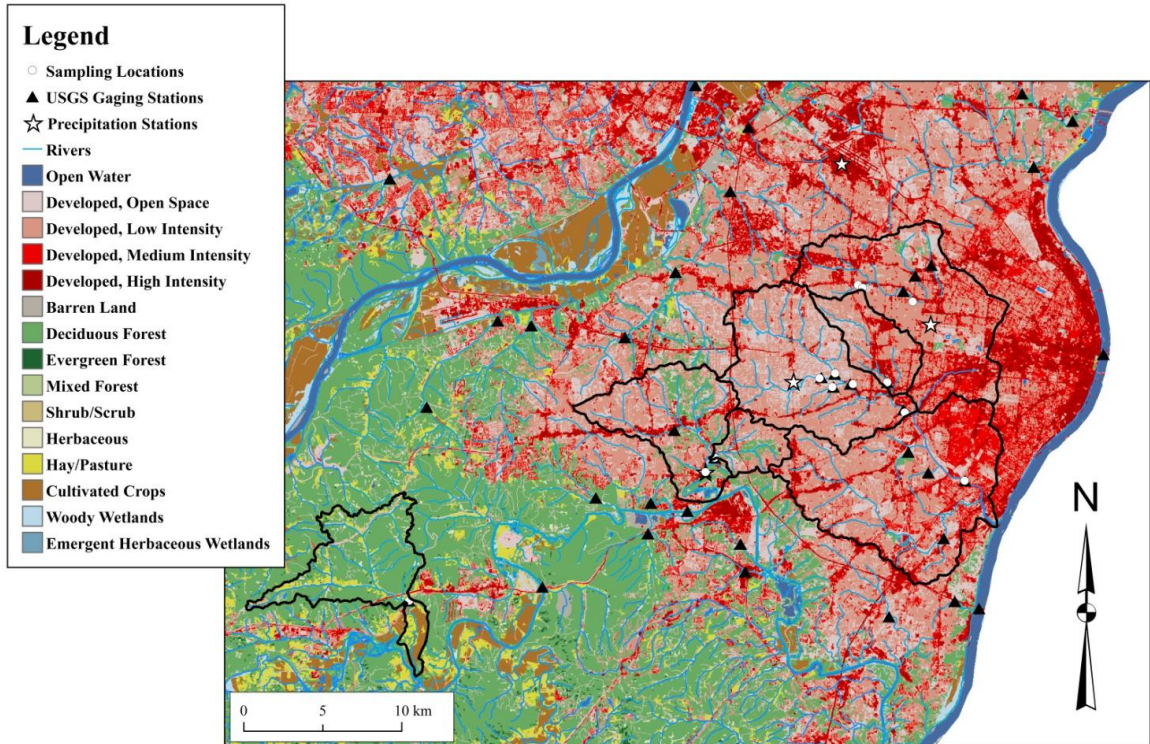


Figure 3.7. Delineated watershed boundaries on a land use map of east-central Missouri. The River des Peres watershed in the City of St. Louis and surrounding metro is highly developed, the Grand Glaize Creek watershed is moderately developed, and Fox Creek is mostly undeveloped. Land use/land area data are from the 2006 National Land Cover Database (USGS; MSDIC, 2011).



Figure 3.8. Fox Creek during normal flow (photo by Elizabeth Hasenmueller). Note that unlike the urban end-members in this study (Figures 3.9-3.11), Fox Creek's channel is not dissociated from its floodplain, and stream waters are clear and have abundant fauna.



Figure 3.9. Grand Glaize Creek during normal flow (photo by Elizabeth Hasenmueller).

The channel is incised approximately 1.5 m at this location and the green hue of the water is due to algae.

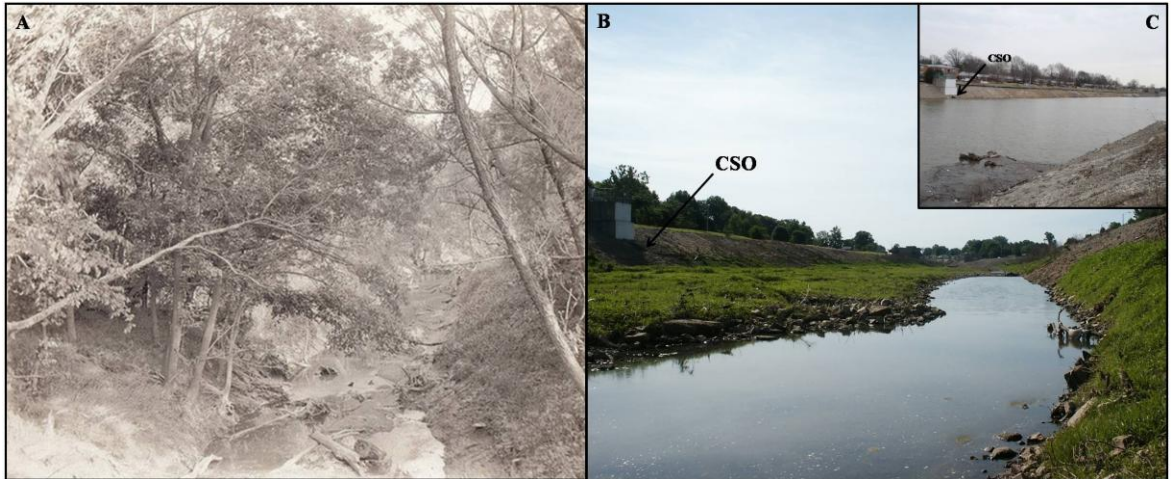


Figure 3.10. (A) The River des Peres near the Mississippi River, 1916 (uncredited photo, St. Louis City Planning Commission, 2011) and the River des Peres at the Morgan Ford Rd. monitoring site near the Mississippi River during (B) normal flow in 2007 (photo by William Winston) and (C) high flow in 2008 (photo by Elizabeth Hasenmueller). Note the CSO location in Figure 3.7B-C.



Figure 3.11. Black Creek during normal flow (photo by William Winston). The photo shows the highly entrenched channel (3.5 m) and the large quantities of trash and debris from the nearby shopping and industrial areas.

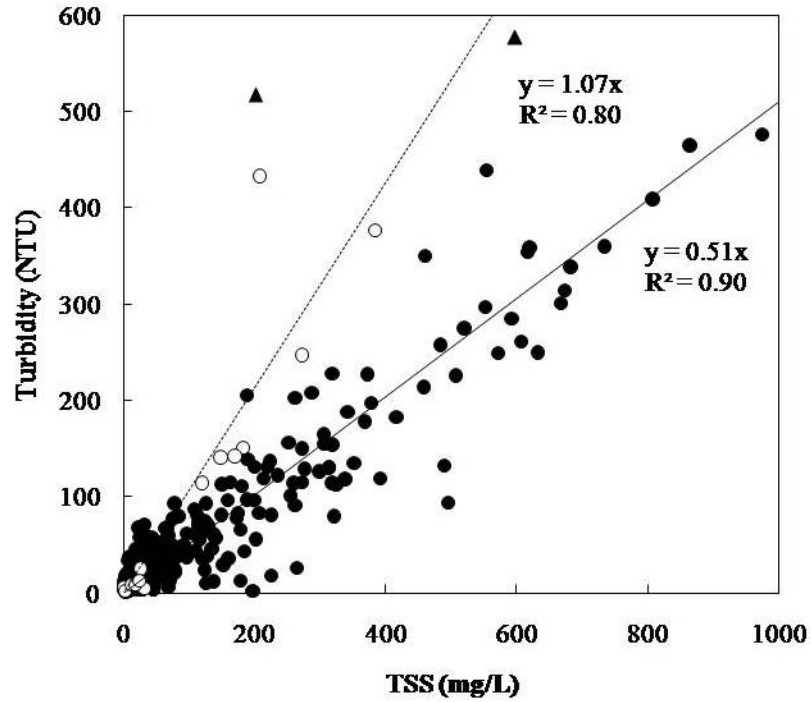


Figure 3.12. A plot of turbidity (NTU) versus TSS (ppm) for a variety of samples: large rivers, streams, springs, and surface runoff (black circles); mulching leachate (black triangles); and both untreated and treated municipal wastewaters (open circles). Surface and groundwaters show a strong, unique correlation between the two parameters, while organic rich waters have a different trend. Turbidity measured in the field and by continuous monitoring devices can be a proxy for TSS as long as these waters conform to the properties observed in typical surface waters and groundwaters.

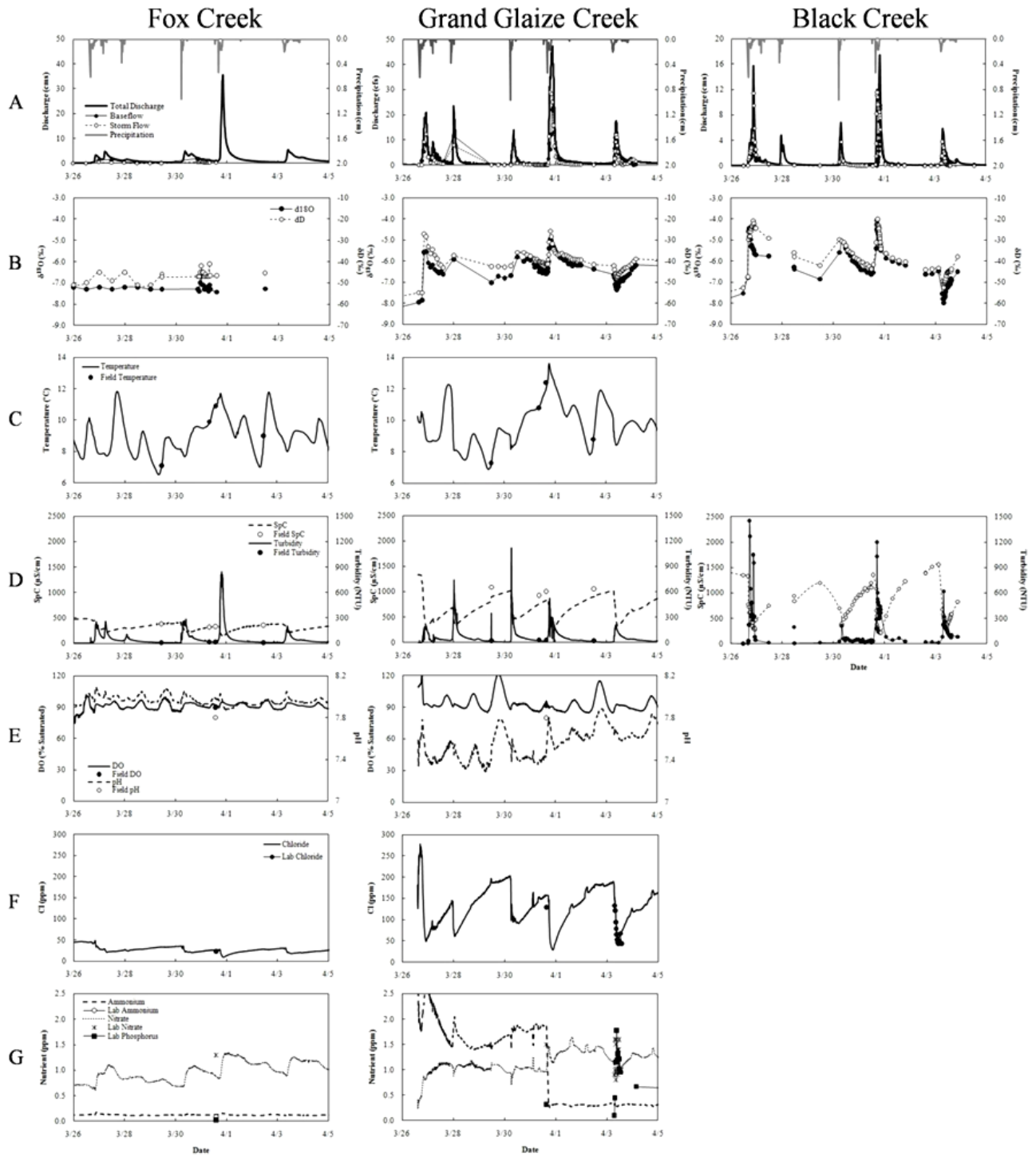


Figure 3.13. The hydrologic, isotopic, and geochemical responses for Fox, Grand Glaize, and Black Creeks during five rainfall events that occurred at the end of March and beginning of April in 2008. Results include: (A) total discharge, baseflow and storm flow proportions (determined by isotopic hydrograph separation), and precipitation totals; (B) δD and $\delta^{18}O$ results; in situ and field measurements for: (C) temperature; (D) SpC and turbidity; (E) DO and pH; and in situ and lab measurements of (F) Cl and (G) NH_4^+-N , $NO_3^- -N$, and total PO_4^{3-} for Fox Creek (first column) and Grand Glaize Creek (second column). Black Creek was not outfitted with continuous monitoring devices during this period; lab measurements for (A), (B), and (D) are shown for Black Creek (third column). All parameters are on the same scale except for discharge of the small Black Creek watershed. Symbols for each parameter are shown in the legend and are consistent for all subsequent figures. All data are from this study except for the total discharge and 15-minute rainfall records (USGS, 2011).

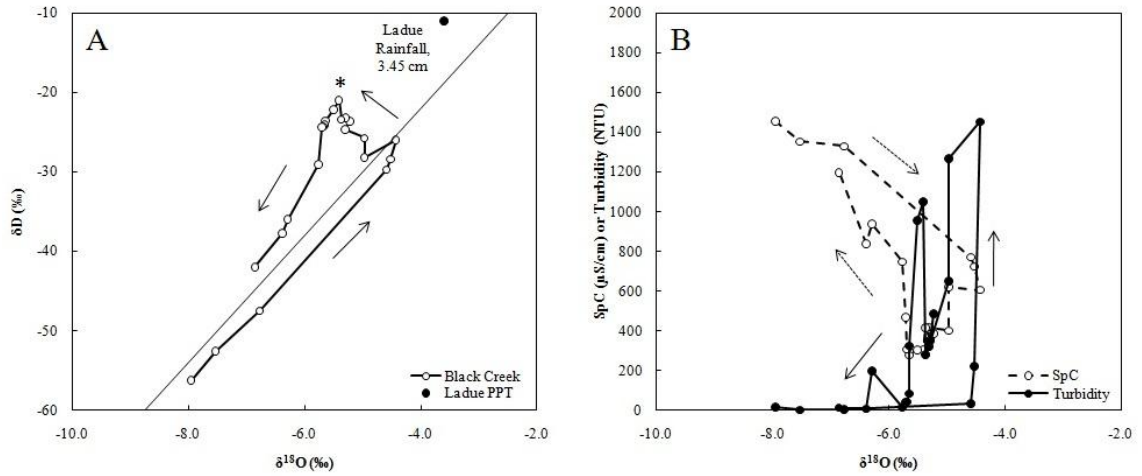


Figure 3.14. (A) The δD and $\delta^{18}O$ hysteresis loop for the March 26 discharge event at Black Creek. The thin black line is the MWL, the open circles are individual storm samples collected during the event, the arrows depict temporal progression, and the closed circle is the isotopic composition of the total rainfall. The asterisk indicates peak discharge. (B) SpC (open circles and dashed line) and turbidity (close circles and solid line) plotted against $\delta^{18}O$.

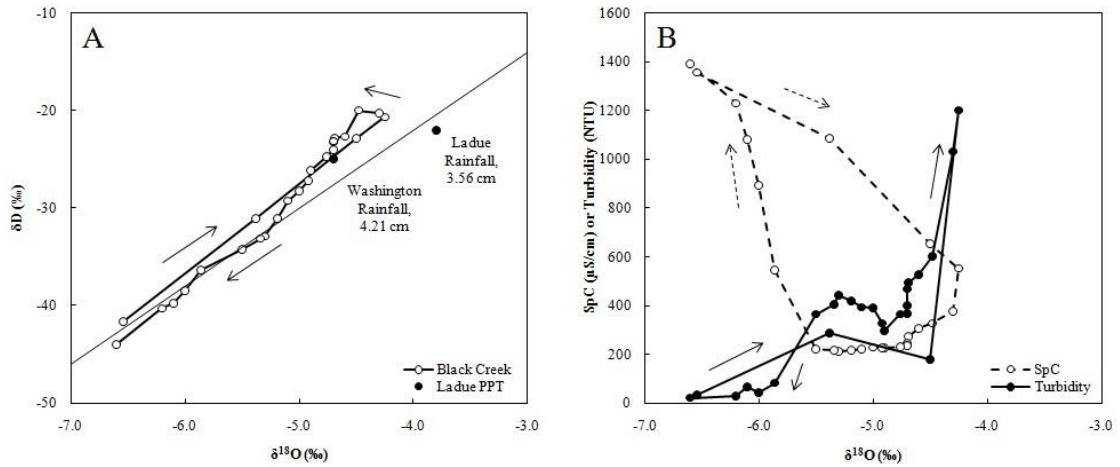


Figure 3.15. (A) The δD and $\delta^{18}\text{O}$ hysteresis loop for the March 31 – April 1 discharge event at Black Creek compared to the rainfall. (B) SpC and turbidity plotted against $\delta^{18}\text{O}$. Symbols as in Figure 3.14.

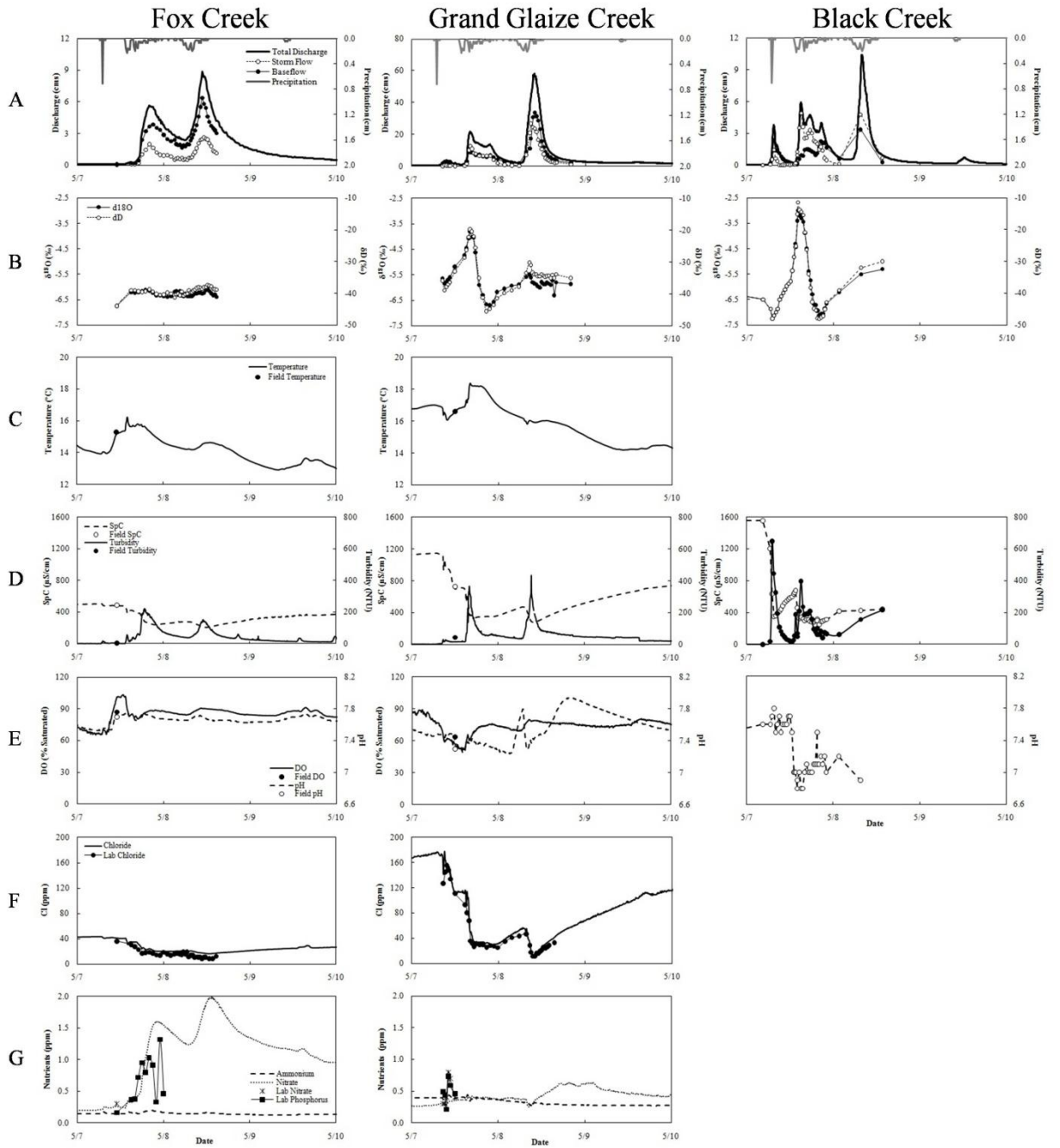


Figure 3.16. The hydrologic, isotopic, and geochemical responses for Fox, Grand Glaize, and Black Creeks during a May 7 – 8, 2008 rainfall event. Results include: (A) total discharge, baseflow and storm flow amounts (determined by isotopic hydrograph separation), and precipitation totals; (B) δD and $\delta^{18}O$ results; in situ and field measurements for (C) temperature; (D) SpC and turbidity; (E) DO and pH; and in situ and lab measurements of (F) Cl and (G) NH_4^+-N , NO_3^--N , and total PO_4^{3-} for Fox Creek (first column) and Grand Glaize Creek (second column). Lab measurements of (A), (B), and (D) are show for Black Creek (third column). All parameters are on the same scale except for discharge at Grand Glaize Creek due to its large magnitude. All data are from this study except for the total discharge and 15-minute rainfall records (USGS, 2011).

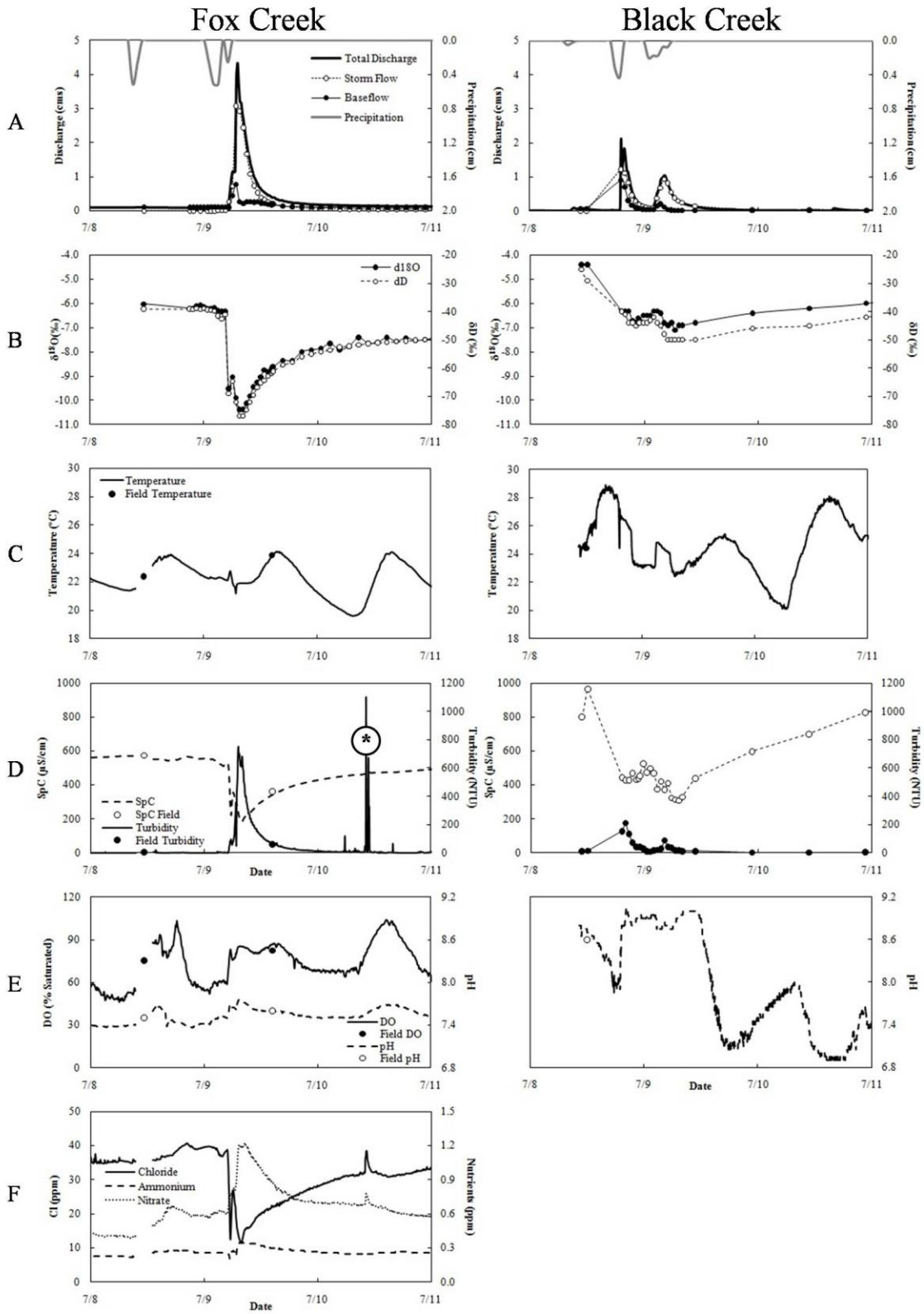
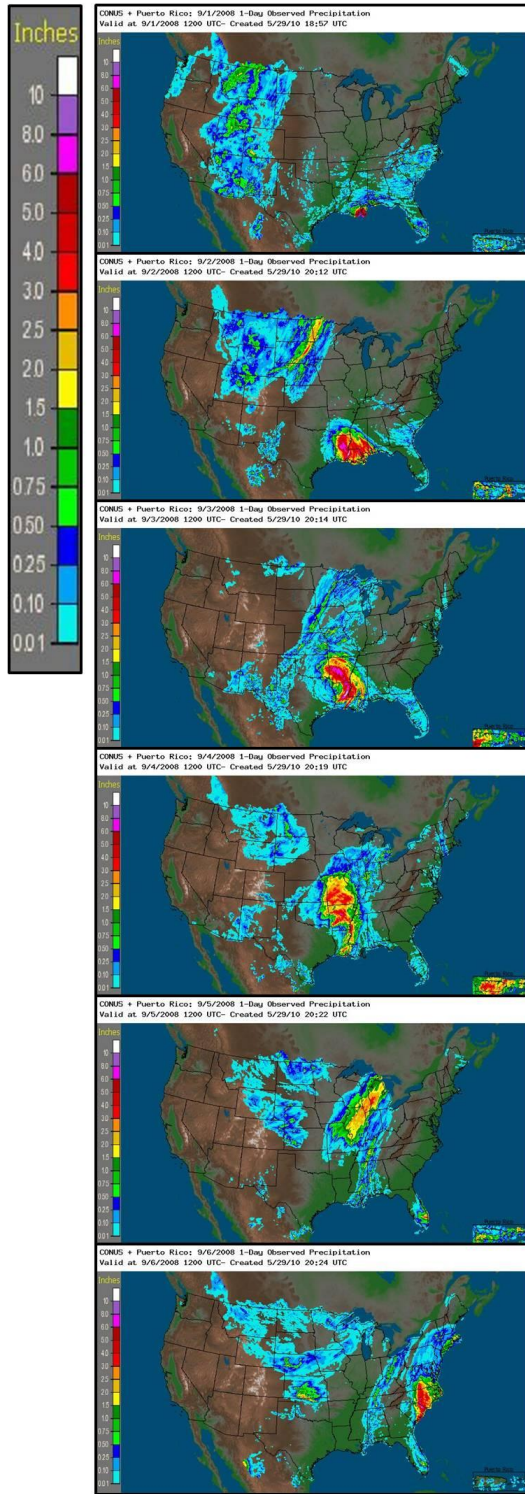


Figure 3.17. The hydrologic, isotopic, and geochemical responses for Fox and Black Creeks for a July 9, 2008 rainfall event. Results include: (A) total discharge, baseflow and storm flow amounts (determined by isotopic hydrograph separation), and precipitation totals; (B) δD and $\delta^{18}O$ results; in situ and field measurements for (C) temperature; (D) SpC and turbidity; (E) DO and pH for Fox Creek (first column) and Black Creek (second column); and in situ and lab measurements of (F) Cl, NH_4^+ -N, NO_3^- -N, and total PO_4^{3-} for Fox Creek. The gap in water quality data on July 8 is a result of temporarily removing the probes for calibration prior to the rainfall event, and anomalous turbidity measurements are indicated by an asterisk. All parameters are on the same scale. All data are from this study except for the total discharge and 15-minute rainfall records (USGS, 2011).



1

Fox Creek

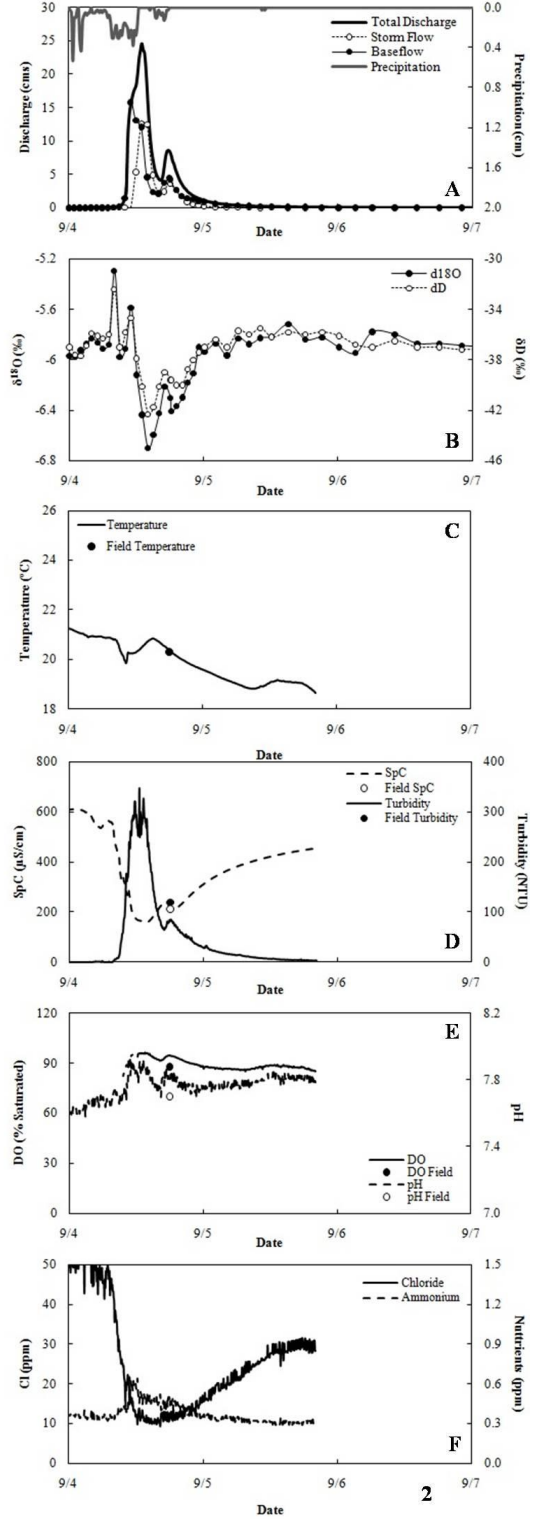


Figure 3.18. (1) The observed precipitation for September 1 – 6, 2008 in the continental United States during Hurricane Gustav (NOAA, 2011a). The event followed a relatively dry period during which only 0.36 cm of rain had fallen in the preceding two weeks. (2) The resulting hydrologic, isotopic, and geochemical responses from Hurricane Gustav at Fox Creek: (A) total discharge, baseflow and storm flow amounts (determined by isotopic hydrograph separation), and precipitation totals; (B) δD and $\delta^{18}O$ results; in situ and field measurements for (C) temperature; (D) SpC and turbidity; (E) DO and pH; and (F) Cl and NH_4^+ -N. All data are from this study except for the total discharge and 15-minute rainfall records (USGS, 2011).

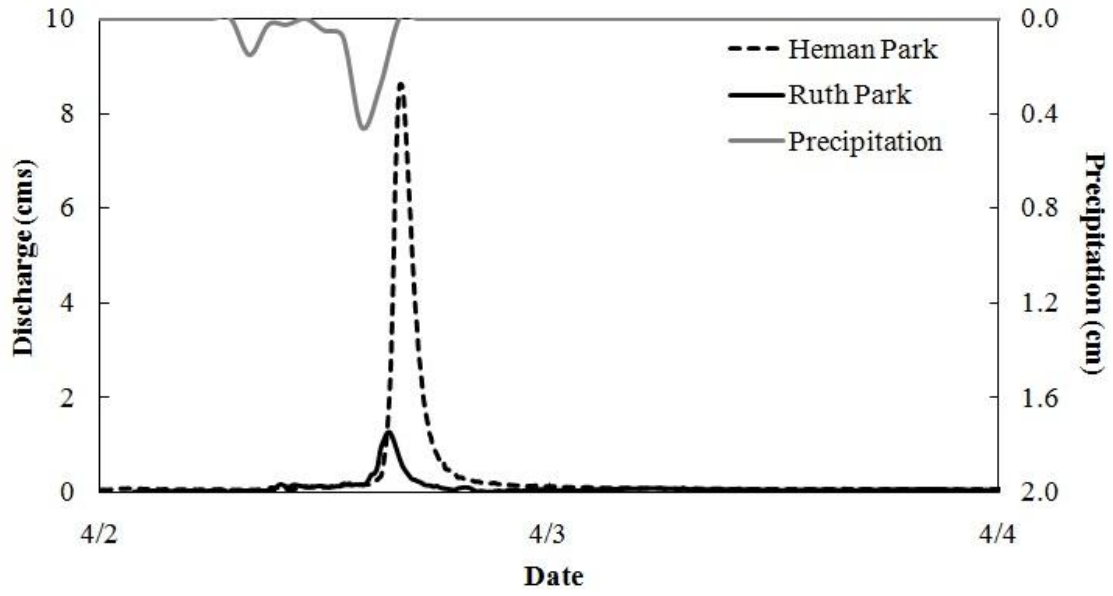


Figure 3.19. The relative discharge (cms) at Ruth Park estimated by this study and at Heman Park (USGS, 2011) in response to an April 2 – 3, 2010 rainfall event.

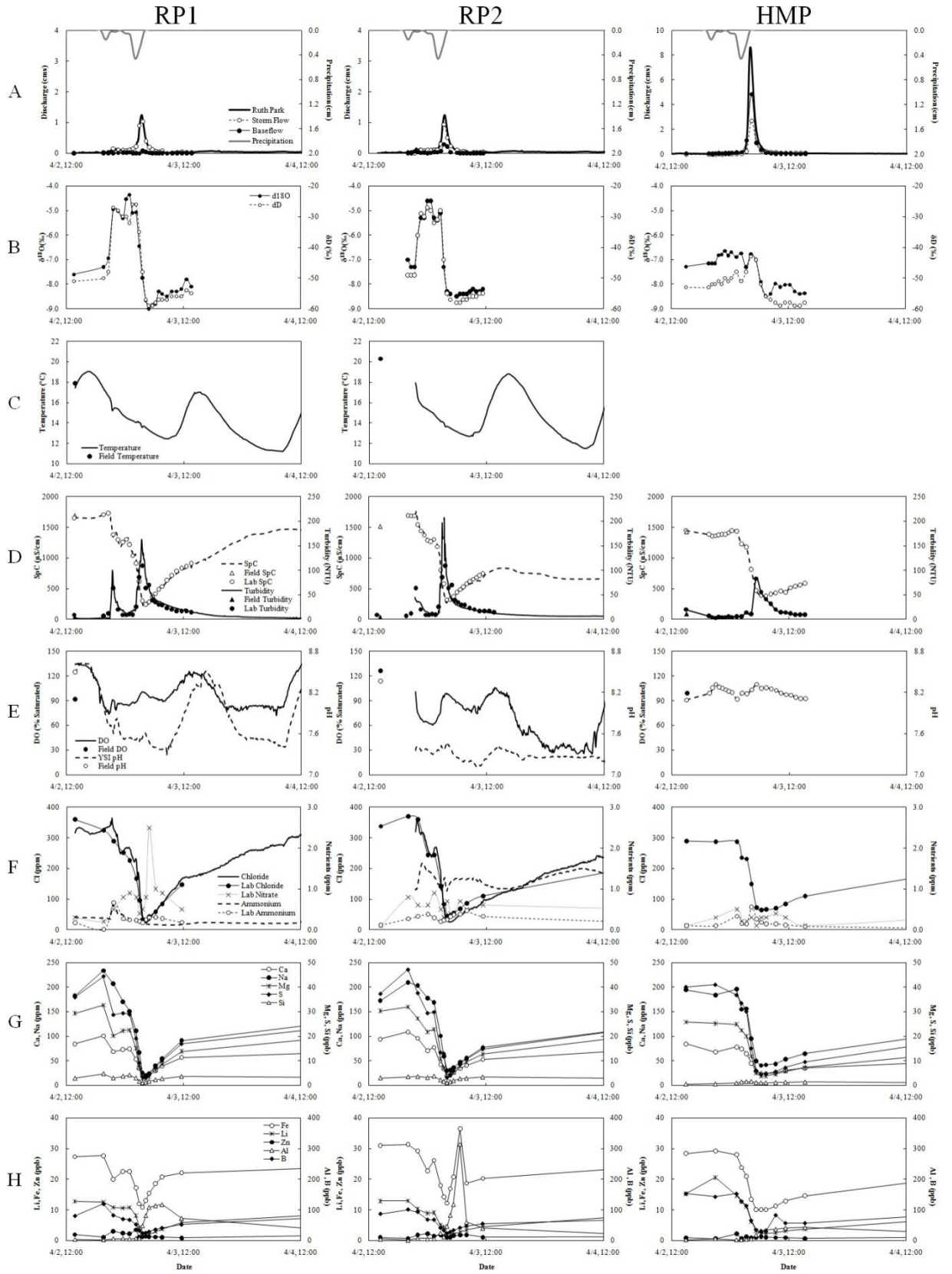


Figure 3.20. The hydrologic, isotopic, and geochemical responses for the Southwest Branch and the Upper River des Peres (RP1, RP2, and HMP) for April 2, 2010 rainfall events. Results include: (A) total discharge, baseflow and storm flow amounts (determined by isotopic hydrograph separation), and precipitation totals; (B) δD and $\delta^{18}O$ results, in situ and field measurements for (C) temperature; (D) SpC and turbidity; (E) DO and pH; in situ and lab measurements of (F) Cl, NH_4^+ -N, and NO_3^- -N; and lab measurements of (G) several major elements including Ca, Na, Mg, Si, and Si; and (H) select minor elements Fe, Li, Zn, Al, and B for RP1 (first column), RP2 (second column), and HMP (third column). A continuous monitoring device at HMP had not yet been installed when this rainfall event occurred. All parameters are on the same scale except for discharge at HMP because of its higher discharge response, but the Ruth Park and Heman Park discharge responses are shown to scale in Figure 3.19. All data from this study except for total discharge at HMP (USGS, 2011) and hourly rainfall (NOAA, 2011a).

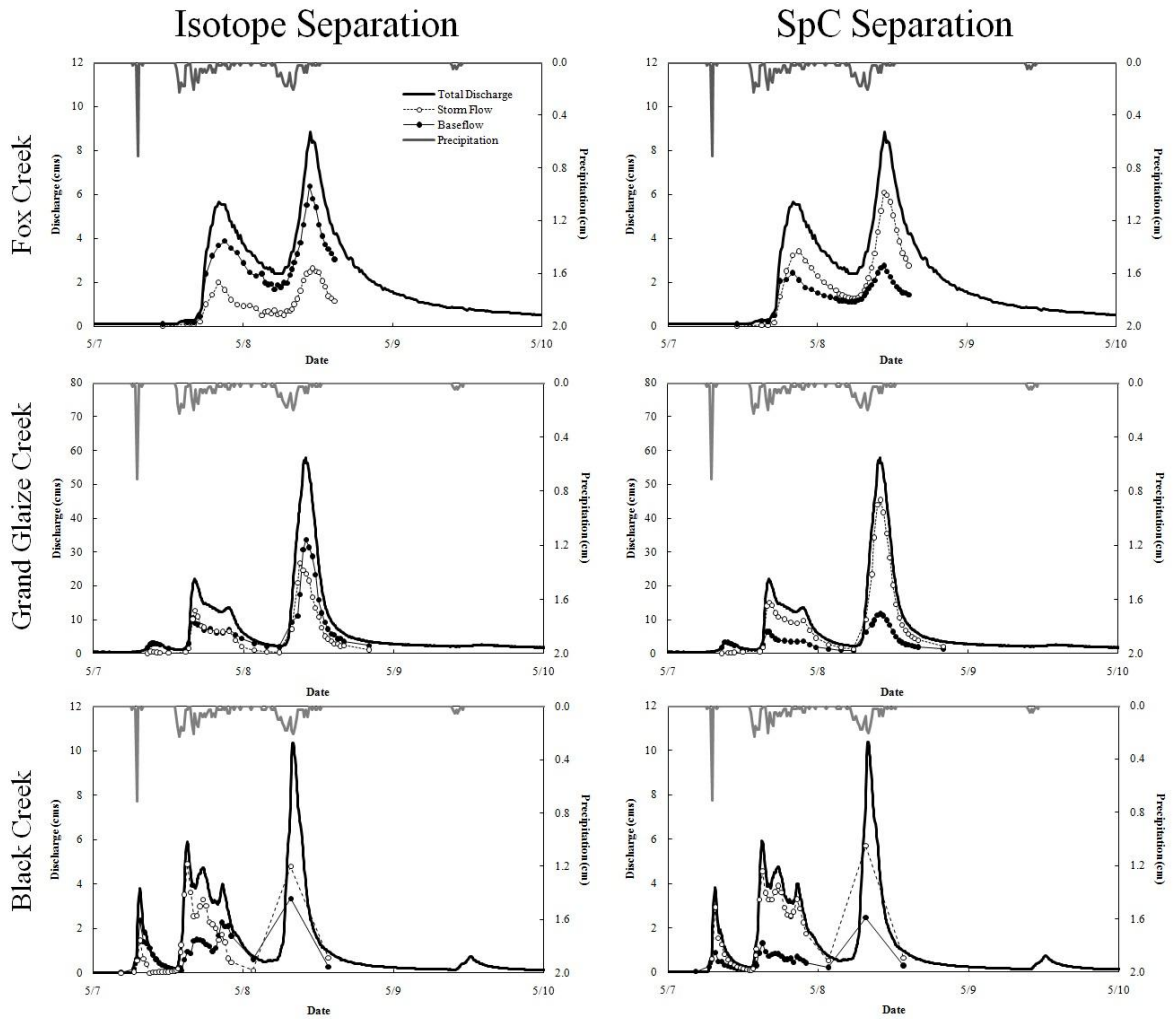


Figure 3.21. Isotope (first column) and SpC (second column) hydrograph separation comparison for the May 2008 storm perturbation at Fox, Grand Glaize, and Black Creeks. The results consistently demonstrate that the baseflow fraction is highest in the rural Fox Creek watershed. The hydrograph separation for SpC was made assuming that measurements of the pre-event stream water are typically of baseflow and that “event water” has a value of $100 \mu\text{S}/\text{cm}$. Discharge data from USGS (2011).

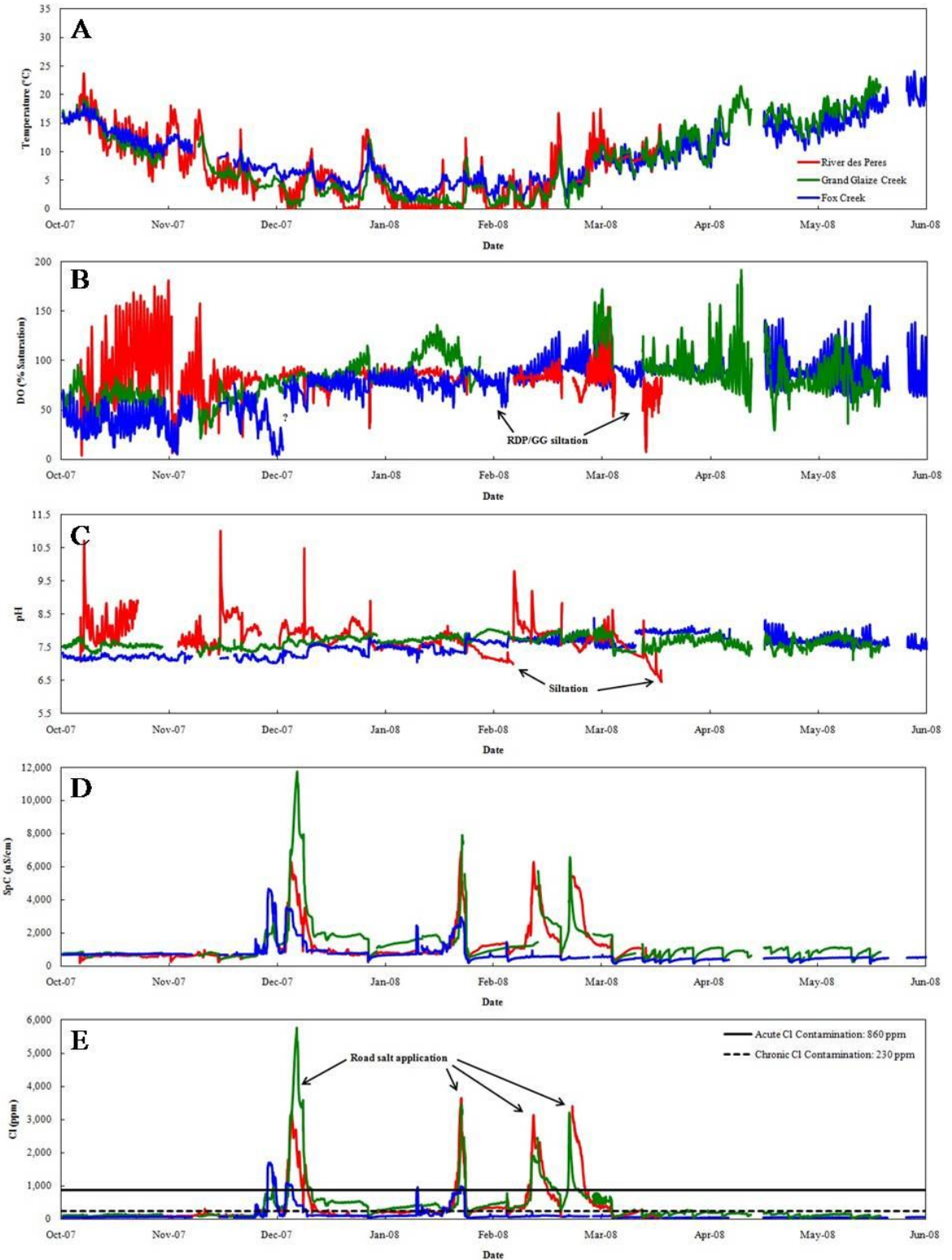


Figure 3.22. A portion of continuous monitoring data for Fox Creek (blue), Grand Glaize Creek (green), and the River des Peres (red) for October 2007 to June 2008. Several parameters are shown including: (A) temperature; note that Fox Creek never reaches freezing temperatures; (B) DO, on several occasions siltation at the Grand Glaize Creek and River des Peres installation sites caused damage to the DO sensor; (C) pH, during siltation events pH decreases and on the rising limb of discharge pulses the pH increases in the River des Peres for unknown reasons; (D) SpC; and (E) Cl, observe several road salt applications that also correlate to SpC spikes. Background levels of Cl in Grand Glaize Creek and River des Peres are frequently over EPA's chronic contamination level (230 ppm), and during periods of road salt application, Cl concentrations exceed regulatory limits for acute Cl contamination (860 ppm) by nearly an order of magnitude for all the basins.

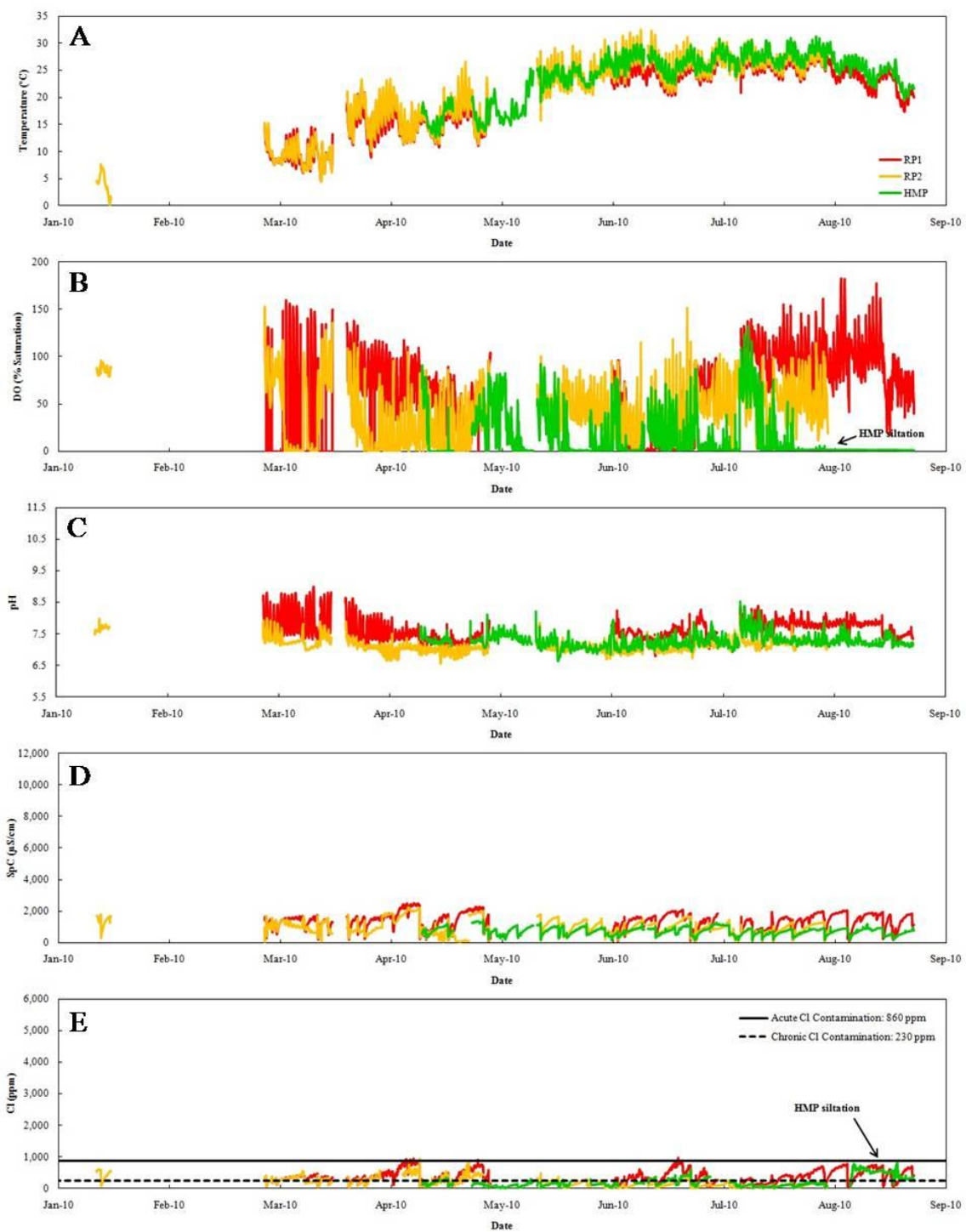


Figure 3.23. A portion of continuous monitoring data for RP1 (red), RP2 (yellow), and HMP (green) for part of January 2010 and all of March through September 2010.

Sensors could not be deployed during the winter months because the stream froze solid at these sites. There is also a portion of data missing for the RP1 site when continuous monitoring sensor electronics were damaged by water leaks. Several parameters are shown including: (A) temperature; (B) DO, on several occasions siltation caused anoxia in sensor housing unit; (C) pH, during siltation events pH decreases; (D) SpC; and (E) Cl, observe that the Cl concentration remains above regulatory limits for chronic Cl contamination (230 ppm) even in the spring and summer months, and on several occasions exceeds the acute Cl contamination level (860 ppm). This indicates extensive Cl contamination of the shallow groundwater.

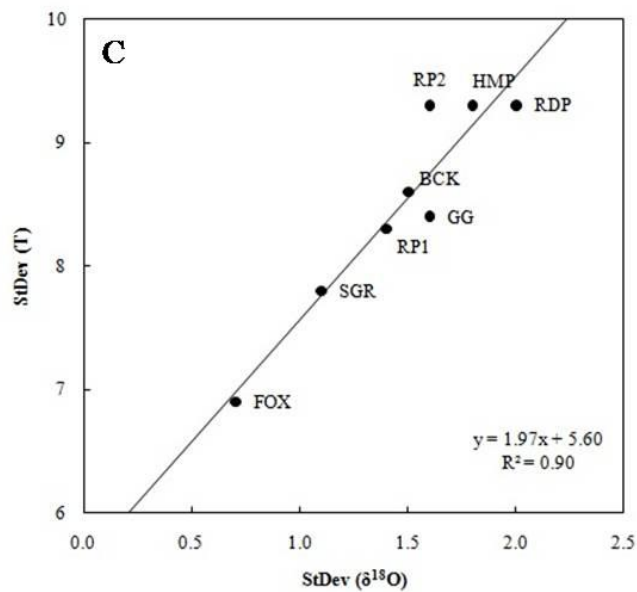
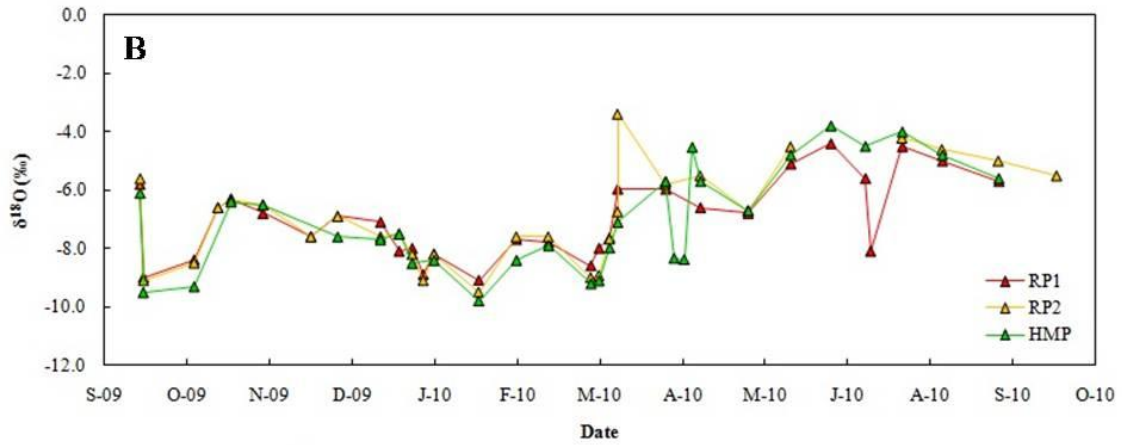
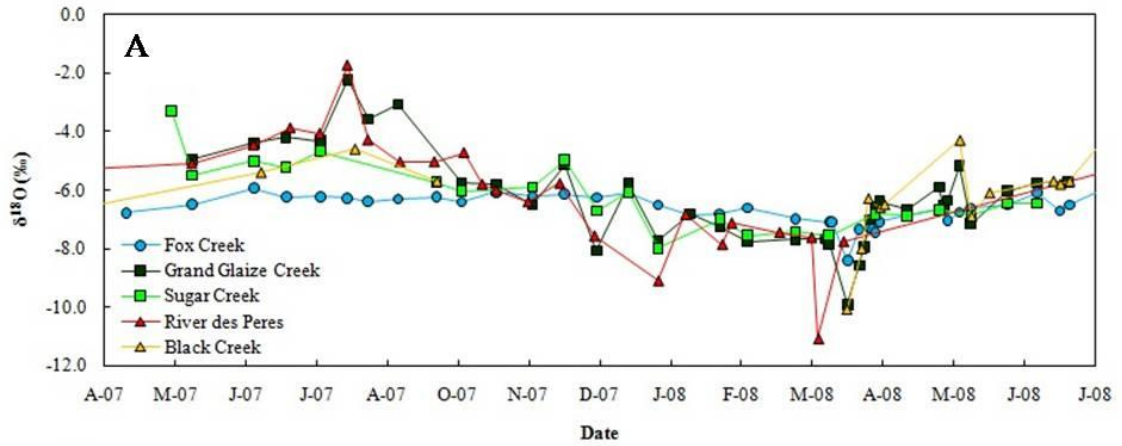


Figure 3.24. Seasonal isotopic data from grab samples at (A) Fox Creek (blue), Grand Glaize Creek (dark green), Sugar Creek (light green), River des Peres (red), and Black Creek (orange) from April 2007 to July 2008 and (B) RP1 (red), RP2 (yellow), and HMP (green) from September 2009 to October 2010. (C) The standard deviation for temperature is plotted against the standard deviation of $\delta^{18}\text{O}$ for the monitored sites, quantitatively illustrating a correlation between the extent of urbanization in the watershed and the amount of physical and isotopic variability.

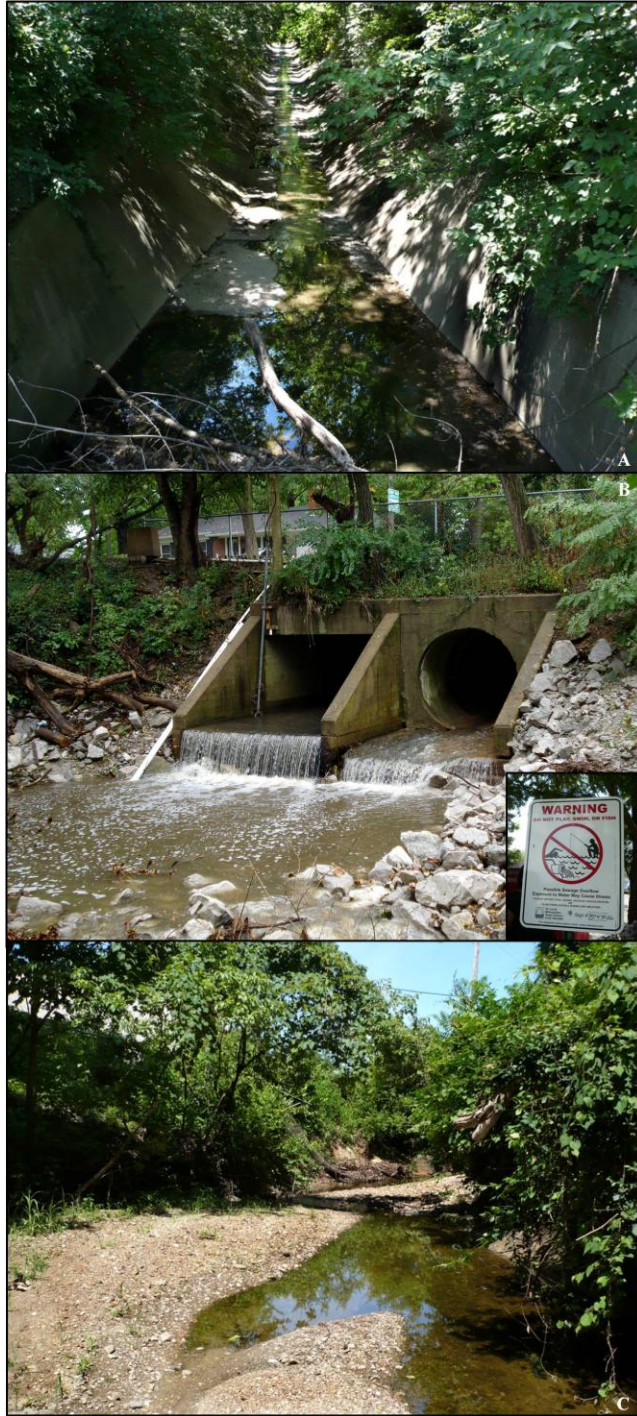


Figure 3.25. The Southwest Branch of the Upper River des Peres: (A) looking upstream of the McKnight Rd. monitoring site (photo by Elizabeth Hasenmueller); (B) the McKnight Rd. monitoring site, with an inset of the CSO warning posted by MSD (note the white PVC pipe along the culvert, which is part of the sampling installation; large photo by Robert Criss, inset by Elizabeth Hasenmueller); and (C) the second monitoring installation in Ruth Park (photo by Elizabeth Hasenmueller). The banks are highly incised, but the stream is not as heavily modified as it is upstream.

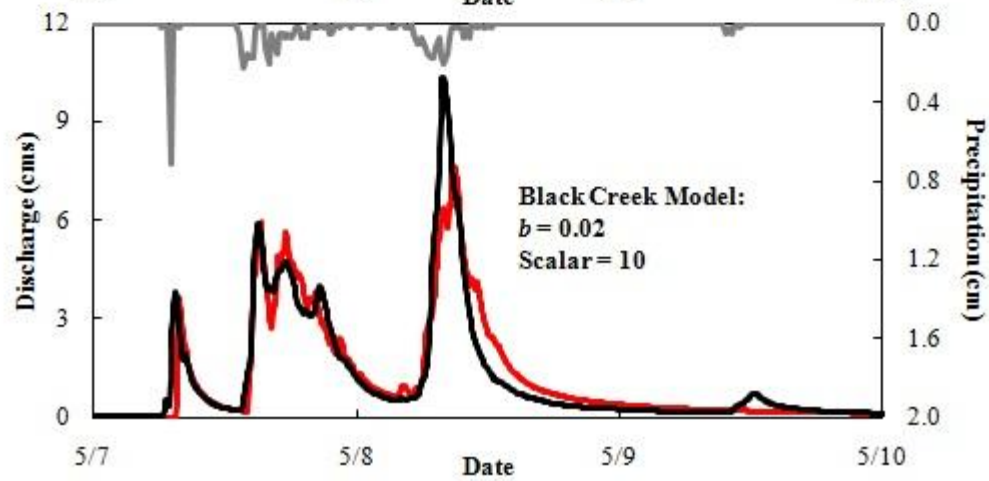
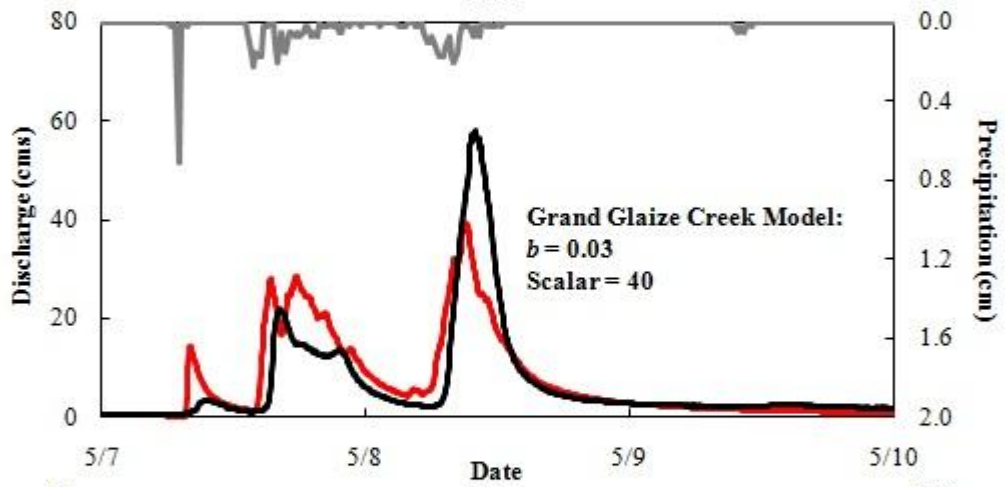
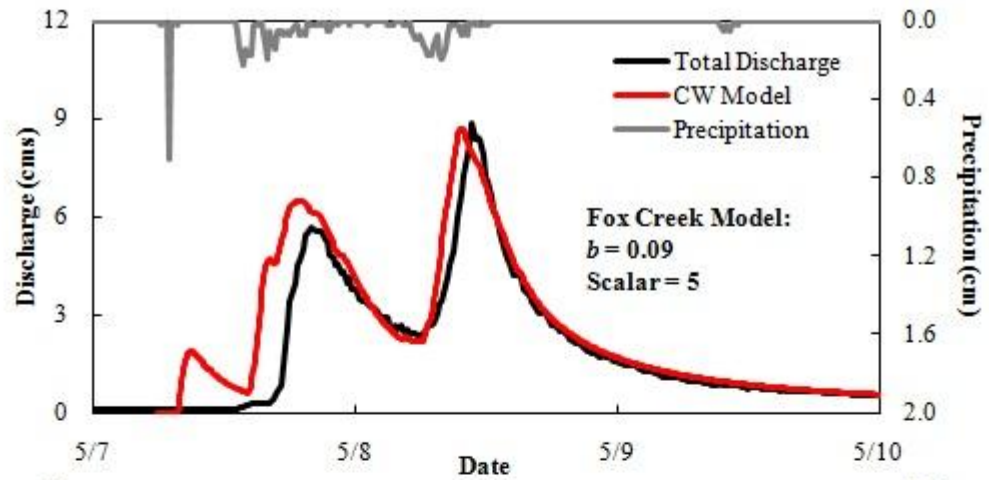


Figure 3.26. Graphs illustrating the measured (black line; USGS, 2011) and predicted (red line; see equations in Chapter 2) discharge variations of Fox Creek (top), Grand Glaize Creek (middle), and Black Creek (bottom) for the same May 2008 precipitation event. Note the differing b values used for the rainfall-runoff models.

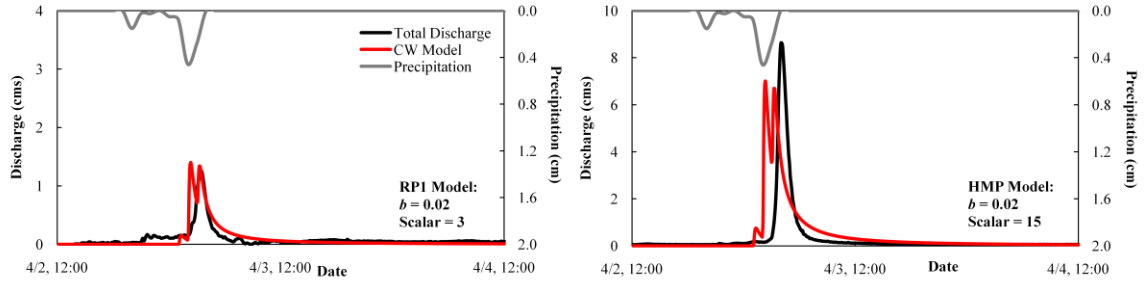


Figure 3.27. Graphs illustrating the measured (black line) and predicted (red line; see equations in Chapter 2) discharge variations of RP1 (left) and HMP (right) for the same April 2010 precipitation event. Note that the b values are the same despite the difference in basin area.

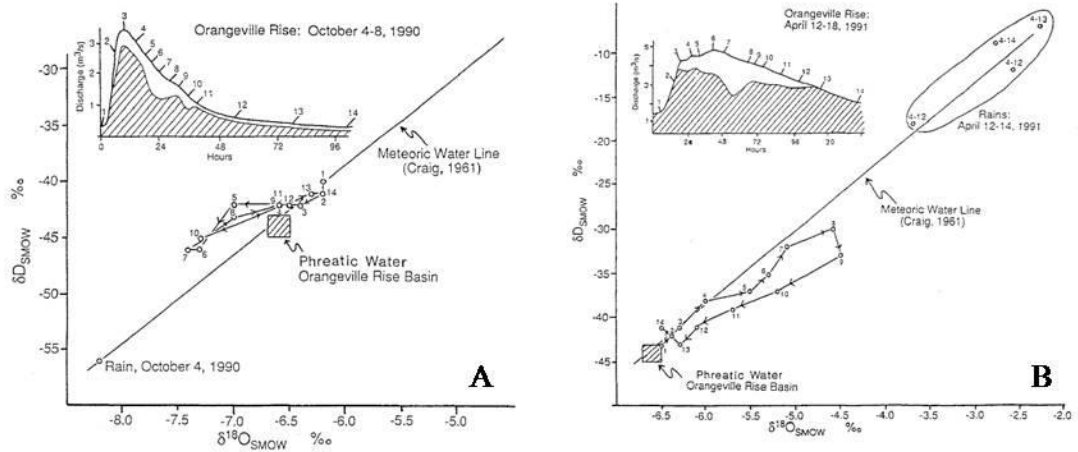


Figure 3.28. Lakey and Krothe (1996). The isotopic hydrograph separation of storm flow and $\delta D - \delta^{18}O$ plots for an (A) October 1990 and (B) April 1991 discharge event at the Orangeville Rise, a perennial spring in south central Indiana. The open circles on the $\delta D - \delta^{18}O$ plot show the isotopic progression throughout the storm perturbation (as indicated by the numbers next to the circles and arrows) and shaded areas indicate phreatic water contributions.

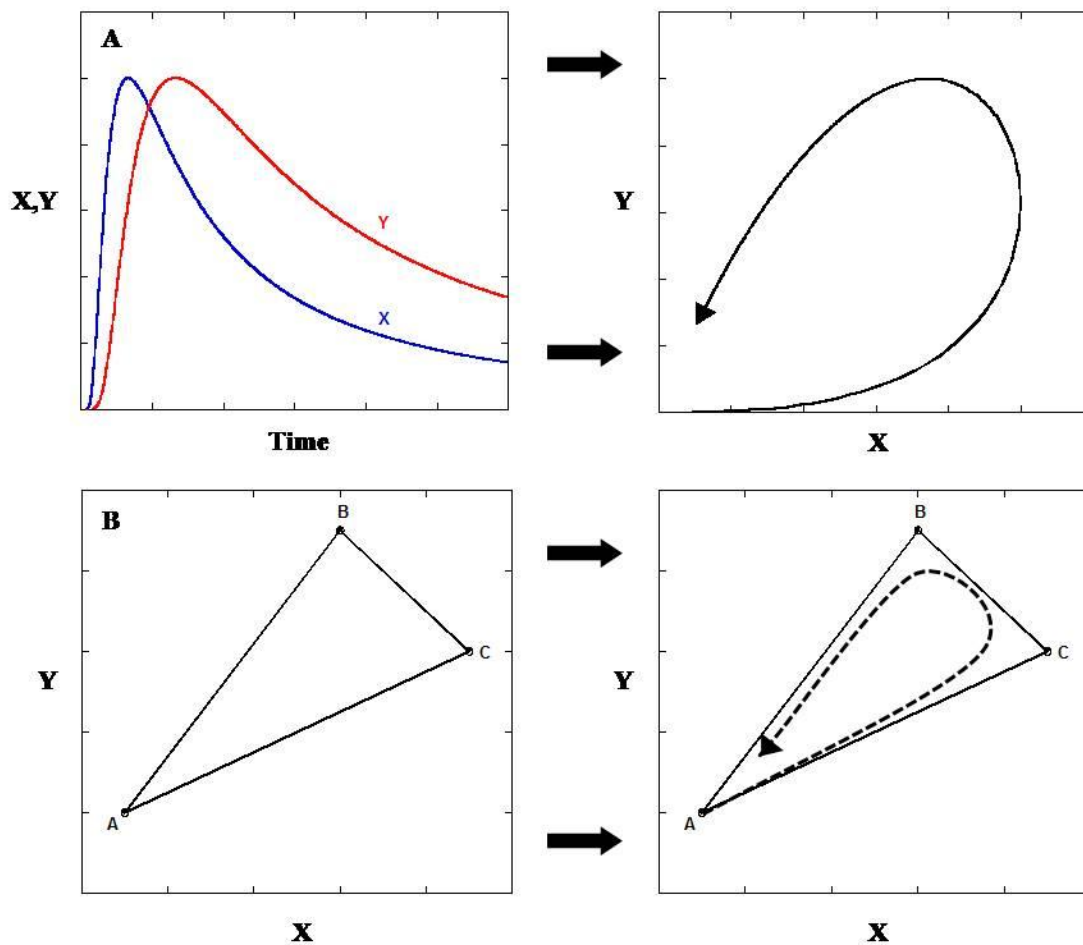


Figure 3.29. Possible causes of hysteresis: (A) Timing differences between parameters X and Y can result in hysteresis loops in an X-Y plot and (B) mixing of multiple components can allow for numerous paths, by individually varying relative proportions of end members A, B, and C. The area inside the triangle represents all mixing combinations of the three end members.

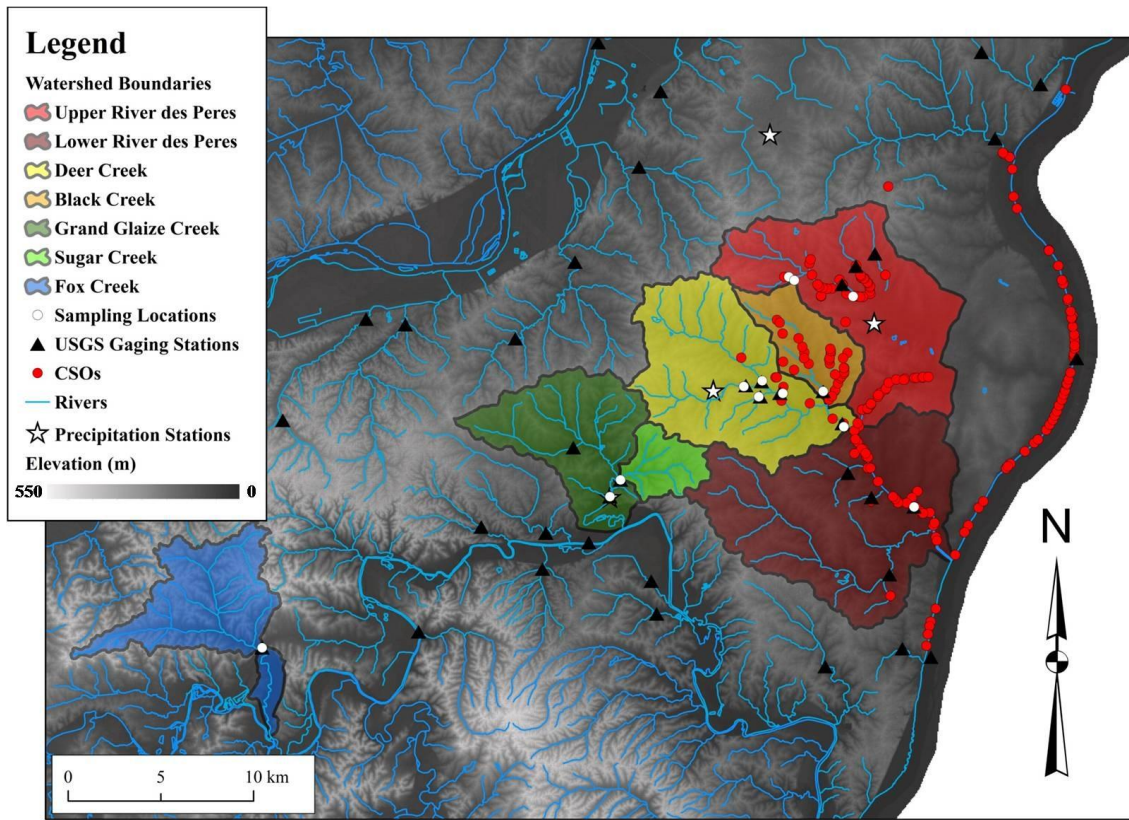


Figure 3.30. CSO locations in St. Louis City and County (MSD, 2011).

Chapter 4: Determining the source of boron in east-central Missouri surface waters and groundwaters

Abstract

Previous studies have attributed high B levels in streams and groundwaters to wastewater and fertilizer inputs. However, this study shows that urban irrigation waters can contribute substantially to the geochemical character of surface waters and groundwaters in the St. Louis, MO area. A variety of freshwater environments in east-central Missouri were sampled, including surface runoff, streams, rivers, several dozen springs that represent local shallow groundwaters, and potential B end-member sources including local rainfall samples, wastewaters, and fertilizers. Urban surface waters and groundwaters are enriched with respect to B (up to almost 250 ppb) compared to background levels (< 25 ppb) found in pristine carbonate-hosted streams and springs. Municipal drinking waters derived from the Missouri River have a high average B concentration (259 ppb) and are used to irrigate urban lawns, a practice that contributes substantial loads of B to local waters. The B concentrations in St. Louis area waters correlate well with ions characteristic of municipal tap water. Detailed storm series show that B decreases with increased discharge; thus, elevated B levels are not primarily derived from combined sewer overflows (CSOs) during flooding. Instead, the B is associated with the baseflow fraction, derived from the shallow groundwater reservoir that through time has accumulated B from lawns irrigated with drinking water.

4.1. Introduction

Sources of anthropogenic contamination in natural waters are often difficult to decipher because many natural and anthropogenic sources may contribute to loads. B makes an ideal tracer of anthropogenic input because it behaves conservatively, is highly soluble, and is found in low concentrations in most natural waters (Christ and Harder, 1978; Barth, 1998). B concentrations in surface waters vary widely, but in most cases the concentration of B in a given aquatic environment is dominated by anthropogenic contributions (Neal et al., 1998; Wyness et al., 2003).

4.1.1. Sources of B

B occurs naturally as borax, borates, boric acid ($B(OH)_3$), and certain borosilicates. Natural sources of B in surface and groundwaters are predominantly derived from weathering of B-bearing minerals from host rock and soil. The highest observed B concentrations in natural waters are a result of the leaching of B-bearing salt deposits (Christ and Harder, 1978). Italy (e.g., Sasso), Turkey (e.g., Kirka and Emet), and California (e.g., Kramer District) have the largest quantities of B-bearing rock, mostly in the form of Na-borates, and groundwaters in these regions can contain B in excess of 100 ppm (Waggott, 1969; Harben and Bates, 1984). The Turkish and American deposits were formed in Neogene lacustrine environments that had proximal volcanic activity (Harben and Bates, 1984; Palmer and Helvacı, 1995). Weathering of igneous rocks can also produce elevated B concentrations in local waters (Christ and Harder, 1978). In coastal areas, rain containing sea salt from ocean spray provides another natural B source, but the importance of this source declines with increasing distances from the coast (Jahiruddin et al., 1998). Thus, because the majority of the

interior of the United States has few B-bearing lithologies, most natural, unpolluted waters have low average B concentrations of 10 – 20 ppb (Drever, 1997; Langmuir, 1997).

Mobilization of B is highly dependent on soil pH (Yermiyahu et al., 1995). B is most readily available to plants in acid soils, but is likewise most easily leached from these soil types. Soluble B is present mostly as $B(OH)_3$, which is formed when borax dissociates in dilute solutions; the acid itself does not readily dissociate (Brady and Weil, 2008). $B(OH)_3$ can exchange with the OH groups on the edges and surfaces of variably charged clays like kaolinite and especially on Fe and Al oxides at circum neutral pH. $B(OH)_3$ interaction with hydrous Fe oxides occurs by both physical adsorption and ligand exchange reactions (Peak et al., 2003), and both Palmer et al. (1987) and Peak et al. (2003) concluded that because physically bound $B(OH)_3$ can be readily leached, it moves with the flow of soil water. Evidence of B mobility in soils has been confirmed by Stueber and Criss (2005).

Elevated B levels in surface waters most commonly occur in industrial and urban areas. Anthropogenic B is introduced into aqueous environments through several sources, including bleaching agents in detergents and soaps, fertilizers, insecticides, glass manufacturing, $B(OH)_3$ solutions for the control of nuclear reactions, the production of fire retardant materials, corrosion inhibitors in antifreeze for cooling systems, ceramics, cosmetics, production of leather, carpets, metal and brazing agents, landfill leachates, coal mine leachates, fly ash, and petroleum products (Waggott, 1969; Adriano et al., 1980; Davidson and Bassett, 1993; Hebblethwaite and Emberson, 1993; Vengosh et al., 1994; Bassett et al., 1995; Barth 1998; Hogan and Blum, 2003; Bayless et al., 2004;

Chetelat and Gaillardet, 2005). Organic-rich sources of B include sewage sludge, manure, compost, and similar materials (Waggott, 1969). Because $B(OH)_3$ has mild bactericidal and fungicidal properties, it is sometimes used as a food preservative, and it can also be used for weed control (Waggott, 1969). There are many other applications for B, but most of these do not result in increased B concentrations in natural waters.

Among these numerous possible sources, wastewaters enriched in B from bleaching agents and fertilizers that contain B as a micronutrient for plants are considered to be the largest sources of anthropogenic B to riverine and groundwater environments (Waggott, 1969; Barth, 1998; Chetelat and Gaillardet, 2005; Neal et al., 2010). The concentrations and isotopic composition of B have been used to trace municipal, agricultural, industrial, slag, landfill leachate, and irrigation contamination in several studies (Davidson and Bassett, 1993; Vengosh et al., 1994; Bassett et al., 1995; Leenhouts et al., 1998).

4.1.1.1. Wastewaters

Industrial and domestic effluents are extremely enriched in B, with concentrations varying from several hundred ppb to several ppm (Barth, 2000; Fox et al., 2000). By far the most common reason for this enrichment is the use of sodium perborate, which is added to bleaching agents in detergents and cleaning products. These perborate compounds are discharged with domestic aqueous effluents into sewage treatment plants, where little or no B is removed during the conventional processing of the waste waters (Waggott, 1969; Stueber and Criss, 2005; this study). Previous authors have asserted that almost the entire anthropogenic B load is released into the environment through the wastewater treatment process (Vengosh et al., 1994; Bassett et al., 1995; Barth, 1998;

Chetelat and Gaillardet, 2005; Neal et al., 2010). Vengosh et al. (1994) used boron isotopes to determine that the Coastal Plain aquifer of Israel was contaminated with sewage effluent. A study of B isotopic composition of the Seine River in France showed high B concentrations around Paris were a result of wastewaters, while lower B concentrations in the headwaters were from agricultural inputs, although the B isotopic composition of the fertilizers was not well constrained (Chetelat and Gaillardet, 2005).

4.1.1.2. Fertilizers

Cultivated soils are often deficient in macro- and micronutrients, and it becomes necessary to fertilize the soil to maintain the proper ranges of these elements for plants. B is an essential micronutrient for plants that activates dehydrogenase enzymes, facilitates sugar translocation and synthesis of nucleic acids and plant hormones, and is essential for cell division and development. Consequently, B is sometimes a necessary additive to fertilizer in B-deficient soils (Brady and Weil, 2008), and the most common form of B used in fertilizers is borax (Bohn et al., 2001).

Few studies have dealt with B-bearing fertilizer contributions to natural waters, but those that have found that contributions of B from fertilizers are generally small. Trauth and Xanthopoulos (1997) measured average B concentrations of 40 ppb in agricultural runoff, Stueber and Criss (2005) observed B concentrations as high as 52 ppb in agricultural runoff in Illinois, and Chetelat and Gaillardet (2005) observed agricultural inputs of 10 to 20 ppb in the headwaters of the Seine River. However, Wyness et al. (2003) found that rivers in agricultural areas of southeastern England can have average B concentrations of almost 400 ppb. They note that the surrounding watersheds have

relatively low rainfall and high evapotranspiration, and therefore, these rivers have low dilution potential.

Because B is taken up by plants as an essential micronutrient, there can be slight changes in B concentrations in vegetated areas that can affect this tracer. This is a minimal factor in groundwater systems, but potentially is more important for surficial waters (Marschner, 1986).

4.1.2. Use of B Isotopes

Previous studies have relied predominantly on B isotopes to determine sources of B contamination (Davidson and Bassett, 1993; Vengosh et al., 1994; Barth, 1998; Hogan and Blum, 2003; Bayless et al., 2004). An isotopic approach can be used successfully to decipher anthropogenic B contributions in a given aquatic environment if the background B signal is distinct from the anthropogenic source. The isotopic composition of B used in detergents and fertilizers depends mainly on the origin of the borates, and studies of B isotopes in borate deposits report ranges of -17‰ to 1‰ for the Turkish Kirka deposit and -25‰ to -8‰ for the Turkish Emet deposit (Palmer and Helvaci, 1997). American borates from the Kramer deposit range from -8‰ to 3‰ (Swihart et al., 1996).

However, constraining B inputs from wastewaters, fertilizers, and other exotic sources can be difficult given that often the same B source material is used for multiple purposes in industry, including fertilizers and detergents, and in other cases, mixtures of parent materials result in intermediate isotopic ranges (Barth, 1998). Previous studies indicate the B isotopic composition in wastewaters and fertilizers do not have consistent ranges: Vengosh et al. (1994) found that wastewaters had B isotopic compositions of 10 to 20‰ and fertilizers ranged from -15 to 7‰; Bassett et al. (1995) found that

wastewaters ranged from 6 to 10‰, and Chetelat and Gaillardet (2005) found almost the exact opposite, where wastewaters were around -10‰ and fertilizers ranged from 10 to 15‰.

4.1.3. Urban Irrigation

Irrigation is often an important part of the urban soil moisture balance. Turf grasses are the most commonly used type of plant in residential and commercial landscape and have high water requirements (Haley, 2007). Irrigation protocols for these grasses as well as urban gardens are very different in urban settings compared to agricultural areas, with significantly higher application rates for amenity land uses such as golf courses and gardens (Lerner, 2002). Irrigation systems are common in many residential communities, urban parks, golf courses, and other landscaped areas.

Despite the relatively humid climate in Missouri, with an average precipitation rate of 97 cm/year (National Oceanic and Atmospheric Administration; NOAA, 2011) and an evapotranspiration rate of 71 cm/year (Vandike, 1995), lawn irrigation is quite common and accounts for up to 60% of the household water use in St. Louis, averaging 443 L per home per day (City of St. Louis Water Division, 2011). This is similar to irrigation rates in drier areas such as Utah, where Aurasteh et al. (1984) found that homeowners used 61% of their total water supply for irrigation. Much of this water is wasted, and previous studies regarding water use indicate that irrigation water in residential landscapes is often excessively applied. Barnes (1977) found that residential irrigation rates range from 122% to 156% of the seasonal evapotranspiration (ET) rate (more than 150 cm/year) in two Wyoming cities. No research is known that identifies the

significance of localized recharge from irrigation waters in urban areas. However, it is very likely that significant localized recharge from lawn irrigation occurs in urban areas.

The City of St. Louis Water Division maintains two water treatment plants that draw water from the Mississippi and Missouri Rivers. The Chain of Rocks Plant is located on the Mississippi River 8 km south of the confluence of the Missouri and Mississippi Rivers. While the plant is located on the Mississippi River, the water intake is located on the side where the Missouri River joins the Mississippi River. Due to slow mixing between the two rivers, intake water for the Chain of Rocks Plant has the isotopic and chemical character of the Missouri River rather than the Mississippi River (Criss, 1999). The second plant (e.g., the Howard Bend Treatment Facility), is located on the Missouri River, 60 km above the confluence of the Missouri and Mississippi Rivers. Thus, the majority of the municipal drinking water supply has the chemical and isotopic character of the Missouri River.

4.1.4. Study Design

A monitoring network for the determination of non-point sources of surface water pollution in the urban areas of St. Louis was implemented and operated from March 2009 to July 2011, and B concentrations were monitored for a year within that period. The main concept of the network lay in the collection of a consistent series of samples that define temporal variations of surface water quality and the relationship between B concentrations and anthropogenic pollutants derived from non-point sources. This study uses B concentrations along with a suite of other elements to identify urban irrigation input in streams and springs in east-central Missouri. Careful analyses of end-member concentrations were used to distinguish sources of B, rather than relying on highly

variable isotopic compositions for these waters. The study shows that irrigation waters have a substantial input to the River des Peres, which drains the majority of the St. Louis City and County, as well as other surface waters and shallow groundwaters. As discussed previously, B has largely been associated with wastewater input to urban streams; however, this work demonstrates that the prevailing source of B in small urban streams and springs in the St. Louis metropolitan area is institutional and homeowner lawn irrigation rather than sewer leaks, CSO contributions, or fertilizer applications. Along with B, a suite of other physical and chemical water quality parameters were analyzed in this study. The results show that B trends systematically match those of the major elements, demonstrating that B is related to baseflow and is indicative of the input of municipal drinking water sources in the local surface waters and groundwaters.

4.2. Description of Study Sites

4.2.1. Continuously Monitored Sites

Two sets of sites were continuously monitored in the River des Peres watershed. Three sites were selected along the Upper River des Peres to capture the variations in B concentrations in surface waters, and three additional sites in the River des Peres basin were selected to monitor the B concentrations in surface runoff.

4.2.1.1. Upper River des Peres

The River des Peres is a highly impacted urban stream that drains 214 km² (see Chapter 3) of the City of St. Louis and parts of St. Louis County, MO. The subsurface lithology is dominated by carbonates, which are B-poor. Biweekly water samples were collected from three sites in the Upper River des Peres watershed (Figures 4.1, 4.2) and analyzed for a suite of parameters (see Chapter 2). The sites were also continuously

monitored (at 5-min intervals) using automated YSI 6600 V2 Sondes for multiple water quality parameters (see Chapters 2 and 3). Grab samples were augmented by rapid sequence sampling by autosamplers during storm perturbations. One of the autosampler units used to collect discharge events (at the most upstream sampling location, Figures 4.1, 4.2) was outfitted with an ultrasonic stage sensing module to measure stage (see Chapter 2). The most downstream site was proximal to the River des Peres at University City, MO U.S. Geological Survey (USGS) gaging station (station number 07010097) that monitored stage and discharge data for this site.

4.2.1.1.1. Ruth Park 1 (RP1)

Ruth Park 1 (RP1) is located in Ruth Park, University City, MO. The site is located at the McKnight Rd. culvert and has a contributing drainage area of 2.8 km². Upstream of the monitoring site the stream flows through cement-walled channels, resulting in rapid changes in discharge during storm perturbations as evidenced by extensive erosion of the rehabilitated channel in Ruth Park. There is one combined sewer overflow upstream of the site.

4.2.1.1.2. Ruth Park 2 (RP2)

Ruth Park 2 (RP2) is also located in Ruth Park about 320 m downstream of RP1. In the 320 m reach between the two stations, the stream occupies a more natural channel that allows stream water to communicate with the local groundwater. The natural stream bed slows the water velocity because of the rougher bed, and channel incision is not as severe at this site. Upstream of the monitoring site is a mulching operation that intermittently contributes leachate to the stream above the monitoring station. Leachate discharge volume ranged from zero during dry conditions to about 0.3 cms (30 L/s)

following precipitation events of 2.5 cm or more. The site also receives surface runoff from a golf course.

4.2.1.1.3. *Heman Park (HMP)*

The Heman Park monitoring station (HMP) is farthest downstream (4.5 km), located below the confluence of the Southwest Branch, the Upper River des Peres main stem, and an unnamed tributary. There are 11 CSO locations upstream of the site including the one upstream of RP1 (Metropolitan St. Louis Sewer District; MSD, 2011). Several sections of the upstream reaches are channelized, but the stream bed in Heman Park is unlined. The channel is deeply entrenched and a Gabian wall has been installed to prevent further erosion. Total drainage area upstream of the site is 23.2 km².

4.2.1.2. Surface Runoff

Surface runoff from three small (< 2 ha) suburban areas in the western River des Peres watershed was also monitored (Figures 4.1, 4.2). Sites were selected to reflect a variety of land development, including street runoff from residential and institutional land use. Surface runoff discharge was measured with pressure transducer stage sensors and water samples were collected by autosamplers at the three locations from November 2009 to July 2011. Samples were collected at storm sewer inlet; site descriptions are summarized in Table 4.1 and described below.

4.2.1.2.1. *10920 Chalet Court (CHA)*

Chalet Court is a suburban neighborhood in the Deer Creek watershed where yard erosion is occurring at a storm pipe outlet. The total drainage area at the monitoring site is 3,500 m² (UTM coordinates: 0724457, 4282986, elevation: 188 m). Surface runoff is

predominantly composed of street runoff, but there are contributions from the nearby residential yards.

4.2.1.2.2. 8360 Cornell Avenue (CORN)

Homes along Cornell Avenue are located within a suburban neighborhood, where the storm water flow path is behind the homes. Surface runoff at this site is comprised exclusively of yard runoff, and the total drainage area at the monitoring site is 4,300 m² (UTM coordinates: 0730272, 4282615, elevation: 167 m). The home at the lowest point of the neighborhood has experienced repeated yard flooding and other yards have experienced erosion.

4.2.1.2.3. Mt. Calvary Church and Adjacent Neighborhood (MTC)

Mt. Calvary Church and its adjacent suburban neighborhood are located near a developed area of Brentwood, MO. The total drainage area at the monitoring site is 15,100 m² (UTM coordinates: 0729913, 4277911, elevation: 148 m). The monitoring location drains the church's parking lot and a large soccer field. The low-lying neighborhood homes that are in the storm water flow path have experienced repeated yard and structure flooding.

4.2.2. Grab Sample Sites: Surface Waters, Groundwaters, and End-members

In addition to the continuously monitored sites, water samples from several other St. Louis area streams, rivers, springs, resurgences, and lakes were collected on multiple occasions between June and October 2010 (Figure 4.1). These samples represent a broad range of catchment size and land development, and were collected under a range of hydrologic conditions including both low and high flow conditions. Springs sampled for this study have mean discharges ranging from about 0.0001 to 4.1 cms, which represent

effective catchment areas that vary from about 0.01 to 430 km² (Vineyard and Feder, 1982). Sampled rural and suburban stream mean discharges range from approximately 0.07 to 0.4 cms, which represent catchment areas that vary from about 10 to 45 km². Additionally, samples from the large Mississippi and Missouri Rivers were also collected. Water samples were collected at 38 springs, seven streams, two rivers, one lake, and one pond in the St. Louis area. In addition, potential B end-member sources were also sampled, and include wood ash, fertilizers, road salt melt runoff, agricultural runoff, wastewaters (from the St. Louis, MO, treatment plants operated by MSD: Coldwater Creek, Missouri River, Grand Glaize, Lemay, Bissell Point, Lower Meramec, and Fenton Treatment Plants and two St. Charles, MO, treatment plants: Duckett Creek Plants 1 and 2), and meteoric precipitation.

4.2.3. Additional Data

B data collected in this study were augmented by archived data maintained by the USGS for a number of regional sites. Composite samples monitored by the Howard Bend and Chain of Rocks Water Treatment Plants provide data for the Missouri River and treated water from the two plants.

4.3. Methods

Field sampling techniques, field equipment specifications and periods of operations, laboratory procedures, and data processing procedures are outlined in Chapter 2. The complete set of analytical data collected during this project is too large for tabulation here. Selected data and statistical summaries of B concentrations in various waters are presented in Table 4.2, 4.4-4.6. A copy of the entire analytical dataset can be found in Appendices F-H, K, and L.

V-notch weirs were installed alongside the stage monitoring devices at the surface runoff monitoring locations. The weirs were used to calculate discharge with the empirically-derived relationship (Fetter, 2001):

$$Q = 1.389H^{5/2}$$

where Q is discharge (m^3/s) and H is the height of the backwater above the weir crest (m).

Because *Escherichia coli* (*E. coli*) and total coliform colonies were chronically off-scale for stream and wastewater samples using the IDEXX Colilert reagent and 97-well Quanti-Tray® (most probable number range limit of 1 to 2420 cfu/100 mL) system, even after diluting samples 1:20, the Coliscan® EasyGel® agar plate system was used to count the *E. coli* and total coliform colonies. Wastewater aliquots of 1 to 10 μL were added to agar gel mix and incubated for 24 hours.

4.4. Results and Discussion

4.4.1. Regional B Concentrations

To determine sources of B for local waters, a suite of water samples including urban and rural surface waters and groundwaters, runoff samples, lakes, ponds, and wastewaters along with other potential B sources were collected and analyzed for this study (Table 4.2). These data were compared to archives of USGS B analyses in various water bodies throughout Missouri. Unpolluted waters in central Missouri that exhibited minimal agricultural and urban development (Figures 4.1, 4.2) had an average B concentration of 25 ppb (Table 4.2), close to the global average of 20 ppb (Drever, 1997; Langmuir, 1997). USGS measurements of rural surface waters and groundwaters typically had values less than 20 ppb, confirming the naturally low concentrations of B in

Missouri waters. The USGS statewide average, including both rural and urban areas, was 33 ppb.

In this study, surface and groundwater samples collected from the suburban and urban areas of St. Louis had B values ranging from natural background levels to almost 250 ppb in the River des Peres. The B concentrations in phreatic and vadose springs ranged from 20 to 120 ppb, rural and suburban streams ranged from 31 to 46 ppb, and a lake was slightly above regional background levels (28 ppb; Table 4.2). The shallow groundwaters in the St. Louis metropolitan area had higher B levels than their rural counterparts, indicating the anthropogenic inputs of B to these systems. The relationships between B and discharge, B end-members, and sources for elevated B concentrations in regional waters are discussed in the following sections.

4.4.2. Relationship between B Concentrations and Discharge

4.4.2.1. Urban Watersheds: The River des Peres

The River des Peres had the highest concentrations of B of all the surface streams and groundwater samples, and the average B concentrations were 88 ppb at RP1, 92 ppb at RP2, and 129 ppb at HMP (see Table 4.2). The B concentration was positively correlated with specific conductivity (SpC) and the other major elements (including Ca, Mg, K, and Na, among others; Figure 4.3), indicating that B concentrations were associated with the baseflow fraction of stream flow, and B concentrations are diluted with increased discharge following rainfall.

This result is confirmed by a time series of samples collected during a discharge event on April 2 – 3 (Figure 4.4; see Chapter 3 for more detail). The initial B concentration was approximately the same at the RP1 and RP2 stations; however, the

concentration at the most downstream site, HMP, was 154 ppb; almost 80 ppb higher than the upstream sites. All stations experienced B dilution, and the lowest value observed at RP1 and RP2 was 23 ppb, while the minimum B value observed at HMP was 35 ppb during the flooding event. The dilution trend demonstrates the relatively low contribution of B from rainfall, and indicates that elevated B concentrations originate from baseflow.

A more detailed representation of the relationship between B concentrations and discharge is illustrated in the Figure 4.5). Here, the B concentrations in the River des Peres sites are plotted against the dynamic variations in flow. Again, concentrations are highest during low flow and become diluted during flood perturbations. This result is in agreement with observations made by Wyness et al. (2003), who found that B concentrations in a suite of English and French rivers were highest under low flow conditions and were diluted with increasing flow. The authors concluded that this reflects the dilution of urban point sources, such as wastewater effluent, with increased flow; however, findings in this study indicate that non-point sources of B are responsible, as discussed in more detail in subsequent sections.

4.4.2.2. Surface Runoff

This study observed unusually high concentrations of B in surface runoff, with an average of 58 ppb for a residential area (CORN) and 89 ppb for institutional and residential land use (MTC). Concentrations of B in surface runoff following rainfall events at these sites were extremely variable, ranging from 33 – 69 ppb at CORN and from 28 ppb to extraordinarily high values of 246 ppb for MTC. High B levels in runoff samples for these sites were observed at the onset of overland flow during the initial

flushing event, and were followed by dilution. Figure 4.6 demonstrates typical B behavior in surface runoff at both of the sites, where B concentrations are initially high and positively correlated to SpC and are then followed by dilution. When B concentrations were plotted against discharge, a trend similar to the one observed at the River des Peres was noted (Figure 4.5B).

4.4.2.3. Examples of Positive Correlations between B and Discharge

In contrast to the negative correlation between B concentration and discharge observed in this study, Winston and Criss (2004) found that the B levels for Bluegrass Spring, a perennial karst spring 40 km west of St. Louis, were positively correlated with discharge and negatively correlated to SpC and other major ions. They also found that the B values were relatively low in Bluegrass Spring (14 – 33 ppb) under a range of discharge conditions (e.g., 1.4 – 280 L/s). The authors concluded that the positive correlation of B with discharge was likely associated with the event water and its path, and that B could be mobilized by pulses of acidic soil water. Measurements of Bluegrass Spring in this study yielded similar results with B concentration ranging from 37 – 38 ppb during average flow conditions (8.5 L/s).

A positive correlation between discharge and B was also found in a study on several Illinois springs and streams (Stueber and Criss, 2005). Surface runoff into a sinkhole from a large agricultural field planted in corn and soybeans had an average B concentration of 52 ppb, higher than the mean B level of 23 ppb for the nearby Auctioneer and Camp Vandeventer Springs and 30 ppb for Fountain, Bond, and Andy's Run Creeks (Stueber and Criss, 2005). Concentrations of B at Auctioneer Spring covaried with discharge, and during high flow events B levels as high as 45 ppb were

observed, confirming the immediate source from fertilizers applied to the nearby agricultural fields (Stueber and Criss, 2005).

Differences between this study and the Winston and Criss (2004) and Stueber and Criss (2005) studies are likely a result of lower B loads in the other authors' study areas, and the lack of lawn irrigation at those sites. The lowest B concentrations found in surface runoff and the River des Peres are about the same as the maximum values observed during peak discharge in the previous studies.

4.4.3. B Sources and End-members

4.4.3.1. Atmospheric Deposition

Previous studies have found that the major global sources of atmospheric B are volcanic emissions and sea salt aerosol production, but in urban areas, atmospheric concentrations of B can be elevated by coal burning (Fogg and Duce, 1985). However, this study found that B levels in rainwater were relatively low (24 ppb; Table 4.2), and close to the average B concentrations found in uncontaminated surface and groundwaters in this study, demonstrating that meteoric deposition cannot explain the high B levels in St. Louis streams. Moreover, surface runoff samples collected 10 km east (e.g., downwind) of the Ameren Missouri coal-fired power plant in Labadie, MO, had B values of 21 ppb, indicating that B contributions from coal fly ash to surface and groundwaters are not large in this area.

4.4.3.2. Road Salt Contamination

Road salt contamination during the winter in the area is a chronic problem (see Chapters 3 and 5). Street runoff was collected from the CHA monitoring site during a winter snow melt event to test whether road salt is a significant B source. Runoff

collected immediately following snow melt was highly enriched in Na and Cl from road salting activities, and SpC was 36,000 $\mu\text{S}/\text{cm}$, which corresponded to high Na and Cl values of 13,457 ppm and 13,875 ppm, respectively. The B concentration, however, was only slightly elevated (57 ppb) considering that the SpC level was almost 25 times higher than normal background for the River des Peres watershed, and Na and Cl levels were more than 40 times higher. This indicates that road salt contamination is not the primary source of elevated B levels in urban streams such as the River des Peres.

4.4.3.3. Organic Rich Leachates

Leachate from a mulching operation located 30 m from the RP2 study site showed elevated levels of B (301 to 492 ppb). However, leachate from the mulching operation had a maximum flow rate of less than 0.03 cms, and therefore, could contribute only a small volume to the River des Peres, which had peak discharges of more than 9 cms at RP2. It should also be noted that when there were large volumes of runoff discharging from the mulching facility, these waters were substantially diluted with recent rainfall. Furthermore, the average B concentration for the site upstream of the mulching facility was 92 ppb during low flow conditions and is similar to that of the site downstream of this facility (88 ppb), demonstrating the minimal effect of this operation on the B concentration in the Southwest Branch of the Upper River des Peres. The leachate also had substantially different relationships between B and $\text{SO}_4^{2-}\text{-S}$ as well as B and Zn (Figure 4.7A, D), with the leachate having lower average $\text{SO}_4^{2-}\text{-S}$ values and higher average Zn values than the RP2 monitoring station.

4.4.3.4. Wastewaters

Elevated B levels were found in municipal wastewaters. Two treatment plants in St. Charles had an average B composition of 240 ppb, while the seven treatment plants operated by MSD that serve St. Louis and the surrounding metropolitan area had an average value of 247 ppb for the influent and 285 ppb for the effluent (Tables 4.2, 4.4).

St. Louis wastewater samples were collected from the entry points of the main sewer lines that carry influent into the seven wastewater treatment facilities. Additional samples from both the St. Charles and St. Louis treatment plants were collected from the post-treatment plant effluent lines (Table 4.3, 4.4), and permitted comparison of influent and effluent concentrations, revealing any changes due to the sewage treatment processes. The ultimate source of the bulk of the water in the sanitary sewer lines is the St. Louis municipal water supply provided by the Howard Bend and Chain of Rock Facilities to the Coldwater Creek, Missouri River, Grand Glaize, Lemay, and Bissell Point Treatment Plants. The Fenton and Lower Meramec Treatment Plants receive water from municipal sources from the Meramec River, which can clearly be observed in their different $\delta^{18}\text{O}$ values (Table 4.3).

The B concentrations in water samples from the wastewater treatment plant effluent were consistent with the B concentrations in the influent. B concentrations in both the influent and effluent were surprisingly similar to the concentrations in municipal water samples from the Missouri River collected in this study, which indicates that B loads in the drinking water also contribute to the B load in wastewaters. Fe, Al, Li, and Zn are all elevated in wastewater influent, but Fe, Al, Cu, and Zn are reduced in the finished water. The NO_3^- -N concentration in plant effluent was more than an order of

magnitude larger than that in any of the influent sewer lines and exceeded the U.S. Environmental Protection Agency (EPA) maximum contaminant level (MCL) of 10 ppm for drinking water (U.S. Environmental Protection Agency; EPA, 2011). This high concentration was related to the aeration process that regulates the amount of NH_4^+ produced by the microbial decomposition of organic matter during sewage treatment.

Na and Cl concentrations in water samples from the combined sewer lines were comparable with those in treatment plant effluents but were elevated considerably above the Na and Cl levels in municipal supply water (Table 4.2, 4.3). Thus, appreciable amounts of Na and Cl have been added during the use of the supply water. Additional contributions of Na and Cl come from the treatment process and MSD's Grand Glaize Plant uses sodium hypochlorite for sterilization by chlorination and sodium bisulfite for dechlorination; all of the plants operated by MSD use ferrous chloride for flocculation. Still, the Na and Cl concentrations in the wastewaters are significantly less than those found in urban surface and groundwaters and the River des Peres has on average twice the Na and Cl concentrations of the wastewaters.

While wastewaters are potentially important B-rich end-members, none of the receiving waters for the effluents from these treatment plants are located in the River des Peres watershed or in the rest of the study area. The receiving waters are typically large, and include the Mississippi River, Missouri River, Meramec River, and Coldwater Creek. Therefore, wastewater effluent is not a B source in the River des Peres, and the only viable sources of wastewater in the River des Peres are CSOs and sewer leaks. There are CSOs located upstream of the River des Peres sampling sites (Figures 4.1, 4.2); however, CSOs debauch during high flow conditions when B concentration would be diluted with

storm water. Further, there are no CSOs or sanitary sewers located in drainage areas of the surface runoff monitoring sites. Thus, CSOs are not sources for increased B concentrations in surface runoff and are not likely to be the major source for elevated B concentrations in the River des Peres.

4.4.3.5. Fertilizers

Another possible B end-member that was examined in this study was B-bearing fertilizers. Initially, it was thought that B in lawn fertilizers may significantly influence the concentration of B in surface runoff, and subsequently, in the receiving surface waters and shallow groundwaters. However, the analyses of several household fertilizers commonly used for turf grasses, along with analyses by the Oregon Department of Agriculture (2010) of agricultural fertilizers (Table 4.5), revealed an insignificant concentration of B in surface runoff when the dilution factor of fertilizer with rainfall is considered. Leenhouts et al. (1998) reached a similar conclusion when examining the B isotope ratios of irrigation waters recharging groundwater in Avra Valley, Arizona, where higher B concentrations were attributed to the use of wastewaters for irrigation rather than from fertilizers used on the agricultural fields.

Urban fertilizer application and intensity are more variable than in agricultural landscapes, with fertilized areas (lawns) occupying discrete portions of the landscape and application rates varying with the preferences of multiple land managers. Analyses suggested that the fertilizer application rate is affected by social economic factors (including market value of the house and age of development) and soil characteristics (including soil bulk density and soil nitrogen contents).

There are no known studies of contributions of B from urban lawn fertilizers, though application rates of B-containing fertilizers are likely similar to or less than agricultural application rates (Gold et al., 1990; Liu et al., 1997). A study by Law et al. (2004) found a wide range in the application rates of N-fertilizers to residential lawns, golf courses, and public parks. Survey data from the study estimated a mean annual fertilizer application rate of 97.6 kg/ha with a standard deviation of 88.3 kg/ha. This rate can be used to estimate the average load of B from fertilizers. If one assumes an application rate of 97.6 kg/ha, that the fertilizer with the highest B concentration is used (Miracle-Gro; 0.06%; Table 4.5), and that the average rainfall in the area is 100 cm/year, then fertilized lawn runoff would have a B concentration of approximately 6 ppb, substantially less than what is observed. Further, because the monitoring operations require close cooperation from homeowners and institutions, it is known that there has been no fertilizer application in the homeowners' yards at CORN and at the church soccer field at MTC. The application rates in other portions of the drainage areas to the sites are unknown.

4.4.3.6. Lawn Irrigation

Measurements of tap water from several locations in River des Peres watershed were made in this study ($n = 10$). The average B concentration in these waters was 259 ppb (Table 4.2), one of the highest concentrations of all the B end-members. It should be noted that this concentration is twice as high as those observed by the Howard Bend Treatment Plant (Table 4.2). This disparity may be due to the shorter time frame in which samples were collected for this study. As mentioned before, lawn irrigation can be a substantial portion of household water use (on average 443 L/day per household),

meaning that these municipal waters could potentially contribute up to 0.42 kg/ha of B annually (compared to the estimated 0.06 kg/ha contributed annually from fertilizers; see pervious section). The relationships of B with SO_4^{2-} -S, Li, Na, and Zn (Figure 4.7A-D) clearly demonstrate that the concentration of B in surface runoff, surface streams, and groundwaters are related to municipal irrigation waters. Figure 4.7A shows that the municipal drinking waters and wastewaters from the Missouri River and the Missouri River itself have a similar trend in B and SO_4^{2-} -S contents to that of local surface runoff, surface streams, and shallow groundwaters, demonstrating that local groundwaters have developed a chemical signature similar to the Missouri River. Similarly, data collected by Stueber and Criss (2005) show that the Mississippi River and wastewaters from the Waterloo Treatment Plant in Illinois (which are derived from Mississippi River municipal sources) have a distinct relationship between B and SO_4^{2-} -S.

4.4.3.6.1. B Concentrations along the Missouri River

Concentrations of B along the Missouri River were determined by compiling USGS data from sites along the river (Table 4.6). The upper Missouri River has about the same concentration of B as the lower Missouri River near Hermann, MO. However, a sharp increase in B contents occurs just below the confluence of the Missouri and Yellowstone Rivers (Figure 4.8), and B remains high in the monitoring stations along the large reservoirs in the Dakotas. A dilution trend is observed downstream of the reservoirs, which asymptotically approaches a value of about 55 ppb, appropriate for lower basin waters. Again, B concentrations in the Missouri River measured by the USGS at Hermann, MO, are half the concentration measured in this study, and this may be due to the longer USGS sampling period.

High B concentrations in the Missouri River are likely derived from natural rock weathering in the basin, although wastewater treatment plants along the river may provide additional inputs. However, these contributions should be relatively small (less than 2%). For example, the MSD operated Bissell Point and Lemay Wastewater Treatment Plants continuously discharge an average of 11 cms and 15 cms (MSD, 2011) into the Mississippi River, respectively, and the average discharge of the Mississippi River at St. Louis is 5,500 cms (USGS, 2011). Thus, wastewater effluent comprises less than 1% of the flow for the Mississippi River. Similarly, no more than a few percent of the flow of the Missouri River could be wastewater effluent. Other B contributions in the Missouri River watershed may come from B-rich fertilizers.

4.5. Conclusions

This study has established the regional B concentrations in surface runoff, surface streams and rivers, and springs representative of the shallow groundwater using a large suite of B data generated by this study, which was augmented by data from the Howard Bend and Chain of Rocks Water Treatment facilities and by regional USGS data. Previous studies have largely attributed high concentrations of B to treated wastewaters, sewer leaks, and fertilizer use. However, in the study area, treated wastewaters are debauched into large rivers and are unable to directly affect their upstream tributaries. Moreover, CSO and sewage contributions of B are impossible at the small, residential runoff sites as these features do not exist at these sites. Wastewater contributions are also unlikely to be the dominant B source in local creeks, where B contributions from CSOs would only occur during heavy storms when their B contents would be highly diluted by ordinary storm water runoff. Fertilizer contributions were also found to be unlikely

sources due to the trace amounts of B they contain; other studies have confirmed that B concentrations in agricultural field runoff are small.

The work establishes that municipal drinking waters derived from the Missouri River retain and possibly augment the high B concentrations in the river, and may have an average concentration of more than 250 ppb. Urban lawn irrigation in the area comprises up to 60% of household water use, and the B-rich irrigation water contributes large amounts of B to surface waters and groundwaters. The highest levels of B were observed during low flow conditions, when applications of irrigation water would be necessary. B likely accumulates as residual salts in the irrigated soils and soil water. These salts are rapidly flushed out during precipitation events, with the first runoff having the highest B concentrations.

4.6. References

- Adriano, D.C., Page, A.L., Elseewi, A.A., Chang, A.C., and Straughan, I., 1980, Utilization and disposal of fly ash and other coal residues in terrestrial ecosystems, a review: *Journal of Environmental Quality*, v.9, p. 333-344.
- Aurasteh, M.R., Jafari, M., and Willardson, L.S., 1984, Residential lawn irrigation management: *Transactions of the American Society of Agricultural Engineers*, v. 27, p. 470-472.
- Barnes, J.R., 1977, Analysis of residential lawn water use [Master thesis]: Laramie, University of Wyoming, 78 p.
- Barth, S.R., 1998, Application of boron isotopes for tracing sources of anthropogenic contamination in groundwater: *Water Research*, v. 32, p. 685-690.
- Barth, S.R., 2000, Utilization of boron as a critical parameter in water quality evaluation: implications for thermal and mineral water resources in SW Germany and N Switzerland: *Environmental Geology*, v. 40, p. 73-89.
- Bassett, R.L., Buszka, P.M., Davidson, G.R., and Chong-Diaz, D., 1995, Identification of groundwater solute sources using boron isotopic composition: *Environmental Science & Technology*, v. 29, p. 2,915-2,922.
- Bayless, E.R., Bullen, T.D., and Fitzpatrick, J.A., 2004, Use of $^{87}\text{Sr}/^{86}\text{Sr}$ and $\delta^{11}\text{B}$ to identify slag-affected sediment in southern Lake Michigan: *Environmental Science & Technology*, v. 38, p. 1,330-1,337.
- Bohn, H. L., McNeal, B.L., and O'Connor, G.A., 2001, *Soil chemistry*: New York, N.Y., John Wiley and Sons, 307 p.
- Brady, N., and Weil, R., 2008, *The nature and properties of soils*, 14th ed.: Upper Saddle River, New Jersey, Prentice Hall, 975 p.
- Chetelat, B., and Gaillardet, J., 2005, Boron isotopes in the Seine River, France: A probe of anthropogenic contamination: *Environmental Science & Technology*, v. 39, p. 2,486-2,493.
- Christ, C.L., and Harder, H., 1978, Boron, in Wedepohl, K.H., ed., *Handbook of geochemistry*, v. II/1, elements H(1) to Al(13): Berlin, Springer, p. 5-A-1-5-O-10.
- City of St. Louis Water Division, 2011, St. Louis Water Division: Water Treatment Web page, <http://www.stlwater.com/>.
- Criss, R.E., 1999, *Principles of stable isotope distribution*: Oxford, Oxford University Press, 254 p.

Criss, R.E., Davisson, M.L., and Kopp, J.W., 2001, Nonpoint sources in the lower Missouri River: *Journal of American Water Works Association*, v. 93, p. 112-122.

Davidson, G.R., and Bassett, R.L., 1993, Application of boron isotopes for identifying contaminants such as fly ash leachate in groundwater: *Environmental Science & Technology*, v. 27, p. 172-176.

Drever, J.I., 1997, *The geochemistry of natural waters: Upper Saddle River, New Jersey*, Prentice Hall, 436 p.

Fetter, C.W., 2001, *Applied hydrogeology*, 4th ed.: Upper Saddle River, New Jersey, Prentice Hall, 598 p.

Fogg, T.R., and Duce, R.A., 1985, Boron in the troposphere: distribution and fluxes: *Journal Geophysical Research*, v. 90, p. 3,781-3,796.

Fox, K.K., Daniel, M., Morris, G., and Holt, M.S., 2000, The use of measured boron concentration data from the GREATER-ER UK validation study (1996-1998) to generate predicted regional boron concentrations: *Science of the Total Environment*, v. 251-252, p. 305-316.

Gold, A.J., DeRagon, W.R., Sullivan, W.M., and Lemunyon, J.L., 1990, Nitrate-nitrogen losses to groundwater from rural and suburban land uses: *Journal of Soil and Water Conservation*, v. 45, p. 305-310.

Haley, M.B., Dukes, M.D., and Miller, G.L., 2007, Residential irrigation water use in central Florida: *Journal of Irrigation and Drainage Engineering*, v. 133, p. 427-434.

Harben, P.W., and Bates, R.L., 1984, *Geology of the non-metallics: New York*, Metal Bulletin Inc., 392 p.

Hebblethwaite, R.L., and Emberson, P., 1993, Rising from the ashes: *Landscape Design*, v.10, p. 31-34.

Hogan, J.F., and Blum, J.D., 2003, Boron and lithium isotopes as groundwater tracers: a study at the Fresh Kills Landfill, Staten Island, New York, USA: *Applied Geochemistry*, v. 18, p. 615-627.

Jahiruddin, M., Smart, R., Wade, A.J., Neal, C., and Cresser, M.S., 1998, Factors regulating the distribution of boron in water in the River Dee catchment in north east Scotland: *Science of the Total Environment*, v. 210-211, p. 53-62.

Langmuir, D., 1997, *Aqueous environmental geochemistry: Upper Saddle River, New Jersey*, Prentice Hall, 600 p.

Law, N.L., Band, L.E., and Grove, J.M., 2004, Nutrient input from residential lawn care practices: *Journal of Environmental Planning and Management*, v. 47, p. 737-755.

Leenhouts, J., Bassett, R. L., and Maddock, T., 1998, Utilization of intrinsic boron isotopes as co-migrating tracers for identifying potential nitrate contamination sources: *Ground Water*, v. 36, p. 240-250.

Lerner, D.N., 2002, Identifying and quantifying urban recharge: a review: *Hydrogeology Journal*, v. 10, p. 143-152.

Liu, H., Hull, R.J., and Duff, D.T., 1997, Comparing cultivars of three cool-season turfgrasses for soil water NO_3^- concentration and leaching potential: *Crop Science*, v. 37, p. 526-534.

Marschner, H., 1986, Mineral nutrition of higher plants, 1st ed.: Waltham, Massachusetts, Academic Press, 651 p.

Metropolitan St. Louis Sewer District, 2011, Metropolitan St. Louis Sewer District: Metropolitan St. Louis Sewer District Web page, <http://www.stlmsd.com/home>.

Missouri Spatial Data Information Service. Data Resources (MSDIS), 2011, Missouri Spatial Data Information Service: University of Missouri Web site, <http://www.msdis.missouri.edu>.

Neal, C., Fox, K.K., Harrow, M.L., and Neal, M., 1998, Boron in the major UK rivers entering the North Sea: *The Science of the Total Environment*, v. 210-211, p. 41-52.

Neal, C., Williams, R.J., Bowes, M.J., Harrass, M.C., Neal, M., Rowland, P., Wickham, H., Thacker, S., Harman, S., Vincent, C., and Jarvie, H.P., 2010, Decreasing boron concentrations in UK rivers: Insights into reductions in detergent formulations since the 1990s and within-catchment storage issues: *Science of the Total Environment*, v. 408, p. 1,374-1,385.

National Oceanic and Atmospheric Administration (NOAA), 2011, National Weather Service (NWS) Weather: NWS Web page, <http://www.weather.gov/>.

Oregon Department of Agriculture, 2010, Oregon Department of Agriculture: Fertilizer Program Web page, <http://oregon.gov/oda/pest/fertilizer.shtml>.

Palmer, M.R., and Helvacı, C., 1995, The boron isotope geochemistry of the Kirka borate deposit, western Turkey: *Geochimica and Cosmochimica Acta*, v. 59, p. 3,599-3,605.

Palmer, M.R., and Helvacı, C., 1997, The boron isotope geochemistry of the Neogene borate deposits of western Turkey: *Geochimica and Cosmochimica Acta*, v. 61, p. 3,161-3,169.

Palmer, M.R., Spivack, A., and Edmond, J.M., 1987, Temperature and pH controls over isotopic fractionation during adsorption of boron on marine clay: *Geochimica et Cosmochimica Acta*, v. 51, p. 2,319-2,323.

Peak, D., Luther, G.W., III, and Sparks, D.L., 2003, ATR-FTIR spectroscopic studies of boric acid adsorption on hydrous ferric oxide: *Geochimica et Cosmochimica Acta*, v. 67, p. 2,551-2,560.

Stueber, A.M., and Criss, R.E., 2005, Origin and transport of dissolved chemicals in a karst watershed, southwestern Illinois. *Journal of American Water Resources Association*, v. 41, p. 267-290.

Swihart, G.H., McBay, E.H., Smith, D.H., and Siefke, J.W., 1996, A boron isotopic study of a mineralogically zoned lacustrine borate deposit: the Kramer deposit, California, U.S.A.: *Chemical Geology*, v. 127, p. 241-250.

Trauth, R., and Xanthopoulos, C., 1997, Non-point pollution of groundwater in urban areas: *Water Research*, v. 31, p. 2,711-2,718.

U.S. Department of Agriculture, 2011, USDA Web Soil Survey: Web Soil Survey Web page, <http://websoilsurvey.nrcs.usda.gov/app/HomePage.htm>.

U.S. Environmental Protection Agency, 2011, Drinking water contaminants: Drinking water contaminants Web page, <http://water.epa.gov/drink/contaminants/index.cfm>.

U.S. Geological Survey, 2011, USGS Real-time data for Missouri: USGS Real-time data for Missouri Web page, <http://waterdata.usgs.gov/mo/nwis/rt>.

Vandike, J.E., 1995, Surface water resources of Missouri (Missouri State Water Plan Series - Volume 1): Missouri Department of Natural Resources Water Resources Report 45, 121 p.

Vengosh, A., Heumann, K. G., Juraske, S., and Kasher, R., 1994, Boron isotope application for tracing sources of contamination in groundwater: *Environmental Science & Technology*, v. 28, p. 1,968-1,974.

Vineyard, J., and Feder, G.L., 1982, Springs of Missouri: Missouri Department of Natural Resources Water Resources Report 29, 266 p.

Waggott, A., 1969, An investigation of the potential problem of increasing boron concentrations in rivers and watercourses: *Water Research*, v. 3, p.749-765.

Winston, W.E., and Criss, R.E., 2004, Dynamic hydrologic and geochemical response in a perennial karst spring: *Water Resources Research*, v. 40, W05106.

Wyness, A.J., Parkman, R.H., and Neal, C., 2003, A summary of boron surface water quality data throughout the European Union: *The Science of the Total Environment*, v. 314-316, p. 255-269.

Yermiyahu, U., Keren R., and Chen, Y., 1995, Boron sorption by soil in the presence of composted organic matter: *Soil Science Society America Journal*, v. 59, p. 405-409.

Table 4.1. Site descriptions for runoff sampling locations.

Parameter	10920 Chalet Ct.	8360 Cornell Ave.	Mt. Calvary Church
Type of Land Use Influencing Runoff	Residential Yards and Streets	Residential Yards	Institutional: Playing Field and Parking Lot
BMP Drainage Area (m ²)	3,500	4,300	15,100
Soil Unit*	60223: Urban land-Harvester complex, 9 to 20 percent slopes 60190: Menfro-Urban land complex, 5 to 9 percent slopes	60223: Urban land-Harvester complex, 9 to 20 percent slopes	60224: Urban land-Harvester complex, karst, 2 to 9 percent slopes
Soil Hydrologic Unit	D†	D†	D†
Number of septic tanks	0	0	0

*Soil data from the U.S. Department of Agriculture (USDA; 2011).

†Group D: Soils in this group have high runoff potential when thoroughly wet. Water movement through the soil is restricted or very restricted. Group D soils typically have > 40% clay, < 50% sand, and have clayey textures. All soils with a depth to a water impermeable layer less than 50 cm and all soils with a water table within 60 cm of the surface are in this group. Group D is common in the study area.

Table 4.2. Average values for various water quality parameters for surface runoff, municipal drinking and wastewaters, surface streams, groundwaters, runoff, and other potential B end-members.

Feature	Description	Number of Measurements	SpC (µS/cm)	pH	B (ppb)	Ca (ppm)	Mg (ppm)	Na (ppm)	Cl (ppm)	Si (ppm)	K (ppm)	NO ₃ ⁻ -N (ppm)	PO ₄ ³⁻ -P (ppm)	SO ₄ ²⁻ -S (ppm)	Al (ppb)	Fe (ppb)	Li (ppb)	Cu (ppb)	Zn (ppb)
Rainwater	St. Louis	10	54	4.78	24	6.7	0.5	0.9	0.6	0.2	0.4	0.0	0.01	1.9	37	5.3	0.2	13.9	28.5
Runoff	Near Labadie Power Plant	2	523	7.82	21	41.7	13.8	8.0	12.0	5.7	4.5	-	0.50	2.5	420	49.2	0.7	8.0	83.9
	Parking Lot and Field (MTC)	126	406	8.3	89	37.3	7.6	26.0	55.1	3.5	6.5	0.5	0.23	10.9	87	19.3	3.1	2.8	16.6
	Residential (CORN)	25	178	7.55	58	20.8	4.3	5.5	5.6	3.1	12.8	0.1	0.54	2.8	200	23.1	2.2	6.9	41.0
	Agricultural Runoff*	43	-	-	52	26.1	6.3	2.7	17.4	-	24.0	11.5	3.70	1.1	-	-	-	6.3	9.9
	Street Runoff (CHA)	1	110	7.38	37	12.9	2.1	12.0	2.8	2.8	3.9	0.2	0.26	2.4	228	20.3	1.8	3.3	10.2
	Street Runoff (WU)	1	-	-	88	31.9	9.0	32.6	32.6	6.1	2.8	-	0.07	26.8	226	42.4	35.2	22.2	206.0
	Road Salt-Rich Melt Waters	1	36,000	7.38	57	71.3	15.7	13,457	13,875	1.8	152.5	0.0	0.46	17.6	116	54	68.5	351.8	36.4
Municipal Water	Tap Water	15	558	9.74	259	20.1	16.4	65.6	16.0	3.1	8.1	0.5	0.04	58.5	0.39	10.5	104.9	96.7	26.4
	Howard Bend	28	417	9.51	150	24.0	13.7	34.4	23.0	6.2	5.7	1.5	0.01	38.1	0.01	0.004	-	-	-
	Chain of Rocks	28	412	9.18	100	22.8	15.1	34.4	23.7	6.0	5.8	1.7	0.01	37.3	0.01	0.003	-	-	-
Wastewaters	St. Charles Effluent	3	797	8.15	146	54.3	17.0	73.5	72.0	5.2	11.7	11.4	1.06	24.6	12	19.6	8.9	3.1	44.1
	St. Louis Influent	7	932	-	247	47.5	22.2	125.3	39.4	4.8	19.6	1.0	1.70	58.0	673	343.0	70.1	15.3	734.3
	St. Louis Effluent	7	810	-	285	40.3	20.4	113.1	87.9	5.0	18.4	12.4	1.26	48.1	66	81.8	73.3	10.1	367.0
	Monroe Co., IL Effluent*	7	-	-	430	66.6	21.7	94.0	129.0	-	15.8	9.9	2.48	25.0	-	-	-	8.3	73.0
Local Waters	RP1 (Grab)	40	1,570	8.21	88	93.4	25.3	217.2	287.5	5.1	6.4	1.1	0.07	31.1	22	29.0	11.7	5.4	28.0
	RP2 (Grab)	34	1,484	8.08	92	91.9	24.6	202.6	298.5	4.8	9.1	1.2	0.09	29.9	13	31.4	11.8	5.4	20.1
	HMP (Grab)	29	1,383	8.21	129	73.2	19.6	231.4	273.1	4.0	6.5	0.7	0.03	28.4	22	24.8	13.2	5.4	28.9
	Suburban Streams	9	483	7.9	43	63.0	11.7	34.2	24.4	4.1	3.5	1.0	0.11	9.7	26	19.7	1.9	2.4	12.4
	Missouri River	1	715	8.23	189	58.2	19.9	65.2	11.0	3.8	8.9	0.2	0.34	53.5	20	31.4	116.4	4.4	37.7
	Missouri River (Howard Bend)	28	545	8	110	52.1	16.3	35.8	18.0	7.2	5.9	1.5	0.09	34.8	0.08	0.06	-	-	-
	Mississippi River	1	523	8.42	220	50.0	20.4	23.2	28.0	2.0	3.6	2.9	0.26	12.7	25	21.0	9.5	2.9	12.4
	Mississippi River† (Chain of Rocks)	28	541	8.06	100	54.4	16.6	36.8	20.5	7.1	5.9	1.6	0.09	36.2	0.02	0.03	-	-	-
	Springs	59	748	7.49	42	93.7	17.6	44.6	53.6	6.8	2.5	2.0	0.08	13.0	40	32.5	6.8	1.3	16.8
	Lakes	1	104	9.66	28	9.6	2.0	0.4	0.5	0.8	2.1	0.3	0.05	1.3	73	37.0	BDL	1.8	2.7
Forest Park Pond	1	546	9.1	133	24.4	16.7	57.4	12.0	3.3	9.8	1.5	1.65	44.6	5	2.3	42.8	2.3	14.6	
Organic-Rich Samples	Wood Ash (%)	1	NA	NA	58	32.3	0.7	0.3	4.8	0.0	3.6	-	0.33	0.3	0.08	0.02	0.01	0.006	0.035
	Mulching Leachate	3	2,036	7.02	375	176.2	47.6	31.6	38.8	19.8	137.4	1.2	14.33	12.1	119	266.4	53.7	15.8	181.8
Fertilizers	Scott's Turf Builder with Halts (%)	1	NA	NA	0.06	BDL	0.025	BDL	0.333	0.002	1.8	0.533*	0.01	9.69	BDL	0.0004	0.0002	BDL	0.0005
	Miracid (Miracle Grow, %)	1	NA	NA	0.06	BDL	0.004	BDL	0.083	0.001	4.7	0.033	2.31	0.20	BDL	0.0120	0.0002	0.033	0.0390

*Stueber and Criss (2005); †Samples have the chemical signature of the Missouri River; NA = Not applicable or not available; BDL = Below detection limits.

Table 4.3. Field measurements, major element, isotope, and bacterial analyses of wastewater influent and effluent (this study).

Site	Water Type	SpC (μS/cm)	Turbidity (NTU)	TSS (ppm)	Ca (ppm)	Mg (ppm)	Calculated HCO ₃ ⁻ (ppm)	Na (ppm)	Cl (ppm)	NH ₄ ⁺ -N (ppm)	NO ₃ ⁻ -N (ppm)	PO ₄ ³⁻ -P (ppm)	SO ₄ ²⁻ -S (ppm)	K (ppm)	Si (ppm)	δ ¹⁸ O (‰)	δD (‰)	<i>E. coli</i> Easygel (cfu/100mL)	Coliforms Easygel (cfu/100mL)
Duckett Creek #2	Effluent	773	4		46.1	16.0	217	76.9	68	0.27	16.8	1.73	29.7	14.4	5.9	-7.2	-50	-	-
Duckett Creek #1	Effluent	795	9	35	65.3	18.2	269	50.5	54	0.44	3.2	0.26	19.0	6.1	4.3	-9.3	-62	-	-
Duckett Creek #2	Effluent	822	4	10	51.6	16.9	255	93.0	94	0.59	14.2	1.26	25.1	14.6	5.3	-8.8	-60	-	-
Coldwater Creek	Influent	883	114.0	120	45.3	21.9	299	108.0	30	34.00	3	1.50	56.3	19.2	5.5	-10.3	-81	2,800,000	25,100,000*
	Effluent	818	6.0	0	34.9	20.6	200	113.8	74	10.40	3.1	0.96	56.6	20.0	5.3	-10.6	-82	0	100,000
Missouri River	Influent	968	151.0	182	45.0	21.6	271	114.1	44	33.20	0	1.76	61.1	20.2	5.6	-10.6	-78	7,800,000	59,000,000*
	Effluent	873	25.0	26	41.7	21.6	273	121.5	77	8.30	11.7	1.40	49.3	22.6	5.7	-11.0	-79	100,000	2,100,000
Grand Glaize	Influent	956	247.0	272	49.4	21.0	370	147.1	27	37.10	0.2	1.44	70.7	25.0	5.3	-10.4	-82	1,310,000	7,710,000*
	Effluent	781	5.0	32	43.0	20.1	240	123.7	84	0.40	20.6	0.96	55.5	22.8	4.9	-10.4	-80	0	0
Fenton	Influent	746	141.0	148	32.6	20.4	331	68.6	10	20.10	0.8	1.99	15.9	15.9	3.3	-5.7	-40	16,500,000	82,100,000*
	Effluent	661	2.0	2	35.5	20.8	210	74.4	95	1.23	19.7	1.88	16.0	15.8	3.3	-5.7	-40	0	0
Lower Meramec	Influent	813	142.0	170	52.2	18.6	308	69.6	10	21.60	0.8	1.77	34.8	13.2	3.6	-5.8	-40	17,100,000	104,300,000*
	Effluent	675	9.0	12	44.0	17.8	168	66.4	89	0.71	9.9	1.25	25.9	13.0	3.5	-5.7	-40	200,000	2,200,000
Lemay	Influent	831	377.0	384	55.6	21.1	285	102.3	50	16.90	1.6	1.82	53.2	17.3	5.0	-9.5	-74	2,800,000	30,000,000*
	Effluent	762	9.0	18	42.9	19.9	232	99.4	51	4.37	3.8	1.38	52.2	15.4	4.8	-9.6	-74	200,000	1,100,000
Bissell Point	Influent	1328	433.0	208	52.3	30.4	448	267.2	105	4.65	0.8	1.86	114.0	26.7	5.0	-10.8	-81	600,000	6,400,000
	Effluent	1099	13.0	24	40.4	22.1	216	192.5	145	0.99	18	1.19	81.2	19.1	7.7	-12.7	-85	0	0

*Estimated because of high colony density.

Table 4.4. Minor and trace element analyses of wastewater influent and effluent (this study).

Site	Water Type	Al (ppb)	B (ppb)	Cd (ppb)	Co (ppb)	Cr (ppb)	Cu (ppb)	Fe (ppb)	Li (ppb)	Mn (ppb)	Mo (ppb)	Ni (ppb)	Pb (ppb)	Zn (ppb)
Duckett Creek #2	Effluent	6.9	240	0.04	0.24	1.2	2.8	13.8	15.0	20.2	3.6	3.5	0.1	38.5
Duckett Creek #1	Effluent	25.1	51	0.24	0.31	0.6	3.0	25.1	3.6	22.9	2.4	4.4	0.2	32.8
Duckett Creek #2	Effluent	4.8	147	0.26	0.60	0.7	3.5	20.0	8.0	9.6	2.4	3.9	0.2	61.1
Coldwater Creek	Influent	426.3	228	0.85	0.86	8.2	16.8	285.4	90.2	190.8	5.2	12.1	12.1	430.1
	Effluent	48.0	347	0.16	0.74	1.7	6.8	40.8	99.5	144.4	4.3	8.9	1.3	312.1
Missouri River	Influent	327.8	274	0.44	1.11	4.5	17.6	630.9	87.1	292.4	0.7	12.8	2.3	674.4
	Effluent	98.7	355	0.13	0.77	2.4	16.4	251.5	94.3	205.5	4.6	12.2	0.8	216.1
Grand Glaize	Influent	822.3	340	0.69	0.97	2.9	14.4	309.3	83.2	378.8	3.7	11.3	16.9	1933.9
	Effluent	50.4	341	0.35	0.65	0.1	8.2	37.6	88.7	54.1	6.0	10.4	2.8	224.2
Fenton	Influent	348.7	209	0.18	0.70	2.6	17.6	65.3	15.0	107.4	2.6	10.4	4.3	519.3
	Effluent	34.0	231	0.13	0.60	0.2	8.5	26.9	30.5	31.2	2.7	8.8	1.1	349.6
Lower Meramec	Influent	939.4	191	0.31	0.73	4.2	7.9	91.8	18.6	132.6	1.7	13.5	1.7	244.7
	Effluent	67.1	216	0.14	0.49	0.4	11.4	52.5	20.7	36.7	5.8	10.1	1.0	964.9
Lemay	Influent	1722.6	249	0.97	3.57	7.0	10.8	481.8	54.3	772.9	3.2	12.8	15.1	551.7
	Effluent	56.7	260	0.09	1.31	0.1	6.6	50.5	80.5	201.7	4.7	11.0	0.6	166.1
Bissell Point	Influent	124.0	238	0.88	1.88	2.2	22.1	539.6	142.3	77.2	10.0	19.0	1.9	786.2
	Effluent	103.4	246	1.55	0.61	5.2	12.9	113.0	99.0	208.8	7.5	15.1	1.1	336.0

Table 4.5. Chemical composition of selected homeowner fertilizers (this study) and agricultural fertilizers (Oregon Department of Agriculture, 2010). All analyses in weight percent.

Agricultural Product	Analysis or Guarantee	B	Total N	Phosphate (P ₂ O ₅)	Soluble Potash (K ₂ O)	Ca	Mg	S	Co	Cu	Fe	Mn	Mo	Zn
Advanced Floriculture (1.365-0.122-1.205) Seafuel Bloom	Lab Analysis	0.0007	0.90	0.44	0.70	0.29	0.05	0.15	0.00004	0.0031	0.003	0.0001	0.00003	0.001
	Label Guarantee	0.0015	1.36	0.12	1.21	0.10	0.11	0.14	0.00003	0.00003	0.010	0.0009	0.00003	0.005
Advanced Floriculture 0.17-0.027-3.278 Seaweed Bloom	Lab Analysis	0.0003	0.17	0.06	1.33	0.04	0.04	0.04	0.00003	0.0001	0.0001	0.0000	0.00003	0.000
	Label Guarantee	0.0008	0.17	0.03	3.28	0.13	0.09	0.09	0.00005	0.0001	0.001	0.0008	0.00079	0.000
Age Old 12-6-6 Grow	Lab Analysis	0.0195	12.80	6.07	6.32	-	-	-	-	0.0613	0.11	0.0494	-	0.060
	Label Guarantee	0.0200	12.00	6.00	6.00	-	-	-	-	0.0500	0.10	0.0500	-	0.050
9-50-10 Cha Ching	Lab Analysis	0.0221	10.30	51.70	9.33	-	-	-	-	0.1080	0.13	0.5510	-	0.674
	Label Guarantee	0.0200	9.00	50.00	10.00	-	-	-	-	0.0500	0.10	0.0500	-	0.050
General Hydroponics 7-4-10 Flora Nova Grow One-Part Plant Food	Lab Analysis	0.0154	7.11	4.73	11.90	4.34	1.42	2.46	0.00220	0.0082	0.11	0.0261	0.00251	0.012
	Label Guarantee	0.0100	7.00	4.00	10.00	4.00	1.50	2.00	0.00200	0.0100	0.10	0.0300	0.00300	0.020
General Organics BioThrive Vegan Plant Food 2-4-4 Bloom	Lab Analysis	0.0148	2.37	4.36	3.69	-	0.51	-	-	0.0066	0.12	0.0258	0.00237	0.012
	Label Guarantee	0.0100	2.00	4.00	4.00	-	0.05	-	-	0.0100	0.10	0.0300	0.00200	0.010
Bio-Genesis 0-0-1 Mineral Matrix	Lab Analysis	0.0231	-	-	1.38	-	0.71	3.46	-	0.4340	1.72	2.0500	0.00165	2.680
	Label Guarantee	0.0200	-	-	1.00	-	0.50	3.00	-	0.0500	2.00	2.0000	0.00500	3.000
Maxsea 3-20-20 Bloom Water Soluble Concentrate	Lab Analysis	0.0213	8.45	26.30	25.10	-	-	3.19	-	0.0860	0.27	0.0770	0.21100	0.077
	Label Guarantee	0.0200	3.00	20.00	20.00	-	-	2.00	-	0.0500	0.10	0.0500	0.00050	0.050
Dutch Master Gold Range 0.6-8-5 Nutrient B Flower Two Part Nutrient	Lab Analysis	0.0079	0.56	7.96	5.35	-	0.64	1.73	-	0.0006	-	0.0001	0.00168	0.000
	Label Guarantee	0.0070	1.00	8.00	5.00	-	0.90	14.00	-	0.0010	-	0.0100	0.00100	0.010
Dutch Master Gold Range 0-3-5 Nutrient B Flower Two Part Nutrient	Lab Analysis	0.0066	-	11.10	7.25	-	0.61	1.56	-	-	-	-	0.00143	-
	Label Guarantee	0.0010	-	3.00	5.00	-	0.50	1.20	-	-	-	-	0.00100	-
Homeowner Product	Analysis*	B	NO ₃ ⁻ -N	PO ₄ ³⁻ -P	K	Ca	Mg	S	Co	Cu	Fe	Mn	Mo	Zn
Scotts Turf Builder with Halts Crabgrass Preventer	Lab Analysis	0.0620†	0.533‡	0.01	1.83	BDL	0.03	9.69	BDL	BDL	0.0004	0.0001	0.00005	0.001
Miracid (Miracle-Gro)	Lab Analysis	0.0630	0.03	2.31	4.68	BDL	0.00	0.20	BDL	0.0327	0.0124	0.0170	0.00048	0.039

*Lab analysis performed by this study; †Label guarantee is 0.02%; ‡Urea interference with NO₃⁻-N analysis; BDL = below detection limit.

Table 4.6. B concentrations along the Missouri River.

Missouri River Station	State	USGS Gaging Station Number	River Kilometer	Discharge* (cms)	Average B (ppb)	Number of Samples
Toston	MT	06054500	3695	158	108	31
Fort Benton	MT	06090800	3336	216	76	29
Virgelle	MT	06109500	3274	236	80	1
Landusky	MT	06115200	3093	255	91	26
Wolf Point	MT	06177000	2738	276	102	68
Culbertson	MT	06185500	2608	285	104	150
Williston	ND	06330000	2270	576	132	169
Bismarck	ND	06342500	2115	626	138	74
Schmidt	ND	06349700	2089	NA	120	48
Pierre	SD	06440000	1716	NA	129	111
Yankton	SD	06467500	1297	NA	124	93
Omaha	NE	06610000	991	926	107	168
St. Joseph	MO	06818000	721	1339	95	17
Sibley	MO	06894100	557	NA	90	12
Hermann	MO	06895700	158	2528	75	202

*Data from USGS (2011); NA = Not available.

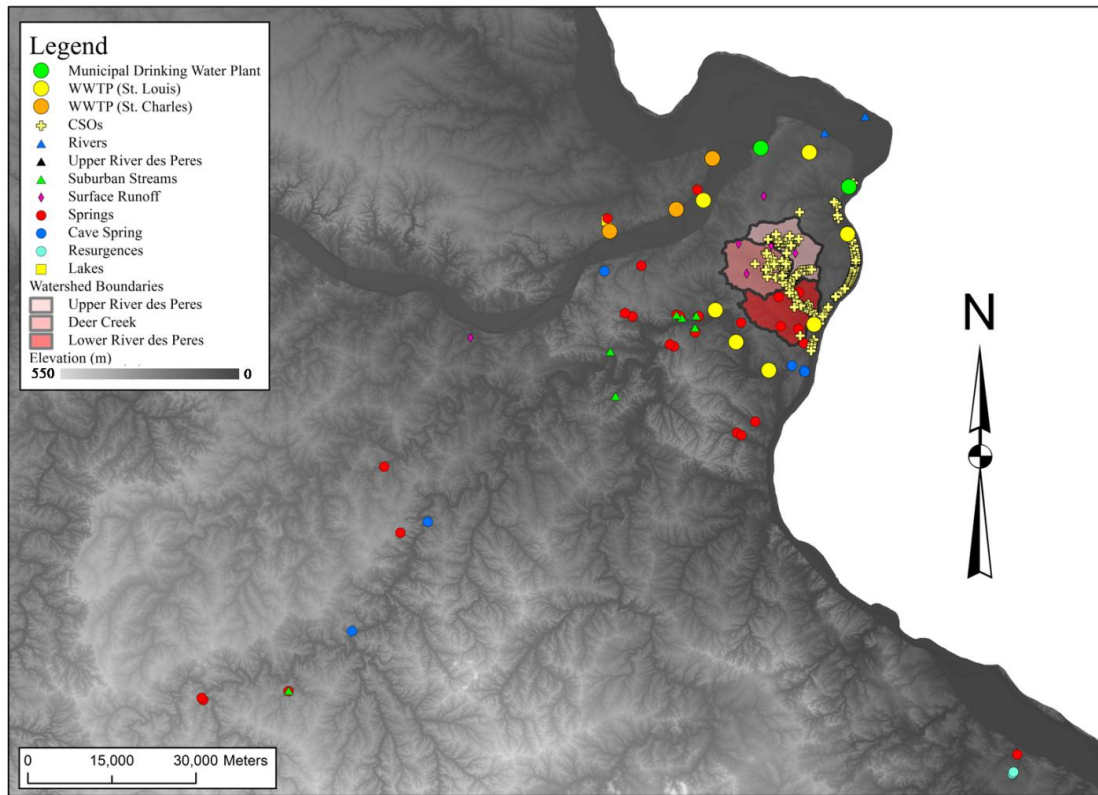


Figure 4.1. Relief map of east-central Missouri showing sampling locations. The elevation ranges from 390 m in the southwest to 110 m along the Mississippi River in the southeast. The 60 m digital elevation model basemap data are from the USGS (Missouri Spatial Data Information Service; MSDIS, 2011). The delineated watershed boundaries for the Upper River des Peres, Deer Creek, and Lower River des Peres, on a digital elevation model for east-central Missouri.

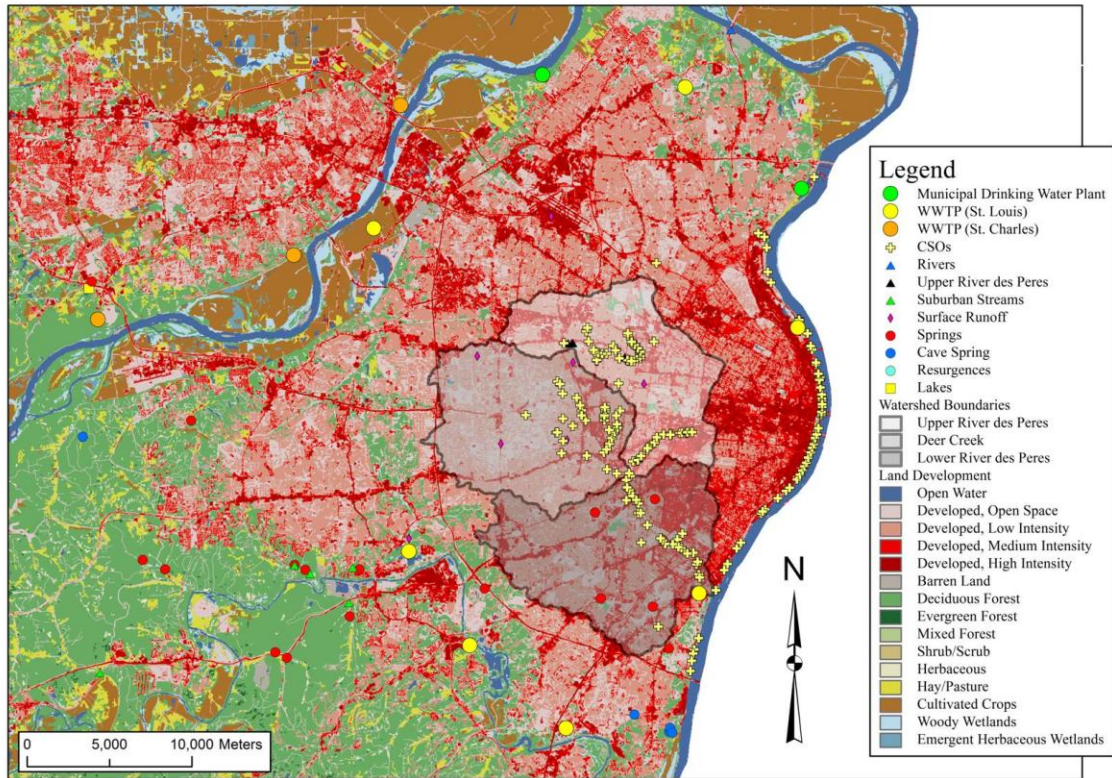


Figure 4.2. Enlarged view of the sample sites and the delineated watershed boundaries for the Upper River des Peres, Deer Creek, and Lower River des Peres on a land use map of east-central Missouri. Land use/land area data are from the 2006 National Land Cover Database (USGS, 2011).

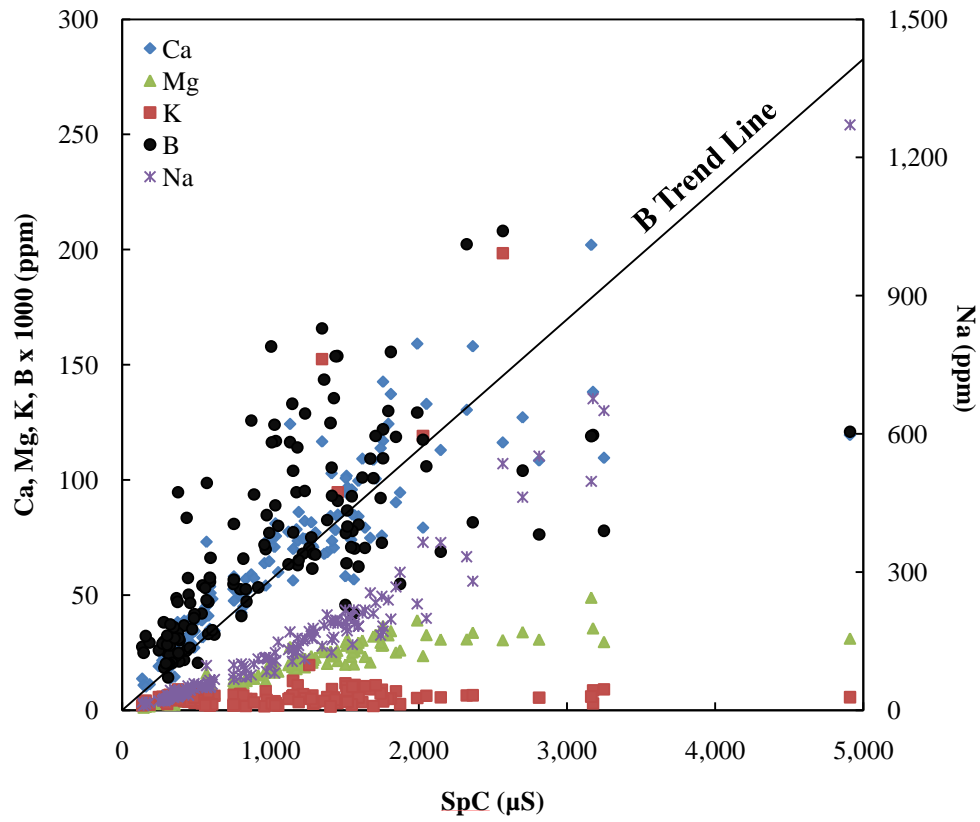


Figure 4.3. A graph depicting the positive correlation of B and major elements (Ca, Mg, K, and Na) with SpC.

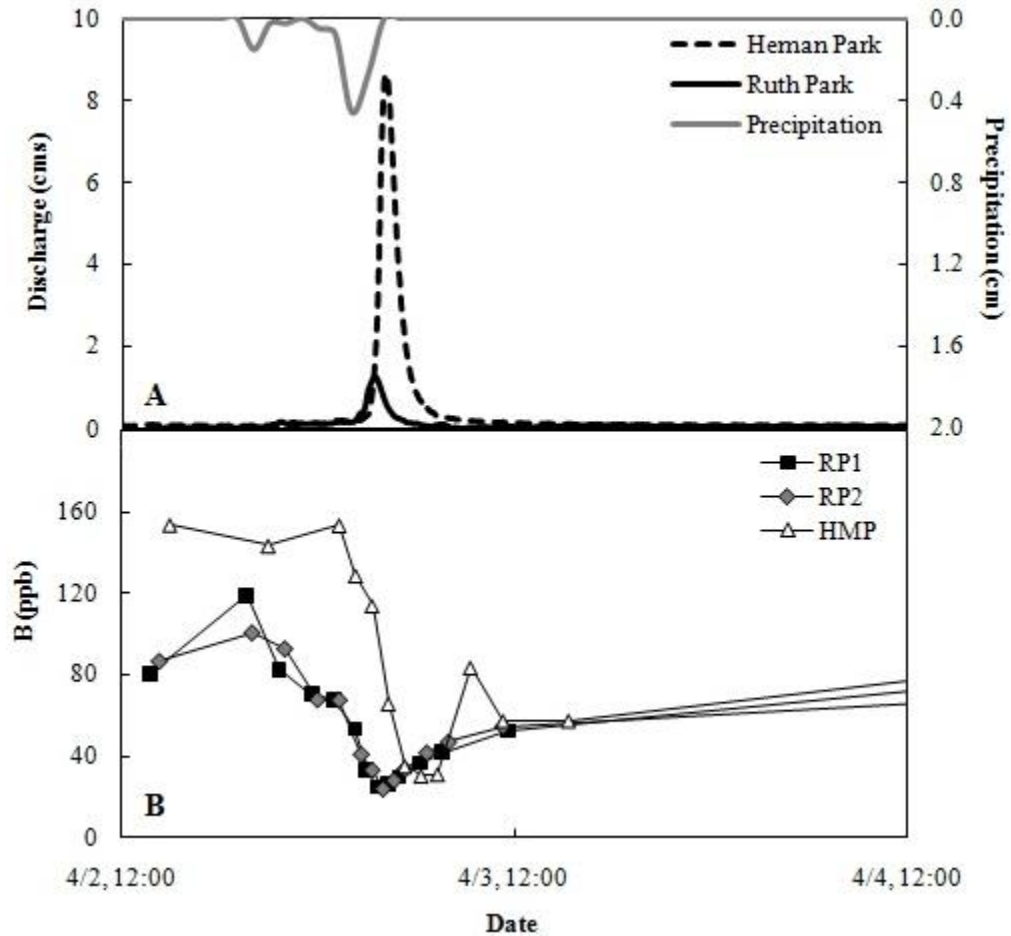


Figure 4.4. (A) An April 2 to 3 discharge event at all three monitoring locations on the River des Peres. Discharge measurements from the USGS gaging station near HMP (dashed line) and from the Washington University monitoring station at RP1 (solid line) are shown. Hourly precipitation from National Weather Service (NWS) at Lambert-St. Louis International Airport (NOAA, 2011) is also shown (gray line). Peak discharge at RP1 occurs 35 min before peak discharge at HMP. (B) The B concentrations for RP1 (black squares), RP2 (gray diamonds), and HMP (open triangles) are shown.

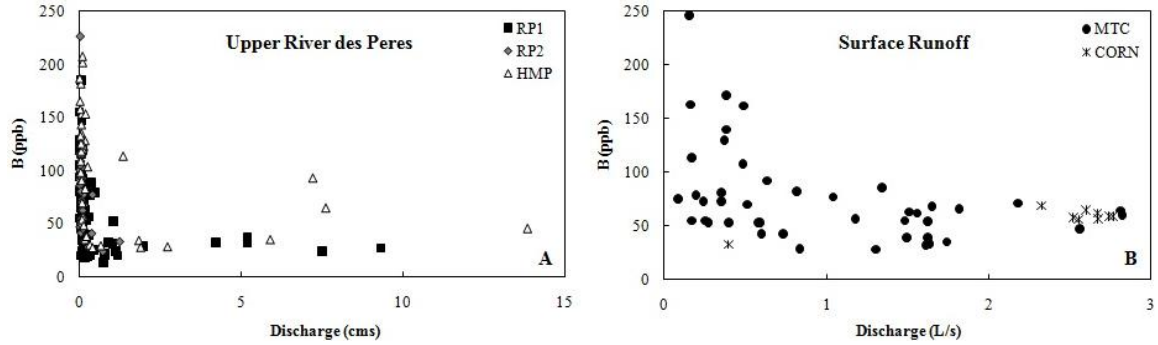


Figure 4.5. The relationship between B concentration and discharge for (A) the Upper River des Peres sample sites and (B) the surface runoff sites. Graph (A) clearly shows that baseflow B concentrations for the Upper River des Peres are higher than storm flow concentrations. For the surface runoff in figure (B), the B concentrations are initially high, but become diluted with increased discharge. Possible B sources for these small watersheds include lawn fertilizers or residual salts from lawn irrigation water, but CSOs and sewer leaks are not possible at these sites (see text).

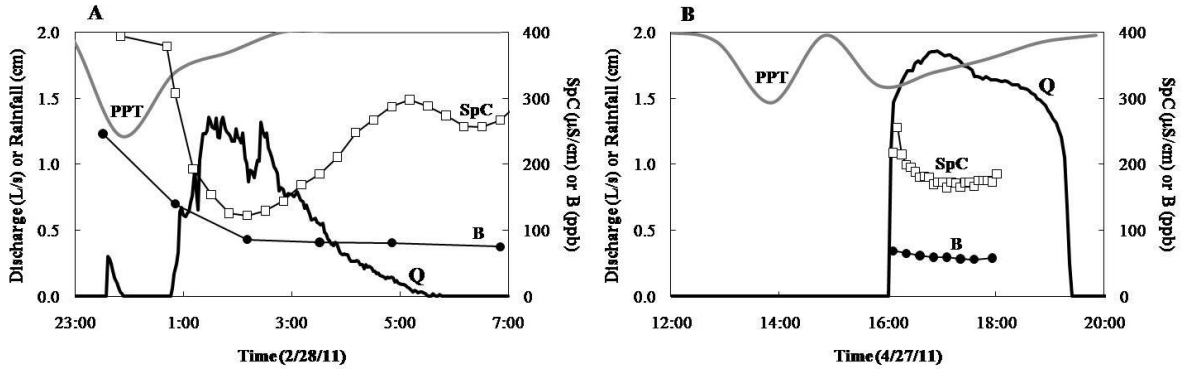


Figure 4.6. Examples of typical surface runoff responses at (A) the parking lot and field at MTC (February 2011) and (B) the residential neighborhood at CORN (April 2011).

Discharge for the drainage area (black line), hourly rainfall records from NWS (gray line, scale is inverted; i.e., 2.0 cm is equal to 0.0 cm), SpC (open squares), and B (solid circles) are shown. Total rainfall amounts were similar: (A) 1.40 cm and (B) 1.65 cm. The first SpC measurement in (A) is off-scale at 611 $\mu\text{S}/\text{cm}$ and is associated with a small discharge peak from parking lot runoff at the church.

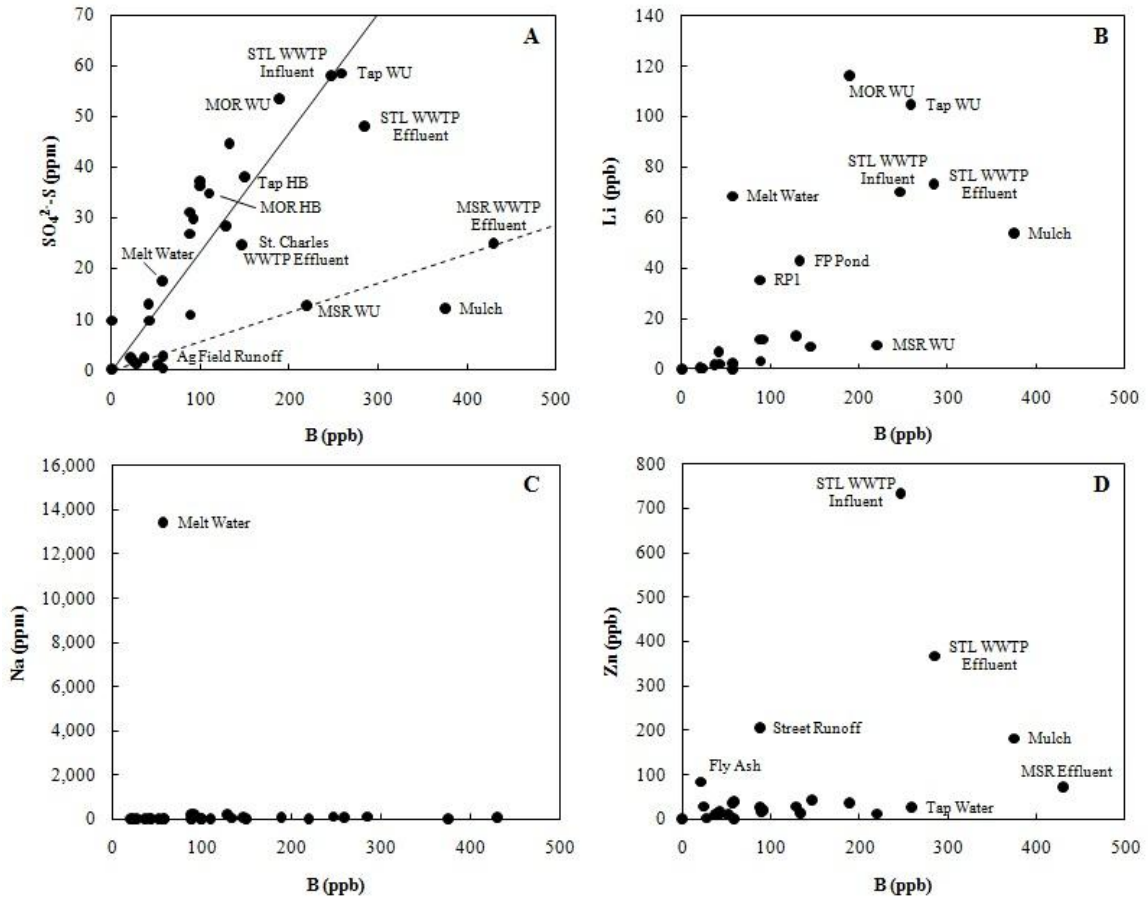


Figure 4.7. The relationship between B and (A) SO₄²⁻-S; (B) Li; (C) Na; and (D) Zn. In (A) there is a distinct relationship between waters with a Missouri River (MOR) signature (solid line) and those with a Mississippi River (MSR) signature (dotted line).

Measurements of the municipal drinking water (Tap) made in this study (WU) and by the Howard Bend Treatment Plant (HB) are shown. The characteristic differences between the Missouri and Mississippi Rivers are also observed in Figure (B). Figure (C) demonstrates that melt waters that come in contact with road salt are responsible for the high Na and Cl contents in the local streams, but are not the source of the high B concentrations. Figure (D) shows that wastewaters, street runoff, coal fly-ash fall out (Fly Ash), and organic-rich mulching leachates (Mulch) are high in Zn, but this signature is not imparted on local waters.

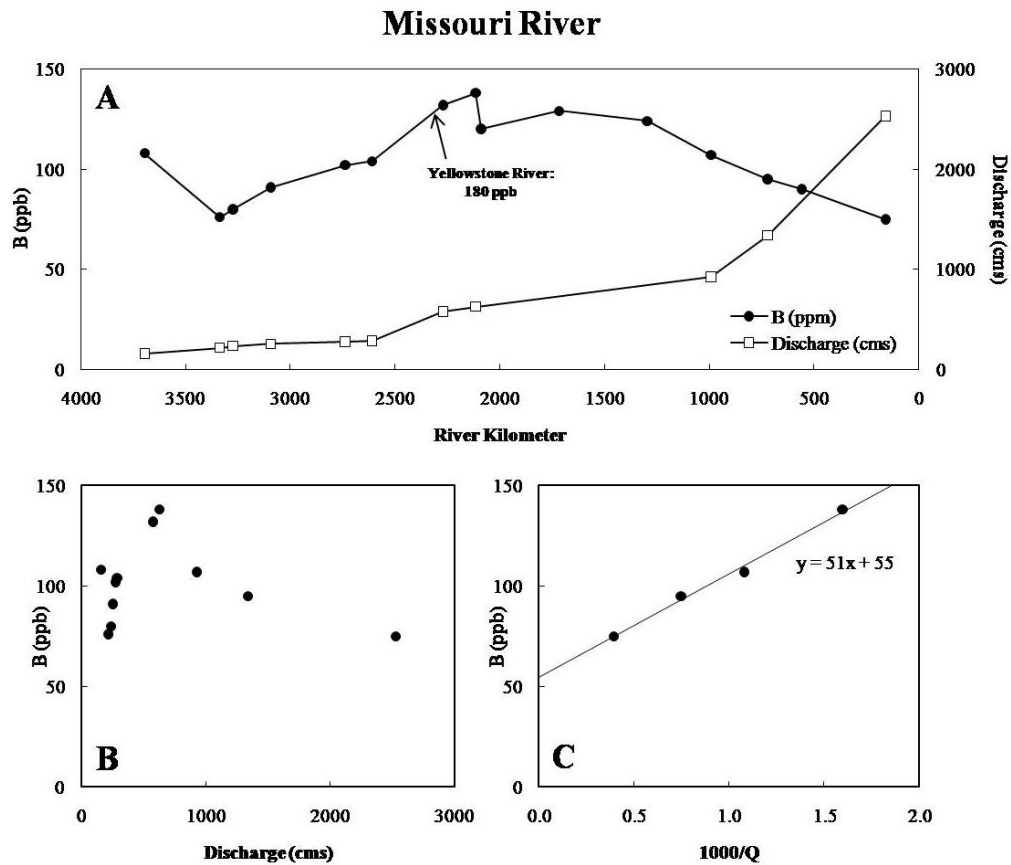


Figure 4.8. (A) The discharge and B concentration (USGS, 2011) along the Missouri River; data correspond to those presented in Table 4.6. Note the increased B concentration below the confluence of the Yellowstone and Missouri Rivers. All data are compiled from USGS records and the Yellowstone River station is located near Forsyth, MT (station number: 06295000). (B) The relationship between B concentration and discharge for the Missouri River. Based on dilution trends in Ca, Mg, HCO_3^- , Na, Cl, and SO_4^{2-} observed by Criss et al. (2001), B concentrations in the Missouri River at Hermann, MO, should be diluted to approximately one-third the concentrations in the headwaters. However, concentrations observed at Hermann, MO, are similar to the headwaters, but

show a dilution trend (C) beginning downstream of the reservoirs, asymptotically approaching a value of about 55 ppb, appropriate for lower basin waters.

Chapter 5: Magnitude, timescales, and geographic variations of groundwater contamination

Abstract

A comparative study of springs in east-central Missouri establishes contaminant background levels and shows that: (1) springs proximal to St. Louis and adjoining suburbs have the most degraded water quality, (2) the time constants for contaminants typically range from a few months to two years and approximate stable isotope residence times, and (3) impacted springs display water quality problems similar to impacted surface waters including high Cl (> 230 ppm), low dissolved oxygen (DO; < 5 ppm), and high *Escherichia coli* (*E. coli*; > 206 cfu/100 mL). Na and Cl contamination from winter road salt applications is attenuated in the springs compared to surface waters, but persists well into the summer and fall, confirming estimates for groundwater residence time. Urban springs commonly have higher NO_3^- -N, NH_4^+ -N, and heavy metal contents compared to rural springs and surface waters.

5.1. Introduction

Karst landscapes facilitate the rapid exchange of water and contaminants between the surface and subsurface, providing a mechanism for the degradation of groundwater quality (Boyer and Pasquarell, 1996; White, 2002; Younos et al., 2001). It is therefore important to identify pollution sources, timescales, and transport mechanisms that affect karst springs. Potential sources of contamination in spring recharge areas include non-point sources such as agrichemicals (e.g. Ryan and Meiman, 1996) and street runoff (Pitt et al., 1996; Zhou et al., 2003), and point sources such as contaminated sites (Singleton et al., 2005), landfills (MacFarlane et al., 1983; Murray et al., 1981), and wastewater discharge (Murray et al., 2007).

Water quality degradation is particularly pronounced in karst regions that are urbanized or intensively farmed. Case studies demonstrate abnormally-high levels of many contaminants in surface waters and/or shallow groundwaters including nutrients (Katz, 2004; Panno et al., 2001), Na and Cl (Buttle and Labadia, 1999; Howard and Maier, 2007; Williams et al., 2000), total suspended solids (TSS; Nightingale and Bianchi, 1977), metals (Page, 1981; Stueber and Criss, 2005), oil and grease (Zhou et al., 2003), and coliform bacteria (Eisena and Anderson, 1979; Mahler et al., 2000). Challenging issues in such investigations include establishing the natural levels of constituents in these systems, quantifying individual contaminant sources, and identifying the timescales on which these pollutants persist.

This study provides a novel and comprehensive comparison of important water quality parameters along a transect progressing from mostly natural, rural systems to highly urbanized areas. Using springs of variable catchment size and land use, the study

shows that urban groundwaters are degraded for nearly all parameters, including: elevated Na and Cl concentrations, increased nutrient and heavy metal contents, increased bacterial counts, and higher and more variable temperature, specific conductivity (SpC), and TSS. It also demonstrates that both karst springs and surface waters are similarly contaminated, but have different time constants. In addition to quantifying the geochemical makeup of perennial karst springs, the response of these features to contaminant perturbations has been modeled. This work attempts to identify potential sources of contaminants, in part by using Na and Cl as tracers of road salt applications.

5.1.1. Regional Hydrologic Setting

East-central Missouri (Figure 5.1) is a densely vegetated region with abundant rainfall (~ 100 cm/yr) and rugged topography (Vandike, 1995). The region lies in the northern part of the Ozark Plateau province and is predominantly underlain by Paleozoic limestone and dolostone units that dip away from the St. Francois Mountains (Fenneman, 1938). This combination of factors promotes interactions between flowing, aggressive groundwaters and soluble carbonate rocks, and has led to the extensive development of karst features including abundant sinkholes, caves, springs, seeps, and losing and gaining streams. In particular, the region shown in Figure 5.1 includes thousands of sinkholes, more than 500 caves, and several hundred springs including the first-magnitude Maramec Spring (e.g., Vineyard and Feder, 1982).

Karst landscapes facilitate vertical penetration of surface waters making groundwaters highly susceptible to contamination. East-central Missouri is ideal for a

contamination study because a large number of springs, seeps, streams, and rivers that differ in size and land use can be compared.

5.2. Methods

5.2.1. Samples

Water samples representing a broad range of catchment size and land development were collected under a range of hydrologic conditions including both low and high flow conditions. Springs sampled for this study have mean discharges ranging from about 0.0001 to 4.1 cms, which represent effective catchment areas that vary from about 0.01 to 430 km² (Vineyard and Feder, 1982). Sampled stream mean discharges range from about 0.07 to 0.4 cms, which represent effective catchment areas that vary from about 10 to 45 km². Water samples were collected at 38 springs, five streams, a lake, and wastewater treatment plants in the St. Louis area, and some were sampled regularly (typically once a month) from 1995 to 2010 (Figure 5.1). The temperature, SpC, turbidity, DO, and pH were measured with portable meters concurrent with sample collection. All samples collected in 2010 were measured for major and minor cations and anions, trace elements, and *E. coli* and total coliform bacteria, and most were measured for TSS. Isotopic, chemical, and bacterial procedures are outlined in Chapter 2.

5.3. Results and Discussion

5.3.1. Water Quality Results

Surface streams in populated areas of east-central Missouri are degraded due to high Cl, low DO, and high *E. coli* (EPA 303d list; see Missouri Department of Natural Resources (MoDNR), 2009). The following sections document that springs are similarly impacted by urban land use, and that they can be analyzed to establish probable sources

for several contaminants and estimate the subsurface residence time. Nutrient levels are elevated and concentrations for several trace metals are near or exceed regulatory levels. The concentration means and ranges for each measured parameter are listed in Table 5.1 and compared to average global values. Several of these water quality parameters are plotted in Figure 5.2 against the Easting, which is used as a proxy for urbanization since St. Louis has largely expanded westward (cf. Figure 5.1).

5.3.1.1. SpC, Na, and Cl

In this study, “urban waters” correspond to samples collected between eastings of roughly 710000 to 745000 and “rural waters” correspond to easting values west of 710000 (Figure 5.1). The SpC of waters in the St. Louis metropolitan area is much higher than that of shallow groundwaters outside of the city and surrounding suburbs (Figure 5.1), and is strongly correlated with Na and Cl concentrations (Figures 5.2A – C, 5.3). Spring and cave spring SpC ranges from 261 to 1,259 $\mu\text{S}/\text{cm}$ and the Na and Cl contents range from nearly 0 to 122 ppm and 208 ppm, respectively, with SpC values generally increasing by an order of magnitude and Na and Cl values increasing nearly three orders of magnitude toward the metropolitan area (Table 5.1; Figures 5.2A – C). The lowest SpC values were measured at Weldon Spring, which is anomalous because its flow includes large contributions from Prairie Lake, a leaky impoundment (Criss et al., 2001).

The SpC values for rural springs typically range from 320 to 600 $\mu\text{S}/\text{cm}$ and Na and Cl concentrations are low (< 10 ppm). Urban springs have higher SpC (greater than 600 $\mu\text{S}/\text{cm}$) and Na and Cl contents (> 10 ppm), with the exception of Weldon Spring (Table 5.1; Figures 5.2A – C). Sampled surface streams have lower mean values for

SpC, Na, and Cl than the urban springs (Figure 5.2A – C), which can be attributed to the shorter residence time of the source waters. Further, the mobility of these constituents is strongly influenced by the flow conditions for both springs and streams (see Chapter 3). Prairie Lake has the lowest SpC, Na, and Cl measurements, while the values in the wastewater effluent are similar to those of the springs.

Linear regressions for Na and Cl versus SpC establish that the former ions are the primary cause of the high SpC values in urban watersheds (Figure 5.3A). Note that the trends do not project to the origin. The x-intercept establishes that the natural SpC for regional waters is between 300 to 420 $\mu\text{S}/\text{cm}$, which is similar to values in rural springs and is attributable to the normally dominant ions Ca, Mg, and HCO_3^- . Given the relatively small contribution of Na and Cl from the host rock and soil in this region, this result shows the large impact of urbanization on water quality, such that these waters commonly are no longer Ca-Mg- HCO_3^- dominated.

High Na and Cl concentrations were observed in wastewaters (Figure 5.3A); however the concentrations of these ions in the springs can be twice as high as those observed in the wastewaters (Figure 5.3A). Further, the wastewater treatment plant effluent is debauched into the larger rivers in the area, and therefore does not represent a non-point source that can affect large numbers of urban springs. Thus, the most likely source for high Na and Cl concentrations in these features is winter road salt application. Runoff collected immediately following snow melt was extremely enriched in Na and Cl from road salting activities, and SpC was 36,000 $\mu\text{S}/\text{cm}$, which corresponded to high Na and Cl values of 13,457 ppm and 13,875 ppm, respectively. Application rates for de-icing salts are difficult to determine given the numerous municipalities in the St. Louis

area and the lack of accurate records. However, data from the Salt Institute (Figure 5.3B) clearly shows that road salting accounts for the majority of the salt use in the United States, and application has increase nearly exponentially with time. Thus, it may be concluded that road salt application is the cause of high Na and Cl levels in the surface waters and groundwaters in this study.

5.3.1.2. DO

The DO for the springs range from 12 to 94% saturation (Figure 5.4); with urban springs tending to have lower and more variable DO than their rural counterparts, due to decomposition of the higher organic matter loads. However, factors other than the presence of biodegradable and non-biodegradable oxidizable pollutants can influence the DO level in springs and streams and are described in more detail in Chapter 6. For example, the DO in springs with no known vadose cave passage is typically low (generally < 60% saturation), as is common in groundwaters long isolated from the atmosphere. In contrast, springs draining open cave systems generally have higher DO (~ 60 – 90% saturation) due to the equilibration of oxygen with overlying cave air. Further, springs with no known passage tend to have lower pH (< 7.7), while those draining vadose cave systems tend to have higher pH (> 7.7) due to degassing of carbon dioxide (Figure 5.4).

Samples collected along traverses down the spring branch of Rockwoods Spring, a small perennial spring in the Rockwoods Reservation, MO, clarify the difference in chemistry between the two types of springs. Field measurements were made on two separate occasions at 0, 18, 85, 152, 274, and 384 m downstream for Traverse 1 (August 27, 2010) and 0, 6, 15, 30, 61, 152, 381 m downstream for Traverse 2 (October 22, 2010;

Figure 5.4). In particular, exchange with the atmosphere causes an increase in DO only a short distance downstream of the spring orifice, while the pH concurrently increases due to the degassing of CO₂ (Figure 5.4). Further downstream both parameters tend to level off reflecting a general approach to equilibrium under surface conditions, though this process is more rapid for DO than for pH. Moreover, both quantities can be perturbed by secondary factors such as aquatic photosynthesis, organic matter decay, and additional groundwater inflows.

Surface streams have higher DO than the springs with no known cave passage as well (43 to 64%; Table 5.1), which is expected due to their contact with the atmosphere. However, the mean DO for these streams was somewhat lower than the cave springs (ranging from 55 to 94%; Table 5.1), likely due to more decomposition of plant material. Prairie Lake has a high DO saturation (80%) because of enhanced photosynthetic activity high in the water column, and the treated wastewater effluent has DO comparable to surface waters (66%; Table 5.1).

5.3.1.3. *E. coli*

The *E. coli* levels in springs are frequently higher than the EPA regulatory limit (e.g., 206 cfu/100 mL; MoDNR, 2009) where recharge areas are impacted by urbanization or agriculture. The levels also depend on other aspects of the recharge area such as ambient TSS input and rainfall events. Phreatic springs and cave springs range from 6 cfu/100 mL to off scale, while streams range from 31 cfu/100 mL to off scale; and Prairie Lake has low *E. coli* levels (Table 5.1; Figure 5.2D). The wastewater effluent has remarkably low *E. coli* levels due to high intensity UV sterilization (Table 5.1; Figure 5.2D). Bacterial levels are typically high after storms in all samples, because flood water

has high suspended loads to which bacteria are attached (Pronk et al., 2007). Likewise, springs generally have lower *E. coli* levels than cave springs and streams due to reduction of suspended particles in the subsurface (Dussart-Baptista et al., 2003). Animal waste may also contribute to increased bacterial levels in these waters.

5.3.1.4. Nutrients

Natural NO_3^- -N background levels for the springs and cave springs are below detection limits (< 0.1 ppm) but high NO_3^- -N levels of up to 5.0 ppm occur in some urban springs (Table 5.1; Figure 5.2E). However, even the nearly pristine Maramec Spring can occasionally have very high levels of NO_3^- -N, as exemplified by the 1981 catastrophic leak of a liquid fertilizer pipeline into a losing stream in its recharge area (Vandike, 2007). This event underscores the vulnerability of karst groundwater systems to surface contamination. More commonly, widespread NO_3^- -N contamination of shallow groundwater originates from fertilized agricultural lands as demonstrated for Illinois karst (Panno et al., 2001; Panno et al., 2003).

Surface streams have a narrower NO_3^- -N range of 0.4 to 1.7 ppm (Table 5.1; Figure 5.2E). During high discharge events, both springs and streams typically have very low NO_3^- -N levels, a common result for areas where NO_3^- has become concentrated in shallow groundwaters (Spalding and Exner, 1993; Stueber and Criss, 2005). Prairie Lake has a relatively low NO_3^- -N concentration while the wastewater effluent has the highest levels of NO_3^- -N at 16.8 ppm (Table 5.1; Figure 5.2E), well above the EPA Maximum Contaminant Level (MCL) of 10 ppm for drinking water (EPA, 2011). This high concentration is related to the production of NH_4^+ by the microbial degradation of organic matter during the treatment process. Excess NH_4^+ produced during treatment is

converted to NO_3^- by aeration processes intended to help prevent anoxic conditions that would inhibit the activity of the microbial communities that decompose the waste. Thus, NO_3^- in the plant effluent is more concentrated than in any spring or stream samples collected, and could be a source of elevated NO_3^- in the springs.

Spring and cave spring NH_4^+ -N range from below the detection limit (less than 0.01 ppm) up to 1.32 ppm (Table 5.1), which occurred during a high flow event at urban Kiefer Spring. Surface streams typically have lower NH_4^+ -N than the springs, and range from 0.04 to 0.48 ppm (Table 5.1). The NH_4^+ -N values for both Prairie Lake and the treated wastewater fall in the range of springs and streams (Table 5.1) and the effluent NH_4^+ -N concentration is lower than the NO_3^- -N concentration for the aforementioned reason.

Total PO_4^{3-} levels range from 0.06 to 0.85 ppm in the springs and cave springs, and vary from 0.11 to 1.07 ppm in surface streams (Table 5.1). Springs with the highest total PO_4^{3-} levels had the largest quantities of organic debris in the orifice, while the highest total PO_4^{3-} levels in the streams occurred during flood events. Prairie Lake has a low total PO_4^{3-} concentration (Table 5.1). High concentrations of P are also a byproduct of the treatment process at wastewater treatment facilities, as exhibited by the wastewater effluent which has the highest total PO_4^{3-} (5.2 ppm). Rural, first-magnitude Maramec Spring has the lowest measured total PO_4^{3-} (0.6 ppm; Table 5.1). A potential source of P contamination in the urban features, along with K (see Table 5.1) and NO_3^- , (three primary plant nutrients) is fertilizer.

5.3.1.5. B

B is an essential micronutrient to plants and is sometimes added to fertilizers in the form of borax to combat soil deficiencies (Bohn et al., 2001). Borax is readily leached as boric acid in solution (Peak et al., 2003), and Stueber and Criss (2005) found slightly higher B concentrations in surface runoff from agricultural fields (52 ppb) in the Illinois sinkhole plains. However, the mean B level in proximal creeks was lower (e.g., 30 ppb; Stueber and Criss, 2005) and not significantly above the worldwide average background level of 10 to 20 ppb for streams (Drever, 1997; Langmuir, 1997).

The measured B concentrations range from 20 to 120 ppb in all the springs and from 31 to 46 ppb in streams (Table 5.1; Figure 5.2F). The B concentration in Prairie Lake is slightly above background (28 ppb; Table 5.1; Figure 5.2F). The highest concentrations occurred in the most urbanized areas are related to lawn irrigation (see Chapter 4).

5.3.1.6. Trace Metals

Concentrations of trace metals in unpolluted natural waters are typically very low, reflecting natural processes of rock weathering and soil leaching, but can become dramatically increased by human activities. Fortunately, high metal concentrations typically do not persist in aquatic systems because of adsorption by hydrous Fe and Mn oxides and organic compounds in the soil, or co-precipitation as minor components of relatively insoluble solid phases (Drever, 1997).

Analyses of 17 trace and minor elements, mostly transition metals (Table 5.1), show that their concentrations tend to be highest proximal to St. Louis, as exemplified by Pb (Figure 5.2G). Mean concentrations in streams are comparable to springs in the same

area, reflecting the importance of karst groundwater contributions to local stream flow. Toxic metal (Cd, Cr, and Pb) concentrations in springs are higher than in streams, a result which is either due to sampling bias, such as over representation of streams in less developed areas, or to rainfall events diluting the baseflow concentration (Table 5.1).

It is difficult to determine specific sources for individual trace metals given their variable character and mobilities. However, the background levels of these elements established by this study show that increased urban land use including non-point sources (fertilizers, street runoff, and atmospheric fallout) and point sources (contaminated sites, landfills, and wastewater infiltration) greatly influence the concentrations of these elements in springs and streams.

5.3.1.7. Stable Isotopes

The sampled springs have a mean $\delta^{18}\text{O}$ value of -6.7‰ (Table 5.1), which is close to the average values of local meteoric precipitation in St. Louis, MO (Criss, 1999). This similarity indicates that these waters are derived from local meteoric precipitation that has become variably homogenized in shallow groundwater systems. It also suggests that these waters have a relatively long residence time within the aquifer according to a linear reservoir model (Table 5.2; Criss, 1999; Criss et al., 2007). An exception is Weldon Spring, whose elevated average $\delta^{18}\text{O}$ value of -5.5‰ reflects the large contributions of evaporated lake water to its flow. In detail, the isotopic values of springs fluctuate seasonally, and are perturbed following large rainfall events (Winston and Criss, 2004).

The isotopic values of surface streams, on the other hand, are more variable and consistently higher than the values for springs ($\delta^{18}\text{O} = -6.2\text{‰}$; Table 5.1). This is consistent with evaporative enrichment of ^{18}O and D in surface and soil waters during the

summer and fall (Criss, 1999). The $\delta^{18}\text{O}$ and δD values and their variability suggest that base flow is dominated by meteoric water with a relatively short residence time (approximately 100 days). Cave springs have an intermediate mean $\delta^{18}\text{O}$ value of -6.5‰ and mean δD value of -44‰ , which indicates that these systems may include higher contributions of surface runoff than other springs. Cave spring waters also are consistently more evaporated as they commonly plot below the meteoric water line (MWL).

These isotopic data corroborate both similarities and differences in the physical and geochemical character of springs and surface streams. For example, groundwater typically has lower DO and pH and higher Na and Cl concentrations than surface streams during the summer and fall. These characteristics are consistent with water that has resided in the subsurface and been cut-off from the atmosphere for sufficient time to become comparatively anoxic, interact with carbonate host rock, and become more isotopically and chemically homogenized.

5.3.1.8. Timescales of Contaminant Residence

Contaminants respond on considerably different time scales in the various springs. The effect of road salt contamination on shallow groundwater has been modeled by combining the linear reservoir model of Frederickson and Criss (1999) with an assumed “square wave” input function to simulate winter salt application. The maximum ($C_{\text{max GW}}$) and minimum ($C_{\text{min GW}}$) concentrations in groundwater, and the corresponding amplitude (A) of the variations depend on the maximum (C_{max}), minimum (C_{min}), and average (\bar{C}) values of the input contaminate, as well as on the year fraction of

contaminant loading (F) and the subsurface residence time (a). Approximate relationships are:

$$C_{\max \text{ GW}} \approx \frac{a\bar{C} + FC_{\max}}{a + F} \quad (1)$$

$$C_{\min \text{ GW}} \approx \frac{a\bar{C}}{a + (1 - F)} \quad (2)$$

$$A \approx \frac{F}{a + F} (C_{\max} - C_{\min}) \quad (3)$$

It was assumed that for SpC $C_{\max} = 3000 \mu\text{S/cm}$ and $F = 0.2$ years during the winter months. The normal background SpC (C_{\min}) was assumed to be $200 \mu\text{S/cm}$. It is recognized that there are profound irregularities of salt applications in space and time, and that dilution of the salt occurs before it reaches the groundwater reservoir via variable flow paths. However, an ample number of examples demonstrate that the model yields a reasonable approximation of the time constants for road salt contamination of these groundwaters (Table 5.2).

Using these equations in conjunction with detailed modeling, it is concluded that the time constants for road salt contamination in groundwater vary from 0.25 to 2.0 years. This estimate corresponds well with stable isotope estimates of residence times (Table 5.2). Rockwoods Spring and Lewis Spring exemplify these differences in response times (Figure 5.5). Rockwoods Spring has a ~ 1 year time constant for both its isotopic and SpC response and shows a more dampened response, while Lewis Spring has an approximately 0.25 year time constant and consequently has a much larger isotopic and SpC amplitude. Despite the large differences in amplitude, both springs exhibit similar annual patterns.

No long term fluctuations were observed in the SpC data for Lewis Spring (Figure 5.5.). However, a slight increasing trend in SpC was observed in the Rockwoods Spring data (Figure 5.5), which may correlate to increasing trend in road salt application rates (Figure 5.3B), demonstrating the deleterious effects of increased application rates on shallow groundwaters.

5.4. Conclusions

Intercomparison of springs, streams, a lake, and treated wastewater in the karstified region of east-central Missouri establishes the background levels of chemical constituents and helps identify the sources and magnitude of adverse impacts. Urban springs display similar water quality problems as degraded surface waters including high Cl, low DO, and high *E. coli*, but they also tend to display higher trace metal contents. Additionally, water quality problems persist in springs longer than in surface waters as a result of their longer residence times, as exemplified by the persistence of road salt contamination into the summer months. Contaminant and salt concentrations strongly depend on the flow conditions in both springs and streams.

Specific sources for pollutants can be difficult to determine due to the myriad of possibilities. A few contaminants have obvious sources; for example, increased Na and Cl levels and high SpC in urban areas arise from road salt, and can overwhelm the natural Ca-Mg- HCO_3^- character. The persistence of high Na and Cl concentrations in springs well into the summer and fall, along with oxygen isotope data reflect the substantial residence times of shallow groundwaters. However, modeling shows that the residence time of these groundwaters can be variable. High nutrient contents likely arise from

fertilizer use, while high B concentrations are a result of the accumulation of B-salts in recharge area soils from lawn irrigation with municipal drinking water.

Finally, it is also challenging to determine specific sources for trace metals given their variable character and mobility. However, the background levels of these elements established by this study are low; confirming that increased urban land use including non-point sources (fertilizers, street runoff, and atmospheric fallout) and point sources (contaminated sites, landfills, and wastewater infiltration) can greatly influence the concentrations of these elements.

5.5. References

Bohn, H.L., McNeal, B.L., and O'Connor, G.A., 2001, Soil chemistry: New York, N.Y., John Wiley and Sons, 307 p.

Boyer, D.G., and Pasquarell, G.C., 1996, Agricultural land use effects on nitrate concentrations in a mature karst aquifer: *Journal of American Water Resources Association*, v. 32, p. 565-573.

Buttle, J.M., and Labadia, C.F., 1999, Deicing salt accumulation and loss in highway snowbanks: *Journal of Environmental Quality*, v. 28, p. 155-164.

Criss, R.E., 1999, Principles of stable isotope distribution: Oxford, U.K., Oxford University Press, 254 p.

Criss, R.E., Davisson, L., Surbeck, H., and Winston, W.E., 2007, Isotopic methods, *in* Goldscheider, N., and Drew, D., eds., *Methods in karst hydrogeology*: London, Taylor and Francis, 123 p.

Criss, R.E., Fernandes, S.A., and Winston, W.E., 2001, Isotopic, geochemical and biological tracing of the source of an impacted karst spring, Weldon Spring, Missouri: *Environmental Forensics*, v. 2, p. 99-103.

Drever, J.I., 1997, *The geochemistry of natural waters: surface and groundwater environments*: Upper Saddle River, New Jersey, Prentice-Hall, 436 p.

Dussart-Baptista, L., Massei, N., Dupont, J.-P., and Jouenne, T., 2003, Transfer of bacteria-contaminated particles in a karst aquifer: Evolution of contaminated materials from a sinkhole to a spring: *Journal of Hydrology*, v. 284, p. 285-295.

Eisena, C., and Anderson, M.P., 1979, The effects of urbanization on ground-water quality – a case study: *Ground Water*, v. 17, p. 456-462.

Fenneman, N.M., 1938, *Physiography of the eastern United States*: New York, McGraw-Hill, 714 p.

Frederickson, G.C., and Criss, R.E., 1999, Isotope hydrology and time constants of the unimpounded Meramec River basin, Missouri: *Chemical Geology*, v. 157, p. 303-317.

Howard, K.W.F., and Maier, H., 2007, Road de-icing salt as a potential constraint on urban growth in the Greater Toronto Area, Canada: *Journal of Contaminant Hydrology*, v. 91, p. 146-170.

Katz, B.G., 2004, Sources of nitrate contamination and age of water in large karstic springs of Florida: *Environmental Geology*, v. 46, p. 689-706.

- Langmuir, D., 1997, *Aqueous environmental geochemistry: Upper Saddle River, New Jersey*, Prentice-Hall, 600 p.
- MacFarlane, D.S., Cherry, J.A., Gillham, R.W., and Sudicky, E.A., 1983, Migration of contaminants in groundwater at a landfill: A case study: 1. Groundwater flow and plume delineation: *Journal of Hydrology*, v. 63, p. 1-29.
- Mahler, B.J., Personné, J.C., Lods, G.F., and Drogue, C., 2000, Transport of free and particulate-associated bacteria in karst: *Journal of Hydrology*, v. 238, p. 179-193.
- Missouri Department of Natural Resources, 2009, *Methodology for the development of the 2010 Section 303(d) List in Missouri*:
<http://www.dnr.mo.gov/ENV/wpp/docs/final2010-lmd.pdf>.
- Missouri Spatial Data Information Service. Data Resources (MSDIS), 2011, *Missouri Spatial Data Information Service: University of Missouri Web site*,
<http://www.msdis.missouri.edu>.
- Murray, J.P., Rouse, J.V., and Carpenter, A.B., 1981, Groundwater contamination by sanitary landfill leachate and domestic wastewater in carbonate terrain: Principal source diagnosis, chemical transport characteristics and design implications: *Water Resources*, v. 15, p. 745-757.
- Murray, K., Straud, D., and Hammond, W., 2007, Characterizing groundwater flow in a faulted karst system using optical brighteners from septic systems as tracers: *Environmental Geology*, v. 53, p. 769-776.
- Nightingale, H.I., and Bianchi, W.C., 1977, Ground-water turbidity resulting from artificial recharge: *Ground Water*, v. 15, p. 146-152.
- Page, G.W., 1981, Comparison of groundwater and surface water for patterns and levels of contamination by toxic substances: *Environmental Science & Technology*, v. 15, p. 1,475-1,481.
- Panno, S.V., Hackley, K.C., Hwang, H.H., and Kelly, W.R., 2001, Determination of the sources of nitrate contamination in karst springs using isotopic and chemical indicators: *Chemical Geology*, v. 179, p. 113-128.
- Panno, S.V., Kelley, W.R., Weibel, C.P., Krapac, I.G., and Sargent, S.L., 2003, Water quality and agrichemical loading in two groundwater basins of Illinois' sinkhole plain: *Illinois State Geological Survey Environmental Geology* 156, 36 p.
- Peak, D., Luther, III, G.W., and Sparks, D.L., 2003, ATR-FTIR spectroscopic studies of boric acid adsorption on hydrous ferric oxide: *Geochimica et Cosmochimica Acta*, v. 67, p. 2,551-2,560.

Pitt, R., Field, R., Clark, S., and Parmer, K., 1996, Groundwater contamination from stormwater infiltration: Chelsea, Michigan, Ann Arbor Press, Inc., 519 p.

Pronk, M., Goldscheider, N., and Zopfi, J., 2007, Particle-size distribution as indicator for fecal bacteria contamination of drinking water from karst springs: *Environmental Science & Technology*, v. 41, p. 8,400-8,405.

Ryan, M., and Meiman, J., 1996, An examination of short-term variations in water quality at a karst spring in Kentucky: *Ground Water*, v. 34, p. 23-30.

Salt Institute, 2011, Salt Uses and Benefits: Salt Uses and Benefits Web page, <http://www.saltinstitute.org/>.

Singleton, M.J., Woods, K.N., Conrad, M.E., DePaolo, D.J., and Dresel, P.E., 2005, Tracking sources of unsaturated zone and groundwater nitrate contamination using nitrogen and oxygen stable isotopes at the Hanford Site, Washington: *Environmental Science & Technology*, v. 39, p. 3,563-3,570.

Spalding, R.F., and Exner, M.E., 1993, Occurrence of nitrate in groundwater: *Journal of Environmental Quality*, v. 22, p. 392-402.

Stueber, A.M., and Criss, R.E., 2005, Origin and transport of dissolved chemicals in a karst watershed, southwestern Illinois. *Journal of American Water Resources Association*, v. 41, p. 267-290.

U.S. Environmental Protection Agency, 2011, Drinking water contaminants: Drinking water contaminants Web page, <http://water.epa.gov/drink/contaminants/index.cfm>.

Vandike, J.E., 1995, Surface water resources of Missouri (Missouri State Water Plan Series - Volume 1): Missouri Department of Natural Resources Water Resources Report 45, 121 p.

Vandike, J.E., 2007, The effects of the November 1981 liquid-fertilizer pipeline break on groundwater in Phelps County, Missouri: Missouri Department of Natural Resources Water Resources Report 75, 29 p.

Vengosh, A., Heumann, K.G., Juraske, S., and Kasher, R., 1994, Boron isotope application for tracing sources of contamination in groundwater: *Environmental Science & Technology*, v. 28, p. 1,968-1,974.

Vineyard, J., and Feder, G.L., 1982, Springs of Missouri: Missouri Department of Natural Resources Water Resources Report 29, 266 p.

White, W.B., 2002, Karst hydrology: recent developments and open questions: *Engineering Geology*, v. 65, p. 85-105.

Williams, D.D., Williams, N.E., and Cao, Y., 2000, Road salt contamination of groundwater in a major metropolitan area and development of a biological index to monitor its impact: *Water Research* v. 34, p. 127-138.

Winston, W.E., and Criss, R.E., 2004, Dynamic hydrologic and geochemical response in a perennial karst spring: *Water Resources Research*, v. 40, W05106.

Younos, T., Kaurish, F W., Brown, T., and de Leon, R., 2001, Determining the source of stream contamination in a karst-water system, southwest Virginia, USA: *Journal of American Water Resources Association*, 2001, v. 37, p. 327-334.

Zhou, W., Beck, B.F., and Green, T.S., 2003, Evaluation of a peat filtration system for treating highway runoff in a karst setting: *Environmental Geology*, v. 44, p. 187-202.

Table 5.1. Concentration means and ranges for selected water quality parameters compared to global average values.

Chemical Constituent ^a	SI units	Springs	Cave Springs	Streams	Prairie Lake	Treated Wastewater	Global SW and GW ¹	Global GW ²
Temp	°C	14.8 12.5 – 19.4	14.5 11.9 – 16.7	16.6 14.3 – 20.1	35.0	24.6	–	–
SpC	µS/cm	731 261 – 1259	732 443 – 1014	540 191 – 805	104	773	350 ^d	–
δ ¹⁸ O	‰	-6.7 -8.0 – -3.4	-6.5 -7.3 – -5.7	-6.2 -6.8 – -5.5	-3.2	-7.2	–	–
<i>E. coli</i>	cfu/100 mL	_{-b} 6 – >2420	_{-b} 15 – >2420	_{-b} 31 – >2420	14	73	–	–
Coliforms	cfu/100 mL	_{-b} 147 – >2420	_{-b} 1414 – >2420	_{-b} 1733 – >2420	>2420	1120	–	–
pH		7.43 6.94 – 8.13	7.96 7.70 – 8.18	7.92 7.75 – 8.07	9.66	8.15	7.4	–
DO	ppm	4.50 1.23 – 7.64	7.28 5.64 – 10.04	5.6 4.02 – 6.53	5.44	5.53	–	–
TSS	ppm	23 1 – 225	44 1 – 225	92 1 – 598	–	–	–	–
NO ₃ ⁻ -N	ppm	2.0 BDL ^c – 5.0	1.1 BDL ^c – 2.1	1.0 0.4 – 1.7	0.3	16.8	–	–
NH ₄ ⁺ -N	ppm	0.17 BDL ^c – 1.32	0.15 0.03 – 0.32	0.12 0.04 – 0.48	0.41	0.27	–	–
Total PO ₄ ³⁻	ppm	0.26 0.06 – 0.85	0.25 0.10 – 0.47	0.30 0.11 – 1.07	0.14	5.19	0.020	–
Cl	ppm	54.3 0.6 – 208.0	46.4 0.1 – 114.0	22.2 10.4 – 56.0	0.5	68.0	20	–
Ca	ppm	94.8 32.6 – 163.5	92.0 47.2 – 125.7	67.5 21.0 – 103.6	9.6	46.1	50 (Ca ²⁺)	–
K	ppm	2.5 1.1 – 4.1	1.8 0.6 – 4.1	3.2 2.5 – 3.8	2.2	14.4	3 (K ⁺)	–
Mg	ppm	15.8 6.5 – 28.1	20.7 13.4 – 31.6	12.5 3.4 – 16.6	2.0	16.0	7 (Mg ²⁺)	–
Na	ppm	48.2 0.3 – 121.7	35.0 1.0 – 72.9	34.0 11.9 – 61.6	0.4	76.9	30 (Na ⁺)	–
S	ppm	15.0 1.3 – 41.5	11.7 1.2 – 18.8	9.5 3.8 – 17.0	1.3	29.7	30 (SO ₄ ²⁻)	–
Si	ppm	5.6 3.1 – 8.8	7.9 3.7 – 12.3	4.3 2.5 – 5.4	0.8	5.9	16 (SiO ₂)	–
Al	ppb	45.3 1.3 – 393.1	83.4 25.35 – 236.8	24.1 0.6 – 158.0	73.3	6.9	10	50
B	ppb	40.3 19.8 – 95.5	51.3 19.9 – 119.5	41.8 35.8 – 46.0	28.0	240.3	10	20
Ba	ppb	91.9 43.7 – 131.8	100.7 44.6 – 135.5	96.6 33.9 – 129.4	35.3	39.2	20	50
Cd	ppb	0.08 0.01 – 0.45	0.04 0.01 – 0.08	0.08 0.04 – 0.12	0.03	0.04	0.03	–
Co	ppb	0.22 0.07 – 0.88	0.19 0.09 – 0.34	0.19 0.15 – 0.27	0.49	0.24	0.1	0.2
Cr	ppb	2.6 0.3 – 11.4	1.3 0.5 – 3.45	1.5 0.8 – 2.4	1.0	1.2	1	1
Cu	ppb	1.3 0.3 – 4.0	1.3 0.3 – 2.3	1.9 1.1 – 4.2	1.8	2.8	3	7
Fe	ppb	32.6 10.2 – 80.2	28.7 14.1 – 41.7	20.3 15.4 – 27.7	37.0	13.8	100	40
Ga	ppb	2.1 1.3 – 3.1	2.1 1.1 – 2.8	2.2 0.9 – 2.8	1.1	1.1	–	0.1
Li	ppb	2.0 BDL ^c – 5.8	2.5 0.1 – 5.7	1.6 0.5 – 3.3	BDL ^c	15.0	3	170

Mn	ppb	$\frac{55.1}{0.7 - 602.8}$	$\frac{9.3}{1.5 - 17.3}$	$\frac{30.5}{47.5 - 80.8}$	66.3	20.2	15	8
Mo	ppb	$\frac{1.13}{0.09 - 12.80}$	$\frac{0.65}{0.17 - 1.90}$	$\frac{0.74}{0.37 - 1.69}$	0.3	3.6	1.5	0.5
Ni	ppb	$\frac{4.0}{1.6 - 8.4}$	$\frac{3.6}{2.2 - 4.6}$	$\frac{3.3}{1.9 - 4.6}$	0.9	3.5	1.5	2
Pb	ppb	$\frac{0.37}{0.02 - 3.35}$	$\frac{0.44}{0.07 - 0.92}$	$\frac{0.09}{0.04 - 0.21}$	0.75	0.08	3	1
Rb	ppb	$\frac{0.74}{0.29 - 1.32}$	$\frac{0.60}{0.26 - 0.89}$	$\frac{0.76}{0.53 - 0.88}$	1.08	7.89	1	1
Sr	ppb	$\frac{181.8}{40.5 - 387.7}$	$\frac{176.9}{47.0 - 291.3}$	$\frac{140.5}{68.4 - 221.1}$	32.3	207.8	400	60
Zn	ppb	$\frac{10.8}{0.03 - 43.5}$	$\frac{8.39}{1.1 - 22.6}$	$\frac{10.4}{6.3 - 15.4}$	2.7	38.5	20	30

^aDetection limits reported in Chapter 2.

^bObtaining a mean was not possible due to off-scale measurements.

^cBDL represents measurement below detection limits.

^dTDS reported in ppm.

Table 5.2. Time constants of isotopic and SpC response for select springs rounded to the nearest 0.25 years.

Spring	Isotopic Time Constant (years)	SpC Time Constant (years)
Cliff Cave	0.25	0.25
Lewis	0.25	0.25
Weldon	0.25	0.25
Burgermeister	0.5	-
Kiefer	0.5	0.5
Petty	0.5	0.5
Bluegrass	1.0	1.0
Rockwoods	1.0	1.0
House	1.0	1.5
Maramec	2.0	2.0

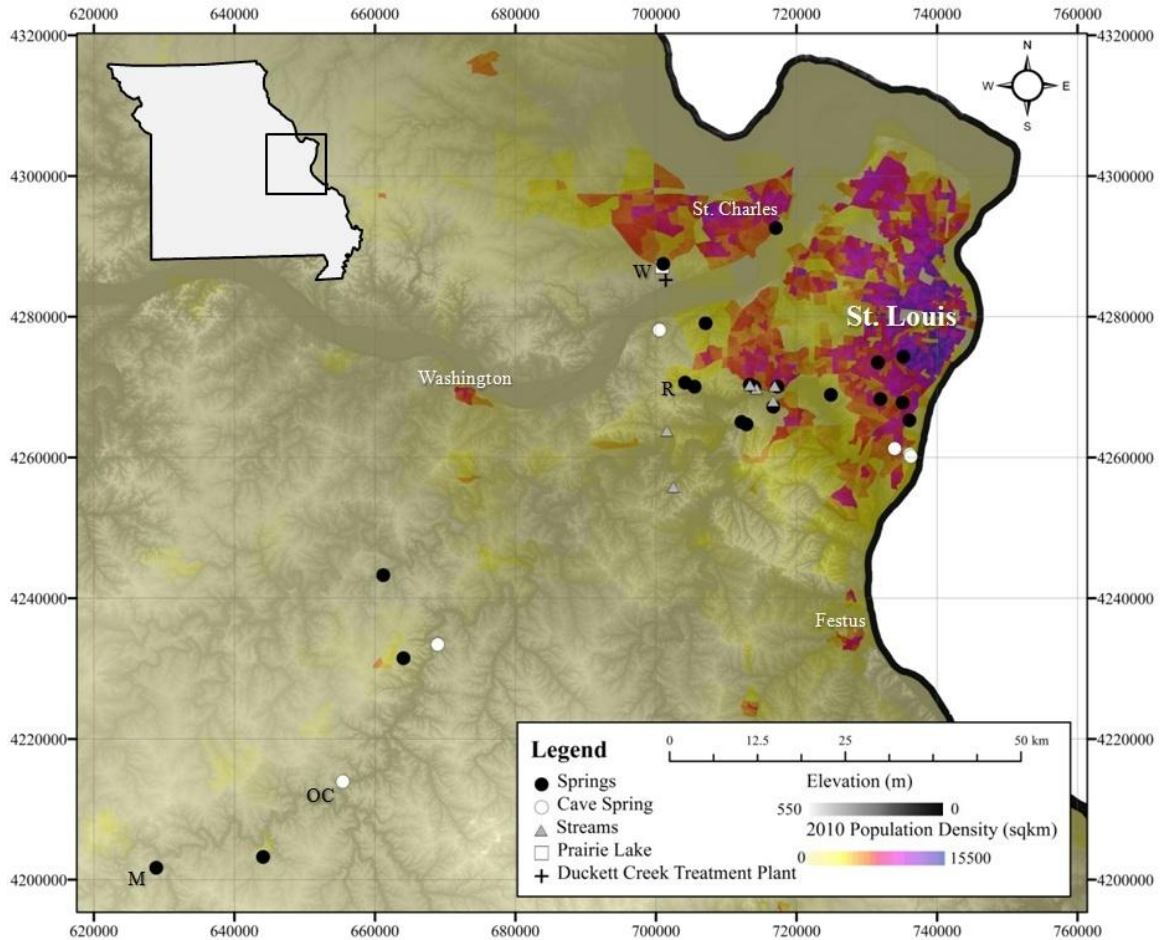


Figure 5.1. Relief map of east-central Missouri showing sampling locations. The elevation ranges from 390 m in the southwest to 110 m along the Mississippi River in the southeast. Cities, including St. Louis, St. Charles, Washington, and Festus, MO, are shown for reference as well as a few features of note: M is Maramec Spring, OC is Onondaga Cave, W is Weldon Spring, and R is Rockwoods Spring. Digital elevation model basemap data are from the U.S. Geological Survey (USGS; MSDIS, 2011); overlain on the DEM is population density data from the 2010 U.S. Census. Gridlines are in UTM eastings and northings (Zone 15, NAD 83; MSDIS, 2011).

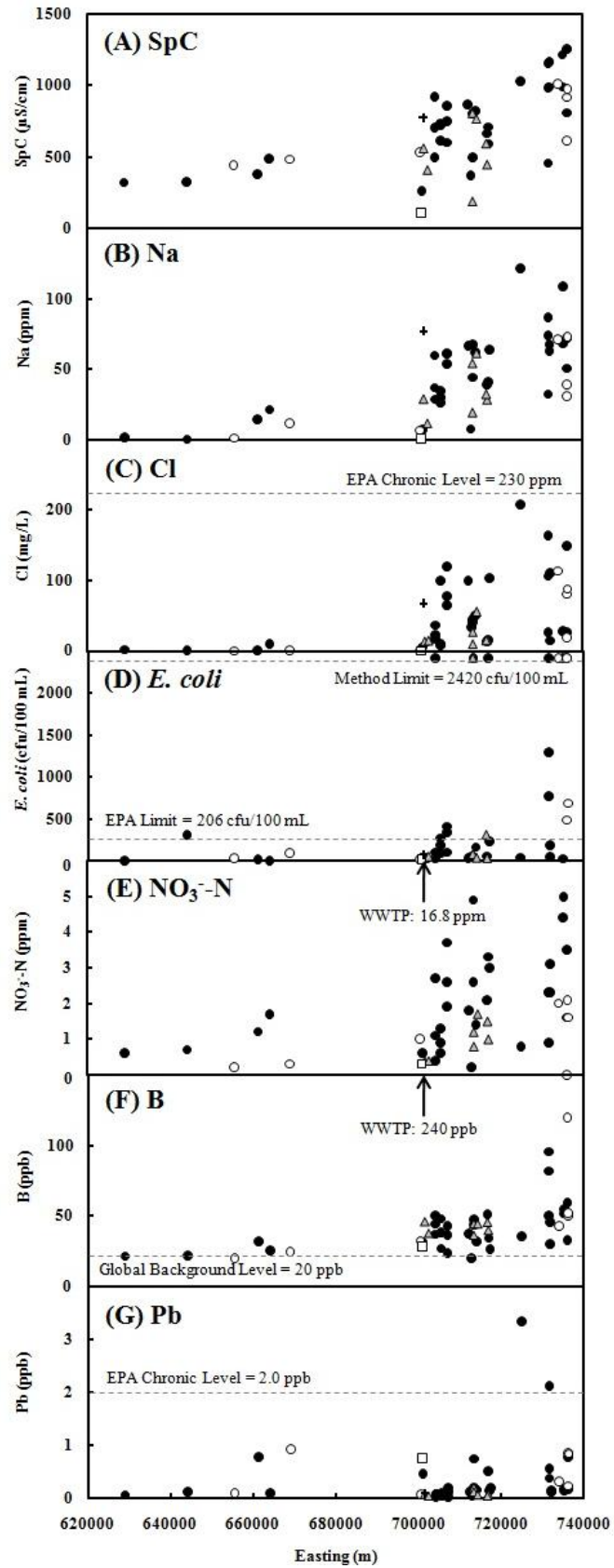


Figure 5.2. (A) SpC ($\mu\text{S}/\text{cm}$), (B) Na (ppm), (C) Cl (ppm), (D) *E. coli* (cfu/100 mL), (E) NO_3^- -N (ppm), (F) B (ppb), and (G) Pb (ppb) for the springs (closed circles), cave springs (open circles), surface streams (gray triangles), Prairie Lake (open square), and wastewater effluent (cross) plotted against their east-west position in UTM eastings (m). Regulatory limits for Cl, *E. coli*, and Pb are plotted on relevant diagrams, as are the *E. coli* method limit and the global background level of B. Arrows indicate off-scale values for the wastewater treatment plant (WWTP).

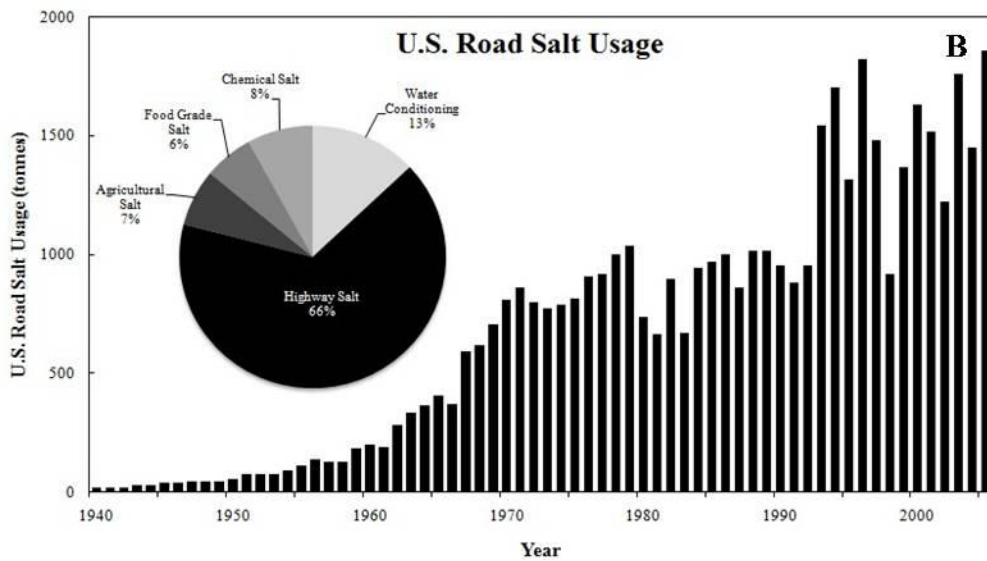
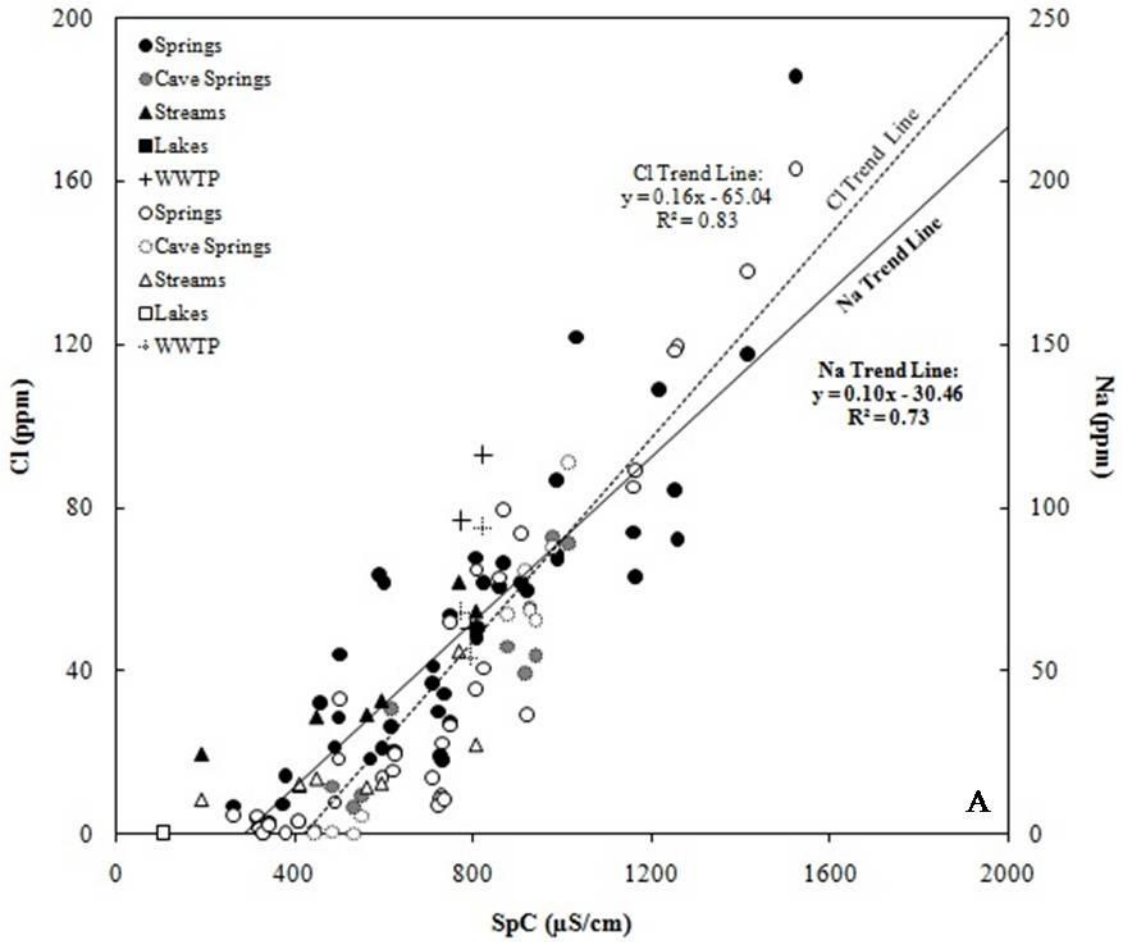


Figure 5.3. (A) Na (closed shapes) and Cl (open shapes) concentrations in ppm for springs (circles), cave springs (circles with dashed borders), streams (triangles), Prairie

Lake (square), and treated wastewater effluent (cross) plotted against SpC for all samples. Note that the trend lines do not project to the origin; the x-intercept establishes the typical SpC of unimpacted springs. (B) Road salt application rates for the United States over time (Salt Institute, 2011).

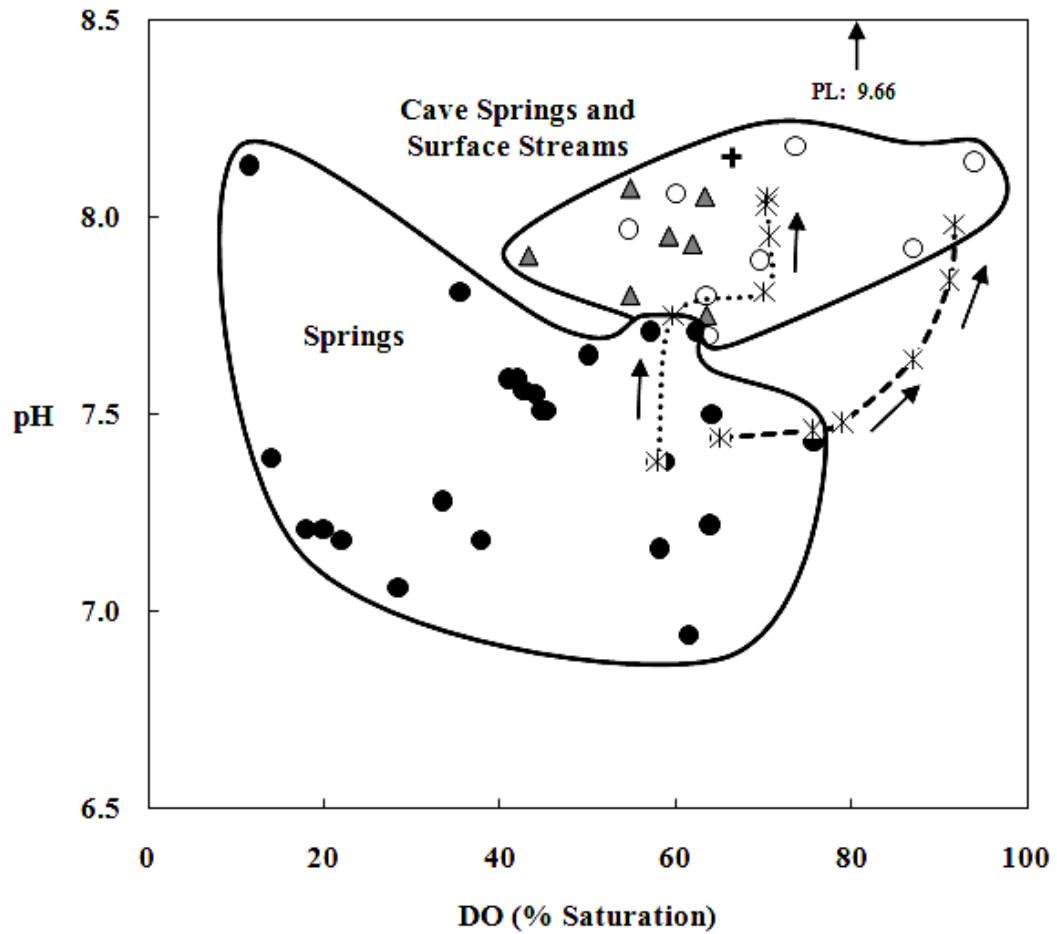


Figure 5.4. The pH versus DO for springs (closed circles), cave springs (open circles), surface streams (gray triangles), wastewater effluent (cross), and Prairie Lake (PL; off scale with pH = 9.66). Also shown are variations along two traverses (asterisks; Traverse 1 is indicated by the dotted line and Traverse 2 is indicated by the dashed line; arrows indicate downstream direction) below Rockwoods Spring. Both DO and pH rapidly equilibrate with air below the spring orifice, with DO responding fastest.

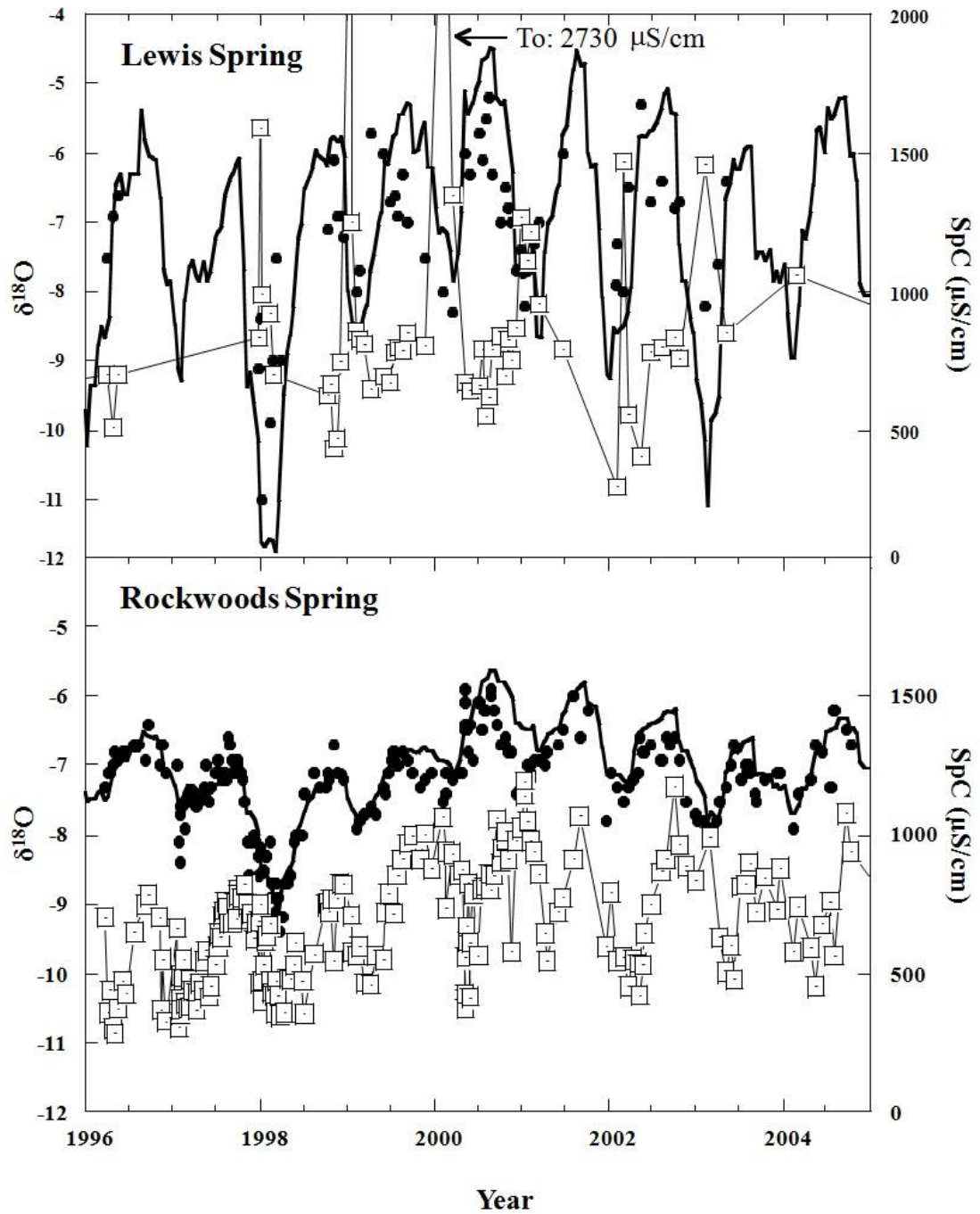


Figure 5.5. Comparison of $\delta^{18}\text{O}$ values (closed circles, left axis) of samples of Lewis Spring and Rockwoods Spring. The heavy solid line represents an independent estimation of isotope variations based solely on precipitation data and the linear reservoir model (Criss *et al.*, 2007). Variations of SpC (open squares) are also shown along with

an interpolated line. Note that the amplitudes of the isotopic and SpC variations at Rockwoods Spring are much smaller than those in Lewis Spring, reflecting a significant difference in subsurface residence time.

Chapter 6: A novel technique to discover open cave passage in karst spring systems

Abstract

Dissolved oxygen (DO) and pH data provide a novel, inexpensive means to detect open cave passage in karst spring systems. Karst springs in east-central Missouri that have no known air-filled passages (“phreatic” springs) typically have low DO and pH values (< 80% saturation and < 7.7, respectively), which is characteristic of groundwaters that do not communicate with the atmosphere. In contrast, springs draining vadose cave passages have higher DO and pH values (> 60% saturation and > 7.7, respectively), which resemble surface waters due to the equilibration of DO with the overlying cave atmosphere and the simultaneous degassing of dissolved CO₂. Traverses down several spring branches clarify the difference in chemistry between the two types of springs. In particular, exchange with the atmosphere causes an increase in DO only a short distance downstream of the spring orifice, while the pH concurrently increases due to the degassing of CO₂. Further downstream both parameters tend to level off reflecting a general approach to equilibrium under surface conditions, though this process is more rapid for DO than for pH. In contrast, the DO and pH along cave spring branches changes little from values at the orifice. Degassing processes also affect the saturation state of minerals such as calcite, with cave springs being the most saturated with respect to calcite. These chemical responses are corroborated by total suspended solids (TSS), bacterial, and oxygen and hydrogen stable isotope data. The phreatic springs typically have lower TSS and *Escherichia coli* (*E. coli*) levels than open cave springs due to slower and less variable flow delivery, longer residence times, and less turbulent flow. Phreatic springs also tend to plot on the meteoric water line (MWL), while waters from open cave

systems can plot below the MWL, indicating isotopic enrichment by evaporation into the overlying cave atmosphere.

6.1. Introduction

Discovery and exploration of underground passages are important for ecosystem conservation, to delineate their potential as collapse hazards, and to identify subsurface avenues for the transport of shallow groundwater and their pollutants. Most known caves have been found by chance discovery of passages that breach the surface. Systematic methods for finding caves have relied predominantly on mapping and geophysical techniques. Solution caves are by far the most abundant type of cave and occur in soluble rocks such as limestones and dolostones. Because cave formation is dependent on rock type, familiarity with the bedrock is essential to cave discovery. In detail, knowledge of stratigraphic contact locations is crucial, because where insoluble rock overlies soluble rock there is a larger potential for dissolution (Palmer, 2007). Once stratigraphy is determined, karst topography including the presence of sinkholes, valleys, and springs can help indicate the presence of underlying cave passages.

Less conventional methods, such as air movement through openings at the ground surface, have been used to detect caves. Jewel Cave, Lechuguilla Cave, and Wind Cave were all discovered by investigating air drafts on the surface generated as subsurface voids respond to changes in atmospheric pressure (Davis, 2000; Horrocks and Szukalski, 2002). On cold winter days, such changes can generate visible condensation clouds at cave entrances, an effect that led to the discovery of Valentine Cave in northeastern California. More recently, infrared mapping has facilitated cave discovery by exploiting the temperature contrast between the relatively warm cave exhalations and the ambient air (Brown 1972; Campbell et al., 1996; Thompson and Marvin, 2005).

6.1.1. Geophysical Cave Detection

Geophysical techniques are often employed to locate and map subsurface passages. Like most cave detection methods, these techniques require a priori knowledge, from topography and lithology, of potential open passage locations, but often also involve expensive equipment and extensive work to set up instrumentation and gather the data in the field. Gravity surveys have detected caves by identifying local decreases in Earth's gravitational field caused by the subsurface voids (Butler, 1984; Smith and Smith, 1987; Linford, 1998). Unfortunately, gravity data must be corrected for elevation, latitude, topography, and variations with time (including instrument drift and changes in the position of the moon and sun), and its use for this purpose is depth limited; thus, as a "rule of thumb," the surveys cannot detect a cave if its depth is greater than the square of the passage diameter. Further, the presence of water in cave passages and local anomalies in the bedrock can decrease the depth at which caves can be detected.

Another geophysical method that has been employed to detect subsurface voids is electrical resistivity (Noel and Xu, 1992; Manzanilla et al., 1994). McLean and Luke (2006) made a resistivity survey across Fort Stanton Cave, NM, and many of their profiles showed evidence for known underlying passages. Additional surveys performed in areas without known caves showed similar anomalies, perhaps indicating undiscovered caves. Nevertheless, limestone has a very high resistivity, and this method is likely to be less successful for features in carbonate rock. Natural potential surveys have been utilized as well, but relationships between the anomaly pattern and cave locations are not always clear (Lange, 1999).

Magnetic surveys are useful for detecting open voids in iron-rich rocks that produce differences in magnetism, and this method has been able to detect lava tubes in volcanic rocks (Green, 2003). However, the scarcity of magnetic minerals in typical soluble rocks renders this technique inadequate. Ground-penetrating radar (GPR) is well suited for finding and mapping the shallow soil-bedrock interface and shallow cave systems (Chamberlain et al., 2000; Murphy et al., 2005), but much like gravity surveys it is depth-limited. Open voids must be relatively shallow (typically < 30 m), but the effective depth is often much less than this due to the clay rich soil layers associated with most carbonate-hosted caves.

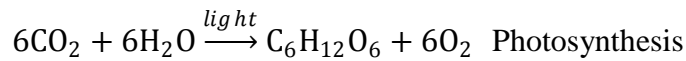
Seismic surveys are commonly used to map subsurface anomalies (Cook, 1965). However, neither reflection nor refraction seismology is well suited for detecting open subsurface caverns, but three-dimensional mapping with shallow reflection has shown some promise (Stierman, 2004). Nevertheless, these methods are associated with extensive computer processing, and placement of the geo- and hydrophones is time consuming and laborious for prospecting for caves. This technique is likely better suited for determining the location of geologic structures that can influence the location and pattern of caves, rather than for precisely delineating passages.

6.1.2. Chemical Basis

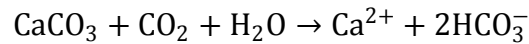
This study presents a novel, inexpensive, and straightforward geochemical technique for detecting open cave passage in carbonate-hosted spring systems using DO and pH measurements. Recharge and subsurface waters are depleted in O₂ and enriched in CO₂ by respiration and decomposition, but re-equilibrate when they contact open air, either inside the cave or above ground (Palmer, 2007). The degassing of CO₂ when

saturated groundwaters encounter open air is well established (Drever, 1997; Langmuir, 1997; Baldini et al., 2006), and the depletion of DO in recharge waters has also been observed (Jacobson and Langmuir, 1974; Boulding and Ginn, 2004). Thus, using DO and pH as a means to find vadose cave passages can be applied in carbonate-hosted caves, and it is proposed that field meters can be used at spring orifices to elucidate whether the upstream passages are open or closed.

This method is centered on the basic biochemical processes of O₂ removal and CO₂ production by respiration, and the reverse by photosynthesis:



as well as the abiotic process of dissolution and precipitation in carbonate-hosted springs:



In addition, other processes play a role in the relative gas contents of spring water such as chemical oxygen demand.

The pH of pure water in equilibrium with the atmosphere ($P_{\text{CO}_2} = 10^{-3.5}$ bar) is 5.66 and is representative of unpolluted rain water, but if calcite is present the pH of the equilibrated open system is 8.26 (i.e., carbonate-hosted waters). However, dissolved CO₂ concentrations in limestone aquifers are almost always above the 10^{-3.5} bar expected for waters in equilibrium with the atmosphere (Back and Hanshaw, 1970; Holland et al., 1964; Langmuir, 1971). This is the result of P_{CO_2} mediation by the soil atmosphere in the recharge area. The soil atmosphere has a much higher concentration of CO₂, and is usually 10^{-2.5} to 10^{-1.5} bar (Troester and White, 1984; White, 1988), as a result of microbial and plant root respiration, decay of organic matter (OM), and the restricted

circulation of soil air. Moreover, the O₂ content is 5 to 20% of the soil atmosphere (or 10^{-1.3} to 10^{-0.7} bar) but can drop to almost zero in poorly drained soils (Brady and Weil, 2008). Thus, as rain percolates through the soil, its CO₂ content typically increases to an equivalent *f*CO₂ of 10⁻² bar in typical humid, temperate climate soils (Langmuir, 1997) and the O₂ content is reduced. These high CO₂-low O₂ soil waters then recharge local aquifers, where OM decay can continue.

CO₂-rich waters are largely responsible for the high content of total dissolved CO₂ in subsurface water. In closed systems, limestone dissolution occurs until CO₂ is consumed while open systems retain high CO₂ concentrations and can dissolve more calcite. If closed system waters return to an open system, such as air-filled cave passages or they emerge as springs, they degas their high CO₂ content and take up O₂ to achieve equilibrium with the lower *P*_{CO₂} and higher *P*_{O₂} of the overlying air. This commonly leads to calcite deposition, sometimes evidenced by the development of speleothems (Dreybrodt, 2005), and can lead to dramatic increases in pH. This process has been observed in groundwater seeps in Paulter Cave, which generally had a lower pH than water in the cave streams (Friedrich et al., 2011).

The *P*_{CO₂} in cave air generally increases with increased distance into caves (Baldini et al., 2006), though the rate at which the CO₂-rich cave air mixes with outside air depends on cave size and cave entrance size (James, 2004; Herman, 2005). Previous unpublished studies on Cliff Cave and 23° Cave by Steiner et al. (2007) found a similar increase in *P*_{CO₂} of cave air and also found that the δ¹³C values of the cave air CO₂ varied from approximately -9‰ at the entrance to -18‰ deeper into the cave during the summer months. The distance into the cave at which -18‰ values were measured varied between

caves (300 m for Cliff Cave and 60 m for 23° Cave), but were consistently in the deepest, narrowest passages in the cave. The depleted $\delta^{13}\text{C}$ values deep inside these caves were similar to those for C3 plants (-38‰ to -22‰; Farquahar et al., 1989), demonstrating the contribution of the CO_2 derived from the decay of C3 plants in the overlying soils. However, the P_{CO_2} and $\delta^{13}\text{C}$ values can vary seasonally, and Steiner et al. (2007) found that samples collected near the main entrance of Cliff Cave (up to 250 m inside) during cold, winter conditions have homogeneous P_{CO_2} and $\delta^{13}\text{C}$ values. The homogenous P_{CO_2} and $\delta^{13}\text{C}$ values suggests that cave exhalation is more pronounced during the winter, and that the mixing of air within the cave enhances exchange between the isotopically light CO_2 in groundwater with the heavier atmospheric CO_2 .

6.2. Description of Study Sites

A total of 46 features including phreatic springs, cave springs, resurgences, surface streams, wastewater treatment plant (WWTP) effluents, and a lake were sampled on multiple occasions to document variations in DO and pH over a wide range of hydrologic, lithologic, and land use conditions (Figure 6.1). In the following, the term “phreatic spring” is applied to features that lack known cave passage, although there is the possibility that undiscovered, air-filled passages exist. In contrast, the term “cave spring” is used to describe streams issuing from enterable caves. Only perennial, flowing phreatic and cave springs were selected; mean discharges ranged from 0.0001 to 4.1 cms, which equates to effective catchment areas of 10 to 450 km^2 (Vineyard and Feder, 1982). Samples were collected during high and low flow conditions.

Mississippian and Ordovician limestones host the majority of the features studied here, though one watershed is underlain by St. Peter Sandstone and one spring issues

from Quaternary alluvium. Most features are located in sinkhole plains or in their highly modified, urban remnants, and several mapped caves of varying size were included in the study: Cliff Cave, Double Drop Cave, Onondaga Cave, and Babler Cave (Vineyard and Feder, 1982; Criss et al., 2006; Figure 6.2).

Features corresponding to a variety of land use, including urban, agricultural, and rural, were included in the study. Extensive chemical datasets were collected over a two-year period (2010-2011), and further contributions were made to a series of field and isotope measurements that have been maintained for the last 16 years for numerous phreatic and cave springs. Most samples in this study were collected during the summer months when soil respiration effects would be largest, but archival samples were collected throughout the year.

6.3. Methods

Standard field sampling techniques and lab analyses were employed for all the samples (see Chapter 2 for details). The DO was measured in both ppm and % saturation. However, % saturation was used for comparison between features since overall dissolved O₂ concentration depends on temperature, altitude, and salinity. Concentrations of HCO₃⁻ were calculated using ion balancing for the measured major ions (including cations: Ca²⁺, Mg²⁺, Na⁺, K⁺, and NH₄⁺-N and anions: Cl⁻, NO₃⁻-N, PO₄³⁻, SO₄²⁻-S, and SiO₄⁴⁻-Si) and pH, and *f*CO₂, *f*O₂, and carbonate alkalinity were calculated using Geochemist's Workbench Standard 8.0.

Multiple traverses along several spring branches were made to establish dynamic changes in water chemistry downstream of the orifice. These traverses were selected based on the length of the spring branch. Short spring branches, including those that

traveled only a few meters before joining a surface stream or returning to the subsurface via a swallow hole, or those artificially dammed near the orifice, were not selected for traverse studies. Traverses within the caves were not possible due to the limited access to these features as a measure to curtail the spread of white nose syndrome in bats. Measurements at the spring orifice were repeated at the end of each series to determine if any instrumental drift occurred during the sampling interval; these duplicate measurements consistently showed minimal drift. In particular, the DO varied less than 0.2 ppm and 1.5%, pH varied less than 0.02 units, and SpC varied less 0.3%, all within error of the instruments (± 0.3 ppm or 2% of reading, 0.02 pH units, and 0.5% of the reading, respectively).

6.4. Results and Discussion

Results are discussed in the following subsections. All relevant chemistry for the features is compiled in Table 6.1 and further chemical analyses are presented in Appendix K.

6.4.1. Dissolved Oxygen and pH

The DO and pH values plotted in Figure 6.3 show distinct differences between phreatic springs and cave springs. For the aforementioned reasons, gas equilibration in open cave systems results in systemically higher DO and pH contents in these waters. However, due to different chemistries among the recharge waters and their subsequent subsurface paths and the fact that some of the “phreatic” springs may be incorrectly classified, there is a continuum of DO and pH values with some overlap (gray box, Figure 6.3A).

Archival data from the Washington University Stable Isotopes Laboratory (WUSIL; e.g., Criss and Winston, 2007) show a similar trend to the data in this study (Table 6.2; Figure 6.3B). Spring pH data for these archived measurements are similar to those in this study, but can be more than 0.5 pH units higher for cave streams. Most of the archived phreatic spring pH values are below 7.5. The DO measurements for archival spring data are substantially higher than those measured in this study, with many samples above 80% saturation. Similarly, the DO exceeds 100% saturation for many of the cave springs. Given that these measurements were made by numerous people with different levels of field experience, the accuracy of their data is unknown. Likewise, the sampling distance from the orifice of these springs is not always known, and if these measurements were made some distance from the orifice, changes in dissolved gas content may have occurred. However, DO values for the archived samples are often higher in the winter than in the summer months; thus, some of the chemical differences observed between the samples in this study and the archived data may be the result of seasonal variations in DO contents. This seasonal effect is likely the result of reduced biological activity in recharge waters during colder periods.

Spring branch traverses for both types of springs further established that gas equilibration processes occur in these waters (Figure 6.4). These equilibration rates are comparable to the surface residence time for these features, and, thus, both kinetic and equilibrium concepts apply; that is, gas solution-exsolution rates typically have half-times on the order of minutes (Langmuir and Mahoney, 1985), which is comparable to spring discharge rates. These degassing equilibrium processes were observed in all the phreatic spring traverses.

Equilibration of pH was typically slower than for DO, a phenomenon that has been observed in other carbonate springs (Omelson et al., 2006), and most springs did not reach steady pH values by the end of the traverse (Figures 6.5A, B). On the other hand, DO equilibration was quite rapid for the springs; typically, steady state was attained in the first 150 m of the traverse. Phreatic springs showed large increases in pH, sometimes by almost a pH unit, and similar behavior has been observed in other carbonate-hosted springs (Usdowski et al., 1979; Dandurand, 1981). In contrast, cave springs generally showed only small increases in pH (less than 3%) within the first 30 m of the traverse, with the exception of Babler Cave Spring. Concomitant decreases in DO of > 10% usually occurred, presumably due to microbial activity. Small caves systems, such as Babler Cave Spring (Figure 6.2A), which has a maximum length of 30 m and diameter of 3 m (but its passage is commonly much narrower than this), had lower DO and pH and varied more along a traverse down its spring branch. This is likely a result of the small atmospheric volume with which the cave stream can equilibrate.

These equilibration rates can be represented by the equation:

$$\frac{C - C_{eq}}{C_i - C_{eq}} = e^{-ad}$$

where C is the concentration at a given distance, C_i is the orifice concentration, C_{eq} is the concentration at equilibrium, d is the distance from the orifice, and a is a constant.

However, the final equilibrium concentrations are unknown and can be unique for each feature because multiple and complex processes affect the equilibrium endpoint (Dandurand et al., 1981). Consequently, one cannot assume that these features equilibrate completely with the atmosphere by the end of the traverses.

The DO and pH data for these springs are simultaneously influenced by variable rates of photosynthesis and respiration. Photosynthetic activities during the hours of maximum solar radiance remove CO₂ and add O₂ from the spring waters, while respiration has the opposite effect. Respiration is the dominant biologic control on these dissolved gases during the night when photosynthetic organisms are inactive. Accordingly, diurnal DO and pH cycles have been noted (Parker et al., 2005; this study, Chapter 3). Photosynthetic processes such as these were found to have a profound effect on springs with high nutrient contents. Specifically, springs that have high nutrient loads (typically NH₄⁺-N > 0.2 ppm; PO₄³⁻ > 0.5 ppm; e.g., urban Blackburn Spring; Figures 6.4, 6.5) have lower DO and pH at the orifice (less than 60% saturation and 7.0, respectively) due to enhanced microbial activity fostered by high nutrient availability. There was no discernible trend in the NO₃⁻-N contents for the springs with higher nutrient concentrations. However, the most dramatic expression of high nutrient availability was noticed several meters away from the spring orifice, where large algal mats were evolving visible gas bubbles, presumably via photosynthetic oxygen production. This effect is minimal at the spring orifices themselves as they were often heavily shaded and subsurface conditions do not permit photosynthetic activity.

Aquifer properties play an important role in determining the relative amounts of dissolved CO₂ and O₂. The gas contents in the recharge waters depend on whether these waters percolate through soils rich in OM, which enhance decomposition and create more anoxic conditions, or whether they travel through bare rock fractures that have less OM content, and foster the retention of lower CO₂ and higher O₂ contents. The distribution and reactivity of OM and other potential reductants in the aquifer can also have

differential effects on CO₂ and O₂ concentrations. The distribution of potential redox materials such as MnO₂, Fe(OH)₃, and Fe₂O₃ in the aquifer can affect the DO content.

The circulation rate of groundwater determines the extent to which DO and pH values can be modified in the subsurface. If residence times are short, then the relatively slow bacterial reactions have insufficient time to alter the DO and pH of the water. Despite this complication, residence times for these features tend to be rather long (Frederickson and Criss, 1999) and OM appears to be metabolized similarly in the area as these trends reliably predict the presence of air filled passage in these subsurface systems. Once the groundwater reaches the surface, the amount of aeration (including rapids and waterfalls) can exert significant control on the rate of gas equilibration. Similarly, the discharge of the spring influences the rate of equilibration. For instance, Maramec Spring, a first magnitude spring with the average discharge volume of 4.1 cms (Vineyard and Feder, 1982) during the study, requires significant time to mix fully, and, consequently, to equilibrate (see Figures 6.5A, B).

6.4.2. Calcite Saturation

Further chemical analysis in conjunction with chemical modeling determined the influence of CO₂ degassing on the saturation state of carbonate minerals in phreatic springs and cave springs. Figure 6.6 shows the relationship between Ca²⁺ and *f*CO₂ contents and calcite saturation. Cave spring waters are typically supersaturated with respect to calcite, and their saturation indices are typically greater than 0.5, but can reach over 1.2, while phreatic springs have saturation indices under 0.5, and are commonly undersaturated (Figure 6.6). Supersaturation in both types of spring water is, in part, attributed to elevated dissolved carbonate species in recharge area soil waters, but in cave

systems is also a result of CO₂ degassing that leaves the Ca²⁺ concentration unchanged until precipitation of calcite occurs. However, the cave air was not always fully equilibrated with the surface air, and evidence of further degassing was observed at a waterfall below Double Drop Spring, where tufa deposition had occurred. Another minor effect on these cave waters is evaporation, which causes the Ca²⁺ concentration to increase. Evaporative and degassing processes are the driving forces in the formation of speleothems (Baldini et al., 2008), and evaporative processes are seen in stable isotope data (see 6.4.4 Stable Isotopes section).

Two of the stream samples are undersaturated with respect to calcite. LaBarque Creek is undersaturated (Figure 6.6) because its watershed is underlain by St. Peter Sandstone, an extremely pure sandstone with > 98% Si₂O. Kiefer Creek was sampled during high flow conditions dominated by event water that is typically undersaturated with respect to calcite (Figure 6.6). Despite these exceptions, surface and cave waters are almost always supersaturated with respect to calcite.

6.4.3. Total Suspended Solids and *E. coli*

Phreatic springs generally have lower *E. coli* levels than cave springs and surface streams due to reduction of suspended particles and less turbulent flow in the subsurface (Dussart-Baptista et al., 2003). Moreover, this study documents that the TSS in phreatic springs was half that of the cave springs and a quarter that of the surface streams (Table 6.1). Values for phreatic springs range from 6 cfu/100 mL to off scale (18% of the measurements were off-scale), while cave springs range from 15 cfu/100 mL to off scale (25% of the measurements were off-scale; Table 6.1). However, when off-scale measurements were excluded, the cave springs had average *E. coli* levels 100 cfu/100 mL

higher than the phreatic springs. Bacterial levels are typically high after storms in all samples, because flood waters have high suspended loads to which bacteria are adhered (Pronk et al., 2007).

6.4.4. *Stable Isotopes*

Stable isotope data show that cave springs have undergone more evaporation than phreatic springs (Figure 6.7). Phreatic springs have an average $\delta^{18}\text{O}$ value of -6.7‰ and average δD value of -43‰ (Table 6.1), which is close to the average values of local meteoric precipitation in St. Louis, MO (Criss, 1999). Archival data show similar results (Table 6.2). These similarities indicate that all these waters are derived from local meteoric precipitation that has become variably homogenized in shallow groundwater systems. It also suggests that these waters have a relatively long residence time within the aquifer according to a linear reservoir model (Criss, 1999; Criss et al., 2007), but residence times tend to be longer for the phreatic springs than for the cave springs. An exception is Weldon Spring, whose elevated average $\delta^{18}\text{O}$ value of -5.5‰ reflects the large contributions of evaporated lake water to its flow (Criss et al., 2001). In detail, the isotopic values of springs fluctuate seasonally, and are perturbed following large rainfall events (Lakey and Krothe, 1996).

The isotopic values of surface streams, on the other hand, are more variable and consistently higher than the values for springs ($\delta^{18}\text{O} = -6.2\text{‰}$; $\delta\text{D} = -41\text{‰}$; Table 6.1). This result is consistent with evaporative enrichment of ^{18}O and D in surface and soil waters during the summer and fall (Criss, 1999). The $\delta^{18}\text{O}$ and δD values and their variability suggest that base flow is dominated by meteoric water with a relatively short residence time (approximately 100 days). Cave springs have an intermediate average

$\delta^{18}\text{O}$ value of -6.5‰ and average δD value of -43‰, which indicates that these systems may include higher contributions of surface runoff than phreatic springs. Cave springs also are consistently more evaporated as they commonly plot below the meteoric water line (MWL; Figure 6.7).

6.5. Conclusions

Open cave passages are difficult to discover. Geophysical methods for cave detection are expensive and also require that the general location of the passage is previously known. Once a spring orifice is discovered, the geochemical approach outlined in this study exploits the well-established changes in dissolved CO_2 and O_2 that occur when phreatic groundwaters encounter open air. These equilibrium processes can be used to detect open cave passage in spring systems with conventional water quality equipment. Cave springs have elevated DO and pH compared to phreatic springs, and these cave spring systems have calcite saturation indices over 0.5. Cave spring waters are also typically higher in TSS and *E. coli* due to more turbulent flow in the subsurface, and they experience more evaporative isotopic enrichment than their phreatic spring counterparts.

6.6. References

- Back, W.B., and Hanshaw, B.B., 1970, Comparison of chemical hydrogeology of the carbonate peninsulas of Florida and Yucatan: *Journal of Hydrology*, special issue 10, p. 77-93.
- Baldini, J.U.L., Baldini, L.M., McDermott F., and Clipson, N., 2006, Carbon dioxide sources, sinks, and spatial variability in shallow temperate zone caves: Evidence from Ballynamintra Cave, Ireland: *Journal of Cave and Karst Studies*, v. 68, p. 4-11.
- Baldini, J.U.L., McDermott, F., Hoffmann, D.L., Richards, D.A., and Clipson, N., 2008, Very high-frequency and seasonal cave atmosphere PCO₂ variability: Implications for stalagmite growth and oxygen isotope-based paleoclimate records: *Earth and Planetary Sciences Letters*, 272, p. 118-129.
- Brady, N.C., and Weil R.R., 2008, *The nature and properties of soils*, 14th ed.: Ohio, Prentice Hall, Inc., 975 p.
- Boulding, J.R., and Ginn, J.S., 2004, *Practical handbook of soil, vadose zone, and ground-water contamination: Assessment, prevention, and remediation: Florida*, Lewis Publishers, 693 p.
- Brod, L., and Lyon, J., 1965, Double drop cave: File Map St. Louis County (SLO) 065.
- Brown, M.C., 1972, Karst hydrogeology and infrared imagery, an example: *Geological Society of America Bulletin*, v. 83, p. 3,151-3,154.
- Butler, D.K., 1984, Microgravimetric and gravity gradient techniques for detection of subsurface cavities: *Geophysics*, v. 49, p. 1,084-1,096.
- Campbell, C., Latif, M., and Foster, J., 1996, Application of thermography to karst hydrology: *Journal of Cave and Karst Studies*, v. 58, p. 163-167.
- Chamberlain, A.T., Sellers, W., Proctor, C., and Coard, R., 2000, Cave detection in limestone using ground penetrating radar: *Journal of Archaeological Science*, v. 27, p. 957-964.
- Cook, J.C., 1965, Seismic imaging of underground cavities using reflection amplitude: *Geophysics*, v. 30, p. 527-538.

Cravens, T., Heier, R., Thenhaus, P., and Victor, F., 1971 Babler Spring Cave: File Map St. Louis County (SLO) 004. Missouri: Missouri Speleology, v. 45, p. 1-16.

Criss, R.E., 1999, Principles of stable isotope distribution: Oxford, U.K., Oxford University Press, 254 p.

Criss, R.E., Davisson, M.L., Surbeck, H., and Winston, W.E., 2007, Isotopic techniques, *in* Drew, D., and Goldscheider, N., eds., Methods in karst hydrogeology: London, Taylor & Francis, Ch. 7, p. 123-145.

Criss, R.E., Fernandes, S.A., and Winston, W.E., 2001, Isotopic, geochemical and biological tracing of the source of an impacted karst spring, Weldon Spring, Missouri: Environmental Forensics, v. 2, p. 99-103.

Criss, R.E., Lippmann, J.L., Criss, E. M., and Osburn, G.R., 2006, Caves of St. Louis County, Missouri: Missouri Speleology, v. 45, p. 1-18.

Criss, R.E., and Winston, W.E., 2007, Chemical and isotopic measurements of springs: unpublished raw data.

Dandurand, J.L., Gout, R., Hoefs, J., Menschel, G., Schott, J., and Usdowski, E., 1981, Kinetically controlled variations of major components and carbon and oxygen isotopes in a calcite-precipitating spring: Chemical Geology, v. 36, p. 299-315.

Davis, D.G., 2000, Extraordinary features of Lechuguilla Cave, Guadalupe Mountains, New Mexico: Journal of Cave and Karst Studies, v. 62, p. 147-157.

Drever, J.I., 1997, The geochemistry of natural waters: Surface and groundwater environments: Upper Saddle River, New Jersey, Prentice-Hall, 436 p.

Dreybrodt, W., 2005, Speleothem deposition, *in* Culver, D.C. and White, W.B., eds., Encyclopedia of caves: New York, Elsevier Academic Press, p. 543-549.

Dussart-Baptista, L., Massei, N., Dupont, J.-P., and Jouenne, T., 2003, Transfer of bacteria-contaminated particles in a karst aquifer: Evolution of contaminated materials from a sinkhole to a spring: Journal of Hydrology, v. 284, p. 285-295.

Farquahar, G.D., Ehleringer, J.R., and Hubick, K.T., 1989, Carbon isotope discrimination and photosynthesis: Annual Review of Plant Physiology and Plant Molecular Biology, v. 40, p. 503-537.

- Frederickson, G.C., and Criss, R.E., 1999, Isotope hydrology and time constants of the unimpounded Meramec River basin, Missouri: *Chemical Geology*, v. 157, p. 303-317.
- Friedrich, A.J., Hasenmueller, E.A., and Catalano, J.G., 2011, Composition and structure of nanocrystalline Fe and Mn oxide deposits: Implications for contaminant mobility in a shallow karst system: *Chemical Geology*, v. 284, p. 82-96.
- Green, D.J., 2003, The effects of lava on compass readings: Salt Lake City, Salt Lake Grotto: National Speleological Society, Technical Note 99, p. 75-84.
- Herman, J.S., 2005, Water chemistry in caves, *in* Culver, D.C., and White, W.B., eds., *Encyclopedia of caves*: New York, Elsevier Academic Press, p. 609-614.
- Holland H.D., Kirsipu, T., Huebner, J., and Oxburgh, U., 1964, On some aspects of the chemical evolution of cave waters: *Journal of Geology*, v. 72, p. 36-67.
- Horrocks, R.D. and Szukalski B.W., 2002, Using geographic information systems to develop a cave potential map for Wind Cave, South Dakota: *Journal of Cave and Karst Studies*, v. 64, p. 63-70.
- House, S., 1985, Onondaga Cave; surveyed by House, S., Butts, L., Hauck, P., Baker, D., Wagner, J., Sutton, M., Hagan, S., Compas, E., et al.: File Map Crawford County (CRD) 001.
- Jacobson, R.L., and Langmuir, D., 1974, Controls on the quality variations of some carbonate spring waters: *Journal of Hydrology*, v. 23, p. 247-265.
- James, J., 2004, Carbon dioxide-enriched cave air, *in* J. Gunn, ed., *Encyclopedia of caves and karst science*: New York, Fitzroy Dearborn, p. 183-184.
- Lakey, B., and Krothe, N.C., 1996, Stable isotopic variation of storm discharge from a perennial karst spring, Indiana: *Water Resources Research*, v. 32, p. 721-731.
- Lange, A.L., 1999, Geophysical studies at Kartchner Caverns State Park, Arizona: *Journal of Cave and Karst Studies*, v. 61, p. 68-72.
- Langmuir, D., 1971, The geochemistry of some carbonate ground waters in central Pennsylvania: *Geochimica et Cosmochimica Acta*, v. 35, p. 1,023-1,045.

Langmuir, D., 1997, *Aqueous environmental geochemistry: Upper Saddle River, New Jersey*, Prentice-Hall, 600 p.

Langmuir, D., and Mahoney, J., 1985, Chemical equilibrium and kinetics of geochemical processes in ground water studies, *in* Hitchon, B., and Wallick, E.I., eds., *Practical applications of ground water geochemistry*, Proceedings 1st Canadian/American Conference on Hydrogeology: Worthington, Ohio, National Water Well Association, p. 69-95.

Linford, N.T., 1998, Geophysical survey at Boden Vean, Cornwall, including an assessment of the microgravity technique for the location of suspected archaeological void features: *Archaeometry*, v. 40, p. 187-216.

Manzanilla, L., Barba, L., Cha´vez, R., Tejero, A., Cifuentes, G. and Peralta, N., 1994, Caves and geophysics: An approximation to the underworld of Teotihuacan, Mexico: *Archaeometry*, v. 36, p. 141–157.

Marty, A., Marty, J., and Bielawski, S., 1982, *Cliff Cave: File Map St. Louis County (SLO) 013*.

McLean, J., and Luke, B., 2006, Electrical resistivity surveys of karst features near Fort Stanton, Lincoln County, New Mexico: *New Mexico Geological Society, Guidebook to 57th Annual Field Conference*, p. 227-232.

MSDIS (Missouri Spatial Data Information Service. Data Resources), 2011, *Missouri Spatial Data Information Service: University of Missouri Web page*, <http://www.msdis.missouri.edu>.

Murphy, P.J., Parr, A., Strange, K., Hunter, G., Allshorn, S., Halliwell, R., Helm, J., and Westerman, R., 2005, Investigating the nature and origins of Gapping Gill Main Chamber, North Yorkshire, UK, using ground penetrating radar and lidar: *Cave and Karst Science*, v. 32, p. 25-38.

Noel, M., and Xu, B., 1992, Cave detection using electrical resistivity tomography: *Cave Science*, v. 19, p. 91-94.

Omelon, C.R., Pollard, W.H., and Andersen, D.T., 2006, A geochemical evaluation of perennial spring activity and associated mineral precipitates at Expedition Fjord, Axel Heiberg Island, Canadian High Arctic: *Applied Geochemistry*, v. 21, p. 1-15

Palmer, A.N., 2007, Cave geology: Dayton, OH, Cave Books, 454 p.

Parker, S.R., Poulson, S.R., Gammons, C.H., and DeGrandpre, M.D., 2005, Biogeochemical controls on diel cycling of stable isotopes of dissolved O₂ and dissolved inorganic carbon in the Big Hole River, Montana: *Environmental Science & Technology*, v. 39, 7,134-7,140.

Pronk, M., Goldscheider, N., and Zopfi, J., 2007, Particle-size distribution as indicator for fecal bacteria contamination of drinking water from karst springs: *Environmental Science & Technology*, v. 41, p. 8,400-8,405.

Smith, D.L., and Smith, G.L., 1987, Use of vertical gravity gradient analyses to detect near-surface dissolution voids in karst terranes, *in* Beck, B.F., and Wilson, W.L., eds., *Karst hydrology: Engineering and environmental applications*: Rotterdam, Balkema, p. 205-210.

Steiner, A., Marlow, J., Orland, I., and Wiseman, S., 2007, Unpublished data: Department of Earth and Planetary Sciences, Washington University in St. Louis, St. Louis, MO.

Stierman, D.J., 2004, Geophysical detection of caves and karstic voids, *in* Gunn, J., ed., *Encyclopedia of caves and karst science*: New York, Fitzroy Dearborn, p. 377-380.

Thompson, J., and Marvin, M., 2005, Experimental research on the use of thermography to locate heat signatures from caves *in* *Proceedings of the 17th National Cave and Karst Management Symposium*: Huntsville AL, National Speleological Society, p. 102-115.

Troester, J.W., and White, W.B., 1984, Seasonal fluctuations in the carbon dioxide partial pressure in a cave atmosphere: *Water Resources Research*, v. 20, p. 153-156.

2010 U.S. Census, 2010, Population Density Data: 2010 U.S. Census Web page, <http://2010.census.gov/2010census/>.

Uzdowski, E., Hoefs, J., and Menschel, G., 1979, Relationship between ¹³C and ¹⁸O fractionation and changes in major element composition in a recent calcite-depositing spring; a model of chemical variations with inorganic CaCO₃ precipitation: *Earth and Planetary Science Letters*, v. 42, p. 267-276.

White, W.B., 1988, *Geomorphology and hydrology of karst terrains*: New York, Oxford University Press, 464 p.

Vineyard, J., and Feder, G.L., 1982, Springs of Missouri: Missouri Department of Natural Resources Water Resources Report 29, 266 p.

Table 6.1. Concentration means and ranges for selected water quality constituents for various types of waters.^a

	Phreatic Springs	Resurgences	Cave Springs	Streams	Treated Wastewater	Lake
Total Sampling Sites	25	4	7	7	2	1
Temperature (°C)	14.7	15.3	14.5	16.8	17.9	35.0
	12.5 – 19.4	14.6 – 15.8	11.9 – 16.9	14.3 – 20.1	14.4 – 24.6	
SpC (µS/cm)	760	613	809	515	797	104
	261 – 1524	595 – 624	481 – 1014	191 – 805	773 – 822	
DO (% saturation)	53.9	77.0	76.9	60.7	88.5	80.1
	11.5 – 84.6	72.0 – 86.5	60.1 – 98.5	43.3 – 84.1	66.4 – 107.8	
DO (ppm)	5.50	7.62	7.87	5.96	8.54	5.44
	1.23 – 8.72	7.01 – 8.58	6.08 – 10.16	4.02 – 8.21	5.53 – 10.92	
pH	7.35	7.69	7.95	7.88	8.15	9.66
	6.93 – 8.13	7.65 – 7.72	7.70 – 8.18	7.62 – 8.07	8.00 – 8.30	
TSS (ppm)	22	-	52	92	23	-
	1 – 225		6 – 126	1 – 598	10 – 35	
<i>E. coli</i> (cfu/100 mL)	^b	33	^b	^b	687	14
	6 – >2420	0 – 100	15 – >2420	31.3 – >2420	3 – 1986	
δ ¹⁸ O (‰)	-6.7	-5.2	-6.5	-6.2	-8.4	-3.2
	-8.0 – -3.4	-5.2 – -5.2	-7.3 – -5.7	-6.8 – -5.5	-9.3 – -7.2	
δD (‰)	-43	-34	-43	-41	-57	-30
	-58 – -18	-33 – -34	-49 – -40	-46 – -35	-62 – -50	
Carbonate Alkalinity (ppm) ^c	269	227	278	214	154	23
	107 – 442	224 – 232	216 – 320	65 – 317	110 – 203	
Ca ²⁺ (ppm)	95.5	59.4	100.0	67.5	53.3	9.6
	32.6 – 163.5	59.0 – 59.9	75.2 – 125.7	21.0 – 103.6	46.1 – 65.3	
Mg ²⁺ (ppm)	16.7	24.4	19.9	12.5	17.0	2.0
	6.5 – 34.2	23.3 – 25.1	13.4 – 31.6	3.4 – 16.6	16.0 – 18.2	
HCO ₃ ⁻ (ppm) ^c	384	290	351	285	190	23
	160 – 744	287 – 296	269 – 410	101 – 434	135 – 253	
logfCO ₂ (bar) ^c	-1.928	-2.327	-2.462	-2.584	-2.959	-5.346
	-2.820 – -1.307	-2.362 – -2.287	-2.716 – -1.973	-2.983 – -2.266	-3.130 – -2.693	
logfO ₂ (bar) ^c	-1.018	-0.822	-0.818	-0.945	-0.765	-0.823
	-1.620 – -0.717	-0.856 – -0.765	-0.959 – -0.706	-1.066 – -0.896	-0.885 – -0.668	

^aSee Chapter 2 for performance ranges, errors, and detection limits.

^bObtaining an average was not possible due to off scale measurements.

^cCalculated using Geochemist's Workbench Standard 8.0.

Table 6.2. Concentration means and ranges for selected water quality constituents for archival phreatic and cave spring data.

	Phreatic Springs	Cave Springs
Total Sampling Sites	5	1
Temperature (°C)	12.6	13.0
	6.0 – 19.2	6.0 – 18.6
SpC (µS/cm)	674	803
	148 – 2729	306 – 1235
DO (% saturation)	77.7	93.0
	23.1 – 117.3	62.2 – 111.9
DO (ppm)	8.12	9.66
	2.15 – 12.01	6.03 – 11.47
pH	7.18	8.30
	5.53 – 8.28	7.26 – 8.80
δ ¹⁸ O (‰)	-6.6	-6.3
	-11.0 – -3.3	-7.5 – -4.6

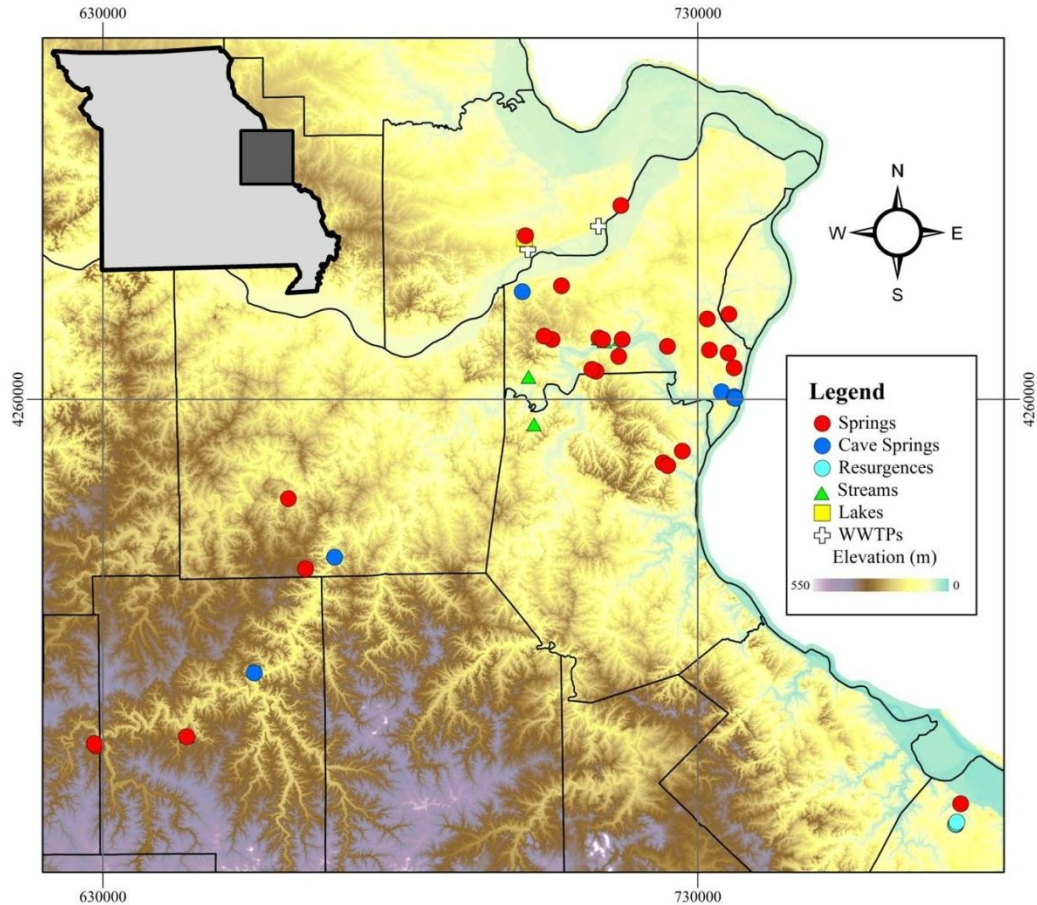


Figure 6.1. Relief map of east-central Missouri showing sample locations. The elevation ranges from 390 m in the southwest to 110 m along the Mississippi River in the southeast. Digital elevation model basemap data are based on the U.S. Geological Survey (USGS) data and provided by MSDIS (2011); overlain on the DEM are the county lines from the 2010 U.S. Census. Gridlines are in UTM eastings and northings (Zone 15, NAD 83; MSDIS, 2011).

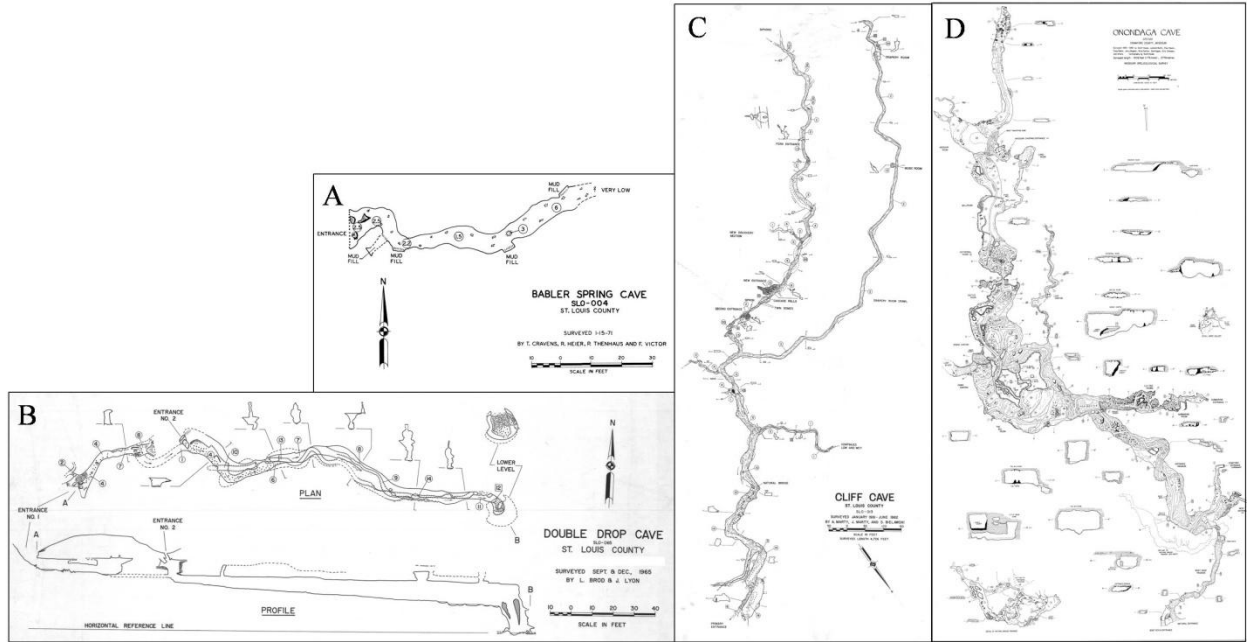


Figure 6.2. Cave maps for (A) Babler Cave (Cravens et al., 1971), (B) Double Drop (Brod and Lyon, 1965), (C) Cliff Cave (Marty et al., 1982), and (D) Onondaga Cave (House et al., 1985) demonstrating the variety in size and form. Samples were collected at the mouth of each feature.

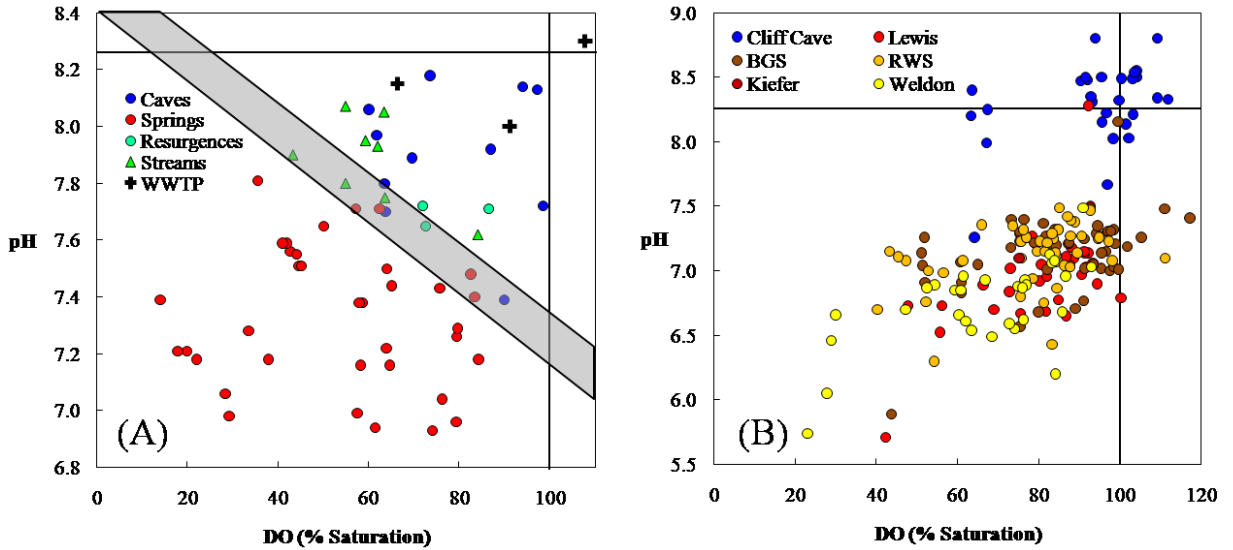


Figure 6.3. (A) The pH versus DO (% saturation) for phreatic springs (red circles), cave springs (blue circles), resurgences (light blue circles), and surface streams (green triangles) in this study and (B) for data acquired by the WUSIL from 1995 to 2008 for phreatic springs (warm colored circles) and cave springs (blue circles). All samples shown in (A) were measured at the orifice; Prairie Lake is off scale with a pH of 9.66 and DO of 80%. Lines for DO saturation (100%) and the pH of pure water in equilibrium with the atmosphere and calcite (8.26) are plotted for reference in both (A) and (B). Note the minor overlap (gray box, 6.3A) of the fields for phreatic springs and cave springs.

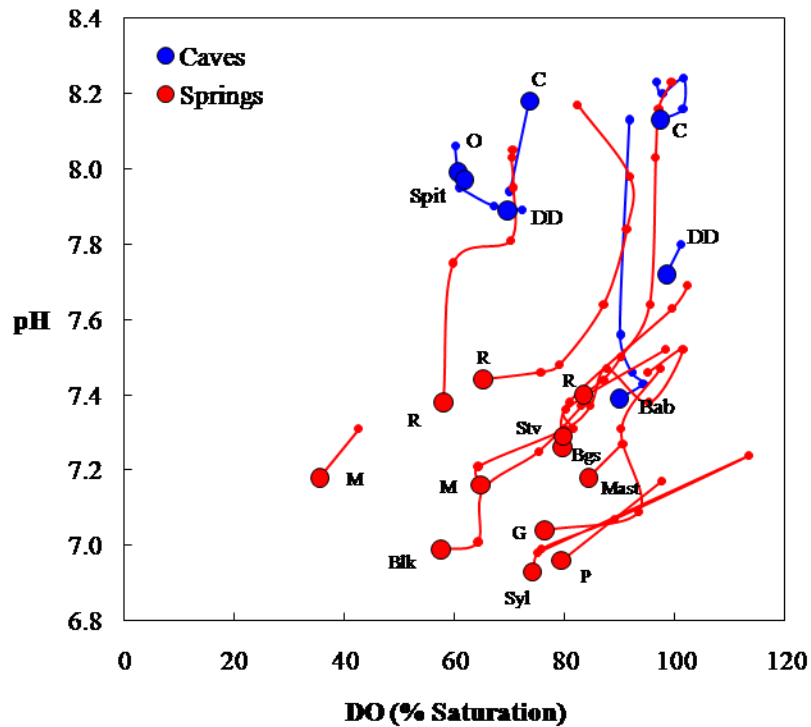


Figure 6.4. The pH versus DO (% saturation) for phreatic springs (red circles) and cave springs (blue circles) for traverses made in this study. Measurements were made at the orifice (larger circles) and along the spring branch (smaller circles). Phreatic springs exhibit rapid increases in DO and pH to reach equilibrium with the atmosphere; cave springs, however, generally increase very little, maintaining their DO and pH values, or even decreasing somewhat due to biological activity. All cave springs (Babler Cave, B; Cliff Cave, C; Double Drop Cave, DD; Onondaga Cave, O; and Spit Cave, Spit) and phreatic springs (Blackburn, Blk; Bluegrass, Bgs; Rockwoods, R; Glatt's, G; Maramec, M; Mastodon, Mast; Pevely Milkhouse, P; Steelville, Stv; and Sylvan, Syl) are labeled. Distances between sampling locations along the traverses are shown in Figure 6.5A, B.

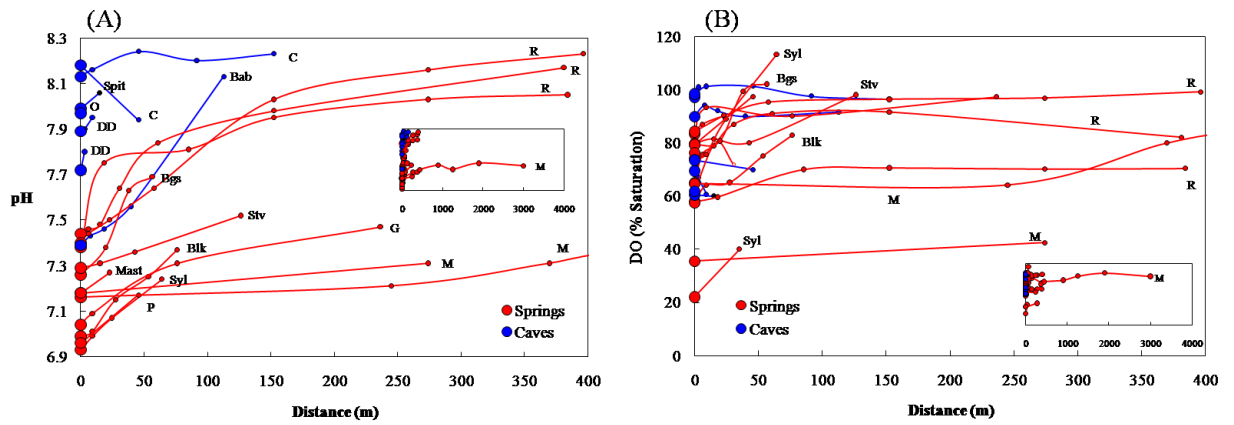


Figure 6.5. (A) The pH and (B) DO (% saturation) versus distances for phreatic springs and cave springs (symbols as in Figure 6.4) for traverses made in this study. Maramec Spring (M) distances are off-scale, but data are shown to scale in the inset.

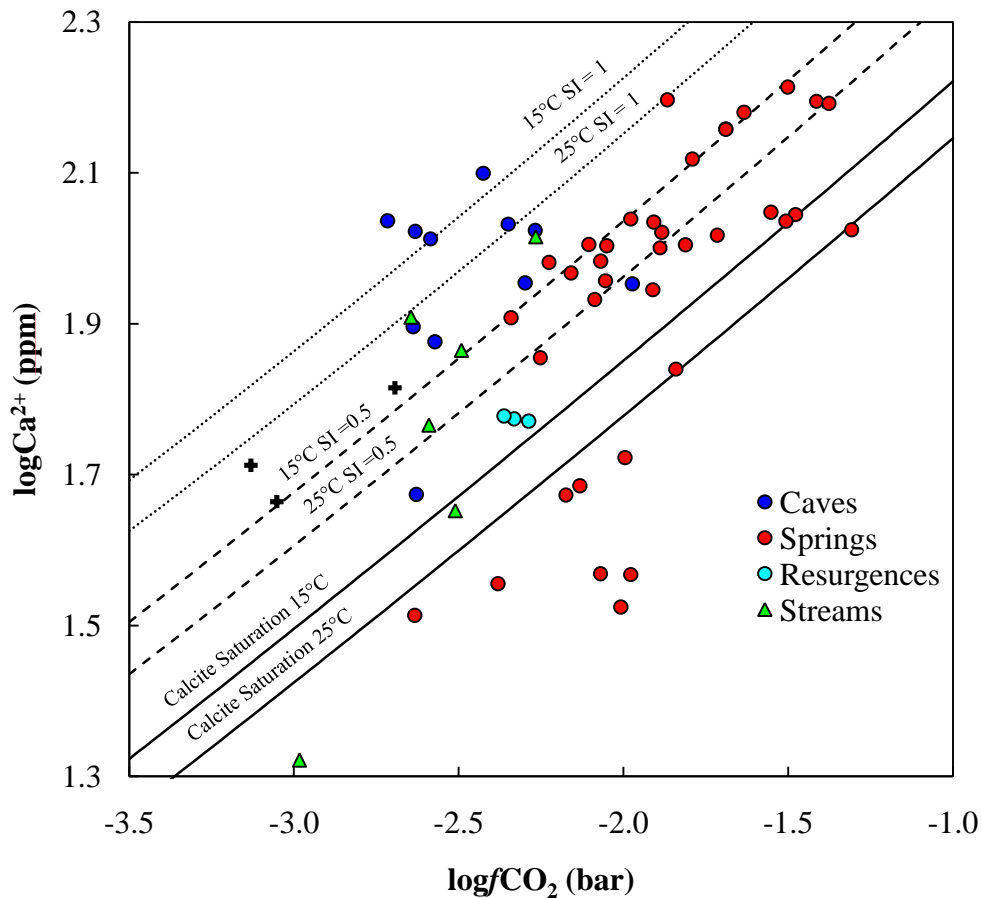


Figure 6.6. The $\log Ca^{2+}$ (ppm) versus $\log fCO_2$ (bar) for various water samples (symbols as in Figure 6.3). Calcite saturation lines are plotted for 15° and 25°C. Lines representing saturation indices of 0.5 (dashed line) and 1.0 (dotted line) for 15° and 25°C are plotted for reference. Note that most cave springs and surface streams have saturation indices above 0.5 due to degassing of CO_2 into the cave atmosphere; however, outliers, including Babler Cave Spring (Bab), LaBarque Creek (L), and Kiefer Creek (K), are labeled. Prairie Lake is off-scale with a $\log Ca^{2+}$ (ppm) of 0.981 and $\log fCO_2$ (bar) of -5.346.

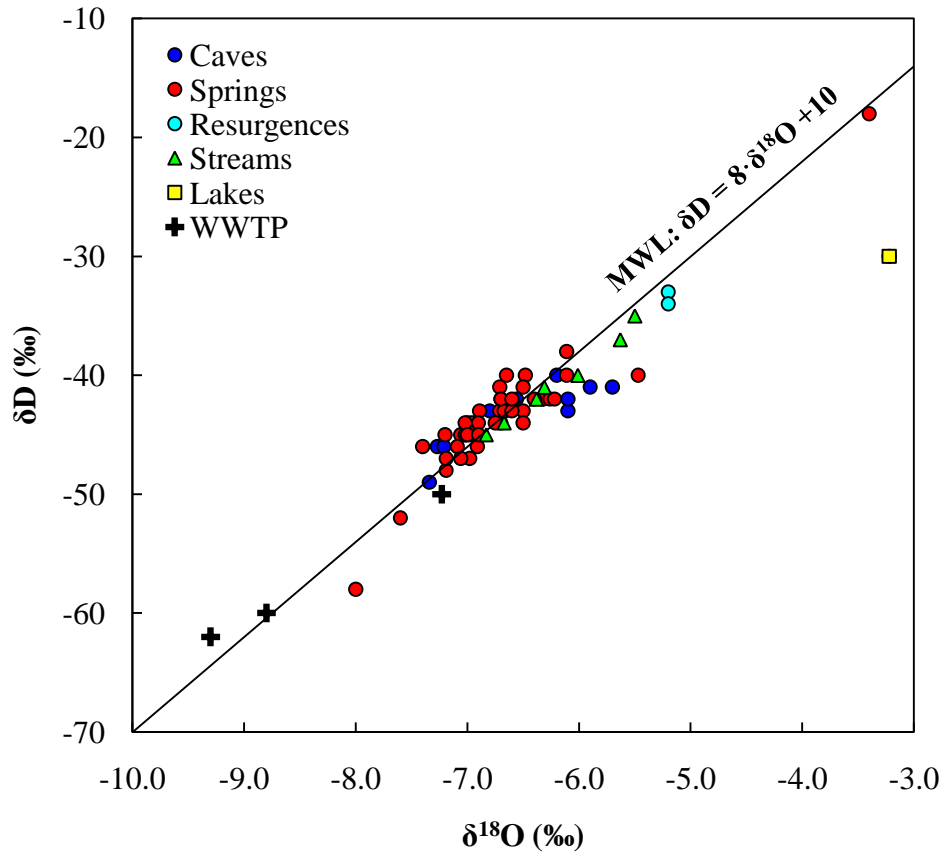


Figure 6.7. The $\delta^{18}O$ (‰) and δD (‰) for the various water samples (symbols as in Figure 6.3). The MWL is shown for reference. Most phreatic springs lie on the line, while the cave springs tend to lie below the line indicating evaporative enrichment. Prairie Lake shows the most enrichment, a common occurrence in lakes. WWTP water is isotopically depleted due to the use of Missouri River water as a municipal water source.

Chapter 7: Conclusions and Future Work

7.1. Conclusions

The diverse hydrologic features of east-central Missouri provide a unique opportunity to study the effects of anthropogenic activities on surface waters and shallow groundwaters. Proximal watersheds spanning a wide range of size and land use can be intercompared in terms of flow variability and water quality. This study used hydrologic, isotopic, and geochemical data to identify factors that control the dynamic response of these hydrologic features to storm perturbations, seasonal and diurnal fluctuations, and the hydrologic and geochemical differences between natural and impacted systems. An extensive database for these features has been created and includes physical and chemical parameters such as stage, discharge, temperature, specific conductivity (SpC), total suspended loads (TSS), pH, major and minor elements, and D and ^{18}O isotopes. These records extend over long periods for a diverse suite of aquatic environments, and they represent an array of hydrologic conditions ranging from low sustained baseflow to the dramatic variations associated with storm-driven flash floods.

Through careful analysis of these data it is possible to understand the climatic, physiographic, and anthropogenic factors that influence surface and shallow groundwater hydrology and chemistry. The results from this study quantify the flow components that combine to produce total streamflow in these features. The long-term component is derived from groundwater while flash floods are comprised of significant amounts of recent rainfall. Peak discharge and recession rate are strongly influenced by land use. This study found that urban streams had reduced baseflow components, higher discharge peaks, and faster recession than their rural counterparts.

Urban streams are also characterized by greater variability in their chemical and isotopic responses to storm perturbations, and invariably exhibit higher contaminant levels in both baseflow and storm flow components. A hierarchy of transport timescales was found for the different chemical and physical parameters, and in each of the basins in this study, SpC and the major elements had the longest response times while turbidity had the shortest response time. The transport of individual solutes depends on storm and basin characteristics and also can be affected by the time of year, antecedent moisture conditions, and land use, but in general, urbanization shortens the transport timescales and amplifies the variability of all individual parameters. The major elements, including Ca, Mg, Na, Cl, Si, and S are most closely associated with the isotopically-identified baseflow fraction. However, the behavior of Na and Cl becomes more complicated following winter road salt applications, as these ions are highly concentrated in melt waters and in the runoff from the first few spring storm events. In contrast, sharp perturbations of temperature, turbidity, dissolved oxygen (DO), pH, and NO_3^- -N correlate most closely with the event water fraction.

Continuous monitoring data collected in this study establish that an infrequent sampling protocol does not accurately quantify the loads of particulates and individual solutes transported by streams in small basins. High resolution data document rapid changes in solutes and other physical parameters that are missed by arbitrary, infrequent sampling regimes.

This work also characterized the dynamic interchanges between surface waters and groundwaters in karst landscapes. The interconnectivity of surface and subsurface waters in these landscapes makes tracing and identifying contaminant sources important.

Human activity degrades surface and groundwater quality, and impacted waters often have elevated SpC, TSS, Cl, nutrient and trace element content, and low DO levels. Pollutants are mobilized by surface waters that penetrate shallow groundwater reservoirs, and because of the longer residence time of groundwaters, these constituents are reintroduced to surface waters as baseflow throughout the year. For example, road deicing salt applied in the winter months can increase the Cl levels nearly 200-fold in surface waters. This study has shown that high Cl concentrations in streams and springs persist into the summer, many months after road salt application, because of widespread contamination of shallow groundwater.

The idea that urban waters are more polluted than rural waters is a platitude, yet few regional studies have quantitatively addressed the impacts of urban development on shallow groundwater systems. In this study, a regional and comparative approach was used by incorporating measurements of a suite of physical and geochemical constituents to address the impact of different types of land use on shallow groundwater springs at numerous hydrologic sites. The results corroborate the findings from other aspects of the study that show that the hydrology and geochemistry of urban watersheds are more impacted, and that the interconnectivity of surface and groundwater systems leads to widespread and persistent water quality issues.

Some trace elements, including B, make ideal conservative tracers of anthropogenic contamination of water. Previous studies have attributed high B concentrations to fertilizer use and/or wastewater effluent or sewer leaks. However, the detailed monitoring of B end-members, surface water runoff, stream water, and shallow groundwaters in this study clearly demonstrates that the dominant source of B

contamination in the St. Louis area is urban irrigation water. Municipal water sources in the St. Louis metropolitan area have distinctively higher B concentrations than natural waters. The use of this water for irrigation purposes dramatically increases the concentration of B in surface runoff; thus, this study has identified another source of B in urban environments.

In addition to documenting the impact of human activities on hydrology and hydrochemistry, this study developed a novel chemical method to detect the nature of the groundwater environment. The subsurface environment imparts a unique geochemical signal on these waters; in particular, the equilibration of O₂ and CO₂ in emergent groundwaters combined with other physical and chemical parameters provides a novel means to detect subterranean, air-filled passages.

Identifying the sources and relative contributions of pollutants allows us to better understand how to remediate many environmental problems. Thoughtful analysis of the role of land use and development will facilitate the improvement of urban watersheds, which will require reducing high flows, increasing low flows, and decreasing pollutant concentrations.

7.2. Future Research

Although this study has quantified several processes that control the hydrological and geochemical responses of surface streams and identified specific sources of pollutants, it has also raised many questions. Continuing lines of research are proposed that could address these questions.

This study established an extensive database on the hydrologic and geochemical variability of regional waters that has just begun to reveal the complexity of these

systems. Continuous monitoring has produced long-term datasets for seven sites for an extensive suite of physical and geochemical parameters. Autosampling coupled with grab sampling efforts produced nearly 2,500 individual samples that represent a wide range of hydrologic features with differing behaviors and anthropogenic influences. Several of the storm pulse sample suites have not yet been thoroughly studied. These samples will facilitate further investigations of both hydrologic and geochemical behavior. The theoretical hydrograph could be applied to more pulse events to enhance understanding of the model and to quantify how variations in event parameters such as storm intensity and basin saturation affect lag time.

In addition, the application of the theoretical hydrograph to individual solutes will characterize the time constants of these parameters and may identify the elements responsible for the slower response of the geochemical system. The separation of real hydrographs into baseflow and event flow constituents will facilitate further applications of the model and allow estimates of the time constants inherent in each type of flow. Trace element compositions have been determined for many existing samples, and further analysis is necessary to positively identify the species that consistently correlate with baseflow or event water components.

Monitoring of additional end-member components (including soil water, forest throughfall, and wastewater components, among others) during pulses in these systems would further understanding of the hydrologic and chemical responses of watersheds. The simplistic two end-member hydrograph separations proposed by Sklash and Farvolden (1979), where only baseflow and storm flow are considered, has substantial limitations (Lee and Krothe, 2001). Often the isotopic and chemical characteristics of

other end-members are unique and identifiable. Future work would entail characterizing these end-members, and determining their relative influence in watersheds with differing land use.

An important contribution to the hydrologic modeling and assessment of the urban impacts on surface waters would be to compare archival U.S. Geological Survey (USGS) discharge data with recent discharge measurements. The author has recently accessed USGS discharge records from the 1970s (Spencer and Alexander, 1978), which were measured prior to the extensive development and expansion of St. Louis County. The theoretical hydrograph model would provide an excellent means to determine how hydrologic response of surface waters has changed over time.

Additional samples from around the region are needed to further characterize B, including more samples from agricultural areas and of wastewaters and lakes. Moreover, diurnal and seasonal cycling of B, and of other major and minor elements, is an important topic for future work. Previous studies using B as a tracer for wastewater and fertilizer inputs have made the assumption that B is a conservative tracer (Bassett et al., 1995; Chetelat and Gaillardet, 2005; this study). However, B is a micronutrient for plants, shows pH dependence, and other trace elements have been observed to undergo diurnal cycling, which indicates that B concentrations may not truly be conserved. Thus, it is important to quantify the influence of such factors on B concentrations.

Regulations intended to curtail the spread of white nose syndrome in bats have restricted access to cave interiors. If permission to enter local caves is obtained in the future, an important contribution to the cave detection method would be to make traverses inside caves to assess groundwater O₂ and CO₂ degassing processes and their

resultant effects on other variables (e.g., pH and Ca). Complementary measurements of CO₂ concentrations in the cave atmosphere, along with isotopic and dissolved inorganic carbon (DIC) concentration data, would shed further light on these processes.

Finally, the continued study of surface runoff quality and quantity, and means to remediate these waters, is important future work. Preliminary efforts to reduce surface runoff volume and to improve its quality using constructional bioretention areas demand further evaluation. There is currently a large suite of hydrological and geochemical data for pre-best management (BMP) practices for several proposed rain garden sites, and future monitoring will assess the effectiveness of such installations.

7.3. References

Bassett, R. L., Buszka, P. M., Davidson, G. R., and Chong-Diaz, D., 1995, Identification of groundwater solute sources using boron isotopic composition: *Environmental Science & Technology*, v. 29, p. 2,915-2,922.

Chetelat, B., and Gaillardet, J., 2005, Boron isotopes in the Seine River, France: A probe of anthropogenic contamination: *Environmental Science & Technology*, v. 39, p. 2,486-2,493.

Lee, E. S., and Krothe, N. C., 2001, A four-component mixing model for water in a karst terrain in south-central Indiana, USA. Using solute concentration and stable isotopes as tracers: *Chemical Geology*, v. 179, p. 129-143.

Sklash, M. G., and Farvolden, R. N., 1979, The role of groundwater in storm runoff: *Journal of Hydrology*, v. 43, p. 45-65.

Spencer, D. W., and Alexander, T. W., 1978, Techniques for estimating the magnitude and frequency of floods in St. Louis County, Missouri: U.S. Geological Survey Water-Resources Investigations Report 78-139, p. 23 p.

Appendix A: Ladue Rainfall

Sample	Precipitation (cm)	$\delta^{18}\text{O}$ (‰)	δD (‰)
6A95L	6.86	-5.7	-34
6B95L	2.29	-6.2	-37
7A95L	2.03	-6.0	-41
7B95L	3.05	-3.9	-16
8A95L	13.97	-5.5	-36
8B95L	3.30	-4.3	-20
9A95L	0.00	NA	NA
9B95L	1.78	-5.6	-35
10A95L	2.26	-6.0	-36
10B95L	3.81	-8.3	-50
11A95L	2.79	-7.5	-48
11B95L	0.00	NA	NA
12A95L	7.37	-15.6	-113
12B95L	0.00	NA	NA
1A96L	1.91	-19.4	-141
1B96L	5.03	-6.6	-33
2A96L	0.00	NA	NA
2B96L	1.80	-4.0	-23
3A96L	0.89	-3.9	-17
3B96L	6.96	-9.0	-58
4A96L	1.57	-5.1	-31
4B96L	22.86	-6.1	-38
5A96L	6.93	-4.0	-20
5B96L	6.71	-5.6	-31
6A96L	8.89	-7.8	-48
6B96L	0.00	NA	NA
7A96L	7.72	-5.1	-29
7B96L	0.00	NA	NA
8A96L	0.00	NA	NA
8B96L	8.28	-2.8	-10
9A96L	4.01	-8.5	-57
9B96L	7.26	-7.0	-40
10A96L	0.38	-7.6	-48
10B96L	6.25	-6.2	-35
11A96L	9.68	-8.1	-50
11B96L	8.31	-11.4	-76
12A96L	2.18	-11.3	-72
12B96L	1.02	-6.4	-37
1A97L	3.02	-13.9	-128
1B97L	5.59	-11.8	-83
2A97L	1.32	-12.6	-95
2B97L	9.17	-5.3	-31
3A97L	4.95	-5.0	-30
3B97L	3.15	-6.8	-45
4A97L	3.99	-9.1	-61

Sample	Precipitation (cm)	$\delta^{18}\text{O}$ (‰)	δD (‰)
4B97L	2.97	-8.5	-56
5A97L	3.15	-5.6	-36
5B97L	6.53	-8.9	-60
6A97L	3.99	-6.7	-38
6B97L	4.55	-4.8	-32
7A97L	0.91	-4.0	-23
7B97L	0.25	-1.0	-1
8A97L	3.68	-4.5	-21
8B97L	6.22	-5.7	-34
9A97L	0.41	-1.3	1
9B97L	3.20	-5.6	-29
10A97L	1.47	-4.7	-26
10B97L	4.65	-13.5	-94
11A97L	5.23	-15.2	-108
11B97L	1.40	-6.1	-39
12A97L	2.01	-13.5	-83
12B97L	3.68	-12.8	-86
1A98L	7.11	-15.2	-111
1B98L	0.53	-14.4	-106
2A98L	3.20	-11.0	-73
2B98L	6.27	-11.6	-81
3A98L	4.75	-12.5	-88
3B98L	13.82	-9.9	-53
4A98L	6.68	-2.8	-7
4B98L	6.02	-5.8	-30
5A98L	2.69	-5.5	-35
5B98L	2.77	-4.0	-25
6A98L	18.52	-5.9	-39
6B98L	5.23	-5.2	-36
7A98L	4.93	-2.7	-19
7B98L	8.23	-5.7	-33
8A98L	3.30	-4.8	-29
8B98L	5.28	-4.4	-25
9A98L	2.77	-7.0	-48
9B98L	1.47	-7.2	-46
10A98L	2.57	-7.1	-54
10B98L	4.22	-3.6	-16
11A98L	5.99	-5.6	NA
11B98L	1.24	-7.4	-47
12A98L	0.66	-3.1	-10
12B98L	1.14	-11.0	-78
1A99L	5.72	-14.1	-100
1B99L	7.95	-9.6	-65
2A99L	8.61	-8.7	-61
2B99L	2.31	-10.0	-62
3A99L	3.35	-6.0	-32
3B99L	3.53	-7.4	-39

Sample	Precipitation (cm)	$\delta^{18}\text{O}$ (‰)	δD (‰)
4A99L	5.03	-5.4	-32
4B99L	6.76	-6.7	-45
5A99L	6.02	-5.1	-27
5B99L	0.69	0.6	15
6A99L	6.15	-3.3	-16
6B99L	3.94	-6.6	-43
7A99L	6.96	-4.4	-22
7B99L	0.25	0.3	8
8A99L	2.84	-3.4	-15
8B99L	0.28	-4.0	-17
9A99L	0.94	-2.4	-3
9B99L	1.85	-5.5	-29
10A99L	4.88	-8.2	-56
10B99L	0.53	-4.3	-29
11A99L	1.27	-2.6	-6
11B99L	0.64	-2.7	-4
12A99L	5.82	-7.6	-44
12B99L	0.00	NA	NA
1A00L	2.49	-9.8	-67
1B00L	2.11	-9.6	-56
2A00L	0.74	-5.7	-29
2B00L	6.78	-7.3	-46
3A00L	1.57	-9.9	NA
3B00L	4.29	-9.3	-66
4A00L	1.80	-4.0	-16
4B00L	3.91	-4.6	-26
5A00L	10.41	-2.4	-6
5B00L	7.37	-6.5	-43
6A00L	2.74	-3.8	-25
6B00L	19.18	-4.9	-32
7A00L	1.42	-1.5	-6
7B00L	10.44	-3.7	-13
8A00L	5.08	-4.3	-28
8B00L	4.37	-3.5	-22
9A00L	2.44	-4.7	-23
9B00L	3.86	-10.7	-72
10A00L	6.27	-5.7	-28
10B00L	0.53	-2.1	-7
11A00L	5.28	-7.9	-45
11B00L	1.75	-14.9	-107
12A00L	3.94	-15.7	-115
12B00L	0.23	-13.7	-98
1A01L	0.69	-11.3	-76
1B01L	2.39	-7.6	-45
2A01L	2.26	-7.0	-47
2B01L	3.73	-5.2	-30
3A01L	3.45	-15.7	-120

Sample	Precipitation (cm)	$\delta^{18}\text{O}$ (‰)	δD (‰)
3B01L	0.56	-9.3	-74
4A01L	5.08	-3.8	-19
4B01L	1.14	-0.9	2
5A01L	0.25	0.1	4
5B01L	9.07	-6.1	-39
6A01L	5.38	-6.1	-41
6B01L	4.80	-2.7	-11
7A01L	3.20	-4.7	-29
7B01L	4.27	-2.7	-9
8A01L	1.73	-1.1	1
8B01L	1.78	-1.3	1
9A01L	4.98	-5.6	-34
9B01L	2.74	-4.4	-18
10A01L	12.32	-8.0	-47
10B01L	2.84	-8.1	-55
11A01L	0.51	-4.1	-19
11B01L	7.92	-9.6	-66
12A01L	4.47	-13.7	NA
12B01L	5.08	-14.5	-113
1A02L	0.25	-16.8	-128
1B02L	8.05	-6.5	-40
2A02L	0.30	-15.6	-118
2B02L	2.29	-7.7	-45
3A02L	6.78	-8.3	-53
3B02L	4.01	-7.3	-43
4A02L	2.26	-4.4	-27
4B02L	9.04	-3.3	-14
5A02L	11.79	-4.1	-24
5B02L	4.57	-5.6	-28
6A02L	4.52	-5.9	-36
6B02L	1.52	-3.9	-29
7A02L	0.25	-2.2	-22
7B02L	1.96	-4.6	-31
8A02L	1.68	-2.8	-15
8B02L	2.67	-3.7	-25
9A02L	0.25	0.0	1
9B02L	4.32	-6.6	-39
10A02L	5.49	-5.5	-32
10B02L	7.62	-12.0	-83
11A02L	3.05	-11.8	-80
11B02L	0.00	NA	NA
12A02L	0.69	-22.5	-159
12B02L	4.19	-9.4	-60
1A03L	1.27	-18.3	-133
1B03L	0.69	-18.0	-138
2A03L	1.98	-13.9	-101
2B03L	4.88	-13.7	-98

Sample	Precipitation (cm)	$\delta^{18}\text{O}$ (‰)	δD (‰)
3A03L	3.94	-5.0	-33
3B03L	3.91	-9.3	-64
4A03L	1.65	-7.0	-43
4B03L	11.20	-6.4	-38
5A03L	8.84	-2.6	-16
5B03L	4.62	-5.1	-24
6A03L	13.94	-5.4	-33
6B03L	9.02	-6.8	-41
7A03L	2.54	-6.4	-40
7B03L	4.93	-4.0	-24
8A03L	2.34	-5.3	NA
8B03L	3.00	-5.9	NA
9A03L	18.01	-10.0	NA
9B03L	5.23	-6.9	NA
10A03L	3.94	-7.4	NA
10B03L	3.68	-8.8	NA
11A03L	4.37	-6.1	NA
11B03L	10.16	-9.3	NA
12A03L	3.89	-6.3	-23
12B03L	3.05	-9.7	NA
1A04L	5.33	-6.0	NA
1B04L	4.88	-12.8	NA
2A04L	2.92	-15.5	-96
2B04L	0.00	NA	NA
3A04L	5.82	-5.2	-27
3B04L	7.98	-3.8	-16
4A04L	0.51	-14.2	-106
4B04L	7.54	-5.7	-32
5A04L	9.17	-5.3	-32
5B04L	14.48	-4.1	-23
6A04L	2.11	-4.5	-32
6B04L	5.38	-8.4	-59
7A04L	10.97	-3.4	-20
7B04L	11.23	-6.1	-38
8A04L	1.22	-3.5	-16
8B04L	6.17	-3.8	-20
9A04L	0.00	NA	NA
9B04L	0.13	-1.3	-8
10A04L	6.07	-9.7	-69
10B04L	4.45	-5.6	-34
11A04L	7.72	-7.8	-45
11B04L	9.55	-12.3	-81
12A04L	3.99	-9.5	-65
12B04L	0.00	NA	NA
1A05L	22.86	-9.2	-61
1B05L	0.81	-17.3	-127
2A05L	4.65	-11.0	-74

Sample	Precipitation (cm)	$\delta^{18}\text{O}$ (‰)	δD (‰)
2B05L	0.64	-12.9	-91
3A05L	0.36	-10.3	-77
3B05L	4.32	-11.6	-77
4A04L	2.79	-7.0	-44
4B05L	5.92	-6.2	-37
5A05L	0.66	-5.5	-38
5B05L	2.18	-3.9	-25
6A05L	8.64	-2.3	-13
6B05L	0.00	NA	NA
7A05L	4.45	-5.7	-39
7B05L	1.80	-4.4	-23
8A05L	5.97	-4.2	-23
8B05L	7.85	-3.6	-17
9A05L	5.89	-7.2	-45
9B05L	9.65	-4.8	-25
10A05L	0.00	NA	NA
10B05L	4.85	-7.5	-42
11A05L	3.68	-7.2	-42
11B05L	4.55	-6.8	-37
12A05L	1.32	-13.6	-89
12B05L	1.55	-16.4	-121
1A06L	2.26	-11.8	-81
1B06L	2.54	-7.0	-41
2A06L	0.48	-17.8	-139
2B06L	0.33	-4.1	-12
3A06L	5.08	-6.5	-42
3B06L	2.62	-9.2	-60
4A06L	1.80	-4.1	-23
4B06L	3.61	-2.1	-4
5A06L	7.32	-7.7	-51
5B06L	0.20	-3.9	-34
6A06L	7.29	-3.5	-21
6B06L	1.14	-3.8	-25
7A06L	4.57	-5.7	-36
7B06L	6.58	-3.4	-22
8A06L	3.35	-2.6	-14
8B06L	4.09	-2.7	-13
9A06L	0.69	-5.1	-29
9B06L	3.10	-5.7	-35
10A06L	5.44	-11.6	NA
10B06L	4.22	-9.9	-71
11A06L	5.18	-10.0	-64
11B06L	5.99	-9.4	-66
12A06L	1.65	-6.8	-36
12B06L	4.52	-6.6	-41
1A07L	8.00	-9.2	-61
1B07L	0.91	-12.1	-90

Sample	Precipitation (cm)	$\delta^{18}\text{O}$ (‰)	δD (‰)
2A07L	3.81	-13.8	-99
2B07L	3.15	-5.5	-28
3A07L	3.18	-7.0	-45
3B07L	5.41	-3.9	-21
4A07L	5.66	-6.4	-37
4B07L	1.78	-5.0	-33
5A07L	9.96	-3.4	-17
5B07L	2.72	-0.5	6
6A07L	2.21	-4.6	-29
6B07L	5.84	-2.9	-14
7A07L	3.35	-5.7	-39
7B07L	2.82	-4.9	-32
8A07L	1.19	-0.5	1
8B07L	1.35	-2.1	-12
9A07L	6.45	-8.8	-57
9B07L	0.00	NA	NA
10A07L	3.33	-4.4	-20
10B07L	2.54	-7.7	-45
11A07L	2.13	-3.9	-12
11B07L	2.18	-9.9	-62
12A07L	5.77	-10.3	-69
12B07L	2.03	-8.8	-51
1A08L	4.11	-6.9	-37
1B08L	1.40	-10.9	-66
2A08L	6.27	-5.9	-17
2B08L	4.57	-9.4	-60
3A08L	3.78	-11.4	-77
3B08L	19.33	-8.7	-51
4A08L	7.01	-5.9	-36
4B08L	4.45	-6.5	-36
5A08L	11.63	-6.2	-38
5B08L	13.97	-5.3	-30
6A08L	5.94	-4.8	-30
6B08L	5.66	-7.1	-48
7A08L	6.17	-4.5	-29
7B08L	10.19	-3.8	-22
8A08L	1.30	-4.2	-26
8B08L	2.92	-3.9	-24
9A08L	21.46	-7.3	-48
9B08L	0.97	-4.6	-24
10A08L	0.99	-4.2	-23
10B08L	2.01	-5.8	-27
11A08L	3.56	-12.7	-89
11B08L	0.56	-16.0	-120
12A08L	2.34	-6.8	-30
12B08L	8.08	-4.4	-21
1A09L	0.00	NA	NA

Sample	Precipitation (cm)	$\delta^{18}\text{O}$ (‰)	δD (‰)
1B09L	1.45	-14.1	-100
2A09L	6.43	-6.4	-33
2B09L	0.84	-4.2	-20
3A09L	1.02	-3.6	-19
3B09L	6.12	-9.3	-59
4A09L	6.32	-7.1	-41
4B09L	4.65	-5.7	-35
5A09L	7.21	-4.8	-34
5B09L	4.52	-7.3	-50
6A09L	16.38	-6.2	-39
6B09L	1.30	-3.8	-27
7A09L	11.84	-5.1	-27
7B09L	1.02	-6.1	-42
8A09L	1.55	-3.7	-17
8B09L	5.05	-3.3	-8
9A09L	6.81	-6.5	-39
9B09L	4.45	-9.1	-59
10A09L	17.12	-9.0	-60
10B09L	17.12	-8.2	-52
11A09L	2.01	-5.0	-21
11B09L	5.23	-7.4	-39
12A09L	5.08	-10.1	-67
12B09L	5.94	-9.0	-54
1A10L	0.58	-17.3	-127
1B10L	3.10	-11.7	-82
2A10L	3.43	-22.9	-172
2B10L	2.24	-13.2	-91
3A10L	3.25	-11.7	-81
3B10L	3.15	-10.2	-62
4A10L	2.26	-4.7	-27
4B10L	6.88	-5.7	-37
5A10L	6.15	-4.7	-28
5B10L	4.83	-5.9	-36
6A10L	7.75	-3.5	-23
6B10L	3.38	-3.4	-17
7A10L	2.64	-8.2	-54
7B10L	8.38	-4.4	-27
8A10L	3.58	-2.8	-9
8B10L	7.54	-5.8	-34
9A10L	9.88	-6.0	-34
9B10L	5.21	-4.0	-29
10A10L	0.13	2.4	7
10B10L	0.20	-4.1	-21
11A10L	0.00	NA	NA
11B10L	14.78	-5.8	-33
12A10L	0.94	-10.2	-60
12B10L	2.21	-8.4	-38

Sample	Precipitation (cm)	$\delta^{18}\text{O}$ (‰)	δD (‰)
1A11L	0.66	-13.0	-98
1B11L	2.72	-15.5	-107
2A11L	3.00	-12.6	-84
2B11L	4.01	-6.3	-39
3A11L	10.01	-9.9	-65
3B11L	3.02	-8.9	-58
4A11L	3.73	-3.4	-23
4B11L	11.71	-5.6	-40
5A11L	4.17	-6.9	-47
5B11L	6.99	-4.1	-25
6A11L	1.30	-0.6	4
6B11L	12.37	-6.2	-41
7A11L	7.70	-3.0	-13
7B11L	0.10	-1.3	-6
8A11L	1.12	-3.5	-22
8B11L	1.30	-2.7	-21
9A11L	6.99	-5.9	-34
9B11L	4.57	-4.6	-23
10A11L	0.58	-5.5	-31
10B11L	4.95	-8.5	-54
11A11L	5.46	-4.8	-27
11B11L	4.95	-10.9	-74
12A11L	4.14	-5.3	-35
12B11L	4.93	-13.1	-93

Appendix B: Fox Creek Data

Sample ID	Site	Date and Time	USGS Stage (m)	USGS Discharge (cms)	SpC ($\mu\text{S}/\text{cm}$)	Temperature ($^{\circ}\text{C}$)	DO (ppm)	DO (% sat)	Turbidity (NTU)	Calculated TSS (ppm)	pH	$\delta^{18}\text{O}$ (‰)	δD (‰)	$\text{NH}_4^+\text{-N}$ (ppm)	Cl (ppm)	$\text{NO}_3^-\text{-N}$ (ppm)	Total PO_4^{3-} (ppm)	<i>E. coli</i> (cfu/100mL)	Total Coliforms (cfu/100mL)
070508G	FOX	5/8/2007 11:00:00	*	*	480	18.0	10.80	114.0	3.5	1.8		-6.8	-44						
070606D	FOX	6/6/2007 11:45:00	*	*	474	19.4	7.30	80.2*	3.4	1.7		-6.5	-42						
070703B	FOX	7/3/2007 11:00:00	*	*	526	21.1	7.00	79.5*	1.7	0.9	7.90	-5.9	-38						
070717H	FOX	7/17/2007 13:00:00	*	*	611	23.4	3.02	36.0*	13.7	7.0	7.80	-6.2	-41						
070801B	FOX	8/1/2007 11:00:00	*	*	300	22.5	4.75	58.6*	8.1	4.1	7.70	-6.2	-41						
070813B	FOX	8/13/2007 11:00:00	*	*	605	24.9	1.55	18.7*	10.2	5.2	7.60	-6.3	-41	0.02	36.6	0.3	0.18	20.7	>200.5
070813B - lab duplicate	FOX	8/13/2007 11:00:00												0.00		0.6	0.20		
070822C	FOX	8/22/2007 11:20:00	*	*	625	24.7	3.40	41.0*	5.2	2.7	7.29	-6.4	-41	0.14	53.6	0.1	0.13	6	>20050
070822D - field duplicate	FOX	8/22/2007 11:20:00												0.14	56.8	0.0	0.21	7	>20050
070822E - lab duplicate	FOX	8/22/2007 11:20:00																5.1	>20050
070904A	FOX	9/4/2007 12:30:00	*	*	625	23.1	3.94	46.4*	4.4	2.2	7.40	-6.3	-41	0.07	56.4	0.3	0.08	0	>20050
070921C	FOX	9/21/2007 11:45:00	*	*	615	22.1	2.89	33.2*	12.9	6.6	7.38	-6.2	-44	0.02	50.0	0.7	0.20	136.4	7820.0
071002C	FOX	10/2/2007 11:30:00	*	*	680	18.5	4.30	46.7*	3.4	1.7	7.00	-6.4	-42	0.06		0.1	0.17	38.3	5910.0
071012A	FOX	10/12/2007 11:48:00	1.25	0.01	633	16.1	6.60	67.3*	2	1.0									
071017B	FOX	10/17/2007 13:40:00	1.22	0.01	635	16.2	3.14	32.0*	2.2	1.1	6.80	-6.1	-40	0.06	55.6	1.0	0.21	24.7	11840.0
071102A	FOX	11/2/2007 11:15:00	1.18	0.01	680	11.5	6.50	60.0	2.8	1.4	7.10	-6.2	-41	0.03	62.0	0.7	0.18	1	889.7
071116A	FOX	11/16/2007 11:00:00	1.16	0.01	698	11.6	6.90	63.3	2	1.0	7.10	-6.1	-42	0.07	56.0	0.0	0.23	3.1	>200.5
071130A	FOX	11/30/2007 12:20:00	1.17	0.01	695	8.4	8.90	76.7*	2	1.0	6.80	-6.3	-42	0.06	59.2	0.0	0.02	6.3	120.1
071214A	FOX	12/14/2007 11:00:00	1.39	0.02	690	5.4	9.00	73.2*	2	1.0	6.60	-6.1	-40	0.03	75.0	1.0	0.03	20.1	1553.1
071227A	FOX	12/27/2007 9:25:00	1.39	0.02	805	5.3	9.00	70.7	1	0.5	7.70	-6.5	-42	0.24	92.0	0.8	0.20	14.2	1732.9
080110A	FOX	1/10/2008 10:05:00	1.43	0.03	634	6.7	8.93	73.0	11	5.6	7.00	-6.9	-42	0.08	76.0	1.4	0.31	131.7	>2419.6
080123A	FOX	1/23/2008 11:09:00	1.36	0.01	755	2.1	12.40	87.2	1	0.5	7.00	-6.8	-42	0.10	88.0	1.5	0.23	3.1	135.4
080204A	FOX	2/4/2008 13:30:00	1.38	0.02	763	5.5	11.68	92.3	2	1.0	6.10	-6.6	-42	0.06	94.8	1.0	0.62	3.1	387.3
080225A	FOX	2/25/2008 13:25:00	1.43	0.03	579	6.3	12.83	106.0	3	1.5	6.70	-7.0	-45	0.15	71.5	1.0	0.30	8.6	920.8
080311F	FOX	3/11/2008 14:00:00	1.36	0.01	558	6.1	14.70	118.5	2	1.0	7.30	-7.1	-46	0.03	57.2	0.2		6.3	191.8

Sample ID	Site	Date and Time	USGS Stage (m)	USGS Discharge (cms)	SpC ($\mu\text{S/cm}$)	Temperature ($^{\circ}\text{C}$)	DO (ppm)	DO (% sat)	Turbidity (NTU)	Calculated TSS (ppm)	pH	$\delta^{18}\text{O}$ (‰)	δD (‰)	$\text{NH}_4^+\text{-N}$ (ppm)	Cl (ppm)	$\text{NO}_3^-\text{-N}$ (ppm)	Total PO_4^{3-} (ppm)	<i>E. coli</i> (cfu/100mL)	Total Coliforms (cfu/100mL)
080312B	FOX	3/12/2008 13:15:00	1.44	0.04	540	10.8			2	1.0		-7.1	-46						
080319B	FOX	3/19/2008 13:15:00	1.95	3.77	164.6	7.1	11.43	94.3	46	23.5	7.20	-8.4	-57	0.34	18.3	1.0	0.39	920.8	>2419.6
080324A	FOX	3/24/2008 12:00:00	1.47	0.06	317.9	7.2	11.36	93.3	3	1.5	7.40	-7.3	-54	0.06	33.2	1.3	0.23	9.8	547.5
080329-11F	FOX	3/24/2008 12:00:00	1.47	0.06								-7.3	-49						
080329-12F	FOX	3/25/2008 0:00:00	1.47	0.06								-7.4	-51						
080329-13F	FOX	3/25/2008 12:00:00	1.46	0.05								-7.3	-50						
080329-14F	FOX	3/26/2008 0:00:00	1.45	0.05								-7.2	-51						
080329-15F	FOX	3/26/2008 12:00:00	1.44	0.04								-7.3	-50						
080329-16F	FOX	3/27/2008 0:00:00	1.80	1.59								-7.2	-45						
080329-17F	FOX	3/27/2008 12:00:00	1.80	1.56								-7.3	-49						
080329-18F	FOX	3/28/2008 0:00:00	1.69	0.65								-7.2	-45						
080329-19F	FOX	3/28/2008 12:00:00	1.64	0.40								-7.2	-51						
080329-110F	FOX	3/29/2008 0:00:00	1.58	0.22								-7.3	-51						
080329-111F	FOX	3/29/2008 10:45:00	1.55	0.16								-7.3	-46						
080329A	FOX	3/29/2008 10:45:00	1.55	0.16	388	7.1			9	4.6		-7.3	-47						
080331-11F	FOX	3/30/2008 20:30:00	1.79	2.27								-7.3	-47						
080331-21F	FOX	3/30/2008 21:30:00	1.77	2.10								-7.4	-47						
080331-31F	FOX	3/30/2008 22:30:00	1.76	1.98								-7.0	-45						
080331-41F	FOX	3/30/2008 23:30:00	1.75	1.81								-6.7	-42						
080331-51F	FOX	3/31/2008 0:30:00	1.73	1.64								-7.1	-45						
080331-61F	FOX	3/31/2008 1:30:00	1.73	1.59								-7.1	-45						
080331-71F	FOX	3/31/2008 2:30:00	1.72	1.53								-7.3	-47						
080331-81F	FOX	3/31/2008 3:30:00	1.71	1.44								-7.2	-46						
080331-91F	FOX	3/31/2008 4:30:00	1.70	1.33								-7.3	-47					488.4	1553.1
080331-101F	FOX	3/31/2008 5:30:00	1.69	1.30								-7.2	-47					517.2	1986.3
080331-111F	FOX	3/31/2008 6:30:00	1.68	1.19								-7.4	-47					456.9	2419.6
080331-121F	FOX	3/31/2008 7:30:00	1.67	1.10								-7.1	-41						
080331A - BW	FOX	3/31/2008 8:00:00	1.68	1.13	319	9.9			18	9.2		-7.3	-47					>1	1.0

Sample ID	Site	Date and Time	USGS Stage (m)	USGS Discharge (cms)	SpC (µS/cm)	Temperature (°C)	DO (ppm)	DO (% sat)	Turbidity (NTU)	Calculated TSS (ppm)	pH	δ ¹⁸ O (‰)	δD (‰)	NH ₄ ⁺ -N (ppm)	Cl (ppm)	NO ₃ ⁻ -N (ppm)	Total PO ₄ ³⁻ (ppm)	<i>E. coli</i> (cfu/100mL)	Total Coliforms (cfu/100mL)
080331A	FOX	3/31/2008 14:00:00	1.64	0.85	331.2	10.9	10.07	89.9	15	7.7	7.40	-7.4	-47	0.09	23.2	1.3	0.02	112.6	>2419.6
080331A field blank	FOX																	>1	1.0
080402A	FOX	4/2/2008 11:15:00	1.60	0.59	360.7	9.0			10	5.1		-7.1	-45						
080414A	FOX	4/14/2008 13:45:00	1.49	0.21	418.9	11.9	10.32	94.4	3	1.5	6.60	-6.9	-45	0.05	30.4	1.2	0.31	30.5	2419.6
080428A	FOX	4/28/2008 14:10:00	1.47	0.17	437.5	13.4	13.10	125.5	2	1.0	6.90	-6.7	-44	0.01	20.0	0.7	0.17	54.8	1732.9
080430A	FOX	4/30/2008 11:00:00	1.45	0.14	466.9	12.9	12.30	115.7	1	0.5	8.10	-6.6	-43	0.04	33.6	0.1	0.22	157.6	2419.6
080502A	FOX	5/2/2008 7:50:00	1.44	0.12								-7.0	-43	0.13	32.0	0.6	0.16	63.1	>2419.6
080507A	FOX	5/7/2008 11:00:00	1.42	0.10	485.8	15.3	8.90	87.1	4	2.0	7.90	-6.8	-44	0.06	36.0	0.3	0.16	148.3	>2419.6
080508A-11F	FOX	5/7/2008 15:00:00	1.49	0.28	426.2	15.6	8.49		22.3	11.4	7.81	-6.2	-39	0.18	30.8		0.37		
080508A-11F - lab duplicate	FOX	5/7/2008 15:00:00												0.24	29.6		0.47		
080508A-12F	FOX	5/7/2008 16:00:00	1.49	0.28	410.4	15.7	8.26		30.5	15.6	7.66	-6.2	-39	0.29	27.2		0.38		
080508A-12F - lab duplicate	FOX	5/7/2008 16:00:00												0.36	31.2		0.26		
080508A-13F	FOX	5/7/2008 17:00:00	1.61	0.65	387.2	15.8	8.07		62	31.6	7.68	-6.2	-39	0.41	22.8		0.72		
080508A-13F - lab duplicate	FOX	5/7/2008 17:00:00												0.64	25.6				
080508A-14F	FOX	5/7/2008 18:00:00	1.87	3.40	333.8	15.7	8.34		182.6	93.1	7.73	-6.2	-40	0.86	17.2		0.95		
080508A-14F - lab duplicate	FOX	5/7/2008 18:00:00												1.45	19.6				
080508A-15F	FOX	5/7/2008 19:00:00	1.94	4.64	277.5	15.6	8.65		213	108.6	7.73	-6.1	-39	1.21	18.0		0.80		
080508A-15F - lab duplicate	FOX	5/7/2008 19:00:00												1.69	16.8				
080508A-16F	FOX	5/7/2008 20:00:00	1.98	5.66	265.3	15.4	8.83		184.8	94.2	7.73	-6.2	-39	1.08	18.4		1.03		
080508A-16F - lab duplicate	FOX	5/7/2008 20:00:00												1.32					
080508A-17F	FOX	5/7/2008 21:00:00	1.98	5.52	247	15.1	8.87		152.4	77.7	7.70	-6.2	-40	1.00	16.8		0.91		
080508A-17F - lab duplicate	FOX	5/7/2008 21:00:00												1.23					
080508A-18F	FOX	5/7/2008 22:00:00	1.94	4.76	243.5	15.0	8.95		119.6	61.0	7.68	-6.3	-40	0.96	14.4		0.33		
080508A-18F - lab duplicate	FOX	5/7/2008 22:00:00												0.96					
080508A-19F	FOX	5/7/2008 23:00:00	1.92	4.33	249.2	14.8	8.89		92.4	47.1	7.68	-6.3	-41	0.85	14.0		1.32		
080508A-110F	FOX	5/8/2008 0:00:00	1.89	3.79	254.5	14.6	8.93		73.7	37.6	7.67	-6.4	-40	0.70	18.4		0.46		
080508A-111F	FOX	5/8/2008 1:00:00	1.87	3.40	259.2	14.5	8.87		62.6	31.9	7.67	-6.4	-40	0.55	16.0				
080508A-112F	FOX	5/8/2008 2:00:00	1.85	3.11	264.1	14.5	8.83		59.7	30.4	7.67	-6.4	-40	0.51	13.6				

Sample ID	Site	Date and Time	USGS Stage (m)	USGS Discharge (cms)	SpC (µS/cm)	Temperature (°C)	DO (ppm)	DO (% sat)	Turbidity (NTU)	Calculated TSS (ppm)	pH	δ ¹⁸ O (‰)	δD (‰)	NH ₄ ⁺ -N (ppm)	Cl (ppm)	NO ₃ ⁻ -N (ppm)	Total PO ₄ ³⁻ (ppm)	<i>E. coli</i> (cfu/100mL)	Total Coliforms (cfu/100mL)
080508A-I13F	FOX	5/8/2008 3:00:00	1.83	2.89	269.1	14.4	8.78		52	26.5	7.67	-6.2	-41	0.45	15.6				
080508A-I14F	FOX	5/8/2008 3:30:00	1.81	2.63	271.7	14.4	8.76		49.1	25.0	7.66	-6.2	-40	0.45	16.4			2419.6	>2419.6
080508A-I15F	FOX	5/8/2008 4:00:00	1.81	2.58	274.3	14.3	8.70		49	25.0	7.66	-6.3	-40	0.48	17.2			>2419.6	>2419.6
080508A-I16F	FOX	5/8/2008 4:30:00	1.80	2.49	276.7	14.3	8.69		45.2	23.1	7.66	-6.2	-41	0.25	16.0			>2419.6	>2419.6
080508A-I17F	FOX	5/8/2008 5:00:00	1.80	2.41	279	14.3	8.70		42.2	21.5	7.66	-6.3	-40	0.23	14.8			>2419.6	>2419.6
080508A-I18F	FOX	5/8/2008 5:30:00	1.80	2.41	280.6	14.3	8.68		40.7	20.8	7.66	-6.4	-41	0.22	18.8			>2419.6	>2419.6
080508A-I19F	FOX	5/8/2008 6:00:00	1.80	2.38	281.5	14.2	8.67		40	20.4	7.66	-6.3	-40	0.22	16.0			1553.1	>2419.6
080508A-I20F	FOX	5/8/2008 6:30:00	1.80	2.49	281.6	14.2	8.70		38.4	19.6	7.66	-6.4	-40	0.24	19.2			2419.6	>2419.6
080508A-I21F	FOX	5/8/2008 7:00:00	1.82	2.66	278.6	14.2	8.73		39.1	19.9	7.66	-6.4	-39	0.15	11.2			>2419.6	>2419.6
080508A-I22F	FOX	5/8/2008 7:30:00	1.84	3.03	277.8	14.2	8.81		40.9	20.9	7.67	-6.4	-40	0.18	14.0			2419.6	>2419.6
080508A-I23F	FOX	5/8/2008 7:50:00	1.86	3.37	275.3	14.9	8.89		44.8	22.8	7.69	-6.4	-40	0.21	13.6			2419.6	>2419.6
080508A-I24F - field duplicate	FOX	5/7/2008 11:00:00										-6.7	-43					195.6	>2419.6
080508A-BW	FOX	5/8/2008 7:50:00	1.86	3.37															
080508C-I1F	FOX	5/8/2008 8:10:00	1.90	3.91	270.1	14.2	8.97		49	25.0	7.70	-6.3	-39	0.07	13.6				
080508C-I2F	FOX	5/8/2008 8:40:00	1.93	4.53	259.6	14.2	9.03		60.2	30.7	7.71	-6.3	-39	0.12	10.0				
080508C-I3F	FOX	5/8/2008 9:10:00	1.97	5.41	248.8	14.3	9.15		67.3	34.3	7.71	-6.3	-38	0.20	11.2				
080508C-I4F	FOX	5/8/2008 9:40:00	2.03	6.71	239.6	14.3	9.21		81.4	41.5	7.71	-6.2	-38	0.30	10.8			>2419.6	>2419.6
080508C-I5F	FOX	5/8/2008 10:10:00	2.07	7.90	229.6	14.4	9.27		113.7	58.0	7.72	-6.2	-38	0.44	11.2				
080508C-I6F	FOX	5/8/2008 10:40:00	2.10	8.83	220.4	14.5	9.22		136.5	69.6	7.71	-6.3	-39	0.56	8.0			>2419.6	>2419.6
080508C-I7F	FOX	5/8/2008 11:10:00	2.09	8.44	213.5	14.6	9.23		140.5	71.7	7.70	-6.2	-38	0.55	10.8				
080508C-I8F	FOX	5/8/2008 11:40:00	2.07	7.90	209.8	14.6	9.19		136.8	69.8	7.68	-6.1	-38	0.62	10.8			>2419.6	>2419.6
080508C-I9F	FOX	5/8/2008 12:10:00	2.04	7.05	209.6	14.6	9.16		121.7	62.1	7.67	-6.1	-37	0.60					
080508C-I10F	FOX	5/8/2008 12:40:00	2.01	6.17	212.4	14.6	9.14		107.8	55.0	7.66	-6.2	-38	0.50	8.8			>2419.6	>2419.6
080508C-I11F	FOX	5/8/2008 13:10:00	1.98	5.52	216.5	14.6	9.14		89.2	45.5	7.66	-6.3	-38	0.36					
080508C-I12F	FOX	5/8/2008 13:40:00	1.95	4.87	221.6	14.6	9.11		80.3	41.0	7.65	-6.3	-39	0.32	8.4			>2419.6	>2419.6
080508C-I13F	FOX	5/8/2008 14:10:00	1.93	4.59	226.7	14.6	9.11		69.7	35.5	7.66	-6.3	-39	0.25					
080508C-I14F	FOX	5/8/2008 14:40:00	1.91	4.19	232.1	14.5	9.10		62.1	31.7	7.66	-6.4	-39	0.23	12.4			>2419.6	>2419.6
080508A	FOX	5/8/2008 15:00:00	1.91	4.22															

Sample ID	Site	Date and Time	USGS Stage (m)	USGS Discharge (cms)	SpC (µS/cm)	Temperature (°C)	DO (ppm)	DO (% sat)	Turbidity (NTU)	Calculated TSS (ppm)	pH	δ ¹⁸ O (‰)	δD (‰)	NH ₄ ⁺ -N (ppm)	Cl (ppm)	NO ₃ ⁻ -N (ppm)	Total PO ₄ ³⁻ (ppm)	<i>E. coli</i> (cfu/100mL)	Total Coliforms (cfu/100mL)
080512A	FOX	5/12/2008 11:04:00	1.62	0.71	351.5	12.6	10.03	94.7	13	6.6	7.80	-6.6	-43	0.10	15.6	0.3	0.21	146.7	>2419.6
080528A	FOX	5/28/2008 10:18:00	1.44	0.12	595	15.1	10.70	103.0	3	1.5	6.70	-6.5	-43	0.09	29.2	0.4	0.01	162.4	2419.6
080610A	FOX	6/10/2008 10:27:00	1.43	0.17	517	19.6	8.75	98.3	7	3.6	7.20	-6.1	-41	0.04	28.8	0.5	0.23	75.9	>2419.6
080610A - matrix spike	FOX	6/10/2008 10:27:00												0.59	28.4	0.9	1.23		
080610A - matrix spike 2	FOX	6/12/2008 10:27:00												2.88	48.4	1.9			
080610B - field duplicate	FOX	6/13/2008 10:27:00												0.04	25.2	0.3	0.16	70.3	>2419.6
080610B - field duplicate matrix spike	FOX	6/14/2008 10:27:00												0.56	27.2	1.0	1.61		
080610B - field duplicate matrix spike 2	FOX	6/15/2008 10:27:00												2.71	46.8	2.2			
080620A	FOX	6/20/2008 13:00	1.40	0.12								-6.7	-42						
080624B	FOX	6/24/2008 13:00	1.40	0.12								-6.5	-41						
080708B	FOX	7/8/2008 11:20:00	1.39	0.11	574	22.4	6.50	75.6	4	2.0	7.70	-6.0	-39						
080709-11F	FOX	7/8/2008 21:00:00	1.38	0.10								-6.2	-39						
080709-12F	FOX	7/8/2008 21:45:00	1.38	0.10								-6.2	-39						
080709-13F	FOX	7/8/2008 22:30:00	1.38	0.10								-6.1	-39						
080709-14F	FOX	7/8/2008 23:15:00	1.38	0.10								-6.1	-39						
080709-15F	FOX	7/9/2008 0:00:00	1.38	0.10								-6.1	-39						
080709-16F	FOX	7/9/2008 0:45:00	1.38	0.10								-6.2	-39						
080709-17F	FOX	7/9/2008 1:30:00	1.39	0.11								-6.2	-40						
080709-18F	FOX	7/9/2008 2:15:00	1.40	0.12								-6.2	-40						
080709-19F	FOX	7/9/2008 3:00:00	1.40	0.12								-6.3	-41						
080709-110F	FOX	7/9/2008 3:45:00	1.40	0.12								-6.3	-42						
080709-111F	FOX	7/9/2008 4:30:00	1.40	0.12								-6.3	-41						
080709-112F	FOX	7/9/2008 5:15:00	1.52	0.37								-9.5	-69						
080709-113	FOX	7/9/2008 6:00:00	1.66	1.16								-9.0	-65						
080709-114F	FOX	7/9/2008 6:45:00	1.89	3.85								-9.9	-72						
080709-115F	FOX	7/9/2008 7:30:00	1.85	3.20								-10.4	-77						
080709-116F	FOX	7/9/2008 8:15:00	1.82	2.66								-10.4	-77						

Sample ID	Site	Date and Time	USGS Stage (m)	USGS Discharge (cms)	SpC (µS/cm)	Temperature (°C)	DO (ppm)	DO (% sat)	Turbidity (NTU)	Calculated TSS (ppm)	pH	δ ¹⁸ O (‰)	δD (‰)	NH ₄ ⁺ -N (ppm)	Cl (ppm)	NO ₃ ⁻ -N (ppm)	Total PO ₄ ³⁻ (ppm)	<i>E. coli</i> (cfu/100mL)	Total Coliforms (cfu/100mL)
080709-I17F	FOX	7/9/2008 9:00:00	1.75	1.93								-10.1	-75						
080709-I18F	FOX	7/9/2008 9:45:00	1.69	1.36								-9.8	-72						
080709-I19F	FOX	7/9/2008 10:30:00	1.64	0.99								-9.4	-70						
080709-I20F	FOX	7/9/2008 11:15:00	1.61	0.79								-9.2	-67						
080709-I21F	FOX	7/9/2008 12:00:00	1.58	0.62								-9.0	-65						
080709-I22F	FOX	7/9/2008 12:45:00	1.56	0.54								-8.8	-64						
080709-I23F	FOX	7/9/2008 13:30:00	1.54	0.45								-8.8	-63						
080709-I24F	FOX	7/9/2008 14:15:00	1.53	0.40								-8.7	-62						
080709A	FOX	7/9/2008 14:25:00	1.52	0.40	360.9	23.9	7.08	82.5	58	29.6	7.90	-8.6	-61						
080711-I1F	FOX	7/9/2008 14:38:00	1.52	0.40								-8.6	-61						
080711-I2F	FOX	7/9/2008 16:38:00	1.49	0.28								-8.4	-59						
080711-I3F	FOX	7/9/2008 18:38:00	1.47	0.24								-8.4	-58						
080711-I4F	FOX	7/9/2008 20:38:00	1.46	0.22								-8.0	-56						
080711-I5F	FOX	7/9/2008 22:38:00	1.44	0.19								-7.9	-55						
080711-I6F	FOX	7/10/2008 0:38:00	1.44	0.18								-7.9	-54						
080711-I7F	FOX	7/10/2008 2:38:00	1.43	0.18								-7.7	-54						
080711-I8F	FOX	7/10/2008 4:38:00	1.43	0.16								-7.9	-53						
080711-I9F	FOX	7/10/2008 6:38:00	1.42	0.16								-7.8	-52						
080711-I10F	FOX	7/10/2008 8:38:00	1.42	0.15								-7.4	-52						
080711-I11F	FOX	7/10/2008 10:38:00	1.42	0.15								-7.6	-51						
080711-I12F	FOX	7/10/2008 12:38:00	1.42	0.15								-7.6	-51						
080711-I13F	FOX	7/10/2008 14:38:00	1.41	0.14								-7.4	-51						
080711-I14F	FOX	7/10/2008 16:38:00	1.43	0.14								-7.6	-51						
080711-I15F	FOX	7/10/2008 18:38:00	1.41	0.14								-7.4	-50						
080711-I16F	FOX	7/10/2008 20:38:00	1.41	0.14								-7.5	-50						
080711-I17F	FOX	7/10/2008 22:38:00	1.41	0.14								-7.5	-50						
080711-I18F	FOX	7/11/2008 0:38:00	1.41	0.13								-7.4	-50						
080711-I19F	FOX	7/11/2008 2:38:00	1.41	0.13								-7.4	-49						

Sample ID	Site	Date and Time	USGS Stage (m)	USGS Discharge (cms)	SpC (µS/cm)	Temperature (°C)	DO (ppm)	DO (% sat)	Turbidity (NTU)	Calculated TSS (ppm)	pH	δ ¹⁸ O (‰)	δD (‰)	NH ₄ ⁺ -N (ppm)	Cl (ppm)	NO ₃ ⁻ -N (ppm)	Total PO ₄ ³⁻ (ppm)	<i>E. coli</i> (cfu/100mL)	Total Coliforms (cfu/100mL)
080711-I20F	FOX	7/11/2008 4:38:00	1.41	0.13								-7.2	-49						
080711-I21F	FOX	7/11/2008 6:38:00	1.41	0.14								-7.2	-49						
080711-I22F	FOX	7/11/2008 8:38:00	1.41	0.13								-7.2	-49						
080711-I23F	FOX	7/11/2008 10:38:00	1.41	0.13								-7.1	-49						
080711-I24F	FOX	7/11/2008 12:38:00	1.40	0.12								-7.1	-49						
080711A	FOX	7/11/2008 13:55:00	1.40	0.12	519	24.4	7.06	83.0	2	1.0	7.40	-7.1	-49						
080902A	FOX	9/2/2008 14:46:00	1.37	0.02	597	23.4	6.93	82.5	2	1.0	6.30	-4.4	-37						
080904-I1F	FOX	9/3/2008 20:00:00	1.37	0.02								-6.0	-37						
080904-I2F	FOX	9/3/2008 21:00:00	1.37	0.02								-6.0	-37						
080904-I3F	FOX	9/3/2008 22:00:00	1.37	0.02								-6.0	-38						
080904-I4F	FOX	9/3/2008 23:00:00	1.37	0.02								-6.0	-37						
080904-I5F	FOX	9/4/2008 0:00:00	1.37	0.02								-6.0	-37						
080904-I6F	FOX	9/4/2008 1:00:00	1.38	0.02								-6.0	-38						
080904-I7F	FOX	9/4/2008 2:00:00	1.38	0.02								-5.9	-38						
080904-I8F	FOX	9/4/2008 3:00:00	1.39	0.02								-5.9	-37						
080904-I9F	FOX	9/4/2008 4:00:00	1.42	0.03								-5.8	-36						
080904-I10F	FOX	9/4/2008 5:00:00	1.43	0.04								-5.9	-36						
080904-I11F	FOX	9/4/2008 6:00:00	1.43	0.03								-5.9	-36						
080904-I12F	FOX	9/4/2008 7:00:00	1.43	0.04								-5.9	-36						
080904-I13F	FOX	9/4/2008 8:00:00	1.51	0.09								-5.3	-32						
080904-I14F	FOX	9/4/2008 9:00:00	1.61	0.31								-6.0	-37						
080904-I15F	FOX	9/4/2008 10:00:00	1.79	1.53								-5.9	-36						
080904-I16F	FOX	9/4/2008 11:00:00	2.31	15.29								-5.6	-35						
080904-I17F	FOX	9/4/2008 12:00:00	2.37	18.41								-6.1	-38						
080904-I18F	FOX	9/4/2008 13:00:00	2.50	24.64								-6.4	-40						
080904-I19F	FOX	9/4/2008 14:00:00	2.34	17.05								-6.7	-42						
080904-I20F	FOX	9/4/2008 15:00:00	2.10	7.28								-6.6	-42						
080904-I21F	FOX	9/4/2008 16:00:00	1.98	4.39								-6.4	-40						

Sample ID	Site	Date and Time	USGS Stage (m)	USGS Discharge (cms)	SpC (µS/cm)	Temperature (°C)	DO (ppm)	DO (% sat)	Turbidity (NTU)	Calculated TSS (ppm)	pH	δ ¹⁸ O (‰)	δD (‰)	NH ₄ ⁺ -N (ppm)	Cl (ppm)	NO ₃ ⁻ -N (ppm)	Total PO ₄ ³⁻ (ppm)	<i>E. coli</i> (cfu/100mL)	Total Coliforms (cfu/100mL)
080904-I22F	FOX	9/4/2008 17:00:00	2.06	6.17								-6.2	-39						
080904A	FOX	9/4/2008 18:00:00	2.14	8.44	211.2	20.3	7.97	88.0	119	60.7	6.20	-6.3	-40						
080911-I11F	FOX	9/4/2008 18:10:00	2.12	7.90								-6.4	-40						
080911-I2F	FOX	9/4/2008 19:10:00	2.03	5.27								-6.4	-40						
080911-I3F	FOX	9/4/2008 20:10:00	1.93	3.45								-6.3	-40						
080911-I4F	FOX	9/4/2008 21:10:00	1.87	2.41								-6.2	-39						
080911-I5F	FOX	9/4/2008 22:10:00	1.82	1.81								-6.1	-38						
080911-I6F	FOX	9/4/2008 23:10:00	1.78	1.42								-5.9	-37						
080911-I7F	FOX	9/5/2008 0:10:00	1.75	1.13								-5.9	-37						
080911-I8F	FOX	9/5/2008 2:10:00	1.70	0.74								-5.9	-36						
080911-I9F	FOX	9/5/2008 4:10:00	1.67	0.54								-6.0	-37						
080911-I10F	FOX	9/5/2008 6:10:00	1.64	0.42								-5.8	-36						
080911-I11F	FOX	9/5/2008 8:10:00	1.62	0.34								-5.9	-36						
080911-I12F	FOX	9/5/2008 10:10:00	1.60	0.27								-5.8	-36						
080911-I13F	FOX	9/5/2008 12:10:00	1.58	0.23								-5.8	-36						
080911-I14F	FOX	9/5/2008 15:10:00	1.57	0.19								-5.7	-36						
080911-I15F	FOX	9/5/2008 18:10:00	1.55	0.15								-5.8	-36						
080911-I16F	FOX	9/5/2008 21:10:00	1.54	0.14								-5.8	-36						
080911-I17F	FOX	9/6/2008 0:10:00	1.52	0.12								-5.9	-36						
080911-I18F	FOX	9/6/2008 3:10:00	1.51	0.11								-5.9	-37						
080911-I19F	FOX	9/6/2008 6:10:00	1.51	0.09								-5.8	-37						
080911-I20F	FOX	9/6/2008 10:10:00	1.50	0.08								-5.8	-37						
080911-I21F	FOX	9/6/2008 14:10:00	1.48	0.07								-5.9	-37						
080911-I22F	FOX	9/6/2008 18:10:00	1.48	0.07								-5.9	-37						
080911-I23F	FOX	9/6/2008 22:10:00	1.47	0.06								-5.9	-37						
080911-I24F	FOX	9/7/2008 14:10:00	1.45	0.05								-5.9	-37						
080911F	FOX	9/11/2008 17:30:00	1.42	0.03	557	20.3	5.74	60.4			7.60	-6.1	-38						
101002C	FOX	10/2/2010 12:45:00	*	*	561	16.1	6.12	62.0	5	2.6	7.93	-6.3	-41	0.05	14.2	0.4	0.14	31.3	5500

Appendix C: Grand Glaize Creek Data

Sample ID	Site	Date and Time	USGS Stage (m)	USGS Discharge (cms)	SpC (µS/cm)	Temperature (°C)	DO (ppm)	DO (% sat)	Turbidity (NTU)	Calculated TSS (ppm)	pH	δ ¹⁸ O (‰)	δD (‰)	NH ₄ ⁺ -N (ppm)	Cl (ppm)	NO ₃ ⁻ -N (ppm)	Total PO ₄ ³⁻ (ppm)	<i>E. coli</i> (cfu/100mL)	Total Coliforms (cfu/100mL)
070606B	GG@Q	6/6/2007 10:35:00	0.77	0.11	803	22.3	6.20	72.1	19.1	9.7		-5.0	-33						
070703C	GG@Q	7/3/2007 11:40:00	0.76	0.13	704	23.8	6.30	75.9	16.7	8.5	8.20	-4.4	-29						
070717E	GG@Q	7/17/2007 11:40:00	0.85	0.59	774	27.1			10.3	5.3	8.20	-4.2	-30						
070801C	GG@Q	8/1/2007 12:00:00	0.73	0.04	397	27.4			7.7	3.9	8.30	-4.3	-31						
070813C	GG@Q	8/13/2007 12:00:00	0.85	0.54		26.7	3.75	46.9	4.2	2.1	7.80	-2.2	-14	0.01	56.6	1.20	0.48	>200.5	>200.5
070822B	GG@Q	8/22/2007 10:30:00	0.70	0.02	738	26.8	4.10	51.9	9.5	4.8	7.74	-3.6	-26	0.29	111.0	0.60	0.34	66.2	5040.0
070822B -lab duplicate	GG@Q	8/22/2007 10:30:00																53.6	5040.0
070904B	GG@Q	9/4/2007 13:15:00	0.70	0.02	693	26.5	4.80	60.0	9.2	4.7	7.83	-3.1	-24	0.18	101.6	0.80	0.40	42.8	5040.0
070904B - lab duplicate	GG@Q	9/4/2007 13:15:00												0.16	102.4	1.60	0.23		
070921B	GG@Q	9/21/2007 11:00:00	0.73	0.08	375	25.2	7.50	93.8	12.3	6.3	7.60			0.08	92.0	0.70	0.34	35.4	2880.0
071002A	GG@Q	10/2/2007 10:15:00	0.71	0.04	885	20.1	5.07	57.0	8.6	4.4	7.40	-5.8	-44	0.12	105.0	1.10	0.06	42.5	3640.0
071012B	GG@Q	10/12/2007 13:05:00	0.72	0.06	717	16.7	6.20	63.9	7.2	3.7	7.10								
071017C	GG@Q	10/17/2007 14:30:00			798	16.8	8.40	86.6	10.2	5.2	7.40	-5.8	-44	0.15	96.4	1.10	0.33	266.8	9450.0
071017C - lab duplicate	GG@Q	10/17/2007 14:30:00																383.6	8850.0
071102C	GG@Q	11/2/2007 13:15:00	0.77	0.13	664	10.4	7.90	70.0	11.5	5.9	7.00	-6.5	-46	0.19	76.8	1.10	0.02	62.4	1953.6
071102C - lab duplicate	GG@Q	11/2/2007 13:15:00																36.6	1540.2
071116C	GG@Q	11/16/2007 13:15:00	0.89	0.82	560	10.5	4.10	37.0	8.0	4.1	7.20	-5.1	-30	0.23	56.8	0.50	0.62	53.8	>200.5
071116D - field duplicate	GG@Q	11/16/2007 13:20:00			560	10.6	4.10	36.0			7.20			0.24	52.8	1.50	0.51	50.4	>200.5
071130B	GG@Q	11/30/2007 14:10:00	0.75	0.15	596	6.5	10.70	87.0	20.0	10.2	6.90	-8.1	-55	0.16	54.1	1.90	0.52	31.5	727.0
071130B - lab duplicate	GG@Q	11/30/2007 14:10:00												0.16	53.0	2.00	0.55		
071214B	GG@Q	12/14/2007 12:40:00	0.73	0.10	843	4.6	11.53	90.1	16.0	8.2	7.00	-5.8	-36	0.21	301.0	1.20	0.39	238.2	>2419.6
071227C	GG@Q	12/27/2007 13:50:00	0.78	0.31	1746	3.6	11.70	88.0	31.0	15.8	7.60	-7.7	-52	0.27	373.0	1.40	0.37	46.9	1119.9
080110B	GG@Q	1/10/2008 11:45:00	0.80	0.34	1149	5.7	9.29	75.3	1.3	0.7	7.20	-6.8	-42	0.15	199.0	1.90	0.23	2419.6	>2419.6
080110B - lab duplicate	GG@Q	1/10/2008 11:45:00																1733.0	>2419.6
080123C	GG@Q	1/23/2008 13:30:00	0.72	0.05	1351	1.7	17.00	125.0	5.0	2.6	7.60	-7.3	-48	0.15	278.0	1.30	0.28	6.3	365.4

Sample ID	Site	Date and Time	USGS Stage (m)	USGS Discharge (cms)	SpC (µS/cm)	Temperature (°C)	DO (ppm)	DO (% sat)	Turbidity (NTU)	Calculated TSS (ppm)	pH	δ ¹⁸ O (‰)	δD (‰)	NH ₄ ⁺ -N (ppm)	Cl (ppm)	NO ₃ ⁻ -N (ppm)	Total PO ₄ ³⁻ (ppm)	<i>E. coli</i> (cfu/100mL)	Total Coliforms (cfu/100mL)
080204B	GG@Q	2/4/2008 15:00:00	0.91	1.02	6450	3.9	13.40	104.9	51.0	26.0	7.00	-7.8	-49	0.43	1766.0	1.90	0.34	1732.9	>2419.16
080225B	GG@Q	2/25/2008 14:15:00	0.78	0.21	6070	4.0	12.01	92.1	11.0	5.6	6.50	-7.7	-50	0.34	1785.0	1.30	0.36	980.4	>2419.16
080309D-GG5	GG@Q	3/9/2008 12:00:00	0.80	0.28								-7.7	-49						
080311A	GG@Q	3/11/2008 10:00:00	0.80	0.28	2080	4.2	13.70	99.6	11.0	5.6	6.80	-7.8	-53	0.12	436.0	0.00		118.7	1203.3
080312A	GG@Q	3/12/2008 11:00:00	0.79	0.24															
080319D	GG@Q	3/19/2008 14:10:00	1.04	2.29	425	7.3	10.90	91.0	95.0	48.5	7.40	-9.9	-72	0.30	21.2	2.10	0.58	2419.6	>2419.6
080324B	GG@Q	3/24/2008 14:00:00	0.69	0.01	965	7.6	13.15	111.8	9.0	4.6	7.80	-8.6	-60	0.20	221.0	1.60	0.21	307.6	1732.9
080326C	GG@Q	3/26/2008 15:00:00	0.68	0.00								-8.0	-55						
080329-I1GG	GG@Q	3/26/2008 18:00:00	0.99	1.76								-7.9	-55						
080329-I2GG	GG@Q	3/26/2008 20:00:00	1.62	14.58								-5.6	-27						
080329-I3GG	GG@Q	3/26/2008 22:00:00	1.81	20.30								-5.5	-28						
080329-I4GG	GG@Q	3/27/2008 0:00:00	1.29	6.17								-6.1	-33						
080329-I5GG	GG@Q	3/27/2008 2:00:00	1.04	2.27								-6.3	-36						
080329-I6GG	GG@Q	3/27/2008 4:00:00	1.28	6.06								-6.2	-35						
080329-I7GG	GG@Q	3/27/2008 6:00:00	1.20	4.53								-6.4	-37						
080329-I8GG	GG@Q	3/27/2008 8:00:00	1.09	2.92								-6.5	-39						
080329-I9GG	GG@Q	3/27/2008 10:00:00	1.06	2.52								-6.6	-41						
080329-I10GG	GG@Q	3/27/2008 12:00:00	0.98	1.64								-6.5	-42						
080329-I11GG	GG@Q	3/27/2008 14:00:00	0.93	1.13								-6.6	-43						
080329-I17GG	GG@Q	3/28/2008 0:00:00	1.78	19.40								-5.9	-37						
080329B-BW	GG@Q	3/29/2008 11:40:00	0.74	0.07	1091	7.3			21.0	10.7		-7.0	-43					>1	>1
080331-I1GG	GG@Q	3/29/2008 18:00:00	0.73	0.05								-6.7	-43						
080331-I2GG	GG@Q	3/30/2008 0:00:00	0.73	0.04								-6.8	-43						
080331-I3GG	GG@Q	3/30/2008 6:00:00	0.84	0.54								-6.7	-42						
080331-I4GG	GG@Q	3/30/2008 12:00:00	1.01	1.93								-5.8	-36						
080331-I5GG	GG@Q	3/30/2008 18:00:00	0.88	0.79								-6.0	-36						
080331-I6GG	GG@Q	3/30/2008 21:00:00	0.84	0.51								-5.9	-37						

Sample ID	Site	Date and Time	USGS Stage (m)	USGS Discharge (cms)	SpC (µS/cm)	Temperature (°C)	DO (ppm)	DO (% sat)	Turbidity (NTU)	Calculated TSS (ppm)	pH	δ ¹⁸ O (‰)	δD (‰)	NH ₄ ⁺ -N (ppm)	Cl (ppm)	NO ₃ ⁻ -N (ppm)	Total PO ₄ ³⁻ (ppm)	<i>E. coli</i> (cfu/100mL)	Total Coliforms (cfu/100mL)
080331-17GG	GG@Q	3/31/2008 0:00:00	0.81	0.34								-5.9	-38						
080331-18GG	GG@Q	3/31/2008 3:30:00	0.79	0.27								-6.1	-39						
080331-19GG	GG@Q	3/31/2008 4:30:00	0.79	0.24								-6.3	-39						
080331-110GG	GG@Q	3/31/2008 5:30:00	0.78	0.21								-6.1	-40					1553.1	>2419.6
080331-111GG	GG@Q	3/31/2008 6:30:00	0.78	0.19								-6.2	-39					1553.1	>2419.6
080331-112GG	GG@Q	3/31/2008 7:30:00	0.78	0.18								-6.3	-40					1732.9	>2419.6
080331-113GG	GG@Q	3/31/2008 8:30:00	0.77	0.16								-6.3	-40					1732.9	>2419.6
080331B-BW	GG@Q	3/31/2008 8:30:00	0.77	0.16	928	10.8			33.0	16.8		-6.5	-40						
080331-114GG	GG@Q	3/31/2008 9:30:00	0.77	0.15								-6.4	-40						
080331-115GG	GG@Q	3/31/2008 10:30:00	0.77	0.14								-6.4	-41						
080331-116GG	GG@Q	3/31/2008 11:30:00	0.77	0.14								-6.6	-41					980.4	>2419.6
080331-117GG	GG@Q	3/31/2008 12:30:00	0.77	0.14								-6.5	-41					1119.9	>2419.6
080331-118GG	GG@Q	3/31/2008 13:30:00	0.77	0.14								-6.4	-41					816.4	2419.6
080331-119GG	GG@Q	3/31/2008 14:30:00	0.77	0.14								-6.6	-41					1046.2	>2419.6
080331B	GG@Q	3/31/2008 15:15:00	0.77	0.16	1002	12.4	8.88	91.2	28.0	14.3	7.80	-6.6	-42	0.15	129.2	1.50	0.32	1203.3	2419.6
080402-11GG	GG@Q	3/31/2008 15:30:00	0.78	0.18								-6.4	-41						
080402-12GG	GG@Q	3/31/2008 16:00:00	0.79	0.24								-6.5	-42						
080402-13GG	GG@Q	3/31/2008 16:30:00	0.82	0.40								-6.5	-41						
080402-14GG	GG@Q	3/31/2008 17:00:00	0.89	0.82								-6.4	-39						
080402-15GG	GG@Q	3/31/2008 17:30:00	1.13	3.51								-6.0	-37						
080402-16GG	GG@Q	3/31/2008 18:00:00	1.79	19.85								-5.4	-31						
080402-17GG	GG@Q	3/31/2008 19:00:00	2.24	35.11								-5.0	-26						
080405-18GG	GG@Q	3/31/2008 20:00:00	2.38	40.49								-5.0	-28						
080402-19GG	GG@Q	3/31/2008 21:00:00	2.53	47.01								-5.3	-32						
080402-110GG	GG@Q	3/31/2008 22:00:00	2.33	38.51								-5.3	-34						
080402-111GG	GG@Q	3/31/2008 23:00:00	1.81	20.50								-5.4	-35						
080402-112GG	GG@Q	4/1/2008 0:00:00	1.45	9.85								-5.6	-36						

Sample ID	Site	Date and Time	USGS Stage (m)	USGS Discharge (cms)	SpC (µS/cm)	Temperature (°C)	DO (ppm)	DO (% sat)	Turbidity (NTU)	Calculated TSS (ppm)	pH	δ ¹⁸ O (‰)	δD (‰)	NH ₄ ⁺ -N (ppm)	Cl (ppm)	NO ₃ ⁻ -N (ppm)	Total PO ₄ ³⁻ (ppm)	<i>E. coli</i> (cfu/100mL)	Total Coliforms (cfu/100mL)
080402-113GG	GG@Q	4/1/2008 2:00:00	1.20	4.56								-5.7	-37						
080402-114GG	GG@Q	4/1/2008 4:00:00	1.11	3.17								-5.8	-37						
080402-115GG	GG@Q	4/1/2008 6:00:00	1.05	2.35								-5.9	-36						
080402-116GG	GG@Q	4/1/2008 8:00:00	1.01	1.98								-6.0	-37						
080402-117GG	GG@Q	4/1/2008 10:00:00	0.97	1.56								-6.0	-37						
080402-118GG	GG@Q	4/1/2008 12:00:00	0.96	1.44								-6.1	-38						
080402-119GG	GG@Q	4/1/2008 14:00:00	0.95	1.33								-6.1	-39						
080402-120GG	GG@Q	4/1/2008 16:00:00	0.94	1.22								-6.2	-39						
080402-121GG	GG@Q	4/1/2008 18:00:00	0.92	1.08								-6.2	-39						
080402-122GG	GG@Q	4/1/2008 20:00:00	0.91	0.99								-6.2	-39						
080402-123GG	GG@Q	4/1/2008 22:00:00	0.89	0.85								-6.2	-40						
080402-124GG	GG@Q	4/2/2008 0:00:00	0.90	0.88								-6.2	-40						
080402B	GG@Q	4/2/2008 12:10:00	0.75	0.09	1060	8.8			20.0	10.2		-6.4	-42						
080403A-11GG	GG@Q	4/3/2008 7:02:00	0.94	1.25								-6.7	-42	0.31	133.0	0.90	0.10	1553.1	>2419.6
080403A-12GG	GG@Q	4/3/2008 7:32:00	1.12	3.28								-6.8	-44	0.59	122.0	1.60	0.45	>2419.6	>2419.6
080403A-13GG	GG@Q	4/3/2008 8:02:00	1.42	9.12								-7.1	-46	0.80	121.6	1.00		>2419.6	>2419.6
080403A-14GG	GG@Q	4/3/2008 8:32:00	1.63	14.70								-7.1	-46	0.85	94.0	0.80		>2419.6	>2419.6
080403B-EH	GG@Q	4/3/2008 8:35:00	1.68	16.23								-6.9	-46						
080403B-11GG	GG@Q	4/3/2008 8:41:00	1.68	16.23								-7.2	-47	0.27	78.8	1.50	1.15	>2419.6	>2419.6
080403B-12GG	GG@Q	4/3/2008 9:11:00	1.71	17.41								-7.3	-48	0.16	64.8	1.60	1.78	>2419.6	>2419.6
080403B-13GG	GG@Q	4/3/2008 9:41:00	1.67	16.11								-7.4	-48	0.32	52.8	1.20	1.19	>2419.6	>2419.6
080403B-14GG	GG@Q	4/3/2008 10:11:00	1.57	12.88								-7.3	-48	0.25	46.0	0.90	1.32	>2419.6	>2419.6
080403B-15GG	GG@Q	4/3/2008 10:41:00	1.47	10.17								-7.2	-47	0.24	43.2	1.40	1.30	>2419.6	>2419.6
080403B-16GG	GG@Q	4/3/2008 11:11:00	1.39	8.33								-7.2	-46	0.25	42.8	1.40	1.02	>2419.6	>2419.6
080403B-17GG	GG@Q	4/3/2008 11:41:00	1.32	6.80								-7.0	-46	0.25	50.4	1.60	1.21	>2419.6	>2419.6
080403B-18GG	GG@Q	4/3/2008 12:41:00	1.21	4.73								-7.0	-45	0.24	67.6	1.00	0.95	>2419.6	>2419.6
080403B-19GG	GG@Q	4/3/2008 13:41:00	1.14	3.65								-6.9	-45	0.38	44.0	1.00		>2419.6	>2419.6

Sample ID	Site	Date and Time	USGS Stage (m)	USGS Discharge (cms)	SpC (µS/cm)	Temperature (°C)	DO (ppm)	DO (% sat)	Turbidity (NTU)	Calculated TSS (ppm)	pH	δ ¹⁸ O (‰)	δD (‰)	NH ₄ ⁺ -N (ppm)	Cl (ppm)	NO ₃ ⁻ -N (ppm)	Total PO ₄ ³⁻ (ppm)	<i>E. coli</i> (cfu/100mL)	Total Coliforms (cfu/100mL)
080404A-I10GG	GG@Q	4/3/2008 14:41:00	1.09	2.94								-6.8	-45						
080404A-I11GG	GG@Q	4/3/2008 15:41:00	1.05	2.46								-6.9	-44						
080404A-I12GG	GG@Q	4/3/2008 16:41:00	1.04	2.24								-6.8	-43						
080404A-I13GG	GG@Q	4/3/2008 17:41:00	1.02	2.10								-6.8	-43						
080404A-I14GG	GG@Q	4/3/2008 19:41:00	1.00	1.87								-6.7	-43						
080404A-I15GG	GG@Q	4/3/2008 21:41:00	1.04	2.27								-6.6	-42						
080404A-I16GG	GG@Q	4/3/2008 23:41:00	1.08	2.72								-6.4	-41						
080404A-I17GG	GG@Q	4/4/2008 1:41:00	1.02	2.04								-6.3	-40						
080404A-I18GG	GG@Q	4/4/2008 3:41:00	0.98	1.61								-6.2	-39	0.15	88.0	2.60	0.67	>2419.6	>2419.6
080414B	GG@Q	4/14/2008 15:15:00	0.83	0.76	1244	11.1	10.90	99.5	8.0	4.1	7.60	-6.7	-44	0.11	159.6	0.90	0.46	110.6	1119.9
080428B	GG@Q	4/28/2008 15:10:00	0.85	0.88	1069	13.0	10.45	100.0	17.0	8.7	7.20	-5.9	-38	0.15	110.0	0.00	0.47	>2419.6	>2419.6
080430B	GG@Q	4/30/2008 12:30:00	0.79	0.54	1178	14.2	9.67	95.9	9.0	4.6	7.30	-6.5	-43	0.08	147.0	1.00	0.25	275.5	>2419.6
080502B	GG@Q	5/2/2008 8:20:00	0.79	0.54								-6.4	-42	0.35	159.6	0.40	0.19	770.1	>2419.6
080505-11GG	GG@Q	5/2/2008 11:08:00	0.98	1.98								-6.3	-40						
080505-21GG	GG@Q	5/2/2008 11:38:00	1.06	2.89								-6.0	-39						
080505-31GG	GG@Q	5/2/2008 12:08:00	1.06	2.89								-5.9	-40						
080505-41GG	GG@Q	5/2/2008 12:38:00	1.05	2.61								-6.3	-35						
080507-15GG	GG@Q	5/7/2008 8:40:00	0.96	1.84								-5.6	-36	0.42	126.8	0.30	0.49	>2419.6	>2419.6
080507-16GG	GG@Q	5/7/2008 9:10:00	1.10	3.34								-5.8	-39	0.34	145.2	0.30	0.44	>2419.6	>2419.6
080507-17GG	GG@Q	5/7/2008 9:40:00	1.11	3.43								-5.8	-38	0.52	155.6	0.40	0.21	>2419.6	>2419.6
080507-18GG	GG@Q	5/7/2008 10:10:00	1.08	3.11								-5.7	-37	0.51	148.0	0.80	0.73	>2419.6	>2419.6
080507-19GG	GG@Q	5/7/2008 10:40:00	1.05	2.72								-5.6	-36	0.49	134.0	0.70	0.59	>2419.6	>2419.6
080507B	GG@Q	5/7/2008 12:00:00	0.93	1.61	729	16.6	6.40	63.8	45.0	23.0	8.10	-5.2	-33	0.61	110.8	0.40	0.46	>2419.6	>2419.6
080508B-11GG	GG@Q	5/7/2008 14:43:00	0.94	1.67								-4.7	-29	0.14	92.8				
080508B-12GG	GG@Q	5/7/2008 15:13:00	1.19	4.53								-4.5	-26	0.66	80.4				
080508B-13GG	GG@Q	5/7/2008 15:53:00	1.82	20.67								-4.1	-22	1.86	67.6				
080508B-14GG	GG@Q	5/7/2008 16:13:00	1.85	21.52								-3.8	-20	2.44	35.6				

Sample ID	Site	Date and Time	USGS Stage (m)	USGS Discharge (cms)	SpC (µS/cm)	Temperature (°C)	DO (ppm)	DO (% sat)	Turbidity (NTU)	Calculated TSS (ppm)	pH	δ ¹⁸ O (‰)	δD (‰)	NH ₄ ⁺ -N (ppm)	Cl (ppm)	NO ₃ ⁻ -N (ppm)	Total PO ₄ ³⁻ (ppm)	<i>E. coli</i> (cfu/100mL)	Total Coliforms (cfu/100mL)
080508B-15GG	GG@Q	5/7/2008 16:43:00	1.78	19.57								-4.0	-20	2.21	32.0				
080508B-16GG	GG@Q	5/7/2008 17:13:00	1.68	16.31								-4.0	-22	2.36	26.8				
080508B-17GG	GG@Q	5/7/2008 17:43:00	1.63	14.78								-4.6	-26	1.84	30.4				
080508B-18GG	GG@Q	5/7/2008 18:43:00	1.60	13.96								-5.9	-35	1.35	29.6				
080508B-19GG	GG@Q	5/7/2008 19:43:00	1.56	12.80								-6.3	-41	1.15	30.0				
080508B-110GG	GG@Q	5/7/2008 20:43:00	1.55	12.46								-6.7	-45	0.95	25.6				
080508B-111GG	GG@Q	5/7/2008 21:43:00	1.59	13.51								-6.7	-45	0.92	28.0				
080508B-112GG	GG@Q	5/7/2008 22:43:00	1.44	9.54								-6.6	-43	0.96	27.2				
080508B-113GG	GG@Q	5/7/2008 23:43:00	1.30	6.48								-6.2	-41	0.96	24.8				
080508B-114GG	GG@Q	5/8/2008 1:43:00	1.15	3.96								-6.0	-40	0.95	34.8			>2419.6	>2419.6
080508B-115GG	GG@Q	5/8/2008 3:43:00	1.05	2.69								-5.9	-39	0.80	40.8			>2419.6	>2419.6
080508B-116GG	GG@Q	5/8/2008 5:43:00	1.00	2.24								-5.9	-38	0.64	43.6			>2419.6	>2419.6
080508B-117GG	GG@Q	5/8/2008 7:43:00	1.68	16.42								-5.6	-33	1.50	46.8			>2419.6	>2419.6
080508B-118GG	GG@Q	5/8/2008 8:39:00	2.31	32.00								-5.5	-30	3.06	28.8			>2419.6	>2419.6
080508B-124GG	GG@Q	5/7/2008 14:40:00										-5.0	-32					>2419.6	>2419.6
080508D-11GG	GG@Q	5/8/2008 9:00:00	2.47	44.17								-5.6	-31	3.32	17.6				
080508D-12GG	GG@Q	5/8/2008 9:30:00	2.72	55.22								-5.8	-33	4.20	11.2				
080508D-13GG	GG@Q	5/8/2008 10:00:00	2.76	57.20								-5.8	-34	3.08	11.6				
080508D-14GG	GG@Q	5/8/2008 10:30:00	2.67	52.95								-5.9	-34	2.60	16.4				
080508D-15GG	GG@Q	5/8/2008 11:00:00	2.49	45.31								-6.0	-35	2.56	16.0				
080508D-16GG	GG@Q	5/8/2008 11:30:00	2.28	36.81								-6.0	-35		18.8				
080508D-17GG	GG@Q	5/8/2008 12:00:00	2.01	26.65								-5.8	-34		21.2				
080508D-18GG	GG@Q	5/8/2008 12:30:00	1.78	19.57								-5.9	-34	1.51	26.0			>2419.6	>2419.6
080508D-19GG	GG@Q	5/8/2008 13:00:00	1.62	14.33								-5.9	-35		24.4				
080508D-110GG	GG@Q	5/8/2008 13:30:00	1.52	11.61								-5.8	-34		26.4				
080508D-111GG	GG@Q	5/8/2008 14:00:00	1.44	9.54								-5.8	-34	1.08	28.8			>2419.6	>2419.6
080508D-112GG	GG@Q	5/8/2008 14:30:00	1.39	8.38								-5.9	-35						

Sample ID	Site	Date and Time	USGS Stage (m)	USGS Discharge (cms)	SpC (µS/cm)	Temperature (°C)	DO (ppm)	DO (% sat)	Turbidity (NTU)	Calculated TSS (ppm)	pH	δ ¹⁸ O (‰)	δD (‰)	NH ₄ ⁺ -N (ppm)	Cl (ppm)	NO ₃ ⁻ -N (ppm)	Total PO ₄ ³⁻ (ppm)	<i>E. coli</i> (cfu/100mL)	Total Coliforms (cfu/100mL)
080508D-113GG	GG@Q	5/8/2008 15:00:00	1.34	7.25								-5.7	-34						
080508D-114GG	GG@Q	5/8/2008 15:30:00	1.31	6.68								-6.3	-35	0.86	33.2			>2419.6	>2419.6
080512-11GG	GG@Q	5/8/2008 16:03:00	1.28	5.95								-5.8	-34						
080512-12GG	GG@Q	5/8/2008 20:03:00	1.12	3.51								-5.9	-35						
080512-13GG	GG@Q	5/10/2008 18:40:00	1.04	2.69								-6.2	-39						
080512-14GG	GG@Q	5/10/2008 22:40:00	2.62	50.97								-6.0	-35						
080512-15GG	GG@Q	5/11/2008 2:40:00	1.37	7.90								-5.9	-35						
080512-16GG	GG@Q	5/11/2008 6:40:00	1.26	5.66								-6.5	-40						
080512-17GG	GG@Q	5/11/2008 10:40:00	1.51	11.19								-10.4	-72						
080512-18GG	GG@Q	5/11/2008 14:40:00	1.17	4.28								-9.3	-63						
080512-19GG	GG@Q	5/11/2008 18:40:00	1.08	3.03								-8.5	-57						
080512B	GG@Q	5/12/2008 12:35:00	0.98	2.04	828	14.0	9.26	95.0	22.0	11.2	7.20	-7.1	-48	0.38	80.8	1.40	0.26	1986.3	>2419.6
080528B	GG@Q	5/28/2008 11:43:00	0.84	0.82	809	17.3	10.94	72.4	21.0	10.7	7.10	-6.0	-40	0.25	90.4	1.10	0.06	1986.3	>2419.6
080610C	GG@Q	6/10/2008 12:31:00	0.78	0.48	996	24.8	6.05	75.0	11.0	5.6	7.40	-5.7	-41	0.16	93.2	1.10	0.41	316.9	>2419.6
080624B	GG@Q	6/24/2008 0:00:00	1.38									-5.7	-39						

Appendix D: Sugar Creek

Sample ID	Site	Date and Time	USGS Stage (m)	USGS Discharge (cms)	SpC (µS/cm)	Temperature (°C)	DO (ppm)	DO (% sat)	Turbidity (NTU)	Calculated TSS (ppm)	pH	δ ¹⁸ O (‰)	δD (‰)	NH ₄ ⁺ -N (ppm)	Cl (ppm)	NO ₃ ⁻ -N (ppm)	Total PO ₄ ³⁻ (ppm)	<i>E. coli</i> (cfu/100mL)	Total Coliforms (cfu/100mL)
070528A	SGR	5/28/2007 10:40:00	1.24	0.02	905	19.6						-3.3	-19						
070606C	SGR	6/6/2007 10:50:00	1.21	0.01	1070	19.1	7.40	80.4	10.5	5.4		-5.5	-36						
070703D	SGR	7/3/2007 12:03:00	1.20	0.01	921	21.3	6.90	78.4	6.4	3.3	8.30	-5.0	-33						
070717F	SGR	7/17/2007 12:00:00	1.19	0.01	1044	24.9			9.8	5.0	8.30	-5.2	-36						
070801D	SGR	8/1/2007 11:45:00	1.18	0.01	866	24.7			7.0	3.6	8.40	-4.7	-32						
070813D	SGR	8/13/2007 11:45:00	1.27	0.05			5.80	72.5	31.4	16.0	8.00				27.5			>200.5	>200.5
070921A	SGR	9/21/2007 10:30:00	1.20	0.01	1225	22.9	6.89	80.1	5.4	2.8	8.18	-5.7	-45	0.10	195.2	1.10	0.40	1077.2	11840.0
071002B	SGR	10/2/2007 10:40:00	1.19	0.01	1140	17.8	5.90	62.8	3.9	2.0	7.60	-6.0	-45	0.12		0.50	0.35	45.6	20050.0
071102B	SGR	11/2/2007 12:45:00	1.28	0.02	1059	8.2	7.90	69.0	6.8	3.5	7.00	-5.9	-42	0.08	144.6	0.50	0.46	24.8	740.3
071116B	SGR	11/16/2007 12:45:00	1.28	0.02	940	8.1	9.70	82.0	2.0	1.0	7.40	-5.0	-33	0.11	116.0	0.90	0.01	56.5	>200.5
071130C	SGR	11/30/2007 15:00:00	1.23	0.01	1057	5.4	12.60	100.8	20.0	10.2	7.20	-6.7	-46	0.07	130.9	0.50	0.35	33.5	920.8
071214C	SGR	12/14/2007 13:10:00	1.22	0.01	1790	3.6	15.38	116.5	3.0	1.5	7.20	-6.1	-41	0.14	371.0	0.90	0.22	74.3	1203.3
071227B	SGR	12/27/2007 13:00:00	1.23	0.01	3018	5.0	13.90	109.0	5.0	2.6	7.40	-8.0	-54	0.07	741.0	1.30	0.27	488.4	>2419.6
071227B - lab duplicate	SGR	12/27/2007 13:00:00													723.0				
080110C	SGR	1/10/2008 12:45:00	1.26	0.03	1493	5.8	12.31	98.7	19.0	9.7	6.90			0.29	268.0	2.30	0.39	1413.6	>2419.6
080123B	SGR	1/23/2008 13:00:00	1.22	0.01	1732	1.0	17.80	125.7	3.0	1.5	7.40	-7.0	-46	0.10	340.0	2.80	0.02	16.0	248.1
080204C	SGR	2/4/2008 15:30:00	1.33	0.10	4750	4.3	14.80	110.7	9.0	4.6	7.40	-7.6	-47	0.25	1300.0	0.90	0.04	260.3	>2419.6
080225C	SGR	2/25/2008 15:30:00	1.27	0.04	4686	4.7	14.85	116.7	9.0	4.6	6.90	-7.4	-48	0.12	1325.0	0.30	0.36	104.3	>2419.6
080311B	SGR	3/11/2008 10:00:00	1.27	0.04	2226	3.4	17.05	132.0	6.0	3.1	7.10	-7.6	-50	0.07	440.0	0.70		290.9	1732.9
080331C	SGR	3/31/2008 16:00:00	1.38	0.16	1211	12.3	10.44	97.3	10.0	5.1	8.00	-6.8	-42	0.14	174.0	2.30	0.20	1119.9	>2419.6
080414C	SGR	4/14/2008 15:50:00	1.29	0.11	1288	12.1	15.50	145.1	3.0	1.5	8.10	-6.9	-44	0.07	188.4	1.70	0.46	47.3	770.1
080428C	SGR	4/28/2008 15:30:00	1.29	0.11	1219	13.5	16.43	158.0	4.0	2.0	8.40	-6.7	-43	0.16	177.0	0.90	0.17	648.8	>2419.6
080512C	SGR	5/12/2008 13:06:00	1.35	0.21	1033	14.6	10.74	105.9	6.0	3.1	7.80	-6.9	-46	0.17	115.6	1.30	0.35	920.8	>2419.6
080528C	SGR	5/28/2008 12:12:00	1.32	0.15	1038	16.6	9.47	97.3	12.0	6.1	7.30	-6.5	-41	0.11	135.2	1.40	0.31	1413.6	>2419.6
080610D	SGR	6/10/2008 13:10:00	1.26	0.08	967	22.6	8.56	98.2	3.0	1.5	8.40	-6.5	-42	0.12	114.8	0.80	0.55	816.4	>2419.6

Appendix E: River des Peres at Morgan Ford Rd. Data

Sample ID	Site	Date and Time	USGS Stage (m)	USGS Discharge (cms)	SpC (µS/cm)	Temperature (°C)	DO (ppm)	DO (% sat)	Turbidity (NTU)	Calculated TSS (ppm)	pH	δ ¹⁸ O (‰)	δD (‰)	NH ₄ ⁺ -N (ppm)	Cl (ppm)	NO ₃ ⁻ -N (ppm)	Total PO ₄ ³⁻ (ppm)	<i>E. coli</i> (cfu/100mL)	Total Coliforms (cfu/100mL)	
060405B	RDP	38812.42				23.50						-6.80	-							
070606A	RDP	39239.42	1.86	32.00	4920.00	23.50	2.70	32.14	23.50	11.99		-5.09	-	0.24						
070703A	RDP	39266.38	0.59	0.02	319.00	23.20	9.40	110.59	5.30	2.70	9.20	-4.46	-	2.54						
070719A	RDP	39282.42	0.61	0.03	638.00	27.70	7.25	92.95	3.10	1.58	9.00	-3.88	-	0.11						
070801A	RDP	39295.42	0.61	0.03	471.00	28.50	7.60	98.70	4.80	2.45	8.90	-4.06	-	0.67						
070813A	RDP	39307.42	1.33	10.93	241.00	26.10	3.38	42.25	96.80	49.37	8.10	-1.74	-8.20	0.47	27.70				>200.5	>200.5
070813A	RDP	39307.42													27.50				>200.5	>200.5
070822A	RDP	39316.41	0.61	0.03	723.00	28.60	6.10	79.22	3.30	1.68	8.57	-4.29	-	0.09	113.20	-0.40	0.23	561.00	14450.00	
070905A	RDP	39330.50	0.59	0.02	550.00	25.10	0.65	7.93	6.00	3.06	7.73	-5.04	-	0.24	59.20	0.60	0.68	862.00	2380.00	
070920A	RDP	39345.50	0.59	0.03	604.00	27.70	11.90	152.56	4.50	2.30	9.43	-5.03	-	0.11	104.00	0.30	0.36	91.10	>20050	
071003A	RDP	39358.42	1.12	0.06	324.00	21.50	4.70	54.02	79.00	40.29	7.30	-4.72	-	0.67	16.30	0.00	1.29	>2419.6	>20050	
071011A	RDP	39366.42	0.61	0.06	668.00	18.70	11.70	127.17	36.60	18.67		-5.80	-							
071017A	RDP	39372.48			694.00	16.40	7.80	79.59	6.80	3.47	8.30	-6.00	-	0.10	79.20	0.80	0.25	2866.00	>20050	
071031A	RDP	39386.50	0.63	0.03	630.00	14.30	12.20	119.61				-6.40	-	0.06	86.00	0.80	0.18	146.90	4512.00	
071114A	RDP	39400.42	0.67	0.08	653.00	15.00	5.46	54.60	7.00	3.57	7.50	-5.77	-	2.54	68.00	2.00	1.02	>2419.6	>2419.6	
071129A	RDP	39415.58	0.66	0.24	621.00	7.90	12.40	103.00	12.00	6.12	8.30	-7.56	-	0.49	57.20	3.10	0.49	19.90	2419.60	
071213A	RDP	39429.42	0.70	0.42	1235.00	4.20	12.40	95.38	17.00	8.67	6.20		-	0.53	220.00	2.40	0.56	57.40	>2419.6	
071227D	RDP	39443.60	0.76	0.79	1030.00	6.80	8.60	70.00	20.00	10.20	7.50	-9.09	-	1.73	180.00	2.00	1.06	>2419.6	>2419.6	
080108A	RDP	39455.42	1.97	37.10	445.00	11.90	9.60	87.20	243.00	123.93	9.60	-6.83	-	0.89	30.00	2.90	1.35	>2419.6	>2419.6	
080124A	RDP	39471.54	0.61	0.11	652.00	1.20	14.15	98.60	5.00	2.55	6.80	-7.85	-	0.72	121.00	2.90	0.38	8.40	387.30	
080128A	RDP	39475.64	0.62	0.14	469.00	2.40	12.94	92.60	16.00	8.16	6.20	-7.12	-	0.73	108.00	2.00	0.31	3.10	344.80	
080218A	RDP	39496.58	0.75	0.74	1150.00	7.00	11.05	91.50	55.00	28.05	7.30	-7.44	-	1.67	147.50	3.20		1986.30	>2419.6	
080303A	RDP	39510.55	1.37	12.21	1065.00	8.20	10.68	106.10	263.00	134.13	7.80	-7.61	-	0.53	246.00	1.00	0.90	>2419.6	>2419.6	
080303B - field duplicate	RDP	39510.55											-	0.05	242.00	1.30	0.95			
080306A	RDP	39513.61			4980.00	5.80	9.00	70.70				-11.07	-	0.89						
080317A	RDP	39524.60	0.69	0.42	1292.00	9.10	14.53	123.20	17.00	8.67	7.40	-7.75	-	0.59	226.00	0.90	0.52	>2419.6	>2419.6	
080317B - field duplicate	RDP	39524.60										-7.70	55.00							

Sample ID	Site	Date and Time	USGS Stage (m)	USGS Discharge (cms)	SpC (µS/cm)	Temperature (°C)	DO (ppm)	DO (% sat)	Turbidity (NTU)	Calculated TSS (ppm)	pH	δ ¹⁸ O (‰)	δD (‰)	NH ₄ ⁺ -N (ppm)	Cl (ppm)	NO ₃ ⁻ -N (ppm)	Total PO ₄ ³⁻ (ppm)	<i>E. coli</i> (cfu/100mL)	Total Coliforms (cfu/100mL)
080319A	RDP	39526.52	3.61	173.32	397.20	8.10	10.35	86.80	65.00	33.15	6.90	-10.77	-77.15	0.82	86.40	3.30	1.18	>2419.6	>2419.6
080326A	RDP	39533.57	2.73	88.08	815.00	10.50	7.80	69.50	17.00	8.67	7.20	-9.28	-67.15	0.41	97.60	3.40	0.78	137.40	>2419.6
080407A	RDP	39545.56	2.08	43.33	1088.00	16.20	6.75	68.90	26.00	13.26	6.60	-6.66	-43.30	0.27	140.80	2.30	0.45	1119.90	>2419.6
080421A	RDP	39559.55	3.76		419.50	16.70	3.58	36.70	35.00	17.85	6.40	-7.85	-48.40	0.62	56.00	1.60	0.74	1732.90	>2419.6
080505A	RDP	39573.53	4.26		518.00	19.30	8.00	88.40	12.00	6.12	7.60	-6.00	-38.00	0.38	51.60	1.00	0.51	831.00	>2419.6
080520A	RDP	39588.43	3.62		542.00	19.20	0.80	24.50	14.00	7.14	7.40	-6.50	-42.00	0.86	56.00	1.30	0.46	461.10	>2419.6
080603A	RDP	39602.41	2.74		301.40	21.30	5.61	63.80	390.00	198.90	8.50	-3.60	-18.15	3.02	21.30	1.00	1.64	>2419.6	>2419.6
080603A - lab duplicate	RDP	39602.41													22.00	0.50	1.65		
080603A - matrix spike	RDP	39602.41													24.10	1.00	1.59		
080603A - matrix spike duplicate	RDP	39602.41													22.00	0.90	2.12		
080715A	RDP	39644.50	3.10		312.50	29.00	3.74	48.30	24.00	12.24	7.70	-3.61	-23.60	0.47	22.00	0.50	0.30	1046.20	>2419.6
080826A	RDP	39686.48	0.62	0.05	648.00	25.70	6.15	73.00	23.00	11.73	6.90	-4.36	-33.20	0.75	65.60	0.50	0.67	816.40	>2419.6

Appendix F: Upper River des Peres Data

Sample ID	Site	Date and Time	USGS Stage (m)	USGS Discharge (cms)	SpC (µS/cm)	Temperature (°C)	DO (ppm)	DO (% sat)	Turbidity (NTU)	Calculated TSS (ppm)	pH	δ ¹⁸ O (‰)	δD (‰)	NH ₄ ⁺ -N (ppm)	Cl (ppm)	NO ₃ ⁻ -N (ppm)	Total PO ₄ ³⁻ (ppm)	<i>E. coli</i> (cfu/100mL)	Total Coliforms (cfu/100mL)
091211A	RP2	12/11/2009 11:45:00	0.11	0.04	1795	0.5	13.90	93.0	6.0		7.91	-7.6	-52.9	1.96	340.0	2.10		>2419.6	>2419.6
091211B	RP1	12/11/2009 12:10:00	0.11	0.04	1620	1.6	11.40	81.7	9.0		8.20	-7.6	-53.2	2.68	295.0	1.30		>2419.6	>2419.6
091221A	RP1	12/21/2009 12:39:00	0.10	0.03	1990	5.2	15.10	120.0	8.0		8.23	-6.9	-48.4	0.30	386.0	2.00		2419.6	>2419.6
091221B	RP2	12/21/2009 13:00:00	0.10	0.03	1759	3.2	9.94	77.1	4.0		8.35	-6.9	-49.3	0.71	304.0	2.60		727.0	>2419.6
091221C	RPMP	12/21/2009 13:20:00			3819	2.8	0.85	6.5	237.0		6.20	-7.8	-47	17.30	42.4	2.90		1553.1	>2419.6
091221D	HMP	12/21/2009 13:50:00	0.10	0.03	1348	2.7	12.64	93.7	10.0		8.10	-7.6	-48.6	0.10	204.0	1.90		290.9	>2419.6
100106A	HMP	1/6/2010 14:50:00	0.11	0.11	2324		15.25	110.0	6.0		8.04	-7.7	-53.7	0.24	490.0	1.30		117.2	1299.7
100106B	RPMP	1/6/2010 15:10:00										-6.1	-37.1						
100106C	RP2	1/6/2010 15:15:00	0.11	0.11	3164		13.10	91.5	2.0		7.60	-7.6	-51.3	0.15	750.0	2.50		74.4	>2419.6
100106D	RP1	1/6/2010 15:33:00	0.11	0.11	2365		9.52	70.0	7.0		8.25	-7.1	-48	0.13	434.0	1.50		86.0	1299.7
100106D - matrix spike	RP1	1/6/2010 15:33:00												1.64	392.0	2.30			
100113B	RP2	1/13/2010 14:15:00	0.11	0.08	2701	0.1	13.39	91.8	8.0		8.17	-7.5	-53.4	0.36	715.0	2.20		1119.9	>2419.6
100113C	RP1	1/13/2010 14:30:00	0.11	0.09	3176	0.3	10.50	73.7	19.0		8.05	-8.1	-57.7	1.22	870.0	1.40		>2419.6	>2419.6
100113C	RP1 - lab dup	1/13/2010 14:30:00																	
100113D	HMP	1/13/2010 14:55:00	0.11	0.10	2567	1.0	15.40	108.5	8.0		8.18	-7.5	-52.4	0.50	625.0	1.50		151.5	1732.9
100118A	RP2	1/18/2010 11:20:00	0.10	0.05	2148	1.0	13.56	95.2	3.0		7.54	-8.2	-56.8	0.63	536.0	1.50		>2419.6	>2419.6
100118B	RP1	1/18/2010 11:50:00	0.10	0.05	1874	2.0	12.93	94.4	8.0		8.27	-8	-55	0.61	480.0	1.50		>2419.6	>2419.6
100118C	HMP	1/18/2010 12:20:00	0.10	0.05	2029	1.4	12.60	89.5	15.0		8.27	-8.5	-57.7	0.48	494.0	1.40		30.1	>2419.6
100122A	RP2	1/22/2010 15:50:00	0.11	0.10	1505		5.84	45.6	7.0		7.75	-9.1	-61.6	0.31	320.0	1.80		>2419.6	>2419.6
100122B	RP1	1/22/2010 16:10:00	0.11	0.10	1562	5.5	12.11	95.2	10.0		8.43	-8.9	-60.9	0.16	344.0	1.60		>2419.6	>2419.6
100126A	RP1	1/26/2010 16:30:00	0.11	0.07	1593	2.6	12.94	94.0	8.0		8.22	-8.2	-52.7	0.03	296.0	1.20		2419.6	>2419.6
100126A - field duplicate (EC/TC)	RP1	1/26/2010 16:30:00										-8.2	-52.7					2419.6	>2419.6
100126B	RP2	1/26/2010 16:45:00	0.11	0.07	1513	1.2	14.51	102.6	3.0		8.15	-8.2	-53.5	0.26	306.0	1.40		201.4	>2419.6
100126C	HMP	1/26/2010 17:15:00	0.11	0.07	1454	1.7	17.97	128.9	4.0		8.39	-8.4	-54.6	0.09	294.0	1.40		88.2	>2419.6
100212A	RPMP	2/12/2010 10:35:00			3178	5.5	0.79	6.0	135.0		6.44	-12.6	-90.3	16.20	260.0	1.70		>2419.6	>2419.6
100212A - lab duplicate	RPMP	2/12/2010 10:35:00										-12.5	-90.3	15.20	250.0	2.40		>2419.6	>2419.6

Sample ID	Site	Date and Time	USGS Stage (m)	USGS Discharge (cms)	SpC (µS/cm)	Temperature (°C)	DO (ppm)	DO (% sat)	Turbidity (NTU)	Calculated TSS (ppm)	pH	δ ¹⁸ O (‰)	δD (‰)	NH ₄ ⁺ -N (ppm)	Cl (ppm)	NO ₃ ⁻ -N (ppm)	Total PO ₄ ³⁻ (ppm)	<i>E. coli</i> (cfu/100mL)	Total Coliforms (cfu/100mL)
100212B	RP2	2/12/2010 10:47:00	0.11	0.11	3250	1.3	12.37	88.0	4.0		7.85	-9.5	-62.2	0.65	815.0	2.50		>2419.6	>2419.6
100212C	RP1	2/12/2010 11:07:00	0.11	0.11	2812	2.8	14.44	110.0	8.0		8.30	-9.1	-60.2	1.21	765.0	1.40		>2419.6	>2419.6
100212D	HMP	2/12/2010 11:34:00	0.11	0.11	4910	0.7	15.00	104.0	6.0		8.17	-9.79	-70.1	0.12	1420.0	0.50		88.6	>2419.6
100226A	RP2	2/26/2010 14:17:00	0.11	0.06	1751	2.9	15.75	121.2	3.0		8.05	-7.6	-56.3	0.30	334.0	1.40		38.4	>2419.6
100226A - field duplicate	RP2	2/26/2010 14:17:00										-7.5	-56.8	0.26	340.0	1.10		41.4	>2419.6
100226A - matrix spike	RP2	2/26/2010 14:17:00												1.54	302.0	2.90			
100226B	RPMP	2/26/2010 14:31:00			3208	10.5	0.65	8.1	129.0		6.90	-9.7	-77.8	8.50	314.0	1.40		>2419.6	>2419.6
100226C	RP1	2/26/2010 14:55:00	0.11	0.06	1567	3.3	12.69	93.1	5.0		8.08	-7.7	-57.1	0.14	320.0	1.50		478.6	>2419.6
100226D	HMP	2/26/2010 15:25:00	0.11	0.07	1846	3.6	21.86	165.5	5.0		8.61	-8.4	-58.4	0.05	412.0	1.10		23.3	2419.6
100226 - field blank		2/26/2010 14:17:00												-0.08	<0.1	-0.50		<1	<1
100310A	RP2	3/10/2010 14:15:00	0.11	0.05	1637	14.2	11.83	115.6	9.0		8.43	-7.6	-52	0.35	348.0	0.90		201.4	>2419.6
100310A - lab duplicate	RP2	3/10/2010 14:15:00										-7.5	-51	0.34	348.0	1.00		155.3	>2419.6
100310B	RPMP	3/10/2010 14:50:00			3797	14.6	0.36	3.6	387.0		7.56	-8.6	-73	10.50	390.0	2.00		>2419.6	>2419.6
100310C	RP1	3/10/2010 15:17:00	0.11	0.05	1544	15.1	9.83	97.6	24.0		9.09	-7.8	-53	0.22	334.0	1.20		1119.9	>2419.6
100310D	HMP	3/10/2010 15:42:00	0.11	0.05	1673	13.8	12.58	121.4	33.0		8.51	-7.9	-53	0.34	376.0	0.20		1299.7	>2419.6
100310D - field duplicate (EC/TC)	HMP	3/10/2010 15:42:00																1203.3	>2419.6
100326A	RPMP	3/26/2010 12:02:00			773	13.0	0.42	3.9	195.0		7.55	-8.3	-48	4.55	16.0	0.40		>2419.6	>2419.6
100326B	RP2	3/26/2010 12:45:00	0.11	0.09	1184	9.0	12.11	103.9	13.0		8.36	-9	-58	0.25	223.0	1.20		1203.3	>2419.6
100326C	RP1	3/26/2010 13:39:00	0.11	0.09	1282	11.2	13.24	114.1	13.4		8.92	-8.6	-57	0.16	245.0	1.00		770.1	>2419.6
100326D	HMP	3/26/2010 14:03:00	0.11	0.09	967	9.9	15.66	137.5	20.0		8.59	-9.2	-60	0.18	178.0	0.80		1413.6	>2419.6
100329A	RP2	3/29/2010 13:30:00	0.11	0.15	1284	12.8	11.11	105.9	5.1		8.67	-8.93	-59						
100329B	RPMP	3/29/2010 13:40:00			1256	18.1	0.40	4.4	152.0		8.12	-8.6	-51						
100329C	RP1	3/29/2010 14:04:00	0.11	0.15	1315	12.5	11.79	116.0	28.0		8.98	-8	-58						
100329D	HMP	3/29/2010 14:37:00	0.11	0.15	913	12.8	15.49	143.0	9.0		8.94	-9.1	-65						
100402A	RP1	4/2/2010 13:45:00	0.00	0.00	1593	17.9	8.80	92.0	5.0		8.50	-7.63	-51	0.17	360.0	0.30		1553.1	>2419.6
100402A - lab duplicate	RP1	4/2/2010 13:45:00												0.13	353.0	0.20		1413.6	>2419.6
100402B	RP2	4/2/2010 14:20:00	0.00	0.00	1517	20.3	11.18	126.5	5.0		8.37	-7.68	-51	0.12	338.0	0.10		>2419.6	>2419.6
100402C	RPMP	4/2/2010 14:28:00			1732	26.1	0.24	3.0	372.0		8.19	-6.66	-46	5.90	90.0	0.80		>2419.6	>2419.6

Sample ID	Site	Date and Time	USGS Stage (m)	USGS Discharge (cms)	SpC (µS/cm)	Temperature (°C)	DO (ppm)	DO (% sat)	Turbidity (NTU)	Calculated TSS (ppm)	pH	δ ¹⁸ O (‰)	δD (‰)	NH ₄ ⁺ -N (ppm)	Cl (ppm)	NO ₃ ⁻ -N (ppm)	Total PO ₄ ³⁻ (ppm)	<i>E. coli</i> (cfu/100mL)	Total Coliforms (cfu/100mL)
100402D	HMP	4/2/2010 15:05:00	0.11	2.30	1427	18.6	9.22	99.3	11.0		8.53	-7.98	-53	0.15	294.5	0.20		387.3	>2419.6
100405RP1-1	RP1	4/2/2010 13:37:00	0.00	0.00	1654				9.0		8.03	-7.6	-51						
100405RP1-2	RP1	4/2/2010 19:37:00	0.01	0.02	1709				7.0		8.02	-7.3	-50	0.01	325.0	0.20			
100405RP1-3	RP1	4/2/2010 20:37:00	0.01	0.02	1734				12.0		7.99	-6.94	-48						
100405RP1-4	RP1	4/2/2010 21:37:00	0.04	0.17	1382				64.0		8.04	-4.95	-27	0.66	290.0	0.50			
100405RP1-5	RP1	4/2/2010 22:37:00	0.03	0.13	1296				20.0		7.94	-5.02	-28						
100405RP1-6	RP1	4/2/2010 23:37:00	0.03	0.12	1261				9.0		7.97	-5.32	-30	0.27	252.0	0.80			
100405RP1-7	RP1	4/3/2010 0:17:00	0.02	0.11	1303				9.0		7.92	-4.53	-30						
100405RP1-8	RP1	4/3/2010 0:57:00	0.03	0.14	1219				11.0		7.99	-4.36	-32	0.24	227.0	0.90			
100405RP1-9	RP1	4/3/2010 1:37:00	0.04	0.16	1039				10.0		8.01	-5.1	-26						
100405RP1-10	RP1	4/3/2010 2:17:00	0.05	0.23	917				26.0		8.07	-5.07	-26	0.23	167.0	0.80			
100405RP1-11	RP1	4/3/2010 2:57:00	0.16	0.90	621				86.0		8.16	-6.45	-35	0.20	96.0	0.40			
100405RP1-12	RP1	4/3/2010 3:37:00	0.19	1.12	305.5				109.0		8.28	-7.74	-48	0.17	34.0	0.50			
100405RP1-13	RP1	4/3/2010 4:17:00	0.09	0.44	246.1				64.0		8.30	-8.65	-57	0.25	29.0	0.80			
100405RP1-14	RP1	4/3/2010 4:57:00	0.05	0.22	282.6				70.0		8.23	-9	-59	0.30	43.0	2.50			
100405RP1-15	RP1	4/3/2010 5:37:00	0.03	0.13	369.4				39.0		8.16	-8.85	-59						
100405RP1-16	RP1	4/3/2010 6:17:00	0.02	0.08	417.5				35.0		8.13	-8.8	-58	0.31	59.0	1.00			
100405RP1-17	RP1	4/3/2010 6:57:00	0.01	0.05	491.5				30.0		8.06	-8.3	-57						
100405RP1-18	RP1	4/3/2010 7:37:00	0.02	0.10	536				29.0		8.05	-8.4	-57	0.28	85.0	0.90			
100405RP1-19	RP1	4/3/2010 8:37:00	0.00	0.00	642				23.0		8.01	-8.5	-57						
100405RP1-20	RP1	4/3/2010 9:37:00	0.00	0.01	719				20.0		8.01	-8.3	-56						
100405RP1-21	RP1	4/3/2010 10:37:00	0.01	0.02	784				17.0		8.01	-8.3	-56						
100405RP1-22	RP1	4/3/2010 11:37:00	0.01	0.05	833				17.0		8.03	-8.2	-56	0.18	147.0	0.50			
100405RP1-23	RP1	4/3/2010 12:37:00	0.01	0.03	867				17.0		8.11	-7.8	-54						
100405RP1-24	RP1	4/3/2010 13:37:00	0.01	0.03	915				15.0		8.17	-8.1	-55						
100405RP2-1	RP2	4/2/2010 20:00:00	0.01	0.03	1694				6.0		7.94	-7	-49	0.27	370.0	0.80			
100405RP2-2	RP2	4/2/2010 20:40:00	0.01	0.02	1689				6.0		7.87	-7.3	-49						
100405RP2-3	RP2	4/2/2010 21:20:00	0.01	0.06	1687				14.0		7.81	-7.3	-49						

Sample ID	Site	Date and Time	USGS Stage (m)	USGS Discharge (cms)	SpC (µS/cm)	Temperature (°C)	DO (ppm)	DO (% sat)	Turbidity (NTU)	Calculated TSS (ppm)	pH	δ ¹⁸ O (‰)	δD (‰)	NH ₄ ⁺ -N (ppm)	Cl (ppm)	NO ₃ ⁻ -N (ppm)	Total PO ₄ ³⁻ (ppm)	<i>E. coli</i> (cfu/100mL)	Total Coliforms (cfu/100mL)
100405RP2-4	RP2	4/2/2010 22:00:00	0.03	0.11	1548				19.0		7.78	-6	-36	0.33	360.0	0.60			
100405RP2-5	RP2	4/2/2010 22:40:00	0.03	0.13	1443				16.0		7.78	-5.3	-29						
100405RP2-6	RP2	4/2/2010 23:20:00	0.02	0.11	1371				13.0		7.83	-5.3	-30						
100405RP2-7	RP2	4/3/2010 0:00:00	0.02	0.11	1288				21.0		7.82	-4.6	-27	0.38	244.0	0.60			
100405RP2-8	RP2	4/3/2010 0:40:00	0.03	0.12	1271				7.0		7.77	-4.6	-28						
100405RP2-9	RP2	4/3/2010 1:20:00	0.03	0.15	1303				14.0		7.74	-5.3	-32	0.29	244.0	0.90			
100405RP2-10	RP2	4/3/2010 2:00:00	0.03	0.15	1186				8.0		7.74	-5.4	-31						
100405RP2-11	RP2	4/3/2010 2:40:00	0.08	0.38	803				46.0		7.85	-5.1	-28	0.20	142.0	0.50			
100405RP2-12	RP2	4/3/2010 3:20:00	0.21	1.23	579				162.0		8.00	-7.3	-44	0.23	83.7	0.30			
100405RP2-13	RP2	4/3/2010 4:00:00	0.13	0.72	317.4				69.0		8.01	-8.3	-55	0.25	46.0	0.70			
100405RP2-14	RP2	4/3/2010 4:40:00	0.06	0.27	321.1				68.0		8.01	-8.4	-57	0.32	47.0	0.40			
100405RP2-15	RP2	4/3/2010 5:20:00	0.03	0.15	376				68.0		7.89	-7.2	-54	0.37	55.0	0.40			
100405RP2-16	RP2	4/3/2010 6:00:00	0.03	0.13	443.7				37.0		7.93	-8.5	-58						
100405RP2-17	RP2	4/3/2010 6:40:00	0.01	0.06	487.6				23.0		8.00	-8.4	-58	0.38	69.0	0.70			
100405RP2-18	RP2	4/3/2010 7:20:00	0.02	0.09	528				30.0		7.96	-8.4	-57						
100405RP2-19	RP2	4/3/2010 8:00:00	0.01	0.03	580				22.0		7.95	-8.4	-57	0.47	87.0	0.50			
100405RP2-20	RP2	4/3/2010 8:40:00	0.00	0.00	620				21.0		8.10	-8.3	-56						
100405RP2-21	RP2	4/3/2010 9:20:00	0.01	0.03	654				21.0		8.19	-8.2	-56						
100405RP2-22	RP2	4/3/2010 10:00:00	0.01	0.03	684				18.0		8.18	-8.3	-56						
100405RP2-23	RP2	4/3/2010 10:40:00	0.01	0.02	718				18.0		8.27	-8.3	-55						
100405RP2-24	RP2	4/3/2010 11:20:00	0.01	0.06	750				12.0		8.35	-8.2	-55	0.33	110.0	0.60			
100405HMP-1	HMP	4/2/2010 14:59:00	0.11	0.07	1450				20.0		8.09	-7.28	-53	0.10	290.0	0.10			
100405HMP-2	HMP	4/2/2010 19:39:00	0.11	0.05	1385				7.0		8.19	-7.15	-53						
100405HMP-3	HMP	4/2/2010 20:19:00	0.11	0.05	1361				4.0		8.27	-7.15	-52						
100405HMP-4	HMP	4/2/2010 20:59:00	0.11	0.06	1362				3.0		8.32	-7.15	-52	0.10	288.0	0.30			
100405HMP-5	HMP	4/2/2010 21:39:00	0.11	0.09	1380				5.0		8.28	-6.82	-51						
100405HMP-6	HMP	4/2/2010 22:19:00	0.11	0.06	1390				4.0		8.26	-6.8	-52						
100405HMP-7	HMP	4/2/2010 22:59:00	0.11	0.10	1385				4.0		8.24	-6.64	-50						

Sample ID	Site	Date and Time	USGS Stage (m)	USGS Discharge (cms)	SpC (µS/cm)	Temperature (°C)	DO (ppm)	DO (% sat)	Turbidity (NTU)	Calculated TSS (ppm)	pH	δ ¹⁸ O (‰)	δD (‰)	NH ₄ ⁺ -N (ppm)	Cl (ppm)	NO ₃ ⁻ -N (ppm)	Total PO ₄ ³⁻ (ppm)	<i>E. coli</i> (cfu/100mL)	Total Coliforms (cfu/100mL)
100405HMP-8	HMP	4/2/2010 23:39:00	0.11	0.11	1413				6.0		8.22	-6.83	-51						
100405HMP-9	HMP	4/3/2010 0:19:00	0.11	0.12	1447				4.0		8.20	-6.69	-50						
100405HMP-10	HMP	4/3/2010 1:19:00	0.11	0.18	1438				6.0		8.10	-6.9	-48	0.33	288.0	0.50			
100405HMP-11	HMP	4/3/2010 2:19:00	0.11	0.16	1233				6.0		8.19	-6.74	-51	0.15	235.0	0.20			
100405HMP-12	HMP	4/3/2010 3:19:00	0.13	1.33	1182				14.0		8.18	-7.3	-48	0.14	231.0	0.20			
100405HMP-13	HMP	4/3/2010 4:19:00	0.17	7.53	817				11.0		8.24	-6.78	-43	0.56	150.0	0.30			
100405HMP-14	HMP	4/3/2010 5:19:00	0.14	1.81	471.1				83.0		8.32	-7	-44	0.26	72.0	0.10			
100405HMP-15	HMP	4/3/2010 6:19:00	0.12	0.65	386.3				56.0		8.26	-7.91	-52	0.18	65.0	0.30			
100405HMP-16	HMP	4/3/2010 7:19:00	0.12	0.31	383.3				41.0		8.27	-8.48	-56	0.14	66.0	0.30			
100405HMP-17	HMP	4/3/2010 8:19:00	0.11	0.20	409.3				32.0		8.25	-8.4	-57						
100405HMP-18	HMP	4/3/2010 9:19:00	0.11	0.17	433.8				20.0		8.23	-7.98	-58	0.14	70.0	0.40			
100405HMP-19	HMP	4/3/2010 10:19:00	0.11	0.14	464.6				15.0		8.19	-8.11	-59						
100405HMP-20	HMP	4/3/2010 11:19:00	0.11	0.13	442.9				14.0		8.17	-8.03	-58	0.12	85.0	0.30			
100405HMP-21	HMP	4/3/2010 12:19:00	0.11	0.12	517				12.0		8.16	-8.03	-58						
100405HMP-22	HMP	4/3/2010 13:19:00	0.11	0.10	537				10.0		8.13	-8.29	-59						
100405HMP-23	HMP	4/3/2010 14:19:00	0.11	0.10	557				10.0		8.11	-8.4	-59						
100405HMP-24	HMP	4/3/2010 15:19:00	0.11	0.09	591				10.0		8.11	-8.37	-58	0.08	110.0	0.10			
100405B	RP1	4/5/2010 14:20:00	0.02	0.09	1415	19.4	8.02	86.5	26.0		8.31	-5.96	-38	0.50	298.0	0.44		>2419.6	>2419.6
100405B - field duplicate	RP1	4/5/2010 14:20:00												1.40	268.0	1.79			
100405B - matrix spike	RP1	4/5/2010 14:20:00												0.50	300.0	0.47		>2419.6	>2419.6
100405C	RPMP	4/5/2010 14:35:00			1070	24.3	1.72	25.0	167.0		7.84	-6.5	-42	-0.10	54.0	2.95		>2419.6	>2419.6
100405D	RP2	4/5/2010 14:50:00	0.08	0.39	1553	19.4	11.51	125.3	66.0		8.13	-6.73	-43	0.10	265.0	0.44		>2419.6	>2419.6
100405E	Street runoff near RP2	4/5/2010 15:00:00			225	23.0	4.30	50.1	57.0			-1.59	-4.2						
100405F	RP2	4/5/2010 15:00:00	0.09	0.48	890	19.9	8.01	87.9	333.0			-3.38	-17						
100405G	Runoff from RPMP	4/5/2010 15:08:00			1039	22.1	3.26	44.4	84.0		8.00	-6.9	-44						
100405H	HMP	4/5/2010 16:00:00	0.12	0.26	1152	21.9	7.70	84.1	34.0		8.58	-7.1	-46	0.00	239.0	0.46		>2419.6	>2419.6
100423RP1-1	RP1	4/5/2010 14:02:00	0.01	0.06	1405				14.0			-6	-40		269.0				
100423RP1-7	RP1	4/5/2010 14:42:00	0.02	0.07	959				120.0			-3.6	-20		169.0				

Sample ID	Site	Date and Time	USGS Stage (m)	USGS Discharge (cms)	SpC (µS/cm)	Temperature (°C)	DO (ppm)	DO (% sat)	Turbidity (NTU)	Calculated TSS (ppm)	pH	δ ¹⁸ O (‰)	δD (‰)	NH ₄ ⁺ -N (ppm)	Cl (ppm)	NO ₃ ⁻ -N (ppm)	Total PO ₄ ³⁻ (ppm)	<i>E. coli</i> (cfu/100mL)	Total Coliforms (cfu/100mL)
100423RP1-8	RP1	4/5/2010 15:01:00	0.09	0.48	1052				116.0			-4.7	-27						
100423RP1-9	RP1	4/5/2010 15:12:00	0.06	0.27	753				122.0			-3.35	-17						
100423RP1-10	RP1	4/5/2010 15:31:00	0.07	0.32	991				38.0			-5.2	-30						
100423RP1-11	RP1	4/5/2010 15:34:00	0.07	0.32	1153				40.0			-5.3	-32						
100423RP1-2	RP1	4/6/2010 14:02:00	0.01	0.04	1275				3.0			-3.6	-30						
100423RP1-12	RP1	4/7/2010 13:08:00	0.04	0.19	1121				104.0			-4.4	-26		202.0				
100423RP1-13	RP1	4/7/2010 13:31:00	0.20	1.18	510				263.0			-2.5	-10		71.0				
100423RP1-3	RP1	4/7/2010 14:02:00	0.14	0.79	417.9				214.0			-2.3	-11		41.0				
100423RP1-14	RP1	4/7/2010 14:03:00	0.14	0.79	383.5				158.0			-2.6	-10						
100423RP1-15	RP1	4/7/2010 14:31:00	0.07	0.33	337.9				85.0			-2.2	-10						
100423RP1-16	RP1	4/7/2010 14:37:00	0.05	0.25	317.5				64.0			-2.4	-10						
100423RP1-4	RP1	4/8/2010 14:02:00	0.01	0.03	1190				4.0			-5.4	-34		212.0				
100423RP1-5	RP1	4/9/2010 14:01:00	0.01	0.05	1508				5.0			-6.7	-44						
100423RP1-6	RP1	4/10/2010 14:01:00	0.01	0.04	1519				5.0			-7.1	-47						
100423A	HMP	4/23/2010 14:25:00	0.11	0.09	541	17.1	6.07	62.8	20.0		8.41	-5.7	-32	0.52	83.0	0.40		>2419.6	>2419.6
100423A - lab duplicate	HMP	4/23/2010 14:25:00												0.51	87.0	0.60		>2419.6	>2419.6
100423B	RPMP	4/23/2010 14:52:00			2338	25.4	0.54	5.0	262.0		8.09	-4.65	-31	9.60	115.0	1.10		>2419.6	>2419.6
100423C	RP2	4/23/2010 15:17:00	0.01	0.04	796	17.8	6.84	72.1	18.0		8.35	-5.8	-33	0.49	129.0	0.40		>2419.6	>2419.6
100423D	RP1	4/23/2010 16:48:00	0.01	0.04	838	17.8	6.31	66.0	15.0		8.40	-5.97	-35	0.58	120.0	0.20		>2419.6	>2419.6
100424RP1-1	RP1	4/23/2010 17:01:00	0.02	0.08	853				20.0			-5.9	-36		115.0				
100424RP1-2	RP1	4/23/2010 19:01:00	0.02	0.07	981				8.0			-5.8	-36						
100424RP1-3	RP1	4/23/2010 19:41:00	0.02	0.08	1059				12.0			-5.8	-36						
100424RP1-4	RP1	4/23/2010 20:21:00	0.03	0.12	991				19.0			-5.3	-32						
100424RP1-5	RP1	4/23/2010 21:01:00	0.03	0.11	860				11.0			-3.8	-23						
100424RP1-6	RP1	4/23/2010 21:41:00	0.03	0.12	727				19.0			2.2	-9						
100424RP1-7	RP1	4/23/2010 22:21:00	0.03	0.11	719				21.0			-3.5	-23						
100424RP1-8	RP1	4/23/2010 23:01:00	0.03	0.12	682				9.0			-4	-25						
100424RP1-9	RP1	4/23/2010 23:41:00	0.00	0.00	589				12.0			-3.7	-25						

Sample ID	Site	Date and Time	USGS Stage (m)	USGS Discharge (cms)	SpC (µS/cm)	Temperature (°C)	DO (ppm)	DO (% sat)	Turbidity (NTU)	Calculated TSS (ppm)	pH	δ ¹⁸ O (‰)	δD (‰)	NH ₄ ⁺ -N (ppm)	Cl (ppm)	NO ₃ ⁻ -N (ppm)	Total PO ₄ ³⁻ (ppm)	<i>E. coli</i> (cfu/100mL)	Total Coliforms (cfu/100mL)
100424RP1-10	RP1	4/24/2010 0:21:00	0.00	0.01	595				11.0			-4.2	-27						
100424RP1-11	RP1	4/24/2010 1:01:00	0.02	0.11	579				11.0			-4.3	-30		82.0				
100424RP1-12	RP1	4/24/2010 13:01:00	0.02	0.10	568				15.0			-5.01	-36		128.0				
100424RP1-13	RP1	4/24/2010 13:41:00	0.02	0.09	955				10.0			-5.2	-37						
100424RP1-14	RP1	4/24/2010 14:21:00	0.02	0.10	976				13.0			-4.9	-36						
100424RP1-15	RP1	4/24/2010 15:01:00	0.02	0.10	653				15.0			-4	-33						
100424RP1-16	RP1	4/24/2010 15:41:00	0.04	0.18	433.6				43.0			-5.5	-38		56.0				
100424RP1-17	RP1	4/24/2010 16:21:00	0.04	0.17	454.8				36.0			-5.3	-39		60.0				
100424RP1-18	RP1	4/24/2010 17:01:00	0.14	0.75	309.2				241.0			-9.3	-64		32.0				
100424RP1-19	RP1	4/24/2010 17:41:00	0.04	0.18	307.2				254.0			-8.5	-59		30.0				
100424RP1-20	RP1	4/24/2010 17:58:00	0.04	0.16	284.4				97.0			-8.9	-62						
100424RP1-21	RP1	4/24/2010 18:27:00	0.03	0.11	284.2				42.0			-9.2	-63		32.0				
100424RP1-22	RP1	4/24/2010 18:57:00	0.02	0.07	295.2				49.0			-9.4	-63						
100424RP1-23	RP1	4/24/2010 19:27:00	0.02	0.09	331.1				23.0			-9	-62						
100424RP1-24	RP1	4/24/2010 19:57:00	0.02	0.08	379.3				20.0			-8.6	-60		43.0				
100424RP1-25	RP1	4/24/2010 20:27:00	0.01	0.06	413.6				7.0			-8.8	-60						
100424RP1-26	RP1	4/24/2010 20:57:00	0.01	0.05	457.4				17.0			-8.3	-59						
100424RP1-27	RP1	4/24/2010 21:27:00	0.01	0.05	490.1				13.0			-8	-59						
100424RP1-28	RP1	4/24/2010 21:57:00	0.02	0.07	524				12.0			-8.2	-58						
100424RP1-29	RP1	4/24/2010 22:27:00	0.02	0.07	573				10.0			-8.2	-58						
100424RP1-30	RP1	4/24/2010 22:57:00	0.02	0.08	607				15.0			-8.1	-57		79.0				
100424RP1-31	RP1	4/24/2010 23:27:00	0.02	0.08	634				11.0			-8	-56						
100424RP1-32	RP1	4/24/2010 23:57:00	0.02	0.08	652				10.0			-7.9	-56						
100424RP1-33	RP1	4/25/2010 0:27:00	0.02	0.07	689				6.0			-8	-56						
100424RP1-34	RP1	4/25/2010 0:57:00	0.02	0.08	712				9.0			-7.8	-55						
100424RP1-35	RP1	4/25/2010 1:27:00	0.02	0.07	736				8.0			-7.7	-55						
100424RP1-36	RP1	4/25/2010 1:57:00	0.02	0.07	766				9.0			-7.8	-54		126.0				
100424RP1-37	RP1	4/25/2010 2:27:00	0.02	0.07	791				6.0			-8.2	-55						

Sample ID	Site	Date and Time	USGS Stage (m)	USGS Discharge (cms)	SpC (µS/cm)	Temperature (°C)	DO (ppm)	DO (% sat)	Turbidity (NTU)	Calculated TSS (ppm)	pH	δ ¹⁸ O (‰)	δD (‰)	NH ₄ ⁺ -N (ppm)	Cl (ppm)	NO ₃ ⁻ -N (ppm)	Total PO ₄ ³⁻ (ppm)	<i>E. coli</i> (cfu/100mL)	Total Coliforms (cfu/100mL)
100424RP1-38	RP1	4/25/2010 2:57:00	0.01	0.06	812				12.0			-7.9	-54						
100424RP1-39	RP1	4/25/2010 3:27:00	0.01	0.06	831				6.0			-8.2	-56						
100424RP1-40	RP1	4/25/2010 3:57:00	0.02	0.08	751				13.0			-10.2	-74						
100424RP1-41	RP1	4/25/2010 4:27:00	0.02	0.09	439.7				24.0			-11.9	-87						
100424RP1-42	RP1	4/25/2010 4:57:00	0.02	0.08	346.9				49.0			-12.2	-88						
100424RP1-43	RP1	4/25/2010 5:27:00	0.03	0.11	495.6				13.0			-10.3	-75						
100501HMP-1	HMP	4/30/2010 13:21:00	0.11	0.05	1177				23.0			-7.9	-55						
100501HMP-2	HMP	4/30/2010 14:00:00	0.11	0.05	1173				5.0			-8.1	-56						
100501HMP-3	HMP	4/30/2010 14:40:00	0.11	0.05	1155				3.0			-8	-56						
100501HMP-4	HMP	4/30/2010 15:20:00	0.11	0.05	1137				4.0			-8	-56						
100501HMP-5	HMP	4/30/2010 16:00:00	0.11	0.05	1118				5.0			-7.9	-56						
100501HMP-6	HMP	4/30/2010 16:40:00	0.11	0.05	1098				5.0			-8.1	-57						
100501HMP-7	HMP	4/30/2010 17:20:00	0.11	0.05	1079				3.0			-7.9	-56						
100501HMP-8	HMP	4/30/2010 18:00:00	0.11	0.05	1057				4.0			-8.2	-57						
100501HMP-9	HMP	4/30/2010 18:40:00	0.11	0.05	1053				4.0			-8.1	-56						
100501HMP-10	HMP	4/30/2010 19:20:00	0.10	0.04	1036				5.0			-8	-57	0.50	133.0	1.00			
100501HMP-11	HMP	4/30/2010 20:00:00	0.11	0.05	1014				5.0			-8	-57						
100501HMP-12	HMP	4/30/2010 20:40:00	0.11	0.05	1009				6.0			-8	-57	0.56	150.0	0.90			
100501HMP-13	HMP	4/30/2010 21:20:00	0.17	7.14	889				66.0			-6.7	-48	0.44	133.0	0.60			
100501HMP-14	HMP	4/30/2010 22:00:00	0.20	13.71	458.2				280.0			-4.6	-29	0.35	68.0	0.40			
100501HMP-15	HMP	4/30/2010 22:40:00	0.16	5.83	347.3				338.0			-4	-24	0.33	42.0	0.60			
100501HMP-16	HMP	4/30/2010 23:20:00	0.14	2.69	287.3				214.0			-3.8	-23	0.37	36.0	0.50			
100501HMP-17	HMP	5/1/2010 0:00:00	0.14	1.87	270.2				140.0			-3.9	-23	0.34	32.0	0.30			
100501HMP-18	HMP	5/1/2010 0:40:00	0.13	0.71	285.1				57.0			-3.9	-23						
100501HMP-19	HMP	5/1/2010 1:20:00	0.12	0.40	303.2				58.0			-4.1	-24	0.34	39.0	0.70			
100501HMP-20	HMP	5/1/2010 2:00:00	0.12	0.26	321.4				35.0			-4.2	-25						
100501HMP-21	HMP	5/1/2010 2:40:00	0.11	0.21	389.4				25.0			-4.4	-28						
100501HMP-22	HMP	5/1/2010 3:20:00	0.11	0.20	352.1				27.0			-4.3	-25						

Sample ID	Site	Date and Time	USGS Stage (m)	USGS Discharge (cms)	SpC (µS/cm)	Temperature (°C)	DO (ppm)	DO (% sat)	Turbidity (NTU)	Calculated TSS (ppm)	pH	δ ¹⁸ O (‰)	δD (‰)	NH ₄ ⁺ -N (ppm)	Cl (ppm)	NO ₃ ⁻ -N (ppm)	Total PO ₄ ³⁻ (ppm)	<i>E. coli</i> (cfu/100mL)	Total Coliforms (cfu/100mL)
100501HMP-23	HMP	5/1/2010 4:00:00	0.11	0.16					23.0			-4.3	-26						
100501HMP-24	HMP	5/1/2010 4:40:00	0.11	0.15	385.3				20.0			-4.4	-26						
100501HMP-25	HMP	5/1/2010 14:28:00	0.11	0.07	524				17.0			-4.9	-30						
100501HMP-26	HMP	5/1/2010 15:07:00	0.11	0.07	544				4.0			-5	-31						
100501HMP-27	HMP	5/1/2010 15:47:00	0.11	0.07	574				8.0			-5.1	-32						
100501HMP-28	HMP	5/1/2010 16:27:00	0.11	0.07	576				13.0			-5	-31						
100501HMP-29	HMP	5/1/2010 17:07:00	0.11	0.07	579				7.0			-5.1	-32						
100501HMP-30	HMP	5/1/2010 17:47:00	0.11	0.07	597				4.0			-5	-32						
100501HMP-31	HMP	5/1/2010 18:27:00	0.11	0.07	593				4.0			-4.1	-29						
100501HMP-32	HMP	5/1/2010 19:07:00	0.11	0.07	601				8.0			-5.1	-32						
100501HMP-33	HMP	5/1/2010 19:47:00	0.11	0.07	608				6.0			-5	-32						
100501HMP-34	HMP	5/1/2010 20:27:00	0.11	0.07	617				7.0			-5.1	-32						
100501HMP-35	HMP	5/1/2010 21:07:00	0.11	0.06	626				7.0			-5	-33						
100501HMP-36	HMP	5/1/2010 21:47:00	0.11	0.06	633				7.0			-5	-33						
100501HMP-37	HMP	5/1/2010 22:27:00	0.11	0.06	635				7.0			-5	-33						
100501HMP-38	HMP	5/1/2010 23:07:00	0.11	0.06	642				4.0			-4.9	-33						
100501HMP-39	HMP	5/1/2010 23:47:00	0.11	0.06	642				7.0			-5.1	-33						
100501HMP-40	HMP	5/2/2010 0:27:00	0.11	0.06	650				7.0			-5.1	-33						
100501HMP-41	HMP	5/2/2010 1:07:00	0.11	0.07	659				7.0			-5	-34						
100501HMP-42	HMP	5/2/2010 1:47:00	0.11	0.15	689				7.0			-5	-33						
100501HMP-43	HMP	5/2/2010 2:27:00	0.12	0.24	757				7.0			-5	-33						
100501HMP-44	HMP	5/2/2010 3:07:00	0.12	0.45	676				9.0			-4.65	-30						
100501HMP-45	HMP	5/2/2010 3:47:00	0.12	0.59	660				23.0			-4.7	-31						
100501HMP-46	HMP	5/2/2010 4:27:00	0.12	0.31	594				20.0			-4.1	-26						
100501HMP-47	HMP	5/2/2010 5:07:00	0.12	0.24	607				14.0			-3.8	-25						
100501HMP-48	HMP	5/2/2010 5:47:00	0.11	0.20	651				9.0			-3.8	-25						
100506A	RPMP	5/6/2010 15:25:00			3052	28.0	0.57	4.3	562.0		8.08	-4.48	-32	17.00	70.0	0.70		>2419.6	>2419.6
100506A - field duplicate (EC/TC)	RPMP	5/6/2010 15:25:00																2419.6	>2419.6

Sample ID	Site	Date and Time	USGS Stage (m)	USGS Discharge (cms)	SpC (µS/cm)	Temperature (°C)	DO (ppm)	DO (% sat)	Turbidity (NTU)	Calculated TSS (ppm)	pH	δ ¹⁸ O (‰)	δD (‰)	NH ₄ ⁺ -N (ppm)	Cl (ppm)	NO ₃ ⁻ -N (ppm)	Total PO ₄ ³⁻ (ppm)	<i>E. coli</i> (cfu/100mL)	Total Coliforms (cfu/100mL)
100506B	RP2	5/6/2010 15:35:00	0.00	0.00	1743	23.2	4.78	57.2	5.0		8.18	-5.5	-37	0.55	320.0	1.30		307.6	>2419.6
100506C	RP1	5/6/2010 16:10:00	0.00	0.00	2052	18.2	6.47	73.0	6.0		8.42	-6.6	-43	0.43	368.0	1.40		>2419.6	>2419.6
100506D	HMP	5/6/2010 16:45:00	0.10	0.04	1147	21.5	4.26	47.4	10.0		8.51	-5.7	-38	1.09	198.0	0.80		1203.3	>2419.6
100512RP1-1	RP1	5/6/2010 15:58:00	0.00	0.00	2160				138.0			-6.8	-45						
100512RP1-2	RP1	5/8/2010 3:58:00	0.00	0.00	2195				122.0			-6.6	-45						
100512RP1-3	RP1	5/9/2010 15:58:00	0.00	0.00	2322				411.0			-6.5	-45						
100512RP1-4	RP1	5/11/2010 3:58:00	0.00	0.00	1022				443.0			-5.9	-38						
100512RP1-13	RP1	5/12/2010 3:55:00	0.07	0.36	1033				263.0			-3.9	-24						
100512RP1-14	RP1	5/12/2010 3:58:00	0.18	1.03	559				376.0			-3.1	-15	1.01	85.0	0.40			
100512RP1-15	RP1	5/12/2010 4:28:00	1.06	9.31	134.4				485.0			-5.1	-32	1.51	13.0	0.60			
100512RP1-16	RP1	5/12/2010 4:58:00	0.30	1.98	184.2				361.0			-5.4	-34	1.60	29.0	0.50			
100512RP1-17	RP1	5/12/2010 5:28:00	0.18	1.03	352.1				161.0			-5.2	-33						
100512RP1-18	RP1	5/12/2010 5:58:00	0.13	0.70	361.5				107.0			-5	-32	0.94	62.0	0.60			
100512RP1-19	RP1	5/12/2010 6:28:00	0.10	0.52	467.3				71.0			-4.8	-32						
100512RP1-20	RP1	5/12/2010 6:58:00	0.06	0.30	468.2				70.0			-4.9	-32						
100512RP1-21	RP1	5/12/2010 7:15:00	0.06	0.26	479.3				60.0			-4.8	-32						
100512RP1-22	RP1	5/12/2010 7:20:00	0.06	0.27	484.8				56.0			-4.8	-33	0.83	88.0	1.00			
100524A	RP1	5/24/2010 13:15:00	0.01	0.02	1759	21.6	7.15	77.0	12.0		8.25	-6.8	-45	0.25	293.0	1.50		2419.6	>2419.6
100524A - lab duplicate	RP1	5/24/2010 13:15:00										-6.8	-46	0.22	306.0	1.70		2419.6	>2419.6
100524B	RPMP	5/24/2010 13:30:00			1955	27.2	0.59	7.0	533.0		8.17	-4.3	-31	4.46	110.0	2.40		>2419.6	>2419.6
100524C	RP2	5/24/2010 13:45:00	0.01	0.02	1412	24.2	6.11	72.3	21.0		8.36	-6.7	-44	0.47	232.0	1.70		547.5	>2419.6
100524D	HMP	5/24/2010 15:30:00	0.11	0.13	1027	25.2	5.56	57.2	9.0		8.12	-6.7	-44	0.95	150.0	0.60		>2419.6	>2419.6
100609A	HMP	6/9/2010 13:28:00		0.05	571	23.0	7.26	84.4	8.0	4.5	8.11	-4.8	-33	0.54	58.0	0.90	0.31	>2419.6	>2419.6
100609B	RP1	6/9/2010 14:06:00	0.01	0.05	974	22.9	6.18	66.0	8.0	21.0	8.10	-5.1	-45	2.56	125.0	0.30	0.83	>2419.6	>2419.6
100609B - field duplicate	RP1	6/9/2010 14:06:00								12.5		-5.2	-38	2.46	125.0	0.60	0.78	>2419.6	>2419.6
100609B - matrix spike	RP1	6/9/2010 14:06:00												2.95	113.0	1.50	1.18		
100609C	RPMP	6/9/2010 14:33:00			1788	33.4	1.55	22.1	517.0	201.0	8.39	-2.3	-23	7.35	65.0	2.50	12.80	>2419.6	>2419.6
100609D	RP2	6/9/2010 14:50:00	0.01	0.04	753	25.6	10.70	131.8	17.0	5.5	8.62	-4.5	-35	0.49	96.0	0.90	0.37	2419.6	>2419.6

Sample ID	Site	Date and Time	USGS Stage (m)	USGS Discharge (cms)	SpC (µS/cm)	Temperature (°C)	DO (ppm)	DO (% sat)	Turbidity (NTU)	Calculated TSS (ppm)	pH	δ ¹⁸ O (‰)	δD (‰)	NH ₄ ⁺ -N (ppm)	Cl (ppm)	NO ₃ ⁻ -N (ppm)	Total PO ₄ ³⁻ (ppm)	<i>E. coli</i> (cfu/100mL)	Total Coliforms (cfu/100mL)	
100609 - field blank		6/9/2010 14:50:00																	<1	<1
100624A	RP2	6/24/2010 14:35:00	0.00	0.00	1231	29.0	3.13	42.1	4.0	12.0	7.51	-0.4	-11	1.08	185.0	1.00	0.50	>2419.6	>2419.6	
100624A - lab duplicate	RP2	6/24/2010 14:35:00													192.0					
100624B	RP1	6/24/2010 15:02:00	0.00	0.00	1175	25.9	1.74	21.4	6.0	5.0	7.51	-4.4	-27	3.48	120.0	2.40	0.79	>2419.6	>2419.6	
100624B - lab duplicate	RP1	6/24/2010 15:02:00										-4.4	-28		120.0					
100624C	HMP	6/24/2010 15:30:00	0.11	0.06	870	28.8	4.52	59.8	11.0	13.0	7.59	-3.8	-22	0.54	102.0	0.60	0.22	>2419.6	>2419.6	
100707A	HMP	7/7/2010 13:39:00			1005	29.1	4.44	54.9	6.0	8.0	7.60	-4.5	-33	0.60	154.0	0.30	0.29	1413.6	>2419.6	
100707B	RP1	7/7/2010 14:25:00	0.00	0.00	1812	25.6	3.37	41.3	5.0	4.5	7.70	-5.6	-38	0.56	347.0	0.00	0.30	517.2	>2419.6	
100707C	RP2	7/7/2010 14:38:00	0.00	0.00	1132	28.3	3.43	44.7	3.0	2.5	8.17	-0.7	-17	0.29	282.0	0.60	0.63	1413.6	>2419.6	
100707C - lab duplicate	RP2	7/7/2010 14:38:00								6.7		-0.7	-17	0.39		0.80	0.33			
100709RP1-1	RP1	7/7/2010 14:00:00	0.00	0.00	180				13.0			-5.4	-39							
100709RP1-13	RP1	7/8/2010 18:13:00	0.56	4.22	302.5				130.0	314.0		-9.1	-67	0.33	50.0	0.60	0.55			
100709RP1-14	RP1	7/8/2010 18:29:00	0.89	7.49	143.9				249.0	572.0		-8.55	-65	0.82	19.0	0.60	1.19			
100709RP1-15	RP1	7/8/2010 18:59:00	0.66	5.18	157.7				178.0	368.0		-9	-66	0.69	26.0	1.20	1.04			
100709RP1-16	RP1	7/8/2010 19:29:00	0.66	5.18	323.8				119.0	214.0		-8.5	-63	0.56	60.0	1.10	1.00			
100709RP1-17	RP1	7/8/2010 22:54:00	0.66	5.11	169.9				115.0	272.0		-9.9	-69							
100709RP1-18	RP1	7/8/2010 22:59:00	0.68	5.39	143.4				118.0	338.0		-10.3	-73							
100709RP1-19	RP1	7/8/2010 23:29:00	0.65	5.07	155.9				111.0	181.0		-10.5	-75							
100709RP1-20	RP1	7/8/2010 23:59:00	0.51	3.71	262.9				70.0	129.0		-10.1	-73							
100709RP1-2	RP1	7/9/2010 2:00:00	0.04	0.21	568.1				25.0			-9.1	-66							
100709RP1-21	RP1	7/9/2010 5:04:00	0.45	3.23	165.3				135.0	352.0		-8.5	-58							
100709A	RP1	7/9/2010 11:30:00	0.02	0.11	595	24.3	5.51	64.1	14.0	8.0	7.77	-8.1	-55	0.37	60.0	2.20	0.66	>2419.6	>2419.6	
100721A	HMP	7/21/2010 9:33:00	0.11	0.14	365.5	25.1	4.26	51.1	16.0		7.49	-4	-25	0.32	37.3	0.60		>2419.6	>2419.6	
100721B	RP1	7/21/2010 10:11:00	0.00	0.02	592	24.3	4.37	52.4	15.0		7.82	-4.5	-30	0.31	63.9	0.50		>2419.6	>2419.6	
100721C	RPMP	7/21/2010 10:24:00			1203	27.8	0.31	5.3	39.0		7.70	-3.6	-25	4.62	32.0	0.40		>2419.6	>2419.6	
100721D	RP2	7/21/2010 10:43:00	0.01	0.03	447	25.4	3.32	40.5	15.0		8.35	-4.2	-26	0.44	40.7	0.30		>2419.6	>2419.6	
100805A	HMP	8/5/2010 10:05:00	0.12	0.22	280.1	26.7	3.38	42.5	28.0		7.77	-4.8	-30	0.25	36.0	0.20		>2419.6	>2419.6	
100805B	RP1	8/5/2010 10:39:00	0.01	0.05	372.6	26.1	2.63	32.3	11.0		7.72	-5	-32	0.42	27.0	0.30		>2419.6	>2419.6	

Sample ID	Site	Date and Time	USGS Stage (m)	USGS Discharge (cms)	SpC ($\mu\text{S/cm}$)	Temperature ($^{\circ}\text{C}$)	DO (ppm)	DO (% sat)	Turbidity (NTU)	Calculated TSS (ppm)	pH	$\delta^{18}\text{O}$ (‰)	δD (‰)	$\text{NH}_4^+\text{-N}$ (ppm)	Cl (ppm)	$\text{NO}_3^-\text{-N}$ (ppm)	Total PO_4^{3-} (ppm)	<i>E. coli</i> (cfu/100mL)	Total Coliforms (cfu/100mL)
100805C	RPMP	8/5/2010 10:56:00			1087	27.9	0.12	1.5	133.0		7.17	-3.7	-26	5.84	42.0	0.20		>2419.6	>2419.6
100805D	RP2	8/5/2010 11:05:00	0.01	0.05	376.3	27.4	3.91	49.3	22.0		7.62	-4.6	-30	0.99	24.0	0.30		>2419.6	>2419.6
100826A	RP1	8/26/2010 14:38:00	0.11	0.06	1829	22.1	5.79	65.4	4.0	45.0	7.83	-5.7	-39	0.17	176.0	0.30		613.1	>2419.6
100826A - lab duplicate	RP1	8/26/2010 14:38:00								31.0		-5.7	-39	0.16	174.0	0.20		648.8	>2419.6
100826B	RP2	8/26/2010 14:50:00	0.11	0.06	1200	21.5	3.19	36.2	3.0	13.0	7.92	-5	-34	0.26	156.0	0.10		579.4	>2419.6
100826B - lab duplicate	RP2	8/26/2010 14:50:00								11.0		-5.1	-34	0.23	150.0	0.10		613.1	>2419.6
100826C	HMP	8/26/2010 15:20:00	0.11	0.05	933	24.4	4.72	56.4	6.0	4.0	7.98	-5.6	-40	0.93	104.0	0.30		>2419.6	>2419.6
100826C - lab duplicate	HMP	8/26/2010 15:20:00								8.0		-5.6	-40	0.93	104.0	0.30		>2419.6	>2419.6
100826 - field blank		8/26/2010 15:20:00								2.0				0.04	<0.1	-0.10		<1	<1
100917A	RPMP	9/17/2010 12:15:00			1571	27.2	2.52	33.8											
100917B	RP2	9/17/2010 12:30:00	0.11	0.07	951	18.6	3.85	40.4	3.0	2.0	7.53	-5.5	-39	0.15	100.0	0.10	0.54	224.7	>2419.6
100917C	RP1	9/17/2010 13:00:00	0.11	0.08	1546	19.6	3.84	42.7	3.0	8.0	7.85			0.17	211.0	0.90	0.24	1119.9	>2419.6
101012A	HMP at low water cross	10/12/2010 15:00:00	0.11	0.01	1080	19.0	5.50	60.4	8.0	8.0		-6	-43	0.22	142.0	0.10	0.22	152.9	>2419.6
110715A	RP2	7/15/2011 9:39:00	0.11	0.01	885	24.9			3.0	28.0	7.97	-4.3	-30	0.47	166.4	0.40	2.68	>2419.6	>2419.6
110715B	FP Golf Pond	7/15/2011 10:56:00			546	28.6			4.0	4.0	9.13	-10.5	-83	0.43	12.0	1.50	5.07	4.1	1203.3

Appendix G: Upper River des Peres ICP-MS Data (all values in ppb)

Sample ID	Site	Al	Co	Cr	Cu	Fe	Ga	Li	Mn	Ni	Rb	Zn	Mo	Cd	Ba	Pb
091211A	RP2	28.9	0.6	0.8	13.4	60.3	2.3	12.5	292.6	9.3	3.9	86.8	22.4	0.4	112.6	2.4
091211B	RP1	29.3	0.5	1.2	9.7	56.5	1.9	12.3	238.6	6.4	2.8	19.6	19.1	0.1	91.8	1.9
091221A	RP1	8.7	0.5	0.1	3.5	37.7	2.6	11.3	328.6	8.0	1.8	301.2	24.2	0.1	130.0	0.1
091221B	RP2	7.8	0.8	0.0	3.2	41.9	2.7	13.6	420.6	10.1	2.1	51.8	14.1	0.1	128.8	0.1
091221C	RPMP	338.0	6.1	9.9	27.4	691.4	11.9	62.9	0.5	47.8	77.6	459.7	1.4	1.1	386.8	13.1
091221D	HMP	1.9	0.8	0.6	3.9	28.9	2.1	11.1	346.6	6.7	1.8	46.6	5.7	0.1	94.4	0.4
100106A	HMP	17.3	1.4	BDL	6.8	39.3	2.7	17.5	850.6	9.7	2.5	55.4	19.3	0.2	126.8	0.3
100106C	RP2	15.5	0.9	0.0	5.6	68.7	5.0	15.2	406.6	15.7	1.4	24.0	12.7	0.2	255.6	0.7
100106D	RP1	5.5	0.4	0.1	6.0	43.9	2.8	9.1	74.2	9.9	1.5	34.0	10.5	0.2	129.8	0.2
100113B	RP2	88.9	0.7	0.4	19.4	47.1	3.0	16.8	294.6	9.9	2.0	13.2	11.5	0.1	149.4	2.7
100113C	RP1	163.3	0.6	0.2	10.9	39.7	2.8	18.9	181.2	8.7	3.3	20.8	12.7	0.1	142.6	79.9
100113C	RP1 - lab dup	164.9	0.6	0.3	10.9	39.5	2.8	19.1	181.8	8.7	3.3	21.4	12.8	0.6	142.8	79.7
100113D	HMP	87.7	1.1	BDL	15.3	40.1	3.9	17.0	BDL	8.5	2.3	17.5	3.7	0.2	134.2	5.1
100118A	RP2	BDL	0.6	BDL	6.4	36.6	3.1	13.5	BDL	8.3	2.0	31.4	11.3	0.3	108.5	2.0
100118B	RP1	BDL	0.5	BDL	9.4	25.6	2.6	11.4	183.1	5.6	1.6	44.7	10.3	0.2	90.0	6.7
100118C	HMP	111.6	0.8	BDL	9.3	25.1	3.0	18.8	BDL	6.7	2.0	53.2	3.9	0.2	99.8	16.2
100122A	RP2	29.7	0.3	BDL	4.6	29.1	2.5	10.5	182.0	5.6	1.9	3.0	13.0	0.1	82.6	0.3
100122B	RP1	12.8	0.3	0.1	3.6	22.7	2.4	10.5	106.2	4.7	1.3	5.5	14.6	0.1	81.0	0.1
100126A	RP1	BDL	0.3	BDL	4.2	27.0	2.8	9.3	149.4	5.1	1.7	20.2	13.5	0.1	93.9	0.5
100126A - field duplicate (EC/TC)	RP1	BDL	0.3	BDL	4.4	27.1	2.7	9.5	149.7	5.1	1.6	19.7	13.5	0.1	93.4	0.5
100126B	RP2	BDL	0.5	0.0	10.5	33.1	2.9	10.0	194.3	6.1	1.5	30.8	12.2	0.2	96.6	1.4
100126C	HMP	86.8	0.6	BDL	4.0	24.0	2.5	10.6	218.0	5.3	1.4	16.6	6.0	0.1	84.2	0.2
100212B	RP2	1.7	0.5	BDL	6.3	31.7	3.2	19.7	286.2	7.0	2.3	16.8	9.3	0.1	115.7	0.1
100212C	RP1	2.0	0.5	0.1	7.5	30.3	2.8	18.6	284.0	6.1	2.3	50.9	9.3	0.1	101.9	0.1
100212D	HMP	5.5	1.0	0.0	9.1	36.9	3.8	24.6	0.5	7.3	2.3	23.7	5.5	0.2	150.9	0.1
100226A	RP2	2.1	0.5	0.1	3.3	26.8	2.4	13.1	227.0	6.2	1.3	13.0	7.3	0.1	87.1	0.1
100226A - field duplicate	RP2	1.9	0.5	BDL	3.2	26.5	2.3	13.0	233.4	6.1	1.3	7.8	7.3	0.1	86.8	0.0
100226C	RP1	2.4	0.4	0.0	3.8	25.3	2.2	13.4	168.8	5.5	1.4	19.5	7.4	0.1	82.7	0.7
100226D	HMP	3.5	0.9	0.0	4.1	26.9	2.4	13.5	0.4	6.2	1.5	23.0	5.5	0.1	88.3	0.7

Sample ID	Site	Al	Co	Cr	Cu	Fe	Ga	Li	Mn	Ni	Rb	Zn	Mo	Cd	Ba	Pb
100310A	RP2	7.7	0.5	0.5	5.6	24.7	2.0	14.4	49.9	5.3	1.7	21.4	6.7	0.1	79.6	0.5
100310C	RP1	8.5	0.4	0.5	4.7	23.7	1.8	13.9	0.2	4.5	1.9	9.0	8.0	0.1	71.0	0.3
100310D	HMP	9.9	0.7	0.8	5.8	26.3	2.1	14.5	0.3	5.6	2.3	26.9	4.8	0.1	83.9	0.2
100326B	RP2	12.9	0.3	1.5	4.5	22.3	1.7	8.3	131.6	4.8	1.2	11.4	11.9	0.1	70.6	0.2
100326C	RP1	9.9	0.3	2.5	3.9	21.2	1.7	8.8	111.7	4.3	1.1	8.8	16.5	0.1	70.9	0.2
100326D	HMP	55.3	0.4	0.5	4.1	21.1	1.4	6.4	117.4	3.5	1.1	21.6	6.3	0.1	55.3	0.4
100402A	RP1	3.3	0.4	0.2	3.5	27.3	2.0	12.8	82.7	5.2	1.5	19.7	12.2	0.1	85.3	0.1
100402B	RP2	5.4	0.4	0.6	2.9	31.0	2.2	12.9	0.2	6.0	1.5	10.6	10.0	0.1	93.0	0.2
100402D	HMP	2.8	0.7	1.1	3.7	34.0	2.0	17.1	0.3	5.0	2.2	11.7	5.8	0.1	82.1	0.2
100405RP1-2	RP1	1.6	0.3	1.6	3.6	27.7	1.8	12.6	1.6	6.1	1.7	10.9	11.9	0.1	94.3	0.1
100405RP1-4	RP1	5.7	0.2	3.1	10.9	20.0	1.4	10.8	5.8	5.6	2.6	31.0	9.8	0.1	66.7	0.1
100405RP1-6	RP1	6.5	0.2	3.6	13.0	22.6	1.5	10.6	5.1	5.4	2.2	24.2	6.8	0.1	71.4	0.2
100405RP1-8	RP1	5.0	0.2	3.7	12.7	22.5	1.5	10.8	3.4	5.2	1.9	22.3	7.0	0.2	70.2	0.1
100405RP1-10	RP1	7.0	0.1	3.1	10.5	17.2	1.1	8.2	2.3	3.8	1.7	35.3	5.7	0.1	50.9	0.2
100405RP1-11	RP1	6.5	0.1	2.2	6.9	12.0	0.8	4.2	1.7	2.5	1.7	10.5	2.9	0.0	32.8	0.1
100405RP1-12	RP1	48.0	0.1	1.6	8.5	10.9	0.5	2.3	1.7	1.7	1.8	11.6	1.5	0.0	19.4	0.2
100405RP1-13	RP1	81.9	0.1	1.3	9.9	13.1	0.5	1.7	3.3	1.7	1.1	13.4	4.7	0.1	18.1	0.5
100405RP1-14	RP1	109.0	0.1	1.4	6.1	15.4	0.5	1.9	3.0	1.8	1.1	12.8	6.4	0.1	21.1	0.6
100405RP1-16	RP1	114.0	0.1	2.1	5.0	18.6	0.7	2.9	2.7	2.3	1.2	11.7	8.8	0.1	30.2	0.4
100405RP1-18	RP1	118.0	0.1	1.4	4.6	20.8	0.9	3.7	2.9	2.7	1.3	10.8	11.1	0.1	38.3	0.4
100405RP1-22	RP1	73.0	0.2	1.8	6.1	22.1	1.1	5.9	2.6	3.6	1.3	9.2	14.5	0.1	49.7	0.3
100405RP2-1	RP2	1.5	0.3	1.7	3.8	31.4	1.9	13.0	5.5	7.0	1.7	7.2	12.3	0.1	93.1	0.0
100405RP2-4	RP2	8.1	0.3	2.7	8.3	29.2	1.7	10.3	13.7	6.2	2.3	18.5	14.8	0.1	83.0	0.1
100405RP2-7	RP2	6.9	0.2	3.1	8.7	22.8	1.4	8.9	2.2	5.1	2.2	22.7	8.8	0.1	66.4	0.1
100405RP2-9	RP2	7.0	0.2	2.7	7.5	26.2	1.5	9.2	2.0	5.2	1.9	15.0	8.4	0.1	71.0	0.1
100405RP2-11	RP2	25.2	0.1	1.6	8.5	18.0	1.0	5.0	13.2	2.9	1.4	19.0	5.0	0.1	39.5	0.2
100405RP2-12	RP2	13.0	0.1	1.3	4.8	14.3	0.6	4.4	5.6	3.2	2.3	13.4	2.7	0.1	25.3	0.1
100405RP2-13	RP2	47.3	0.1	0.6	3.8	12.2	0.5	1.6	3.2	1.5	1.3	10.2	1.9	0.0	18.3	0.2
100405RP2-14	RP2	83.3	0.1	0.8	3.5	16.9	0.5	1.8	2.7	1.7	1.3	9.7	5.1	0.1	20.0	0.2
100405RP2-15	RP2	119.0	0.1	0.5	3.8	20.8	0.6	2.2	5.2	2.0	1.5	16.3	6.7	0.1	24.0	0.3
100405RP2-17	RP2	315.0	0.2	1.1	11.9	36.5	0.8	2.8	27.3	2.7	1.8	17.6	8.5	0.2	32.7	0.8

Sample ID	Site	Al	Co	Cr	Cu	Fe	Ga	Li	Mn	Ni	Rb	Zn	Mo	Cd	Ba	Pb
100405RP2-19	RP2	60.9	0.1	1.0	10.0	18.7	0.9	3.5	4.4	3.1	1.6	18.6	10.0	0.2	36.1	0.2
100405RP2-24	RP2	40.5	0.1	1.3	8.8	20.3	1.0	4.5	2.6	3.7	1.6	11.2	12.4	0.2	44.0	0.2
100405HMP-1	HMP	2.3	0.6	2.9	4.9	28.4	1.8	15.3	2.1	5.1	2.1	8.8	7.0	0.1	77.0	0.1
100405HMP-4	HMP	6.7	0.7	3.4	4.8	29.3	1.5	20.6	11.3	4.6	3.3	6.7	8.3	0.1	62.8	0.1
100405HMP-10	HMP	2.5	0.5	2.4	7.0	28.0	1.8	14.7	2.7	5.5	3.1	22.3	6.0	0.1	76.4	0.2
100405HMP-11	HMP	2.3	0.5	2.1	5.0	23.8	1.8	12.6	1.4	5.1	2.5	7.8	5.2	0.0	71.6	0.1
100405HMP-12	HMP	3.9	0.5	2.1	5.2	20.9	1.6	11.1	1.9	4.8	2.3	12.9	5.3	0.1	63.6	0.1
100405HMP-13	HMP	5.3	0.3	2.0	4.4	13.5	1.2	6.2	6.6	3.6	1.7	9.8	3.8	0.0	45.5	0.1
100405HMP-14	HMP	18.5	0.2	1.5	3.9	10.1	0.8	3.2	2.0	2.1	1.1	10.8	2.4	0.0	27.5	0.1
100405HMP-15	HMP	32.4	0.1	1.5	3.9	10.1	0.7	2.4	1.2	1.7	0.9	12.4	2.3	0.0	21.9	0.2
100405HMP-16	HMP	34.4	0.1	1.4	3.6	10.1	0.7	2.3	1.4	1.8	0.8	11.0	2.6	0.1	22.0	0.2
100405HMP-18	HMP	37.5	0.1	1.4	3.4	11.3	0.7	2.6	1.4	1.9	0.8	9.9	3.3	0.0	24.8	0.2
100405HMP-20	HMP	41.5	0.1	1.5	5.6	12.9	0.8	3.2	1.5	2.2	0.9	9.8	3.8	0.0	26.9	0.2
100405HMP-24	HMP	42.9	0.2	1.7	4.1	14.6	0.8	3.8	2.4	2.4	1.0	6.8	4.6	0.1	29.2	0.2
100405B	RP1	7.9	0.4	0.9	6.3	25.0	1.9	10.4	142.4	5.1	2.3	21.3	11.0	0.1	77.3	0.2
100405D	RP2	4.4	0.4	0.2	3.6	26.1	2.1	10.7	0.2	5.4	1.9	13.9	9.4	0.5	87.3	0.2
100405H	HMP	10.8	0.5	0.2	3.7	24.4	1.5	9.4	120.5	4.1	1.9	14.6	5.8	0.4	59.7	0.2
100423RP1-1	RP1	2.9	0.2	1.7	5.0	20.9	1.8	8.2	2.1	4.8	2.5	13.1	11.0	0.2	69.4	0.0
100423RP1-7	RP1	8.7	0.1	1.2	4.7	16.3	1.5	4.7	27.0	3.7	2.2	15.8	6.8	0.1	51.5	0.1
100423RP1-8	RP1	6.9	0.1	1.6	4.6	14.0	1.7	5.5	1.3	3.0	1.7	10.1	5.8	0.0	60.1	0.1
100423RP1-9	RP1	8.0	0.1	1.4	5.7	10.7	1.3	3.9	0.9	2.5	1.7	11.1	4.2	0.0	42.9	0.0
100423RP1-10	RP1	3.9	0.1	3.0	4.3	15.5	1.5	5.9	0.6	3.2	1.8	5.6	3.0	0.0	53.0	0.0
100423RP1-11	RP1	2.4	0.1	2.4	4.4	15.8	1.6	6.3	0.4	3.2	1.8	4.5	3.0	0.1	55.9	0.0
100423RP1-2	RP1	1.3	0.2	1.1	3.5	19.2	1.7	7.8	0.6	4.1	1.6	19.2	10.1	0.1	66.0	0.0
100423RP1-12	RP1	7.1	0.4	2.0	1.8	28.4	2.0	5.5	0.3	3.9	3.7	14.6	3.4	0.0	67.6	0.2
100423RP1-13	RP1	7.9	0.4	1.1	1.2	17.6	1.4	1.4	0.3	2.1	1.9	4.5	1.5	0.1	44.9	0.2
100423RP1-3	RP1	5.0	0.4	1.8	6.4	20.3	1.3	1.8	0.2	2.5	2.2	14.0	1.0	0.0	44.8	0.2
100423RP1-14	RP1	2.7	0.2	0.9	1.9	15.6	1.1	1.6	132.0	2.0	2.0	4.6	0.9	0.0	34.5	0.1
100423RP1-15	RP1	2.9	0.1	0.9	1.7	8.1	0.8	1.6	9.4	2.2	1.6	8.4	1.9	0.3	26.0	0.1
100423RP1-16	RP1	2.6	0.1	1.0	1.9	7.2	0.7	1.5	2.9	1.9	1.6	8.3	1.9	0.0	21.0	0.1
100423RP1-4	RP1	1.7	0.2	2.7	3.5	20.1	1.8	6.8	0.4	4.3	1.5	5.8	12.6	0.1	66.8	0.0

Sample ID	Site	Al	Co	Cr	Cu	Fe	Ga	Li	Mn	Ni	Rb	Zn	Mo	Cd	Ba	Pb
100423RP1-5	RP1	0.5	0.3	0.4	3.3	24.0	2.0	8.7	0.4	4.5	1.6	8.9	10.1	0.1	77.0	0.0
100423RP1-6	RP1	0.4	0.2	2.0	3.1	23.7	2.1	9.7	2.3	4.5	1.6	7.4	8.8	0.1	78.5	0.0
100423A	HMP	28.6	0.4	1.2	5.9	21.0	1.0	3.6	0.4	2.7	1.5	25.4	3.0	0.1	30.0	0.8
100423C	RP2	19.6	0.6	1.3	9.6	24.8	1.4	6.1	178.0	4.1	1.9	27.0	5.6	0.1	44.5	0.5
100423D	RP1	20.6	0.5	1.4	7.9	25.9	1.4	6.7	82.3	3.8	2.4	29.6	4.5	0.1	45.8	0.5
100424RP1-12	RP1	4.4	0.2	1.7	7.6	21.6	1.7	5.4	85.4	4.2	2.1	11.6	5.7	0.1	56.1	0.2
100424RP1-16	RP1	14.4	0.1	1.6	6.8	11.4	0.8	2.4	66.8	2.1	1.6	15.3	2.8	0.1	24.6	0.4
100424RP1-17	RP1	12.0	0.1	1.4	5.3	14.7	0.9	3.0	4.9	2.3	1.9	14.4	2.7	0.1	28.2	0.3
100424RP1-18	RP1	23.2	0.3	1.0	3.3	12.3	0.6	1.0	0.3	1.3	1.0	8.7	1.4	0.1	17.0	0.4
100424RP1-19	RP1	26.9	0.4	0.8	3.2	24.2	0.7	1.2	0.3	1.7	1.3	7.9	2.5	0.1	21.2	0.5
100424RP1-20	RP1	23.7	0.2	1.2	3.2	17.9	0.7	1.1	130.0	1.7	1.3	10.9	2.9	0.1	20.1	0.4
100424RP1-22	RP1	25.6	0.1	1.1	4.2	12.5	0.7	1.5	24.8	1.7	1.3	10.9	3.9	0.1	20.4	0.4
100424RP1-24	RP1	20.6	0.1	1.7	4.2	13.5	0.8	2.0	6.5	2.1	1.4	9.9	5.4	0.1	25.2	0.4
100424RP1-30	RP1	13.5	0.1	1.5	4.6	17.0	1.2	3.1	5.5	2.7	1.6	9.6	8.3	0.1	38.0	0.4
100501HMP-10	HMP	2.4	0.4	1.9	3.3	21.7	1.8	12.4	4.6	5.1	2.2	12.2	5.4	0.1	70.6	0.0
100501HMP-12	HMP	2.3	0.4	2.2	3.7	21.3	1.7	12.2	7.7	5.2	2.2	14.8	5.2	0.1	68.2	0.1
100501HMP-13	HMP	4.0	0.3	1.0	2.7	17.8	1.4	9.8	51.4	4.0	1.9	11.9	3.9	0.0	53.1	0.1
100501HMP-14	HMP	12.4	0.5	0.7	2.6	30.4	1.0	4.1	368.0	2.8	1.4	8.9	3.2	0.0	37.3	0.2
100501HMP-15	HMP	16.1	0.4	0.8	2.5	18.6	0.9	2.6	343.0	2.5	1.1	11.0	2.9	0.0	31.5	0.3
100501HMP-16	HMP	35.4	0.3	1.1	4.9	16.4	0.7	2.2	203.0	2.5	1.1	15.4	2.6	0.1	25.2	0.4
100501HMP-17	HMP	28.3	0.2	1.1	3.6	11.9	0.7	2.0	50.3	2.0	1.1	14.4	2.6	0.1	22.1	0.3
100501HMP-19	HMP	25.6	0.1	1.3	3.9	11.0	0.7	2.2	4.3	1.9	1.1	11.8	3.0	0.0	21.9	0.3
100501HMP-23	HMP	24.4	0.1	1.3	4.0	12.8	0.8	2.6	4.7	2.3	1.2	10.9	3.6	0.0	26.4	0.3
100506B	RP2	1.9	0.8	1.5	3.0	36.5	2.9	13.5	0.4	9.3	1.9	11.1	11.6	0.2	99.8	0.1
100506C	RP1	2.1	0.5	1.4	3.2	41.5	2.8	11.0	110.0	6.8	2.0	7.4	17.4	0.1	101.0	0.1
100506D	HMP	3.4	0.5	1.1	2.8	27.5	1.9	13.1	0.4	6.2	2.6	19.6	4.5	0.1	60.2	0.1
100512RP1-13	RP1	5.2	1.2	2.5	2.5	57.9	1.8	5.0	1440.0	4.6	2.1	15.7	6.9	0.1	84.6	0.5
100512RP1-14	RP1	5.4	0.7	1.6	2.2	31.3	1.1	3.0	714.0	2.9	1.7	16.4	5.5	0.1	46.4	0.2
100512RP1-15	RP1	24.9	0.2	0.1	2.2	10.3	0.4	0.5	36.7	1.5	0.7	7.7	1.8	0.1	15.7	0.3
100512RP1-16	RP1	40.8	0.1	0.4	3.0	9.2	0.4	0.6	17.8	1.6	1.0	9.4	2.7	0.1	17.5	0.2
100512RP1-17	RP1	63.4	0.1	0.3	3.4	11.9	0.5	1.0	11.6	1.7	1.2	9.8	3.9	0.1	21.1	0.3

Sample ID	Site	Al	Co	Cr	Cu	Fe	Ga	Li	Mn	Ni	Rb	Zn	Mo	Cd	Ba	Pb
100512RP1-22	RP1	48.3	0.3	0.6	7.5	14.4	0.7	2.2	15.8	2.5	1.4	28.9	8.3	0.2	31.0	22.5
100524A	RP1	3.4	0.3	1.6	3.1	32.2	2.5	12.2	59.7	5.7	2.5	9.8	25.7	0.2	111.2	0.1
100524A - lab duplicate	RP1	3.5	0.3	1.5	3.1	32.0	2.5	12.4	59.3	5.6	2.5	9.8	25.5	0.2	110.5	0.1
100524C	RP2	2.6	0.6	1.5	2.9	31.4	2.6	12.6	0.2	6.6	2.7	12.6	15.6	0.2	114.2	7.5
100524D	HMP	6.8	0.6	1.1	2.9	23.9	2.0	10.2	0.2	4.8	2.3	17.5	5.4	2.0	79.7	0.1
100609A	HMP	15.8	0.3	1.1	4.1	20.9	1.3	6.5	0.2	3.0	1.8	17.9	4.8	0.2	47.8	0.3
100609B	RP1	5.6	0.4	1.1	3.2	24.3	1.9	9.4	0.2	3.7	3.0	13.6	8.7	0.2	73.5	0.2
100609D	RP2	5.5	0.5	0.8	3.5	17.0	1.3	8.8	0.2	3.9	2.2	14.8	8.6	0.1	52.0	1.3
100624A	RP2	8.9	0.5	1.6	4.2	29.0	2.1	10.8	0.2	4.2	3.6	11.4	9.8	0.1	85.0	0.2
100624B	RP1	7.9	0.7	1.4	6.1	23.2	1.8	10.8	0.2	5.5	2.8	21.2	11.7	0.2	73.9	5.6
100624C	HMP	11.6	0.3	1.0	3.2	18.2	1.8	9.3	132.6	3.4	2.5	13.5	4.9	0.2	66.5	0.3
100707A	HMP	4.2	0.4	1.1	2.7	19.5	1.8	16.6	102.2	4.1	2.9	11.8	5.6	0.6	69.8	0.1
100707B	RP1	4.4	0.4	2.6	7.0	34.7	2.8	17.9	80.5	6.6	3.4	16.9	13.0	0.2	121.5	0.4
100707C	RP2	0.9	0.7	1.5	2.1	28.8	2.6	13.4	0.3	6.1	2.0	11.7	8.1	0.1	109.4	0.2
100709RP1-13	RP1	4.3	0.1	2.3	17.1	6.2	0.5	1.2	40.1	4.5	1.0	31.8	2.7	0.1	19.7	0.1
100709RP1-14	RP1	43.9	0.1	1.9	3.2	8.1	0.4	0.4	17.3	1.3	0.7	12.7	1.9	0.0	15.2	0.2
100709RP1-15	RP1	81.2	0.2	1.9	3.2	11.4	0.5	0.6	14.5	1.5	1.0	12.4	3.1	0.1	17.1	0.4
100709RP1-16	RP1	62.3	0.1	2.1	5.4	10.6	0.5	1.2	6.3	1.9	1.3	21.8	5.4	0.2	20.0	0.3
100709A	RP1	33.4	0.2	0.7	4.2	12.8	1.1	4.1	30.8	2.5	1.3	9.2	16.0	0.2	43.9	0.2
100721A	HMP	17.6	0.2	1.6	5.6	11.2	1.0	3.2	46.6	2.7	1.3	22.1	5.6	0.2	37.0	0.2
100721B	RP1	26.1	0.2	2.3	7.8	18.6	1.7	6.2	29.9	4.0	1.8	23.6	20.7	0.2	58.7	1.0
100721C	RPMP	6.2	2.4	9.9	7.9	55.8	2.4	81.8	1129.0	17.6	54.7	38.3	23.6	4.7	65.6	3.8
100721D	RP2	18.9	0.3	1.6	4.5	15.7	1.2	5.2	85.4	4.4	1.8	21.4	13.8	0.2	41.4	0.3
100805A	HMP	23.5	0.2	2.4	5.4	9.5	0.8	2.8	52.8	2.4	1.4	20.4	6.1	0.3	27.8	0.2
100805B	RP1	18.4	0.2	3.0	5.9	14.5	1.2	4.7	53.8	3.3	1.5	22.8	11.3	0.3	42.8	2.1
100805C	RPMP	13.2	1.8	12.7	12.0	51.9	2.1	16.3	674.7	18.1	32.9	47.3	17.9	0.3	53.9	6.0
100805D	RP2	22.5	0.6	2.4	7.5	29.2	1.1	6.7	243.7	4.7	6.6	27.6	9.2	0.2	38.6	0.8
100826A	RP1	2.1	0.4	0.3	3.0	36.4	2.3	16.1	32.1	11.7	2.4	14.8	23.5	0.4	108.4	0.1
100826B	RP2	2.5	0.5	0.3	3.1	30.8	2.0	12.2	265.6	12.1	1.4	19.0	16.3	0.3	86.8	0.1
100826C	HMP	5.9	0.4	0.3	2.8	21.7	1.6	18.0	80.4	4.7	2.9	8.8	7.1	0.1	68.4	0.1
100917B	RP2	5.1	0.3	0.1	2.9	23.0	1.2	8.2	105.5	3.5	1.2	2.5	15.4	0.1	64.7	0.1

Sample ID	Site	Al	Co	Cr	Cu	Fe	Ga	Li	Mn	Ni	Rb	Zn	Mo	Cd	Ba	Pb
100917C	RP1	8.0	0.4	0.2	4.4	36.2	1.9	13.3	76.1	5.1	2.3	8.9	24.7	0.2	111.6	0.2
101012A	HMP at low water cross	5.3	0.8	2.1	12.2	31.4	1.6	23.0	319.1	8.4	3.5	81.4	6.2	0.6	81.9	168.9
110715A	RP2	5.7	0.8	1.7	4.0	27.7	1.4	15.5	192.2	7.9	3.0	15.3	10.2	0.4	99.9	2.6
110715B	FP Golf Pond	5.2	0.2	1.0	2.3	7.9	0.7	42.8	42.1	2.6	2.2	14.6	3.8	0.1	32.9	0.3

Appendix H: Upper River des Peres ICP-OES Data (all values in ppm)

Sample ID	Site	B	Ca	K	Mg	Na	S	Si	Sr
091211A	RP2	0.130	124.3	11.7	32.5	239.2	39.7	6.3	1.2
091211B	RP1	0.101	109.2	8.3	30.2	211.0	37.3	6.4	1.0
091221A	RP1	0.129	159.1	6.5	39.0	230.5	48.0	6.3	1.5
091221B	RP2	0.109	142.6	10.3	36.5	182.5	47.1	5.8	1.2
091221C	RPMP	0.301	361.5	198.4	91.5	29.6	11.0	24.3	1.1
091221D	HMP	0.166	116.7	5.6	26.9	138.8	39.4	4.9	0.7
100106A	HMP	0.202	130.4	8.2	30.8	333.1	47.3	5.9	0.7
100106C	RP2	0.119	202.1	9.1	48.9	496.7	63.7	6.7	1.6
100106D	RP1	0.082	158.0	5.4	33.6	280.2	49.4	5.8	1.0
100113B	RP2	0.104	127.1	8.9	33.9	462.5	42.7	5.0	0.9
100113C	RP1	0.119	138.2	11.0	35.5	676.4	39.4	5.2	1.1
100113D	HMP	0.208	116.2	9.0	30.4	535.3	43.2	5.6	0.7
100118A	RP2	0.069	112.9	10.5	30.7	364.1	33.1	7.7	1.1
100118B	RP1	0.055	94.5	6.3	26.0	299.6	26.9	5.1	1.0
100118C	HMP	0.117	79.2	8.2	23.5	364.4	28.7	3.9	0.6
100122A	RP2	0.046	58.1	10.9	19.8	217.5	20.7	4.0	0.8
100122B	RP1	0.042	56.7	6.4	19.9	218.2	21.1	4.0	0.9
100126A	RP1	0.062	99.6	5.5	26.9	182.2	32.5	9.4	1.1
100126A - field duplicate (EC/TC)	RP1	0.067	104.5	5.9	28.7	197.9	34.5	10.1	1.1
100126B	RP2	0.064	101.7	8.5	28.0	180.9	32.5	10.0	1.0
100126C	HMP	0.091	84.9	5.6	21.4	188.3	26.6	4.3	0.7
100212B	RP2	0.078	109.6	10.2	29.6	650.2	35.1	4.9	1.1
100212C	RP1	0.076	108.4	9.1	30.7	551.6	34.2	5.2	1.1
100212D	HMP	0.121	119.5	12.7	31.1	1270.7	32.5	3.2	1.0
100226A	RP2	0.073	75.8	7.0	28.0	247.0	33.2	4.9	0.9
100226A - field duplicate	RP2	0.072	77.9	7.0	28.2	236.9	33.0	4.9	0.9
100226C	RP1	0.070	84.6	4.8	25.6	187.2	32.4	4.9	0.8
100226D	HMP	0.119	90.2	5.7	25.1	267.6	32.8	3.1	0.7
100310A	RP2	0.070	79.2	7.3	23.2	217.6	28.1	3.6	0.6

Sample ID	Site	B	Ca	K	Mg	Na	S	Si	Sr
100310C	RP1	0.071	74.0	6.2	23.2	204.1	29.2	3.7	0.7
100310D	HMP	0.109	74.8	6.1	20.8	255.1	27.5	2.2	0.6
100326B	RP2	0.063	73.5	5.5	19.8	134.0	23.5	4.3	0.9
100326C	RP1	0.061	71.5	4.3	20.7	156.0	25.2	4.5	1.0
100326D	HMP	0.070	54.0	3.9	12.8	114.6	16.3	2.7	0.4
100402A	RP1	0.081	84.2	4.4	29.3	182.4	35.9	2.9	0.9
100402B	RP2	0.087	94.1	6.6	30.3	172.7	37.3	3.0	0.9
100402D	HMP	0.136	70.5	5.7	23.7	158.3	32.9	0.4	0.6
100405RP1-2	RP1	0.119	100.5	6.2	32.7	233.5	44.4	4.7	1.1
100405RP1-4	RP1	0.083	68.6	6.2	20.2	207.0	28.7	3.0	0.7
100405RP1-6	RP1	0.070	72.9	5.7	22.3	170.6	29.4	3.6	0.6
100405RP1-8	RP1	0.068	74.6	5.0	22.5	150.9	28.9	4.1	0.6
100405RP1-10	RP1	0.053	53.4	3.9	15.1	111.4	19.1	3.0	0.4
100405RP1-11	RP1	0.033	34.5	3.0	7.1	66.6	9.2	1.6	0.2
100405RP1-12	RP1	0.025	21.7	1.8	2.7	25.6	3.4	1.0	0.1
100405RP1-13	RP1	0.026	19.1	1.5	2.7	19.9	3.3	1.2	0.1
100405RP1-14	RP1	0.030	21.2	1.8	3.6	24.4	4.4	1.6	0.1
100405RP1-16	RP1	0.037	30.1	2.4	6.2	40.5	7.5	2.2	0.2
100405RP1-18	RP1	0.042	38.9	2.8	8.6	54.2	10.0	2.7	0.3
100405RP1-22	RP1	0.053	56.9	3.4	13.9	91.1	16.9	3.5	0.5
100405RP2-1	RP2	0.101	108.7	7.3	32.0	209.7	47.1	3.5	1.0
100405RP2-4	RP2	0.093	95.8	6.6	27.2	203.3	37.6	3.6	1.1
100405RP2-7	RP2	0.068	70.7	6.1	21.8	177.9	29.4	3.1	0.6
100405RP2-9	RP2	0.068	77.1	5.8	22.8	169.3	29.9	3.7	0.6
100405RP2-11	RP2	0.041	42.3	3.3	10.7	100.9	13.4	2.2	0.3
100405RP2-12	RP2	0.033	33.9	3.1	7.2	59.5	13.0	1.6	0.2
100405RP2-13	RP2	0.024	19.2	1.9	2.9	29.8	3.3	1.1	0.1
100405RP2-14	RP2	0.028	21.6	2.5	3.9	30.7	4.3	1.5	0.1
100405RP2-15	RP2	0.034	25.8	3.1	5.3	35.9	5.9	2.0	0.2
100405RP2-17	RP2	0.042	34.3	4.0	7.7	47.2	8.6	2.7	0.2
100405RP2-19	RP2	0.047	41.0	4.5	9.5	55.7	10.7	2.9	0.3

Sample ID	Site	B	Ca	K	Mg	Na	S	Si	Sr
100405RP2-24	RP2	0.055	52.6	5.1	12.7	76.8	14.8	3.3	0.4
100405HMP-1	HMP	0.154	84.2	6.4	25.8	194.8	40.1	0.5	0.7
100405HMP-4	HMP	0.144	67.8	7.7	25.2	184.0	41.0	0.6	0.6
100405HMP-10	HMP	0.154	78.2	7.1	24.9	196.1	36.8	0.9	0.6
100405HMP-11	HMP	0.129	74.3	6.1	22.4	154.9	33.5	1.4	0.6
100405HMP-12	HMP	0.114	64.6	5.8	20.0	156.2	30.1	1.5	0.5
100405HMP-13	HMP	0.066	44.9	3.6	11.7	95.3	15.1	1.5	0.3
100405HMP-14	HMP	0.035	28.6	1.9	5.1	49.4	6.1	1.1	0.2
100405HMP-15	HMP	0.030	23.7	1.6	3.7	40.2	4.6	1.0	0.1
100405HMP-16	HMP	0.031	23.8	1.6	3.8	41.4	4.7	1.0	0.2
100405HMP-18	HMP	0.084	25.3	1.6	4.5	43.6	5.7	1.1	0.2
100405HMP-20	HMP	0.057	30.0	2.0	5.7	53.1	7.3	1.3	0.2
100405HMP-24	HMP	0.057	35.2	2.4	7.3	64.5	9.6	1.3	0.2
100405B	RP1	0.093	73.6	4.9	23.4	153.0	28.0	2.8	0.8
100405D	RP2	0.078	84.9	5.7	25.1	142.5	28.9	2.3	0.8
100405H	HMP	0.104	56.3	4.8	16.7	133.8	23.8	0.7	0.4
100423RP1-1	RP1	0.125	84.3	6.5	25.5	189.5	34.0	2.6	0.9
100423RP1-7	RP1	0.072	63.8	4.9	16.2	112.9	21.9	2.4	0.6
100423RP1-8	RP1	0.080	59.9	4.8	16.8	147.9	22.5	2.1	0.5
100423RP1-9	RP1	0.057	47.5	4.2	11.4	98.0	15.8	1.7	0.3
100423RP1-10	RP1	0.077	64.6	4.3	20.1	114.8	24.9	3.2	0.4
100423RP1-11	RP1	0.077	70.0	4.5	21.6	123.2	26.9	3.5	0.4
100423RP1-2	RP1	0.075	81.5	4.5	23.5	161.3	29.6	3.0	0.7
100423RP1-12	RP1	0.063	77.5	6.5	19.6	131.3	22.2	2.7	0.7
100423RP1-13	RP1	0.021	39.3	3.5	4.3	55.4	3.6	1.4	0.2
100423RP1-3	RP1	0.022	38.8	3.7	4.3	35.8	2.7	1.6	0.2
100423RP1-14	RP1	0.021	34.7	3.6	4.3	33.9	3.3	1.4	0.1
100423RP1-15	RP1	0.020	30.7	3.2	3.9	29.0	4.7	1.1	0.1
100423RP1-16	RP1	0.020	27.9	3.0	3.8	27.4	4.5	1.2	0.1
100423RP1-4	RP1	0.065	86.0	4.4	22.4	140.3	27.3	3.0	0.7
100423RP1-5	RP1	0.077	100.8	4.9	29.6	191.5	37.0	3.4	0.8

Sample ID	Site	B	Ca	K	Mg	Na	S	Si	Sr
100423RP1-6	RP1	0.080	96.8	5.2	30.7	199.5	40.2	3.0	0.8
100423A	HMP	0.054	31.6	3.3	6.2	51.1	7.9	1.3	0.2
100423C	RP2	0.053	50.1	5.3	12.3	72.7	13.8	2.2	0.4
100423D	RP1	0.047	51.6	5.1	12.7	72.3	14.5	3.1	0.4
100424RP1-12	RP1	0.048	73.1	5.4	15.9	96.9	17.7	2.8	0.5
100424RP1-16	RP1	0.026	28.4	3.7	5.3	45.9	6.8	1.4	0.2
100424RP1-17	RP1	0.027	33.0	4.3	6.9	44.7	8.1	2.1	0.2
100424RP1-18	RP1	0.014	17.7	2.5	2.6	25.4	3.4	0.9	0.1
100424RP1-19	RP1	0.020	20.2	3.1	3.4	24.6	4.2	1.3	0.1
100424RP1-20	RP1	0.018	20.9	3.0	3.2	23.5	4.0	1.1	0.1
100424RP1-22	RP1	0.020	24.2	2.9	4.0	23.6	4.9	1.3	0.1
100424RP1-24	RP1	0.025	31.4	3.3	5.7	31.5	6.9	1.6	0.2
100424RP1-30	RP1	0.035	48.3	4.2	9.9	56.4	11.8	2.3	0.4
100501HMP-10	HMP	0.117	75.6	5.7	19.1	107.3	29.3	3.0	0.5
100501HMP-12	HMP	0.116	74.8	5.8	18.9	104.4	29.4	3.1	0.5
100501HMP-13	HMP	0.094	57.3	5.0	13.7	100.3	23.5	2.6	0.4
100501HMP-14	HMP	0.047	32.6	3.3	6.6	43.2	10.6	1.6	0.2
100501HMP-15	HMP	0.036	26.0	2.5	4.8	27.8	6.4	1.3	0.2
100501HMP-16	HMP	0.029	21.4	2.1	3.6	20.3	4.6	1.1	0.1
100501HMP-17	HMP	0.029	21.6	2.2	3.3	20.5	4.5	1.1	0.1
100501HMP-19	HMP	0.028	21.6	2.1	3.3	25.1	4.4	1.1	0.1
100501HMP-23	HMP	0.036	25.7	2.3	4.2	32.4	5.5	1.3	0.2
100506B	RP2	0.092	113.8	8.2	29.3	162.4	29.0	4.5	1.0
100506C	RP1	0.106	133.0	5.8	32.6	199.4	34.0	5.3	1.6
100506D	HMP	0.133	77.4	5.9	18.8	105.9	24.7	3.7	0.5
100512RP1-13	RP1	0.089	81.1	5.5	18.0	124.8	15.6	3.7	0.7
100512RP1-14	RP1	0.053	44.6	3.5	9.0	52.9	9.8	1.9	0.4
100512RP1-15	RP1	0.028	13.6	2.7	3.1	17.4	3.6	0.6	0.1
100512RP1-16	RP1	0.029	11.2	3.6	1.7	16.9	2.7	0.9	0.1
100512RP1-17	RP1	0.031	14.5	4.2	2.4	45.0	3.7	1.2	0.1
100512RP1-22	RP1	0.040	27.1	4.6	5.5	57.6	7.9	2.2	0.2

Sample ID	Site	B	Ca	K	Mg	Na	S	Si	Sr
100524A	RP1	0.122	117.0	5.7	28.2	171.4	34.2	6.1	1.5
100524A - lab duplicate	RP1	0.120	116.4	5.6	27.6	164.4	33.3	5.9	1.5
100524C	RP2	0.105	102.8	9.0	23.9	125.2	30.6	5.4	0.9
100524D	HMP	0.124	70.9	4.3	16.3	80.7	24.6	4.1	0.5
100609A	HMP	0.099	45.5	3.5	9.2	48.8	12.0	3.3	0.3
100609B	RP1	0.085	73.5	6.1	16.8	83.9	19.6	5.1	0.6
100609D	RP2	0.081	58.0	7.2	13.5	67.0	17.1	4.8	0.5
100624A	RP2	0.095	82.1	7.5	18.6	111.1	21.3	5.4	0.7
100624B	RP1	0.095	78.5	8.7	17.9	126.4	19.9	5.2	0.6
100624C	HMP	0.126	58.9	5.3	13.8	76.5	16.7	3.5	0.5
100707A	HMP	0.158	71.4	6.5	18.3	97.9	29.3	2.7	0.5
100707B	RP1	0.156	137.3	8.6	34.4	197.8	38.2	6.9	1.2
100707C	RP2	0.116	124.3	10.9	27.4	169.9	30.2	5.2	1.0
100709RP1-13	RP1	0.032	20.3	1.5	3.1	32.4	3.5	0.7	0.1
100709RP1-14	RP1	0.025	10.9	1.3	1.1	10.0	1.6	0.7	0.0
100709RP1-15	RP1	0.032	10.2	2.8	1.5	13.2	2.3	1.2	0.0
100709RP1-16	RP1	0.037	13.8	4.2	2.3	43.2	3.7	1.7	0.1
100709A	RP1	0.066	50.9	5.8	10.4	51.4	13.8	5.4	0.6
100721A	HMP	0.049	30.8	2.9	5.1	29.7	6.4	2.4	0.2
100721B	RP1	0.056	53.7	5.0	10.8	49.7	14.1	5.2	0.6
100721C	RPMP	0.492	106.9	119.1	31.9	35.7	16.4	25.2	0.4
100721D	RP2	0.050	39.1	5.7	7.5	32.2	9.3	4.2	0.3
100805A	HMP	0.038	23.4	2.6	3.9	22.3	5.4	1.6	0.2
100805B	RP1	0.047	38.2	3.7	7.4	31.7	10.2	3.4	0.3
100805C	RPMP	0.331	60.2	94.6	19.4	29.6	9.0	10.0	0.2
100805D	RP2	0.095	36.7	19.6	8.4	28.7	7.9	4.6	0.2
100826A	RP1	0.186	122.5	6.3	31.8	228.2	34.1	8.0	1.3
100826B	RP2	0.115	93.7	9.9	20.6	116.2	27.8	4.9	0.8
100826C	HMP	0.182	65.1	7.0	15.8	96.2	33.2	4.9	0.5
100917B	RP2	0.122	74.8	7.0	16.9	93.7	25.7	4.3	0.7
100917C	RP1	0.148	116.6	7.1	26.1	175.3	34.4	6.6	NA

Sample ID	Site	B	Ca	K	Mg	Na	S	Si	Sr
101012A	HMP at low water cross	0.187	87.0	9.1	21.6	87.5	36.3	3.5	0.7
110715A	RP2	0.227	87.3	17.1	20.8	127.4	21.7	5.9	0.8
110715B	FP Golf Pond	0.133	24.4	9.8	16.7	57.4	44.5	3.3	0.2

Appendix I: Deer Creek Data

Sample ID	Site	Date and Time	USGS Stage (m)	USGS Discharge (cms)	SpC (µS/cm)	Temperature (°C)	DO (ppm)	DO (% sat)	Turbidity (NTU)	Calculated TSS (ppm)	pH	δ ¹⁸ O (‰)	δD (‰)	NH ₄ ⁺ -N (ppm)	Cl (ppm)	NO ₃ ⁻ -N (ppm)	Total PO ₄ ³⁻ (ppm)	<i>E. coli</i> (cfu/100mL)	Total Coliforms (cfu/100mL)
080911E	DC@BB	9/11/2008 14:46:00	0.271272	0.079296	885	21	7.39	90.5	NA	NA	6.2	-6.3	-46	0.44	108	1.2	0.24	613.1	2419.6
080911E-Field Duplicate	DC@BB	9/11/2008 14:46:00	0.271272	0.079296	885	21	7.39	90.5	NA	NA	6.2			0.44		1.5			
080925G	DC@BB	9/25/2008 13:35:00	0.283464	0.096288	1286	21.8	7.75	91	11	5.61	7.6	-6.7	-46	0.52	149.2	0.867	0.27	149.1	2419.6
081009F	DC@BB	10/9/2008 10:51:00	0.283464	0.096288	714	16.4	4.1	44.8	5	2.55	7.4	-6.2	-42	0.55	84	1.54	0.34	920.8	2419.6
081023F	DC@BB	10/23/2008 12:10:00	0.920496	4.02144	389	12.1	9.6	90.1	148	75.48	7.7	-5.6	-31	1.267	42.8	0.54	1.17	2419.6	2419.6
081106F	DC@BB	11/6/2008 11:05:00	0.283464	0.04248	949	13.8	3.71	33.3	90	45.9	7.6		-41	0.87	166.4	1.81	0.53	75.4	2419.6
081120F	DC@BB	11/20/2008 12:22:00	0.234696	0.00708	462	5.3	10.6	81.2	62	31.62	7.6			0.72	90.4	0.7	0.763	866.4	2419.6
081204F	DC@BB	12/4/2008 12:45:00	0.268224	0.0274704	556	4.2	7.85	61.2	85	43.35	7.6								
081218F	DC@BB	12/18/2008 12:38:00	0.231648	0.0059472	898	1.5	11.41	81.3	14	7.14	6.6								
080916A	DC@Mac	9/16/2008 15:15:00	0.615696	0.09912	715	18.9	NA	NA	NA	NA	NA	-6.5	-45	NA	NA	NA	NA	NA	NA
080925C	DC@Mac	9/25/2008 12:58:00	0.551688	0.002832	746	20.9	11.56	130.1	3	1.53	7.9	-6.3	-43	2.3	103.2	0	0.38	116.2	2419.6
081009B	DC@Mac	10/9/2008 9:37:00	0.551688	0.002832	827	12.4	8.14	78.3	2	1.02	7.8	-5.8	-39	0.343	104.4	0.47	0.26	1046.2	2419.6
081023B	DC@Mac	10/23/2008 10:37:00	0.826008	1.16112	238.2	11.4	10.7	96	42	21.42	8.2	-5.2	-2	0.94	24.4	1.21	1.18	2419.6	2419.6
081106B	DC@Mac	11/6/2008 9:15:00	0.566928	0.0065136	460	13.1	2.45	22.4	84	42.84	8.1		-39	0.51	49.6	0.34	0.59	37.3	1553.1
081120B	DC@Mac	11/20/2008 10:45:00	0.557784	0.001416	373.6	4.6	8.37	64.4	239	121.89	7.6			0.37	57.6	0.567	0.833	123.4	2419.6
081204B	DC@Mac	12/4/2008 10:28:00	0.56388	0.0045312	555	0.6	9.87	69.2	66	33.66	7.6								
081218B	DC@Mac	12/18/2008 10:35:00	0.612648	0.0708	968	1.1	13.49	94	9	4.59	7.5								
100113E	DC@Mac	1/13/2010 15:30:00	0	0	1993	0	15.93	109.5	3	1.53	8.05		-49	0.26	448	2.1	NA	30.5	488.4
080911B	DCL	9/11/2008 12:50:00	0.362712	0	704	19.6	10.98	119.6	7	3.57	7	-4.8	-35	0.22	86.4	1	0.39	285.1	2419.6
080925B	DCL	9/25/2008 12:41:00	0.393192	0.0025488	820	22.6	11.14	127	5	2.55	7.6	-5.6	-39	0.2	71.2	0.334	0.4	125.6	2419.6
081009C	DCL	10/9/2008 9:59:00	0.390144	0.0019824	923	13.7	6.4	58.8	4	2.04	7.5	-5.5	-38	0.21	103.6	0.61	0.32	129.6	2419.6
081023C	DCL	10/23/2008 11:07:00	0.435864	0.0246384	774	11.1	7.2	66.5	76	38.76	5.1	-5.2	-31	0.51	74.4	0.21	1.06	2419.6	2419.6
081106C	DCL	11/6/2008 9:40:00	0.359664	0	650	14.5	5.1	54.6	96	48.96	7.6		-32	0.14	67.2	0.47	0.677	18.9	1011.2
081120C	DCL	11/20/2008 11:07:00	0.381	0.0005664	429.5	5.6	12.42	98.3	30	15.3	7.7			0.13	71.2	1.833	1.06	16.4	920.8
081204C	DCL	12/4/2008 11:15:00	0.374904	0	419.5	2.1	8.2	60.5	46	23.46	7.6								
081218C	DCL	12/18/2008 11:00:00	0.374904	0	1070	2	11.23	81.3	20	10.2	7.4								

Sample ID	Site	Date and Time	USGS Stage (m)	USGS Discharge (cms)	SpC (µS/cm)	Temperature (°C)	DO (ppm)	DO (% sat)	Turbidity (NTU)	Calculated TSS (ppm)	pH	δ ¹⁸ O (‰)	δD (‰)	NH ₄ ⁺ -N (ppm)	Cl (ppm)	NO ₃ ⁻ -N (ppm)	Total PO ₄ ³⁻ (ppm)	<i>E. coli</i> (cfu/100mL)	Total Coliforms (cfu/100mL)
080911C	SEB	9/11/2008 13:20:00	0.74676	0.0022656	1181	22	12.87	116	NA	NA	7.8	-6.4	-46	0.14	190.8	0.1	0.21	410.6	2419.6
080916D	SEB	9/16/2008 16:40:00	0.749808	0.0031152	1080	27	NA	NA	NA	NA	NA	-7.0	-48	NA	NA	NA	NA	NA	NA
080925F	SEB	9/25/2008 13:20:00	0.725424	0	1700	21.1	10.6	139.6	3	1.53	7.6	-5.9	-42	0.19	313.2	0.5	0.17	72	2419.6
081009E	SEB	10/9/2008 10:28:00	0.740664	0.0005664	672	14.9	4.5	41.1	4	2.04	7.5	-5.6	-36	0.37	75.2	1.11	0.38	2419.6	2419.6
081023E	SEB	10/23/2008 11:47:00	0.874776	0.2832	152.8	11.6	11.3	120.6	21	10.71	8	-6.3	-33	0.7	8	0.81	0.83	2419.6	2419.6
081106E	SEB	11/6/2008 10:27:00	0.722376	0	888	14.4	1.48	14.8	280	142.8	7.5		-27	0.707	143.2	1.37	1.66	167	2419.6
081120E	SEB	11/20/2008 11:30:00	0.734568	0.0002832	562	5	9.3	72	25	12.75	7.7			0.16	111.2	1.5	0.18	151	2419.6
081204E	SEB	12/4/2008 12:15:00	0.749808	0.0031152	579	3.8	12.12	91.1	29	14.79	7.5								
081218E	SEB	12/18/2008 11:56:00	0.762	0.0093456	2800	0.8	14.95	104.3	2	1.02	7.4		-52						
080911D	TMW	9/11/2008 14:15:00	-0.048768	0	431.6	21.8	9.96	115.6	NA	NA	8.5	-6.3	-41	0.19	28.8	0.7	0.36	105	2419.6
080916C	TMW	9/16/2008 16:30:00	0.039624	0	510	21.8	NA	NA	NA	NA	NA	-8.5	-59	NA	NA	NA	NA	NA	NA
080925D	TMW	9/25/2008 13:12:00	-0.033528	0	537	23.5	8.4	87.5	27	13.77	7.9	-7.1	-49	0.43	28.8	0.94	0.52	116.2	2419.6
080925E - Lab Duplicate	TMW	9/25/2008 13:12:00	0	0						0				0.44	37.2	1.2			
081009D	TMW	10/9/2008 10:14:00	-0.082296	0	552	16.5	6.01	62.5	11	5.61	7.6	-5.3	-41	0.23	37.2	0.04	0.28	14.5	2419.6
081023D	TMW	10/23/2008 11:25:00	-0.06096	0	531	10.8	8.76	77.4	7	3.57	7.8	-4.4	-33	0.28	33.6	0.04	0.54	156.5	2419.6
081106D	TMW	11/6/2008 10:08:00	-0.09144	0	426.5	14.5	5.31	51.1	42	21.42	7.7		-28	0.413	49.2	0.61	1.033	7.3	1413.6
081120D	TMW	11/20/2008 11:30:00	-0.06096	0	307.7	5.6	8.8	69.5	42	21.42	7.9			0.28	40.4	1.1	0.623	11.9	2419.6
081204D	TMW	12/4/2008 11:45:00	0.070104	0	326.5	3.5	11.01	90.1	33	16.83	7.5								
081218D	TMW	12/18/2008 11:30:00	4.8768	0	542	2.1	8.65	67	11	5.61	7.4								

Appendix J: Black Creek Data

Sample ID	Site	Date and Time	USGS Stage (m)	USGS Discharge (cms)	SpC (µS/cm)	Temperature (°C)	DO (ppm)	DO (% sat)	Turbidity (NTU)	Calculated TSS (ppm)	pH	δ ¹⁸ O (‰)	δD (‰)	NH ₄ ⁺ -N (ppm)	Cl (ppm)	NO ₃ ⁻ -N (ppm)	Total PO ₄ ³⁻ (ppm)	<i>E. coli</i> (cfu/100mL)	Total Coliforms (cfu/100mL)
061213A	BCK	12/13/2006 10:15:00	0.73	0.04	924.0	6.7	13.80	113.1*	16	8.2	8.4	-7.7	-51						
061227A	BCK	12/27/2006 14:22:00	0.71	0.02	528.0	7.0	4.56	38.0*			8.4	-8.0	-58						
070109A	BCK	1/9/2007 14:50:00			748.0	6.0	5.36	43.6*			8.5	-7.9	-58						
070117A	BCK	1/17/2007 9:45:00			901.0	0.8	11.12	78.9*			9.0	-8.1	-57						
070130A	BCK	1/30/2007 9:43:00	0.70	0.01	6000.0	-0.1	14.21	98.0*			8.3	-7.8	-58						
070706A	BCK	7/6/2007 12:30:00	0.72	0.01	1294.0	25.4	3.10	37.3*	8.5	4.3	8.6	-5.4	-35						
070816A	BCK	8/16/2007 14:10:00	0.70	0.02	1240.0	28.6	8.21	106.6*	4.7	2.4	8.9	-4.6	-34						
070921A	BCK	9/21/2007 11:35:00	0.69	0.02	1246.0	22.5						-5.7	-45						
080319E	BCK	3/19/2008 0:00:00	1.92	14.61	724.0	7.5	10.77	87.1	95	48.5	7.5	-10.1	-71						
080325-BCK1	BCK	3/22/2008 0:21:04	0.74	0.05	1940.0				9	4.6		-8.2	-57						
080325-BCK2	BCK	3/22/2008 12:21:04	0.76	0.08	1565.0				67	34.2		-7.7	-56						
080325-BCK3	BCK	3/23/2008 0:21:04	0.72	0.03	2060.0				10	5.1		-7.6	-53						
080325-BCK4	BCK	3/23/2008 12:21:04	0.76	0.08	1555.0				10	5.1		-7.4	-53						
080325-BCK5	BCK	3/24/2008 0:21:04	0.73	0.04	1800.0				17	8.7		-8.3	-58						
080325-BCK6	BCK	3/24/2008 12:21:04	0.72	0.03	1790.0				12	6.1		-8.8	-62						
080325-BCK7	BCK	3/25/2008 0:21:04	0.73	0.04	1800.0				8	4.1		-8.4	-58						
080325-BCK8	BCK	3/25/2008 10:21:00	0.73	0.04	1685.0				16	8.2		-8.9	-61						
080325A	BCK	3/25/2008 11:00:00	0.73	0.03	1160.0	9.0			31	15.8		-8.0	-54						
080328-BCK1	BCK	3/25/2008 11:20:04	0.73	0.03	1456.0				15	7.7		-8.0	-56						
080328-BCK2	BCK	3/26/2008 11:20:04	0.73	0.03	1353.0				2	1.0		-7.5	-53						
080328-BCK9	BCK	3/26/2008 15:47:04	0.78	0.10	1330.0				6	3.1		-6.8	-48						
080328-BCK10	BCK	3/26/2008 16:17:04	1.13	1.78	771.0				33	16.8		-4.6	-30						
080328-BCK11	BCK	3/26/2008 16:47:04	1.18	2.24	725.0				223	113.7		-4.5	-28						
080328-BCK12	BCK	3/26/2008 17:17:04	1.32	3.62	606.0				1453	741.0		-4.4	-26						
080328-BCK13	BCK	3/26/2008 17:47:04	1.30	3.45	623.0				1268	646.7		-5.0	-28						
080328-BCK14	BCK	3/26/2008 18:17:04	1.30	3.48	401.5				651	332.0		-5.0	-26						

Sample ID	Site	Date and Time	USGS Stage (m)	USGS Discharge (cms)	SpC (µS/cm)	Temperature (°C)	DO (ppm)	DO (% sat)	Turbidity (NTU)	Calculated TSS (ppm)	pH	δ ¹⁸ O (‰)	δD (‰)	NH ₄ ⁺ -N (ppm)	Cl (ppm)	NO ₃ ⁻ -N (ppm)	Total PO ₄ ³⁻ (ppm)	<i>E. coli</i> (cfu/100mL)	Total Coliforms (cfu/100mL)
080328-BCK15	BCK	3/26/2008 18:47:04	1.35	4.08	418.5				321	163.7		-5.3	-25						
080328-BCK16	BCK	3/26/2008 19:17:04	1.48	5.78	387.7				485	247.4		-5.2	-24						
080328-BCK17	BCK	3/26/2008 19:47:04	1.47	5.64	355.1				350	178.5		-5.3	-23						
080328-BCK18	BCK	3/26/2008 20:17:04	1.47	5.64	415.9				279	142.3		-5.4	-23						
080328-BCK19	BCK	3/26/2008 20:47:04	1.93	14.84	302.7				1052	536.5		-5.4	-21						
080328-BCK20	BCK	3/26/2008 21:17:04	1.84	12.77	304.8				956	487.6		-5.5	-22						
080328-BCK21	BCK	3/26/2008 21:47:04	1.63	8.33	296.0				324	165.2		-5.6	-24						
080328-BCK22	BCK	3/26/2008 22:17:04	1.44	5.32	278.8				84	42.8		-5.7	-24						
080328-BCK23	BCK	3/26/2008 22:47:04	1.32	3.71	306.4				42	21.4		-5.7	-24						
080328-BCK24	BCK	3/26/2008 23:17:04	1.20	2.44	466.8				43	21.9		-5.7	-24						
080328-BCK3	BCK	3/27/2008 11:20:04	0.92	0.51	748.0				15	7.7		-5.8	-29						
080328A	BCK	3/28/2008 11:00:00	0.85	0.28	937.0	7.5			199	101.5		-6.3	-36						
080331-1BCK	BCK	3/28/2008 11:20:04	0.85	0.27	838.0				8	4.1		-6.4	-38						
080331-2BCK	BCK	3/29/2008 11:20:04	0.78	0.10	1197.0				13	6.6		-6.9	-42						
080331-7BCK	BCK	3/30/2008 5:42:04	1.00	0.91	699.0				30	15.3		-5.6	-30						
080331-8BCK	BCK	3/30/2008 7:42:04	1.52	6.48	383.9				211	107.6		-5.0	-31						
080331-9BCK	BCK	3/30/2008 9:42:04	1.08	1.36	484.7				58	29.6		-5.1	-31						
080331-3BCK	BCK	3/30/2008 11:20:04	0.96	0.68	575.0				41	20.9		-5.4	-33						
080331-10BCK	BCK	3/30/2008 11:42:04	0.94	0.59	517.0				69	35.2		-5.4	-33						
080331-11BCK	BCK	3/30/2008 13:42:04	0.89	0.40	622.0				58	29.6		-5.6	-35						
080331-12BCK	BCK	3/30/2008 15:42:04	0.86	0.31	675.0				34	17.3		-5.7	-36						
080331-13BCK	BCK	3/30/2008 17:42:04	0.84	0.25	766.0				28	14.3		-6.0	-36						
080331-14BCK	BCK	3/30/2008 19:42:04	0.83	0.22	843.0				34	17.3		-6.0	-38						
080331-15BCK	BCK	3/30/2008 21:42:04	0.82	0.20	901.0				48	24.5		-6.1	-39						
080331-16BCK	BCK	3/30/2008 23:42:04	0.81	0.18	962.0				48	24.5		-6.3	-39						
080331-17BCK	BCK	3/31/2008 1:42:04	0.80	0.15	957.0				20	10.2		-6.4	-41						
080331-18BCK	BCK	3/31/2008 3:42:04	0.80	0.14	1021.0				49	25.0		-6.4	-40						
080331-19BCK	BCK	3/31/2008 5:42:04	0.80	0.14	1087.0				17	8.7		-6.4	-42						

Sample ID	Site	Date and Time	USGS Stage (m)	USGS Discharge (cms)	SpC (µS/cm)	Temperature (°C)	DO (ppm)	DO (% sat)	Turbidity (NTU)	Calculated TSS (ppm)	pH	δ ¹⁸ O (‰)	δD (‰)	NH ₄ ⁺ -N (ppm)	Cl (ppm)	NO ₃ ⁻ -N (ppm)	Total PO ₄ ³⁻ (ppm)	<i>E. coli</i> (cfu/100mL)	Total Coliforms (cfu/100mL)
080331-20BCK	BCK	3/31/2008 7:42:04	0.79	0.13	1044.0				31	15.8		-6.5	-42						
080331-21BCK	BCK	3/31/2008 9:42:04	0.80	0.14	1104.0				34	17.3		-6.5	-43						
080331-4BCK	BCK	3/31/2008 11:20:04	0.79	0.13	1197.0				42	21.4		-6.6	-44						
080331-22BCK	BCK	3/31/2008 11:42:04	0.79	0.13	1108.0				18	9.2		-6.6	-44						
080331C-BW	BCK	3/31/2008 13:25:00	0.79	0.13															
080402-1BCK	BCK	3/31/2008 13:27:04	0.79	0.13	1356.0				33	16.8		-6.5	-42						
080402-7BCK	BCK	3/31/2008 16:21:04	0.87	0.34	1085.0				289	147.4		-5.4	-31						
080402-8BCK	BCK	3/31/2008 16:36:04	1.10	1.56	653.0				180	91.8		-4.5	-23						
080402-9BCK	BCK	3/31/2008 16:51:04	1.31	3.60	553.0				1202	613.0		-4.3	-21						
080402-10BCK	BCK	3/31/2008 17:06:04	1.62	8.27	376.0				1032	526.3		-4.3	-20						
080402-11BCK	BCK	3/31/2008 17:21:04	1.77	11.13	328.3				602	307.0		-4.5	-20						
080402-12BCK	BCK	3/31/2008 17:36:04	1.80	11.95	306.1				528	269.3		-4.6	-23						
080402-13BCK	BCK	3/31/2008 17:51:04	1.78	11.33	272.2				493	251.4		-4.7	-23						
080402-14BCK	BCK	3/31/2008 18:06:04	1.74	10.48	246.4				468	238.7		-4.7	-23						
080402-15BCK	BCK	3/31/2008 18:21:04	1.73	10.22	238.5				402	205.0		-4.7	-23						
080402-16BCK	BCK	3/31/2008 18:36:04	1.72	10.17	237.5				367	187.2		-4.7	-24						
080402-17BCK	BCK	3/31/2008 18:51:04	1.73	10.31	232.0				366	186.7		-4.8	-25						
080402-18BCK	BCK	3/31/2008 19:06:04	1.76	11.02	225.2				296	151.0		-4.9	-26						
080402-19BCK	BCK	3/31/2008 19:21:04	1.80	11.81	225.6				328	167.3		-4.9	-27						
080402-2BCK	BCK	3/31/2008 19:27:04	1.82	12.29	228.7				390	198.9		-5.0	-28						
080402-20BCK	BCK	3/31/2008 19:36:04	1.87	13.42	221.3				394	200.9		-5.1	-29						
080402-21BCK	BCK	3/31/2008 19:51:04	1.95	15.38	216.5				420	214.2		-5.2	-31						
080402-22BCK	BCK	3/31/2008 20:06:04	2.02	17.39	213.8				444	226.4		-5.3	-33						
080402-23BCK	BCK	3/31/2008 20:21:04	2.01	17.05	218.2				406	207.1		-5.3	-33						
080402-24BCK	BCK	3/31/2008 20:36:04	1.92	14.67	221.4				365	186.2		-5.5	-34						
080402-3BCK	BCK	4/1/2008 1:27:04	0.98	0.82	547.0				83	42.3		-5.9	-36						
080402-4BCK	BCK	4/1/2008 7:27:04	0.87	0.34	894.0				43	21.9		-6.0	-38						
080402-5BCK	BCK	4/1/2008 13:27:04	0.84	0.24	1082.0				66	33.7		-6.1	-40						

Sample ID	Site	Date and Time	USGS Stage (m)	USGS Discharge (cms)	SpC (µS/cm)	Temperature (°C)	DO (ppm)	DO (% sat)	Turbidity (NTU)	Calculated TSS (ppm)	pH	δ ¹⁸ O (‰)	δD (‰)	NH ₄ ⁺ -N (ppm)	Cl (ppm)	NO ₃ ⁻ -N (ppm)	Total PO ₄ ³⁻ (ppm)	<i>E. coli</i> (cfu/100mL)	Total Coliforms (cfu/100mL)
080402-6BCK	BCK	4/1/2008 19:27:04	0.81	0.18	1230.0				30	15.3		-6.2	-40						
080402C	BCK	4/2/2008 14:25:00	0.78	0.10	1393.0	13.1			22	11.2		-6.6	-44						
080404-1BCK	BCK	4/2/2008 14:34:04	0.78	0.10	1391.0				21	10.7		-6.6	-44						
080404-2BCK	BCK	4/2/2008 20:34:04	0.77	0.10	1519.0				23	11.7		-6.6	-44						
080404-3BCK	BCK	4/3/2008 2:34:04	0.76	0.08	1559.0				14	7.1		-6.5	-43						
080404-7BCK	BCK	4/3/2008 6:21:04	0.99	0.82	673.0				80	40.8		-7.6	-50						
080404-8BCK	BCK	4/3/2008 6:51:04	1.23	2.66	578.0				224	114.2		-7.8	-51						
080404-9BCK	BCK	4/3/2008 7:21:04	1.45	5.35	393.9				617	314.7		-8.0	-53						
080404-10BCK	BCK	4/3/2008 7:51:04	1.46	5.49	495.5				321	163.7		-7.8	-51						
080404-11BCK	BCK	4/3/2008 8:21:04	1.44	5.32	321.5				265	135.2		-7.7	-50						
080404-4BCK	BCK	4/3/2008 8:34:04	1.41	4.81	369.5				213	108.6		-7.7	-50						
080404-12BCK	BCK	4/3/2008 8:51:04	1.37	4.28	339.7				188	95.9		-7.6	-49						
080404-13BCK	BCK	4/3/2008 9:21:04	1.28	3.26	337.7				184	93.8		-7.5	-48						
080404-14BCK	BCK	4/3/2008 9:51:04	1.22	2.58	331.3				168	85.7		-7.3	-47						
080404-15BCK	BCK	4/3/2008 10:21:04	1.16	2.07	353.5				179	91.3		-7.1	-46						
080404-16BCK	BCK	4/3/2008 10:51:04	1.11	1.64	367.3				149	76.0		-7.1	-45						
080404-17BCK	BCK	4/3/2008 11:21:04	1.07	1.30	389.0				132	67.3		-7.1	-45						
080404-18BCK	BCK	4/3/2008 11:51:04	1.03	1.08	414.8				120	61.2		-7.2	-45						
080404-19BCK	BCK	4/3/2008 12:21:04	1.00	0.91	436.7				106	54.1		-7.1	-45						
080404-20BCK	BCK	4/3/2008 12:51:04	0.98	0.76	466.7				95	48.5		-7.1	-45						
080404-21BCK	BCK	4/3/2008 13:21:04	0.96	0.68	495.0				93	47.4		-7.0	-44						
080404-22BCK	BCK	4/3/2008 13:51:04	0.94	0.59	525.0				90	45.9		-7.1	-45						
080404-23BCK	BCK	4/3/2008 14:21:04	0.93	0.54	555.0				79	40.3		-6.8	-44						
080404-5BCK	BCK	4/3/2008 14:34:04	0.92	0.51	587.0				78	39.8		-7.0	-45						
080404-24BCK	BCK	4/3/2008 14:51:04	0.93	0.54	581.0				103	52.5		-6.9	-44						
080404-6BCK	BCK	4/3/2008 20:34:04	1.00	0.88	830.0				80	40.8		-6.5	-38						
080404A	BCK	4/4/2008 13:20:00	0.81	0.18	1215.0	9.8			43	21.9		-6.5	-42						
080507-1BCK	BCK	5/3/2008 10:27:00	0.72	0.04	1173.0				4	2.0	8.1	-6.5	-42						

Sample ID	Site	Date and Time	USGS Stage (m)	USGS Discharge (cms)	SpC (µS/cm)	Temperature (°C)	DO (ppm)	DO (% sat)	Turbidity (NTU)	Calculated TSS (ppm)	pH	δ ¹⁸ O (‰)	δD (‰)	NH ₄ ⁺ -N (ppm)	Cl (ppm)	NO ₃ ⁻ -N (ppm)	Total PO ₄ ³⁻ (ppm)	<i>E. coli</i> (cfu/100mL)	Total Coliforms (cfu/100mL)
080507-2BCK	BCK	5/3/2008 20:27:00	0.72	0.03	1435.0				1	0.5	8.3	-6.5	-42						
080507-3BCK	BCK	5/4/2008 6:27:00	0.71	0.03	1492.0				2	1.0	8.3	-6.3	-40						
080507-4BCK	BCK	5/4/2008 16:27:00	0.71	0.03	1515.0				2	1.0	8.3	-6.4	-41						
080507-5BCK	BCK	5/5/2008 2:27:00	0.71	0.03	1514.0				3	1.5	8.2	-6.4	-41						
080507-6BCK	BCK	5/5/2008 12:27:00	0.71	0.03	1523.0				1	0.5	8.1	-6.6	-43						
080507-7BCK	BCK	5/5/2008 22:27:00	0.71	0.03	1583.0				5	2.6	8.0	-6.3	-40						
080507-8BCK	BCK	5/6/2008 8:27:00	0.70	0.02	1583.0				2	1.0	7.9	-6.4	-41						
080507-9BCK	BCK	5/6/2008 18:27:00	0.71	0.02	1551.0				2	1.0	7.5	-6.3	-40						
080507-10BCK	BCK	5/7/2008 4:27:00	0.71	0.03	1554.0				1	0.5	7.6	-6.5	-42						
080507-11BCK	BCK	5/7/2008 6:32:00	0.83	0.25	1203.0				18	9.2	7.6	-6.9	-45						
080507-12BCK	BCK	5/7/2008 7:02:00	1.04	1.19	634.0				649	331.0	7.7	-7.3	-48						
080507-13BCK	BCK	5/7/2008 7:32:00	1.33	3.82	350.0				445	227.0	7.8	-7.1	-47						
080507-14BCK	BCK	5/7/2008 8:02:00	1.16	2.04	361.0				326	166.3	7.5	-7.0	-46						
080507-15BCK	BCK	5/7/2008 8:32:00	1.12	1.73	395.0				194	98.9	7.6	-6.9	-45						
080507-16BCK	BCK	5/7/2008 9:02:00	1.03	1.13	412.0				109	55.6	7.7	-6.5	-42						
080507-17BCK	BCK	5/7/2008 9:32:00	0.98	0.85	444.0				81	41.3	7.5	-6.4	-41						
080507-18BCK	BCK	5/7/2008 10:02:00	0.94	0.65	487.0				60	30.6	7.6	-6.3	-40						
080507-19BCK	BCK	5/7/2008 10:32:00	0.91	0.51	521.0				45	23.0	7.6	-6.1	-39						
080507-20BCK	BCK	5/7/2008 11:02:00	0.88	0.40	547.0				31	15.8	7.6	-6.0	-38						
080507-21BCK	BCK	5/7/2008 11:32:00	0.86	0.34	569.0				27	13.8	7.7	-5.9	-37						
080507-22BCK	BCK	5/7/2008 12:02:00	0.84	0.28	583.0				20	10.2	7.7	-5.8	-36						
080507-23BCK	BCK	5/7/2008 12:32:00	0.83	0.25	598.0				16	8.2	7.5	-5.4	-33						
080507-24BCK	BCK	5/7/2008 13:02:00	0.82	0.21	634.0				27	13.8	7.0	-4.8	-29						
080507C	BCK	5/7/2008 13:20:00	0.82	0.21	652.0				55	28.1	7.0	-4.3	-26						
080508-1BCK	BCK	5/7/2008 13:34:00	0.87	0.37	677.0				188	95.9	7.0	-4.4	-25						
080508-7BCK	BCK	5/7/2008 13:59:00	1.04	1.16	458.0				69	35.2	6.8	-3.4	-15						
080508-8BCK	BCK	5/7/2008 14:04:00	1.07	1.36	342.0				48	24.5	6.9	-3.0	-11						
080508-9BCK	BCK	5/7/2008 14:34:00	1.36	4.13	324.1				210	107.1	7.0	-3.2	-14						

Sample ID	Site	Date and Time	USGS Stage (m)	USGS Discharge (cms)	SpC (µS/cm)	Temperature (°C)	DO (ppm)	DO (% sat)	Turbidity (NTU)	Calculated TSS (ppm)	pH	δ ¹⁸ O (‰)	δD (‰)	NH ₄ ⁺ -N (ppm)	Cl (ppm)	NO ₃ ⁻ -N (ppm)	Total PO ₄ ³⁻ (ppm)	<i>E. coli</i> (cfu/100mL)	Total Coliforms (cfu/100mL)
080508-10BCK	BCK	5/7/2008 15:04:00	1.48	5.86	340.6				398	203.0	6.8	-3.3	-14						
080508-11BCK	BCK	5/7/2008 15:34:00	1.39	4.50	321.7				236	120.4	6.8	-3.4	-15						
080508-12BCK	BCK	5/7/2008 16:04:00	1.35	3.99	295.8				188	95.9	7.0	-3.9	-21						
080508-13BCK	BCK	5/7/2008 16:34:00	1.35	4.08	311.9				193	98.4	7.1	-4.5	-26						
080508-14BCK	BCK	5/7/2008 17:04:00	1.38	4.47	306.5				192	97.9	7.0	-5.4	-34						
080508-15BCK	BCK	5/7/2008 17:34:00	1.40	4.73	288.2				208	106.1	7.0	-5.7	-38						
080508-16BCK	BCK	5/7/2008 18:04:00	1.37	4.30	278.5				159	81.1	7.0	-6.3	-43						
080508-17BCK	BCK	5/7/2008 18:34:00	1.30	3.48	278.9				96	49.0	7.1	-6.7	-45						
080508-18BCK	BCK	5/7/2008 19:04:00	1.28	3.17	296.8				79	40.3	7.1	-6.7	-45						
080508-2BCK	BCK	5/7/2008 19:34:00	1.27	3.14	319.9				101	51.5	7.5	-6.9	-48						
080508-19BCK	BCK	5/7/2008 19:35:00	1.27	3.14	302.9				61	31.1	7.1	-6.9	-48						
080508-20BCK	BCK	5/7/2008 20:04:00	1.28	3.17	249.4				61	31.1	7.1	-7.1	-48						
080508-21BCK	BCK	5/7/2008 20:34:00	1.35	3.99	288.9				82	41.8	7.2	-7.1	-48						
080508-22BCK	BCK	5/7/2008 21:04:00	1.30	3.48	290.4				42	21.4	7.1	-7.1	-47						
080508-23BCK	BCK	5/7/2008 21:34:00	1.24	2.78	304.1				74	37.7	7.2	-6.8	-45						
080508-24BCK	BCK	5/7/2008 22:04:00	1.17	2.15	311.9				67	34.2	7.0	-6.7	-43						
080508-3BCK	BCK	5/8/2008 1:34:00	0.96	0.74	419.2				62	31.6	7.2	-6.2	-39						
080508-4BCK	BCK	5/8/2008 7:34:00	1.62	8.16	424.3				157	80.1	6.9	-5.5	-32						
080508-5BCK	BCK	5/8/2008 13:34:00	1.00	0.96	441.1				217	110.7	6.8	-5.3	-30						
080512D	BCK	5/12/2008 14:46:00	0.79	0.14	1130.0	17.2	7.90	84.1	185	94.4	8.2	-6.9	-46						
080520-1BCK	BCK	5/12/2008 14:46:00	0.79	0.14	1105.0				74	37.7	7.6	-7.1	-47						
080520-2BCK	BCK	5/13/2008 0:46:00	0.77	0.10	1185.0				32	16.3	7.9	-6.9	-47						
080520-7BCK	BCK	5/13/2008 7:50:00	0.85	0.31	995.0				61	31.1	8.1	-4.2	-30						
080520-8BCK	BCK	5/13/2008 8:20:00	1.00	0.93	802.0				91	46.4	7.8	-4.7	-32						
080520-9BCK	BCK	5/13/2008 8:50:00	1.18	2.24	495.0				366	186.7	8.0	-4.0	-23						
080520-10BCK	BCK	5/13/2008 9:20:00	1.21	2.52	415.0				182	92.8	7.5	-4.0	-21						
080520-11BCK	BCK	5/13/2008 9:50:00	1.13	1.81	475.0				116	59.2	7.9	-4.1	-23						
080520-12BCK	BCK	5/13/2008 10:20:00	1.07	1.36	435.0				96	49.0	7.5	-4.0	-21						

Sample ID	Site	Date and Time	USGS Stage (m)	USGS Discharge (cms)	SpC (µS/cm)	Temperature (°C)	DO (ppm)	DO (% sat)	Turbidity (NTU)	Calculated TSS (ppm)	pH	δ ¹⁸ O (‰)	δD (‰)	NH ₄ ⁺ -N (ppm)	Cl (ppm)	NO ₃ ⁻ -N (ppm)	Total PO ₄ ³⁻ (ppm)	<i>E. coli</i> (cfu/100mL)	Total Coliforms (cfu/100mL)
080520-3BCK	BCK	5/13/2008 10:46:00	1.03	1.13	500.0				108	55.1	7.5	-4.5	-25						
080520-13BCK	BCK	5/13/2008 10:50:00	1.02	1.08	425.0				101	51.5	7.3	-2.5	-21						
080520-14BCK	BCK	5/13/2008 11:20:00	0.98	0.85	415.0				119	60.7	7.5	-2.3	-20						
080520-15BCK	BCK	5/13/2008 11:50:00	0.95	0.71	820.0				44	22.4	7.5	-4.2	-30						
080520-16BCK	BCK	5/13/2008 12:20:00	0.92	0.57	715.0				95	48.5	7.4	-4.2	-24						
080520-4BCK	BCK	5/13/2008 20:46:00	0.80	0.16	820.0				43	21.9	8.4	-4.6	-31						
080520-5BCK	BCK	5/14/2008 6:46:00	0.87	0.34	700.0				63	32.1	7.7	-4.6	-29						
080520-6BCK	BCK	5/14/2008 16:46:00	0.87	0.34	975.0				29	14.8	8.0	-5.5	-33						
080520B	BCK	5/20/2008 12:28:00	0.74	0.06	1549.0	18.7	7.07	75.3	26	13.3	7.4	-6.1	-42						
080617A	BCK	6/17/2008 12:01:00	0.70	0.02	1387.0	20.9	5.58	62.3	9	4.6	6.9	-5.7	-38						
080620B	BCK	6/20/2008 13:30:00	0.78	0.12	535.0	23.3			18	9.2		-5.8	-40						
080624-11B	BCK	6/20/2008 13:37:00	0.77	0.11	466.0	23.3			19	9.7	8.1	-5.7	-40						
080624-17B	BCK	6/20/2008 14:55:00	1.07	1.36	310.0	23.9			194	98.9	7.7	-7.7	-54						
080624-18B	BCK	6/20/2008 15:25:00	2.42	30.02	174.0	22.8			755	385.1	7.8	-8.9	-63						
080624-19B	BCK	6/20/2008 15:55:00	1.83	12.57	148.0	22.2			632	322.3	7.6	-9.0	-63						
080624-110B	BCK	6/20/2008 16:25:00	1.31	3.54	164.0	22.3			445	227.0	7.5	-8.9	-62						
080624-111B	BCK	6/20/2008 16:55:00	1.12	1.73	188.0	22.3			389	198.4	7.4	-8.8	-62						
080624-112B	BCK	6/20/2008 17:25:00	1.03	1.10	214.0	22.4			274	139.7	7.4	-8.7	-60						
080624-113B	BCK	6/20/2008 17:55:00	0.97	0.76	238.0	22.4			231	117.8	7.3	-8.7	-60						
080624-114B	BCK	6/20/2008 18:25:00	0.93	0.59	258.0	22.4			194	98.9	7.3	-8.6	-59						
080624-115B	BCK	6/20/2008 18:55:00	0.90	0.45	276.0	22.4			167	85.2	7.2	-8.5	-59						
080624-116B	BCK	6/20/2008 19:25:00	0.87	0.37	294.0	22.4			152	77.5	7.2	-8.5	-58						
080624-117B	BCK	6/20/2008 19:55:00	0.86	0.31	310.0	22.4			137	69.9	7.2	-8.4	-58						
080624-118B	BCK	6/20/2008 20:25:00	0.84	0.28	328.0	22.3			90	45.9	7.2	-8.3	-57						
080624-119B	BCK	6/20/2008 20:55:00	0.83	0.25	348.0	22.2			116	59.2	7.2	-8.3	-57						
080624-120B	BCK	6/20/2008 21:25:00	0.82	0.21	368.0	22.2			109	55.6	7.2	-8.2	-56						
080624-121B	BCK	6/20/2008 21:55:00	0.81	0.19	386.0	22.1			104	53.0	7.2	-8.1	-56						
080624-122B	BCK	6/20/2008 22:25:00	0.80	0.18	400.0	22.0			100	51.0	7.2	-8.1	-56						

Sample ID	Site	Date and Time	USGS Stage (m)	USGS Discharge (cms)	SpC (µS/cm)	Temperature (°C)	DO (ppm)	DO (% sat)	Turbidity (NTU)	Calculated TSS (ppm)	pH	δ ¹⁸ O (‰)	δD (‰)	NH ₄ ⁺ -N (ppm)	Cl (ppm)	NO ₃ ⁻ -N (ppm)	Total PO ₄ ³⁻ (ppm)	<i>E. coli</i> (cfu/100mL)	Total Coliforms (cfu/100mL)
080624-123B	BCK	6/20/2008 22:55:00	0.80	0.16	412.0	22.0			96	49.0	7.2	-8.1	-55						
080624-124B	BCK	6/20/2008 23:25:00	0.79	0.15	432.0	21.9			93	47.4	7.2	-7.9	-55						
080624-12B	BCK	6/21/2008 13:37:00	0.73	0.05	690.0	23.7			32	16.3	7.6	-7.4	-50						
080624-13B	BCK	6/22/2008 13:37:00	0.80	0.18	834.0	21.1			27	13.8	7.4	-6.4	-44						
080624-14B	BCK	6/23/2008 13:37:00	0.72	0.03	868.0	23.6			9	4.6	7.4	-5.7	-43						
080624C	BCK	6/24/2008 13:44:00	0.93	0.59	774.0	23.6			4	2.0	7.4	-5.7	-39						
080708A	BCK	7/8/2008 12:00:00	0.75	0.07	965.0	24.4	6.15	74.1	14	7.1	6.9	-4.4	-29						
080711-11B	BCK	7/8/2008 10:46:00	0.74	0.06	800.0	23.8			9	4.6	7.3	-4.4	-25						
080711-17B	BCK	7/8/2008 19:15:00	1.17	2.12	443.4	26.8			152	77.5	7.5	-6.3	-40						
080711-18B	BCK	7/8/2008 20:00:00	1.13	1.81	427.0	26.4			209	106.6	7.7	-6.3	-41						
080711-19B	BCK	7/8/2008 20:45:00	1.03	1.13	428.7	26.1			133	67.8	7.9	-6.3	-44						
080711-110B	BCK	7/8/2008 21:30:00	0.93	0.62	469.1	25.7			70	35.7	7.6	-6.7	-44						
080711-111B	BCK	7/8/2008 22:15:00	0.87	0.37	430.4	23.5			42	21.4	7.7	-6.8	-45						
080711-112B	BCK	7/8/2008 22:46:00	0.84	0.27	437.1	23.3			39	19.9	7.8	-6.6	-44						
080711-112B	BCK	7/8/2008 23:00:00	0.83	0.25	454.2	23.2			40	20.4	7.8	-6.7	-44						
080711-113B	BCK	7/8/2008 23:45:00	0.80	0.18	526.0	23.2			27	13.8	7.8	-6.5	-44						
080711-114B	BCK	7/9/2008 0:30:00	0.79	0.14	473.3	23.2			11	5.6	7.8	-6.5	-44						
080711-115B	BCK	7/9/2008 1:15:00	0.77	0.10	497.2	23.2			8	4.1	7.8	-6.5	-43						
080711-116B	BCK	7/9/2008 2:00:00	0.79	0.14	468.0	23.1			15	7.7	7.9	-6.3	-42						
080711-117B	BCK	7/9/2008 2:45:00	0.91	0.51	374.8	23.3			19	9.7	7.6	-6.3	-44						
080711-118B	BCK	7/9/2008 3:30:00	0.99	0.88	420.6	24.7			27	13.8	7.5	-6.4	-45						
080711-119B	BCK	7/9/2008 4:15:00	1.01	1.05	372.0	24.4			87	44.4	7.7	-6.8	-48						
080711-120B	BCK	7/9/2008 5:00:00	0.98	0.85	409.2	24.2			42	21.4	7.6	-6.9	-50						
080711-121B	BCK	7/9/2008 5:45:00	0.92	0.57	322.6	24.1			35	17.9	7.5	-6.8	-50						
080711-122B	BCK	7/9/2008 6:30:00	0.88	0.40	312.8	22.8			18	9.2	7.6	-7.1	-50						
080711-123B	BCK	7/9/2008 7:15:00	0.85	0.31	307.7	22.7			16	8.2	7.8	-6.9	-50						
080711-124B	BCK	7/9/2008 8:00:00	0.83	0.25	327.5	22.7			12	6.1	7.9	-6.9	-50						
080711-13B	BCK	7/9/2008 10:46:00	0.79	0.14	438.8	23.3			11	5.6	8	-6.8	-50						

Sample ID	Site	Date and Time	USGS Stage (m)	USGS Discharge (cms)	SpC (µS/cm)	Temperature (°C)	DO (ppm)	DO (% sat)	Turbidity (NTU)	Calculated TSS (ppm)	pH	δ ¹⁸ O (‰)	δD (‰)	NH ₄ ⁺ -N (ppm)	Cl (ppm)	NO ₃ ⁻ -N (ppm)	Total PO ₄ ³⁻ (ppm)	<i>E. coli</i> (cfu/100mL)	Total Coliforms (cfu/100mL)
080711-14B	BCK	7/9/2008 22:46:00	0.72	0.03	598.0	23.5			1	0.5	7.4	-6.4	-46						
080711-15B	BCK	7/10/2008 10:46:00	0.72	0.03	700.0	24.6			1	0.5	7.5	-6.2	-45						
080711-16B	BCK	7/10/2008 22:46:00	0.70	0.02	827.0	25.0			4	2.0	7.6	-6.0	-42						
080711B	BCK	7/11/2008 14:46:00	0.73	0.04	881.0	28.4	7.18	94.2	8	4.1	8.4	-5.5	-39						
080715-11B	BCK	7/11/2008 15:00:00	0.73	0.04	880.0	29.5			5	2.6	7	-5.3	-39						
080715-17B	BCK	7/11/2008 15:02:00	0.73	0.04	767.0	29.5			1	0.5	7	-5.5	-39						
080715-18B	BCK	7/11/2008 15:30:00	0.72	0.03	786.0	29.4			4	2.0	7	-5.4	-39						
080715-19B	BCK	7/11/2008 16:00:00	0.72	0.03	769.0	29.3			4	2.0	7	-5.4	-38						
080715-110B	BCK	7/11/2008 16:30:00	0.72	0.03	758.0	29.5			1	0.5	7	-5.4	-39						
080715-111B	BCK	7/11/2008 17:00:00	0.71	0.03	725.0	29.4			4	2.0	6.9	-5.4	-38						
080715-112B	BCK	7/11/2008 17:30:00	0.71	0.03	720.0	29.5			4	2.0	6.9	-5.5	-38						
080715-113B	BCK	7/11/2008 18:00:00	0.71	0.03	683.0	29.2			4	2.0	7.2	-5.4	-38						
080715-114B	BCK	7/11/2008 18:30:00	0.71	0.02	755.0	28.7			4	2.0	7.1	-5.3	-38						
080715-115B	BCK	7/11/2008 19:00:00	0.94	0.65	644.0	24.4			18	9.2	8.2	-4.9	-34						
080715-116B	BCK	7/11/2008 19:30:00	1.30	3.45	433.1	27.5			110	56.1	9.1	-3.5	-24						
080715-117B	BCK	7/11/2008 20:00:00	1.55	6.94	260.6	27.3			312	159.1	9.1	-2.7	-17						
080715-118B	BCK	7/11/2008 20:30:00	1.36	4.16	304.8	26.8			243	123.9	9	-2.9	-17						
080715-119B	BCK	7/11/2008 21:00:00	1.16	2.10	235.9	26.5			172	87.7	9	-2.8	-16						
080715-120B	BCK	7/11/2008 21:30:00	1.05	1.25	345.6	26.3			144	73.4	8.9	-3.2	-20						
080715-121B	BCK	7/11/2008 22:00:00	0.98	0.85	401.0	26.0			137	69.9	8.8	-3.2	-19						
080715-122B	BCK	7/11/2008 22:30:00	0.93	0.59	395.8	25.9			120	61.2	8.8	-3.1	-19						
080715-123B	BCK	7/11/2008 23:00:00	0.90	0.48	386.0	24.7			133	67.8	8.8	-3.1	-18						
080715-124B	BCK	7/11/2008 23:30:00	0.87	0.37	396.6	24.2			117	59.7	8.9	-3.1	-18						
080715-12B	BCK	7/12/2008 15:00:00	0.73	0.04	611.0	27.0			10	5.1	8.7	-3.9	-26						
080715-13B	BCK	7/13/2008 15:00:00	0.71	0.03	584.0	25.5			3	1.5	7.1	-3.8	-25						
080715-14B	BCK	7/14/2008 15:00:00	0.70	0.02	788.0	26.7			3	1.5	7	-4.3	-30						
080715B	BCK	7/15/2008 12:50:00	0.69	0.01	1063.0	26.0	5.80	65.0	4	2.0	7.7	-4.7	-33						
080911A	BCK	9/11/2008 11:40:00	0.71	0.01	1401.0	20.9	7.38	84.5	17	8.7	7.3	-5.2	-38	0.21	194	3.6	0.43	1732.9	>2419.6

Sample ID	Site	Date and Time	USGS Stage (m)	USGS Discharge (cms)	SpC (µS/cm)	Temperature (°C)	DO (ppm)	DO (% sat)	Turbidity (NTU)	Calculated TSS (ppm)	pH	δ ¹⁸ O (‰)	δD (‰)	NH ₄ ⁺ -N (ppm)	Cl (ppm)	NO ₃ ⁻ -N (ppm)	Total PO ₄ ³⁻ (ppm)	<i>E. coli</i> (cfu/100mL)	Total Coliforms (cfu/100mL)
080915A	BCK	9/14/2008 9:00:00	4.58	165.65†	303.1				3820	1948.2		-9.4	-65						
080915B	BCK	9/14/2008 9:00:00	4.58	165.65†	275.3				4012	2046.1		-9.4	-66						
080916B	BCK	9/16/2008 12:30:00	0.70	0.01	1185.0	19.8			4	2.0		-7.5	-52						
080919A	BCK	9/19/2008 9:00:00	0.71	0.01	1390.0	18.4			24	12.2		-7.1	-50						
080920A	BCK	9/20/2008 9:30:00	0.71	0.01	1430.0	19.1													
080925A	BCK	9/25/2008 12:25:00	0.71	0.02	1477.0	20.9	5.70	85.0	13	6.6	6.8	-6.9	-48	0.24	195.2	0.43	0.31	241.1	>2419.6
081009A	BCK	10/9/2008 9:25:00	0.72	0.02	799.0	15.5	5.58	55.0	5	2.6	7.7	-6.4	-43	0.28	88	0.31	0.4	1299.7	>2419.6
081023A	BCK	10/23/2008 10:15:00	1.25	2.89	345.6	11.9	9.26	90.0	391	199.4	9.0	-5.4	-28	1.69	36	0.14	2.7	>2419.6	>2419.6
081106A	BCK	11/6/2008 8:50:00	0.78	0.10	772.0	14.3	5.82	56.7	4.62	2.4	7.7	-7.0	-46	4.75	118.8	1.57	1.59	>2419.6	>2419.6
081120A	BCK	11/20/2008 9:15:00	0.71	0.01	766.0	6.0	5.59	68.8	4.7	2.4	7.8	-8.5	-60	1.53	168	1.367	0.51	344.8	>2419.6
081204A	BCK	12/4/2008 10:05:00	0.73	0.02	930.0	2.8	11.94	86.3	41	20.9	7.6	-9.9	-72	1.02	293	1.37	0.31	517.2	>2419.6
081218A	BCK	12/18/2008 10:05:00	0.71	0.02	4411.0	1.0	11.54	82.0	6.5	3.3	7.1	-7.7	-51	1.42	2440	0.57	0.42	>2419.6	>2419.6

Appendix K: Spring Data

Sample ID	Site	Date and Time	Feature Type	SpC (µS/cm)	Temperature (°C)	DO (ppm)	DO (% sat)	Turbidity (NTU)	TSS (ppm)	pH	δ ¹⁸ O (‰)	δD (‰)	NH ₄ ⁺ -N (ppm)	Cl (ppm)	NO ₃ ⁻ -N (ppm)	Total PO ₄ ³⁻ (ppm)	<i>E. coli</i> (cfu/100mL)	Total Coliforms (cfu/100mL)
100621A	LaSalle Spring	6/21/2010 10:00:00	Spring	616	12.5			6.0			-7.0	-45	0.00	100.0	0.60	0.14	272.3	>2419.6
100621B	Rockwoods Spring	6/21/2010 10:30:00	Spring	568	12.6			5.0			-7.0	-45	0.02	44.0	0.10	0.19	68.3	>2419.6
100621C	Lewis Spring	6/21/2010 11:00:00	Spring	599	15.2			10.0			-6.3	-42	0.03	120.0	2.60	0.29	410.6	>2419.6
100621D	Beaumont Spring	6/21/2010 11:30:00	Spring	371	13.7			4.0			-7.1	-45	0.01	34.0	0.20	0.41	58.3	>2419.6
100621E	Petty Spring	6/21/2010 12:00:00	Spring	590	15.3			10.0			-6.1	-40	0.06	104.0	3.00	0.31	235.9	>2419.6
100621F	Rott Spring	6/21/2010 13:30:00	Spring	1030	14.0			45.0			-6.7	-44	0.09	208.0	0.80	0.15	41.0	>2419.6
100621G	Blackburn Spring	6/21/2010 15:00:00	Spring	987	15.4			5.0			-6.7	-43	0.11	164.0	2.30	0.24	770.1	>2419.6
100709C	Dripping Spring	7/9/2010 12:56:00	Spring	710	16.1	6.08	61.5	9.0	19.0	6.94	-7.2	-48	0.19	16.0	3.30	0.33	2419.6	>2419.6
100709D	Francis Park Spring	7/9/2010 14:36:00	Spring	989	17.4	1.34	14.0	4.0	45.6	7.39	-7.0	-47	0.04	28.0	5.00	0.30	27.9	>2419.6
100709E	Blackburn Spring	7/9/2010 15:00:00	Spring	456	16.5	3.73	37.9	4.0	15.0	7.18	-8.0	-58	0.28	27.0	0.90	0.23	2419.6	>2419.6
100709F	Grants Trail Spring	7/9/2010 15:30:00	Spring	989	16.1	2.02	19.9	3.0	19.0	7.21	-7.0	-44	0.07	15.0	3.10	0.12	191.8	>2419.6
100709G	Grasso Spring	7/9/2010 16:00:00	Spring	1217	19.4	5.35	58.2	8.0	4.0	7.16	-6.7	-43	0.07	29.0	4.40	0.85	2419.6	>2419.6
100709H	Sylvan Spring	7/9/2010 16:30:00	Spring	809	16.5	4.41	45.2	17.0		7.51	-7.6	-52	0.27	27.0	3.50	0.32	2419.6	>2419.6
100716A	Weldon Spring	7/16/2010 14:15:00	Spring	261	13.7	2.83	28.4	20.0		7.06	-5.5	-40	0.23	6.0	0.60	0.30	16.1	1203.3
100716D	Lewis Spring	7/16/2010 15:40:00	Spring	748	15.1	5.77	57.2	5.0		7.71	-6.9	-46	0.05	65.0	1.90	0.14	344.8	>2419.6
100716F	LaSalle Spring	7/16/2010 17:00:00	Spring	722	12.9	6.27	58.7	4.0		7.38	-7.2	-47	0.04	9.0	1.30	0.14	88.0	>2419.6
100824E	Sylvan Spring	8/24/2010 14:15:00	Spring	1259	17.8	2.11	22.0	6.0	11.0	7.18	-6.5	-43	0.89	149.6	1.60	0.48	2419.6	>2419.6
100824Ea	Sylvan Spring 115' Downstream	8/24/2010 14:20:00	Spring			3.98	40.1											
100824F	Grants Trail Spring	8/24/2010 15:00:00	Spring	1163	15.7	1.79	17.9	3.0	20.0	7.21	-6.9	-43	0.09	111.6	2.30	0.13	45.0	>2419.6
100824G	Blackburn Spring	8/24/2010 15:30:00	Spring	1158	16.7	3.22	33.5	8.0	7.0	7.28	-6.7	-42	0.17	106.4	2.30	0.21	1299.7	>2419.6
100827A	Rockwoods Spring	8/27/2010 10:50:00	Spring	707	14.2	5.96	57.9	5.0	2.0	7.38	-6.5	-40	0.08	17.5	0.40	0.20	101.7	>2419.6
100827Aa	Rockwoods Spring 60' Downstream	8/27/2010 10:52:00	Spring	703	14.3	6.11	59.7			7.75								
100827Ab	Rockwoods Spring 280' Downstream	8/27/2010 10:57:00	Spring	703	15.4	7.01	70.1			7.81								
100827Ac	Rockwoods Spring 500' Downstream	8/27/2010 11:00:00	Spring	705	15.0	7.15	70.7			7.95								
100827Ad	Rockwoods Spring 900' Downstream	8/27/2010 11:03:00	Spring	693	15.1	7.00	70.3			8.03								
100827Ae	Rockwoods Spring 1260' Downstream	8/27/2010 11:07:00	Spring	702	15.3	7.04	70.5			8.05								

Sample ID	Site	Date and Time	Feature Type	SpC (µS/cm)	Temperature (°C)	DO (ppm)	DO (% sat)	Turbidity (NTU)	TSS (ppm)	pH	δ ¹⁸ O (‰)	δD (‰)	NH ₄ ⁺ -N (ppm)	Cl (ppm)	NO ₃ ⁻ -N (ppm)	Total PO ₄ ³⁻ (ppm)	<i>E. coli</i> (cfu/100mL)	Total Coliforms (cfu/100mL)
100827B	LaSalle Spring	8/27/2010 11:20:00	Spring	736	13.1	6.57	62.4	4.0	8.0	7.71	-6.8	-44	0.08	10.7	0.90	0.25	184.2	>2419.6
100827D	Steeleville Spring	8/27/2010 14:45:00	Spring	327	13.4	4.29	41.0	4.0	1.0	7.59	-7.0	-45	0.05	0.6	0.70	0.11	307.6	>2419.6
100827E	Maramec Spring	8/27/2010 15:30:00	Spring	319	14.4	3.63	35.5	3.0	1.0	7.81	-7.0	-44	0.03	1.9	0.60	0.06	6.3	222.4
100827Ea	Maramec Spring 900' Downstream	8/27/2010 15:40:00	Spring			4.36	42.5											
100919E	Kiefer Spring	9/19/2010 11:30:00	Spring	499	14.7	6.61	63.9	55.0	31.0	7.22	-3.4	-18	1.32	41.6	4.90	0.21	2419.6	>2419.6
100919G	Rockwoods Spring (filtered)	9/19/2010 12:15:00	Spring	498	14.0	4.34	42.0	68.0	22.0	7.59	-6.1	-38	0.48	23.1	2.70	0.20	2419.6	>2419.6
101002A	Bluegrass Spring	10/2/2010 11:00:00	Spring	868	14.1	4.64	44.7	9.0	6.0	7.51	-7.1	-46	0.06	99.5	1.80	0.10	34.5	>2419.6
101002E	Williams Spring	10/2/2010 14:20:00	Spring	664	14.4	4.45	44.1	18.0	225.0	7.55	-6.3	-42	0.41	13.9	2.10	0.76	56.3	>2419.6
101002G	Kiefer Spring	10/2/2010 15:05:00	Spring	806	14.6	5.09	50.1	4.0	4.0	7.65	-7.1	-47	0.04	44.5	2.60	0.12	51.2	770.1
101002I	Ranger Station Spring	10/2/2010 15:25:00	Spring	822	13.6	4.47	42.7	7.0	11.0	7.56	-7.4	-46	0.05	50.9	1.40	0.27	162.4	2419.6
101022A	Lewis Spring	10/22/2010 11:50:00	Spring	859	14.8	7.64	75.7	4.0	2.0	7.43	-6.7	-43	0.00	78.7	3.70	0.13	101.9	1203.3
101022B	Rockwoods Spring	10/22/2010 12:15:00	Spring	921	13.3	6.66	65.1	5.0	4.0	7.44	-6.7	-40	0.02	36.7	1.10	0.16	24.9	172.0
101022Ba	Rockwoods Spring 20' Downstream	10/22/2010 12:25:00	Spring	918	13.5	7.87	75.6			7.46								
101022Bb	Rockwoods Spring 50' Downstream	10/22/2010 12:30:00	Spring	910	13.6	8.22	79.0			7.48								
101022Bc	Rockwoods Spring 100' Downstream	10/22/2010 12:35:00	Spring	907	13.7	9.03	87.0			7.64								
101022Bd	Rockwoods Spring 200' Downstream	10/22/2010 12:40:00	Spring	918	14.2	9.11	91.2			7.84								
101022Be	Rockwoods Spring 500' Downstream	10/22/2010 12:50:00	Spring	903	15.3	9.23	91.7			7.98								
101022Bf	Rockwoods Spring 1250' Downstream	10/22/2010 13:00:00	Spring	919	14.0	8.51	82.2			8.17								
101022C	Kratz Spring	10/22/2010 15:00:00	Spring	379	14.5	1.23	11.5	20.0	31.0	8.13	-6.2	-42	0.19	0.6	1.20	0.72	23.3	727.0
101022E	Elm Spring	10/22/2010 17:30:00	Spring	489	13.6	7.08	64.1	6.0	9.0	7.50	-6.7	-41	0.02	9.7	1.70	0.06	7.5	146.7
110801Aa	Bluegrass Spring, Spring Orifice	8/1/2011 10:05:00	Spring	808	13.7	8.17	79.5	4.0		7.26	-7.2	-45		81.0	1.00			
110801Ab	Bluegrass Spring Downstream 65'	8/1/2011 10:15:00	Spring	798	14.0	8.36	80.8	3.0		7.38								
110801Ac	Bluegrass Spring Downstream 125'	8/1/2011 10:20:00	Spring	809	14.3	10.15	99.5			7.63								
110801Ad	Bluegrass Spring Downstream 185'	8/1/2011 10:30:00	Spring	777	14.6	10.48	102.3			7.69								
110801Ae	Bluegrass Spring, Spring Orifice (Redo)	8/1/2011 10:40:00	Spring	807	13.4	7.89	76.5			7.33								
110801Af	Bluegrass Spring Sinkhole 30' Behind Orifice	8/1/2011 10:50:00	Spring	818	13.5	8.34	79.1			7.32								
110801Ba	Rockwoods Spring, Spring Orifice	8/1/2011 12:00:00	Spring	906	14.7	8.52	83.4	2.0		7.40	-6.5	-44		92.4	1.10			
110801Bb	Rockwoods Spring 20' Downstream	8/1/2011 12:05:00	Spring	906	15.3	8.77	87.0			7.44								

Sample ID	Site	Date and Time	Feature Type	SpC (µS/cm)	Temperature (°C)	DO (ppm)	DO (% sat)	Turbidity (NTU)	TSS (ppm)	pH	δ ¹⁸ O (‰)	δD (‰)	NH ₄ ⁺ -N (ppm)	Cl (ppm)	NO ₃ ⁻ -N (ppm)	Total PO ₄ ³⁻ (ppm)	<i>E. coli</i> (cfu/100mL)	Total Coliforms (cfu/100mL)
110801Bc	Rockwoods Spring 75' Downstream	8/1/2011 12:10:00	Spring	910	15.8	9.04	90.2			7.50								
110801Bd	Rockwoods Spring 190' Downstream	8/1/2011 12:15:00	Spring	881	18.1	8.07	84.7			7.78								
110801Bd'	Rockwoods Spring 190' Roadside Branch	8/1/2011 12:20:00	Spring	910	15.6	9.48	95.4			7.64								
110801Be	Rockwoods Spring 500' Downstream	8/1/2011 12:25:00	Spring	910	17.3	9.20	96.5			8.03								
110801Bf	Rockwoods Spring 900' Downstream	8/1/2011 12:30:00	Spring	881	18.2	9.25	97.0			8.16								
110801Bg	Rockwoods Spring 1300' Downstream	8/1/2011 12:35:00	Spring	907	18.8	9.13	99.3			8.23								
110801Bh	Rockwoods Spring, Spring Orifice (Redo)	8/1/2011 12:45:00	Spring	909	14.7	8.56	84.6			7.44								
110801Da	Maramec Spring, Spring Orifice	8/1/2011 16:55:00	Spring	314	14.3	6.66	64.7	2.0		7.16	-6.7	-42		5.5	2.30			
110801Db	Maramec Spring 245' Downstream	8/1/2011 17:00:00	Spring	314	14.9	6.65	64.2			7.21								
110801Dc	Maramec Spring 370' Downstream	8/1/2011 17:10:00	Spring	309	14.3	8.13	80.0			7.31								
110801Dd	Maramec Spring 440' Downstream	8/1/2011 17:15:00	Spring	306	14.5	8.65	84.6			7.37								
110801De	Maramec Spring 900' Downstream	8/1/2011 17:25:00	Spring	310	14.5	9.05	87.5			7.47								
110801Df	Maramec Spring 1250' Downstream	8/1/2011 17:35:00	Spring	310	14.4	9.70	95.3			7.38								
110801Dg	Maramec Spring 1900' Downstream	8/1/2011 17:40:00	Spring	309	15.7	10.13	101.4			7.52								
110801Dh	Maramec Spring 3000' Downstream	8/1/2011 17:50:00	Spring	311	14.7	9.66	95.1			7.46								
110801Di	Maramec Spring, Spring Orifice (Redo)	8/1/2011 18:00:00	Spring	311	14.3	6.66	64.8			7.22								
110801E	Second Spring at Maramec Spring Park	8/1/2011 17:45:00	Spring	408	13.2	8.63	82.6	1.0		7.48	-7.0	-45		3.9	0.40			
110801Fa	Steelville Spring, Spring Orifice	8/1/2011 19:00:00	Spring	340	13.3	8.15	79.7	3.0		7.29	-6.9	-44		2.7	0.70			
110801Fb	Steelville Spring 50' Downstream	8/1/2011 19:05:00	Spring	338	13.3	8.52	81.6			7.31								
110801Fc	Steelville Spring 140' Downstream	8/1/2011 19:10:00	Spring	342	13.4	8.59	80.1			7.36								
110801Fd	Steelville Spring 415' Downstream	8/1/2011 19:15:00	Spring	340	13.6	10.05	98.2			7.52								
110803Aa	Blackburn Spring, Spring Orifice	8/3/2011 9:35:00	Spring	1416	15.1	5.64	57.5	3.0		6.99	-6.9	-45		172.5	2.30			
110803Ab	Blackburn Spring 30' Downstream	8/3/2011 9:40:00	Spring	1405	16.2	6.31	64.2			7.01								
110803Ac	Blackburn Spring 90' Downstream	8/3/2011 9:45:00	Spring	1404	16.6	6.43	65.2			7.15								
110803Ad	Blackburn Spring 175' Downstream	8/3/2011 9:55:00	Spring	1406	17.0	7.22	75.2			7.25								
110803Ae	Blackburn Spring 250' Downstream	8/3/2011 10:05:00	Spring	1405	17.3	7.99	83.0			7.37								
110803Da	Sylvan Spring, Spring Orifice	8/3/2011 12:50:00	Spring	1253	16.4	7.22	74.1	2.0		6.93	-6.6	-43		148.0	3.40			
110803Db	Sylvan Spring 30' Downstream	8/3/2011 12:55:00	Spring	1260	17.0	7.00	75.8			6.99								

Sample ID	Site	Date and Time	Feature Type	SpC (µS/cm)	Temperature (°C)	DO (ppm)	DO (% sat)	Turbidity (NTU)	TSS (ppm)	pH	δ ¹⁸ O (‰)	δD (‰)	NH ₄ ⁺ -N (ppm)	Cl (ppm)	NO ₃ ⁻ -N (ppm)	Total PO ₄ ³⁻ (ppm)	<i>E. coli</i> (cfu/100mL)	Total Coliforms (cfu/100mL)
110803De	Sylvan Spring 80' Downstream	8/3/2011 13:00:00	Spring	1260	17.5	8.50	89.0			7.07								
110803Dd	Sylvan Spring 210' Downstream	8/3/2011 13:05:00	Spring	1257	19.6	10.60	113.4			7.24								
110803De	Sylvan Spring, Spring Orifice (Redo)	8/3/2011 13:15:00	Spring	1265	16.3	7.25	75.0			6.98								
110818Aa	Mastodon Spring, Cave Orifice	8/18/2011 10:10:00	Spring	750	13.8	8.72	84.2			7.23								
110818Ab	Mastodon Spring, Spring Orifice	8/18/2011 10:15:00	Spring	747	13.9	8.72	84.3	2.0		7.18	-6.6	-42		33.4	2.60		114.3	400.0
110818Ac	Mastodon Spring 75' Downstream	8/18/2011 10:20:00	Spring	748	14.0	9.33	90.5			7.27								
110818B	Lithium Spring	8/18/2011 12:15:00	Spring	1524	14.3	2.98	29.2	1.0		6.98	-6.5	-41		204.0	1.20		0.0	0.0
110818Ga	Pevely/Milkfarm Spring, Spring Orifice	8/18/2011 15:45:00	Spring	730	14.1	8.14	79.4	2.0		6.96	-6.4	-42		28.0	1.50		0.0	300.0
110818Gb	Pevely/Milkfarm Spring 150' Downstream	8/18/2011 15:50:00	Spring	730	14.5	9.75	97.5			7.17								
110825Aa	Glatt's Spring, Spring Orifice	8/18/2011 15:00:00	Spring	723	14.1	7.82	76.3	1.0	3.0	7.04	-6.4	-42	0.05	11.0	1.50	0.25	36.9	1119.9
110825Ab	Glatt's Spring 30' Downstream	8/18/2011 15:05:00	Spring	724	14.1	9.51	93.4	1.0		7.09								
110825Ac	Glatt's Spring 250' Downstream	8/18/2011 15:20:00	Spring	729	15.3	9.02	90.2			7.31								
110825Ad	Glatt's Spring 775' Downstream	8/18/2011 15:30:00	Spring	728	16.3	9.48	97.4	2.0	8.0	7.47	-6.4	-42	0.07	12.0	1.20	0.15	75.4	>2419.6
110825Ae	Glatt's Spring 775' Downstream (Redo)	8/18/2011 14:45:00	Spring	729	16.5	10.14	104.5			7.26								
100709I	Cliff Cave Spring	7/9/2010 17:15:00	Cave	614	16.7	8.92	87.0	20.0		7.92	-7.3	-49	0.31	19.0	0.00	0.46	2419.6	>2419.6
100716E	Babler Spring	7/16/2010 16:25:00	Cave	532	12.4	6.79	63.7	5.0		7.70	-7.3	-46	0.03	0.1	1.00	0.10	14.5	1413.6
100824A	Double Drop Spring Cave	8/24/2010 11:00:00	Cave	916	14.0	7.20	69.6	7.0	9.0	7.89	-6.1	-43	0.14	80.8	2.10	0.15	488.4	>2419.6
100824Aa	Double Drop Spring Cave 5' Downstream	8/24/2010 11:15:00	Cave	918	14.1	7.42	72.3			7.89								
100824Ab	Double Drop Spring Cave 10' Downstream	8/24/2010 11:30:00	Cave	916	14.2	6.86	67.1			7.90								
100824Ac	Double Drop Spring Cave 30' Downstream	8/24/2010 11:35:00	Cave	917	14.8	6.12	60.8			7.95								
100824B	Cliff Cave Spring	8/24/2010 12:00:00	Cave	875	16.1	7.26	73.6	8.0	6.0	8.18	-5.7	-41	0.12	67.6	1.70	0.22	410.6	>2419.6
100824Ba	Cliff Cave Spring 150' Downstream	8/24/2010 12:10:00	Cave	871	17.1	6.79	70.0			7.94								
100824C	Spit Cave	8/24/2010 12:30:00	Cave	977	15.1	6.08	60.1	21.0	52.0	8.06	-5.9	-41	0.32	88.0	1.60	0.47	686.7	>2419.6
100824Ca	Spit Cave in cave at triangular opening	8/24/2010 12:40:00	Cave	977	13.3	6.18	60.6			7.99								
100824D	Cave of the Falls	8/24/2010 13:30:00	Cave	1014	15.4	6.33	63.5	6.0	68.0	7.80	-6.1	-42	0.13	114.0	2.00	0.25	2419.6	>2419.6
100827C	Onondaga Cave Spring	8/27/2010 13:20:00	Cave	443	14.4	5.64	54.7	5.0	3.0	7.97	-6.6	-42	0.06	0.5	0.20	0.12	36.9	>2419.6
100827Ca	Onondaga Cave Spring Entrance	8/27/2010 13:40:00	Cave			6.46	61.8			7.97								
100827Cb	Onondaga Cave Spring 55' Downstream of 100827C	8/27/2010 13:30:00	Cave			8.08	80.2											

Sample ID	Site	Date and Time	Feature Type	SpC (µS/cm)	Temperature (°C)	DO (ppm)	DO (% sat)	Turbidity (NTU)	TSS (ppm)	pH	δ ¹⁸ O (‰)	δD (‰)	NH ₄ ⁺ -N (ppm)	Cl (ppm)	NO ₃ ⁻ -N (ppm)	Total PO ₄ ³⁻ (ppm)	<i>E. coli</i> (cfu/100mL)	Total Coliforms (cfu/100mL)	
100827Cc	Onondaga Cave Spring near Bridge	8/27/2010 13:35:00	Cave			7.43	72.0												
101022D	Lone Hill Onyx Cave	10/22/2010 16:45:00	Cave	481	11.9	10.04	94.0	10.0	126.0	8.14	-7.2	-46	0.08	0.8	0.30	0.19	90.6	>2419.6	
110801Ca	Babler Spring Orifice	8/1/2011 13:00:00	Cave	549	12.5	9.64	89.9	2.0		7.39	-7.0	-44		5.5	0.50				
110801Cb	Babler Spring 25' Downstream	8/1/2011 13:05:00	Cave	551	12.9	9.96	94.2			7.43									
110801Cc	Babler Spring 60' Downstream	8/1/2011 13:10:00	Cave	551	13.4	9.67	92.2			7.46									
110801Cd	Babler Spring 130' Downstream	8/1/2011 13:15:00	Cave	550	14.3	9.28	90.1			7.56									
110801Ce	Babler Spring 180' Downstream	8/1/2011 13:20:00	Cave	536	15.3	7.82	78.0			7.59									
110801Cf	Babler Spring 370' Downstream	8/1/2011 13:25:00	Cave	545	17.2	8.74	91.8			8.13									
110801Cg	Babler Spring, Spring Orifice (Redo)	8/1/2011 13:30:00	Cave	550	12.4	9.45	89.0			7.41									
110803Ba	Cliff Cave Spring, Spring Orifice	8/3/2011 10:45:00	Cave	927	16.9	9.41	97.3	4.0		8.13	-6.2	-40		68.5	1.80				
110803Bb	Cliff Cave Spring 30' Downstream	8/3/2011 10:55:00	Cave	916	17.0	9.82	101.4			8.16									
110803Bc	Cliff Cave Spring 150' Downstream	8/3/2011 11:05:00	Cave	911	17.5	9.74	101.5			8.24									
110803Bd	Cliff Cave Spring 300' Downstream	8/3/2011 11:15:00	Cave	908	18.1	9.21	97.7			8.20									
110803Be	Cliff Cave Spring 500' Downstream	8/3/2011 11:25:00	Cave	900	19.5	8.88	96.6			8.23									
110803Ca	Double Drop Spring Orifice	8/3/2011 11:35:00	Cave	941	14.0	10.16	98.5	4.0		7.72	-6.8	-43		65.5	2.70				
110803Cb	Double Drop Spring Cave 10' Downstream	8/3/2011 12:00:00	Cave	945	14.5	10.35	101.1			7.80									
110818C	Blue Spring Upper Resurgence	8/18/2011 12:50:00	Resurgence	379	23.6	2.65	30.3			7.91									
110818D	Blue Spring Lower Resurgence	8/18/2011 13:00:00	Resurgence	595	15.4	7.01	72.6	14.0		7.65	-5.2	-33		17.5	6.00		0.0	2000.0	
110818E	Keyhole Spring Upper Resurgence	8/18/2011 13:30:00	Resurgence	619	15.8	8.58	86.5	3.0		7.71	-5.2	-34		19.5	5.40		0.0	571.4	
110818F	Keyhole Spring Lower Resurgence	8/18/2011 13:55:00	Resurgence	624	14.6	7.27	72.0	4.0		7.72	-5.2	-34		24.5	5.90		100.0	5500.0	
100716B	Prairie Lake	7/16/2010 14:40:00	Lake	104	35.0	5.44	80.1	37.0		9.66	-3.2	-30	0.41	0.5	0.30	0.14	14.4	>2419.6	
111007A	LD26	10/7/2011 14:15:00	River	523	18.9	10.43	115.1	94.0	495.0	8.42	-7.4		1.24	28.0	2.90	0.80	1.0	770.1	
111007B	LBS	10/7/2011 15:00:00	River	715	19.8	8.23	102.2	119.0	392.0	8.23	-11.1		1.37	11.0	0.20	1.05	10.6	>2419.6	
100919F	Kiefer Creek upstream USGS gaging station	9/19/2010 11:42:00	Stream	191	20.1	5.45	59.3	577.0	598.0	7.95	-5.5	-35	0.48	10.4	0.80	1.07	2419.6	>2419.6	
101002B	LaBarque Creek	10/2/2010 12:15:00	Stream	410	14.3	6.53	63.6	7.0	1.0	7.75	-6.0	-40	0.10	15.2	0.40	0.11	53.7	>2419.6	
101002C	Fox Creek	10/2/2010 12:45:00	Stream	561	16.1	6.12	62.0	5.0	3.0	7.93	-6.3	-41	0.05	14.2	0.40	0.14	31.3	>2419.6	
101002D	Williams Creek	10/2/2010 14:06:00	Stream	594	15.2	5.49	54.9	8.0	13.0	8.07	-6.4	-42	0.06	15.4	1.50	0.18	313.0	>2419.6	
101002F	Fishpot Creek	10/2/2010 14:45:00	Stream	448	19.2	4.02	43.3	5.0	8.0	7.90	-5.6	-37	0.04	16.9	1.00	0.27	34.1	>2419.6	

Sample ID	Site	Date and Time	Feature Type	SpC (µS/cm)	Temperature (°C)	DO (ppm)	DO (% sat)	Turbidity (NTU)	TSS (ppm)	pH	δ ¹⁸ O (‰)	δD (‰)	NH ₄ ⁺ -N (ppm)	Cl (ppm)	NO ₃ ⁻ -N (ppm)	Total PO ₄ ³⁻ (ppm)	<i>E. coli</i> (cfu/100mL)	Total Coliforms (cfu/100mL)
101002H	Kiefer Creek upstream USGS gaging station	10/2/2010 15:12:00	Stream	805	15.1	5.55	54.9	4.0	7.0	7.80	-6.8	-45	0.04	27.3	1.20	0.17	80.9	>2419.6
101002J	Kiefer Creek swimming hole	10/2/2010 15:35:00	Stream	767	16.2	6.29	63.4	5.0	13.0	8.05	-6.7	-44	0.04	56.0	1.70	0.14	38.8	1732.9
110801G	Stream at Confluence with Steelville Spring Branch	8/1/2011 19:20:00	Stream	345	18.0	8.21	84.1	6.0		7.62								
100621A - Duplicate	LaSalle Spring	6/21/2010 10:00:00	QA/QC														209.8	>2419.6
100716A - lab duplicate with old collert	Weldon Spring	7/16/2010 14:15:00	QA/QC														12.2	1553.1
100716C - lab duplicate	Duckett Creek Treatment Plant #2	7/16/2010 15:00:00	QA/QC										0.27	66.0	16.80	5.20		
100716F - lab duplicate with old collert	LaSalle Spring	7/16/2010 17:00:00	QA/QC									-47					87.8	2419.6
100919G	Rockwoods Spring (unfiltered)	9/19/2010 12:15:00	QA/QC															
101002B	LaBarque Creek	10/2/2010 12:15:00	QA/QC															
101002C	Fox Creek	10/2/2010 12:45:00	QA/QC															
101002D	Williams Creek	10/2/2010 14:06:00	QA/QC															
101002F	Fishpot Creek	10/2/2010 14:45:00	QA/QC															
101002J	Kiefer Creek swimming hole	10/2/2010 15:35:00	QA/QC															

Sample ID	Site	Date and Time	Feature Type	B (ppm)	Ca (ppm)	K (ppm)	Mg (ppm)	Na (ppm)	S (ppm)	Si (ppm)	Sr (ppm)	Calculate HCO ₃ ⁻ (ppm)	Al (ppb)	Ba (ppb)	Cd (ppb)	Co (ppb)	Cr (ppb)	Cu (ppb)	Fe (ppb)	Ga (ppb)	Li (ppb)	Mn (ppb)	Mo (ppb)	Ni (ppb)	Pb (ppb)	Rb (ppb)	Zn (ppb)
100621A	LaSalle Spring	6/21/2010 10:00:00	Spring	0.0	100.6	1.8	11.2	26.4	8.6	4.1	0.1	231	20.5	82.6	0.1	0.1	2.8	0.9	27.3	1.8	0.5	5.5	0.3	3.4	0.0	0.4	2.3
100621B	Rockwoods Spring	6/21/2010 10:30:00	Spring	0.0	93.1	1.8	10.1	18.4	7.8	4.3	0.1	281	22.1	82.8	0.0	0.1	2.1	1.1	26.0	1.9	0.5	3.1	0.3	3.2	0.1	0.4	4.4
100621C	Lewis Spring	6/21/2010 11:00:00	Spring	0.0	76.8	4.0	13.5	61.7	13.4	3.9	0.2	214	47.3	109.0	0.2	0.2	2.1	2.1	23.8	2.3	1.7	7.3	1.1	3.4	0.2	1.1	12.3
100621D	Beaumont Spring	6/21/2010 11:30:00	Spring	0.0	82.7	1.3	10.5	7.4	8.6	4.9	0.1	235	22.3	70.7	0.1	0.1	3.2	0.6	27.3	1.6	0.4	20.9	0.7	7.1	0.0	0.3	1.6
100621E	Petty Spring	6/21/2010 12:00:00	Spring	0.0	73.1	4.1	12.2	63.7	13.4	4.0	0.2	230	63.1	102.0	0.0	0.1	3.3	1.4	24.2	2.0	1.6	6.8	1.3	3.1	0.2	0.9	3.2
100621F	Rott Spring	6/21/2010 13:30:00	Spring	0.0	126.2	2.0	28.1	121.7	22.8	5.4	0.3	407	1.3	115.0	0.5	0.4	6.2	4.0	80.2	2.2	2.7	253.0	2.0	6.2	3.4	0.5	40.8
100621G	Blackburn Spring	6/21/2010 15:00:00	Spring	0.1	154.0	2.0	21.7	86.9	41.5	6.9	0.3	371	25.5	95.3	0.1	0.3	2.6	1.2	53.9	1.9	3.2	79.5	0.4	5.9	0.4	0.6	7.5
100709C	Dripping Spring	7/9/2010 12:56:00	Spring	0.0	110.8	3.6	20.8	41.2	24.4	8.1	0.3	437	88.1	85.0	0.2	0.2	8.6	1.7	34.7	2.5	3.9	67.5	12.8	4.3	0.2	0.7	4.1
100709D	Francis Park Spring	7/9/2010 14:36:00	Spring	0.1	157.3	1.9	15.4	68.5	37.3	7.2	0.4	551	6.8	71.8	0.1	0.2	9.1	1.0	37.6	2.1	3.5	21.3	0.3	4.3	0.2	0.3	2.6
100709E	Blackburn Spring	7/9/2010 15:00:00	Spring	0.0	69.2	2.1	9.5	32.1	14.3	3.1	0.2	246	95.1	43.7	0.1	0.2	4.0	2.9	34.0	1.3	1.7	51.5	0.6	2.6	2.1	0.8	11.6
100709F	Grants Trail Spring	7/9/2010 15:30:00	Spring	0.0	151.5	1.4	23.2	67.3	28.1	7.2	0.3	626	9.7	86.7	0.1	0.2	11.4	0.6	32.7	2.7	3.4	16.9	0.5	4.2	0.2	0.4	36.3
100709G	Grasso Spring	7/9/2010 16:00:00	Spring	0.1	163.5	2.9	17.6	109.0	22.7	7.1	0.4	744	30.9	84.5	0.1	0.2	4.7	1.6	45.9	2.5	2.9	91.7	0.7	6.3	0.1	0.6	4.7

Sample ID	Site	Date and Time	Feature Type	B (ppm)	Ca (ppm)	K (ppm)	Mg (ppm)	Na (ppm)	S (ppm)	SI (ppm)	Sr (ppm)	Calculate HCO ₃ ⁻ (ppm)	Al (ppb)	Ba (ppb)	Cd (ppb)	Co (ppb)	Cr (ppb)	Cu (ppb)	Fe (ppb)	Ga (ppb)	Li (ppb)	Mn (ppb)	Mo (ppb)	Ni (ppb)	Pb (ppb)	Rb (ppb)	Zn (ppb)	
100709H	Sylvan Spring	7/9/2010 16:30:00	Spring	0.0	101.2	2.1	12.4	50.4	16.7	5.2	0.2	397	140.0	66.4	0.0	0.2	4.0	2.0	36.8	2.0	2.7	42.5	0.6	3.2	0.8	0.7	6.5	
100716A	Weldon Spring	7/16/2010 14:15:00	Spring	0.0	33.5	2.5	6.5	6.9	2.5	3.4	0.1	137	122.7	58.1	0.0	0.2	0.6	0.9	49.2	1.3	0.2	78.3	0.3	2.2	0.5	0.8	9.3	
100716D	Lewis Spring	7/16/2010 15:40:00	Spring	0.0	80.9	3.6	13.6	53.7	14.0	5.0	0.2	297	28.3	116.5	0.1	0.2	1.0	1.1	21.4	3.1	2.1	2.9	1.1	3.5	0.1	1.2	24.0	
100716F	LaSalle Spring	7/16/2010 17:00:00	Spring	0.0	100.1	1.9	13.1	30.0	10.1	5.4	0.1	399	13.0	92.6	0.0	0.2	1.0	0.6	26.0	2.5	1.0	9.0	0.7	3.8	0.0	0.5	1.0	
100824E	Sylvan Spring	8/24/2010 14:15:00	Spring	0.1	144.0	1.9	19.6	72.3	23.0	8.8	0.3	386	11.6	125.3	0.2	0.6	0.6	1.7	43.4	2.4	4.6	602.8	0.8	8.4	0.2	0.8	11.8	
100824Ea	Sylvan Spring 115' Downstream	8/24/2010 14:20:00	Spring																									
100824F	Grants Trail Spring	8/24/2010 15:00:00	Spring	0.0	143.7	1.3	22.1	63.1	25.7	8.8	0.3	428	5.5	117.4	0.1	0.2	0.5	1.1	39.1	2.4	4.1	33.8	0.7	5.9	0.1	0.5	6.3	
100824G	Blackburn Spring	8/24/2010 15:30:00	Spring	0.1	131.3	2.6	19.9	74.1	32.9	7.8	0.3	392	32.9	88.4	0.0	0.3	0.3	1.5	42.7	1.9	3.4	66.5	0.7	5.9	0.6	0.9	28.6	
100827A	Rockwoods Spring	8/27/2010 10:30:00	Spring	0.0	88.1	2.8	12.7	36.9	9.5	5.3	0.1	368	22.2	97.8	0.0	0.1	0.4	0.8	24.2	2.2	1.1	1.6	0.5	3.5	0.1	0.7	0.3	
100827Aa	Rockwoods Spring 60' Downstream	8/27/2010 10:52:00	Spring																									
100827Ab	Rockwoods Spring 280' Downstream	8/27/2010 10:57:00	Spring																									
100827Ac	Rockwoods Spring 500' Downstream	8/27/2010 11:00:00	Spring																									
100827Ad	Rockwoods Spring 900' Downstream	8/27/2010 11:03:00	Spring																									
100827Ae	Rockwoods Spring 1260' Downstream	8/27/2010 11:07:00	Spring																									
100827B	LaSalle Spring	8/27/2010 11:20:00	Spring	0.0	95.8	2.6	13.7	34.3	11.7	5.4	0.1	393	20.9	88.6	0.0	0.2	0.4	0.7	26.4	2.1	1.5	2.6	0.3	4.0	0.1	0.6	0.5	
100827D	Steeleville Spring	8/27/2010 14:45:00	Spring	0.0	35.9	1.1	18.7	0.3	1.3	4.1	0.0	200	23.3	49.7	0.0	0.1	0.8	0.4	11.1	1.3	BDL	0.7	0.1	2.0	0.1	0.9	23.9	
100827E	Maramec Spring	8/27/2010 15:30:00	Spring	0.0	32.6	1.2	17.1	1.8	1.5	3.7	0.0	183	13.5	53.2	0.0	0.1	0.4	0.3	10.2	1.4	0.1	0.8	0.2	1.6	0.1	1.0	20.0	
100827Ea	Maramec Spring 900' Downstream	8/27/2010 15:40:00	Spring																									
100919E	Kiefer Spring	9/19/2010 11:30:00	Spring	0.0	52.8	3.8	9.2	44.1	9.0	4.7	0.1	224	393.1	74.5	0.2	0.3	4.4	3.2	34.6	1.5	2.2	24.9	3.1	4.1	0.7	1.0	26.6	
100919G	Rockwoods Spring (filtered)	9/19/2010 12:15:00	Spring	0.1	71.6	3.3	8.8	28.5	6.0	5.4	0.1	280	11.0	72.5	0.2	0.3	4.0	2.5	21.7	1.8	0.9	14.4	4.3	4.5	0.1	0.6	43.5	
101002A	Bluegrass Spring	10/2/2010 11:00:00	Spring	0.0	96.1	2.3	17.1	66.5	8.1	5.6	0.2	357	16.6	116.0	0.0	0.1	1.0	0.9	21.5	2.2	1.0	6.9	0.3	3.2	0.1	0.6	2.1	
101002E	Williams Spring	10/2/2010 14:20:00	Spring	0.1	85.5	3.6	14.4	38.9	12.2	5.5	0.2	371	108.9	116.3	0.1	0.2	0.8	0.9	26.8	2.0	0.7	15.3	0.5	3.1	0.5	0.8	2.8	
101002G	Kiefer Spring	10/2/2010 15:05:00	Spring	0.0	92.7	3.6	16.2	67.7	18.8	5.3	0.2	401	10.4	122.9	0.0	0.2	0.7	1.2	24.2	2.6	4.5	15.5	0.5	3.4	0.2	1.0	1.0	
101002I	Ranger Station Spring	10/2/2010 15:25:00	Spring	0.0	100.8	1.8	16.0	61.8	12.8	6.3	0.1	418	13.1	120.2	0.1	0.1	0.3	0.7	22.9	2.1	0.9	15.6	0.2	3.8	0.2	0.5	2.7	
101022A	Lewis Spring	10/22/2010 11:50:00	Spring	0.0	90.5	3.9	16.4	60.6	20.3	5.0	0.2	312	8.6	131.8	0.0	0.2	1.7	0.7	24.9	2.6	5.8	2.1	0.6	3.7	0.0	1.3	1.0	
101022B	Rockwoods Spring	10/22/2010 12:15:00	Spring	0.0	105.0	3.1	18.2	59.8	11.9	5.6	0.2	466	11.9	121.1	0.0	0.2	1.6	0.6	30.3	2.5	1.6	1.1	0.5	4.0	0.0	0.8	0.0	
101022Ba	Rockwoods Spring 20' Downstream	10/22/2010 12:25:00	Spring																									
101022Bb	Rockwoods Spring 50' Downstream	10/22/2010 12:30:00	Spring																									

Sample ID	Site	Date and Time	Feature Type	B (ppm)	Ca (ppm)	K (ppm)	Mg (ppm)	Na (ppm)	S (ppm)	SI (ppm)	Sr (ppm)	Calculate HCO ₃ ⁻ (ppm)	Al (ppb)	Ba (ppb)	Cd (ppb)	Co (ppb)	Cr (ppb)	Cu (ppb)	Fe (ppb)	Ga (ppb)	Li (ppb)	Mn (ppb)	Mo (ppb)	Ni (ppb)	Pb (ppb)	Rb (ppb)	Zn (ppb)	
101022Bc	Rockwoods Spring 100' Downstream	10/22/2010 12:35:00	Spring																									
101022Bd	Rockwoods Spring 200' Downstream	10/22/2010 12:40:00	Spring																									
101022Be	Rockwoods Spring 500' Downstream	10/22/2010 12:50:00	Spring																									
101022Bf	Rockwoods Spring 1250' Downstream	10/22/2010 13:00:00	Spring																									
101022C	Kratz Spring	10/22/2010 15:00:00	Spring	0.0	39.4	2.6	20.3	14.3	1.6	6.8	0.1	257	39.4	99.7	0.0	0.9	0.5	0.4	75.2	2.1	0.2	253.9	0.4	2.1	0.8	1.0	0.7	
101022E	Elm Spring	10/22/2010 17:30:00	Spring	0.0	48.4	1.5	22.5	21.3	2.1	4.8	0.1	295	15.0	75.5	0.0	0.1	1.5	0.5	14.5	1.7	0.6	1.1	0.1	2.2	0.1	1.1	12.2	
110801Aa	Bluegrass Spring Orifice	8/1/2011 10:05:00	Spring	0.0	101.1	1.9	17.1	48.2	6.7	9.8	0.2	359	22.6	79.5	0.1	0.2	0.0	1.1	23.7	1.2	1.4	4.8	0.3	5.7	0.3	0.5	0.5	
110801Ab	Bluegrass Spring Downstream 65'	8/1/2011 10:15:00	Spring																									
110801Ac	Bluegrass Spring Downstream 125'	8/1/2011 10:20:00	Spring																									
110801Ad	Bluegrass Spring Downstream 185'	8/1/2011 10:30:00	Spring																									
110801Ae	Bluegrass Spring Orifice (Redo)	8/1/2011 10:40:00	Spring																									
110801Af	Bluegrass Spring Sinkhole 30' Behind Orifice	8/1/2011 10:50:00	Spring																									
110801Ba	Rockwoods Spring Orifice	8/1/2011 12:00:00	Spring	0.0	108.3	3.4	18.5	61.8	9.9	13.6	0.3	396	4.5	100.7	0.0	0.2	0.0	1.1	28.3	1.8	2.9	1.1	0.5	7.4	0.0	0.8	0.2	
110801Bb	Rockwoods Spring 20' Downstream	8/1/2011 12:05:00	Spring																									
110801Bc	Rockwoods Spring 75' Downstream	8/1/2011 12:10:00	Spring																									
110801Bd	Rockwoods Spring 190' Downstream	8/1/2011 12:15:00	Spring																									
110801Bd'	Rockwoods Spring 190' Roadside Branch	8/1/2011 12:20:00	Spring																									
110801Be	Rockwoods Spring 500' Downstream	8/1/2011 12:25:00	Spring																									
110801Bf	Rockwoods Spring 900' Downstream	8/1/2011 12:30:00	Spring																									
110801Bg	Rockwoods Spring 1300' Downstream	8/1/2011 12:35:00	Spring																									
110801Bh	Rockwoods Spring Orifice (Redo)	8/1/2011 12:45:00	Spring																									
110801Da	Maramec Spring Orifice	8/1/2011 16:55:00	Spring	0.0	36.9	1.7	16.2	3.9	1.4	3.4	0.1	192	7.1	68.8	3.9	0.2	0.2	2.7	13.0	1.7	5.0	1.3	0.3	6.8	0.5	1.2	140.6	
110801Db	Maramec Spring 245' Downstream	8/1/2011 17:00:00	Spring																									

Sample ID	Site	Date and Time	Feature Type	B (ppm)	Ca (ppm)	K (ppm)	Mg (ppm)	Na (ppm)	S (ppm)	SI (ppm)	Sr (ppm)	Calculate HCO ₃ ⁻ (ppm)	Al (ppb)	Ba (ppb)	Cd (ppb)	Co (ppb)	Cr (ppb)	Cu (ppb)	Fe (ppb)	Ga (ppb)	Li (ppb)	Mn (ppb)	Mo (ppb)	Ni (ppb)	Pb (ppb)	Rb (ppb)	Zn (ppb)		
110801Dc	Maramec Spring 370' Downstream	8/1/2011 17:10:00	Spring																										
110801Dd	Maramec Spring 440' Downstream	8/1/2011 17:15:00	Spring																										
110801De	Maramec Spring 900' Downstream	8/1/2011 17:25:00	Spring																										
110801Df	Maramec Spring 1250' Downstream	8/1/2011 17:35:00	Spring																										
110801Dg	Maramec Spring 1900' Downstream	8/1/2011 17:40:00	Spring																										
110801Dh	Maramec Spring 3000' Downstream	8/1/2011 17:50:00	Spring																										
110801Di	Maramec Spring Orifice (Redo)	8/1/2011 18:00:00	Spring																										
110801E	Second Spring at Maramec Spring Park	8/1/2011 17:45:00	Spring	0.0	47.1	0.8	21.6	3.0	1.1	10.2	0.1	250	10.0	32.8	0.1	0.1	0.1	0.6	16.0	0.8	1.3	1.1	0.1	4.3	0.1	0.6	3.0		
110801Fa	Steelville Spring Orifice	8/1/2011 19:00:00	Spring	0.0	37.0	1.1	18.0	3.0	0.9	4.8	0.1	205	16.7	31.6	0.1	0.1	0.2	0.6	14.2	0.8	1.1	1.1	0.2	3.6	0.0	0.8	10.5		
110801Fb	Steelville Spring 50' Downstream	8/1/2011 19:05:00	Spring																										
110801Fc	Steelville Spring 140' Downstream	8/1/2011 19:10:00	Spring																										
110801Fd	Steelville Spring 415' Downstream	8/1/2011 19:15:00	Spring																										
110803Aa	Blackburn Spring Orifice	8/3/2011 9:35:00	Spring	0.1	156.6	3.2	23.9	117.7	32.4	13.0	0.5	494	2.8	97.7	0.0	0.4	BDL	1.9	53.2	1.8	10.5	37.8	0.4	14.2	0.0	0.8	0.2		
110803Ab	Blackburn Spring 30' Downstream	8/3/2011 9:40:00	Spring																										
110803Ac	Blackburn Spring 90' Downstream	8/3/2011 9:45:00	Spring																										
110803Ad	Blackburn Spring 175' Downstream	8/3/2011 9:55:00	Spring																										
110803Ae	Blackburn Spring 250' Downstream	8/3/2011 10:05:00	Spring																										
110803Da	Sylvan Spring Orifice	8/3/2011 12:50:00	Spring	0.1	155.6	2.1	18.3	84.5	19.7	9.3	0.4	463	4.7	111.1	0.1	0.4	0.2	2.3	56.9	2.1	12.5	16.3	0.5	15.6	0.0	0.5	9.3		
110803Db	Sylvan Spring 30' Downstream	8/3/2011 12:55:00	Spring																										
110803Dc	Sylvan Spring 80' Downstream	8/3/2011 13:00:00	Spring																										
110803Dd	Sylvan Spring 210' Downstream	8/3/2011 13:05:00	Spring																										
110803De	Sylvan Spring Orifice (Redo)	8/3/2011 13:15:00	Spring																										
110818Aa	Mastodon Spring Cave Orifice	8/18/2011 10:10:00	Spring																										
110818Ab	Mastodon Spring, Spring Orifice	8/18/2011 10:15:00	Spring	0.0	104.0	2.3	15.3	27.3	9.1	5.7	0.2	378	41.2	118.6	0.0	0.3	0.5	0.4	42.2	2.3	4.2	0.9	0.4	11.4	0.0	0.6	5.3		
110818Ac	Mastodon Spring 75' Downstream	8/18/2011 10:20:00	Spring																										

Sample ID	Site	Date and Time	Feature Type	B (ppm)	Ca (ppm)	K (ppm)	Mg (ppm)	Na (ppm)	S (ppm)	SI (ppm)	Sr (ppm)	Calculate HCO ₃ ⁻ (ppm)	Al (ppb)	Ba (ppb)	Cd (ppb)	Co (ppb)	Cr (ppb)	Cu (ppb)	Fe (ppb)	Ga (ppb)	Li (ppb)	Mn (ppb)	Mo (ppb)	Ni (ppb)	Pb (ppb)	Rb (ppb)	Zn (ppb)	
110818B	Lithium Spring	8/18/2011 12:15:00	Spring	0.1	105.8	9.9	34.2	185.7	9.5	6.5	0.9	615	2.3	92.8	0.1	0.4	1.6	2.5	43.4	1.4	224.2	4.7	0.4	13.1	0.5	5.2	26.4	
110818Ga	Pevely/Milkfarm Spring Orifice	8/18/2011 15:45:00	Spring	0.0	108.6	2.9	14.8	18.1	12.6	5.8	0.2	362	6.4	112.5	0.1	0.4	0.0	0.7	47.5	2.1	4.1	9.4	0.3	14.0	0.4	0.6	31.5	
110818Gb	Pevely/Milkfarm Spring 150' Downstream	8/18/2011 15:50:00	Spring																									
110825Aa	Glatt's Spring Orifice	8/18/2011 15:00:00	Spring	0.0	111.6	2.1	13.7	19.2	13.7	5.6	0.2	392	0.4	103.4	0.1	0.5	BDL	2.4	42.9	2.1	3.9	69.8	0.3	13.1	0.1	0.5	61.3	
110825Ab	Glatt's Spring 30' Downstream	8/18/2011 15:05:00	Spring																									
110825Ac	Glatt's Spring 250' Downstream	8/18/2011 15:20:00	Spring																									
110825Ad	Glatt's Spring 775' Downstream	8/18/2011 15:30:00	Spring	0.0	109.3	1.7	13.3	19.3	12.8	5.4	0.2	384	4.5	104.6	0.3	0.6	BDL	2.0	47.6	1.9	4.0	55.5	0.3	14.6	0.0	0.4	30.3	
110825Ae	Glatt's Spring 775' Downstream (Redo)	8/18/2011 14:45:00	Spring																									
100709I	Cliff Cave Spring	7/9/2010 17:15:00	Cave	0.1	75.2	2.4	14.7	30.7	12.8	6.0	0.2	307	110.0	79.9	0.0	0.2	3.5	2.2	32.0	2.3	2.6	16.4	0.8	2.8	0.9	0.9	2.5	
100716E	Babler Spring	7/16/2010 16:25:00	Cave	0.0	90.0	0.7	13.4	6.6	9.1	7.0	0.1	325	25.4	101.4	0.0	0.1	0.8	0.4	23.1	2.7	0.5	5.3	0.2	3.3	0.1	0.3	4.6	
100824A	Double Drop Spring Cave	8/24/2010 11:00:00	Cave	0.0	125.7	1.2	20.5	39.4	17.4	12.3	0.2	387	75.5	121.2	0.1	0.2	1.3	1.5	29.1	2.1	4.0	13.2	0.4	4.4	0.2	0.5	6.8	
100824Aa	Double Drop Spring Cave 5' Downstream	8/24/2010 11:15:00	Cave																									
100824Ab	Double Drop Spring Cave 10' Downstream	8/24/2010 11:30:00	Cave																									
100824Ac	Double Drop Spring Cave 30' Downstream	8/24/2010 11:35:00	Cave																									
100824B	Cliff Cave Spring	8/24/2010 12:00:00	Cave	0.1	108.8	1.7	22.0	46.1	18.8	11.3	0.2	379	59.0	118.8	0.0	0.2	0.6	1.6	32.9	2.1	4.2	7.9	0.7	4.3	0.2	0.6	1.1	
100824Ba	Cliff Cave Spring 150' Downstream	8/24/2010 12:10:00	Cave																									
100824C	Spit Cave	8/24/2010 12:30:00	Cave	0.1	102.9	4.1	17.7	72.9	16.3	9.2	0.3	389	236.8	119.5	0.1	0.3	0.7	2.3	41.7	2.0	2.3	17.3	0.6	4.6	0.8	0.8	21.0	
100824Ca	Spit Cave in cave at triangular opening	8/24/2010 12:40:00	Cave																									
100824D	Cave of the Falls	8/24/2010 13:30:00	Cave	0.0	107.6	2.9	19.9	71.3	15.9	8.1	0.3	365	85.2	135.5	0.0	0.2	0.8	1.9	33.3	2.6	5.7	9.0	1.9	4.4	0.3	0.9	5.3	
100827C	Onondaga Cave Spring	8/27/2010 13:20:00	Cave	0.0	47.2	0.8	25.7	1.0	1.2	3.7	0.0	271	25.9	44.6	0.0	0.1	0.5	0.3	14.1	1.0	0.1	1.5	0.2	2.2	0.1	0.6	22.6	
100827Ca	Onondaga Cave Spring Entrance	8/27/2010 13:40:00	Cave																									
100827Cb	Onondaga Cave Spring 55' Downstream of 100827C	8/27/2010 13:30:00	Cave																									
100827Cc	Onondaga Cave Spring near Bridge	8/27/2010 13:35:00	Cave																									
101022D	Lone Hill Onyx Cave	10/22/2010 16:45:00	Cave	0.0	78.7	0.6	31.6	11.7	2.5	5.6	0.1	419	49.6	84.8	0.1	0.2	2.3	0.4	23.8	1.8	0.3	4.1	0.3	2.9	0.9	0.3	3.2	
110801Ca	Babler Spring Orifice	8/1/2011 13:00:00	Cave	0.0	89.7	0.9	13.7	9.5	7.1	10.1	0.2	332	2.8	85.4	0.0	0.2	BDL	0.2	27.4	1.8	1.9	0.4	0.2	6.8	0.0	0.3	BDL	
110801Cb	Babler Spring 25' Downstream	8/1/2011 13:05:00	Cave																									

Sample ID	Site	Date and Time	Feature Type	B (ppm)	Ca (ppm)	K (ppm)	Mg (ppm)	Na (ppm)	S (ppm)	SI (ppm)	Sr (ppm)	Calculate HCO ₃ ⁻ (ppm)	Al (ppb)	Ba (ppb)	Cd (ppb)	Co (ppb)	Cr (ppb)	Cu (ppb)	Fe (ppb)	Ga (ppb)	Li (ppb)	Mn (ppb)	Mo (ppb)	Ni (ppb)	Pb (ppb)	Rb (ppb)	Zn (ppb)		
110801Cc	Babler Spring 60' Downstream	8/1/2011 13:10:00	Cave																										
110801Cd	Babler Spring 130' Downstream	8/1/2011 13:15:00	Cave																										
110801Ce	Babler Spring 180' Downstream	8/1/2011 13:20:00	Cave																										
110801Cf	Babler Spring 370' Downstream	8/1/2011 13:25:00	Cave																										
110801Cg	Babler Spring Orifice (Redo)	8/1/2011 13:30:00	Cave																										
110803Ba	Cliff Cave Spring Orifice	8/3/2011 10:45:00	Cave	0.0	105.3	2.6	20.0	55.6	13.5	12.4	0.3	403	6.8	123.5	0.0	0.3	0.1	1.4	37.9	2.4	11.2	0.8	0.7	10.8	0.0	0.6	0.2		
110803Bb	Cliff Cave Spring 30' Downstream	8/3/2011 10:55:00	Cave																										
110803Bc	Cliff Cave Spring 150' Downstream	8/3/2011 11:05:00	Cave																										
110803Bd	Cliff Cave Spring 300' Downstream	8/3/2011 11:15:00	Cave																										
110803Be	Cliff Cave Spring 500' Downstream	8/3/2011 11:25:00	Cave																										
110803Ca	Double Drop Spring Orifice	8/3/2011 11:35:00	Cave	0.0	105.6	1.4	19.1	43.9	13.4	16.4	0.3	372	3.4	121.6	0.0	0.3	1.2	0.9	39.3	2.4	12.8	1.1	0.3	11.7	0.0	0.4	0.1		
110803Cb	Double Drop Spring Cave 10' Downstream	8/3/2011 12:00:00	Cave																										
110818C	Blue Spring Upper Resurgence	8/18/2011 12:50:00	Resurgence																										
110818D	Blue Spring Lower Resurgence	8/18/2011 13:00:00	Resurgence	0.0	59.0	5.0	23.3	21.2	6.4	6.5	0.2	306	11.1	122.8	0.1	0.4	0.4	1.4	25.0	2.5	9.0	62.0	1.0	7.6	0.3	1.2	16.0		
110818E	Keyhole Spring Upper Resurgence	8/18/2011 13:30:00	Resurgence	0.0	59.4	4.4	24.8	20.4	5.3	7.2	0.2	313	36.5	124.5	0.2	0.4	1.0	2.3	28.3	2.5	3.9	35.1	0.8	9.0	0.4	1.2	209.8		
110818F	Keyhole Spring Lower Resurgence	8/18/2011 13:55:00	Resurgence	0.0	59.9	4.1	25.1	20.3	5.3	7.6	0.2	307	8.1	127.4	0.1	0.3	0.7	1.4	26.1	2.5	3.6	18.5	0.8	8.3	0.3	0.8	20.2		
100716B	Prairie Lake	7/16/2010 14:40:00	Lake	0.0	9.6	2.2	2.0	0.4	1.3	0.8	0.0	38	73.3	35.3	0.0	0.5	1.0	1.8	37.0	1.1	0.0	66.3	0.3	0.9	0.8	1.1	2.7		
111007A	LD26	10/7/2011 14:15:00	River	0.2	50.0	3.6	20.4	23.4	12.7	2.0	0.1	226	24.6	62.0	0.1	0.4	1.4	2.9	21.0	2.5	9.5	99.7	2.2	4.4	0.4	1.3	12.4		
111007B	LBS	10/7/2011 15:00:00	River	0.2	58.2	8.9	19.9	65.2	53.5	3.8	0.5	242	20.2	116.6	0.2	0.4	0.4	4.4	31.4	2.1	116.4	15.4	3.9	12.6	0.1	2.3	37.7		
100919F	Kiefer Creek upstream USGS gaging station	9/19/2010 11:42:00	Stream	0.0	21.0	3.3	3.4	19.6	3.8	2.5	0.1	106	158.0	33.9	0.0	0.2	2.0	4.1	18.1	0.9	1.1	14.3	1.1	1.9	0.2	0.9	12.7		
101002B	LaBarque Creek	10/2/2010 12:15:00	Stream	0.0	44.9	2.5	16.6	11.9	4.4	4.3	0.1	213	0.6	92.9	0.1	0.3	2.4	1.3	17.3	2.1	0.5	80.8	0.4	3.0	0.0	0.7	13.3		
101002C	Fox Creek	10/2/2010 12:45:00	Stream	0.0	73.2	2.9	15.5	29.2	5.8	4.6	0.1	336	2.1	114.8	0.1	0.2	0.8	1.1	19.1	2.6	0.6	32.2	0.4	3.3	0.1	0.5	7.8		
101002D	Williams Creek	10/2/2010 14:06:00	Stream	0.0	81.1	3.0	13.0	32.7	10.2	5.4	0.2	339	3.7	108.1	0.1	0.2	2.3	1.6	19.8	2.3	0.9	15.3	0.6	3.8	0.0	0.8	9.6		
101002F	Fishpot Creek	10/2/2010 14:45:00	Stream	0.0	58.3	3.5	8.4	28.7	8.7	3.7	0.2	239	2.0	73.9	0.0	0.2	0.9	1.4	15.4	1.9	2.2	32.1	1.7	2.7	0.1	0.8	7.3		
101002H	Kiefer Creek upstream USGS gaging station	10/2/2010 15:12:00	Stream	0.0	103.6	3.5	15.7	54.6	16.5	5.2	0.2	435	0.8	129.4	0.1	0.2	1.3	2.2	27.7	2.8	2.3	31.6	0.5	4.6	0.1	0.8	15.4		
101002J	Kiefer Creek swimming hole	10/2/2010 15:35:00	Stream	0.0	90.4	3.8	14.8	61.6	17.0	4.7	0.2	358	1.3	122.9	0.1	0.2	0.8	1.2	24.8	2.6	3.3	7.5	0.6	3.6	0.1	0.9	6.3		

Sample ID	Site	Date and Time	Feature Type	B (ppm)	Ca (ppm)	K (ppm)	Mg (ppm)	Na (ppm)	S (ppm)	SI (ppm)	Sr (ppm)	Calculate HCO ₃ ⁻ (ppm)	Al (ppb)	Ba (ppb)	Cd (ppb)	Co (ppb)	Cr (ppb)	Cu (ppb)	Fe (ppb)	Ga (ppb)	Li (ppb)	Mn (ppb)	Mo (ppb)	Ni (ppb)	Pb (ppb)	Rb (ppb)	Zn (ppb)		
110801G	Stream at Confluence with Steelville Spring Branch	8/1/2011 19:20:00	Stream																										
100621A - Duplicate	LaSalle Spring	6/21/2010 10:00:00	QA/QC																										
100716A - lab duplicate with old colilert	Weldon Spring	7/16/2010 14:15:00	QA/QC																										
100716C - lab duplicate	Duckett Creek Treatment Plant #2	7/16/2010 15:00:00	QA/QC																										
100716F - lab duplicate with old colilert	LaSalle Spring	7/16/2010 17:00:00	QA/QC																										
100919G	Rockwoods Spring (unfiltered)	9/19/2010 12:15:00	QA/QC	0.0	72.6	2.5	8.6	27.1	5.7	5.6	0.1	318	312.5	77.8	0.0	0.2	2.3	1.6	33.6	1.6	0.7	19.7	0.3	2.9	0.9	0.6	6.3		
101002B	LaBarque Creek	10/2/2010 12:15:00	QA/QC	0.0	45.2	2.2	16.6	9.4	4.4	4.3	0.1	233																	
101002C	Fox Creek	10/2/2010 12:45:00	QA/QC	0.0	74.6	2.8	15.4	28.0	5.9	4.6	0.1	361																	
101002D	Williams Creek	10/2/2010 14:06:00	QA/QC	0.0	81.2	3.0	13.0	37.4	10.1	5.4	0.2	378																	
101002F	Fishpot Creek	10/2/2010 14:45:00	QA/QC	0.0	58.4	3.4	8.4	28.0	8.6	3.7	0.1	267																	
101002J	Kiefer Creek swimming hole	10/2/2010 15:35:00	QA/QC	0.0	89.1	3.8	14.7	51.0	16.7	4.7	0.2	422																	

Appendix L: Wastewater Treatment Plant Data

Site	Water Type	SpC (µS/cm)	Turbidity (NTU)	TSS (ppm)	Ca (ppm)	Mg (ppm)	Calculated HCO ₃ ⁻ (ppm)	Na (ppm)	Cl (ppm)	NH ₄ ⁺ -N (ppm)	NO ₃ ⁻ -N (ppm)	PO ₄ ³⁻ -P (ppm)	SO ₄ ²⁻ -S (ppm)	K (ppm)	Si (ppm)	δ ¹⁸ O (‰)	δD (‰)	<i>E. coli</i> Easygel (cfu/100mL)	Coliforms Easygel (cfu/100mL)
Duckett Creek #2	Effluent	773	4		46.1	16.0	217	76.9	68	0.27	16.8	1.73	29.7	14.4	5.9	-7.2	-50	-	-
Duckett Creek #1	Effluent	795	9	35	65.3	18.2	269	50.5	54	0.44	3.2	0.26	19.0	6.1	4.3	-9.3	-62	-	-
Duckett Creek #2	Effluent	822	4	10	51.6	16.9	255	93.0	94	0.59	14.2	1.26	25.1	14.6	5.3	-8.8	-60	-	-
Coldwater Creek	Influent	883	114.0	120	45.3	21.9	299	108.0	30	34.00	3	1.50	56.3	19.2	5.5	-10.3	-81	2,800,000	25,100,000*
	Effluent	818	6.0	0	34.9	20.6	200	113.8	74	10.40	3.1	0.96	56.6	20.0	5.3	-10.6	-82	0	100,000
Missouri River	Influent	968	151.0	182	45.0	21.6	271	114.1	44	33.20	0	1.76	61.1	20.2	5.6	-10.6	-78	7,800,000	59,000,000*
	Effluent	873	25.0	26	41.7	21.6	273	121.5	77	8.30	11.7	1.40	49.3	22.6	5.7	-11.0	-79	100,000	2,100,000
Grand Glaize	Influent	956	247.0	272	49.4	21.0	370	147.1	27	37.10	0.2	1.44	70.7	25.0	5.3	-10.4	-82	1,310,000	7,710,000*
	Effluent	781	5.0	32	43.0	20.1	240	123.7	84	0.40	20.6	0.96	55.5	22.8	4.9	-10.4	-80	0	0
Fenton	Influent	746	141.0	148	32.6	20.4	331	68.6	10	20.10	0.8	1.99	15.9	15.9	3.3	-5.7	-40	16,500,000	82,100,000*
	Effluent	661	2.0	2	35.5	20.8	210	74.4	95	1.23	19.7	1.88	16.0	15.8	3.3	-5.7	-40	0	0
Lower Meramec	Influent	813	142.0	170	52.2	18.6	308	69.6	10	21.60	0.8	1.77	34.8	13.2	3.6	-5.8	-40	17,100,000	104,300,000*
	Effluent	675	9.0	12	44.0	17.8	168	66.4	89	0.71	9.9	1.25	25.9	13.0	3.5	-5.7	-40	200,000	2,200,000
Lemay	Influent	831	377.0	384	55.6	21.1	285	102.3	50	16.90	1.6	1.82	53.2	17.3	5.0	-9.5	-74	2,800,000	30,000,000*
	Effluent	762	9.0	18	42.9	19.9	232	99.4	51	4.37	3.8	1.38	52.2	15.4	4.8	-9.6	-74	200,000	1,100,000
Bissell Point	Influent	1328	433.0	208	52.3	30.4	448	267.2	105	4.65	0.8	1.86	114.0	26.7	5.0	-10.8	-81	600,000	6,400,000
	Effluent	1099	13.0	24	40.4	22.1	216	192.5	145	0.99	18	1.19	81.2	19.1	7.7	-12.7	-85	0	0

*Estimated because of high colony density.

Site	Water Type	Al (ppb)	B (ppb)	Cd (ppb)	Co (ppb)	Cr (ppb)	Cu (ppb)	Fe (ppb)	Li (ppb)	Mn (ppb)	Mo (ppb)	Ni (ppb)	Pb (ppb)	Zn (ppb)
Duckett Creek #2	Effluent	6.9	240	0.04	0.24	1.2	2.8	13.8	15.0	20.2	3.6	3.5	0.1	38.5
Duckett Creek #1	Effluent	25.1	51	0.24	0.31	0.6	3.0	25.1	3.6	22.9	2.4	4.4	0.2	32.8
Duckett Creek #2	Effluent	4.8	147	0.26	0.60	0.7	3.5	20.0	8.0	9.6	2.4	3.9	0.2	61.1
Coldwater Creek	Influent	426.3	228	0.85	0.86	8.2	16.8	285.4	90.2	190.8	5.2	12.1	12.1	430.1
	Effluent	48.0	347	0.16	0.74	1.7	6.8	40.8	99.5	144.4	4.3	8.9	1.3	312.1
Missouri River	Influent	327.8	274	0.44	1.11	4.5	17.6	630.9	87.1	292.4	0.7	12.8	2.3	674.4
	Effluent	98.7	355	0.13	0.77	2.4	16.4	251.5	94.3	205.5	4.6	12.2	0.8	216.1
Grand Glaize	Influent	822.3	340	0.69	0.97	2.9	14.4	309.3	83.2	378.8	3.7	11.3	16.9	1933.9
	Effluent	50.4	341	0.35	0.65	0.1	8.2	37.6	88.7	54.1	6.0	10.4	2.8	224.2
Fenton	Influent	348.7	209	0.18	0.70	2.6	17.6	65.3	15.0	107.4	2.6	10.4	4.3	519.3
	Effluent	34.0	231	0.13	0.60	0.2	8.5	26.9	30.5	31.2	2.7	8.8	1.1	349.6
Lower Meramec	Influent	939.4	191	0.31	0.73	4.2	7.9	91.8	18.6	132.6	1.7	13.5	1.7	244.7
	Effluent	67.1	216	0.14	0.49	0.4	11.4	52.5	20.7	36.7	5.8	10.1	1.0	964.9
Lemay	Influent	1722.6	249	0.97	3.57	7.0	10.8	481.8	54.3	772.9	3.2	12.8	15.1	551.7
	Effluent	56.7	260	0.09	1.31	0.1	6.6	50.5	80.5	201.7	4.7	11.0	0.6	166.1
Bissell Point	Influent	124.0	238	0.88	1.88	2.2	22.1	539.6	142.3	77.2	10.0	19.0	1.9	786.2
	Effluent	103.4	246	1.55	0.61	5.2	12.9	113.0	99.0	208.8	7.5	15.1	1.1	336.0